JP0250084

JAERI-Conf 2001-017

PROCEEDINGS OF THE 2000 WORKSHOP ON THE UTILIZATION OF RESEARCH REACTORS

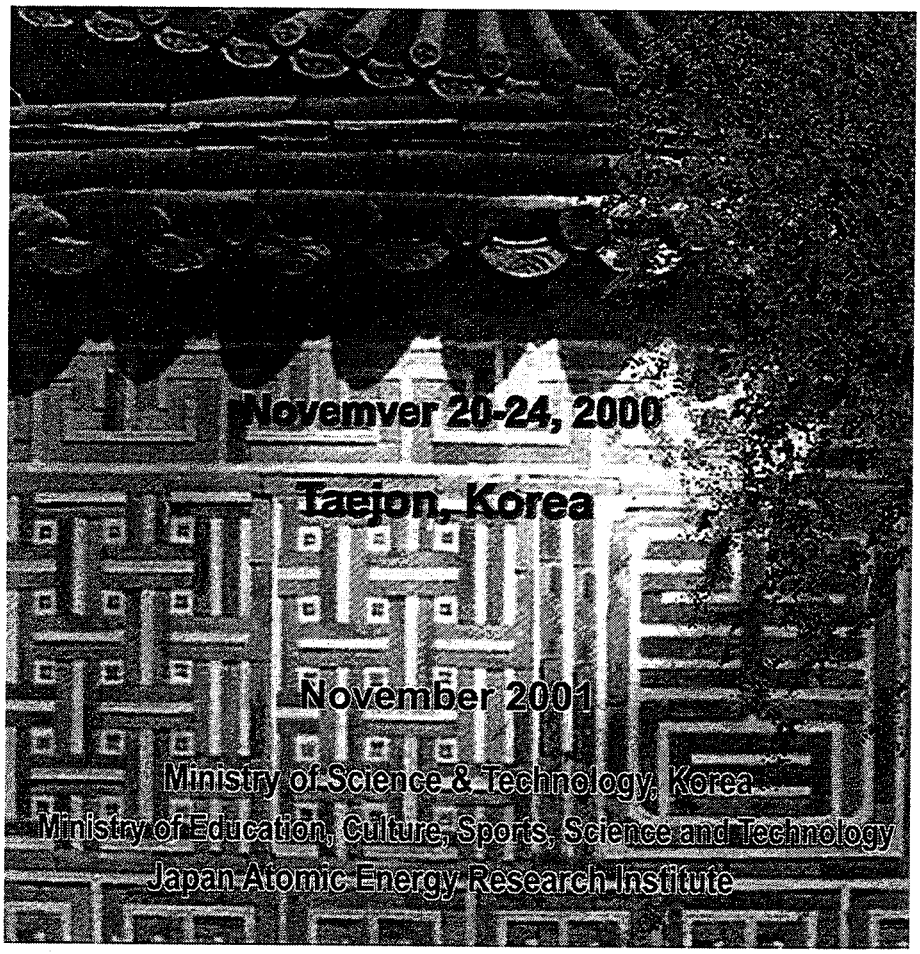

Department of Research Reactor

日 本 原 子 力 研 究 所

Japan Atomic Energy Research Institute

本レポートは、日本原子力研究所が不定期に公刊している研究報告書です。
入手の問合わせは、日本原子力研究所研究情報部研究情報課（〒319-1195　茨城県那珂郡東海村）あて、お申し越し下さい。なお、このほかに財団法人原子力弘済会資料センター（〒319-1195　茨城県那珂郡東海村日本原子力研究所内）で複写による実費領布を行っております。

This report is issued irregularly.
Inquiries about availability of the reports should be addressed to Research Information division, Department of Intellectual Resources, Japan Atomic Energy Research Institute, Tokai-mura, Naka-gun, Ibaraki-ken 319-1195, Japan.

© Japan Atomic Energy Research Institute, 2001

編集兼発行　日本原子力研究所

The 2000 Workshop on the Utilization of Research Reactors

November 20-24,2000 Taejon, Korea

1. Opening (November 20)

Welcome address by Mr. CHANG, KAERI

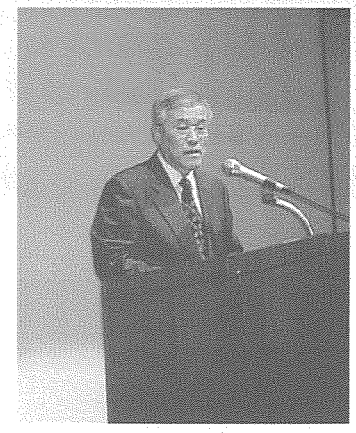

Opening address by
Mr. LEE, MOST, KOREA
& Mr. SHIGEYAMA, STA, JAPAN

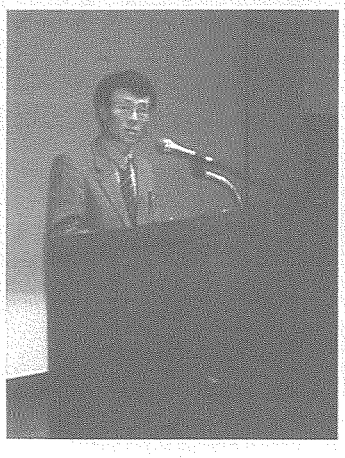

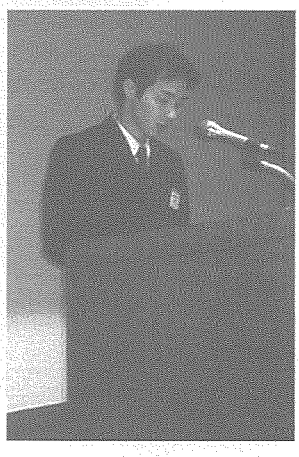

Participants for Workshop on U.R.R.

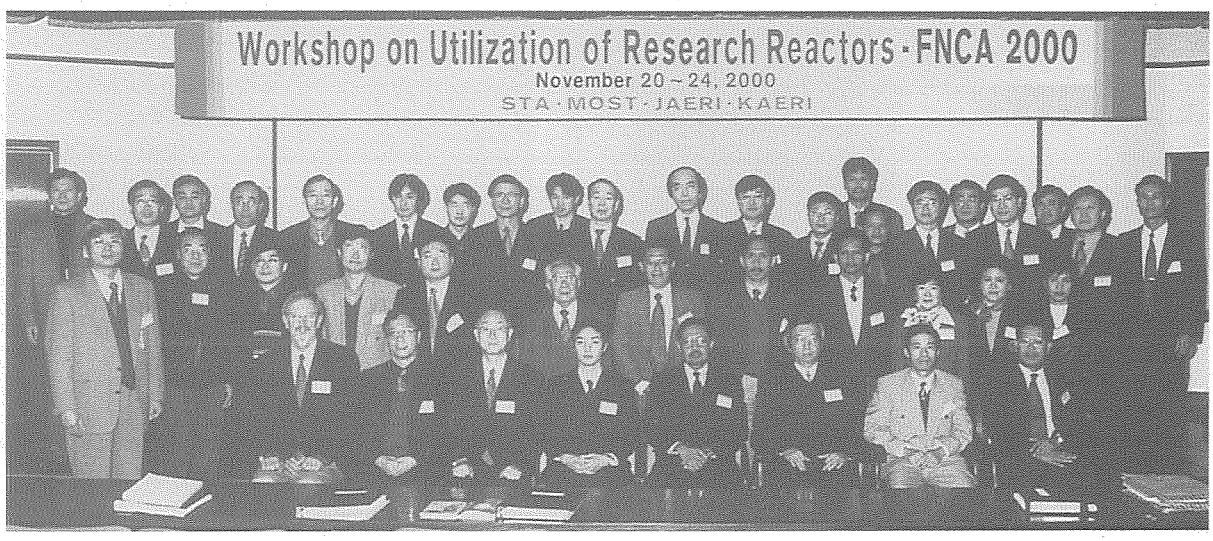

Opening session (November 20, at Seminar room, KAERI)





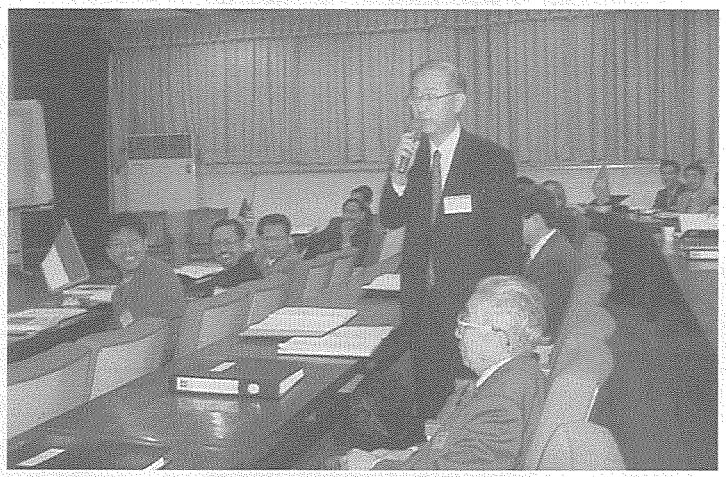

2. Neutron Scattering (November 20 at NSL, KAERI)

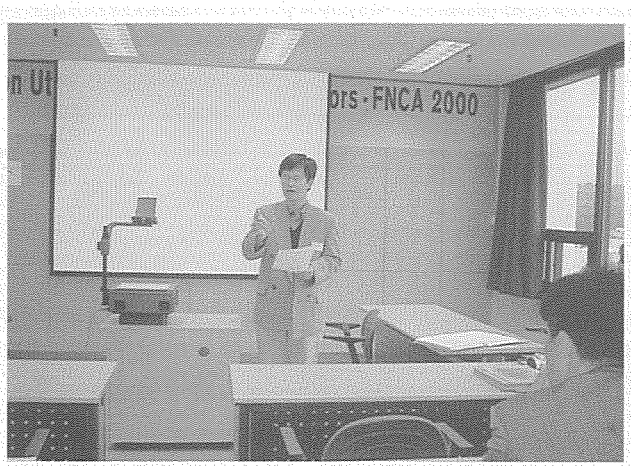



Small Angle Neutron Scattering Experiments (November 20-24 at HANARO Reactor Hall)

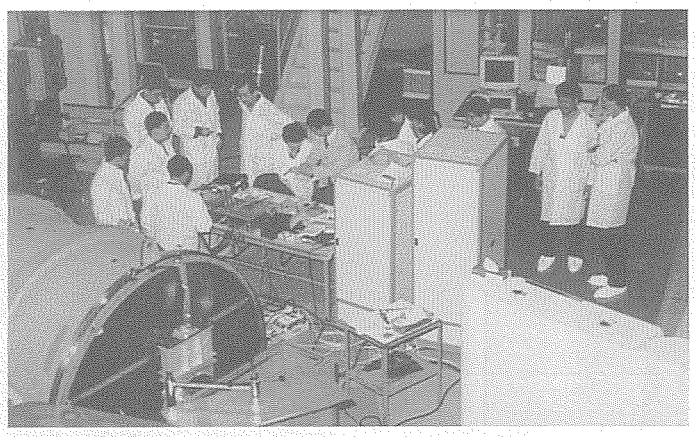

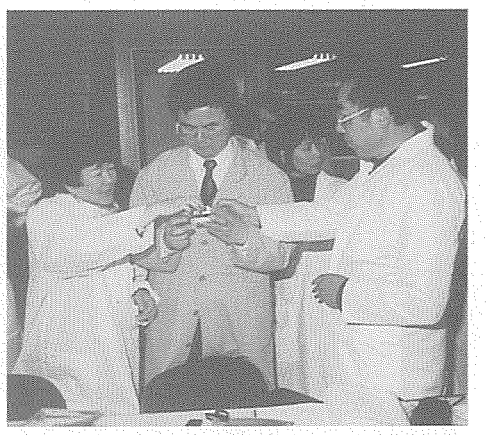

3. Neutron Activation Analysis (November 20-23, KAERI)





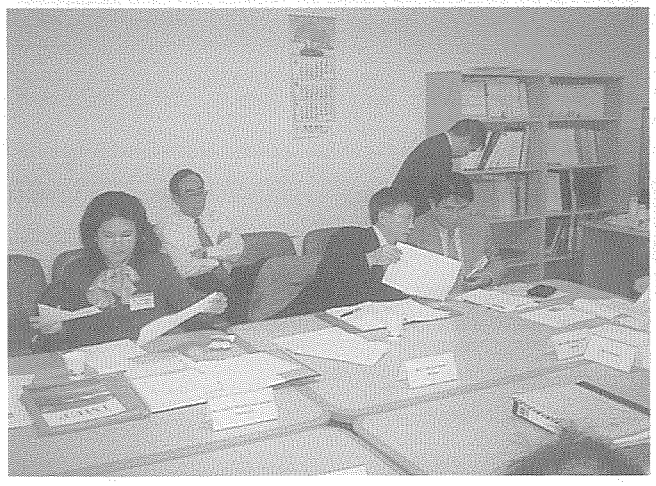



4. Utilization Technology (BNCT) (November 20-23, KAERI)



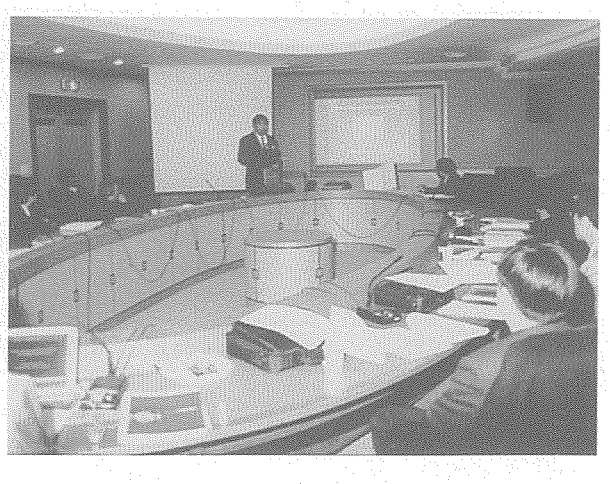

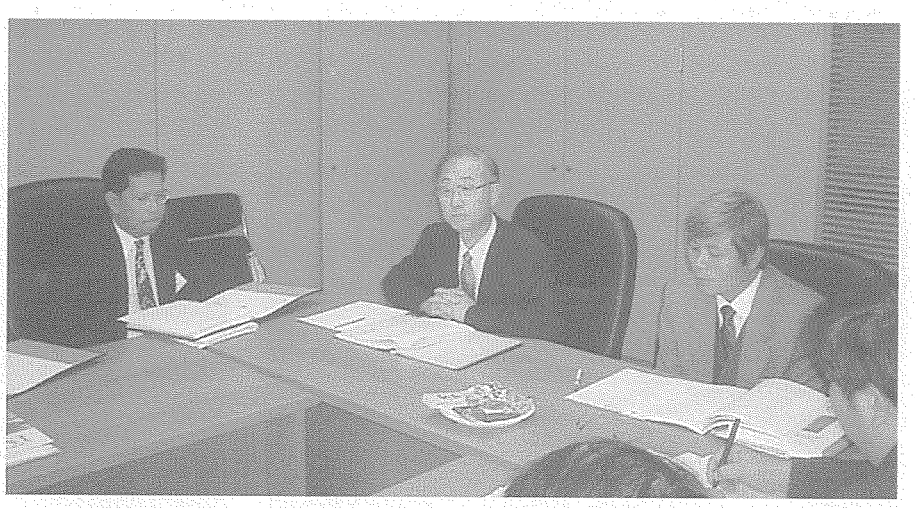





5. Round Table Discussion (November 24, 2000 at SPAPIA HOTEL)



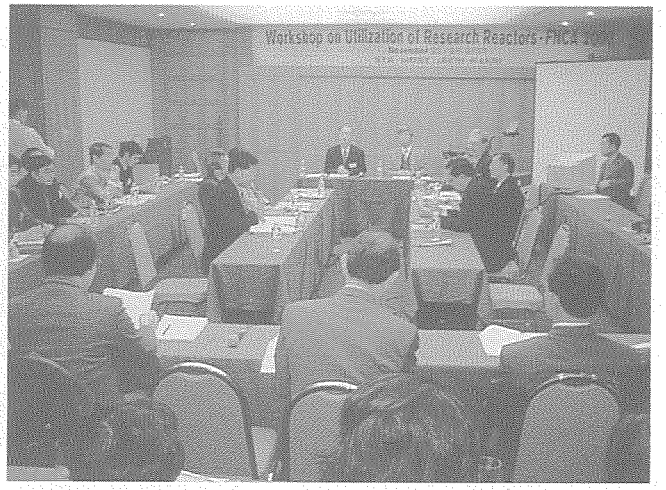





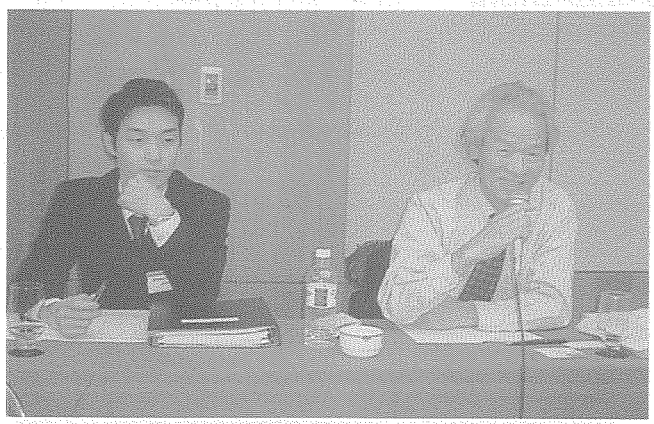

Site Tour : RI Building & Reactor Building (November 22, KAERI)



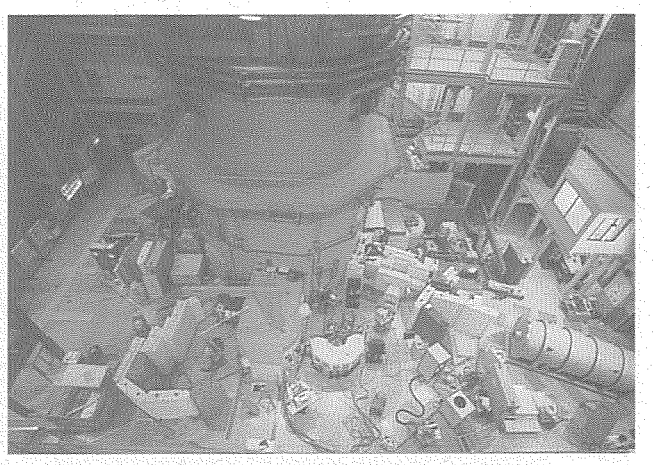

Site Tour : HANARO Reactor Hall (November 22, KAERI)

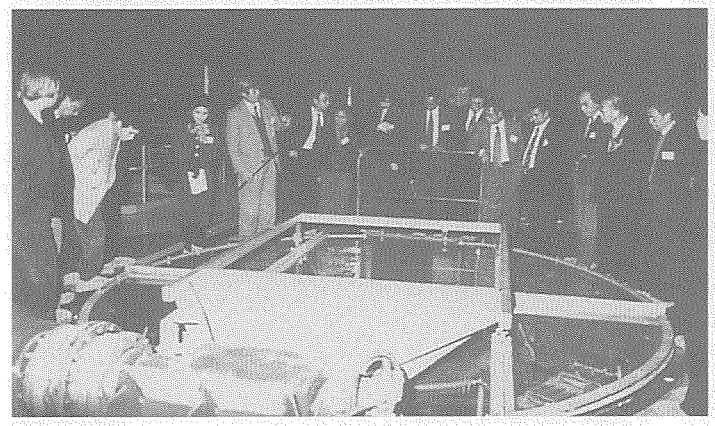



Technical Tour : Yonggwang Nuclear Power Plant

(November 23, 2000)





JAERI－Conf 2001－017

Proceedings of the 2000 Workshop on the Utilization of Research Reactors

November 20 – 24

Taejon, Korea

(Contract Research)

Department of Research Reactor

Tokai Research Establishment

Japan Atomic Energy Research Institute

Tokai-mura, Naka-gun, Ibaraki-ken

(Received November 6, 2001)

The 2000 Workshop on the Utilization of Research Reactors, which is the ninth Workshop on the theme of research reactor utilization, was held in Taejon, Korea from November 20 to 24. This Workshop was executed based on the agreement in the First Coordinator's Meeting of Forum for Nuclear Cooperation in Asia (FNCA) held in Tokyo, March 2000.

The Workshop consists of three groups under the themes of the following fields; 1) Neutron Scattering, 2) Neutron Activation Analysis, and 3) Research Reactor Utilization (BNCT). The total number of participants for the Workshop was about 60 people from 8 countries; Australia, China, Indonesia, Korea, Malaysia, The Philippines, Thailand, Vietnam, and Japan.

This report consists of 13papers for Neutron Scattering, 12 papers for Neutron Activation Analysis, and 12 papers for Research Reactor Utilization (BNCT) and 2 summary reports.

Keywords: Utilization, Research Reactor, Neutron Scattering, Neutron Activation Analysis, Research Reactor Utilization, BNCT, and FNCA.

This Workshop was sponsored by the Ministry of Education, Culture, Sports, Science and Technology (MEXT), and the Japan Atomic Energy Research Institute (JAERI) had been assigned by MEXT as the responsible organization for holding the Workshop. This report includes the results carried out under the contract between JAERI and MEXT under the auspices of the special account law for electric power development promotion.

JAERI－Conf 2001－017

2000年度　研究炉利用ワークショップ　論文集

2000年11月20日～24日

テジョン　韓国

（受託調査）

日本原子力研究所東海研究所

研究炉部

（2001年11月6日受理）

研究炉利用ワークショップは、2000年3月に東京で開催された第1回FNCAコーディネーター会合での合意に基づいて、文部科学省からの受託として11月20日から24日まで、韓国のテジョン市で開催されたものである。

11月20日から5日間、テジョン市において中性子散乱、中性子放射化分析及び研究炉利用技術（BNCT）の3テーマに関するワークショップを開催した。ワークショップには、オーストラリア、中国、インドネシア、韓国、マレーシア、タイ、ベトナム、及び日本の8カ国から約60名が参加した。

本論文集は13編の中性子散乱分野の報告、12編の中性子放射化分析分野の報告、12編の研究炉利用技術(BNCT)分野の報告、及び2編のサマリー報告を収録したものである。

本ワークショップは、韓国原子力研究所及び文部科学省との共催として、文部科学省から原研が受託して実施したものである。この論文集は、電源開発促進対策特別会計法に基づき、文部科学省から受託して行なった調査の結果を含む。

東海研究所：〒319-1195　茨城県那珂郡東海村白方白根2-4

CONTENTS

1. Workshop

Neutron Scattering

1.1 The Acquisition and Reduction of Small Angle Neutron Scattering Data
KNOTT Robert 1

1.2 Neutron Scattering Science at the Australian Nuclear Science and Technology Organisation(ANSTO)
KNOTT Robert 13

1.3 The Investigation of Artificial Articular Cartilage- PVA –hydrogel with SANS
YANG Tong Hua, WANG Hong Li, ZHAO Xin, CHEN Dong Feng GU Zheng Qiu, XIAO Jiu Mei, ZHANG Xiang Hong, LIN Min Yue 31

1.4 Current Status of Neutron Scattering in Indonesia
IKRAM Abarrul 34

1.5 Measurements of PS-PEP Sample in Serpong
IKRAM Abarrul, SUDIRMAN and A. INSANI 42

1.6 Revitalization of Neutron Diffractometers in Serpong
IKRAM Abarrul, M. R. MUSLIH, A. PURWANTO, T. H. PRIYANTO and E. SANTOSO 47

1.7 Progress Report on Neutron Scattering at KAERI
LEE Chang Hee 55

1.8 Enhancement of Small Angle Neutron Scattering Facility and Related Activities in Malaysia
MOHAMED Abdul, A. J. B. A. HAMID and SHUKRI B. Mohd 61

1.9 Current Status of Neutron Scattering in Thailand
SANGARIYAVANICH Archara, PONGKASEM Somchai PATCHAR Suriya, AMPORNRAT Pantip 70

1.10 Progress Report on the Preparation of Co Substitution for Cu in BSCCO(2223) Superconductor
SANGARIYAVANICH Archara, AMPORNRAT Pantip 76

1.11 High Temperature Superconductors of Pb and Sb Doped Bi-Sr-Ca-Cu-O System
TRAN Thi Thu Phuong, TRAN Kim Cuong NGUYEN Thi Cam Phuong 81

1.12 Residual Stress Analysis by Neutron Scattering
MINAKAWA Nobuaki, MORIAI Atushi, OHTOMO Akitoshi 86

1.13 Synchrotron SAXS Facility at the PAL and Its Applications in Materials Science
BOLZE Jorg, KIM Jehan, LEE Byeongdu, SHIN Joo Tae, LEE Jinwon, HUANG Jung-Yun, RAH Seungyu, YOUN Shik Hwa, LEE Ki-Bong, and REE Moonhor 92

Neutron Activation Analysis

1.14 Introduction of the Neutron Activation Analysis Facilities in High Flux Engineering Test Reactor
FENG Mingquan 131

1.15 Current Status and Progress of Research and Development of NAA at GA. Siwabessy Reactor
SUTISNA, YUSUF Saeful, RUKIHATI 137
WARDANI Sri, HAMZAH Amir, M Th Rina

1.16 Application and Facility of Neutron Activation Analysis in HANARO Research Reactor
CHUNG Yong Sam 148

1.17 The Use of Neutron Activation Analysis in Environmental Pollution Studies
MOHD YUSOF Alias, GILL S. K., SALLEH S., ... 160
AKYIL S., HAMZAH S., RAHMAN S. A., WOOD A. K. H.

1.18 Utilization of NAA in Thailand
SRINYAWACH Chastbongkoch 193

1.19 Neutron Activation Analysis at the Dalat Nuclear Research Reactor
NGUYEN Van Minh 203

1.20 NAA Supporting System of JAERI
SASAJIMA F., SAWAHATA H., ONIZAWA K., ICHIMURA S., ... 211
OHTOMO A., HORIGUCHI Y., ITO Y., TAKAYANAGI M.

1.21 Air Pollution Study by NAA in Korea
MOON Jong Hwa 223

1.22 Probabilistic Risk Analysis of Airborne Toxic Metals in Korean Industrial Complex
LEE Jin-Hong, JANG Mi-Suk 242

1.23 Application of NAA in the Field of Environmental Geology
LEE Kil Yong and YOON Yeol Yoon 248

1.24 Application of NAA in High Purity Materials
YOON Yeol Yoon and LEE Kil-Yong 258

1.25 The Study of Trace Element Distribution in Biological Samples with NAA for Human Health
CHO Seung Yeon, KANG Sang Hun, CHUNG Yong Sam 274

Research Reactor Utilization

1.26 Current Status of Operation and Utilization with Several Research Reactors in China
XU Hanming 293

1.27 Present Status of Research and Test Reactors in JAERI
SATO Mitsugu, KOBAYASHI Shinsho 302
TAKAYANAGI Masaji

1.28 Overview of HANARO
JUN Byung Jin, KIM Hark Rho 306

1.29 Utilization of Beam Ports of MINT Research Reactor
BOKHARI Adnan, KASSIM Mohammad Suhaimi 313

1.30 Current Status of Operation and Utilization of the Dalat Research Reactor
NGUYEN Nhi Dien 318

1.31 BNCT Project in Thailand
SAKDA Charoen 327

1.32 Development of BNCT Facility at the Indonesian Research Reactor
HASTOWO Hudi 335

1.33 Development of PGNAA Facility in HANARO
CHOI H. D., BYUN S. H., SUN G. M., KIM M. S., JUN B. J. 344

1.34 JRR-4 Medical Irradiation Facility
TORII Y., YAMAMOTO K., HORI N., KUMADA H., HORIGUCHI Y. 352

1.35 Development of Computational Dosimetry System and Measurement of Dose Distribution in Water Head Phantom for BNCT in JAERI
KUMADA H., YAMAMOTO K., TORII Y., MATSUMURA A., YAMAMOTO T., NAKAGAWA Y., HORIGUCHI Y. 357

1.36 Carboranyl Tetrahydroisoquinolines. Synthesis and the X- ray Structural Study of 1-(*0*-Carboran – 1- ylmethyl)-1,2,3,4-Tetrahydroisoquinolines
LEE Jong Dae, LEE Chai Ho, LEE Seung Hoon LIM Sang Moo, CHO Sungil, KANG Sang Ook 363

1.37 Neutronic Design Approach to a Small Medical Reactor for BNCT
CHO Nam Zin 368

2. Summary Reports

2.1 Workshop 371

2.2 Sub-Workshop 376

Appendix

Schedule 390

List of Participants 393

This is a blank page.

1.Workshop

Abstract & Papers

Neutron Scattering

This is a blank page.

JP0250085

1.1 The Acquisition and Reduction of Small Angle Neutron Scattering Data

Robert Knott
Australian Nuclear Science and Technology Organisation
Private Mail Bag
Menai NSW 2234
Australia.
robert.knott@ansto.gov.au

ABSTRACT

The Small Angle Neutron Scattering (SANS) technique is used to investigate problems in a wide range of fields including chemistry, materials science and biology. Therefore, there is considerable variation in the physical and chemical form of samples, with liquids, hard and soft solids, and gaseous particulates all under investigation. In order to obtain accurate SANS data from these samples, it is very important to design the experiment and configure the instrument appropriately.

Given that the SANS technique will provide structural information on bulk material, the first step is to ensure that the sample has maximum scattering contrast and the correct geometry, and that the sample environment (temperature, pressure etc) is applied with minimum impact on the sample scattered pattern.

The next important step is to configure the SANS instrument. A typical instrument has a variable wavelength and wavelength resolution, and adjustable pre- and post-sample flight paths. The proper configuration for a given sample depends upon many factors, including the sample size and density, the size of the scattering object (which determines the desired q range) in the sample, the neutron scattering and absorption cross-sections of the sample, and desired accuracy of the data. A number of algorithms have been developed to assist with the calculation of the instrument geometry.

A complete SANS experiment requires not only the measurement of the scattered pattern from the sample but also the measurement of the empty cell and blocked beam, plus correction for instrumental effects such as detector uniformity. In addition, data from a standard sample must be collected to place

the sample scattered pattern on an absolute scale. This will often assist with the interpretation of the scattered pattern.

Generally the 2D scattered pattern must be reduced to a 1D (intensity versus q) profile to facilitate fitting of various models and functional forms. A number of algorithms are available for this reduction including radial integration for isotropic scattered patterns, and segment integration for anisotropic scattered patterns.

The final step is the storage and transmission of all the data for further analysis. It is often very convenient to adopt a standard format for data storage particularly when transferring data from one institute to another. There are a number of international standard formats presently under discussion.

SAMPLE PREPARATION

Initial planning. The first step in a SANS experiment is to define the structural feature of interest and then to decide if the feature is accessible with the SANS technique given the length scale of ~10Å to ~5000Å applies. Is there sufficient sample available and what is the neutron scattering contrast within the sample? Can the scattering contrast be readily changed, and finally what environment is required either to maintain a sample in a given state, or to explore a scattering dependence on an external parameter (temperature, pressure, shear etc)?

Neutron scattering contrast. The neutron scattering length density, ρ, is calculated from the chemical composition of the sample, viz:

$$\rho = \frac{\sum_i^n b_i}{\bar{V}} = N_A\left(\frac{\rho_{mass}}{M_W}\right)\left(\sum_i b_i\right)_{molecule}$$

where N_A = Avagardo's number (6×10^{23}), M_W = molecular weight, b_i = bound coherent scattering length of atom i.

The scattering length density is a fundamental parameter that can be calculated for all sample components if the chemical composition and mass density are known. From the ρ of each component the contrast factor for the sample may be calculated and it is this parameter that will indicate the likely success of the SANS experiment. It may also suggest whether the deuteration of the sample, the solvent, or the supporting matrix will provide a higher contrast and therefore improved SANS data.

Sample cells. Samples for SANS experiments come in very different physical and chemical forms and include soft and hard solids, liquids and gel, and even fine gaseous particulates. A range of sample environments is usually available with liquid sample thickness varying from 1 to 5mm and diameter 10 to 25mm (Figure 1). Sample cells usually have quartz (suprasil or equivalent) windows but thin aluminium may also be used. However, if a new material is to be used for a cell window it is advisable to check for any scattering in the small angle region.

Sample size. The area of the sample must be greater than the area of the neutron beam. The area of the neutron beam is calculated to give the highest

neutron intensity for the lowest q_{min} required by the experiment (**Section: SANS Instrument Configuration**). The sample thickness must be selected for maximum scattered intensity and the scattering processes within the sample must be considered (Figure 2). As a general rule a sample with large hydrogen content should not be more than 1mm thick, and a low hydrogen content sample may be up to 5mm thick.

Sample environment. There is an extensive range of sample environments possible. Temperature, pressure, shear and magnetic field are the most commonly varied parameters.

- Furnaces, heating/cooling blocks, and cryostats are used for high, medium, and low temperatures respectively.
- High pressures require a pressure cell and a vacuum is usually readily available for low pressure.
- A Couette cell (Figure 3) is best used for liquids and gels, and a plate shear cell for shearing soft solids (eg polymers in the melt)
- A magnetic field may be applied with either a standard electromagnet or a superconductor magnet for high (several tesla) magnetic fields.

To make the best use of available beam time it is advisable to use an automatic sample changer wherever possible.

SANS INSTRUMENT CONFIGURATION

A typical instrument has a variable wavelength and wavelength resolution, and adjustable pre- and post-sample flight paths[1] (Figure 4). The proper configuration for a given sample depends upon many factors, including the sample size and density, the size of the structural feature (which determines the desired q range) in the sample, the neutron scattering and absorption cross-sections of the sample, and desired accuracy of the data. A number of algorithms have been developed to assist with the calculation of the instrument geometry.

The appropriate q range can be chosen for a given sample by considering the following relations:

$$q_{min} \sim 2\pi / r_{max}$$

$$q_{max} \sim 2\pi / r_{min}$$

where r_{max} and r_{min} are the longest and shortest scale lengths in the sample, respectively. Note that 1, 2 or 3 instrument configurations may be required to cover the entire q range of interest. The beam apertures and distances which determine the instrument resolution (and hence the minimum q) as well as the intensity on the sample are indicated in Figure 4. Collimation is achieved by adjusting the incident flight path using the neutron guide sections that can be

moved into the beam in order to bring the effective neutron source closer to the sample.

The values of q_{min} for a given configuration can be computed from

$$q_{min}=(2\pi/\lambda)\vartheta_{min}$$

where ϑ_{min} is the nominal value of the scattering angle at which the measured incident beam intensity would go to zero. Thus

$$\vartheta_{min}= (B/2+A_3/2)/L_2$$

where A_3 is the FWHM of the detector spatial resolution function and B is the penumbra beam size at the detector given by

$$B=(L_2/L_1)(A_1+A_2)+A_2$$

Therefore,

$$q_{min}=(\pi/\lambda)\{(A_1+A_2)/L_1+(A_2+A_3)/L_2\}$$

Here A_1, A_2 and A_3 are the source aperture, sample aperture and detector resolution respectively, and L_1 and L_2 are the source-to-sample and sample-to-detector distances.

Note that the direct neutron beam image on the detector must be smaller than the beamstop size.

In general, long flight paths rather than long wavelengths should be used first to reduce q_{min}. Neutron intensity values can be calculated for different configurations from one known value assuming that the intensity (n/sec) on the sample, I_s, scales as $(A_1A_2/L_1)^2$ for a given wavelength λ. These intensity values can be extrapolated to longer wavelengths assuming that $I_s\sim(1/\lambda^4)$ at long wavelengths when the wavelength spread $\Delta\lambda/\lambda$ is fixed. Flux can be increased by adding guides (shortening L_1) at the expense of q_{min} and/or by relaxing the wavelength resolution ($\Delta\lambda/\lambda$) at the expense of Δq. When higher resolution is desired then the wavelength should be increased only when the detector is at the furthest distance from the sample and all guides have been moved out of the pre-sample flight path.

When A_1, A_2, L_1 and L_2 have been selected, the beamstop size and position determined, and the sample environment selected, the instrument is ready for the experiment.

SANS Instrument Calibration. An important issue that should be considered when planning an experiment is the absolute calibration of the instrument. Whilst calibration is usually the responsibility of the instrument scientist it is important that the guest scientist is familiar with the concept and whether the process may introduce significant errors into the final reduced data. A SANS instrument requires calibration in q and in scattered intensity, I.

Silver behenate [$CH_3(CH_2)_{20}COOAg$] (AgBE) is a useful standard for q calibration since it is one of the very few materials featuring Bragg reflections in the angular range accessible to SANS instruments[2-4]. AgBE has the following favourable physical and chemical properties:

- reasonable scattering cross-section
- relatively easy to prepare quality powders
- stable over reasonable time scales
- provides a sharp diffraction peak at 1.08nm^{-1}.

AgBE has been assessed as an international standard for the calibration of both X-ray and neutron scattering instruments. It is, therefore, possible to compare the results with those obtained at other institutes around the world[2-4].

One of the major achievements of the FNCA Sub-workshops on Neutron Scattering is the inter-laboratory comparison of the q-calibration of all SANS instruments in the region.

The absolute calibration of intensity presents somewhat of a challenge. There are a number of possibilities and each has their limitations[4-7]. The following have been used for absolute intensity calibration:

- Irradiated aluminium
- Water – incoherent scatterer – inelastic effects must be considered
- Polymer mixtures
- Porous silica – pore size to match q range
- Direct neutron flux (calibrated attenuator)

The standard sample should be selected to match the q range used during the experiment and it should have a large differential cross-section (typical 20-100cm^{-1}) to minimise counting time. As given in more detail in the next section, data from the standard sample is collected under identical conditions and used to normalise the unknown sample data.

SANS DATA ACQUISITION PROTOCOL

A complete SANS experiment requires not only the measurement of the scattered pattern from the sample but also the measurement of the empty cell and blocked beam, plus correction for instrumental effects such as detector uniformity. In addition, data from a standard sample must be collected to place the sample scattered intensity on an absolute scale. This will often assist with the interpretation of the scattered data.

According to counting statistics, the noise level of an experiment decreases with the square root of the measurement time. In any experiment, a judicious choice must be made between number of samples, environmental conditions, counting statistics and the available beam time for the measurement. The counting times needed for different experiments vary widely depending upon how strongly the samples scatter and what kind of information is sought. Total detector counts per measurement may vary from 2×10^4 to 1×10^7 neutrons. The lower limit corresponds to measurements where the intensity is concentrated in the centre of the detector, and where the fit parameters have several percent error. The upper limit corresponds to data fitted over the entire detector to high accuracy. Radially integrated data consists of approximately 100 data points. To achieve a 1% noise level, a total of 1×10^6 detector counts is needed if the intensity is evenly distributed radially.

At the beginning of an experiment, an estimate is made of the time for each experiment. It is recommended to sub-divide long accumulation times into shorter time periods and monitor the neutron beam flux and the scattered intensity for major shifts in instrument parameters and/or sample characteristics.

Background runs such as from the empty cell, blocked beam, solvent or control samples should normally have accumulation times of the same length as that of the sample.

Data Correction. A complete SANS dataset consists of scattered patterns from the sample, I_{sample}, empty cell, I_{empty}, and background, $I_{background}$, viz:

$$I_{sample} = C_0 T_{sample+cell}\left(\left(\frac{d\Sigma(q)}{d\Omega}\right)_{sample} + \left(\frac{d\Sigma(q)}{d\Omega}\right)_{empty}\right) + I_{blocked\cdot beam}$$

$$I_{empty} = C_0 T_{cell}\left(\frac{d\Sigma(q)}{d\Omega}\right)_{empty} + I_{blocked\cdot beam}$$

$$I_{background} = I_{blocked\cdot beam}$$

where

$$C_0 = \phi \cdot A \cdot d \cdot \Delta\Omega \cdot \varepsilon \cdot t$$

Here ϕ = incident neutron flux; A = sample area; d = sample thickness; $\Delta\Omega$ = solid angle of each detector pixel; ε = detector efficiency; t = counting time.

The sample scattered pattern is corrected for backgrounds according to the following relationship:

$$I_{correct} = \left(I_{sample} - I_{background}\right) - \left(\frac{T_{sample+cell}}{T_{cell}}\right)\left(I_{cell} - I_{background}\right)$$

Finally, the corrected data is multiplied by the detector sensitivity matrix to account for the pixel to pixel variation in detector efficiency.

The resultant intensity data is now related to the sample cross-section viz:

$$I(q)_{correct} = \phi \cdot A \cdot d \cdot T_{sample+cell}\left(\frac{d\Sigma(q)}{d\Omega}\right)_{sample} \cdot \Delta\Omega \cdot \varepsilon \cdot t$$

It remains to obtain the differential cross-section for the sample.

Absolute scale. The background corrected scattered intensity may placed on an absolute scale using one of two standard methods[4-7]; direct beam flux method or standard sample calibration. The direct beam flux method requires measuring the direct flux on the detector and knowing the absolute values of neutron flux and the transmission of a standard attenuator.

$$I_{direct} = \phi \cdot A \cdot T_{attenuator} \cdot \Delta\Omega \cdot \varepsilon \cdot t$$

Therefore,

$$\left(\frac{d\Sigma(q)}{d\Omega}\right)_{sample} = \left(\frac{I(q)_{correct}}{I_{direct}}\right)\left(\frac{1}{d}\right)\left(\frac{T_{attenuator}}{T_{sample+cell}}\right)$$

The second method uses a scattered pattern collected under identical conditions to normalise the scattered pattern from the sample.

$$I(q=0)_{standard} = \phi \cdot A \cdot d_{standard} T_{standard+cell}\left(\frac{d\Sigma(q=0)}{d\Omega}\right)_{standard} \Delta\Omega \cdot \varepsilon \cdot t$$

Therefore,

$$\left(\frac{d\Sigma(q)}{d\Omega}\right)_{sample} = \left(\frac{I(q)_{correct}}{I(q=0)_{standard}}\right)\left(\frac{d_{standard}}{d}\right)\left(\frac{T_{standard+cell}}{T_{sample+cell}}\right)\left(\frac{d\Sigma(q=0)}{d\Omega}\right)_{standard}$$

SANS DATA REDUCTION

Generally the 2D scattered pattern must be reduced to a 1D (intensity versus q) profile to facilitate fitting of various models and functional forms. A number of algorithms are available for this reduction including radial integration for isotropic scattered patterns, and segment integration for anisotropic scattering patterns.

For radial integration, the (x, y) coordinates for zero q are usually defined in detector pixel units during positioning the beamstop and also during sample transmission measurements. These coordinates are then used to determine the Δq distance of each detector pixel from zero q to facilitate radial integration (Figure 5). Note that the radial integration function should not have a q resolution greater than the original data.

For segment integration, the coordinates for zero q plus the angular limits for segment integration are required (Figure 6). Depending on the asymmetry of the pattern and the nature of the structural feature causing the asymmetry, a radial

integration algorithm within the angular limits will provide 1D data with acceptable q smearing.

The 1D SANS data is now corrected for all background and instrument effects, placed on an absolute scale and is now ready for detailed data analysis.

DATA STORAGE

The final step is the storage and transmission of all the data for further analysis. It is often very convenient to adopt a standard format for data storage particularly when transferring data from one institute to another.

At present there is no internationally accepted standard although there are a number under discussion[8]. The data files must contain all the information about the experiment (instrument parameters, sample details etc) and must be able to be analysed either by specific software provided by the host institute, or by one of the ever increasingly available general data analysis packages (IDL, IGOR etc). The following are data storage formats under discussion

- ASCI – readable text
- CIF
- NEXUS
- HDF – internally self contained

To a large extent it remains with the host institute to offer to the guest scientist data storage options that are convenient and useable.

SUMMARY

SANS experiments should be well planned and well executed. Since data analysis is complex and in many cases model dependent, it is important that the reduced data used as input to the data analysis process is accurate with well-defined errors.

ACKNOWLEDGEMENTS

SANS experiments benefit from the knowledge and experience of the instrument scientists. The many contributions of scientists at National Institute of Standards and Technology (USA), Brookhaven National Laboratory (USA), Risø National Laboratory (Denmark), Japan Atomic Energy Research Institute (Japan) and Indonesia National Nuclear Energy Agency (BATAN) (Indonesia) are gratefully acknowledged.

REFERENCES

1. The 30m Small-Angle Neutron Scattering Instruments at the National Institute of Standards and Technology. C.J. Glinka, J.G. Barker, B. Hammouda, S. Krueger, J.J. Moyer and W.J. Orts. *Journal of Applied Crystallography* **31**, 430-445 (1998).
2. X-ray powder Diffraction Analysis of Silver Behenate; A possible Low-Angle Diffraction Standard. T.C. Huang, H. Toraya, T.N. Blanton and Y. Wu. *Journal of Applied Crystallography* **26**, 180 – 184 (1993).
3. JCPDS – International Centre for Diffraction Data round robin study of silver behenate. A possible low-angle X-ray diffraction calibration standard. T.N. Blanton, T.C. Huang, H. Toraya, C.R. Hubbard, S.B. Robie, D. Louër, H.E. Göbel, G. Will, R. Gilles and T. Raftery. *Powder Diffraction* **10**, 91 – 95 (1995).
4. Silver behenate powder as a possible low-angle calibration standard for small-angle neutron scattering. R. Gilles U. Keiderling and A. Wiedenmann. *Journal of Applied Crystallography* **31**, 957 – 959 (1998).
5. Assessment of Detector Calibration Materials for SANS Experiments. A.R. Rennie. *Journal of Applied Crystallography* **38**, 35 (1995).
6. The Forward Scattering of Cold Neutrons by Mixtures of Light and Heavy Water. R.P. May, K. Ibel and J. Haas. *Journal of Applied Crystallography* **15**, 15 – 19 (1982).
7. Intercalibration of Small-Angle X-ray and Neutron Scattering Data. T.P. Russell, J.S. Lin, S. Spooner and G.D. Wignall. *Journal of Applied Crystallography* **21**, 629 – 638 (1988).
8. Data Handling for Small-Angle Scattering. J.D. Barnes, M. Capel, J. Skov Pedersen and D. Svergun. ACA Workshop, July 1998.

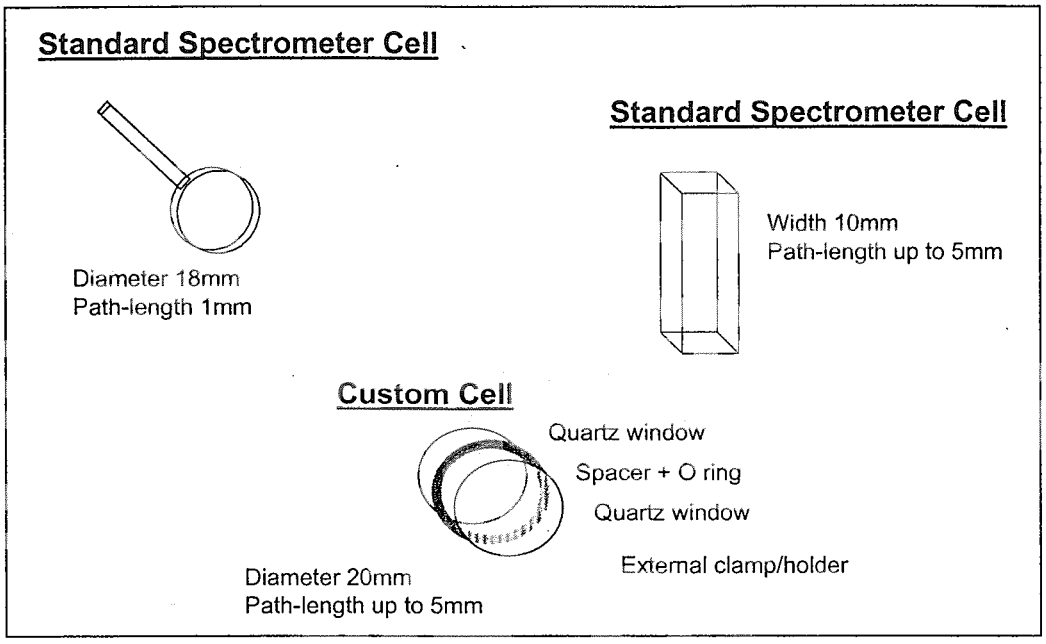

Figure 1. A selection of standard cells used in small angle neutron scattering experiments.

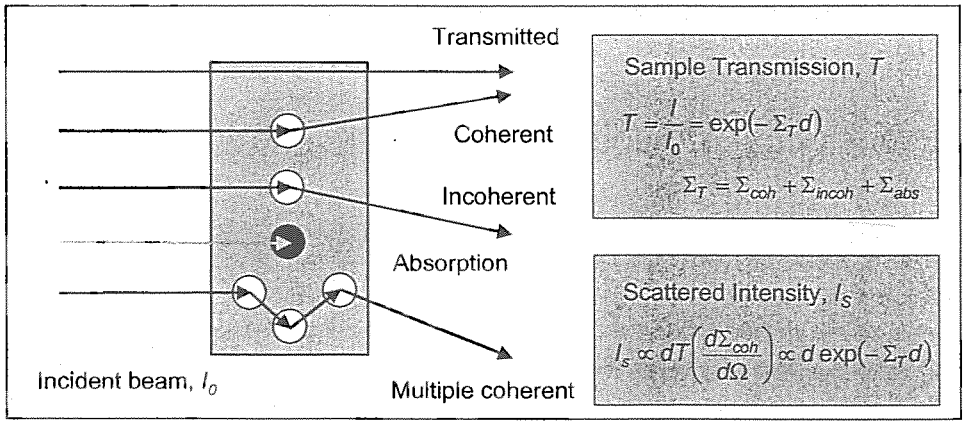

Figure 2. Scattering process within a sample that must be considered when planning a small angle neutron scattering experiment.

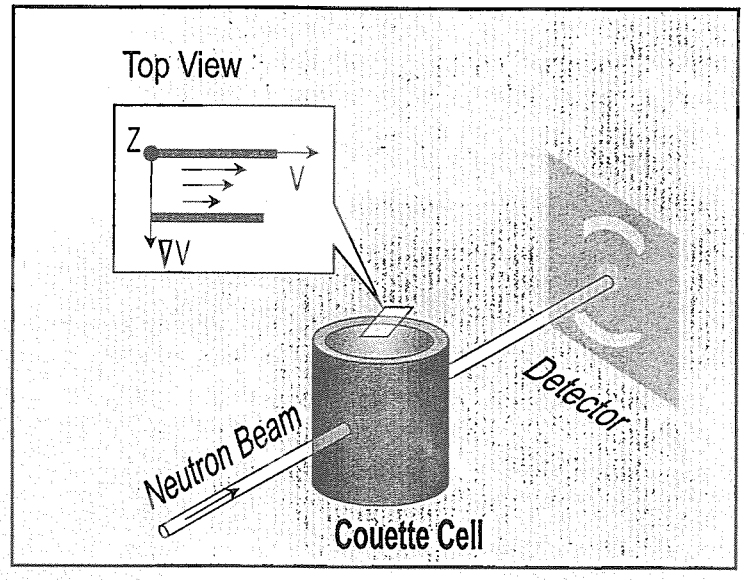

Figure 3. Schematic of a Couette cell for small angle neutron scattering applications

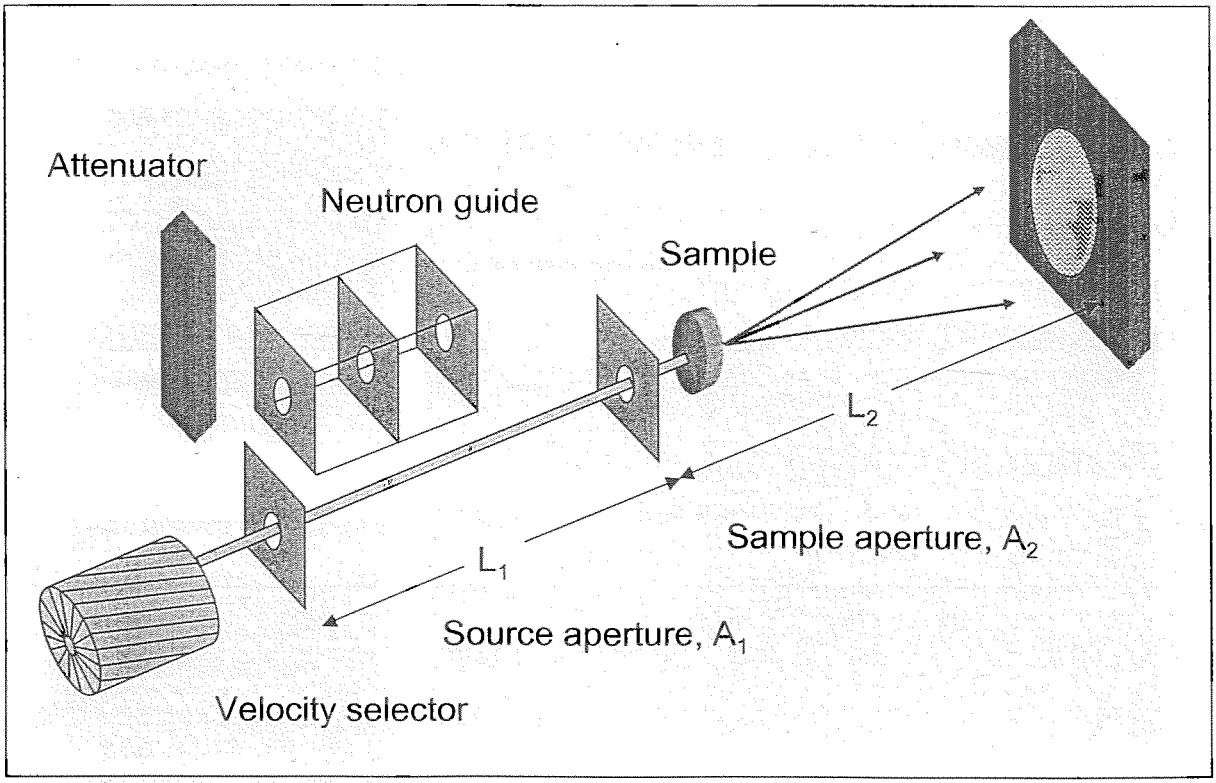

Figure 4. Schematic of a typical small angle neutron scattering instrument.

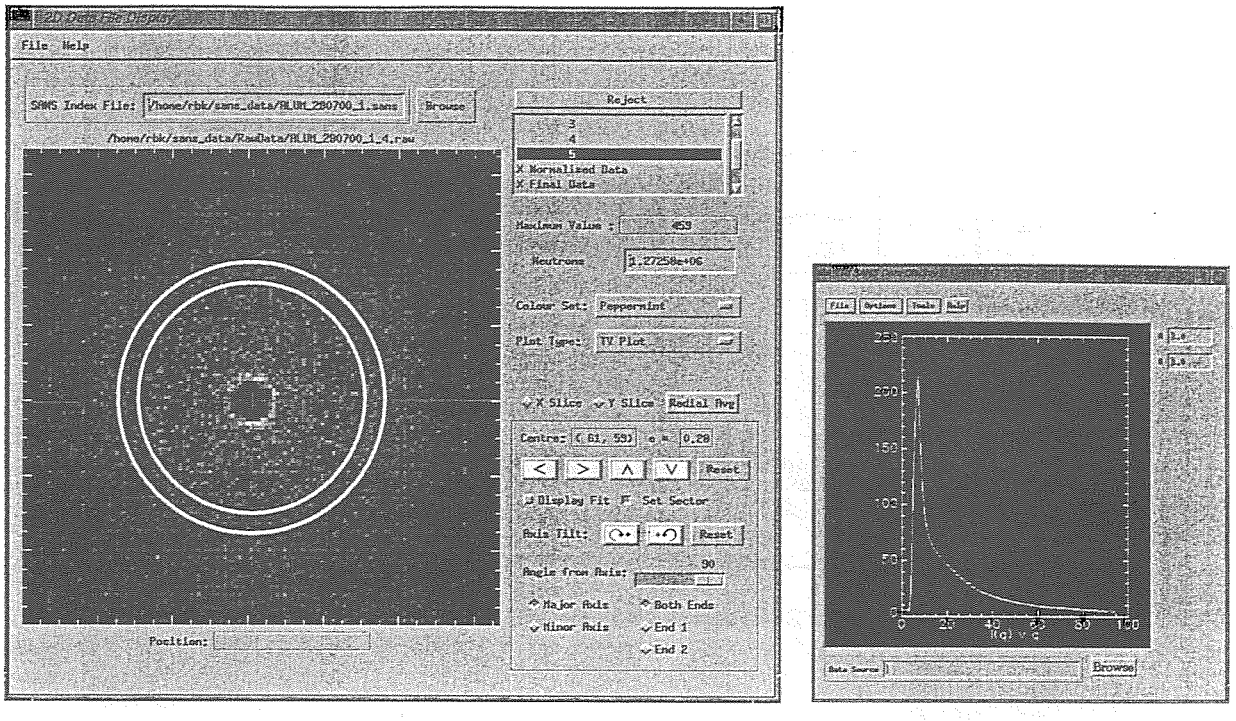

Figure 5.

Radial integration of a 2D SANS scattered pattern results in a 1D function (intensity versus q).

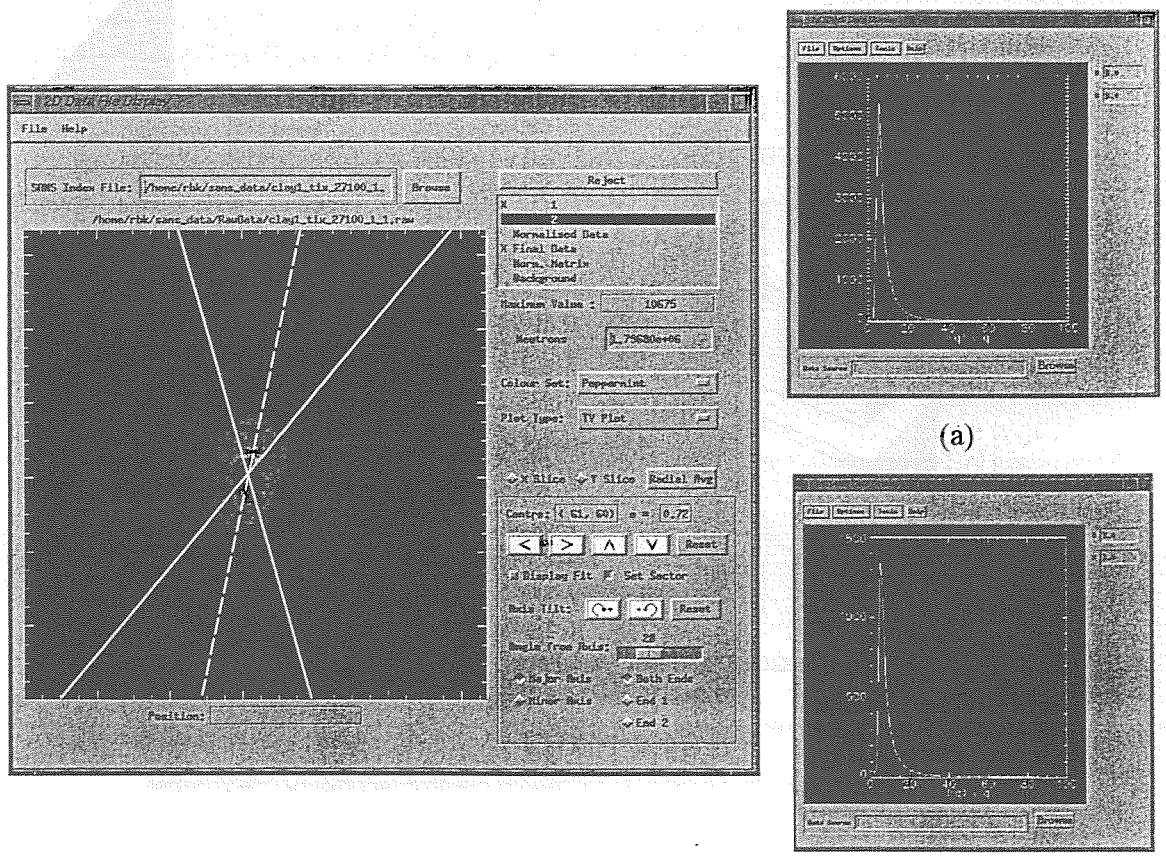

Figure 6.

Segment integration of a 2D SANS scattered pattern results in one or more 1D functions (intensity versus *q*). (a) Major axis; (b) Minor axis.

JP0250086

1.2 Neutron Scattering Science at the Australian Nuclear Science and Technology Organisation (ANSTO)

Robert Knott
Australian Nuclear Science and Technology Organisation
Private Mail Bag
Menai NSW 2234
Australia.
robert.knott@ansto.gov.au

ABSTRACT

Neutron scattering science at the Australian Nuclear Science and Technology Organisation (ANSTO) is being applied to a number of fields in the scientific and industrial research communities. The 10MW research reactor HIFAR at the ANSTO research laboratories has a suite of neutron scattering instruments including a medium and a high resolution powder diffractometer; a small angle neutron scattering facility; a single crystal diffractometer; a polarised neutron spectrometer, and a triple axis spectrometer. A reflectometer suitable for solids and liquids is under development. These instruments are being used to investigate problems in chemistry, materials science, physics, engineering and biology.

The HIFAR research reactor is now forty years old and approaching the end of its useful life certainly as a source for leading-edge neutron scattering science. Therefore by 2005, HIFAR will be replaced with a modern multi-purpose research reactor. The contract for the design and construction of the replacement research reactor has recently been signed. The experimental and analysis equipment associated with a modern research reactor will permit the establishment of a national centre for world class neutron science research focussed on the structure and functioning of materials, industrial irradiations and analyses in support of Australian manufacturing, minerals, petrochemical, pharmaceuticals and information science industries.

A brief overview will be presented of all the instruments available on the HIFAR reactor with emphasis on the small angle neutron scattering facility. A description of the replacement research reactor and the planned neutron scattering instruments will also be presented.

THE HIFAR RESEARCH REACTOR

The High Flux Australian Reactor (HIFAR) is a DIDO-class 10MW(th) research reactor of modest performance (maximum thermal neutron flux $1\times10^{14}cm^{-2}sec^{-1}$) and provides the only neutron source in the country suitable for neutron scattering. HIFAR is operated by the Australian Nuclear Science and Technology Organisation (ANSTO) (http://www.ansto.gov.au), a

government research organisation with the mission to 'ensure that its research, technology transfer, commercial and training activities in nuclear science and associated technologies will advance Australia's innovation, international competitiveness and environmental and health management'.

HIFAR was designed and built in the 1950's primarily as a materials testing reactor and as such has limited facilities for neutron beam studies. Apart from the neutron beam quality discussed below, the reactor building is small (20 metre diameter) and does not provide the space required for modern neutron scattering instruments. In addition, there is no cold source installed. Figure 1 is a photograph of the interior of the HIFAR reactor building. The limitations of HIFAR as a neutron source have been recognised and in September 1997 the Australian government made the decision to replace HIFAR with a multi-purpose pool-type research reactor.

Despite the inherent limitations in HIFAR, the neutron scattering instrument presently in operation are being used to investigate a number of important problems.

NEUTRON SCATTERING INSTRUMENTS ON HIFAR

The present supported instruments located on the HIFAR reactor include a single crystal diffractometer (2tanA), a polarised beam facility (Longpol), two powder diffractometers (HRPD, MRPD) and a small angle neutron scattering (SANS) instrument. A reflectometer is under construction. Except for 2tanA instruments are located on radial beam tubes. The beam tubes have a diameter up to 25cm, and terminate either in the D_2O moderator or the graphite reflector regions of the reactor core. This has an impact on beam quality and has influenced instrument design. Table 1 is a summary of instrument characteristics and Figure 2 illustrates their disposition on the experimental floor.

Single Crystal Diffractometer

The High Resolution Single Crystal Diffractometer (2tanA) is a four circle single crystal diffractometer located at one end of a 'tangential' beamline that passes under the reactor core. The 1.235Å monochromatic neutron beam is selected at a take off angle of 58° by a copper single crystal. The 10mm diameter neutron beam has a flux of 6 x 10^5 $n.cm^{-2}.s^{-1}$ at the sample position with good signal to background characteristics. The maximum 2θ is ~118° and over this range the reflection widths are typically ~0.4° (fwhm) (2θ) at 5° (2θ) increasing to ~0.75° at 105°.

The diffractometer has undergone upgrade (since 1996) in nearly every aspect of the instrument. These upgrades now allow the use of heavy environment stages (such as the new cryorefrigerator) on the sample stage.

The following three detector configurations are now available: a BF_3 single detector suitable for routine single crystal studies; a ^3He single detector with Soller collimator suitable for preferred-orientation/pole-figure studies; a ^3He multidetector (90 mm x 90 mm) particularly suited to diffuse scattering and other studies which need to sample large volumes of reciprocal space.

In single crystal mode Bragg reflection peaks typically have full widths at half maximum of order 0.4° (2q) at 5° scattering angle, 0.2° at 50°, and 0.75° at 105° with a maximum scattering angle of 118°. In pole figure mode powder peaks have a FWHM resolution of approx. 0.7° (2q).

The main applications include general single crystal structure determinations (chemical and magnetic) particularly where accurate information is sought on hydrogen bonding, thermal parameters, etc; preferred-orientation/pole-figure studies; and diffuse scattering studies.

Long Wavelength Polarised Neutron Spectrometer

The long-wavelength polarisation analysis spectrometer (Longpol) (Figure 3) is a 2-axis instrument that uses a neutron beam of wavelength 3.6Å and is equipped with 8 ^{3}He neutron detectors[1]. It incorporates neutron polarisation techniques and timed control of the polarisation direction of the incident neutron beam to produce time-of-flight (TOF) spectra. The instrument is therefore able to simultaneously detect changes in momentum, polarisation and energy of the neutrons after interaction with the sample. Polarisation analysis can be used to separate magnetic scattering from nuclear scattering, providing unambiguous data for determination of atomic and magnetic short-range order. It is also used to isolate the nuclear-spin-incoherent scattering that is caused by elements such as hydrogen. The energy analysis enables measurement of (low energy) inelastic scattering events such as magnons and phonons, and crystal field transitions. The instrument can also be used to measure trapped magnetic flux in superconductors and magnetic domain size in magnetic ribbons by analysing the polarisation of the undeflected portion of the neutron beam after transmission through the sample.

Recent improvements to the instrument include complete replacement of the neutron polariser, the neutron spin flipper, and the TOF data acquisition system, and partial replacement of the neutron spin analysers. The upgrade has so far produced a 10 fold increase in the quality of the polarisation analysis system and has also produced an increase in flux and in resolution. The spectrometer now has a neutron flux at the sample position of about 2 x 10^4 n.cm^{-2}.s^{-1}. It uses supermirror devices to polarise the neutron beam (polarising efficiency about 96%) and also for polarisation analysis in 3 of the 8 detectors (analysing efficiency about 94%). A Pentium PC is used to control the experiments, including neutron spin flipping, data binning, sample and detector positioning and sample temperature. The computer can also perform on line cross-correlation of data with the flipper control sequence to produce the TOF spectrum in real time. The energy resolution is currently <1meV, allowing some measurements of quasi-elastic scattering and further improvements are expected in the near future.

Present applications include the determination of atomic and magnetic distributions in magnetic materials; determination of hydrogen concentration in bulk materials; measurement of paramagnetic correlations in itinerant electron systems; magnon measurements; measurement of critical fields and flux pinning energies in type-II superconductors and flux creep in superconductors[2]; magnetic domain size in metallic ribbons; and determination of low energy crystal field transitions and diffusion processes.

Powder Diffractometers

The two powder diffractometers (Figure 4) were designed specifically to accommodate the conflicting requirements of neutron intensity and resolution[3]. The neutron flux at the sample position on the Medium Resolution Powder Diffractometer (MRPD) is typically five times that of the High Resolution Powder Diffractometer (HRPD) and the resolution is about half. This enables rapid phase transition type patterns to be collected on the MRPD and high resolution structure patterns on the HRPD. The HRPD has a selection of two Soller collimators before the monochromator (0.16 and 0.25°), a take-off angle of 120° and uses a germanium monochromator. Routine wavelengths are 1.371, 1.493 and 1.8834Å. The beam has

dimensions 20mm wide by 50mm high and the neutron flux at 1.8834Å is approximately 8 × $10^4 cm^{-2} sec^{-1}$. Patterns are collected from 5 - 156° (2θ) in a bank of 24 detectors (5° apart), with each detector having its own high efficiency collimator (0.17°). The minimum peak width is 0.25° and the width is less than 0.4° over most of the pattern. Data collected on this instrument is primarily for structure determination and quantitative phase analysis by multiphase Rietveld refinement of known components.

The collimation of the primary neutron beam on the MRPD can be either 0.25 or 0.5°. The monochromator consists of an array of 8 germanium single crystals with total height 80mm and width of 50mm, with vertical focussing to increase the neutron flux at the sample position to ~$10^6 cm^{-2} sec^{-1}$. Currently, 32 ^{3}He neutron detectors are mounted at 4° spacings at a distance of 0.7m on the 2θ drive. Each detector is mounted down-beam from a Soller collimator that has an acceptance angle of 0.35°. The instrument is designed for neutron powder diffractometry, magnetic structure determination, phase transition and residual stress measurements. *In-situ* kinetic studies of structure transformations, hydration mechanisms etc down to time resolution of ~15 minutes are also possible.

Small Angle Neutron Scattering Instrument

The Small Angle Neutron Scattering (SANS) instrument (Figure 5) has a 5m collimation length and sample-to-detector distance range of 1.5 - 5m. The monochromator and first section of the collimator are located within the reactor containment building, and the second section of the collimator, the sample position and the detector system are located in an external laboratory. The monochromator is a double multilayer system[4,5] in a dog-leg configuration. The multilayer monochromators are single d-spacing, planar geometry used in reflection mode. The large 64 × $64cm^2$ active area PSD has been designed in collaboration with BNL and the ILL, and constructed at ANSTO[6]. The detector is mounted in a vacuum tank that can be rotated +5 to -30° in 2θ to expand the accessible q range. The sample position provides a range of environments including a computer controlled sample changer that can operate *in vacuo*, or in the laboratory atmosphere. Since the instrument is located on a thermal neutron source, the flux is modest particularly at longer wavelengths. Nevertheless, considerable useful work is being undertaken on samples with high contrast and large physical dimensions.

A number of sample environments, including a range of temperature controlled cells for liquids, polymers and gels, is presently available. The most recent addition is a temperature controlled Couette cell for investigating the structural changes induced by an applied shear field (Figure 6).

Reflectometer

A reflectometer has been designed and is presently being constructed. The instrument will be suitable for both solid and liquid surface reflectivity measurements, and polarised neutron facilities will be added in a later development phase. The neutron wavelength will be either 1.75Å (Cu) or 4.0Å (pyrolytic graphite) produced by the dog-leg monochromator. The resultant q range (liquids) will be 0.005 - 0.17$Å^{-1}$ and the q resolution ($\Delta q/q$) will be 6%. Accessible reflectivities will be ~10^{-5}. Figure 7 is a schematic of the reflectometer. When complete, the instrument will facilitate a number of useful experiments in surface structure (monolayer surfactants, for example) and enable capability development.

NEUTRON SCATTERING SCIENCE

International scientific assessments rate the neutrons produced by research reactors as a unique and broadly applicable scientific tool for leading edge, basic and applied investigations across a wide range of scientific and technological disciplines in physics, chemistry, biology and medicine. Because neutrons probe in a non-destructive way, they are particularly suited for investigating the microstructure and properties of existing solid and liquid materials and of emerging advanced materials in the aerospace, automotive, biotechnology, petrochemical and telecommunications fields. As each new class of materials (eg, high-temperature superconductors, carbon-cage "fullerene" molecules) has been developed, neutrons have been the primary tool for studying the properties and understanding the behaviour.

Whilst opportunities exist to pursue scientific ideas of a fundamental nature, in general, the neutron scattering science at ANSTO is problem driven. Consistent with ANSTO's mission to contribute to the vitality and competitiveness of Australian industrial research and development, the neutron scattering effort has a focus on science that support this mission. Recent studies of practical significance include the following:

- To estimate the pore structure of rocks intact. Porosity in rock controls the flow of oil to the well head. An ideal bore should have a porosity that allows the oil to flow but does not allow the drill lubricant to penetrate. If possible, therefore, the location of the oil well should take this into account hence porosity needs to be determined. A problem is that conventional methods usually underestimate porosity and require the rock sample to be crushed. SANS is a means to overcome these limitations and at the same time measure the smaller pores that have the major influence on oil flow. SANS measurements are being coordinated with conventional methods.

- To estimate the pore structure of metals and contaminated metals during the refining process. Metal extraction from an ore in a blast furnace obviously requires the addition of a firing agent. Separation of the residual firing agent from the molten metal is the key to the efficiency of the blast furnace. This separation is a wetting problem. Pore size determination of the residual is needed to determine if pore size and distribution is a factor. Pore size determination on the nano-scale must be combined with techniques that determine the interfacial structure on the atomic scale.

- To investigate template/framework interactions during the synthesis of oxides with ordered mesoporosity, controlled wall thickness and domain sizes exceeding 100nm (particularly titania) by surfactant templating. SANS contrast variation will be used for in-situ studies of the evolution of the ordered oxide framework, surfactant self-assembly processes, and surfactant/metal oxide precursor interactions in "isolation".

- Production of mesoporous titanate gel microspheres from sheared sols. To investigate the effect of shearing precursor sols on the microstructure and porosity of spray-dried gel microspheres. Simultaneous SANS/rheology studies on sheared silica sols have indicated that the application of shear during the sol-gel transition profoundly alters the properties of the resulting gels. This work is being extended to titanate-based sols, and the effect of such shearing on the properties of titanate gel microspheres (e.g. porosity) is being determined.

- Crystal growth in contaminated environments. The goal of the study is to measure crystal growth in aqueous solutions contaminated with organic impurities and propose methods to remove the contaminants. Metal refining requires the treatment of complex contaminated ores.

Metals are extracted from the appropriate crystals that must be isolated and grown in this contaminated, organic environment. How these organics affect crystal growth is a major concern to industry.

• Nanocomposites. To prepare and characterise nano-structure organo-clay minerals and organo-colloid composites. The potential of using clay as the filler in a polymeric organic/inorganic composite is well understood and appreciated. The properties, however, of a composite are most influenced when the largest possible clay surface area is presented to the polymer matrix. Ideally, the clay should be fully dispersed into its constituents and bonded to the matrix using an appropriate organic intermediary or the polymeric material itself. Unfortunately, clay platelets tend to form large aggregates in the presence of organics, so normally will not disperse. The problem is to prevent this aggregation. The solution will not only allow the manufacture of nanomaterials, but will impact significantly such divers areas as pollution prevention and remediation, enhanced oil recovery and the treatment of petroleum liquids and the manufacture of cosmetics and pharmaceuticals.

• Deposition in petroleum liquids. The aims of the study are to monitor and measure asphaltenes and waxes in petroleum fluids and propose possible growth arrestors to prevent their formation. Deposition is a major economic problem in oil extraction, transport and refining particularly in Australian oil fields. Deposition can occur any time when the ambient conditions are changed eg changes in temperature and chemical composition of the petroleum fluid itself. There is an urgent need for growth arrestors to prevent the formation of asphaltenes and waxes. It is necessary to understand the physical and chemical nature of asphaltenes before any growth arrestors can be used effectively.

• Inorganic materials with ordered mesoporosity. The synthesis and structure of inorganic materials with ordered mesoporosity and surface areas exceeding $1000m^2/g$, using self-assembled surfactant systems as supramolecular templates, is an important, emerging field in Materials Science. Such materials have applications in areas as diverse as ion exchangers, selective sorption of cations and anions, filtration, catalysis, biomolecule separations, formation of semiconductor nanostructures, etc. They could also form the fundamental building blocks for the development of a range of "Smart Materials" with surfaces functionalised for a range of specific environmental responses. Although there have been numerous reports of the preparation and characterisation of templated silica systems (eg MCM-41), there have been only limited reports of templated mesoporosity in alternative metal oxide systems such as titania, tin oxide, zirconia, niobium oxide, tantalum oxide, alumina, etc. In addition, many of the reported products are not pure metal oxides, and contain residues due to incomplete removal of the templating species during sample washing and/or pyrolysis. They also contain significant quantities of disordered and/or amorphous material.

THE AUSTRALIAN NEUTRON SCATTERING COMMUNITY

The neutron scattering community in Australia is distributed throughout universities, government research organisations and industry. Within this context, neutron scattering is identified as a national facility and this influences the funding for its continued use and expansion. The neutron scattering group at ANSTO undertakes scientific research as well as the development of instruments and techniques for neutron scattering and provides assistance to guest scientists with instrument operation and data analysis.

In order to become more globally competitive, Australian industry is investing in research and development. As a consequence there is an increasing number of industry based scientists becoming involved in neutron scattering science. This is particularly relevant in the mining and mineral processing, environment, polymer and food industries.

The attachment of guest scientists to ANSTO from Australian universities is facilitated by the Australian Institute for Nuclear Science and Engineering (AINSE) (http://www.ainse.gov.au). AINSE is a consortium of 36 Australian and New Zealand universities in partnership with ANSTO, and was established to provide a mechanism for access to all the special facilities at ANSTO by universities and other tertiary institutions.

REPLACEMENT RESEARCH REACTOR

The Australian Government has decided that HIFAR will be replaced to ensure that Australia retains the capabilities to produce its own medical and industrial radioisotopes, to conduct nuclear based research and to maintain the first hand ability to remain abreast of international and regional nuclear developments and regulation. The decision to replace the HIFAR research reactor by the year 2005 will opened up new opportunities for Australia's capabilities in nuclear medicine, neutron scattering science, environmental science, education and industrial support. The modern neutron source will facilitate research and development relating to, for example, polymers, ceramics and other new materials, life sciences and biotechnology, understanding complex industrial processes, advanced therapeutic treatment strategies with radiopharmaceuticals, and advanced environmental management processes.

Therefore, Australia's requirement is for a multipurpose neutron source with adequate facilities for radioisotope and materials irradiation plus the ability to efficiently illuminate a range of neutron beam tubes and sources. A pool-type reactor with its open architecture, adaptable design, and inherent safety and reliability features meets all the design criteria. The contract for the design and construction of a state-of-the-art, multipurpose research reactor was recently signed between ANSTO and the Argentinian company INVAP S.E. and its Australian alliance partners, John Holland Construction and Engineering Pty Ltd and Evans Deakin Industries Limited. The contract is basically for the reactor facility and associated infrastructure, and a large guide hall. In addition, a reference set of eight neutron scattering instruments, scheduled for installation by the time the reactor comes on line in 2005, has been selected by a Beam Facilities Consultative Group. This group represented a cross-section of Australian scientific interests, including industry, academia, CSIRO and other research laboratories. In order to ensure that the neutron scattering instruments will be the most appropriate for the Australian scientific and industrial research community, the consultative group identified present and future research priorities. . As a consequence of extensive deliberations a suite of instruments was formulated. Table 2 lists the range of instruments considered most likely to facilitate the priority research science areas, and Figure 8 is a schematic of the suite of neutron scattering instruments located on the replacement research reactor. The neutron scattering facilities will be built up from the existing expertise and equipment base. Design and construction of the neutron scattering instruments will be carried out by the Neutron Scattering Group at ANSTO.

Figure 9 is a photograph of an architect's model of the proposed design for the replacement research reactor. Table 3 illustrates the difference between HIFAR and the replacement research reactor.

The total project will including reactor island, all associated infrastructure and buildings. It will incorporate modern instrumentation and enhanced experimental access, high intensity neutron beams, and a cold neutron source. Since cold neutron sources provide the basis for many of the current advances in neutron science and technology, the replacement reactor with the most advanced cold neutron source will enable Australia's basic and applied research scientists to enter new areas of endeavour. An example is the field of nanotechnology, which requires multidisciplinary application of knowledge in physics, chemistry, mathematics, biology and electronics and where science and engineering converge at the level of individual atoms. The developments in nanotechnology will require access to intense sources of neutrons to probe the most minute structures of materials.

SUMMARY

Neutron scattering science is an important, integral component of the scientific and industrial research community in Australia. The present neutron source, HIFAR, and the suite of neutron scattering instruments facilitate research programs of a very high standard. The replacement research reactor due to be commissioned in 2005 will build on the strengths developed on HIFAR as well as offer new opportunities particularly in cold neutron scattering science. The combination of four decades of experience and a modern research reactor will assure ANSTO's place as a national and regional centre for neutron scattering science.

ACKNOWLEDGEMENTS

The neutron scattering team at ANSTO is Sandra Leigh Cram, Margaret Elcombe, Tunay Ersez, Yang Fei, Gerard Gadd, Brett Hunter, Michael James, Shane Kennedy, Robert Knott, Venassa Peterson, Ross Piltz, Robert Robinson (Leader), Andrew Studer, Robin Walsh and Howard Hanley (Scientific Advisor). Their contributions are gratefully acknowledged.

REFERENCES

1. L. Cussen, et al., *Nuclear Instr. & Methods* **A314**, 155 (1992).
2. P.A. Miles, et al., *J. Mag. Mag. Materials* **140-144**, 1317 (1995).
3. S.J. Kennedy, in "Advances in X-ray Analysis" (Plenum Press NY) **38**, 35 (1995).
4. A.M. Saxena and B.P. Schoenborn, *Materials Sci. Forum* **27/28**, 313 (1988).
5. B.P. Schoenborn, *SPIE* **1738**, 192 (1992).
6. R.B. Knott, et al., *Nuclear Instr. & Methods* **389**, 62 (1997).
7. E.H. Kisi, et al., *J. Alloys Comp.* (1994)
8. S.J. Kennedy, et al., *J. Phy: Condensed Matter* (1994).
9. R.W. Cheary, *J. Solid State Chem.* **98,** 323 (1992) J. Bartlett, *Prog. Polymer Colloid Sci.* (1999)

Table 1:

Characteristics of neutron scattering instruments located on HIFAR

Instrument		Monochromator	Detectors	Neutron Wavelength (Å)	Maximum Neutron Flux ($cm^{-2}sec^{-1}$)	Resolution	Beam size (mm)
2tanA	High Resolution Single Crystal Diffractometer	Cu single crystal	1 (BF_3) (2D (16^2 elements) ^3He)	1.235	6×10^5	0.4° at 5° (2θ) 0.2° at 50° (2θ) 0.75° at 105° (2θ)	10 diameter
2tanB	Medium Resolution Single Crystal Diffractometer	pyrolytic graphite	1 (BF_3)	1.239	10^6	0.4° at 5° (2θ) 2° at 90° (2θ)	10 diameter
LONGPOL	Long Wavelength Polarised Neutron Spectrometer	pyrolytic graphite	8 (^3He)	3.6	3×10^4	$1 \leq \Delta E \leq 10meV$ $0.3 \leq q \leq 3.0Å^{-1}$	30(H)×20(V)
MRPD	Medium Resolution Powder Diffractometer	Ge multiple single crystals (focussing)	32 (^3He)	1.06 -5.0	3.8×10^5	0.4° - 0.8° (2θ)	20(H)×50(V)
HRPD	High Resolution Powder Diffractometer	Ge single crystal	24 (^3He)	1.2 - 2.96	8×10^4	0.25° - 0.4° (2θ)	20(H)×50(V)
SANS	Small Angle Neutron Scattering Instrument	multilayer	2D (128^2 elements) (^3He)	2.0 - 8.0	$\sim 10^4$	$0.08 \leq q \leq 0.1Å^{-1}$	40(H)×50(V)

Table 2.

List of neutron scattering instruments proposed for the replacement research reactor.

	Instrument
1	Small Angle Neutron Scattering (SANS) Instrument (40 metre)
2	Horizontal Neutron Reflectometer
3	High Intensity Powder Diffractometer
4	High Resolution Powder Diffractometer
5	Polarisation Analysis Spectrometer
6	Residual Stress Diffractometer
7	Quasi Laue Diffractometer
8	3-Axis Spectrometer
9	High Resolution Backscattering Spectrometer
10	Amorphous Materials Diffractometer
11	4-Circle Diffractometer
12	Radiography Station
13	Small Angle Neutron Scattering Instrument (6 metre)
14	Neutron Spin Echo Spectrometer
15	Vertical Neutron Reflectometer
16	4-Circle Diffractometer
17,18	Thermal and Cold Neutron Instrument Development Stations

Table 3.
Comparison of relevant features for the HIFAR reactor and the replacement research reactor.

Feature	HIFAR reactor	Replacement research reactor
Reactor power heat output (MW)	10-15	14-20
Neutron Flux ($\times 10^{14}$ n cm^{-2} s^{-1})	1	At least 3
Number of fuel elements	25	#
Fuel enrichment (% uranium-235)	60%	20%
Fuel load (kg uranium-235)	7	#
Achitecture	Tank	Pool
Core	Loose array of fuel elements	Compact array of fuel elements
Spent fuel elements a year	37	#
Coolant	D_2O	H_2O
Reflector	D_2O	D_2O
Experimental positions*	11	17 (max)
Neutron guide hall	No	Yes
Beamline geometry	Radial	Tangential
Cold source	No	Yes
Hot source	No	Yes

Notes:
* for neutron scattering instruments
# dependent upon design

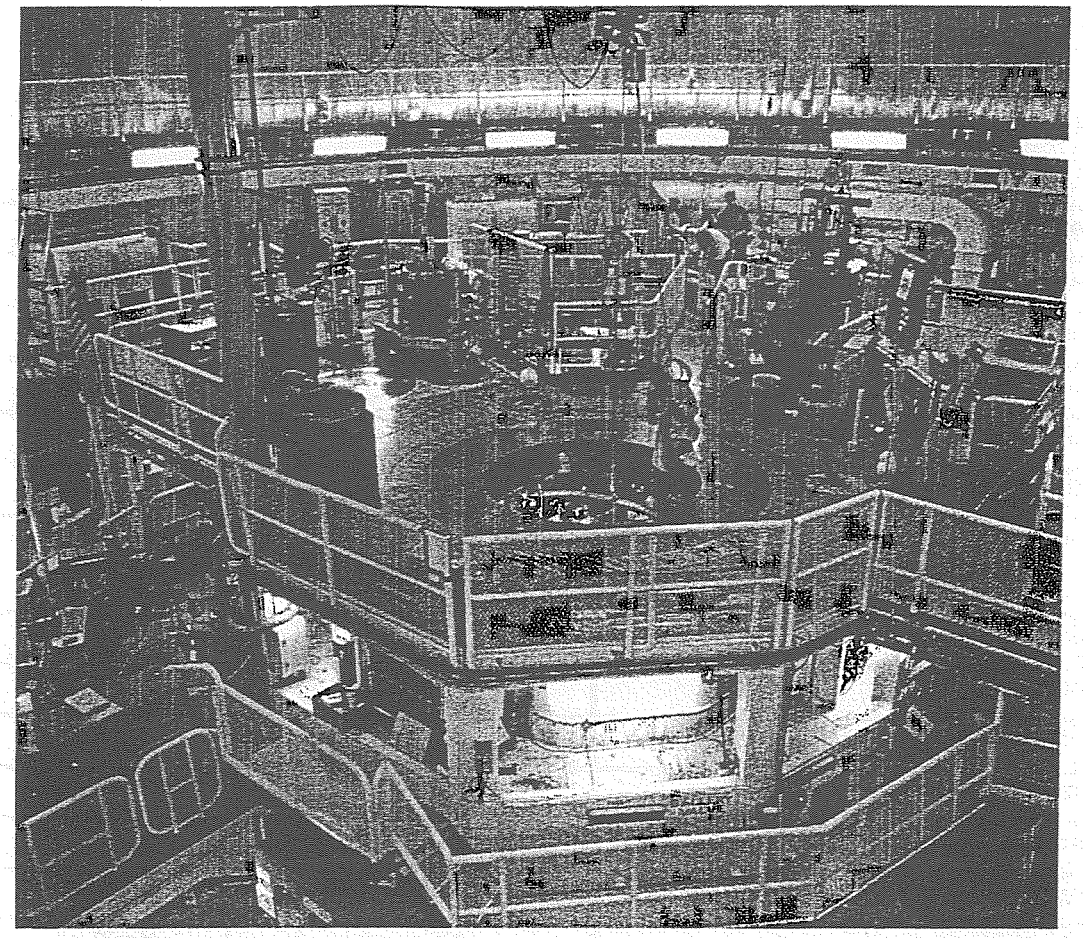

Figure 1

Photograph of the interior of the HIFAR reactor building. The top plate of the reactor tank has been removed for routine maintenance. Note the limited space for neutron scattering instruments.

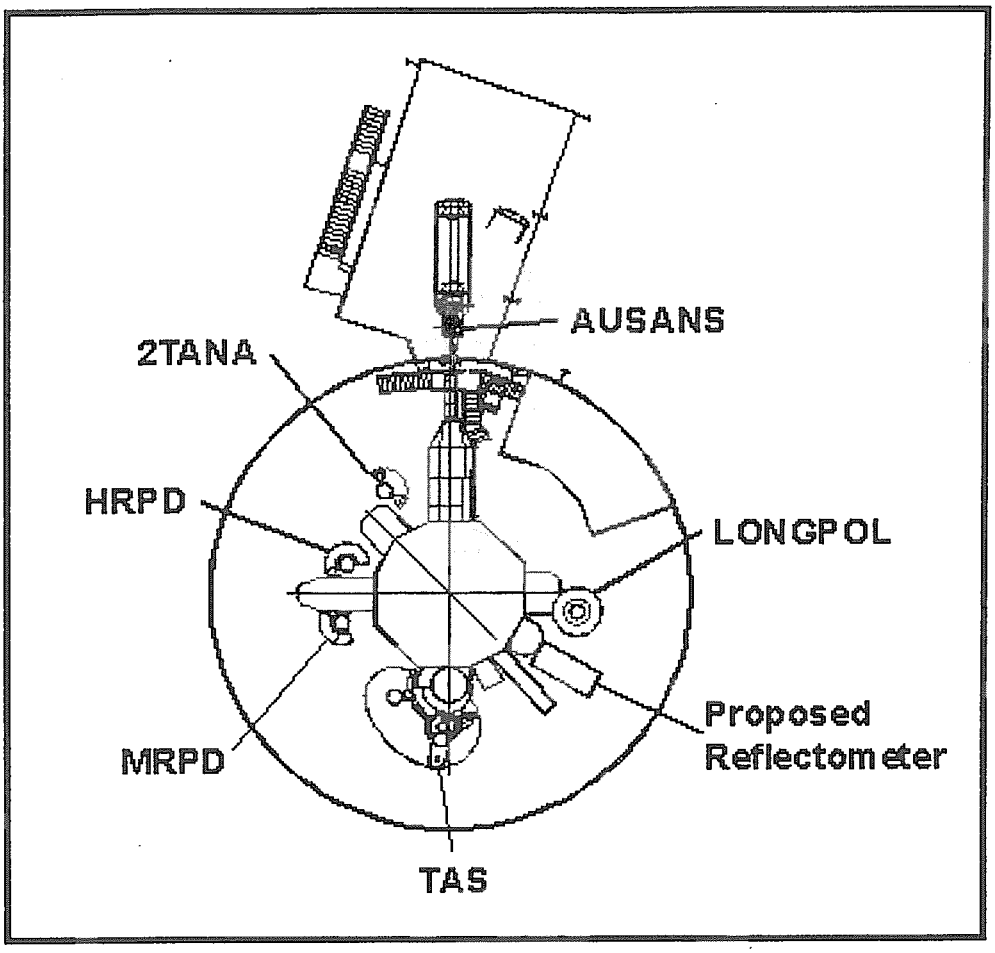

Figure 2.

Disposition of the neutron scattering instruments on HIFAR.

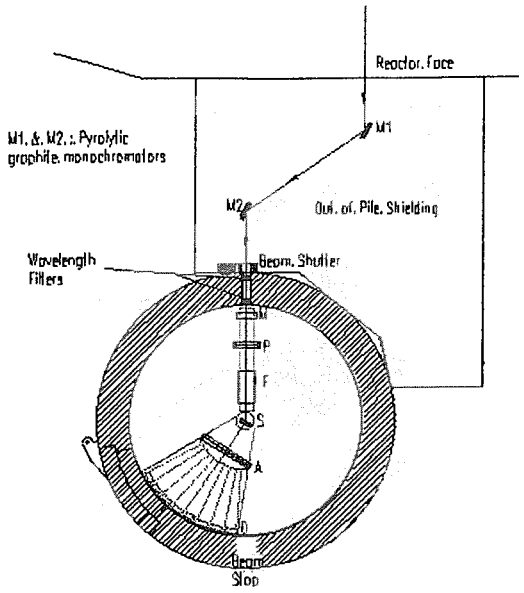

Figure 3.

Schematic of the Long Wavelength Polarised Neutron Spectrometer (LONGPOL) on HIFAR.

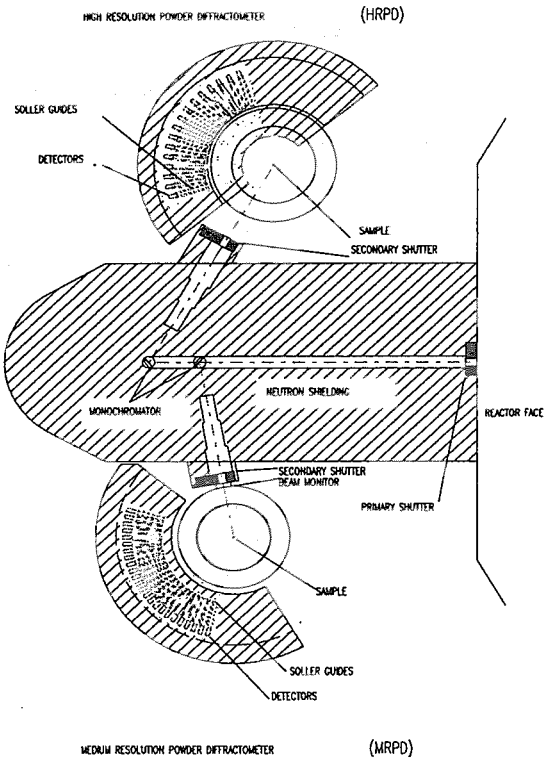

Figure 4.

Schematic of the two powder diffraction instruments (MRPD and HRPD) on HIFAR.

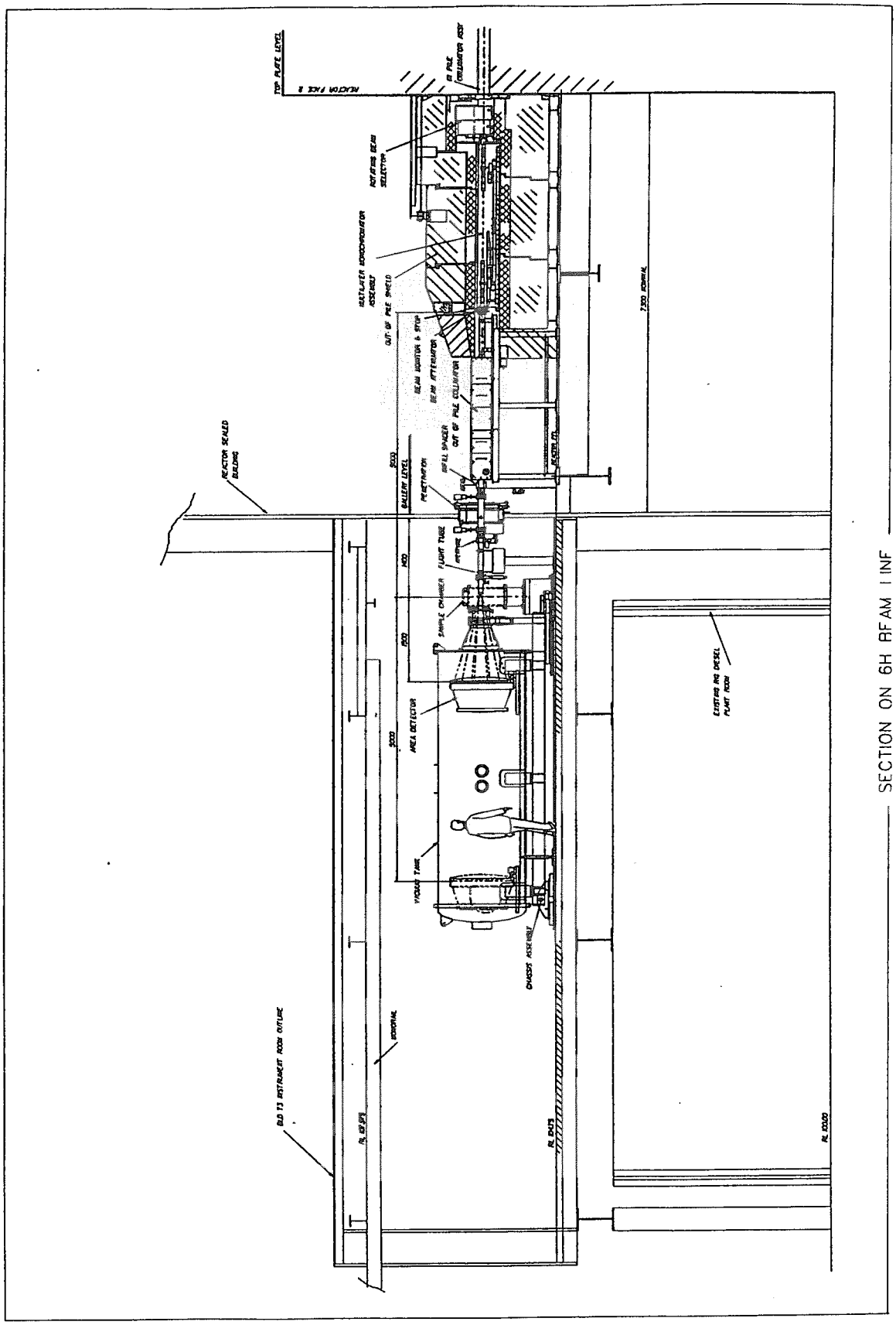

Figure 5.

Schematic of the small angle neutron scattering (SANS) instrument on HIFAR.

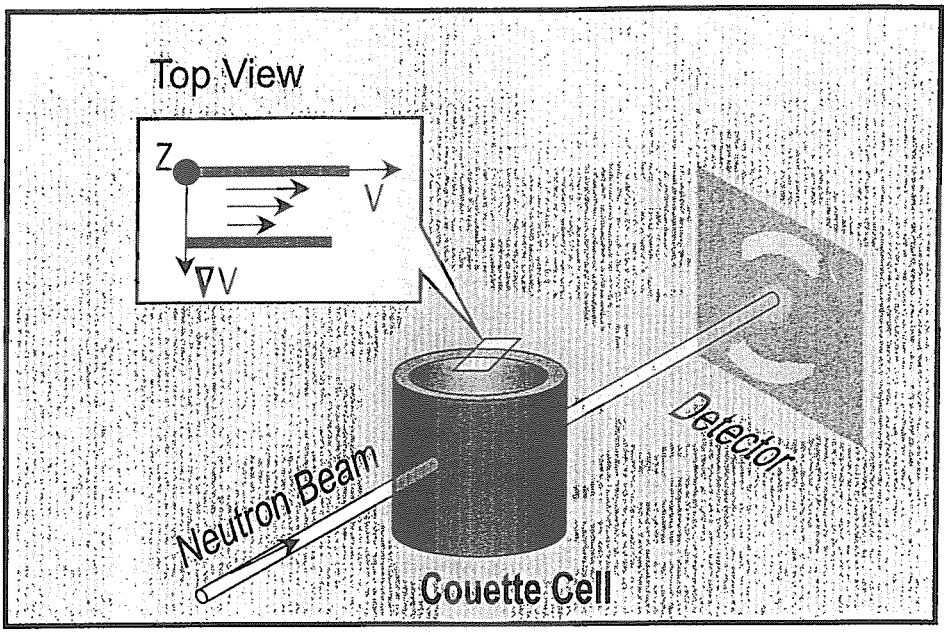

Figure 6

Schematic of the Couette cell used for investigation of structure/rheology relationships.

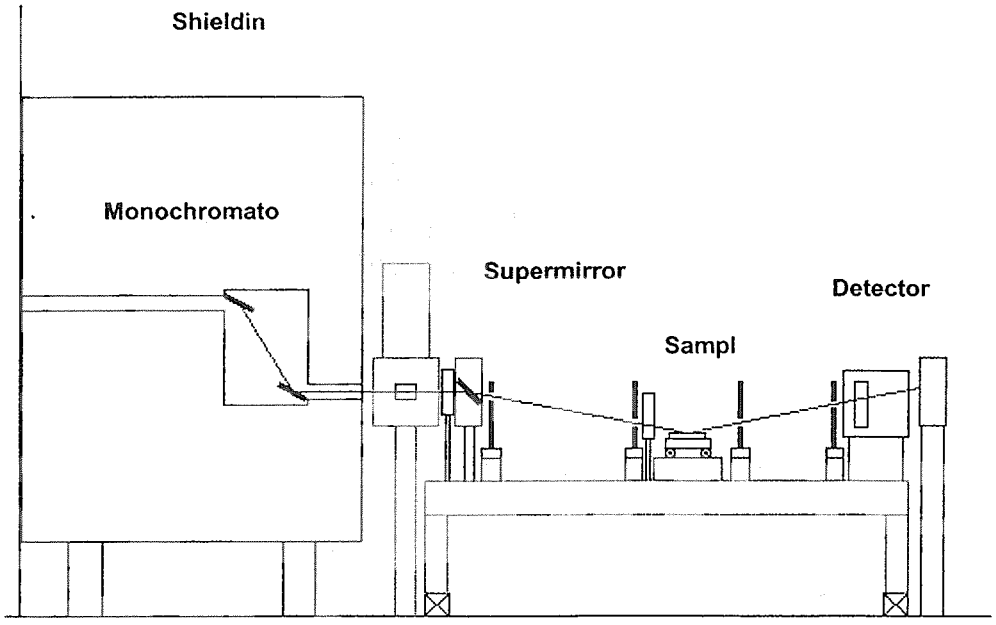

Figure 7.

Schematice of the reflectometr presently under construction on HIFAR.

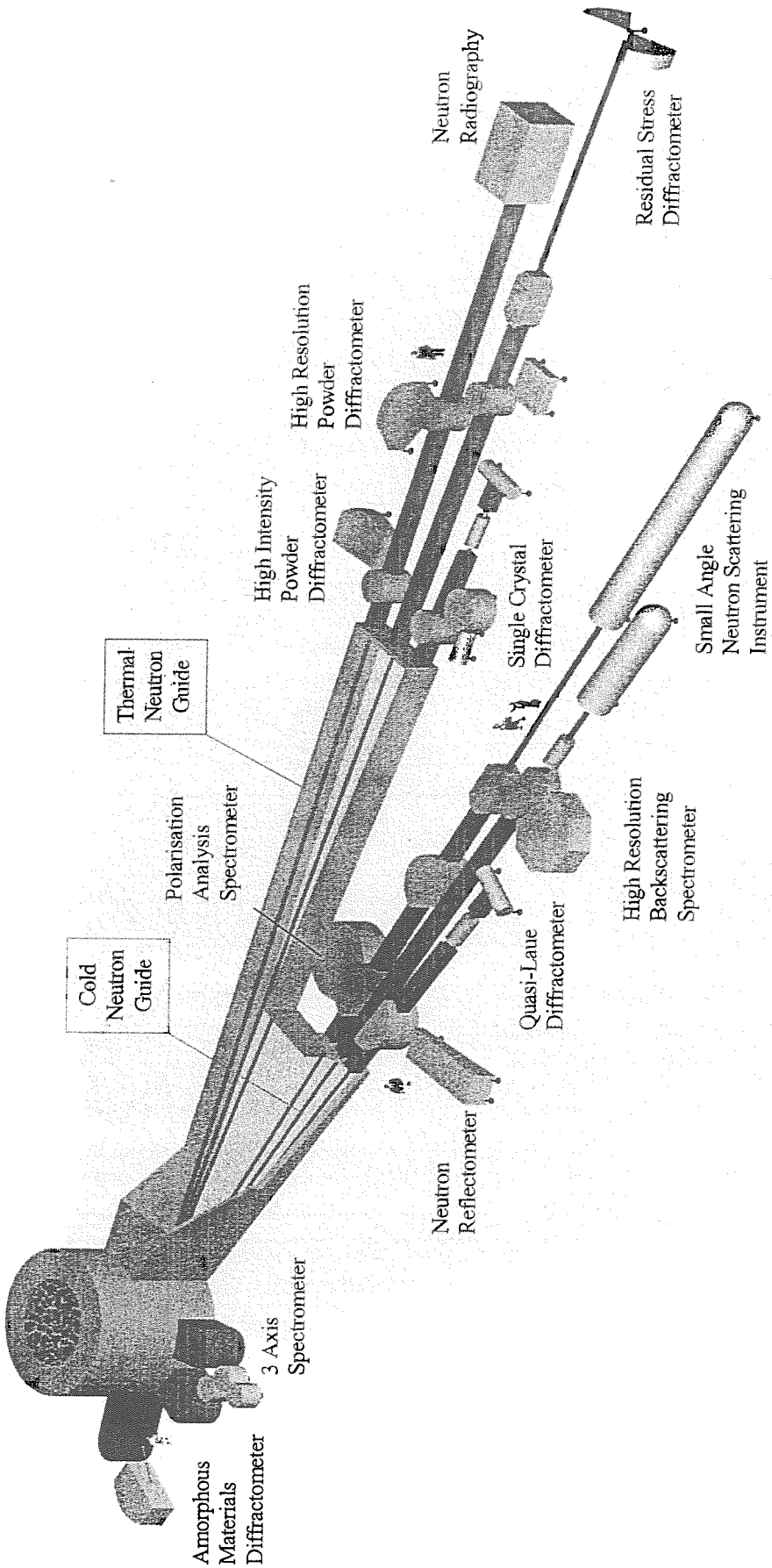

Figure 8.

Schematic of the neutron scattering instruments proposed to be located on the replacement research reactor.

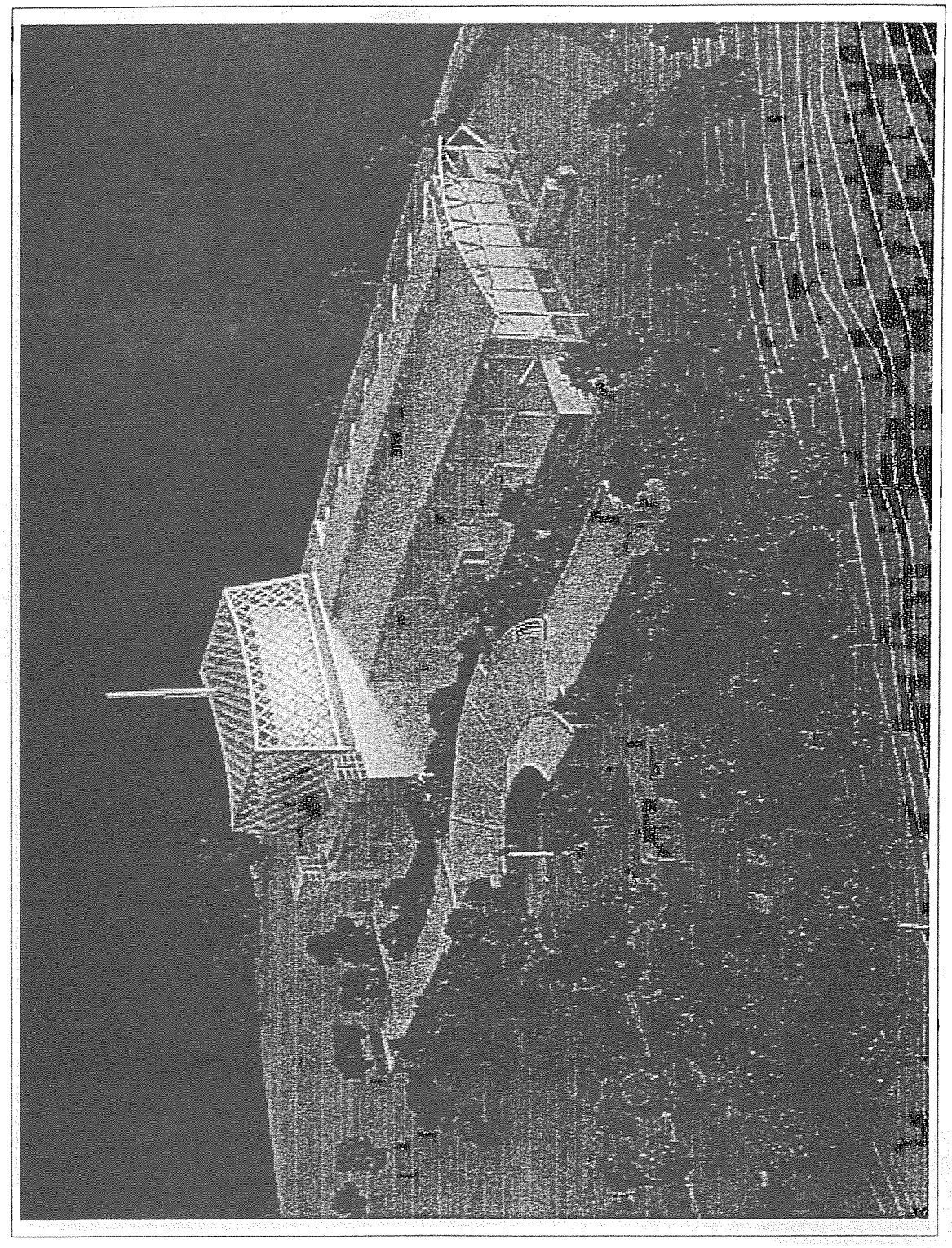

Figure 9.

An architects model of the replacement research reactor to be located at ANSTO.

JP0250087

1.3 The Investigation of Artificial Articular Cartilage-PVA-hydrogel with SANS

Yang Tong-Hua, Wang Hong-Li, Zhao Xin, Chen Dong-Feng
(China Institute of Atomic Energy, 102413 Beijing 275(30) China)

Gu Zheng-Qiu, Xiao Jiu-Mei and Zhang Xiang-Hong
(Department of corrosion Engineering, College of Materials Science and Engineering, University of Science and Technology Beijing, Beijing 100083.P.R.China)

Lin Min-Yue
(National Institute of Standards and Technology center for Neutron Research Gaithersburg, MD 20899 USA)

Abstract

The artificial articulate cartilage-PVA-hydrogel has been developed with being frozen and thawed 1-3 times and dehydrated in vacuum. In order to understand the relationship between the characteristic and structure, SANS was used to get some important structural parameters. The results show the SANS is suitable method to understand the microstructure of PVA- hydrogel.

1. Introduction

PVA-hydrogel is a outstanding biomaterial[1] with the best biocompatibility and good physical and chemical characteristic. It was widely used to clinical application, such as artificial articulate cartilage, because of its special advantage . At the early time of its development, material combinations of metal and ultrahigh molecular weight polyethylene (UHMWPE) have been used for most joint prosthesis. The prosthesis operates generally under unlubricated condition, that is mean, the rubbing surfaces contact directly, which results in high friction and high wear. In addition, wear debris of UHMWPE causes foreign-body reaction, induces the absorption of bone and formation of a granulomatous tissue, and finally results in the necrosis of the bone surrounding the prosthesis. The silicone rubber and polyurethane have also been used as the cushion materials attaching to the surfaces of artificial joints with low elastic modulus. Unfortunately, the silicone rubber is high wear rate material and the polyurethane is apt to degrade. Comparing with above materials, PVA-hydrogel is a very promising material, which meet the requirements of artificial articular cartilage. First it has a great number of infinitesimal pores containing a lot of water in it. Under loading, the fluid in PVA-hydrogel will be squeezed off and filtered into the gap between the sliding pair. The entrained fluid in the gap acts as a lubricant. Second, the PVA-hydrogel has special surface structure, which is similar to that of natural cartilage. Third the biocompatibility is also good.

During the process of developing PVA-hydrogel, the traditional analyses have been used for the structure and mechanical properties, for example, SEM, Dichromatic Microscopy and Differential Scanning Calorimentry. In recent years, new structural investigation methods of gel has been greatly used with development of experimental technologies, such as quasi-elastic light scattering and small angle neutron scattering (SANS) and theoretical progress[2-3].

In order to improve the mechanical properties of PVA-hydrogel as artificial articulate cartilage, we used the SANS to resolve its microstructure parameter, to directly get certain important structure information.

II Sample preparation and Test

Commercially available PVA with a degree of polymerization (DP) of 1800 (1799 PVA) was provided by the Beijing (second) chemical factory, China. The degree of sapouification is 99.9 mol %.

The 1799 PVA was dissolved in 90℃ water in autoclave for about 6h. The PVA solution was poured into the die, frozen at about -20℃ for 6-12h, then thawed at room temperature for 1-2h. The above freezing-thawing process was repeated for 1-3 times. Finally the frozen specimens were dehydrated in vacuum for about 10h.

The PVA-hydrogel was observed by means of dichromatic microscopy and SEM. The specimens were dried in an alcohol environment for 2h, then dehydrated in vacuum for 24h to get rid of all of the water. Differential scanning calorimentry (DSC) was carried out on DSC 7-differential scanning calorimentry analyzer made by Perkin-Elmer Corporation in USA. Aluminum pans with a scanning rate of 10℃ min^{-1} were used for the samples. The specimen was in an environment of flowing argon (Ar).

The ensile tests were conducted on a LLDYD-2000R material testing machine (rate of extention=10mm/min). In addition, the indention test were also performed on the above testing machine and a plain-end cylindrical indented was used to evaluate the elastic compression modulus of the specimens soaked in 0.9% NaCl solutions at 37℃

III Experiment and Results

The neutron-scattering experiment was carried out on the small-angle neutron scattering facility-NG7 at the National Institute of Standards and Technology(NIST), Maryland, USA. The PVA sample was swollen in the heavy water and poured into quartz cells and keep it several hours, in order to get swelling balance before the SANS measurements. A flux of cold neutrons was monochromatized with a velocity selector of wavelength λ=6Å. The scattered intensity was corrected for air scattering, incoherent scattering, fast neutron, and then re-scale to the absolute intensity.

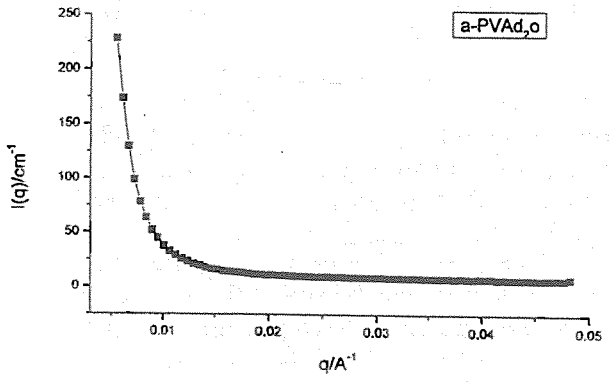

Figure 1. I(q) ~ q curve

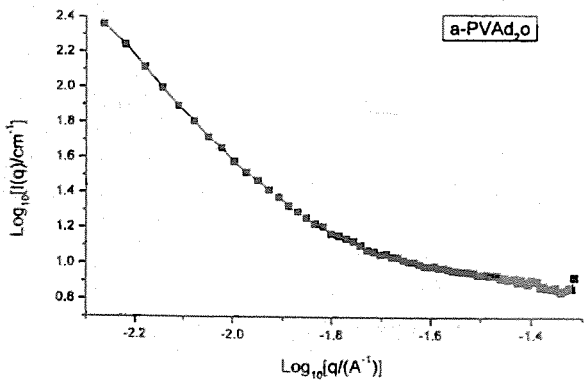

Figure 2. $Log_{10}I(q) \sim Log_{10}q$ curve

Figure 1 shows the scattering intensity profiles of SANS experiment for PVA-hydrogel. The scattering intensity decreases monotonously with q and shows no scattering peaks.

Figure 2 shows double logarithmic plot of the scattering intensity I(q) versus the scattering vector q for the PVA-hydrogel sample. The value of D should be obtained from the slope at the high-q region. We obtained the value of D from the slope of the curve. The fractal dimension D is one of the most important parameters to describe the

gel structure. D, which is 2.8±0.1, is strongly depend on the structure characteristic of amorphous zone.

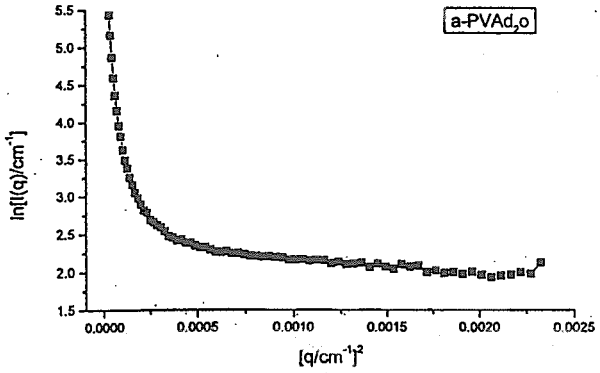

Figure 3. lnI(q)~q^2 curve

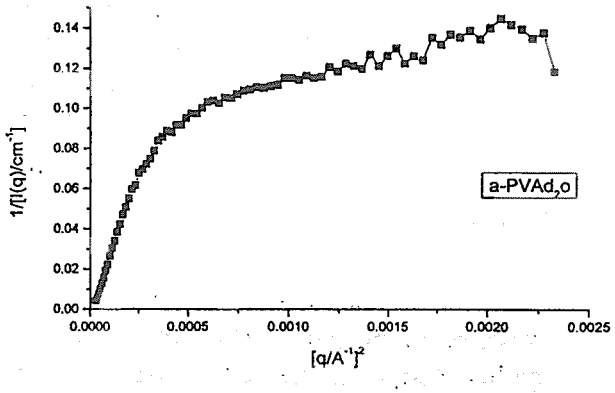

Figure 4. $I(q)^{-1}$~q^2 curve

Figure 3. shows the plot of logarithmic I(q) versus q^2 for PVA-hydrogel sample. From the slope we can obtain the R_G[4], which is interpreted as the radius of gyration of polymer dense or poor domains. In this measurement , the slope is not totally straight, and it demonstrate that there is a tendency size distribution in this system. The maximum $R_{G\,max}$ is around 273.6A.

Figure 4. shows that plot [I(q)-1 vs q2], we can make the asymptotic line for the plot. And get the ξ, which is the correlation length(or blob size[5]).

From the simple treatment of our SANS data we can get certain important parameters of microstructure of gel. So we think that Small-angle neutron scattering is a powerful tool for the investigation of Small-scale structure of polymer gels.[6]

References

[1] Gu Zheng-Qiu,Xiao Jiu-Mei and Zhang Xiang-Hong Bio-Medical Material and Engineering 8 (1998) 75-81

[2] Mitsuhiro shibayama,Hidenobu Kurokawa and Shunji Nomura et. POLYMER,1992,Volume 33,Number 14

[3] Wen-li Wu, Mitsuhiro shibayama,Saroj Roy et. Macromolecules 1990,23,2245-2251

[4]Mitsuhiro shibayama and Toyoichi Tanaka J.Chem.Phys. 97(9) November 1992.

[5] Mistsuhiro shibayama ," Small-angle Neutron Scattering on Polymer Gels"

[6] Simon Mallam,Ferenc, Anne-Marie Hecht, Adrian R, Rennie and Erick Geissler, Macromolecules 1991.24. 543-548

JP0250088

1.4 CURRENT STATUS OF NEUTRON SCATTERING IN INDONESIA

Abarrul Ikram
Neutron Scattering Laboratory
R & D Centre for Materials Science & Technology
National Nuclear Energy Agency
Serpong - Indonesia

ABSTRACT

Neutron Scattering activities in Indonesia during the last one year period are reported in this paper. The National Neutron Scattering Seminar in Serpong as an effort to gather people interested in Neutron Scattering is also described. The neutron beam facilities in Serpong include one diffractometer for residual stress measurement (DN1-M), one diffractometer for single crystal structural determination and texture measurement (FCD/TD), one high resolution powder diffractometer (HRPD), one neutron radiography facility (NRF), one triple axis spectrometer (TAS), one small angle neutron scattering spectrometer (SANS) and one high resolution small angle neutron scattering spectrometer (HRSANS). This paper discuss three out of these seven neutron beam instruments which are related to this workshop. HRSANS is working but not at its best condition. The other two i.e. HRPD and SANS are running well especially HRPD which is heavily used. The latest situation of the reactor and its operation mode is also described briefly in connection with the activities of the neutron scattering instruments.

1. INTRODUCTION

In the last three workshops we have presented the neutron scattering facilities in Serpong together with their problems, guesses of the causes as well as the possibility of overcoming them especially the ones related to the workshop which include three main neutron instruments.

In 1992, BATAN commissioned some instruments utilizing neutrons produced by the Multi-Purpose Reactor (RSG) GA Siwabessy in Serpong. These instruments are neutron powder diffractometer, four circle/texture diffractometer, triple axis spectrometer, neutron radiography facility, small angle neutron scattering (SANS) spectrometer, high resolution SANS spectrometer and high resolution powder diffractometer (HRPD).

The first four instruments were installed in the reactor experimental hall (XHR) while the last three are located in the neutron guide hall (NGH). Those two halls are connected by a tunnel in which two neutron guides are used to take neutrons from the reactor to the instruments in the neutron guide hall. Lay out of the neutron instruments in the reactor hall (XHR) and in the neutron guide hall (NGH) is presented in figure 1.

After five years in operation, some and different problems have come out from each instrument which raised some questions of how to solve them. Many efforts have been done by BATAN with the help from other established neutron scattering centres in the world especially from JAERI. In this paper we present again briefly the current status of three instruments closely related to this workshop together with efforts that have been done in the past one year to find alternative solutions of some problems, and we expect some positive responses from this workshop in utilizing the spectrometers.

2. THE RESEARCH REACTOR

The research reactor, called RSG-GAS (Multipurpose Reactor - GA Siwabessy) in honor to Prof. GA Siwabessy for his contribution in promoting and developing atomic energy in Indonesia, is a light water open pool reactor with a maximum thermal power of 30 MW. It is considered to be the first high-power research reactor in the world, designed and constructed for the use of low enriched (19.75%) uranium MTR-type fuel. It produces an average thermal neutron flux of 2.5×10^{14} n $cm^{-2}sec^{-1}$ at the central irradiation position in its core. An L-shaped beryllium block reflector surrounds one half of the core. Six beam tubes - two tangentials and four radials - are available for neutron experiments. When they are not in use these beam tubes are flooded with water and closed by the insertion of concrete plugs. One of the beam tube has a larger diameter (Ø = 27 cm) than the others (Ø = 24 cm), to accommodate two thermal neutron guides supplying neutron beam for the spectrometers in the external neutron guide hall (NGH). In addition, the reactor provides facilities for nuclear engineering experiments, neutron activation analysis and radioisotopes production. The arrangement of the beam tubes and other facilities in the reactor core is shown in figure 2.

The RSG-GAS has achieved its criticality in 1987 and reached its full power level of 30 MW thermal in 1992. However continuous regular operation was started not earlier than 1995. The delay was due to a long shutdown period owing to the installations of the in-pile engineering loops, radioisotope production equipment, neutron scattering instruments, and also due to other technical problems.

In 1996, the reactor has been operated quite regularly for three cycles per month and nine days per cycle. In order to improve the radioisotope production, in 1997 the reactor operation has been made weekly with 5 operation days with reactor power of 25MW thermal. This was not so convenience for the neutron scattering activities. After some consultations and discussions, the reactor operation mode has been compromised and changed to 12 days operation and followed by 9 days off. This schedule has been settled and started in July 1998 and lasted until July 1999. In return the reactor will only be in operation at 15MW thermal to maintain the length of the operation with the available fuel elements. Due to some more problem in the financial sector, in the past one year the reactor has been in operation for 12 days followed by 16 days off which means we have neutron beams for 12 days monthly which is about 100 days yearly.

So far the neutron beams have been used for most of the scheduled operation days. This continuous and regular monthly scheduled operation days give advantages in planning the experiments in advance and improve the reliability of the neutron instruments.

3. NEUTRON SCATTERING INSTRUMENTS

3.1. SANS SPECTROMETER

This instrument is installed at the end of the 58 m long neutron guide (NG-1), situated in the neutron guide hall (NGH), to benefit from low background environment. The incident beam is monochromatised by a slot-type mechanical velocity selector having a minimum rotational speed of 700 rpm and a maximum rotational speed of 7000 rpm. The selector's tilting angle can be varied from −3.9° to +3.9°. By varying these rotational speed and tilting angle, neutron wavelengths of 2-5 Å and a Q range of $(0.001<Q< 0.6)$ $Å^{-1}$ can be obtained.

The collimator is placed in an 18 m long tube, comprises of four sections of movable guide tube, and one section of a fixed collimator (non-reflecting) tube. Collimation is made by adjustable apertures (pinholes) at discrete distances of 1.5 m, 4 m, 8 m, 13 m and 18 m from the sample position. The detector, which can be moved continuously from 1.5 m to 18 m in another18 m tube, is a 128 x 128 He-3 two dimensional position sensitive detector (2D-PSD) made by RISØ, with three beam stoppers of 40, 80 and 140 mm in diameter. The whole system, excluding the sample position is evacuated to 10^{-3} torr. Variation of collimation length and sample to detector distance are fully computer controlled. An automatic sample changer with six sample holders is provided.

In the last two years, many efforts have been carried out to bring this spectrometer in action, including the SANS subworkshops held together with the workshops. Some of its components have been replaced, but there are still many others need carefull attention and repaired, such as the velocity selector, control motor for the guide tube and beam stopper to mention a few. Last year we reported in Mito, Japan the problem coming from a spurious peak. We have tried to adopt the solution taken in JAERI by covering some part of the guide tube entrance after the velocity selector. It seemed at that time that it was effective, especially for experiments where the detector are placed at a distance which is less than 5 meters from sample position. Some checkings after that proved that actually the method is not working, especially for longer sample to detector distance experiments.

We also have checked some combinations of the pinhole and it seems that the neutron leakage is coming from the second guide tube in the collimation path. Right now we are running the experiment by placing neutron absorber in front of the sample to absorb neutron coming from other source. Eventhough this doesn't solve the problem completely, but for the time being, it works for some number of experimental settings.

3.2. HRSANS SPECTROMETER

This neutron spectrometer, which is similar to the Bonse-Hart type diffractometer for small angle X-ray scattering, extends the Q range covered by SANS spectrometer to lower Q. This increases the sensitivity of inhomogenity on length up to some microns. The instrument has a PG(004) monochromator mounted on the neutron guide (NG-2), 63 m away from the reactor core.

Two nearly perfect Si(311) single crystals are used as monochromator ($\Delta\lambda/\lambda$ = 0.15 %) and analyzer ($\Delta\theta$ = 0.0001°) and installed on goniometers. These goniometers

which provide rotation, translation and tilting movements are mounted on an optical bench moving on air cushions and controlled by a computer or handy terminal (HT). Three detectors are installed for alignment, monitoring and diffracted beam measurements.

The sample with a maximum size of 30x30 mm^2 is placed between the two Si(311) crystals whereas the whole system is installed in a thermostatic room to obtain constant sample temperature within 0.5° C.

This spectrometer has already been in operation since 1992, but we couldn't have utilized it very much. This is due to the problem in performing the calibration everytime we want to start this machine. Even in the middle of running it, we have to start calibration again if there is an electric failure. So, actually we have calibrated this spectrometer so many times or in another word everytime. A solution that we have forseen is by changing the software so we can keep the calibration state even when we turn of the electronics. It would be a great help if this meeting can provide us with suggestions for solving this problem.

3.3. HRPD (HIGH RESOLUTION POWDER DIFFRACTOMETER)

The HRPD, which is the most heavily used instrument for the time being, is installed at the neutron guide (NG2) in the Neutron Guide Hall (NGH) about 71 m away from the reactor core. The monochromator drum has three beam exits corresponding to three different take off angles, $2\theta_M$ = 41.5°, 89° and 130°. At present the instrument is set for $2\theta_M$ =89°.

In the last three years we found so many strange things coming to the diffraction patterns of this diffractometer. The worst problem is that we cannot get the same thing again. This means that it is not reproducible. In order to solve this problem, we replaced some of the 32 detectors with the help of JAERI two years ago. We have reported the results last year in Mito. It did help in some part of the pattern, but the rest still remains unpredictable. At that time we received suggestions to replace the third collimator and check and evaluate the electronics after the detectors. In June this year we had the opportunity to replace the third collimators with the help of JAERI. At that time we replaced our original 10 minutes collimator with the 6 minutes ones from JAERI. Figure 3 presents the diffraction patterns of TiO_2 standard sample taken after the replacement of the third collimators with the 6 minute ones, while figure 4 shows the diffraction pattern taken earlier before the replacement. Eventhough we can see some improvement, especially the elimination of some extra intensities around 130° of 2theta angle, but there is another sharp and strong extra peak below 40° of 2theta angle. We still couldn't find out the origin of this extra peak and some other smaller peaks. On the other hand, as it is predicted before, the intensity of the whole pattern is becoming a bit less for the 6 minutes collimators. The confusing problems are that this diffraction pattern is not constantly be produced everytime.

4. NATIONAL SEMINAR ON NEUTRON SCATTERING

Last June, we held the third National Seminar on Neutron Scattering in Serpong. The first seminar was launched in 1998 to gather people who has interest in neutron scattering in general. We had 20 papers presented orally and in the form of posters. There were about 100 partipants all together discussing many aspects of neutron scattering in Indonesia. Last year this seminar presented 23 papers all together and attended by about 150 participants. At that time the idea of replacing the control system by microcontrollers was raised and gathered strong support from the audience. The seminar this year, which was held on June 28, was presenting 34 papers. Many of the papers related more to the instrumentation since last year we agreed to solve our instrumentation first before launching some neutron scattering experiments. We expected that by handling our instrumentation by ourself will lead to a better state in the operation and maintaining of the instruments. In the second week of August 2000 we held a training course discussing microcontroller as alternative solution for the problem in the instrumentation of our spectrometers. Out of that course, we are pursuing the possibility of replacing some components to the ones that can be produced and repaired by our ownselves in the future. Right now we are planning to implement this on the four circle diffractometer/texture diffractometer (FCD/TD).

5. SUMMARY

The conditions of the three neutron scattering instruments, i.e. SANS spectrometer, HRSANS spectrometer and HRPD have been reported. Problems and shortcomings that attached with each instrument have also been presented together with some efforts in dealing with them. The help from JAERI and the previous workshops and sub-workshops is acknowledged and received with gratefulness.

Right now HRPD is the most heavily used instrument since it is stil capable to run some structural analysis. Some rooms for improvements are still available especially in the area of increasing its electronics capabilities.

The next instrument in line is the SANS spectrometer which is ready for some real experiments. Some of its components need replacement and/or repair due to their ages. Eventhough the spurious peak is still an obstacle in the instrument, some data taken from polymer samples are quite acceptable.

The HRSANS spectrometer is still has the calibration problem but it can handle the tasks good enough, especially when the calibration is already in place. Suggestions and solutions from this workshop will be appreciate.

6. ACKNOWLEDGEMENT

The author would like to thank STA Japan for the financial support so he could attend the workshop to present this paper. He is also very grateful to JAERI, KAERI and MOST for the support. Thank is also due to Mr. Yatno for his help in preparing this paper.

7. REFERENCES

1. A. Ikram, IAEA TCM on Neutron Beam Research, Lisbon, Sept. 10-12 1997
2. A. Ikram, National Symposium on X- Ray and Neutron Scattering, Serpong, May 13, 1998
3. A. Ikram, Workshop on the Utilization of Research Reactor, Mito, Nov 29 - Dec 2, 1999
4. A. Ikram, National Symposium on X-Ray and Neutron Scattering, Serpong, June 28, 2000

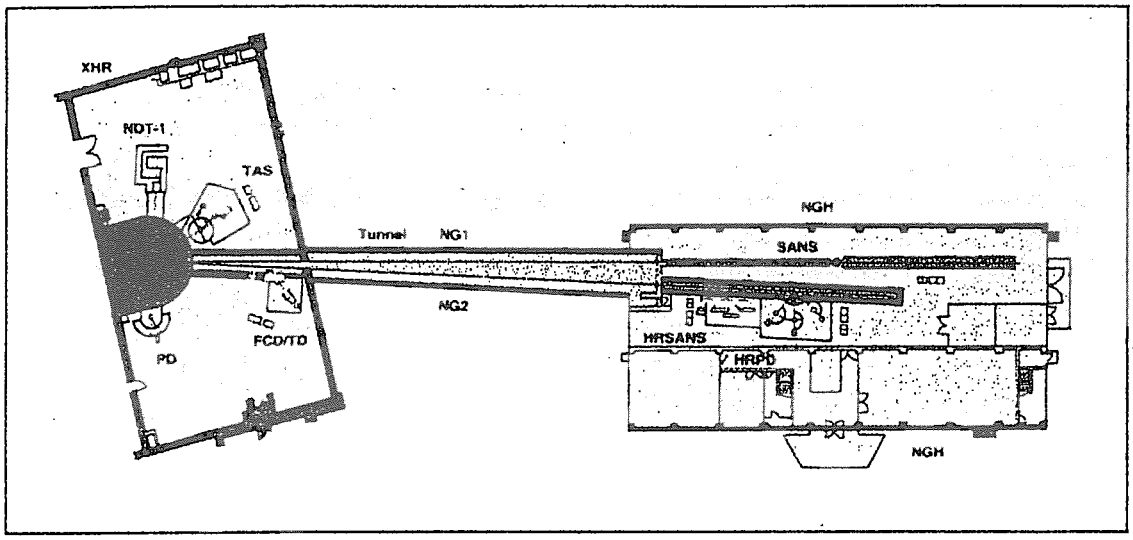

Figure 1. The Layout of the neutron scattering instruments in the reactor experimental hall (XHR) and in the neutron guide hall (NGH)

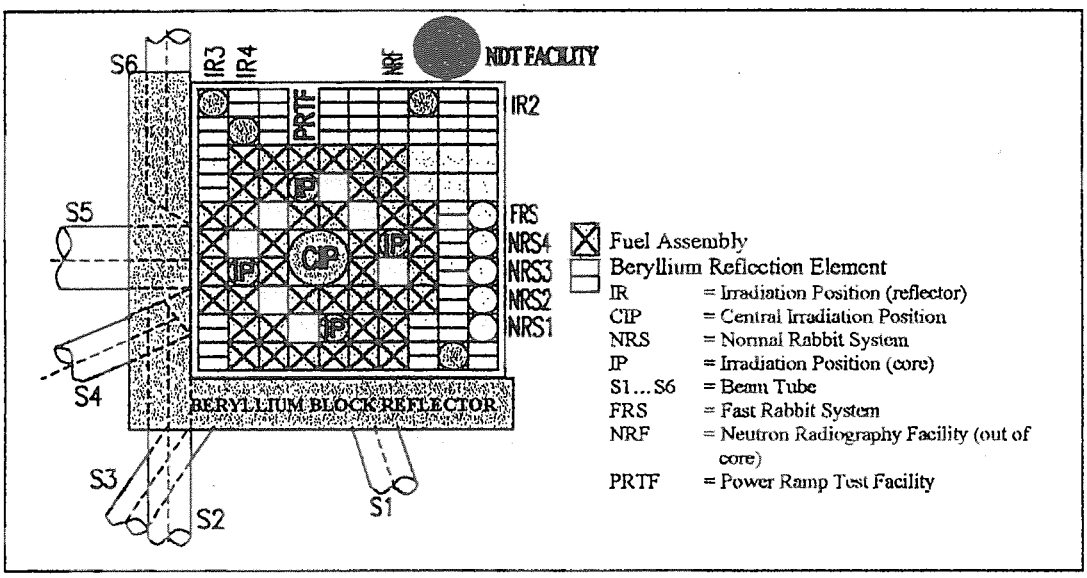

NGH	: Neutron Guide Hall	FCD/TD	: Four Circle Diffractometer/ Texture Diffractometer
NG1	: Neutron Guide #1		
NG2	: Neutron Guide #2	HRPD	: High Resolution Powder Diffractometer
NDT-1	: Neutron Radiography Facility		
SANS	: Small Angle Neutron Spectrometer	TAS	: Triple Axis Diffractometer
HRSANS	: High Resolution Small Angle Neutron Scattering Spectrometer		

Figure 2. The arrangement of the beam tubes and other facilities in the reactor core

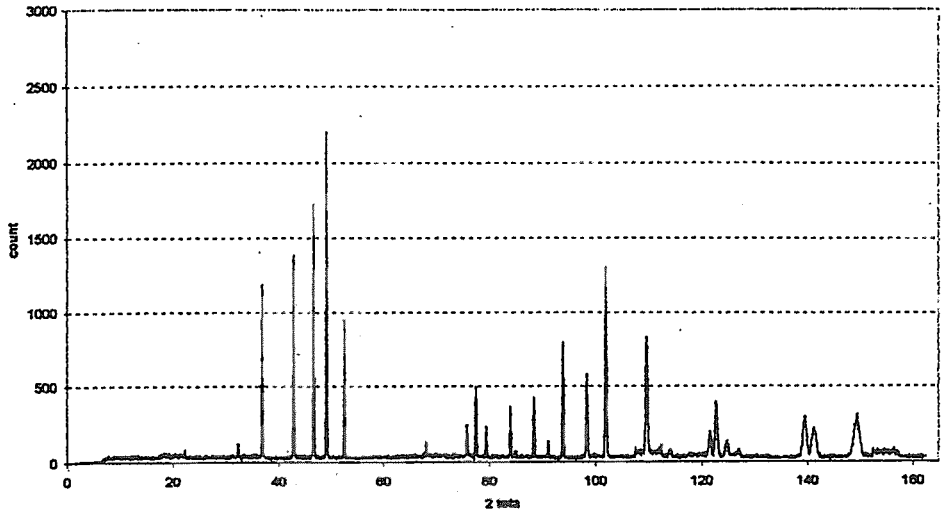

Figure 3. Diffraction Pattern of TiO_2 using 6 minute Collimators

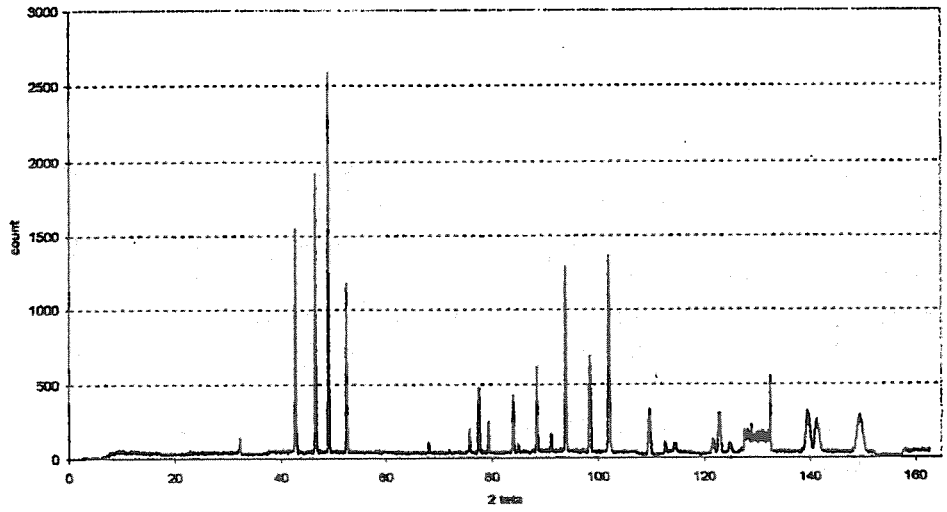

Figure 4. Diffraction Pattern of TiO_2 using 10 minute Collimators

JP0250089

1.5 MEASUREMENTS OF PS-PEP SAMPLE IN SERPONG

A. Ikram, Sudirman and A. Insani
Neutron Scattering Laboratory
R & D Center for Materials Science & Technology
National Nuclear Energy Agency
Serpong - Indonesia

ABSTRACT

SANS spectrometer in Serpong is described briefly. Results from the measurements of PS-PEP standard samples, through and edge views, taken by the instrument are presented and compared with the ones taken by SANS-J in JAERI. The outcome is not very satisfactory but the features are there. Suggestions from the workshop are very invited to improve the results not only from the instrumentation but also from the software.

1. INTRODUCTION

In the last three years SANS technique has been explore in the workshops followed by sub-workshop in Serpong (February 1999) and Tokai (November 1999). Polymer samples have been chosen for the study starting from SPU (segmented polyurethane), polystyrene, PMMA (polymethylmethacrylate), sodium dodecyl sulphate (SDS). The study was intended to find out the capability of the technique as well as the instrument. Last year in Mito, it was decided to run some standard samples with different SANS machines in the region to compare the performances of the instruments in each country. In this paper we reported the results of measuring PS-PEP standard samples, through and edge views, in Serpong.

2. THE SMALL ANGLE NEUTRON SCATTERING SPECTROMETER

This instrument is installed at the end of the 58 m long neutron guide (NG-1), situated in the neutron guide hall (NGH), to benefit from low background environment. The incident beam is monochromatised by a slot-type mechanical velocity selector having a minimum rotational speed of 700 rpm and a maximum rotational speed of 7000 rpm. The selector's tilting angle can be varied from –3.9° to +3.9°. By varying these rotational speed and tilting angle, neutron wavelengths of 2-5 Å and a Q range of ($0.001<Q<0.6$) $Å^{-1}$ can be obtained.

The collimator is placed in an 18 m long tube, comprises of four sections of movable guide tube, and one section of a fixed collimator (non-reflecting) tube. Collimation is made by adjustable apertures (pin-holes) at discrete distances of 1.5 m, 4 m, 8 m, 13 m and 18 m from the sample position. The detector, which can be moved continuously from 1.5 m to 18 m in another 18 m tube, is a 128 x 128 He-3 two dimensional position sensitive detector (2D-PSD) made by RISØ, with three beam stoppers of 40, 80 and 140 mm in diameter. The whole system, excluding the sample position is evacuated to 10^{-3} torr. Variation of collimation length and sample to detector distance are fully computer controlled. An automatic sample changer with six sample holders is provided. Figure 1 shows the schematic block diagram of the instrument.

In the last four years, many efforts have been carried out to bring this spectrometer in action. Some of its components have been replaced but there are still many others need careful attention and repaired such as the velocity selector, control motor for the guide tube and beam stopper to mention a few.

3. EXPERIMENTAL SETTINGS

The experiment is carried out by placing the detector at 12 m position away from the sample position. The beam stopper of 80 mm in diameter was applied. In order to keep the simmetry, we replace the the last three guide tubes with non reflecting tubes to bring the neutron source away from the sample. The combination of pin-hole setting was chosen so the neutron beam is optimized. The first pin-hole was open, the following five pin-holes were set at 30 mm, 20 mm, 14 mm, 10 mm and 10 mm in diameter respectively. The velocity selector was set at 7000 rpm correspnding to producing neutron with lambda at 0.408 nm. The samples, through and edge views, were placed in the air atmosphere at the sample changer. It took 3 days to run the whole experiment including measuring the pattern from water, cell, empty, background and 6 hours for each sample. Eventhough we have taken the data for several time while the reactor at 15 MW thermal power, but the results that we are reporting here in this paper are the best ones and were taken at the time when the reactor was operated at 10 MW thermal power.

4. RESULTS

Figure two presents the results of the measurements. The top picture shows the pattern taken from the through view sample. We can see the first peak at 0.07 nm^{-1} and a very shallow hump at about 0.125 nm^{-1}, while the third is a bit distracted and slash in two humps with the centre at about 0.19 nm^{-1}. The lower figure is presenting the pattern from the edge view sample. It is obvious that there are two peaks with a small hump in the middle. The first peak is at 0.07 nm^{-1}, while the hump is centered at 0.16 nm^{-1}, and the last peak at 2.2 nm^{-1}. Figure 3 shows the results taken by SANS-J, JAERI in the last sub-workshop in Tokai last year. The quality of the results is uncomparable, but we still hope that the instrument in Serpong can be improved.

5. SUMMARY

We have presented the SANS spectrometer in Serpong. We also present results from the measurements of PS-PEP standard sample using that spectrometer. It is obvious that the data were not very satisfactory, eventhough we have taken the best available data from many trial and error experiments. We are still hopeful to improve the data quality taken by this instrument, especially with the help and suggestions coming from this workshop.

In order to do that, we are planning to run again some standard samples in JAERI, with the kind permission of JAERI experts, so we can calibrate the results taken by our instrument. Ms. A. Insani has spent four weeks in JAERI lately and she is very motivated to run some more calibration procedures in Serpong once the reactor is in operation.

6. ACKNOWLEDGEMENT

The authors would like to express their gratitude to JAERI for all the support that has been provided by JAERI to bring the BATAN SANS instrument into its best condition. We'd also like to thank Mr. SM Prasetyo and Mr. IP. Utomo who have been very helpfull in operating the instrument and Mr. Yatno and Ms. AD Puspitasari for preparing this paper.

7. REFERENCES

1. Marsongkohadi et.al., IAEA Regional Expert Workshop on Neutron Scattering and Applications, Serpong, June 16 - 20, 1997.
2. A. Ikram, IAEA TCM on Neutron Beam Research, Lisbon, Sept. 10-12 1997
3. A. Ikram et.al, National Symposium on X- Ray and Neutron Scattering, Serpong, 2000.

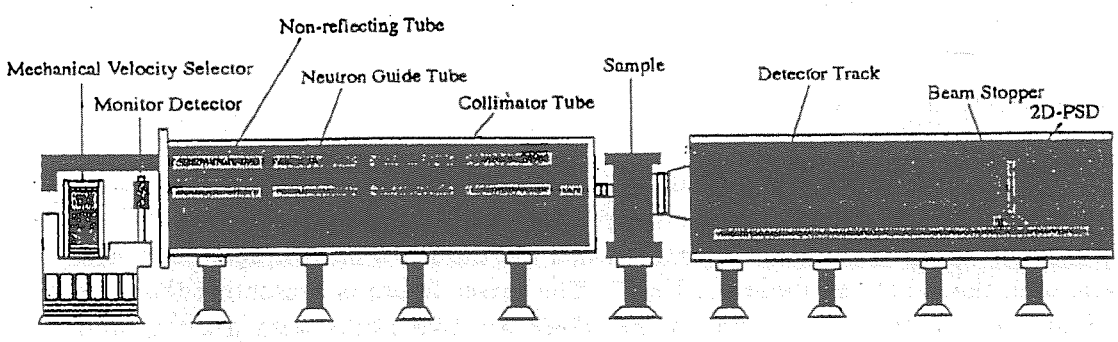

Figure 1. BATAN-SANS Instrument

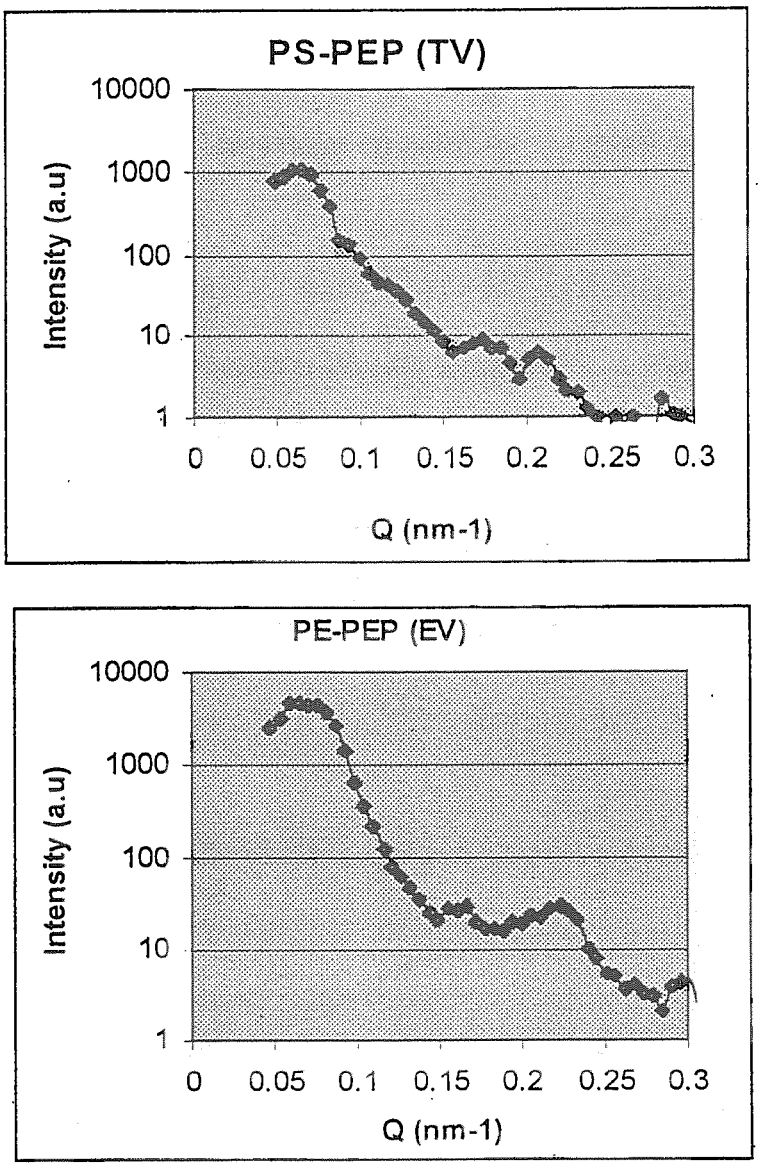

Figure 2. SANS data from PS-PEP Sample, through view (top) and edge view (bottom), taken by BATAN Instrument

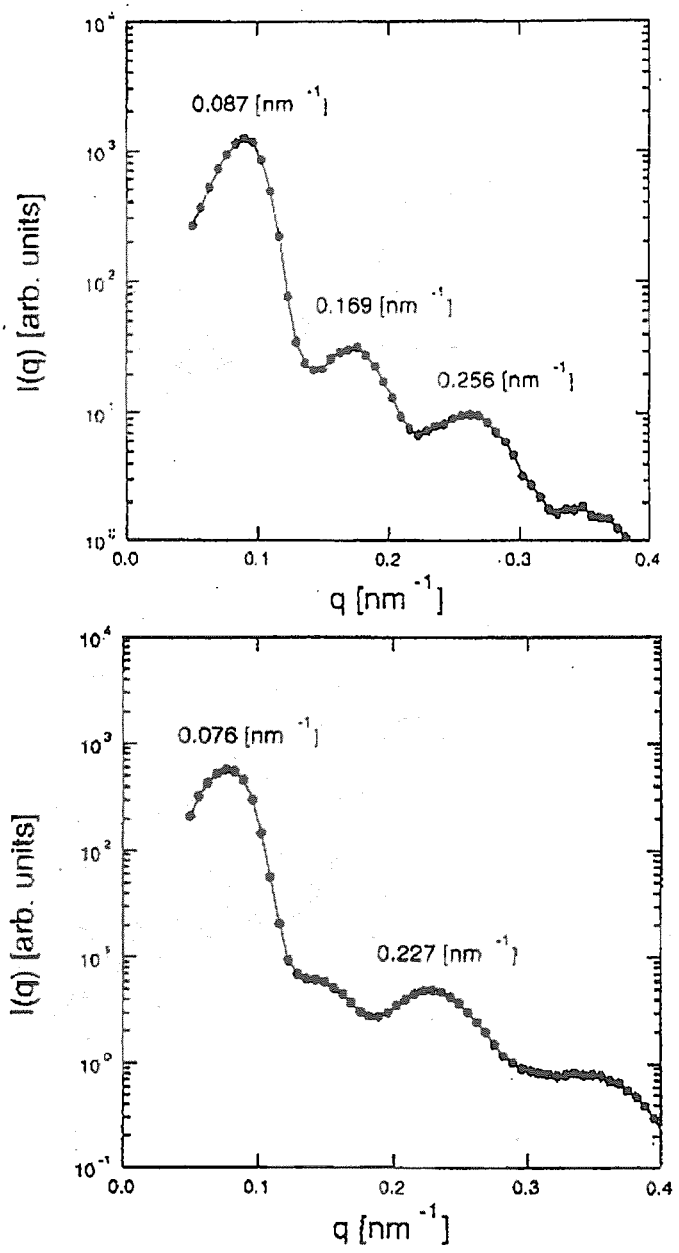

Figure 3. SANS data from PS-PEP Sample, through view (top) and edge view (bottom), taken by SANS-J, JAERI

JP0250090

1.6 REVITALIZATION OF NEUTRON DIFFRACTOMETERS IN SERPONG

A. Ikram, M. R. Muslih, A. Purwanto, T. H. Priyanto and E. Santoso
Neutron Scattering Laboratory
Research & Development Centre of Materials Science & Technology
National Nuclear Energy Agency
Serpong - Indonesia

ABSTRACT

The neutron beam facilities in Serpong include one diffractometer for residual stress measurement and one diffractometer for single crystal structural determination and texture measurement. Current status of these instruments are presented together with the development carried out in the past year to overcome some of their problems. Their performances are also described briefly. The capabilities of the diffractometer for residual stress measurements are also discussed as well as the possibility of running the FCD/TD using a promising modified control system which implement microcontrollers.

1. INTRODUCTION

The RSG-GAS, a very high neutron flux research reactor commissioned in Serpong, has achieved its criticality in 1987 and reached its full power level of 30 MW thermal in 1992. However continuous regular operation was started not earlier than 1995. The delay was due to a long shutdown period owing to the installations of the in-pile engineering loops, radioisotope production equipment, neutron scattering instruments, and also due to other technical problems.

Since 1996, the reactor has been operated quite regularly for three cycles per month and nine days per cycle. In order to improve the radioisotope production, in 1997 the reactor operation has been made weekly with 5 operation days with reactor power at 25MW thermal. This was not so convenience for the neutron scattering activities. After some consultations and discussions, the reactor operation mode has been compromised and changed to 12 days operation and followed by 9 days off. This schedule has been settled and started in July 1998 and lasted until July 1999. In return the reactor will only be in operation at 15MW thermal to maintain the length of the operation with the available fuel elements. Due to some more problem in the financial sector, in the past one year the reactor has been in operation for 12 days followed by 16 days off which means we have neutron beams for 12 days monthly which is about 100 days yearly.

So far the neutron beams have been used for most of the scheduled operation days. This continuous and regular monthly scheduled operation days give advantages in planning the experiments in advance and improve the reliability of the neutron instruments.

During 1992, various neutron scattering instruments have been installed in the NSL-Serpong . Those instruments are :

1) Powder Diffractometer (PD), DN-1
2) High-Resolution Powder Diffractometer (HRPD), DN-2
3) Four-Circle diffractometer for single crystal structural studies and texture analysis (FCD/TD), DN-3
4) Neutron Radiography Facility (NRF) with real time experiment capability, RN-1
5) Triple Axis Spectrometer (TAS), SN-1
6) Small Angle Neutron Scattering (SANS) spectrometer, SN-2
7) High-Resolution Small Angle Neutron Scattering (HRSANS) spectrometer, SN-3

About five years ago, the powder diffractometer was modified to accommodate residual stress measurements (DN-1M) and has been used for some measurements. The powder diffractometer, the triple axis spectrometer and the neutron radiography facility are installed at the beam port S6 (tangential), S4 (radial), and S2 (tangential), respectively in the experimental hall of the reactor (XHR).

Two neutron guides are installed starting from S5 radial beam port, penetrating the reactor confinement building wall and going through a 35 m tunnel into the external neutron guide hall (NGH). The first neutron guide (NG1) is dedicated to the small angle neutron scattering spectrometer, which is installed at the end of the guide. The second neutron guide (NG2) has three beam ports labelled as NG2-1, NG2-2 and NG2-3 at which the four-circle diffractometer, the high-resolution small angle neutron scattering spectrometer and the high-resolution powder diffractometer are installed respectively. In order to shield the radiation coming from the neutron guide, they are confined inside a casemate having concrete walls along their whole length, except those parts, which are inside the tunnel.

In this short paper we presents the last development implemented to the diffractometers, especially related to the residual measurements which will be discussed further in the forthcoming workshops.

2. Neutron Diffractometer (DN-1M)

The powder diffractometer was the first instrument installed and situated in the reactor experimental hall (XHR). It was a standard two axis type diffractometer with a PG (004) focussing monochromator to enhance the neutron flux at the sample position. Mylar films coated with gadolinium are used for collimators with angular divergences of 20' and 40'. In collaboration with the Japan Atomic Energy Research Institute (JAERI), five years ago the diffractometer was modified for residual stress measurements.

Modifications were made by installing a divergent flight tube of 1750 mm long on the diffractometer arm in front of a 256 mm long one-dimensional position sensitive detector (1D-PSD). The distance between the sample and the tip of the flight tube can be varied continuously in the range of 0-190 mm, to allow handling big samples. For sample mounting and positioning the iinstrument is equipped with goniometer having three orthogonal translation as well as a turn table to rotate samples around the incident beam. All sample movements and data collection are controlled by a NEC PC-9821 computer. The size of both incident and scattered beams are defined by apertures having various diameters ranging from 2 to 5 mm. The volume sampled by the diffractometer is then defined by the intersection of the incident and scattered beams in the scattering plane.

Three years ago we replaced the PG (004) monochromator with a bent Si (311) single crystal to obtain higher intensity of monochromatic neutron beam. At that time we reported in the Workshop that there was a double peak coming from the monochromator detected by the 1-D PSD. We have tried many things to overcome this problem. Last year, again with the help from JAERI we replaced the monochromator system with horizontally bent and vertically focussed Ge (311) single crystals. After so many consultations with JAERI's experts we decided to remove the 1-D PSD early this year and replaced it again with the original detector (He3). We also made some modification to the diffractometer such as removing the flight tube, etc ; and went through a calibration procedure starting from the first collimator, monochromator, second and third collimators and so on. Table 1 shows the latest technical specification of the diffractometer. Figure 1 shows a diffraction pattern taken from a standard sample of Alumina after the latest modifications of the diffractometer.

Last June we had an opportunity to run a Ring-Plug sample supplied by JAERI. The plug is develope according to the standard procedure produced by VAMAS. The measurements were also performed according to VAMAS instructions. Figure 2 shows the diffraction pattern of the ring plug taken by the neutron diffractometer. Figure 3 presents the strain calculated from peak (220) for hoop, radial and axial configurations. The results show irregular pattern which roughly representing the strain in the sample. There was a bit of confusion when we perform the experiments since we couldn't find the line on the ring plug indicating where the experiments should be carried out. But, by looking at the results, we are confident that the instrument is capable of handling many other sample containing residual stress. Further development of the instrument will include some modifications so we could measure the stress directly and at the same time measuring the strain through a certain the diffraction peak.

Table 1. Technical Specification of the neutron diffractometer for residual stress measurements

1. Monochromator	: Ge (311), horizontally bent and vertically focussed
2. Collimators	: #1 = 40' (before monochromator) #2 = 40' (between monochromator and sample) #3 = 20' (between sample and main detector)
3. Incoming beam size	: 30(w)*50(h) mm^2
4. Take-off angle	: $0\sim70^0$
5. 2-theta range	: $-100 \sim +100^0$
6. Incident slit to sample	: max. 190 mm
7. Sample to diffraction slit	: max. 310 mm
8. Beam axis height	: 91 mm
9. Sample table translator	: X = -70 ~ 70 mm Y = -70 ~ 70 mm Z = 0 ~ 50 mm
10. Main Detector	: He^3
11. Counting System	: Canberra
12. Control System	: IBM-PC
13. Software	: modified from RESA (JAERI).

3. Four-Circle Diffractometer/Texture Diffractometer (DN-2)

The four-circle diffractometer is installed at the NG2-1 beam port sited in the XHR. This dual purpose instrument was designed for single crystal structural studies and texture measurements, and was constructed robustly to allow heavy attachments. The allowable load on the sample table is 300 kg.

A Cu (220) or PG (004) monochromator with a fixed take off angle of 46° is mounted inside the neutron guide casemate to obtain monochromatic beam having a wavelength of 0.997 Å or 1.311 Å for Cu (220) or PG (004) monochromator, respectively. The maximum beam size at the sample position is 40 x 40 mm^2 and the detector is BF_3 end window counter with 100 mm∅ and 236 mm effective length.

This instrument is operated automatically by an IBM PC 2/70 computer. Ancillary equipment available are full and half circle Eulerian goniometers, a fiber specimen holder and a cryostat. Since October 1998 the computer is out of order, so we were thinking of by passing the computer. In the last two years we have tried to find an alternative way in operating the diffractometer. Last August we started to implement a system using microcontrollers. Figure 4 shows block diagrams of the original and modified configuration of the control system. Using the new configuration we expect to overcome the problems occurred in the instrument. We hope by the end of the year 2001 we already can run some experiments using this diffractometer. From this workshop, we'd like to ask some suggestion in installing the software to control the instrument.

4. SUMMARY

We have presented the modification in our diffractometers, i.e. : the neutron diffractometer for residual stress measurements (DN-1M) and the four circle diffractometer/texture diffractometer (FCD/TD). The calibration of DN-1M using Alumina standard sample showed that the instrument is in good shape, especially to contribute to the next sub-workshop ; and furthermore this is supported and confirmed by the results coming from a ring plug sample provide by JAERI.

The difficulties faced by FDC/TD in the last two years have pushed us in Serpong to find an alternative way in controling the instrument. Application of microcontroller came out as a better choice not only because the components could be obtained easily locally in Indonesia but also we can apply this to other instruments once it works with FCD/TD.

5. ACKNOWLEDGEMENT

We'd like to thank STA, Japan for the financial support so Dr. Ikram could attend the workshop to present this paper. We are also very grateful to JAERI, KAERI and MOST for the support. We'd like to thank Mr. Yatno for the help in preparing this paper.

6. REFERENCES

1. Marsongkohadi et.al., IAEA Regional Expert Workshop on Neutron Scattering and Applications, Serpong, June 16 - 20, 1997.
2. NSL – Serpong, Information Brochure, August 1997
3. A. Ikram, IAEA TCM on Neutron Beam Research, Lisbon, Sept. 10-12 1997
4. A. Ikram, National Symposium on X- Ray and Neutron Scattering, Serpong, 1998
5. A. Ikram, Workshop on the Utilization of Research Reactor, Mito, 1999
6. A. Ikram, National Symposium on X-Ray and Neutron Scattering, Serpong, 2000
7. G. A. Webster, Neutron Diffraction Measurements of Residual Stress in a Shrink-fit Ring and Plug, VAMAS Report No. 38, January 2000

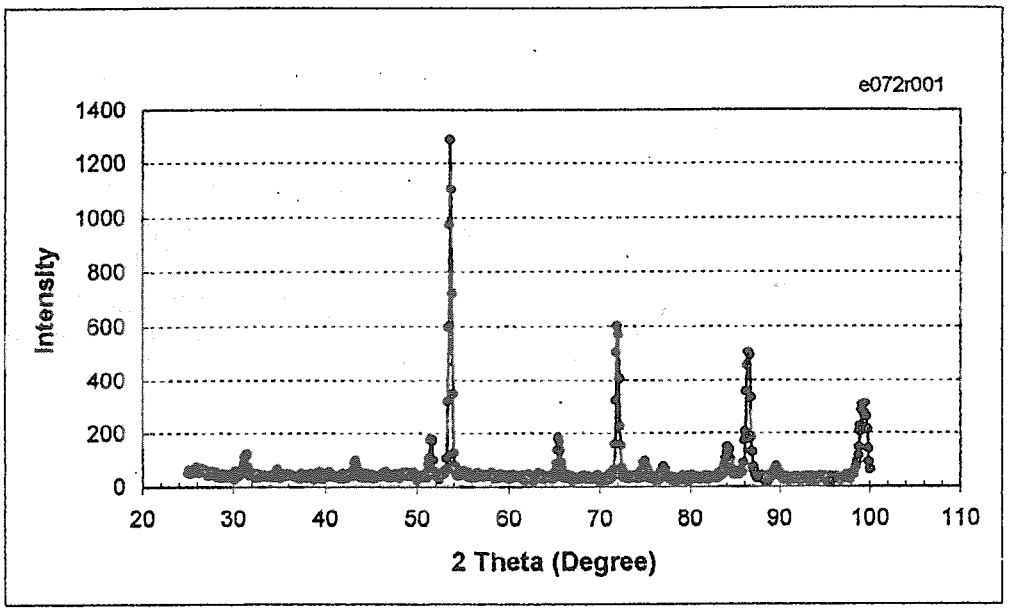

Fig. 1. Neutron Diffraction Pattern of Sample Standard Al_2O_3

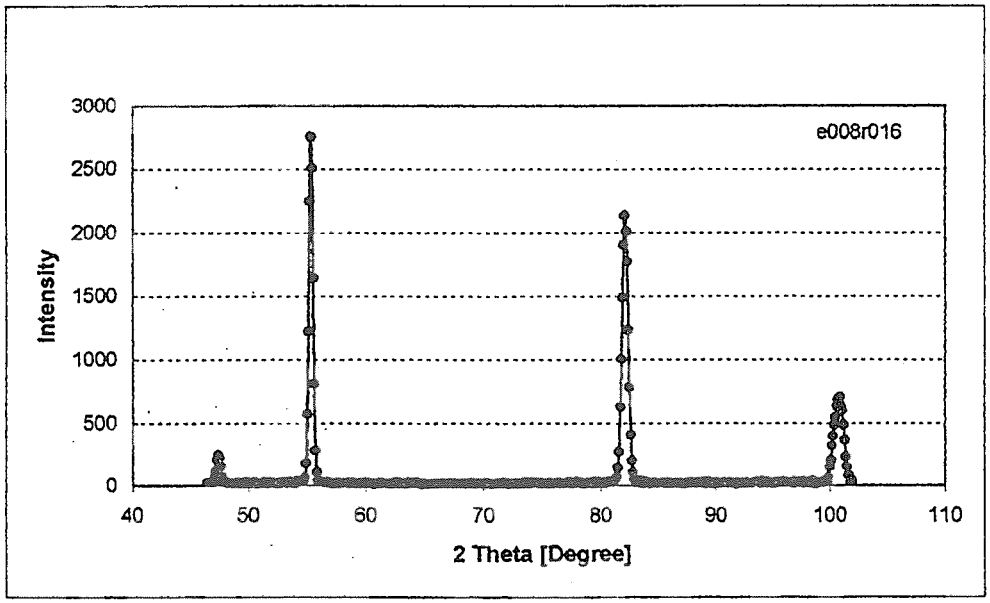

Fig. 2. Neutron Diffraction Pattern of Ring Plug A6063

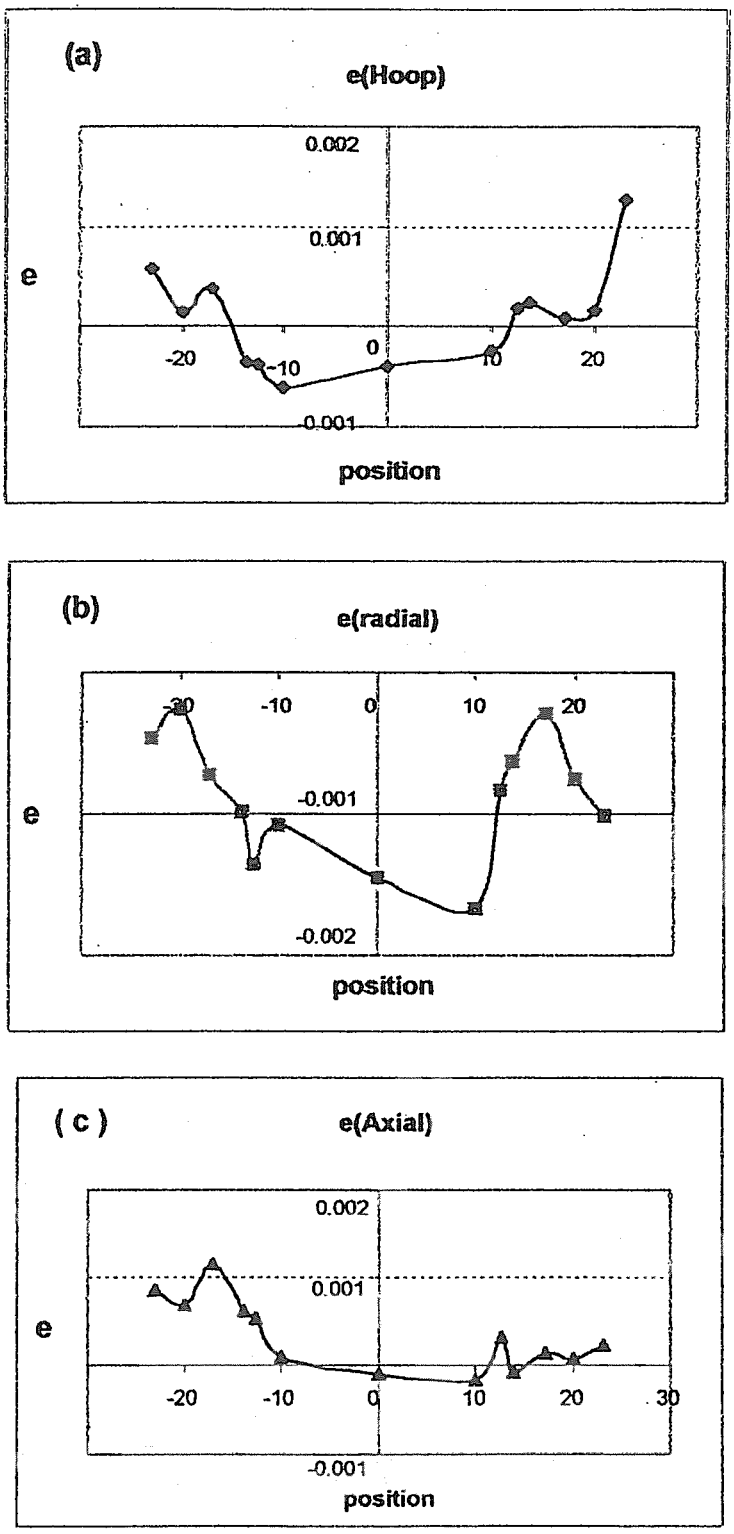

Fig. 3. Strain Distribution of A6063 (220 peak) for (a) Hoop (b) Radial and (c) Axial

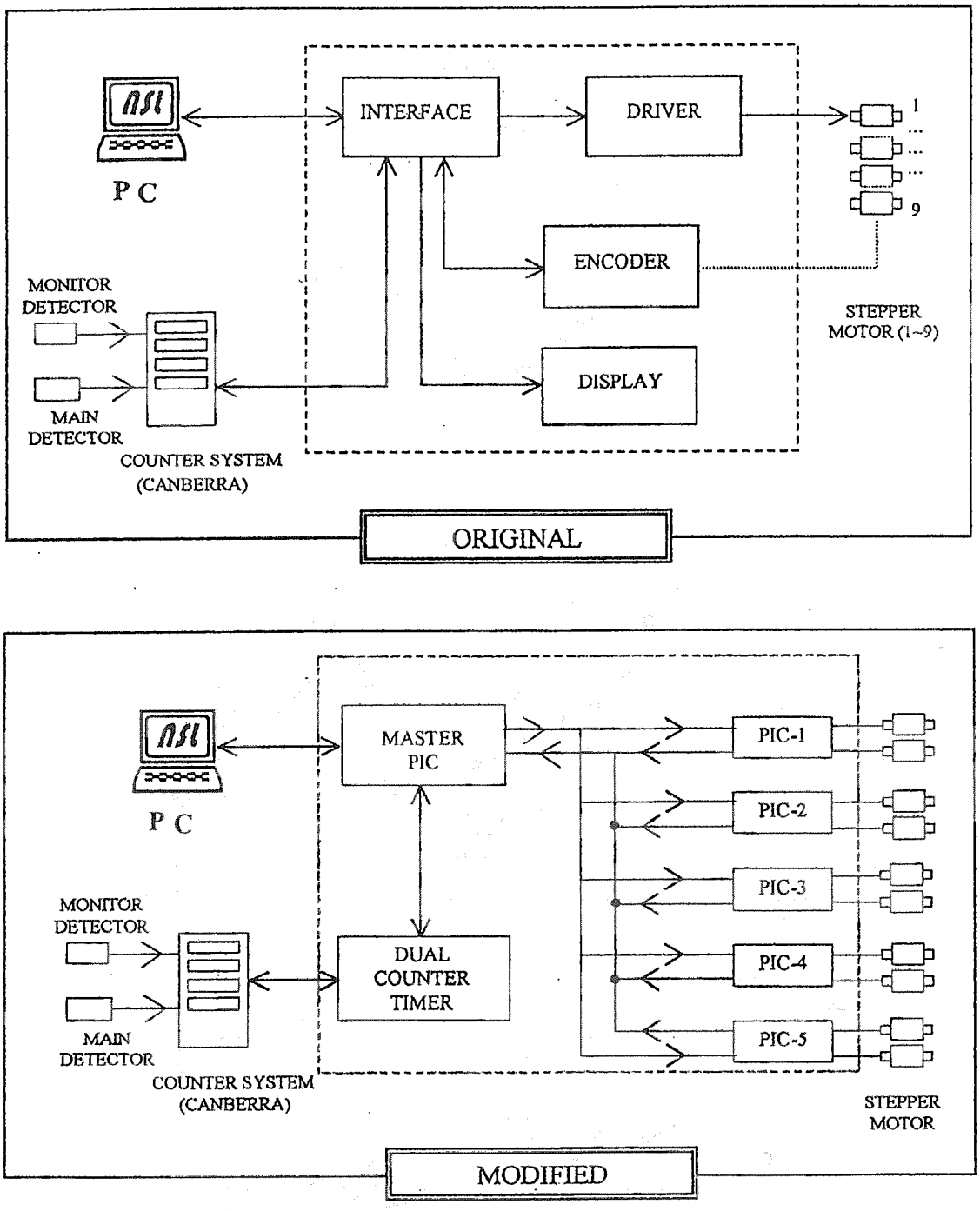

Fig. 4. Block Diagram of Control System of FCD/TD Instrument (a) Original and (b) Modified Version

JP0250091

1.7 Progress Report on neutron scattering at KAERI

Chang-Hee Lee
Korea Atomic Energy Research Institute, Taejon 305-6000, Korea

ABSTRACT

The neutron beam facilities in HANARO are presented and the specification of the research reactor is described. Present status, performance and on-going development with utilization fields of each instrument such as the high resolution powder diffractometer, the four-circle diffractometer, the neutron radiography facility, and the commissioning status of the small angle neutron spectrometer are described. We also present some of technical developments for spectrometer components, and starting-phase users' program and promoting activities.

1. The Research Reactor, HANARO

The specifications of the reactor, HANARO, are summarized in table 1. The HANARO is an open-tank-in-pool type reactor cooled by light water, and moderated by heavy water. Its compact core inside the inner shell is surrounded by a spacious reflector, which accommodates a variety of experimental holes. At its maximum thermal power of 30MW, the maximum thermal neutron flux is expected to be 5 x 10^{14} neutrons/cm^2/sec at the central thimble. In the reflector there are seven horizontal beam tubes and a total of 25 vertical holes. These holes with different sizes are widely used for radioisotope production and neutron activation analyses, and a large vertical hole for the future installation of a cold neutron source is provided.

Table 1. The reactor characteristics

Type	Open-tank-in-pool
Maximum thermal power	30MW thermal
Peak thermal neutron flux	5 x 10^{14} neutrons/cm^2/sec
Coolant / Moderator, Reflector	Light water, Heavy water
Core Cooling	Upward flow forced convection combined with bypass flow
Fuel	LEU 19.75w/o ^{235}U, U_3Si in Al matrix
Horizontal beam ports / Vertical holes	7 / 36
Maximum thermal neutron flux(<0.625 eV)	4.5x10^{14} nv @ core, 2.1x10^{14} nv @ reflector
Operation	28 day x 9 cycles/year

A cold neutron beam port (CN) is equipped with a vertical channel of 160mm diameter with its beam tube nose of 60mm(W) x 50mm(H) for the installation of a liquid hydrogen cold source in the future. The in-pile channel of the CN beam port is designed so that three or four neutron guides of about 20mm width x 150mm height each could be installed reaching up to about 150cm to the cold source. Cold neutron source installation project were decided to be postponed by 2003 after evaluation and re-planning overall aspects including neutron guides and a cold neutron laboratory, a set of spectrometers and users community.

HANARO has been operated for about 150 days a year as before and more than 95% of beam time from the operation days has been serviced to meet the demand from internal and external users. As the SANS commissioning is going well, small modification in the vertical hole, which was supposed to be for CNS installation, is expected in the next year. Because the hole is filled with light water and the estimation for several candidate materials for the insert replacing the light water region showed promising result, we will undertake more detailed flux calculation based on the models and put the insert plugging structure in the vertical hole. As a result, it is expected about two times higher flux gain for the SANS.

As for the IR port, the BNCT installation has been done continuously and a large platform structure attached to the port was constructed. In the ST1 port, neutron beam extraction for PGNAA by adopting 90 degree take-off from PG crystals in vertical direction is under way.

2. Neutron Beam Facilities

2.1 The High Resolution Powder Diffractometer (HRPD)

This instrument has been used most heavily without any serious problems since its commissioning and competition rate for beam time request becomes 1.5 to 2.0 these days and expected to be higher than 2.5 in the next year. The high temperature sample furnace has been used very much higher than expected but more works on sample cans and fine temperature control is needed to reduce beam time loss and easy handing. Overall upgrade of the instrument control program will be done next year for fixing and addition of different measuring modes, integration of computer control of several sample environments, and re-designing of communication between instruments and experiment database management by TCP/IP protocol.

Various chemical structures and magnetic structural studies has been undertaken mostly collaborating with external users from universities by using low and high temperature sample environments. In this year we have tried to do several feasibility works using the HRPD on the accurate determination of hydrogen content in materials by incoherent diffraction, neutron

diffraction of very small sample quantity in high pressure sapphire anvil cell and structure studies on the fullerene and its derivatives. Industrial application by using quantitative phase analysis and by combining texture measurements produced good result and is becoming attractive to industrial researchers.
Another progress is the development of residual stress instrument. Full set of measurements on VAMAS samples and a welded stainless steel plate of 20mm thickness could be done satisfactorily. This instrument is still an optional one to the HRPD and so beam time allocation for the residual stress measurement is to be limited to some extent depending on the users' demand.

2.2. The Four Circle Diffractometer

FCD is a conventional two-axis diffractometer with an Eulerian cradle and has been be used for the structural study of single crystals and for the texture measurements for industrial applications. Ge(331) monochromators with a fixed take-off angle of -45 degree were mounted and the wavelengths of the neutron beam for the three monochromators are 0.99Å. The effective beam size at the sample position is 20mm in diameter. A detector unit with a single He-3 counter is connected to the 2Θ-table by a cantilever type arm with a counter weight.
The early commissioning had been done by August 1999, and it has been routinely used for single crystal diffraction experiments as well as texture measurements. As for single crystals, KDP-DKDP system has been being undertaken and a few university users used it for their structural works as trial base. But texture measurement and analysis has been increased a lot by internal and external researchers related with industries.
Two sample environments fitted with the Euler cradle such as a CCR-type low temperature cryostat and a high temperature furnace are under development. In the end of this year the furnace will be tested first. As for neutron detection, we have a plan to install a 2-D PSD developed by us and/or the image plate for fast and wide measurement in near future depending on the characteristics of requested experiments.

2.3. The Small Angle Neutron Scattering Spectrometer

Until the cold neutron source is available, this SANS instrument would be operated at the CN beam port in the reactor hall. Neutrons filtered by liquid nitrogen cooled beryllium are monochromatized using a high speed Dornier velocity selector to obtain neutrons with a wavelength range of mostly 4Å to 8Å. To avoid gamma radiation from the beam port in a forward direction, a liquid nitrogen cooled Bi filter, an angular divergence of the transmitted beam, can be used in combination or independently depending on the situation. The total length of the SANS is about 8.5m due to the limitation of the reactor hall space. The scattered

neutrons is measured by using an large area 2-D position-sensitive detector of 128 x128 pixels with a resolution of 5mm x 5mm.

For the design goal of Q_{min}~0.005 $Å^{-1}$ and a neutron intensity of $I_s > 10^4 n/cm^2/sec$ at the sample position, the instrumental parameters of the single-aperture collimation are optimized at a wavelength spread of $\Delta\lambda/\lambda = 0.1$. The detector can be moved continuously from 1.5m to 5m inside the detector chamber of 1.7m diameter to change the available Q-range of the instrument. The whole system including the sample chamber would be evacuated down to about 10^{-3} torr. The Q_{max} will be extended to 0.81 $Å^{-1}$ by rotating the detector up to 30° around the sample stage. Its design characteristics are summarized in Table 2. The collimator with the pinhole type apertures, which are changeable with different sizes, is 4.2m long.

Table 2. The design characteristics of SANS

Source	CN beam port without cold neutron source
Gamma/Fast neutron filter	Liquid Nitrogen cooled Bi/Be filter
	Neutron V-bender
Monochromator	Neutron velocity selector with variable speed
Wavelength range	0.45nm to 0.7nm
Wavelength resolution (FWHM)	10 %
Minimum beam divergence	0.003 rad
Sample size	5 to 20 mm in diameter
Sample to Detector distance	1.5 to 4.25m
Q-range	0.06 to 8 nm^{-1}
Detector active area	65cm x 65cm with 128 x 128 pixels
Calculated neutron current(n/sec) at the sample	
Qmin (nm^{-1}) = 0.06	2×10^3
0.1	3×10^4
1.0	3×10^5

The performance test on major components and the neutron beam characteristics of the port had been done mostly last year and an overall testing of the integrated system by SANS experiments using a one-dimensional position sensitive detector done early this year, too. The base structure to rotate scattering angle position of the 2-D PSD, a safety interlock, integration of control and data acquisition system and completion of sample chamber, etc. will be done for next six months. The 2-D SAS measurement had been made since August and is now under full commissioning by first quarter of next year. Two polymer research groups will be joining with us on the test and performance evaluation during the commissioning phase.

2.4 The Neutron Radiography Facility

The neutron radiography facility was installed at the NR beam port late in 1996, as the first neutron facility at HANARO. NRF has been used for the nondestructive testing of components from general mechanics, aerospace, ordnance industries, etc., using both the direct and the indirect methods. The training of university students related to nuclear engineering or non-destructive test is also one of the important utilization of the above

instrument.

As the industrial applications are increasing slowly, we started quality assurance work specifically on neutron radiography test complying with KOLAS and ISO standards and a process of accreditation to the KOLAS is under way. The usage of image plate and real time analysis technique by image processing are also being developed and applied. In addition to this traditional radiography technique, neutron-induced auto-radiography using solid state nuclear track detectors has also been used internally and externally, such as for boron content and distribution in steel or fission fragments. Feasibility studies on neutron tomography and dynamic two-phase flow started, too.

2.5 Development of Spectrometer components and Plan for next phase Spectrometers

Development of a 1-D & 2-D position-sensitive detector with delay-line readout could be mentioned. As a continued work for last three years, now 1-dimensional position-sensitive neutron and X-ray detectors could be fabricated easily. Several wide vertical aperture 1-D neutron PSD of 200mm H x 100mm V, 120mm x 80mm, and 100mm x 200mm, which are receiving neutrons of relaxed vertical collimation from diffractometers were fabricated and applied for residual stress instrument and fast changing measurement. The results showed quite good and complied with the expectation. We are now discussing PSDs for synchrotron SAXS with Pohang Accelerator Laboratory.

Our design of the polarized neutron spectrometer at the ST1 beam port would have both a triple axis and polarized neutron beam capability in its final shape. This instrument will consist of a conventional monochromator drum which can be rotated from 10°to 60°in 2Θ, a filter, polarizing crystals or a PG(002), analyzers, and spin flippers. CoFe or Heusler crystals or a polarizing mirror will produce polarized neutrons. All the tables of the sample, analyzer, and detector move on the dance floor. We have completed the preparation works such as installation of the monochromator drum and dance floor but major parts of the work for instrument development will be done during next 3 years. This instrument will be used for general test station for spectrometer component test and techniques development, too.

In the second phase from 2000 to 2006, a neutron reflectometer and a triple axis spectrometer, which are strongly requested by external users from universities and industries, are to be realized to extend the activity to surface and interface structure and dynamics studies. A medium resolution powder diffractometer, a dedicated instrument for residual stress measurement, or a double crystal diffractometer complementary to the present SANS is under intense discussion.

3. Users program and activities

In the past before 1996, users of neutron scattering research were scattered around and not

organized. KAERI scientists had been developing instruments and doing research for themselves without any serious connection with external researchers, and the number of universities researchers who could be interested in neutron scattering were very few. But since the time of reactor criticality in 1995, there had been many discussions among the researchers in the institutes and the universities. As a result, the first neutron scattering workshop could be held during June 12-13, 1997, before the commissioning of the HRPD. More than 120 participants attended and many of them became the early users of the HRPD. The 2nd workshop was held during June 11-12, 1998, before the commissioning of FCD, and about 100 participants attended. Some of the early users presented their results in this workshop.

With the increasing number of users, the first winter school focused on graduate school students was organized in February 1999. As a result of many discussions and efforts by the institute and outside users, a peer group of 15 members from universities, institutes and industry was formed in October 1999. It is to accommodate the users' demand and to make a body toward users' group or an association in the future if possible. Based on these activities and the record of experiments on operational instruments, the Ministry of science and technology decided to support the users outside the institute in December 1999 and 18 grants were awarded mostly to the university groups. If this trial program worked successful, we could expect a strong, long-term program, which would boost up the neutron scattering research in Korea.

The 3rd neutron scattering workshop (February 16-17) and 2nd winter school (February 18-19, 2000) were organized jointly by the KAERI, the Korea Advanced Institute of Science and Technology (KAIST) and the Garcia Center at the State University of New York at Stony Brook. The subjects were small angle neutron scattering and reflectometry from soft matter. A one-day tutorials on SANS and reflectometry in the winter school for about 100 graduate students was given by the well-known experts in the field.

This year's workshop by users group will be held mid December and a joint workshop with Synchrotron scattering groups is under discussion. More and more researchers are now visiting the HANARO site and Pohang Synchrotron is also available for them. We, therefore, could hope to make strong scattering research community within a short time. By now most of the experiments have been limited to powder diffraction and single crystal diffraction related fields. Small angle scattering works could be included next year depending on the availability of the instrument and then the users' community would be expanded more rapidly.

JP0250092

1.8 Enhancement of Small Angle Neutron Scattering Facility and Related Activities in Malaysia

Abdul Aziz Bin Mohamed, Abd Jalil Bin Abd Hamid and Shukri Bin Mohd

Malaysian Institute for Nuclear Technology Research (MINT), Complex of PUSPATI, Bangi, 43000, Kajang, Malaysia

Abstract

Materials research, together with traditional scientific interest in understanding matter at the atomic scale, requires detail knowledge of the arrangement and the dynamics of the atoms or molecules. To enhance Malaysian research and development in this area, MINT has continually maintained the existing small angle neutron scattering facility. The scope was focussed on the data acquisition system.

The upgraded Malaysian Small Angle Neutron Scattering (MySANS) data acquisition program that is running on personnel computer (PC) platform has been developed by utilising the Super Video Graphic Array (SVGA) graphical user interface (GUI) environment. It is operating in a real mode under MSDOS operating system. The technique used to expand the 640KB conventional memory (base memory for MSDOS) is called flat real mode where linear 32-bit memory accessing method could be employed.

In addition data analysis and a future work planning are also described.

1. Introduction

This report highlights activities that have been carried out in year of 2000. Two main areas are presented, namely, facility upgrading and data acquisition modification. In addition, the work plans from 2001-2004 are presented.

2. Facility Upgrading

Since the system has already reached its five years old, the repairing and enhancement have become a major agenda in further extend the system lifetime. Two areas are targeted, namely, mechanical and data acquisition systems. The latter area was given more attention.

2.1 Mechanical System

Both primary collimator and flight tube had repaired and upgraded. Some minor modifications were made on neutron beam filter cryostat. The system is installed with a new beam shutter at the collimator front and a new shielding cover for the cryostat and the monochromator.

2.2 Data Acquisition

MySANS is using the RISØ Small Angle Neutron Scattering detector - a multi-wire instrument. It uses the Time to Digital Converter (TDC) to process neutron events by determining the rise time difference for pulses arriving at either side of three multi-wire plane. The results form an address to a location in one of the two histogram memories.

The TDC histogramming memories consist of 3 boards, 2 14-bit 500 MHz counter boards and a Z180 micro-processer board. For the microprocessor board, it makes use of two DMA devices as well as one of the timer circuits. One of the internal DMA is used to transfer data to the host computer using built-in routine. In all other communications with the host computer, programmed input/output transfer is used.

Input/outputs from the TDC to host computer is established via IEEE-488 (GPIB) interface bus connector.

TDC communication program uses DMA to read N bytes form histogram 0 or 1 to the host computer. The TDC communication program is activated by an interrupt from the host computer. The program uses a queue structure to prevent cross interruption between sources.

To transfer data from the DMA counting system, the host computer is also installed a GPIB card. The card is set to use DMA mode for moving data from TDC to the host computer device memory. DMA is a method of allowing data transferring from one location to another in a computer without intervention from the central processing (CPU). A limitation of this mode is that the DMA write must be performed onto conventional PC memory since extended memory that is mapped to upper memory blocks is mapped only for CPU accesses due to the 80386 memory mapping is on chip, not on the motherboard.

In SANS data acquisition, most of the time required in to read data from buffers and then display on the screen in form of 2D or 3D graph presentation. The acquired data are also needed fairly amount of space to store in a storage media. To address the first problem, the new program has utilised the flat real mode technique which allows program to treat one or more segments as large (32 bits) segments. With this technique the entire memory available on the

motherboard (maximum 4 GBytes) can be access without special memory managers in a fast and efficient way. The previous software was using pixel by pixel drawing data from the memory. In the current program, the 2D and 3D PSD data images are displaying by using a double buffer approach. The video card is programmed to get video data directly from the double buffer rather than from it regular address (A000:000h). Since the host computer using SVGA video card the approach chosen works very well. It should be noted that there are many different chipsets used by graphics cards, which would make it very convenient to program them all. The VESA specification of the SVGA graphic cards provides many different pixels resolution and colour. This procedure makes programming the graphic card more manageable since under VESA the graphic memories are handled by the bank switching method. Table 1 shows memories required for various graphic resolution under 256 colour. The MySANS is currently configured to 800x600 resolution under the new program. In term of time required to acquire data from counting and display the 2D and 3D images on the computer screen, the new program needs only 2 seconds compare to the previous method which was 10 seconds. The images displayed are considered real-time displayed as in actual time required for PSD to collect all data and put in the DMA is around 2 seconds.

Table 1: Graphic resolution under VESA specification

No.	Resolution	Colour	Memories allocated (Kbytes)
1	640x400	256	250
2	640x480	256	300
3	800x600	256	469
4	1024x768	256	768
5	1280x1024	256	1,280 (1.28 Mbytes)

For storing 2D and 3D data, the binary (single precision) format is used. The experimental set-up parameters are on the first portion of the file data block followed by the image data.

"Window" style input dialogue and output display has been developed; the displaying of scattered neutron data in two or three-dimensional isometric view - utilised VESA. Graphical User Interface (GUI) fast and user friendly. C programming Language and Assembler Tools are chosen for the upgrading the system software development.

3. Data Analysis

Modelling of scattering intensities which was started in early March 1999 is on going work. The hard sphere

particles model is currently under investigation and application is now on degradation in alloy. Multiple scattering method of analysis is under planning and further literatures survey will be followed.

4. Conclusion

The on-going activities related to SANS in Malaysia 2000 has been presented. Main works on the system improvement had been completed. System is ready to be used for experiment for studying related materials.

MINT's Personnel Involved in SANS for 2000

Researcher	Assistant Researcher
Abdul Aziz Mohamed	Razali Kassim
Azali Muhammad	Abd Jalil Hamid
Mohd Ali Sufi	Mohd Arif Hamzah
Shukri Mohd	Ramzah Mohamed
Ishak Mansur	Mohd Syarif

Summary on 2000 activities

No	Item	Period	Remarks
1	Primary & Secondary tubes, Cryostat maintenance and upgrading.	Jun -Oct	Successfully completed
2	Detection verification, calibration and repairment	Oct - Dec	Waiting for budget and component repair
3	MathCad Programming software - version 2000	Jan	Purchased
4	Request expert from IAEA (Dr. Robert Knott from ANSTO)	Nov (1-2 weeks)	Postponed to 2001 (date to be determined soon)

Year 2001 Tentative Programme		
No	Item	Remarks
1	Discussion and formation small laboratory on SANS sample (i.e. polymer and metallic materials) preparation with MINT polymer and metallurgy groups; target material: carbon glassy for catalyst and bio-material for artificial bones.	Waiting for commitment and budget from the higher authority and related groups support
2	Modelling of metallic alloys using a multiple scattering method.	Required depth literature survey on the subject matters
3	National workshop and training course (with expert assistance from IAEA)	June/July
4	2 IAEA fellowship application forms have been submitted; Australia Dr. Robert Knott, ANSTO and Mr. B. Seong, KAERI.	August/September (1-2 months)

Work Plan for 2002-2004		
Year	Focussed area(s)	Remarks
2002	SANS application in failure analysis	• request for more grants from various available sources; • support from materials study group
2003	SANS application in composite materials	support from local industries
2004	SANS application in advanced materials	support from SIRIM advanced material centre.

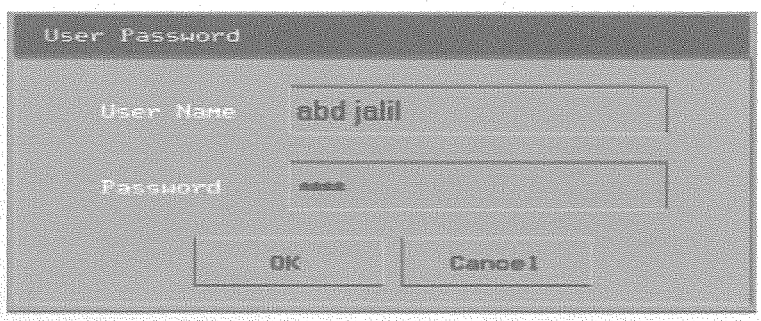

Figure 1: The user name and password scheme employed in MySANS.

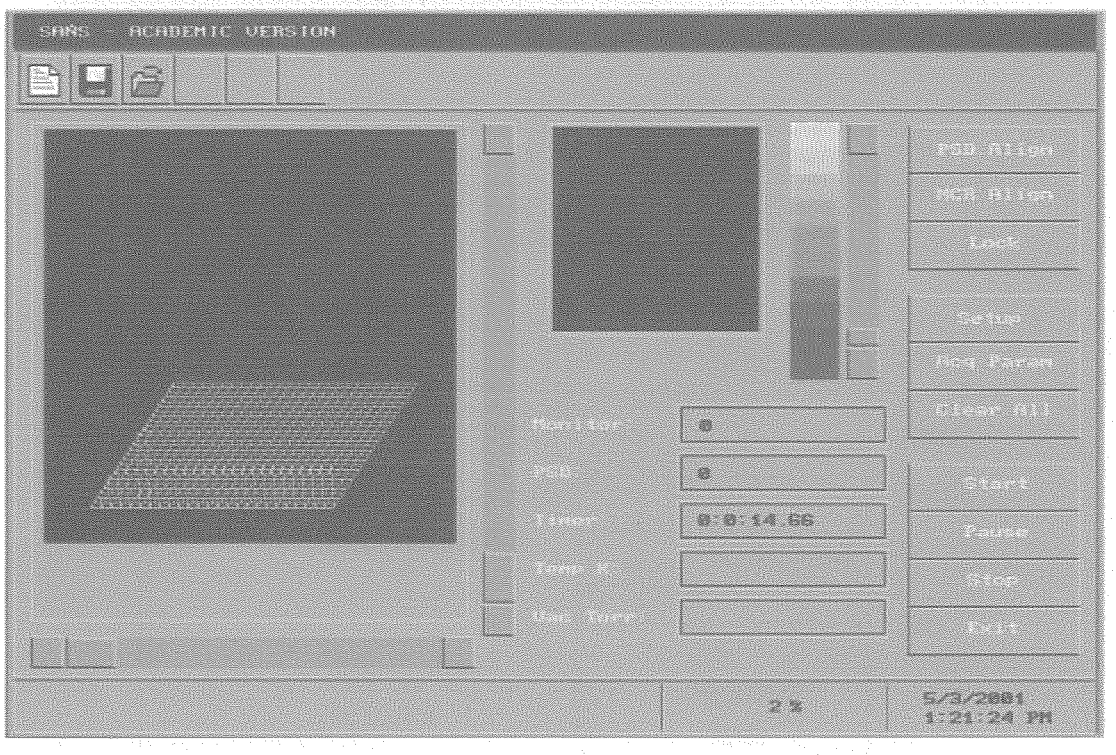

Figure 2: General GUI layout for MySANS.

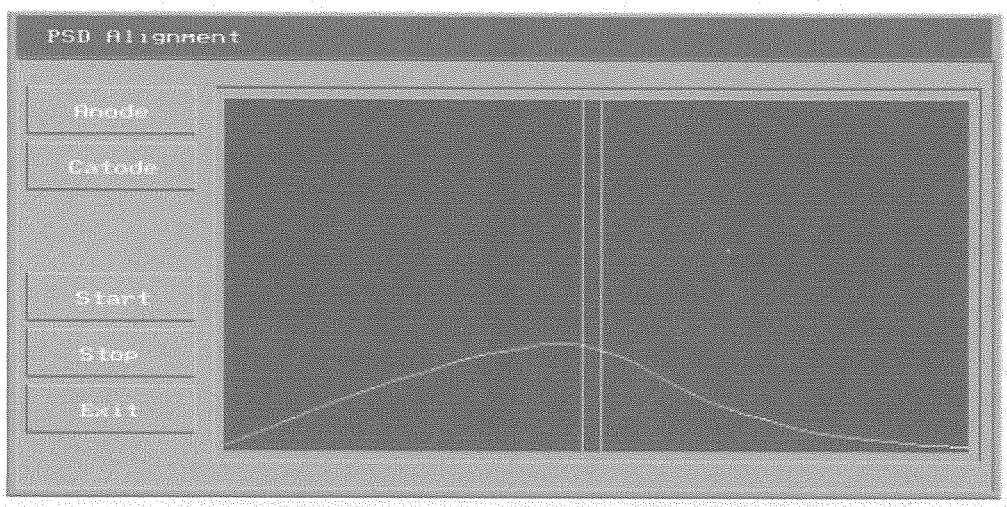

Figure 3: Graphic Presentation for PSD electronic alignment.

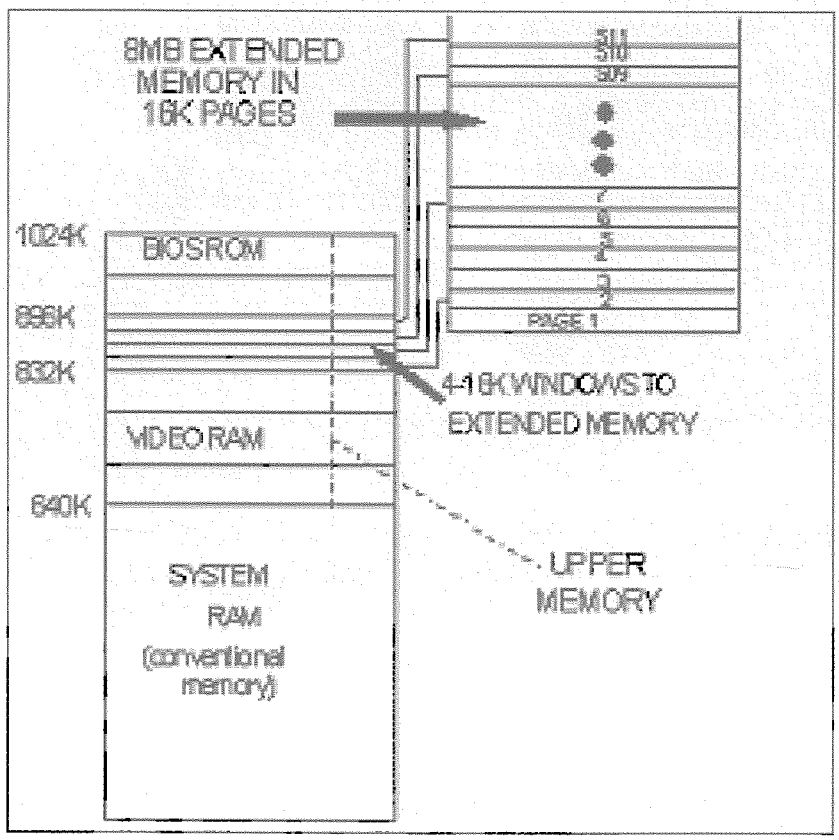

Figure 4: Address and Memory Mapping in MySANS computer interfacing.

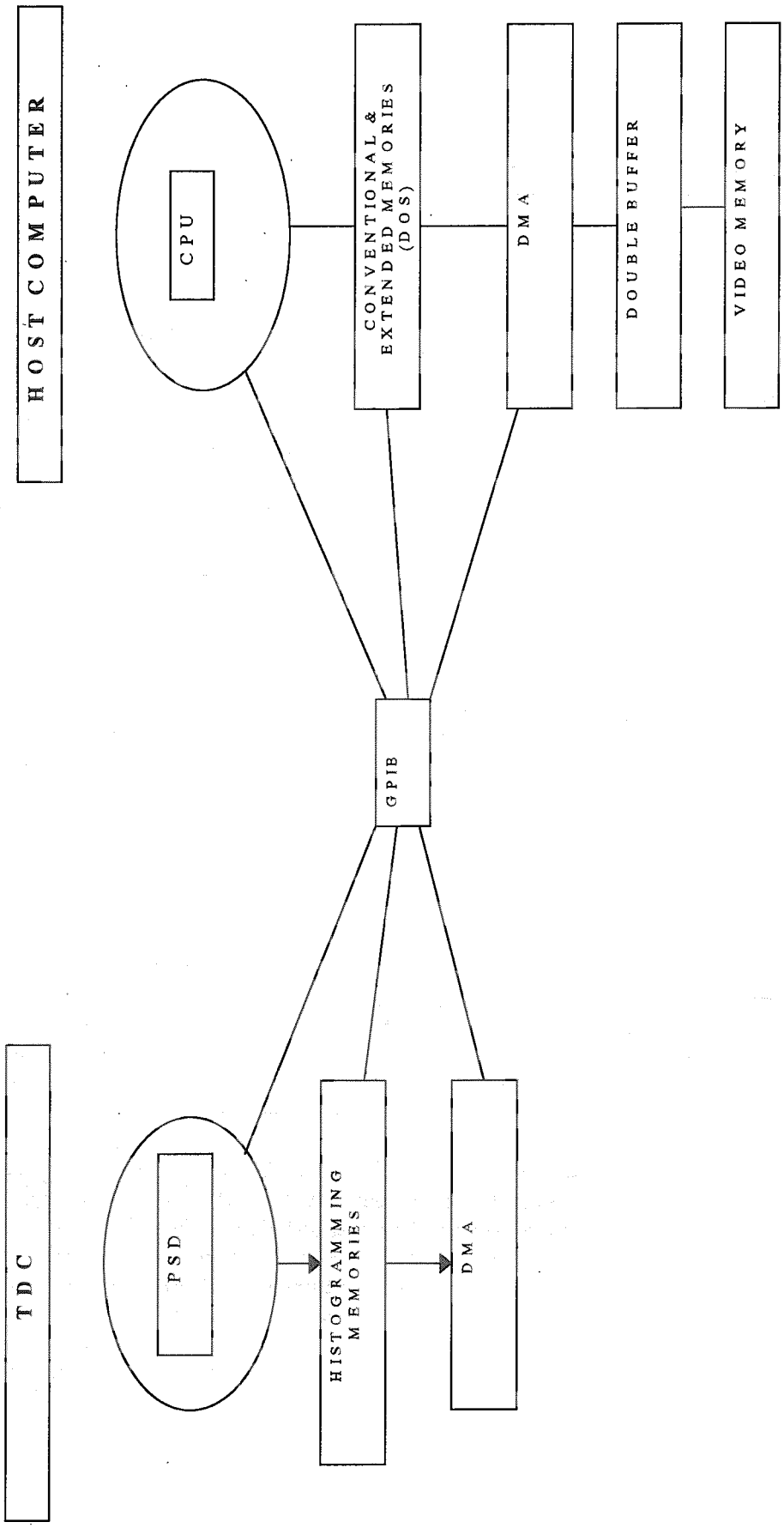

Figure 5. Schematic Diagram Of MySANS Data Communication/Control

JP0250093

1.9 Current Status of Neutron Scattering in Thailand

Archara Sangariyavanich*, Somchai Pongkasem, Suriya Patchar and Pantip Ampornrat

Office of Atomic Energy for Peace
Vibhavadi Rangsit Road, Chatuchak, Bangkok 10900, THAILAND
*e-mail: archara@oaep.go.th ; archaras@yahoo.com

Abstract

The first double-axis neutron spectrometer in Thailand was installed at the Thai Research Reactor (TRR-1) in 1968. It was about a decade that this diffractometer had supported a number of the magnetic materials researches. During 1975-1977, the reactor was modified into a TRIGA MARK III type with nominal power of 2 MW. Meanwhile the diffractometer was dismantled, since then neutron scattering activities had ceased for many years. As the Office of Atomic Energy for Peace recognized the important role of neutron scattering techniques in materials research, therefore in 1992, a spectrometer upgrade program has been setup in order to improve the performance of the obsolete diffractometer. At present, installation and alignment of the diffractometer have been completed. This report gives brief description about the past activities as well as current status of the upgraded diffractometer.

Additionally, the Office of Atomic Energy is in process of establishing a new Nuclear Research Center. Its main facility is a multipurpose 10 MW TRIGA reactor. The reactor will be equipped with a High Resolution Powder Diffractometer. The HRPD is anticipated to be ready for operation soon after the commission of the reactor. Feature of the HRPD including its potential utilization are also presented in this report.

1. Introduction

The Thai Research Reactor TRR1 achieved its first criticality on October 27, 1962. It was a multipurpose 1 MW pool type using plate type HEU fuel. In 1968, the first double-axis neutron spectrometer in Thailand was installed at one of its beam tubes. It was about a decade that this diffractometer had served a number of magnetic materials researches. In 1977, the reactor core was changed into TRIGA MARK III type with nominal power of 2 MW at steady state and pulsing capacity up to 2000 MW. It was designated as TRR-1/M1. At present the reactor is normally operated at 1.2 MW for 3 days a week, about 12 hours a day to meet 40 MW-hours per week as required by radioisotope production.

During the modification of TRR1, the diffractometer was dismantled. Since then neutron scattering activities had ceased for many years. As the Office of Atomic Energy for Peace recognized the important role of neutron scattering technique in broad areas of research particularly in materials science, therefore in 1992, a spectrometer upgrade program has been established. The purpose was to improve the performance of the obsolete existing diffractometer. Implementation of the program included modification of the old monochromator shielding, construction of a new in-pile collimator and a specimen table as well as purchasing a new detection system. At present time, installation of the diffractometer is completed and performance test is being carried on.

2. Description of the Upgraded Neutron Powder Diffractometer

The upgraded diffractometer was aimed to have medium resolution. Optimization of resolution and intensity was conducted through selection of 60° takeoff angle in combination with 30', 30' and 20' for the first, the second and the third collimations, respectively. In order to minimize the background, heavy concrete blocks more than 50 cm. thick were added around the old monochromator shielding. The new detector shielding has been designed to accommodate four He-3 detectors setting at 6° apart. This detector bank was surrounded by a curved fixed-shielding made of 5% borated paraffin. At this moment, because of high background intensity, only a single He-3 detector is in use to provide more room for additional shielding. Automated data acquisition is accomplished by incorporating the motor controller and the counter with a personal computer through the GPIB communication controller system. Detail of the upgraded diffractometer is indicated in Table 1 and its layout is illustrated in Fig. 1.

Table 1 Characteristics of the upgraded neutron diffractometer

Beam size	20 mm.x 100 mm.
First collimation	30'
Second collimation	30'
Third collimation	20'
Monochromator :	
Take-off	59°
Wavelength : Cu(111)	2.0557 Å
PG(004)	1.6524 Å
Neutron detectors	4 x He-3 (4 atm.)
Neutron source to monochromator	400 cm.
Monochromator to specimen	180 cm.
Specimen to detector	70 cm.
Thermal neutron flux at specimen position	2 x 10^4 n.cm^{-2}.sec^{-1}

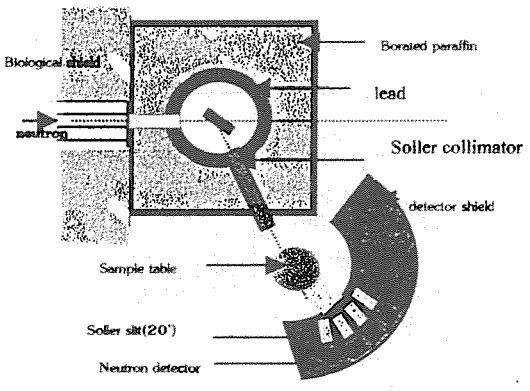

Fig. 1 Layout of the upgraded neutron powder diffractometer

3. Diffractometer Performance

Performance test has been carried out by running a standard silicon powder (NIST Standard Reference Material 640b)and a high purity corundum powder samples (99.999% Al_2O_3, Aldrich Chemical Company) on the diffractometer. The silicon sample was contained in small vanadium tubes, 10 mm. in diameter and 50 mm. high. In an attempt to gain higher peak intensity, the sample size of corundum was increased to 13 mm. in diameter and 60 mm high. Data were collected from 8° to 105° with 2° step size. The counting time was 5 minutes per step. A 75mm.x75 mm.x1 mm. pyrolytic graphite monochromator was employed to provide thermal neutron flux greater than 2 x 10^4 $n.cm^{-2}.sec^{-1}$ at the sample position.

The recorded data were refined by Rietveld method. The Voigt profile function was assigned to fit the diffraction peak shapes. Since examination of the diffraction patterns from silicon and corundum samples revealed severe contamination from 2λ , 2/3λ and ½λ, thus in the refinement both samples were treated as four-phase compounds. It was found that data obtained beyond 100° were ambiguous, therefore they were not taken into account in the analysis. The wavelength using in the refinement was 1.6537 Å

4. Results of Analysis from Silicon and Corundum Diffraction Pattern

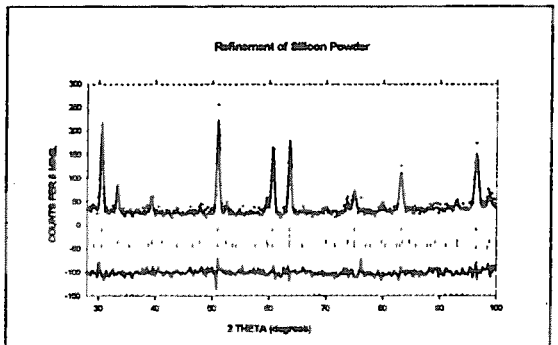

Fig.2 Rietveld refinement of silicon powder sample showing contamination from higher order beams.

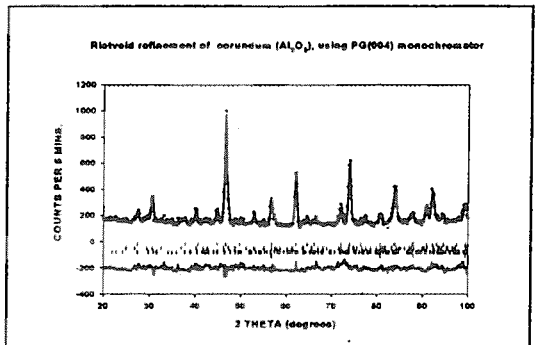

Fig.3 Rietveld refinement of corundum showing contamination from higher order beams.

Table 2 Results of Rietveld Analysis of silicon and corundum samples, data from OAEP ND

Parameters	Silicon				Corundum			
	λ	2λ	2/3λ	1/2λ	λ	2λ	2/3λ	1/2λ
Scale factor	0.32(1)	0.96(8)	0.035(3)	0.003(1)	0.165(3)	0.41(11)	0.019(3)	.0001(0)
Scale factor ratio	1	2.94	0.11	.009	1	2.48	0.11	.006
Cell dimension(Å)	a=5.4300(4)				a=4.759(2) c=12.997(3)			
R_B (%)	2.34	0.91	6.85	7.28	3.45	2.93	3.42	4.73
R_p (%)	13.07				7.60			
R_{wp} (%)	16.91				9.52			
R_{exp} (%)	15.28				7.14			
GOF (%)	1.22				1.78			
U	.4986				0.8712			
V	-.2034				-0.9201			
W	.2957				0.5069			

Fig.2 indicates the results of Rietveld refinement from silicon powder diffraction pattern. The resulting reliability factors shown in Table 2 imply that the observed data do not fit well the calculated values. Nevertheless, its observed cell dimension which is a=5.4300(4) Å agrees closely with the expecting 5.4309Å.

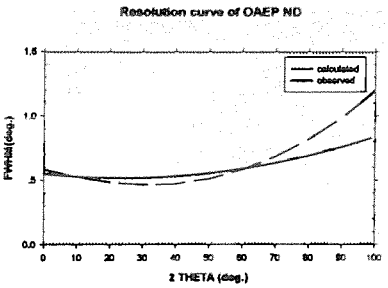

Fig.4 Comparison of the observed and calculated peak widths

The peak widths of silicon derived from the Rietveld analysis were plotted in comparison with the calculated values as indicated in Fig.4. It is obvious that the observed and calculated peak resolutions are consistent for scattering angles below (2θ) 65°. At higher angles, the observed peaks widths are comparable small.

Results of Rietveld refinement from corundum diffraction data are shown in Fig.3 and Table2. Although more than three hundred peaks produced from 2λ , 2/3λ and ½λ. are observed, there is a good agreement between the observed and calculated profiles. The reliability factors obtained from the analysis are included in Table2.

5. Future development of ND and its applications

From the scale factor ratio of the contaminants λ:2λ:2/3λ:½λ. indicated in Table2, interference from the half lamda was less than 1% and could be neglected. Contribution from 2λ was more than 250% but could be reduced by using small unit cell sample. It seemed that contribution from 2/3λ which was about 10% had significant effect on the analytical results particularly on the reliability factors.

Besides the interference from the higher order beams, other significant problems are due to low neutron intensity and high background. It is noted that the peak to background ratio were about 9 at peak(111) of silicon and 7 at peak (113) of corundum.

To improve the neutron intensity at specimen position, the existing monochromator may be replaced with a vertical focusing or a bent focusing crystals. The data acquisition rate could be enhanced by adding more detectors. Meanwhile, better shielding for detectors is needed. Alternatively, the diffractometer could be modified to serve residual stress measurement, which requires smaller data range. However, at the present time the facility could be employed for investigation of small unit cell samples and training university students in the field of neutron scattering.

6. High Resolution Powder Diffractometer at the Ongkharak Nuclear Research Center

The Office of Atomic Energy for Peace is presently in process of constructing a 10 MW TRIGA nuclear research reactor at the Ongkharak Nuclear Research Center (ONRC) site which is about 60 km. from Bangkok. The reactor is a multipurpose, pool type, cooled and moderated by light water using low enriched uranium fuel. Reflectors are heavy water and beryllium. The expecting maximum thermal neutron flux is $2x10^{14}$ $n.cm^{-2}.sec^{-1}$. Six horizontal beam tubes are available for beam experiment, four of them are allocated for experiments in neutron scattering, neutron radiography, prompt gamma neutron activation

analysis and BNCT. The rest are reserved for the future neutron guide tube and unforeseen experiment. Configuration of the reactor core is illustrated in Fig. 5 [1]. Provision of a High Resolution Powder Diffractometer has also been included as part of the ONRC project contract. Installation of the HRPD shall be completed before the commission of the reactor.

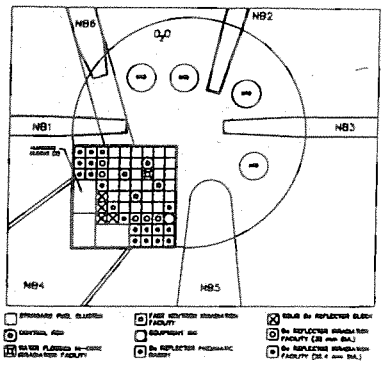

Fig.5 Configuration of the reactor core at ONRC

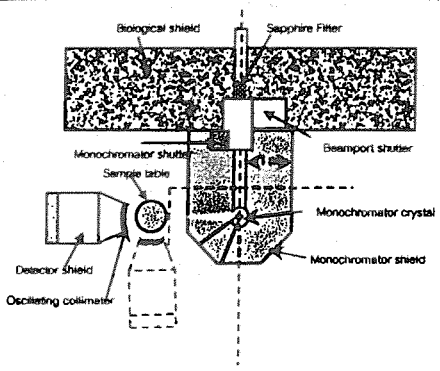

Fig.6 Layout of the HRPD at ONRC

Layout of the HRPD at ONRC is shown in Fig.6. The design basis of the proposed HRPD involves the matching of a bent focusing monochromator, small sample and position sensitive detector[2]. No collimators are required in this system. The monochromator is a doubly focusing bent silicon perfect crystal, which is at 95° takeoff, could be adjusted to provide four wavelengths, that is 2.41 Å, 1.84 Å, 1.54 Å and 1.22 Å, from diffraction planes (311), (331), (511) and (533) respectively. To achieve high peak resolution, the sample diameter needs to be less than 3 mm. The detector bank is consisted of 7 He-3 position sensitive detectors assembled together with 20° horizontal and 6.27° vertical spanning at 160 cm. distance. The detector electronics provide position resolution better than 3 mm. An oscillation collimator is positioned between the sample and the detector bank to reduce background from the environment. The monochromator shielding is designed to provide takeoff angles at 95°, 60 ° and 30°.

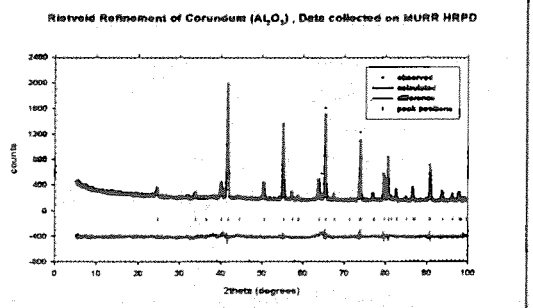

Fig.7 Rietveld refinement of alumina sample showing good agreement between the observed and calculated profiles.

Performance of the proposed facility has been investigated by measuring the diffraction pattern of a standard alumina (Al_2O_3) sample with the High Resolution Neutron Powder Diffractometer at the Missouri University Research Reactor, which is a similar type diffractometer. It took several hours to collect more than 2000 counts at peak (113) of alumina with the peak to background ratio of 10. The result of Rietveld refinement, which is illustrated in Fig.7 shows good agreement between the observed and calculated profiles. The unit cell parameters obtained from the analysis were a= 4.7589(4) Å, c=12.9941(7) Å with the reliability factors R_{wp} = 6.89%, R_{exp} = 6.36%, R_B=1.56% and Goodness of Fit =1.17%.

The High Resolution Powder Diffractometer at the ONRC site would be dedicated for broad range research areas. Potential applications would be in the area of advanced materials research e.g. high temperature superconducting materials, PZT, magnetic materials, structural transitions and training.

7. Neutron Scattering Research Program

At present, our Nuclear Material Science Group has a national joint research project on gemstone enhancement with the Department of Physics of Kasetsart University and the Department of Mineral Resources. We are taking parts in gemstone characterization and coloration by irradiation. Two collaborative projects with Mahidol university in the investigation on the atomic positions in RE-doped PZT and the study of the morphology of elastomer under strain are being planned.

Besides the above projects, an international research program on the investigation of high temperature superconductors is being proceeded in collaboration with BATAN, Indonesia and Vietnam.

Acknowledgement

We would like to extend our sincere gratitude to the late R.L. Davis (ANSTO) for his effort to design the in-pile collimator for our ND and for his kind supervision on our neutron spectrometer upgrade program. We are in debt to N. Minakawa (JAERI) for his strong encouragement and support, without him substantial improvement in the performance of our existing neutron diffractometer would never be achieved. We are grateful to the IAEA and JAERI for their continuous support and funding. Special thanks are given to the OAEP Physics Division, Mechanical Workshop and the Reactor Operation Division staffs for their kind contribution in the spectrometer installation.

References

1. A. Sangariyavanich, Proceedings of the 1997 Workshop on the Utilization of Research Reactors, November 6-13, 1997, Bandung, Indonesia.
2. W.B. Yelon, B. Berliner and M. Popovici, **Physica**, **B241-243**, 237-239 (1998).

JP0250094

1.10 Progress Report on the Preparation of Co Substitution for Cu in BSCCO(2223) Superconductor

Archara Sangariyavanich and Pantip Ampornrat
Nuclear Material Sciences Group, Physics Division
Office of Atomic Energy for Peace
16 Vibhavadi-Rangsit Road, Chatuchak, Bangkok 10900, THAILAND
Tel: (66-2) 562-0119; Fax: (66-2) 562-0118
e-mail: archara@oaep.go.th, archaras@yahoo.com

ABSTRACT

The samples of $Bi_2Sr_2Ca_2(Cu_{(1-x)}Co_x)_3O_y$ when x = 0.0, 0.01, 0.02, 0.04, 0.06, and 0.08 were prepared by solid state reaction. Samples were sintered between 828-853℃ and then quenched in liquid nitrogen. Physical properties of the specimens were examined by standard four-probe technique to determine the critical temperatures. Phase identifications were performed by using X-ray diffraction technique. It was found that at a certain sintering temperature, increasing the amount of cobalt impurities suppressed the critical temperatures. This result agrees with that has been reported by Youwen Xu[1].

Introduction

As agreed in 1999 Workshop on the Utilization of Research Reactor, the Joint Research Project on high temperature superconductor would be continued on the investigation of Co substitution for Cu in BSCCO (2223). A. Santoro[2] has proposed a models for oxygen ordering in $Ba_2YCu_3O_x$ and $Ba_2YCu_{3-y}M_yO_x$. In his model, substitution of copper by impurity metal atoms involved the rearrange of oxygen atoms in the basal plane, which was associated with a change in stoichiometry.

In this experiment, effect of cobalt substitution on the superconductivity properties of $Bi_2Sr_2Ca_2(Cu_{(1-x)}Co_x)_3O_y$ was studied.

Experimental

Samples of $Bi_2Sr_2Ca_2(Cu_{(1-x)}Co_x)_3O_y$ when x = 0.0, 0.01, 0.02, 0.04, 0.06, and 0.08 were synthesized by solid state reaction. The nominal compositions of high-purity grade chemicals (99-99.99%) were mixed together in an agate mortar and ground for 8-10 hours. The mixture was calcined at 720 °C for 24 hours, then ground again for 4 hours and pressed to form pellets with 1.3 mm in diameter and 2 mm thick. The pellets were sintered at 828°C - 853°C for 65 hours in normal atmosphere. The synthesized conditions are shown in Table1. At the end of the sintering process, each specimen was subsequently quenched in liquid nitrogen.

Superconducting transition temperature of the sintered samples was investigated by using standard four-probe technique and the electrical resistivity as a function of temperature was determined. X-ray diffraction technique was employed for phase identification.

Table 1 Synthesized conditions of $Bi_2Sr_2Ca_2(Cu_{(1-x)}Co_x)_3O_y$.

Sample	Co-doped (x)	Cu : Co	Calcine Temp (°C)	Pressure (ton)	Sinter Temp (°C)
#6A/1	0.0	3 : 0	720	1	828 ± 2
#6A/2	0.0			1	840 ± 2
#7A/1	0.01			1	837 ± 2
#7A/2	0.01	2.97 : 0.03	718	1	837 ± 2
#7A/3	0.01			1	844 ± 2
#8A/1	0.02			1	841 ± 2
#8A/2	0.02	2.94 : 0.06	718	1	838 ± 1
#8A/3	0.02			3	842 ± 1
#9A/1	0.04			1	853 ± 3
#9A/2	0.04	2.88 : 0.12	717	1	848 ± 2
#9A/3	0.04			3	850 ± 3
#10A/1	0.06			1	850 ± 2
#10A/2	0.06	2.82 : 0.18	720	1	841 ± 1
#10A/3	0.06			3	843 ± 1
#11A/1	0.08			1	843 ± 1
#11A/2	0.08	2.76 : 0.24	720	1	841 ± 1
#11A/3	0.08			3	846 ± 1

Result and Discussion

The result in Table 2 shows that the appropriate calcining temperature is 720°C for 24 hours, while sintering temperature is around 840°C for 65 hours.

The electrical resistivity property was examined by four-probe technique. The results are indicated in Table 2. It is found that the superconducting transition temperatures diminish with the increasing amount of cobalt and could not be observed at x >0.02. Figure 1 shows sharp superconducting transitions of the undoped samples while Co-doped samples have larger transition widths.

X-ray powder diffraction was used for phase identification. The pattern showed that the 2212, 2223 and 2234 phases were formed in samples. Table 3 shows phase identification by XRD. The highest amount is 2212 phase, 2223 phase and 2234 phase, respectively. These results do not relate to the superconductivity behavior that obtained by resistivity measurement. Therefore, the high resolution neutron diffraction measurement should be done in order to investigate these effects.

Table 2 Superconducting transition temperatures of the samples.

Sample	Co-doped (x)	Electrical Property	T_c (K)	$T_{c,on\ set}$ (k)
#6A/1	0.0	Superconductor	109	114
#6A/2	0.0	Superconductor	98	114
#7A/1	0.01	Conductor	-	
#7A/2	0.01	Superconductor	87	109
#7A/3	0.01	Conductor	-	-
#8A/1	0.02	Conductor	-	-
#8A/2	0.02	Conductor	-	-
#8A/3	0.02	Superconductor	99	121
#9A/1	0.04	NS	-	-
#9A/2	0.04	Conductor	-	-
#9A/3	0.04	NS	-	-
#10A/1	0.06	NS	-	-
#10A/2	0.06	Conductor	-	-
#10A/3	0.06	NS	-	-
#11A/1	0.08	Conductor	-	-
#11A/2	0.08	NS	-	-
#11A/3	0.08	NS	-	-

*NS – Non Superconductor

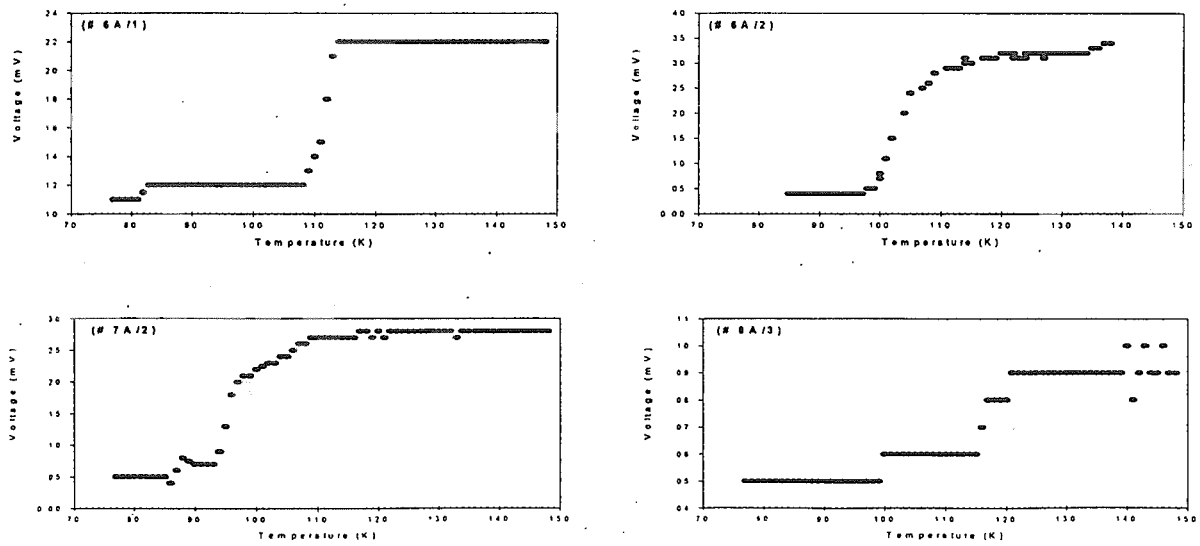

Figure 1 Resistivity curve of samples #6A/1, #6A/2, #7A/2 and #8A/3

Table 3 Phase identification obtained by X-ray diffraction.

Sample	Co-doped (x)	Resistivity result	Phase identification		
			2212	2223	2234
#6A/1	0	Superconductor	1	2	-
#6A/2	0	Superconductor	1	-	-
#7A/1	0.01	Conductor	1	2	-
#7A/2	0.01	Superconductor	1	2	-
#7A/3	0.01	Conductor	1	2	-
#8A/1	0.02	Conductor	1	2	-
#8A/2	0.02	Conductor	1	-	-
#8A/3	0.02	Superconductor	1	2	-
#9A/1	0.04	NS	1	2	-
#9A/2	0.04	Conductor	1	2	-
#9A/3	0.04	NS	2	1	-
#10A/1	0.06	NS	1	2	3
#10A/2	0.06	Conductor	1	2	-
#10A/3	0.06	NS	1	2	-
#11A/1	0.08	Conductor	1	2	3
#11A/2	0.08	NS	1	2	3
#11A/3	0.08	NS	1	2	-

Note 1 : major phase
2 : minor (1) phase
3 : minor (2) phase

Conclusion and Future Plan

From the experimental, 840°C is the best condition in synthesizing the studied samples. The Co-doped BSCCO (2223) samples showed the superconductivity behavior when x = 0, 0.01 and 0.02. Increasing the amount of Co-doped resulted in decreasing the superconductivity property of samples. These effects were clearly shown by the electrical resistivity measurement. X-ray diffraction pattern, nevertheless, could not indicate phase different of a superconductor sample from the other.

The future plan for high Tc superconductor research is to synthesize the bulk samples for high resolution neutron diffraction measurement. Preparation of Sb-doped Pb-BSCCO

specimens which was a Joint research project agreed in 1998 Workshop will be carried on.[3] While investigation of Co-doped BSCCO (2223) will still be an ongoing project.

References

1. Y.Xu. et al. Ibid. pp. 221-224.
2. A.Santoro. Material Research Society Symposium Proceedings,**V 169**, Material Research Society, Pittsburgh, Pensylvania (1990) pp. 185-188.
3. P. Ampornrat and A. Sangariyavanich. Proceedings of the 1998 Workshop on the Utilization of Research Reactors, (1999).

JP0250095

1.11 HIGH TEMPERATURE SUPERCONDUCTORS OF Pb AND Sb DOPED Bi-Sr-Ca-Cu-O SYSTEM

Tran Thi Thu Phuong, Tran Kim Cuong, Nguyen Thi Cam Phuong
Nuclear Physics Department
Dalat Nuclear Research Institute
01, Nguyen Tu Luc, Dalat, Vietnam
Tel. 84 63 829436, Fax. 84 63 821107
Email: luonghoan@fpt.vn

ABSTRACT. From 1996, Dalat Nuclear Research Institute has been participated in the Regional Program with taking of studying " The mechanism of Pb and Sb doping role on superconductivity of 2223 phase of BSCCO system". To achieve this aim, following reports about just Sb or Pb doped Bi-Sr-Ca-Cu-O system (BSCCO system), we investigate a mixing doping Pb+Sb. In fact, we investigated $Bi_{2-x-y}Pb_xSb_ySr_2Ca_2Cu_3O_z$ samples with x ranged from 0.1 to 0.8 and y from 0.1 to 0.4. After processing those samples were measured the resitivity depending on temperature with the four probe technique and studied the phase properties carefully by using X ray diffractometor SIEMENS D5000. Distinguishing with the BSSCCO and BPSCCO samples, there was a new phase in the XRD patterns of the BPSSCCO ones, called 4441, and T_c^{on} attained approximately 140K. Unfortunately, we are unable to determine neutron scattering data from these samples.

Key words. *High temperature superconductor (HTS); Bi-Sr-Ca-Cu-O system (BSCCO); Pb doped Bi-Sr-Ca-Cu-O system (BPSCCO); Sb doped Bi-Sr-Ca-Cu-O system (BSSCCO); X Ray diffraction(XRD); XRD pattern; resitivity dependent temperatute (R-T) characteristic, critical temperature or zero resistance temperature (T_c^o), onset transformation temperature (T_c^{on}), new phase.*

1.Introduction

The doped Pb or Sb BSCCO high temperature superconductive system have a T_c^o of more than 100K [1], [17]. The phase with the highest temperature for this system is $Bi_2Sr_2Ca_2Cu_3O_{10}$ (2223) with T_c = 110K. There were also a few reports [9-16] on the partial substitution of Bi by Sb and Pb simultaneously. Different techniques such as the conventional solid state diffusion reaction [9, 10, 15, 16], melt quenching [11], coprecipitation [12], planar flow casting [13], and the matrix reaction method [14] were adopted for synthesis. Irrespective of the different proportions of Pb and Sb the resultant material was a multi-phase system. However, the values of T_c^{on} and T_c^o were observed to vary to a large extent (between 50K and 132K) [18]. Though addition of Sb along with Pb in Bi systems seems to increase the formation of the high temperature phase or the formation of a 'new phase', there

are many questions that remain unanswered. The role of Sb in high superconductivity, the effect of the presence of the 'new phase' on the superconducting behavior of the Bi-Pb system and the nature of the 'new phase' — superconducting or not, still remain unclear and futher investigations were thought to be necessary. With the hope obtaining answers to these questions, even if only partial ones, systematic investigations of a system 2223 as the starting composition with addition of Sb and Pb, synthesized via the solid state diffusion reaction were carried out. The resulting material was characterized via XRD and temperature dependent resistance studies for various duration of sintering. The effect of heating temperature has been studied. The detailed analysis of these investigations is presented in this report.

2.Experimental procedure

The samples were prepared by the conventional solid state reaction of Bi_2O_3, PbO, Sb_2O_3, $CaCO_3$, CuO, $SrCO_3$ of high purity, in air. The investigating composition was $Bi_{2-x-y}Pb_xSb_ySr_2Ca_2Cu_3O_z$ with x ranged from 0.1 to 0.8 and y from 0.1 to 0.4. There were two steps in the material processing. In the first step, the mixture were calcined at 820°C - 825°C for 24h in open funace and repeat this step. In the final phase, this mixture were sintered at 840-850°C for 100 - 135 h and repeat. The resultant material were cooled in furnace.

Resistance was measured as a function of temperature using the standard four probe technique. Electronical contacts were made by using an air drying silver paste. Temperature was monitored by using a Cooper-Constantan thermocouple. X-ray diffraction analysis was performed by using a SIEMENS D5000 diffractometer with Cu K radiation.

3.Results and discussion

3.1Resistance □ Temperature (R-T) characteristics

In general, the R-T characteristics were observed to depend strongly on the sintering period, with the best superconducting characteristics observed for 100h of sintering.

Samples with Sb = 0.1 and 0.2 and Pb = 0.4 and 0.5 had T_c^{on} vary from 90-105K and $(T_c^{\circ})_{max}$ approximately 90K. The others were semiconductor.

Samples with Sb = 0.3, only $Bi_{1.6}Pb_{0.1}Sb_{0.3}Sr_2Ca_2Cu_3O_z$ had T_c^{on} = 140K and T_c° = 130K(it can be seen in figure 1 and 2). In contrast, if Sb = 0.4, irrespective of the different proportions of Pb, semiconducting behavior was exhibited (it can be seen in table 1).

3.2 X ray diffraction (XRD) investigation

From R-T characteristic studies it was thus quite clear that after an optimum heating time the superconducting characteristics of the resulting material reverted back from a broad single

Table I : Typical Samples

Composition of Samples	Sintering Temperature (°C)	Sintering time (h)	T_c^{on} (K)	T_c° (K)	Behavior in R-T characteristics	Main phases in XRD patterns
Sb =0.1 Pb=0.4& 0.5	820-845	24 - 96	90-105	90	Superconducting	2212 2223
Sb =0.2 Pb=0.4& 0.5	820-845	24 - 96	90-105	90	Superconducting	2212 2223
Sb=0.3 Pb=0.1	825-850	100	140	130	Superconducting	4441 CuO
Sb=0.4	825-850	100-130	—	—	Semiconducting	—

transition to 2-step transitions with distinct decreased in both T_c^{on} and T_c° values. Our XRD investigations also supported these observations as can seen in the following part of this section. It also revealed the development and transition of different phases during the process of heating.

In XRD of the system (Sb=0.3 and Pb=0.1) under consideration it has been observed that irrespective of the sintering or calcine there existed always a cluster of sharp and intense peaks around 2 =30° and a few others that were never obtained earlier in undoped Sb or Pb BSCCO system. The most surprising and interesting observation was the presence of these peaks in XRD pattern of a pellet just calcined at 820° C for 24h.

The position and intensities of all these peaks match with those reported by Tingzhu et al [16] and Agnihotry et al [18]. These authors have attributed these peaks to a 'new phase' belonging to the monoclinic system and identified as $Bi_3Sb_{0.8}Pb_{0.2}Sr_{4.1}Ca_{3.9}CuO_{15}$ represented as 4441.

Our XRD studies also made it evident that there was an optimum sintering time of 100h and calcining time of 25h, when the best superconducting behavior was exhibited. However, exceeding this time may lead to deterioration of the superconducting characteristics.

The most interesting figure to note was the optimum T_c° = 130K, which was comparable to that of only Sb or Pb doped Bi-systems, and T_c^{on} =140K which was much higher. The unusual high value of T_c^{on} can be correlated with the presence of the 'new phase' that has appeared due to doping Sb.

4. Conclusion

Our combined R-T and XRD studies proved that the partial substitution of Bi by Pb+Sb and an appropriate thermal treatment leaded to a material with an unusual high value of T_c^{on} =

140K never achievable in Pb or Sb substituted Bi systems. The important role of Sb seems to be in forming the so-called 'new phase' (4441) from calcination step to the final sintering step, and accelerating the formation of the high temperature phase.

Acknowledgements

The authors are thankful to Director of the Institute ,Dr. Nguyen Nhi Dien, and Vice Director of the Vietnamese Atomic Energy Agency, Dr. Vuong Huu Tan for his keen interest and encouragement. The authors would like to acknowledge the Science and Technology Agency of Japan (STA) and Ministry of Science and Technology (MOST) of Korea who supported for organization of the Workshop.

References

1.Maeda H. et al, 1988 Japan J.Appl. Phys. 27 L209
2.Sunshine S.A. et al 1988 Phys. Rev. B38 893
3.Green S.M. et al. 1988 phys. Rev. B 38 5061
4.Takano M. et al 1988 Japan. J. Appl. Phys. 27 L104
5.Chandra S. et al (communicated to Phys. Status Solidi)
6.Ramesh R. et al 1988 Appl. Phys. Lett. 53 1759
7.Liu H.B et al 1988 physica C 156 804
8.Chandrahood M.R. et al 1989 appl Phys. Lett. 55 1472
9.Hongbao L. et al 1988 Solid State Commun. 69 867
10.Dou S. X. et al 1989 Physica C 158 97
11.Komatsu T. et al 1989 Japan. J.Appl. Phys. 28 L 1159
12.Spencer N.D. et al 1989 Japan. J. Appl. Phys. 28 L1564
13.Luo J.S. et al 1989 . Appl. Phys. Lett.55 1448
14.Sastri P.V. et al 1989 Solid State Commun.71 935
15.Pissas H . et al 1989 Physica C 159 643
16.Tingzhu C. et al 1990 Supercond. Sci. Technol. 3 87
17.Nguyen Thi Kieu Oanh et al 1995, Master Thesis, The Pb doped BSCCO system
18.Agnihotry S.A. et al 1991 Supercond. Sci. Technol. 4 7-12

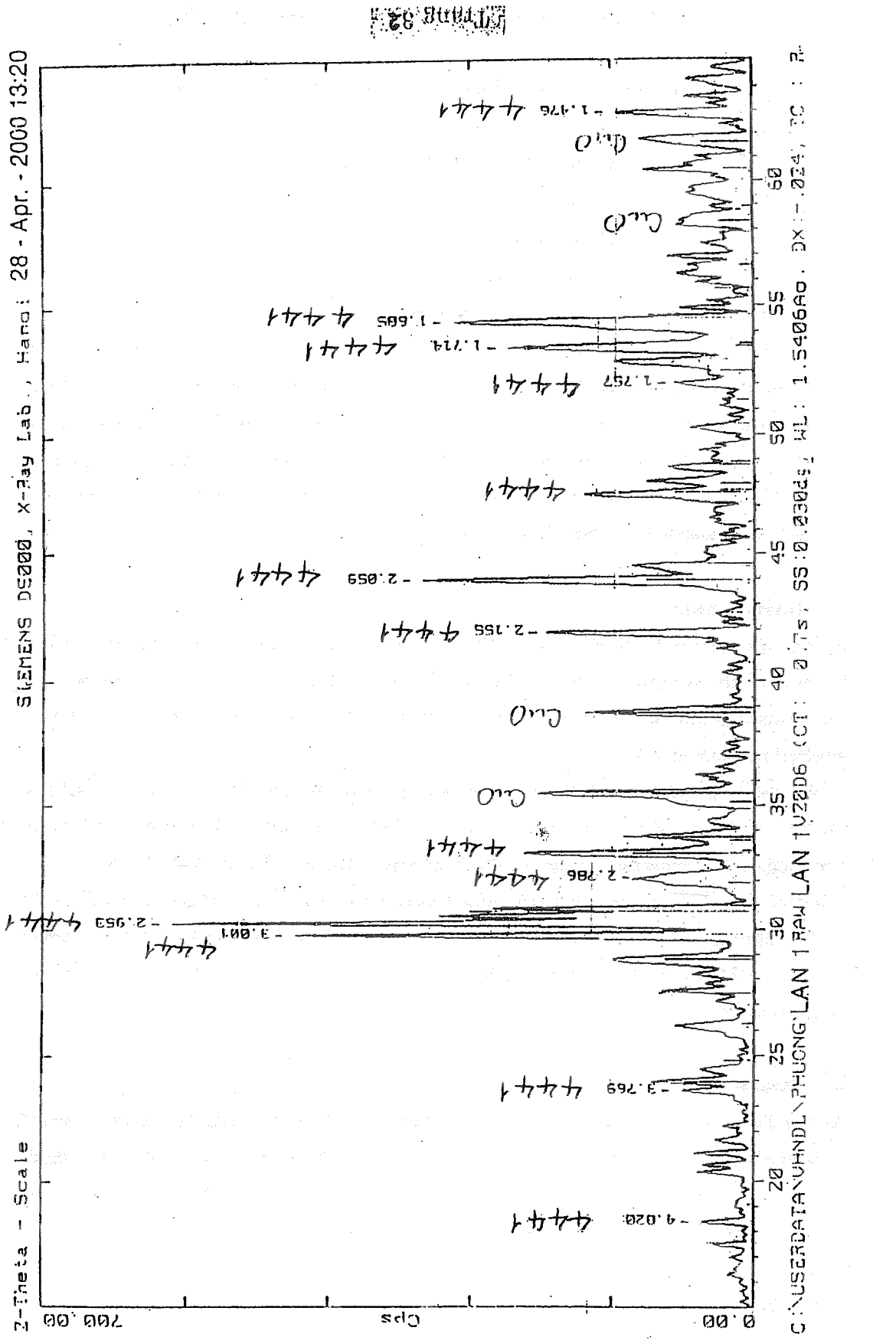
SIEMENS D5000, X-Ray Lab., Hanoi 28 - Apr. - 2000 13:20
Z-Theta - Scale
Cps
700.00
0.00
20
25
30
35
40
45
50
55
60
4.020
3.769
3.001
2.953
2.786
2.155
2.059
1.757
1.714
1.685
1.476
4441
CuO

JP0250096

1.12 Residual Stress Analysis by Neutron Scattering

[1]Nobuaki.Minakawa, [2]Atushi. Moriai, [2]Akitoshi.Ohtomo
[1]Research Group for Neutron Scattering,
Advanced Science Research Center, JAERI
[2]Research Reactor Utilization Division,
Department of Research Reactor, JAERI
Tokai –Mura, Naka-Gun, Ibaraki, Japan 319-1195

Abstract

The structure material of the sample can understand a neutron diffraction measurement, and it can know the structure. The property of material can be known from as a result. A strain measurement is a kind of measurement of physics, and change of a spacing of lattice planes is a strain. It is also highly precise spacing of lattice planes measurement technique. A strain is convertible into a stress with a Hooke's law. Getting to know the strain distribution in material can guess the strength of material, fatigue condition, a life, etc.

1. Introduction

By the measurement of internal residual stress for the material, it is possible to do the lifetime of the structure material, the development of new materials, the safe securing of the structures and so on. It has only a neutron diffraction method that can measure the internal residual stress.

We made a sample for the residual stress measurement by the neutron diffraction method, which is planned from 2002 in this "WS on the utilization of research reactors" and began the manufacturing of the standard sample. We do like to report for the standard shrink-fit sample was manufactured which used an aluminum material A6063 as for sample of the residual stress by the thermal expansion. As for this sample, to measure with the neutron diffractometer in every country, we will introduce the way of measurement.

2. Design

As for the sample to measure with the practice of WS and that the neutron scattering equipment in every country, the sample measurement evaluation can do easily is desirable. Therefore, we manufactured shrink-fit sample, which is easily of the computation of the occurrence stress and it is possible to measure by installing in the sample table directly.

For the inner stress be able to measured even if the incident monochromatic neutron

beam flux was weak, it was necessary to choose material with small neutron absorption coefficient(μ) and we chose an aluminum material. The neutron absorption coefficient of aluminum about the neutron wavelength of 0.2 nm is 0.012. As for the aluminum material, the age hardening chose done A6063 and A7075 of heat-treatment-type alloy in the precipitation process in the Mg-Si layer. This time, we manufactured a sample using A6063. The characteristic of mechanical properties and the chemical composition of A6063 are shown in table 1.

The shrink fit sample is considered neutron attenuates and a manufacturing size is

The chemical composition (mass%)							
Si	Fe	Cu	Mn	Mg	Zn	Cr	Ti
0.2 ～ 0.6	≦ 0.35	≦ 0.10	≦ 0.10	0.45 ～ 0.9	≦ 0.10	≦ 0.10	≦ 0.10

The mechanical properties			
quality	The tensile strength (MPa)	0.2% proof stress	elongation(%)
T6	≧206	≧177	≧8

Table-1 Chemical composition and mechanical properties of A6063

composed of outside diameter 50mm ϕ, 50 mm height, ring with caliber 25mm ϕ and plug. In order to make shrink fit samples the plug is cooled in the liquid nitrogen and the shrunk plug is inserted into the ring immediately. The internal pressure, which occurs by the thermal expansion, was found by the formula (1) and the manufacturing size was found by the formula (2).

$$s = Ee = Ea(t - t_0) \qquad (1)$$

where: σ = stress of the direction of the circumference, E = elastic constant, ε = strain by the thermal expansion, α = expansion coefficient, t = plug cooling temperature, t_0 = normal temperature (20℃)

The 20℃ coefficient of linear expansion α of aluminum is 23.6×10^{-6} and the elastic constant is 70Gpa. Depending on the occurring thermal stress is 281 MPa. Plug temperature rise until inserts in the ring center, which was cooled at the liquid-nitrogen (77.348K). To decide on the operation time and insertion temperature, which plug into the ring, with measured a characteristic of the temperature rises, when leaving in the

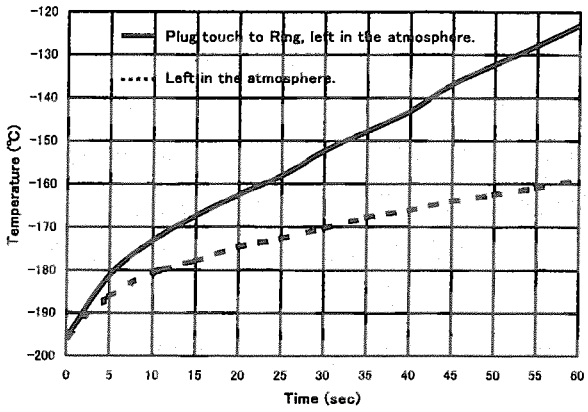

Fig.1: Characteristic of the temperature rises

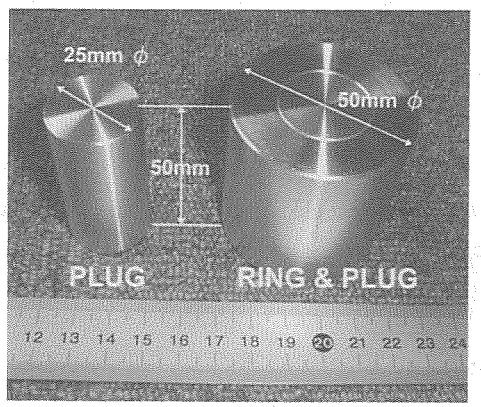

Fig.2: Manufactured Ring and Plug

room temperature and make a plug touch to ring taking out from liquid-nitrogen. It found expansion length by the formula (2). Figure 1 shows a characteristic of the temperature rises.

$$a = \frac{1}{l_R}\left(\frac{dl}{dt}\right) \qquad (2)$$

where: l_R = plug diameter about 20℃ of room temperature, dl = change length with plug diameter at the cooling temperature t℃, dt = change quantity with temperature

As a result, the operation time is about 30 seconds, the plug surface temperature is about -150℃ then it should manufacture a plug diameter 0.1 mm more longer than ring caliber. Even if ring and plug makes by a precise automatic milling machine, but manufacturing precision is becomes 5/1000 mm. Therefore, it made a ring caliber 25.000mm ϕ +0mm, -0.005mm tolerance and plug diameter is 25.100mm ϕ +0mm, -0.005mm, and tolerance. Manufactured Ring and plug is shown in Figure 2.

The stress, which occurred by the thermal expansion, dispersed and estimated a remaining condition as follows.

The stress equivalent condition will be achieved at the contacting boundary of the ring and plug: the ring was pressurized whereas the plug is compressed. The samples are not constrained to the axial direction. In polar coordinates system the axis symmetric stress condition of the elastic body is described by

$$\left.\begin{aligned} \varepsilon_R &= \frac{(\sigma_R - \nu\sigma_H)}{E} \\ \varepsilon_H &= \frac{(\sigma_H - \nu\sigma_R)}{E} \end{aligned}\right\} \qquad (3)$$

where ε_R = radius strain component, ε_H = circumferential strain component, σ_R = radius stress component, σ_H = circumferential stress component, ν = Poisson's ratio and E = Young's modulus. After shrink fit the plug was compressed by the pressure −P(P>0), then its stress state to the radius direction as well as to the circumferential direction is given by $\sigma_R - \sigma_H = -P$ The pressure P is denoted by

$$P = E\delta \frac{(b^2 - c^2)}{b^2 c} \tag{4}$$

where δ = a-b, a= diameter of plug, b= outer diameter of ring, c= inner diameter of ring. A circumferential stress components for the internally pressurized cylinder is obtained:

$$\sigma_H = \frac{P}{4r^2}\left[\frac{b^2 c^2}{(b^2 - c^2)}\right] \tag{5}$$

Substituting P the next equation is easily found

$$\sigma_H = \frac{E\delta c}{4r^2} \tag{6}$$

The measurement method and be expected distribution of stress for hoop direction is shown in Figure 3.

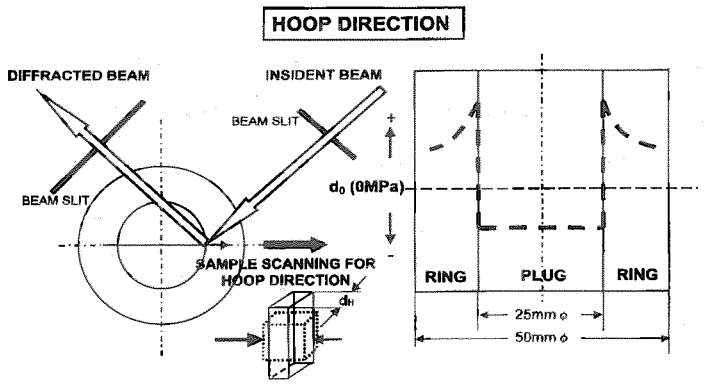

Fig.3: The measurement method and expected of stress for hoop direction

3. Measurement and result by the Neutron Diffraction

It is only a neutron diffraction method, which can measure the state of stress disperse in the sample that occurred at the 281MPa by the thermal expansion.

The inner stress measurement used the neutron diffractometer for residual stress analysis (RESA) that is installed T2-1port in the thermal guide hall at JRR-3M in JAERI. An equipment and strain measurement condition is shown next.

Monochromator crystal : Si(311) Bending and focusing method Crystal mosaicnes : 0.23° Scattering angle of monochromator crystal : 80.00° Wavelength : 2.01nm Collimation : $\alpha 1 = 0.35°$ $\alpha 2 = 0.3°$ $\alpha 3 = 0.33$

Strain was measured 33 points in amount of +-23 mm from the sample center. In the arrow, which was written in the upper part of the sample, according to the direction of the scattering vector, it measured the 3 directions of radial, hoop, and axial, and diffraction plane chose the (220) where the gauge volume is small, but this material had strong texture then could not measurement of axial direction. Therefore, it analyzed a stress in radial and hoop. A texture is shown in Figure 4.

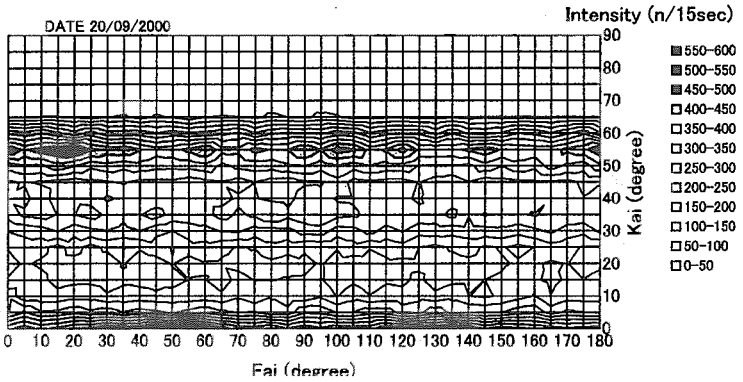

Fig.4: Texture of A6063 (220)

The strain free lattice spacing d_0 was measured by the plug sample.

The stress analysis from the measured strain used formula (7). An analysis of the stress for hoop directions are shown in Figure 5.

$$\sigma_{R,H} = \frac{E}{1-\nu}\left[\varepsilon_{R,H} + \frac{\nu}{1-2\nu}\left(\varepsilon_R + \varepsilon_H\right)\right] \qquad (7)$$

4. Result

The VAMAS TWA 20* was manufacturing the design of the sample for the neutron diffraction, which used stress generation by the thermal expansion already as the Round Robin sample but as for the process of the manufacturing design wasn't published. Therefore, it became manufacturing design from nothing.

The maximum stress for the hoop direction in the boundary part neighborhood of plug and ring is about 200MPa from the measurement result. The analysis result becomes a value with the low of 80MPa than an estimated value. As this cause, the following item is thought of the manufactured plug size was smaller than 25.100 mm

as well as it stores up that there was texture which is strong in the plug to have used for the spacing of lattice planes d_o measurement of the stresses Condition.

It is possible to say that the following item is important in the standard sample manufacturing this time.

① the computation of the thermal expansion occurrence stress, because the plug outward form size, the ring caliber size influence precision mainly, improve manufacturing and size measurement precision.

② The aluminum material is very small neutron absorption coefficient but although the grain orientation is so big.

It is necessary to measure texture every each index in the manufacturing of the standard sample and to fix the plug and ring direction of the cut out from the material.

*: Versailles Project on Advanced Materials and Standards, Technical Working Area 20, it was worked on measurement of residual stress by the neutron diffraction method.

5. Conclusion

An internal residual stress measurement of material can measure only a neutron diffraction. This is an indispensable measurement technique and contributes to the industrial prosperity of each country, in order that to make and develop the excellent manufactured goods.

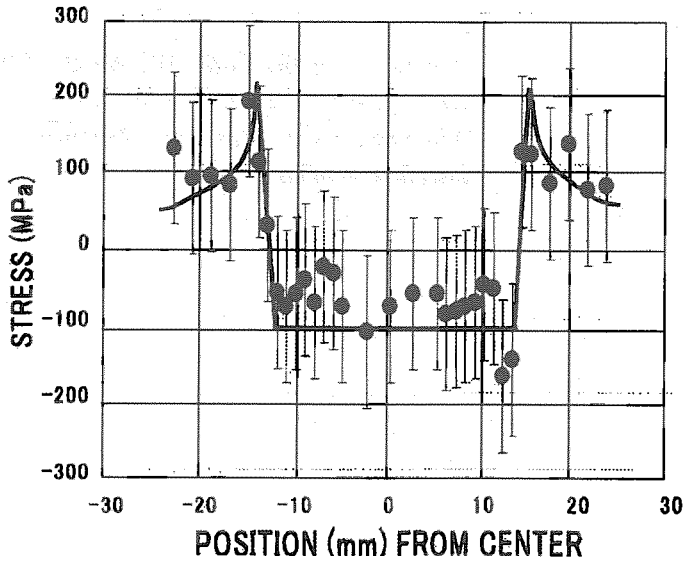

Fig.5: An analysis of stress for hoop and radial directions

JP0250097

1.13 Synchrotron Small-Angle X-ray Scattering Facility at the Pohang Accelerator Laboratory and Its Applications in Materials Science

Jörg Bolze,[1,2] Jehan Kim,[1] Byeongdu Lee,[2] Tae Joo Shin,[2] Jinwon Lee,[2] Jung-Yun Huang[1], Seungyu Rah[1], Hwa Shik Youn[1], Ki-Bong Lee[1] and Moonhor Ree,[1,2*]

[1]Pohang Accelerator Laboratory;
[2]Dept. of Chemistry, Center for Integrated Molecular Systems, BK21 Functional Polymer Thin Film Group, and Polymer Research Institute,
Pohang University of Science and Technology,
San 31, Hyoja-dong, Pohang 790-784, Republic of Korea

presented at the 2000 WS on the Utilization of Research Reactors, 20-24 November 2000, Korea Atomic Energy Research Institute (KAERI), Daejon, Korea

* To whom all correspondence should be addressed:
(Tel) +82-54-279-2120; (Fax) +82-54-279-3399;
(E-Mail) ree@postech.edu

Abstract: The small-angle X-ray scattering (SAXS) beamline BL4C1 at the 2.5 GeV storage ring of the Pohang Accelerator Laboratory (PAL) has been in its first year of operation since August 2000. During this first stage it could meet the basic requirements of the rapidly growing domestic SAXS user community, which has been carrying out measurements mainly on various polymer systems. The X-ray source is a bending magnet which produces white radiation with a critical energy of 5.5 keV. A synthetic double multilayer monochromator selects quasi-monochromatic radiation with a bandwidth of ca. 1.5 %. This relatively low degree of monochromatization is sufficient for most SAXS measurements and allows a considerably higher flux at the sample as compared to monochromators using single crystals. Higher harmonics from the monochromator are rejected by reflection from a flat mirror, and a slit system is installed for collimation. A charge-coupled device (CCD) system, two one-dimensional photodiode arrays (PDA) and imaging plates (IP) are available as detectors. The overall performance of the beamline optics and of the detector systems has been checked using various standard samples. While the CCD and PDA detectors are well-suited for diffraction measurements, they give unsatisfactory data from weakly scattering samples, due to their high intrinsic noise. By using the IP system smooth scattering curves could be obtained in a wide dynamic range. In the second stage, starting from August 2001, the beamline will be upgraded with additional slits, focusing optics and gas-filled proportional detectors. In addition, the second SAXS beamline BL4C2 based on a bending magnet X-ray source and a double crystal monochromator is under construction and this construction will be completed by August of 2002. And, the third SAXS beamline based on an undulator X-ray source and a double crystal monochromator is also planned to construct by 2005. In Korea the SAXS beamlines become very important advanced tools for structural investigations on various commodity and advanced materials. Together with these SAXS facilities, the wide-angle and small-angle neutron scattering (WANS and SANS) beamlines at the Hanaro Center of Korea Atomic Energy Research Institute open a wide view of features to the fundamental and applied researches of materials in Korea.

Keywords: X-ray, small-angle scattering, synchrotron, Pohang Accelerator Laboratory, beamline, detector, polymer, latex.

1. Introduction

Small-angle X-ray scattering from an irradiated specimen arises from electron density fluctuations on a mesoscopic length scale in the range of ca. 10 to 500 Å. This method has become a very important tool for structural studies on a wide variety of materials, such as polymers, fibers, metals and alloys, liquid crystals, and colloidal systems.[1-5] Examples for colloids which have been investigated are biomolecules,[6] synthetic nanoparticles, aggregates of amphiphilic molecules, gels etc. Information about the overall shape and size of the scattering object, its density, orientation, packing with other objects etc. may be obtained. Typical applications in polymer science[7,8] are studies on the nanodomain formation in block copolymer systems as a function of temperature and composition, on the crystallization mechanisms and kinetics of homopolymers and copolymers, on the structure of polymer latexes, on the conformation of polymers in solution etc. Due to the high photon flux which is available at synchrotron sources, the data collection times can be greatly reduced which also allows for time-resolved studies on phase transitions, crystallization kinetics, assembly/disassembly processes, denaturation/renaturation etc. Other merits of synchrotron radiation are the naturally low beam divergence and the available wavelength continuum.

Beamline BL4C1 at the Pohang Accelerator Laboratory (PAL)[9] is the first dedicated synchrotron small-angle X-ray scattering station in Korea. The first phase of construction was started in January 1999 and completed in August 2000. Domestic SAXS user and SAXS working groups were founded in 1994 and 1995, respectively, and have been growing rapidly. To date, simple optical components have been installed

at the beamline, which can meet the basic requirements of the domestic SAXS community. This paper summarizes the current status of the beamline instrumentation and reports about some measurements on standard samples, which were conducted to test the performance of the beamline optics and of the various detector systems. Brief outlooks on to further upgrading plans and on upcoming new SAXS beamlines are also given.

2. X-Ray Source

The Pohang Accelerator Laboratory (PAL) is a 2.5 GeV synchrotron radiation facility in Pohang, Korea. It is operated at a ring current of typically 150 - 200 mA. The radiation source for the SAXS beamline is a bending magnet with a magnetic field of 1.32 T. The size of the source (root mean square deviation ó of the electron beam with respect to the orbit) is $ó_v$ = 0.059 mm vertically and $ó_h$ = 0.160 mm horizontally, and the divergence of the emitted white beam is 0.1 mrad vertically and 3.0 mrad horizontally. At a stored electron energy of 2.5 GeV the critical energy of radiation is 5.5 keV and a usable photon flux up to 15 keV is delivered. The calculated angular photon flux density (which is given in units of the number of photons per unit time (s), per unit solid angle ($mrad^2$), and per 0.1 % relative bandwidth) amounts to 2.15 x 10^{13} photons / sec / $mrad^2$ / 0.1% b.w. at a stored electron energy of 2.5 GeV, a ring current of 200 mA and an energy of radiation of 7.7 keV. The ultra-high vacuum in the storage ring is separated from the high vacuum beamline by a beryllium window. The access of the X-ray beam to the experimental station is controlled by a photon shutter.

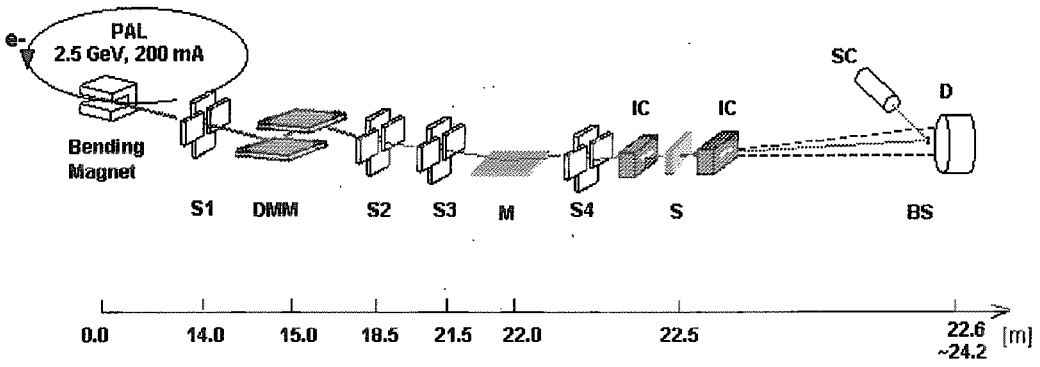

Figure 1. Schematic diagram of the SAXS beamline BL4C1 at the Pohang Accelerator Laboratory: S1-S4: slits; DMM: double mulitlayer monochromator; M: flat mirror; S: sample; IC: ionization chamber; BS: beamstop; SC: scintillation counter; D: detector.

3. Beamline Optics

3.1. Monochromator

The monochromator is located at a distance of 15 m from the source of radiation. It consists of a set of two synthetic multilayers (Osmic Inc.) which are deposited on silicon substrates with a size of 20 x 50 x 5 mm. Each multilayer consist of 200 W/B_4C layers, with a d-spacing of 25 ± 1 Å and a root-mean-square roughness smaller than 1 Å. The first order Bragg reflection of these multilayers is used to obtain a quasi-monochromatic beam. The reflectivity at the Bragg angle amounts to ca. 70 % at

8 keV and the band width of the reflected beam, which is mainly determined by the number of layers, is ca. 1.5 %. In addition to the fundamental, the second harmonic is also present in the same reflected beam. As will be described further below, it is removed downstream using the reflection from a flat mirror. The two multilayers are mounted on a holder in a parallel geometry and offset the incoming beam ca. 3 mm upwards without changing its direction. This optical system yields X-rays with energies E varying from 7.5 to 9.5 keV. The beamline is usually operated at E = 7.709 keV, which corresponds to a wavelength ë of 1.607 Å. Energy calibration is done using the *K*-absorption edge of a cobalt foil. At that energy the Bragg angle of the multilayer is 1.842° and the vertical beam size which is intercepted by the monochromator is 1.6 mm. The resolution of the double multilayer monochromator in terms of Äë / ë, where Äë represents the full width at half maximum of the reflected wavelength distribution, is ca. 1.5 %. This degree of monochromatization is rather poor compared to that of single crystal monochromators, for which Äë / ë is of the order of 10^{-4}. The advantage of a wide-bandpass monochromator as being used here, however, is a considerable gain of photon flux by about a factor of 100.

In the following we discuss how the monochromator characteristics will affect scattering and diffraction data. A wavelength spread in the radiation incident on a specimen leads to a distribution of scattering vectors q (q = 4ð ^{x} sin(è/2) / ë, where è denotes the scattering angle) which are being probed simultaneously at one angle in the detector plane. The scattering curve $\tilde{I}(q)$, which is measured from a sample when using a polychromatic beam with a wavelength distribution W(ë'), is related to the scattering pattern I(q), which would be measured in case of an ideally monochromatic beam (Äë / ë = 0), by the following smearing integral:[2]

$$\tilde{I}(q) = \int_0^\infty W(\lambda') \cdot I(\frac{q}{\lambda'})\, d\lambda' \qquad (1)$$

where ë' = ë / ë$_0$ and ë$_0$ denotes the mean wavelength. From this equation it can be seen, that there is no smearing effect at q = 0 nm^{-1}, and that the width of distribution in q, over which I(q) is being averaged, increases with q. In order to estimate the smearing effect due to the finite energy resolution of the monochromator used at BL4C1, a computer program was written, which applies the smearing integral given in equation (1) on various calculated model scattering patterns.

First we discuss the scattering from an assembly of non-interacting, homogeneous spheres with a mean sphere diameter of 100 nm. A Gaussian particle size distribution with a rather small standard deviation of 3 % was assumed. This kind of model system may represent a dilute polymer dispersion (latex). The scheme for calculating the scattering intensity of such a system was reported elsewhere.[10] Figure 2 displays the scattering patterns which were calculated as a function of Äë / ë, where W(ë') was assumed to be a Gaussian. The model curve calculated for the case of an ideally monochromatic beam exhibits deep minima in the oscillations because symmetric particles with a narrow particle size distribution are being considered. In case of Äë / ë = 1.5 %, no significant smearing of the oscillations occurs, whereas in case of Äë / ë = 10 % (a typical resolution for neutron scattering) considerable smearing is evident. Thus, such a sample can be measured using the double multilayer monochromator at BL4C1, without any drawback in resolution. On the other hand, if the data were measured with a

resolution of Äë / ë = 10 %, a desmearing of the scattering curve would be necessary. Otherwise, the determination of the particle size polydispersity would lead to an erroneous result.

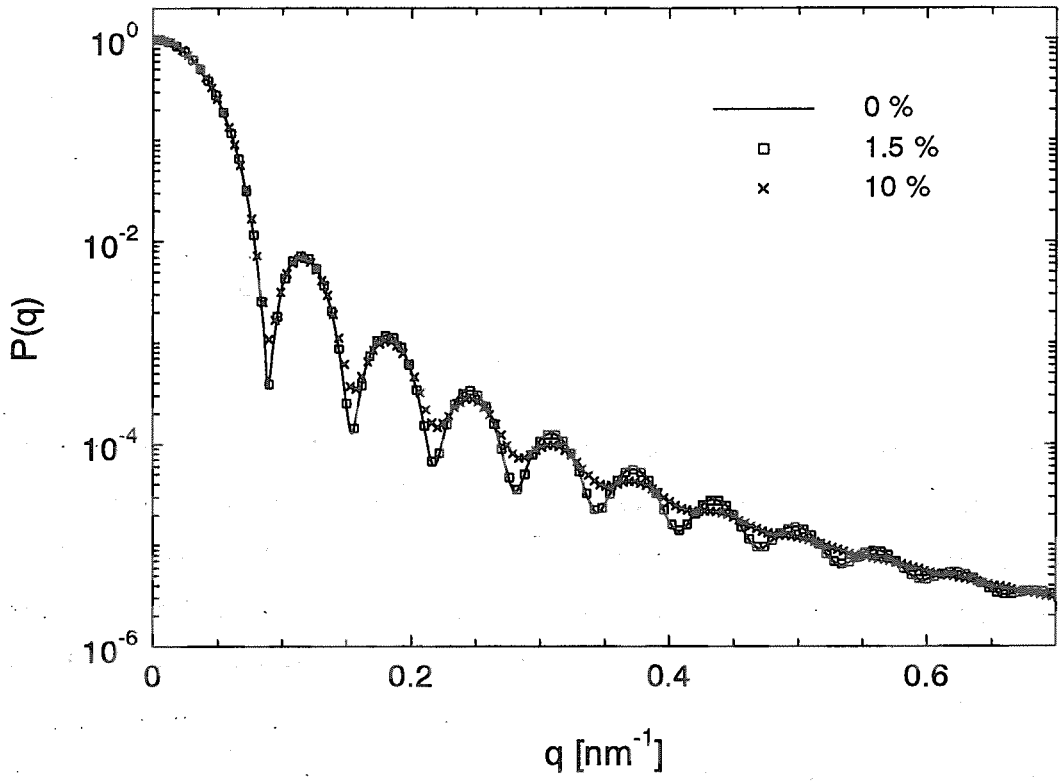

Figure 2. Model calculation demonstrating how SAXS data are affected by a finite wavelength resolution of the monochromator. Shown is the form factor P(q) of a homogenous sphere with a radius of 50 nm. The standard deviation of the Gaussian particle size distribution was set to 1.5 nm or 3 %. Parameter is the width of the wavelength distribution in the incident X-ray beam which is assumed to be Gaussian. The smearing effect due to a bandwidth Äë / ë of 1.5 % (as provided by the double multilayer monochromator) is still negligible, whereas 10 % bandwidth would result in a considerable smearing of the extrema.

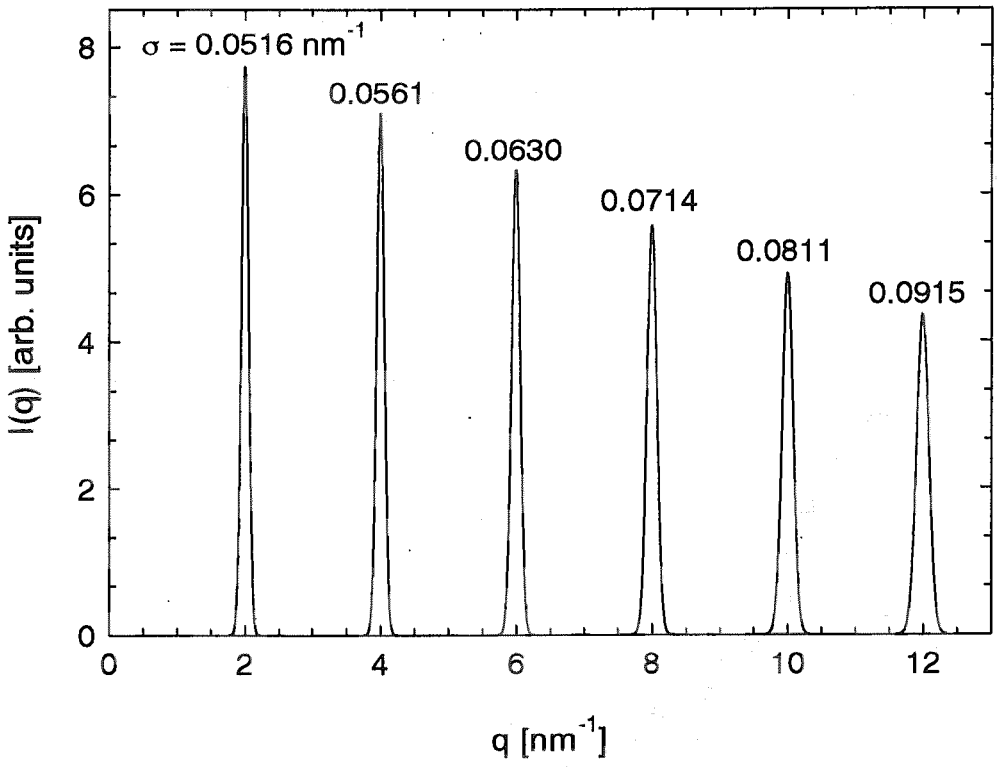

Figure 3. Model calculation demonstrating how the width of a diffraction peak is affected by a finite wavelength resolution of the monochromator. The wavelength distribution in the incident beam was assumed to be Gaussian with Äë / ë = 1.5 % and the intrinsic line width (standard deviation) of the Gaussian peak was set to ó = 0.0500 nm^{-1}. In order to elucidate how the peaks are affected as a function of their angular position, this calculation was done assuming various Bragg spacings. As can be seen, the broadening increases with increasing scattering vector. The figures given in the plot indicate the calculated standard deviation of the broadened Bragg peaks.

Next we consider the diffraction from a sample containing some ordered domains. The Bragg peak originating from this sample is assumed to be Gaussian with an intrinsic line width (standard deviation) of ó = 0.0500 nm^{-1}. This corresponds to a

correlation length of 54 nm in real space. In Figure 3 it is shown, how the width of the Bragg peak is affected by a finite energy resolution of 1.5 %. In order to elucidate how the smearing effect depends on the diffraction angle, various d-spacings were assumed. It can be seen, that significant peak broadening is induced, and that the effect increases considerably with increasing scattering vector. As an example, the peak width is broadened by 3.2 % at q = 2 nm^{-1} (SAXS regime), but at q = 10 nm^{-1} (WAXD regime) by as much as 62 %. Before any quantitative interpretation of such data is done, a desmearing of the raw data is required. Desmearing procedures are discussed in References 2 and 3.

In summary, the bandwidth which is provided by the double multilayer monochromator is sufficient and suitable for most of the SAXS measurements which are typically performed at BL4C1 and no data correction procedures are required. In case of highly ordered samples, however, it is necessary to desmear the raw data, especially when intermediate or wide angles are being considered.

3.2. Mirror

In order to reject the higher harmonics from the beam which is reflected by the multilayer monochromator, a flat, gold-coated mirror (Beamline Technology Corp., USA) is installed 22 m from the source. The dimensions of the mirror are 200 x 30 x 30 mm and the surface roughness is smaller than 1.5 Å. To prevent radiation damage on the mirror surface, it is kept in a box under a helium atmosphere. The tilt angle of the mirror is adjusted so that the beam is reflected under 8 mrad with respect to the mirror surface. At that angle the reflectivity for X-rays with E = 7.7 keV is about 75 %, whereas it is less than 2 % for the second harmonic. Thus, the total reflecting mirror acts as a low-

pass filter which effectively reduces the intensity of the second harmonic to a negligible level. The performance of the mirror is demonstrated in Figure 4. It compares the diffraction patterns from lead stearate which were measured by a charge-coupled device (CCD) detector before and after the installation of the mirror. Without the mirror, an intense diffraction ring was observed in the small-angle region, and in addition a weak ring at half angle. Upon installation of the mirror, only the intense diffraction ring remained. It is thus obvious that the weak ring must be attributed to the diffraction of the second harmonic, which could be effectively suppressed using the mirror.

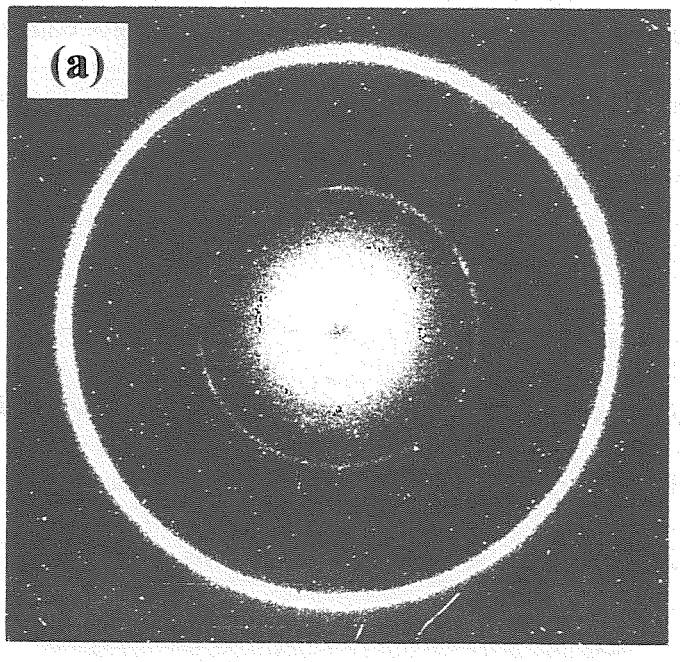

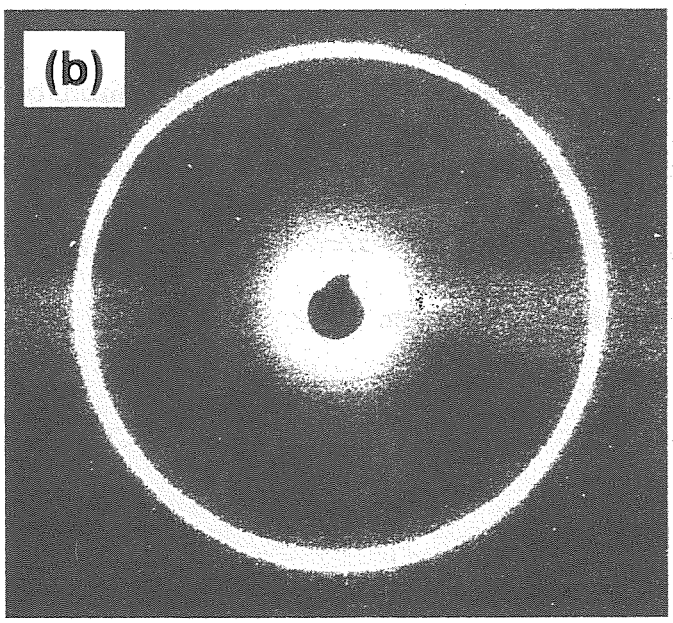

Figure 4. Diffraction pattern from lead stearate before **(a)** and after **(b)** a flat mirror had been installed. The weak diffraction ring in **(a)** corresponds to the diffraction of the second harmonic. It could be rejected upon reflecting the incident beam at the mirror surface.

3.3. Slit Collimation System

A very tight collimation of the X-ray beam and the minimization of any parasitic scattering is essential in small-angle scattering, so that measurements can be done in the immediate vicinity of the direct beam. Several slits are installed along the beam path for that purpose. A primary slit is located 14 m from the source point, in front of the monochromator. It is usually set to 0.5 mm vertically and 1.0 mm horizontally, thus slicing off a rectangular portion from the central cone of the emitted beam. The actual beam size is determined by two more slits behind the monochromator (one of those slits is scheduled to be installed in August 2001), whereas a guard slit just

in front of the sample has the function to cut down any parasitic scattering without touching the main beam. This setting still needs to be optimized, because the parasitic scattering originating from the mirror cannot be completely removed with this configuration. Two viewing ports are installed along the beam path in order to monitor the shape and position of the X-ray beam.

4. SAXS Camera

The SAXS camera is enclosed in a safety hutch and all components are remotely controlled. A motorized sample stage is located 22.5 m from the source and allows users to install various sample cells in a flexible way. The photon flux at the sample position was estimated from the current measured with an ionization chamber to ca. 2 x 10^{10} photons/mm^2/s at a ring current of 200 mA. Attenuators with various thickness may be inserted into the beam in order to control the photon flux on the sample. An evacuated beam path with adjustable length (10, 90, 130, and 170 cm) is mounted on a double optical rail between the sample and the detector stage. It is sealed on both ends with thin Kapton foils and the vacuum level (typically 5 x 10^{-3} Torr) is continuously monitored. The beamstop, which is made of tantalium, is located inside the vacuum path, close to the Kapton window at the end. A motor-controlled detector stage is installed right behind the vacuum path. The intensity of the primary beam may be monitored by ionization chambers before and/or behind the sample, and also by a scintillation counter which measures the back-scattering from the beamstop under an angle of ca. 45°.

5. Detector Systems

At present two one-dimensional photodiode array detectors (PDA), an area-CCD detector, as well as phosphor imaging plates (IP) are available. In the following we will first discuss the properties, merits and demerits of each detector. Afterwards, we present SAXS measurements from some standard samples and compare the performance of the various detection systems.

5.1. Photodiode Array Detector System (PDA)

This is an unintensified solid state detector which is based on an X-ray sensitive, linear silicon photodiode array (Princeton Instruments, USA, Model X/PDA). X-rays directly hit the sensing area after passing through the entrance window, which is made of beryllium. It is a multichannel line-scan camera which consists of two arrays placed one above the other. The total length of the combined arrays is two inches, which is divided in 2048 channels. The light sensing area per pixel is 25 x 25 μm^2. For storing the accumulated charge, however, a much larger area of 25 x 2500 μm^2 is used. This has the advantage that a high charge may be collected before the saturation level of a pixel is reached. Other merits of this type of integrating detector are its high gain (as compared to indirectly illuminated array detectors) and its high count rate capability, which is important when synchrotron radiation is used to measure intense diffraction peaks. According to the manufacturer, the spatial resolution is better than 1.5 pixels, geometric distortion less than one pixel and the uniformity of response is 5 to 10 %. After a preset exposure time, the array is scanned and the charge in each diode is read

out by the preamplifier board in the detector head. An analog signal is created and sent to the detector controller, where it is further shaped and amplified. It is then digitized by an analog-to-digital converter (ADC) with a resolution of 16 bit. The digitized signals are integer numbers measured in analog-to-digital units (ADU). They are sent via Direct Memory Access to the interface board of a personal computer, where data are displayed, further processed and stored.

A main disadvantage of this detector type is its inherently high dark current noise, which varies from pixel to pixel. Main sources of this background are thermally induced, statistical noise (accumulated charge in the array) as well as electronic noise originating from the readout electronics and from the digitizer. As thermally induced dark charge decreases exponentially with temperature, the array is cooled to typically –30°C. The thermoelectric cooler and the array are confined within a static vacuum chamber in order to prevent water condensation and to ensure optimal insulation. The detector is prone to radiation damage which is manifested in a locally increased dark current. Even though damaged areas may be recovered upon annealing the array, this process is not fully reversible. The dark current increases linearly with the integration time, but in damaged pixels it increases much faster than in undamaged areas. The detector dark signal has to be determined carefully each time before a sample is to be measured. It has to be measured using the same integration time as for the sample and with the photon shutter being closed. The dark signal amounts to ca. 800 ADU when measured for 10 s. The detector is controlled using software provided by Princeton Instruments (Winspec 3.1) which automates data acquisition, display, and basic processing. Further data processing, as scaling, background subtraction and model fitting is done using other software developed by ourselves.

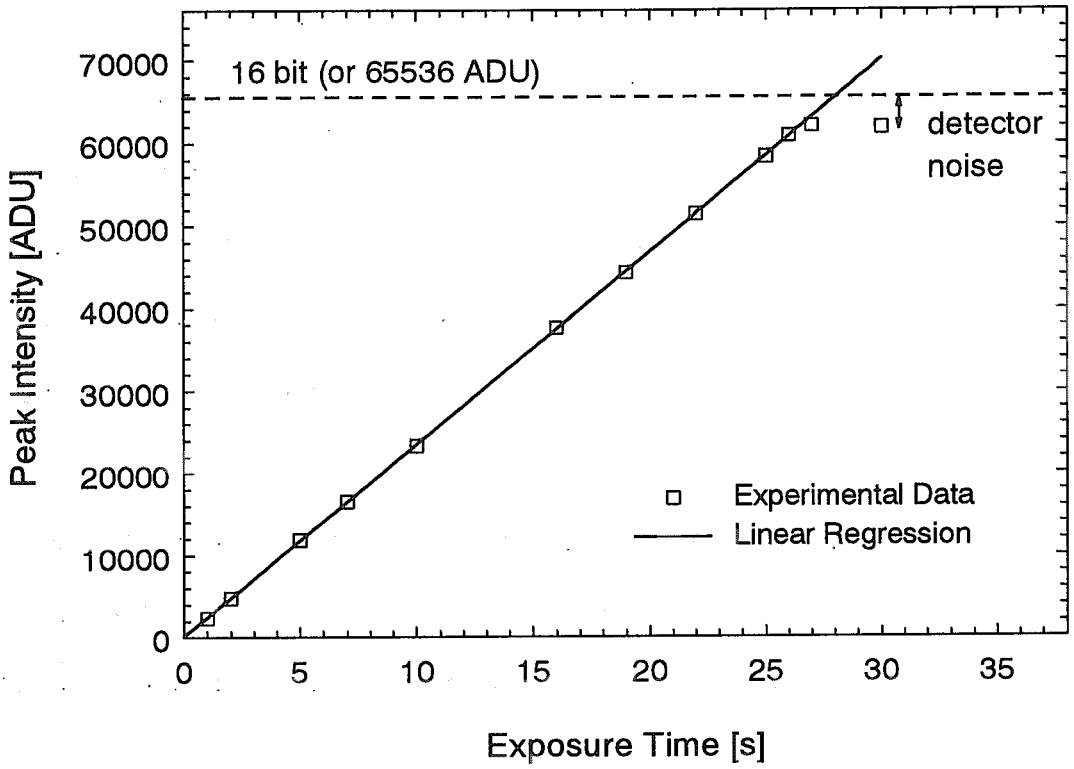

Figure 5. Measured diffraction peak intensity from an ordered block copolymer sample. Shown is the response of the PDA detector as a function of the exposure time. The full-well-capacity per pixel (i.e. the integrated signal which saturates a detector pixel) is 16 bit. Good linearity in the detector response was found until the pixel well capacity is reached. From the intensities which are displayed here, the dark noise was subtracted to yield solely the intensity scattered from the sample. Evidently, the dynamic range which is available for the sample, is diminished due to the dark noise. This is becoming most severe when the scattering intensity from the sample under consideration is low.

The linearity of the detector was checked by measuring the intensity of a Bragg peak from a block copolymer sample with ordered nanodomains as a function of the exposure time. The measured intensity shows good linearity with a relative error of less than

0.5 %. It increases until the saturation level of the detector is reached (16 bit, or 65536 ADU). The dynamic range of the detector is greatly diminished due to the high dark signal, which has to be subtracted from the measured raw data. Thus, as shown in Figure 5, at long exposure times the maximum signal from the sample scattering does not reach the 16 bit level. It is reduced by the dark signal. In particular in case of weakly scattering samples, where long exposure times of several minutes are required for good counting statistics, the dark current may strongly dominate the measured raw data. In such a case the maximum exposure time is mainly determined by the accumulated dark current rather than by the scattering intensity of the sample. The PDA detector is not well-suited to study weakly scattering samples. Data then tend to become noisy after subtraction of the dark signal, because the dark signal itself shows a random fluctuation of ca. 0.5 % when measured repeatedly.

5.2. Charge-Coupled Device (CCD) Area Detector

The unintensified CCD area detection system (Princeton Instruments, USA) is based on a scientific grade CCD image sensor (EEV 1152x1242 CCD, 1.4 Megapixel; EEV, U.K.), where charges are stored in an array of photosensitive capacitors. The entrance window of the detector is made of beryllium and has a diameter of 115 mm. Incident X-rays are converted by an 0.5 mm GdOs phosphor screen into visible scintillation photons which are guided to the CCD image sensor by a demagnifying fiber-optic taper with a reduction ratio of 4.6:1. The pixel size is 104 x 104 μm at the entrance window and 22.5 x 22.5 μm^2 at the CCD image sensor. The sensor has a size of 25.9 x 27.5 mm^2 and is divided into 1152 x 1242 pixels. The diameter of the taper at the CCD is 25 mm. In order to reduce its dark current, the CCD is cooled to –50°C by a

Peltier device in combination with a circulating coolant. Water condensation inside the detector is prevented by evacuation. The output from the CCD is amplified, digitized by a 12- or 16-bit A/D converter, and transferred to the image memory of a Pentium computer via a high speed serial interface. Normal readout speed of the CCD at lowest noise is 200 KHz with a dynamic range of 16 bits per pixel. There also exists an option for a high speed readout at 1 MHz with a dynamic range of 12 bits per pixel. Other possibilities to achieve a faster readout are binning of pixels, partial readout, or a frame transfer mode. To prevent a smearing of the image during readout, an electromagnetic fast shutter, which is triggered by the detector controller, was installed close to the sample. The detector is controlled using software provided by Princeton Instruments (Winview32). It automates data acquisition, display, and basic processing. Further data processing, as e.g. spherical averaging, scaling, background subtraction and model fitting is done using other software developed by ourselves.

As in case of the PDA detector, a precise measurement and subtraction of the dark charge signal is essential, in particular when low intensity patterns are to be measured. Compared to the PDA detector, the dark signal from the CCD is low and shows little fluctuation over the array. Fluctuations are further reduced upon spherical averaging. When measured repeatedly, a stability of the dark signal within ca. 0.2 % was found. The dark signal amounts to ca. 90 ADU within 1 s, most of which are offset counts from the A/D converter. Compared to the PDA detector, the CCD detector has only a very small increase of dark current with integration time, which makes it better suitable for measurements of samples with a low scattering intensity. According to the manufacturer the response nonuniformity is less than ± 3 % over the entire CCD area. The good linearity of the detector within the dynamic range was reconfirmed using the same

method as for the PDA-detector (cf. Figure 5). The detector was checked for spatial distortion effects which could arise e.g. due to a shear distortion of the fiber optics taper. For that purpose the detector was illuminated through a grid patterned mask made of brass which consists of an array of holes 5 mm apart from each other with a hole diameter of 0.25 mm. The image obtained in that way (cf. Figure 6) is to be compared with the real geometry of the grid. We found a fairly good reproduction of the grid; the maximum deviation of a grid point from a straight line was found to be ca. 1 % of the taper diameter at the CCD sensor side. Sophisticated software exists to correct acquired images for such spatial distortion effects.[11]

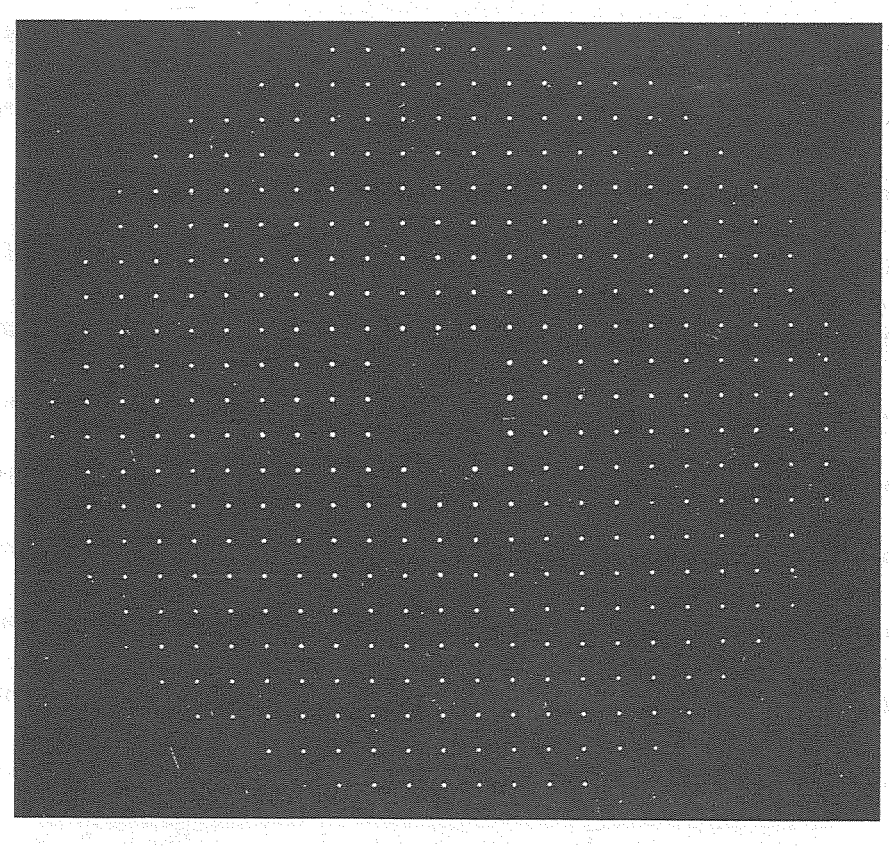

Figure 6. Image of a grid patterned mask measured with the CCD detector.

5.3. Phosphor Imaging Plate System

White image plates (Fuji BAS 2000) with a dimension of 400 x 200 mm^2 and a pixel size of 100 x 100 μm^2 are available. After exposure, the photo-stimulated phosphor screen is read out off-line with a MAC Science IPR-420 reader system and subsequently erased. The advantages of this integrating area detector are its high dynamic range (16 bit), a good detection quantum efficiency, and a very low readout or dark noise. On the other hand it is not well-suited for real time or time-resolved measurements.

6. Experimental Results

We now compare the performance of the various detector systems by discussing experimental data acquired from a polymer latex and from chicken tendon collagen. A latex, which is prepared by emulsion polymerization, consists of an aqueous dispersion of polymer particles with a particle size in the range of ca. 50 - 500 nm.[12] Here we discuss the scattering profiles obtained from highly uniform, spherical poly(methylmethacrylate) (PMMA) latex particles with a diameter of ca. 90 nm. The latex was dried at room temperature and subsequently ground to yield a fine powder. Even in the dried state, the spherical particles keep their identity due to the high glass transition temperature of PMMA.[13] We found that such a dried polymer latex is highly suitable to test critically the performance of detectors, because its scattering curve shows a number of peculiar characteristics: i) a very high scattering intensity, due to the

high electron density contrast between the particles and the surrounding air, ii) a large number of oscillations due to the narrow particle size distribution and due to the symmetry of the particles, and iii) a steep, continuous decay of the intensity over several orders of magnitude within a small angular range. Thus, for the measurement of such a sample, a suitable detector is required to have a high count-rate capability, a good resolution, and a high dynamic range.

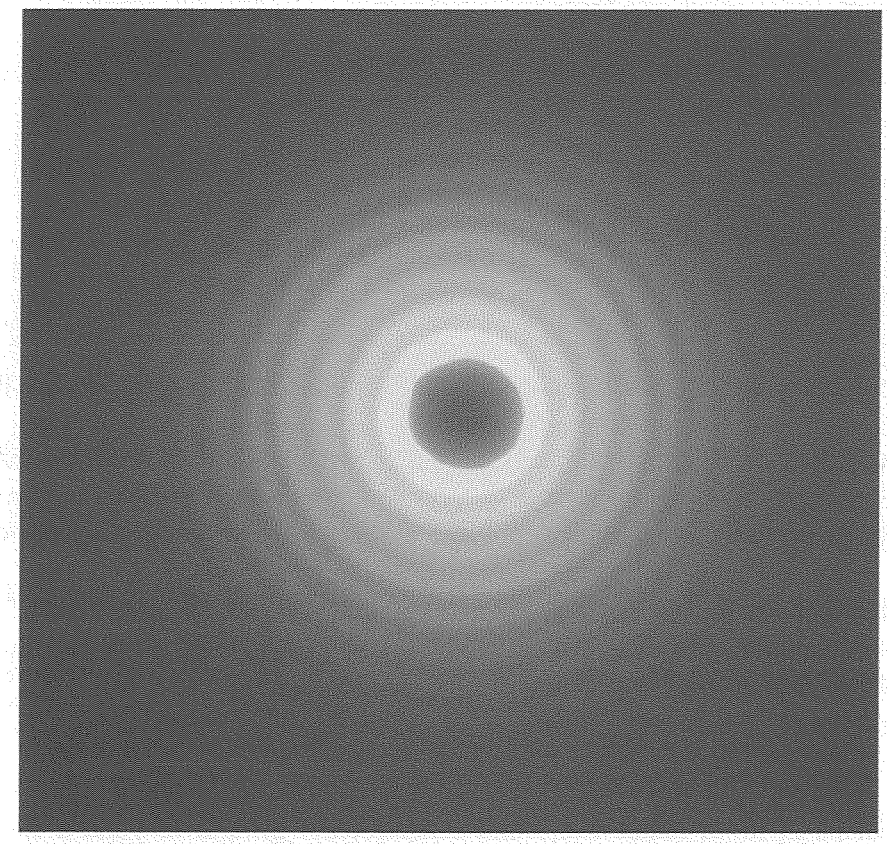

Figure 7. Scattering pattern of a PMMA latex powder acquired by the CCD detector with an exposure time of 2.5 s. The image is displayed on a logarithmic intensity scale in order to visualize the scattering features in the low intensity region more clearly.

Figure 7 displays an image of the scattering pattern which was measured from the dried PMMA latex using the CCD detector system with an exposure time of 2.5 s. The intensity is displayed on a logarithmic scale for a better visualization of the data over the whole intensity range. Several rings of high and low intensity can be seen, due to the oscillations in the form factor of those uniform, spherical particles (cf. Figure 2). Furthermore it was found, that the scattering intensity of this sample is so high, that the contribution of any parasitic scattering to the measured intensity is negligible at all angles. As the sample under consideration is an isotropic powder, we will from now on discuss spherically averaged scattering profiles.

Figure 8 displays the SAXS patterns measured with the PDA, CCD and image plate detection systems, respectively. In all cases, the sample-to-detector distance was ca. 110 cm. Following a procedure given by Fujisawa *et al.*,[14] the dynamic ranges of the detectors were checked by variation of the height (in case of the one-dimensional PDA detector) or diameter (in case of the CCD area detector and IP) of the beamstop, so as to mask increasing parts of the highest intensity region at small angles. In Figure 8 the first data points in the various measurements at different beamstop heights are marked by arrows and numbered consecutively. As can be seen from those data, the scattering intensity decays over nearly five orders of magnitude in the angular range under consideration and displays several maxima and minima at smallest angles.

In case of the PDA detector the decays of the curves measured with various beamstop heights are clearly different. By using attenuators of various thickness it was found, that the shape and decay of the scattering pattern does not depend on the incident photon flux, even though the scattering intensity of this sample is very high. This shows that the detector has a high count rate capability and that the differences in the curves

are due to the insufficient dynamic range of the detector. Using the PDA detector, it is not possible to measure simultaneously the regions of highest and lowest intensities correctly. The curves only superimpose when the beamstop is in positions numbered 3 and 4 in Figure 8). Thus, if such a sample is to be measured with the PDA detector, it is necessary to perform two measurements with the beamstop placed in positions 1 and 3, respectively. It is concluded that the practical dynamic range of this detector is limited to ca. 500 : 1.

In case of the CCD and IP detectors, the respective differences in the scattering curves acquired at various beamstop sizes are only marginal. This means that the dynamic range of those detectors is sufficient to simultaneously acquire data over an intensity range of at least 10^4 : 1. Additional measurements using attenuators have shown, that both detectors are working correctly even at a very high count rates.

In Figure 9 the scattering data from the latex powder, which were acquired with the three different detectors, are shown together in a single plot. The displayed data for the PDA detector were combined from three measurements at different beamstop heights, whereas the data which are shown for the CCD and IP detectors are the single measurements at smallest beamstop size, respectively. As can be seen, all three curves superimpose very well at smallest angles where the oscillations appear, but also the decay of the intensity over more than four orders of magnitude is identical. In conclusion, when carefully applied, all available detectors can yield reliable SAXS data over a wide dynamic range and may reveal fine scattering features, provided that the scattering intensity from the sample is high.

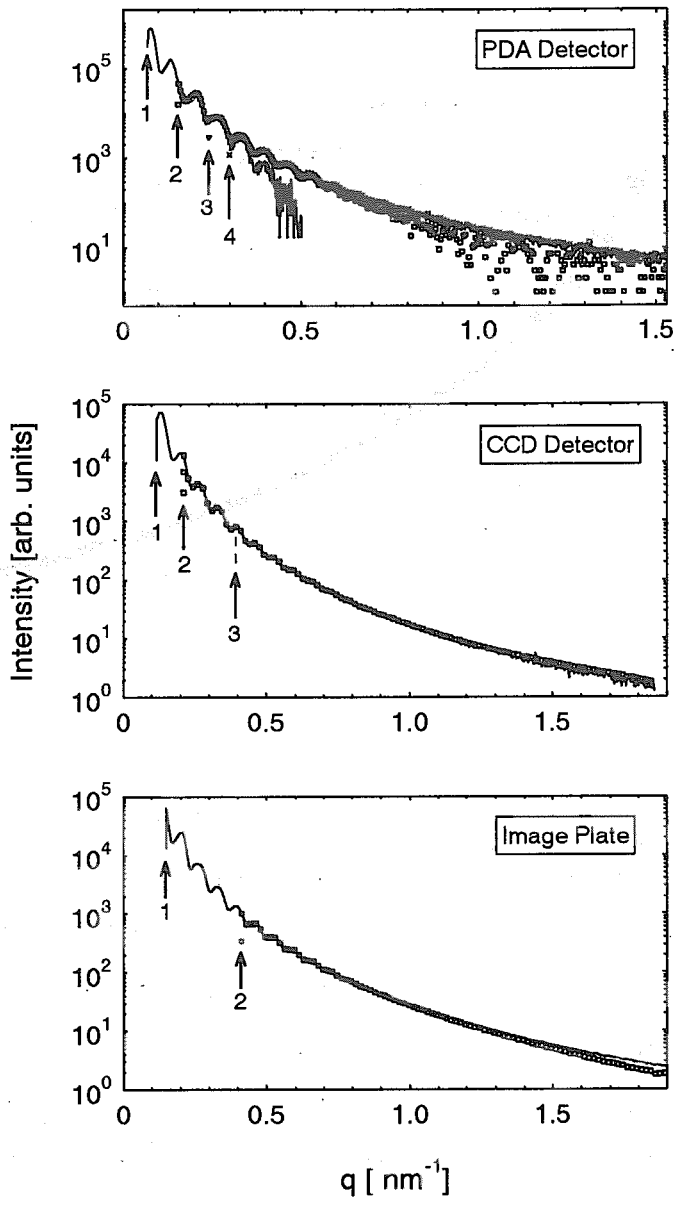

Figure 8. SAXS patterns from a dried PMMA latex measured with PDA and CCD detectors as well as with an image plate (IP). In order to check the dynamic range of the various detection systems the height (in case of the 1-D PDA detector) or diameter (in case of CCD area detector and IP) of the beamstop was varied and increasing parts of the highest intensity region were thus masked at smallest angles. The arrows indicate the first data point for the respective measurements.

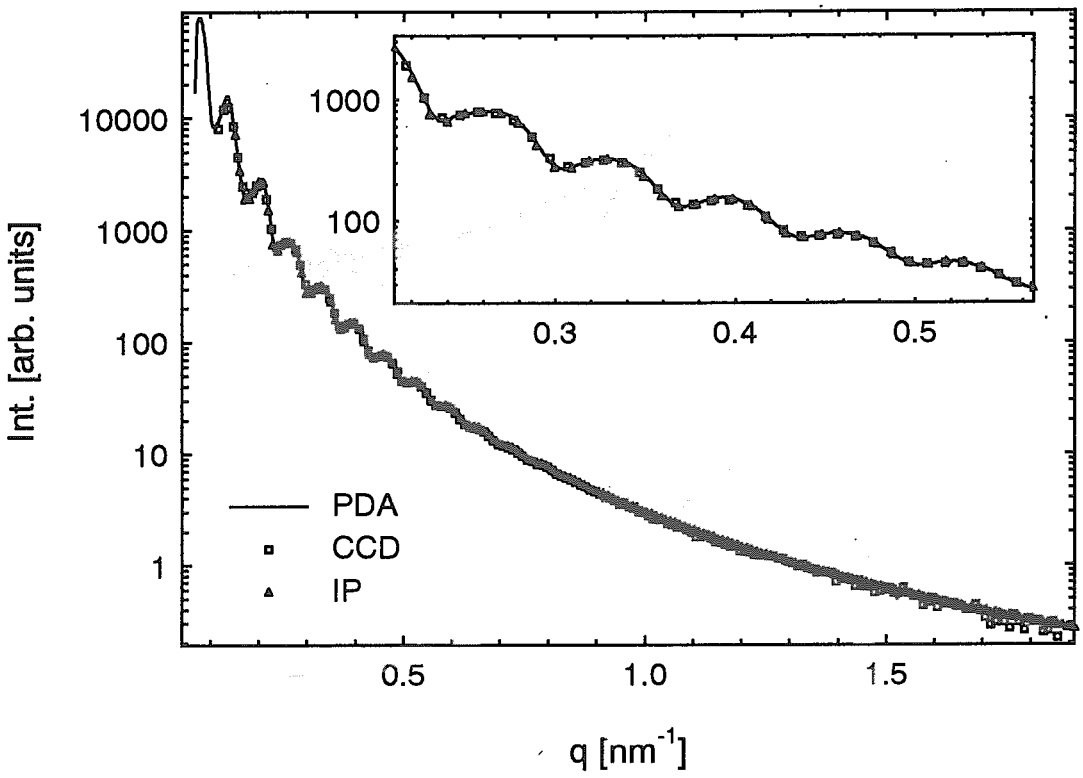

Figure 9. Comparison of the SAXS patterns from a dried PMMA latex measured with the PDA and CCD detectors, as well as with an image plate (IP). The PDA data were combined from three measurements at three different beamstop heights (cf. Figure 8), whereas the CCD and IP data were collected in a single measurement using the smallest beamstop size. The inset shows a magnification of the curves in a small angular region. For sake of clarity, only every third measured data points are displayed for the CCD and IP detectors.

Next we discuss the performance of the detectors when samples with a lower scattering intensity are to be investigated. For that purpose the aqueous PMMA latex was measured at a concentration of 17 vol.%. In that case the scattering intensity is considerably lower than for the dried latex, because of the much lower electron density difference between PMMA and water, as compared to that between PMMA and air. To

yield the scattering intensity from the latex particles only, it is necessary to measure separately the scattering from water and from the empty sample cell, and to subtract those contributions from the gross scattering curve measured from the aqueous dispersion, taking properly into account the respective transmission factors.[10] Figure 10 displays the thus obtained scattering curves which were acquired using the CCD detector and the imaging plate with an exposure time of 600 s, respectively. Like in the case of the latex powder sample, the data coincide well in the angular region of highest intensity where the oscillations occur. At higher angles (q 0.5 nm^{-1}), however, the CCD data become very noisy and at scattering vectors higher than 1 nm^{-1} the data are no more meaningful. On the other hand, the data acquired with the image plate are comparatively smooth and show a reasonable decay in the whole angular range. The main reason for the strong noise in the CCD signal is the instability of its dark current. At high angles, the scattering intensity is considerably lower than the dark current, so that small fluctuations in the dark image can create a high noise level in the scattering curve, even if the data are radially averaged. In case of the one-dimensional PDA detector this problem is even more severe, because the dark current is relatively much higher, especially when it is acquired over the period of a few minutes or longer. In addition, data smoothing by radial averaging is not applicable, of course. For the image plate system, dark and readout noise are negligible compared to the scattering intensity. The efficiency of the image plate is ca. 3.5 times higher as compared to the CCD. This is evident in Figure 10, where the measured scattering curves are displayed in the actual intensity ratio. This example has shown, that among the currently available detector systems, the image plate is the detector of choice when weakly scattering samples are to be investigated.

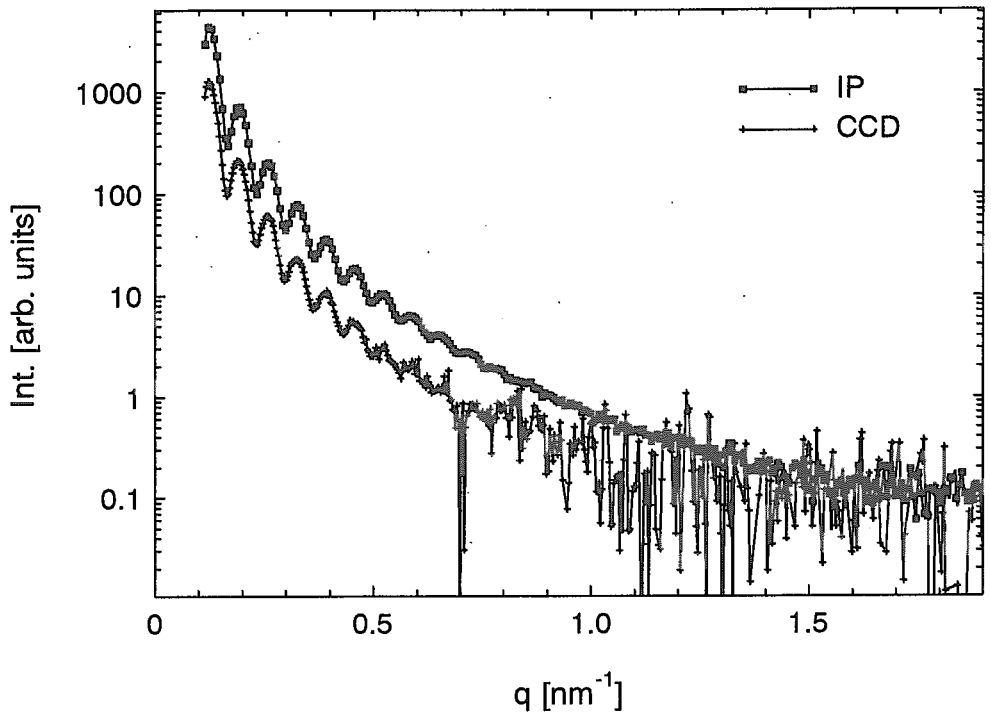

Figure 10. Comparison of the radially averaged SAXS profiles from a PMMA latex dispersion (ca. 17 Vol.%) measured with the CCD detector and an image plate (IP), respectively. In both cases the data collection time was 600 s, the sample-to-detector distance was set to 110 cm and the beamsize at the sample position was ca. 0.40 x 0.20 mm^2. Note that the counting efficiency of the IP is approximately three times higher as compared to the CCD detector. The strong fluctuations of the CCD data at higher angles are mainly due to high contributions of dark and readout noise of the detector, which have to be subtracted.

It was possible to fit the experimental data from the PMMA latex using a model that assumes a system of homogeneous spheres with a mean diameter of 93.1 nm, and a standard deviation of the particle size distribution of 5.6 %. The shape of the assumed particle size distribution function was slightly asymmetric.[10] Figure 11 shows that the data measured with the imaging plate are well fitted by such a model. In particular the

oscillations and the overall decay are well matched. The scattering curve that we measured at BL4C1 also coincides very well with SAXS data which were acquired by others[15] from the same sample at the ESRF (European Synchrotron Radiation Facility, Grenoble, France).

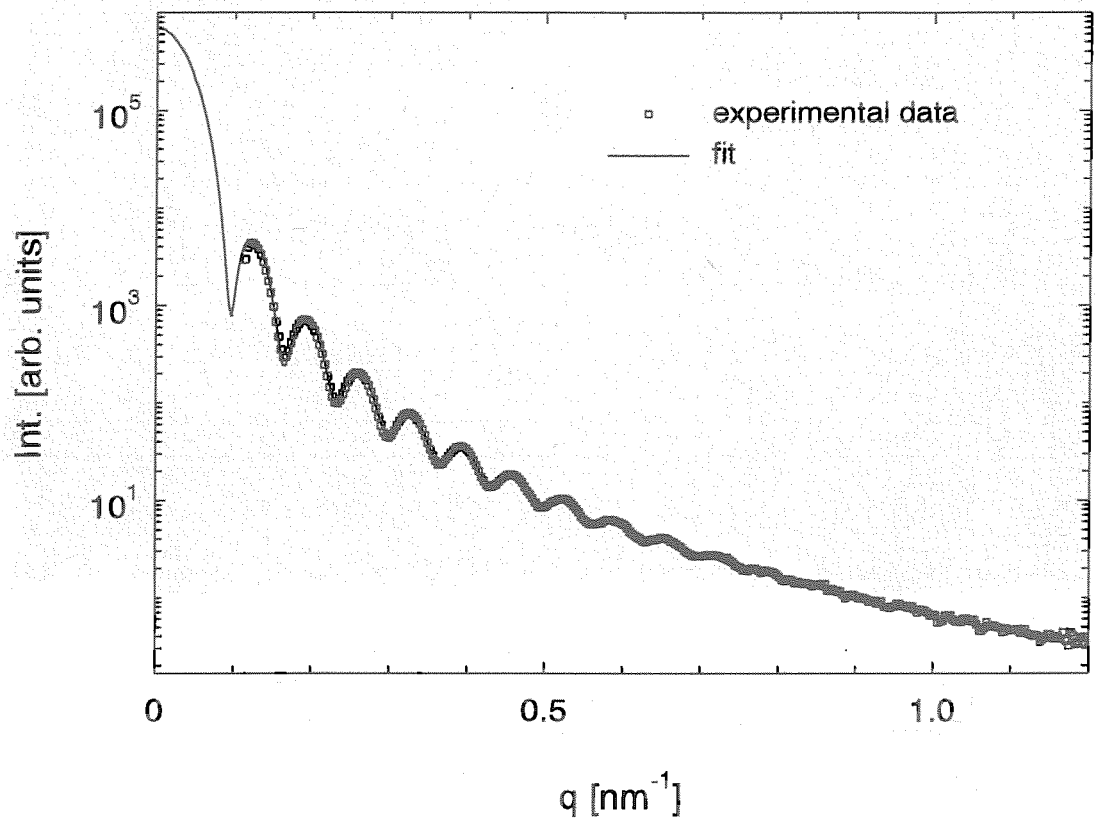

Figure 11. Radially averaged SAXS data acquired from a PMMA latex (18 vol.%) using an image plate detector. The exposure time was 600 s and the sample-to-detector distance was set to 110 cm. The experimental data were fitted with the scattering from a system of noninteracting, homogeneous spheres having an average diameter of 93.1 nm and a standard deviation of the (asymmetric) particle size distribution of 5.6 %.

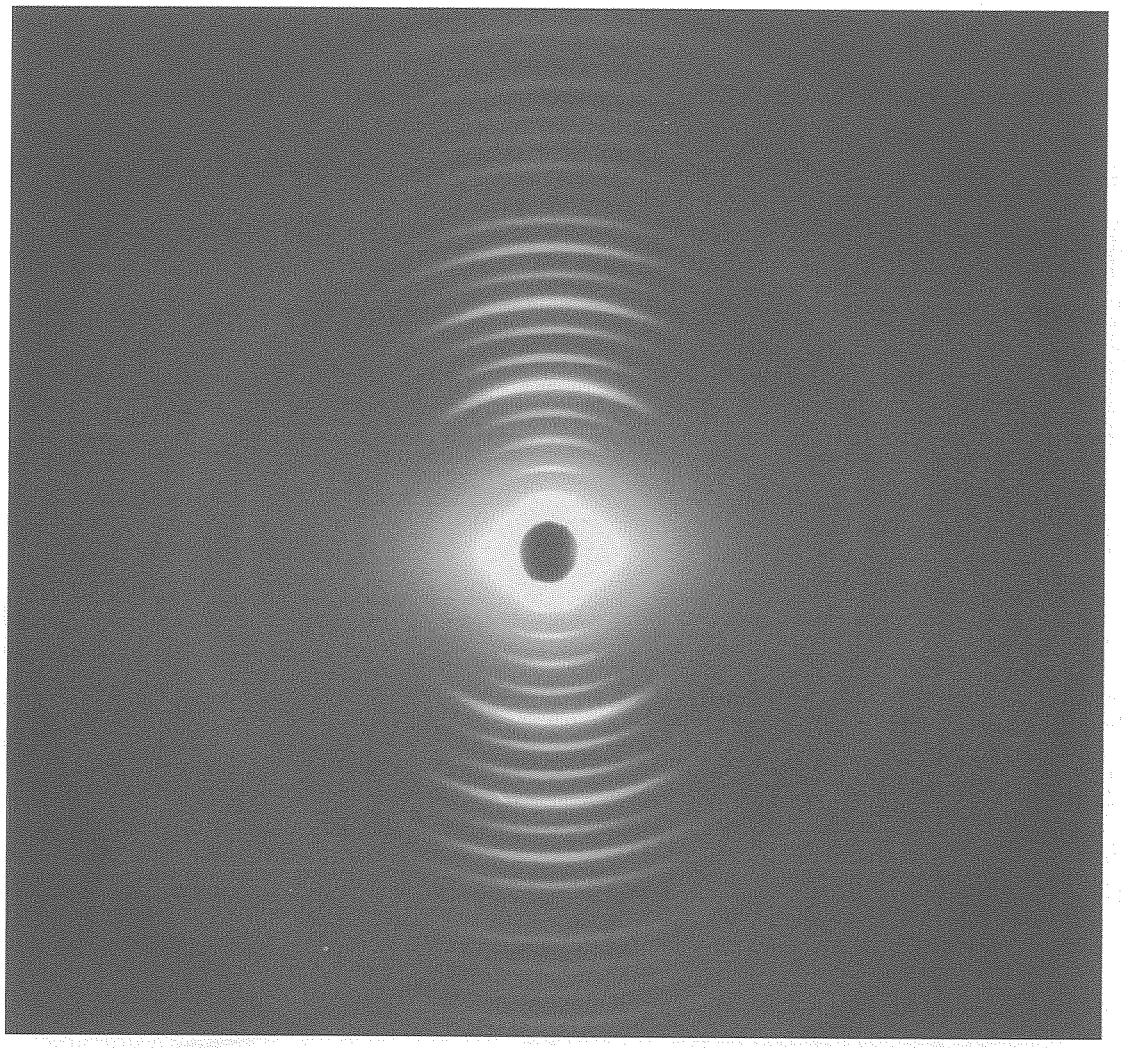

Figure 12. Diffraction pattern from a dry chicken tendon collagen acquired by the CCD detector with an exposure time of 100 s. The image is displayed on a logarithmic intensity scale in order to visualize the weaker diffraction peaks more clearly.

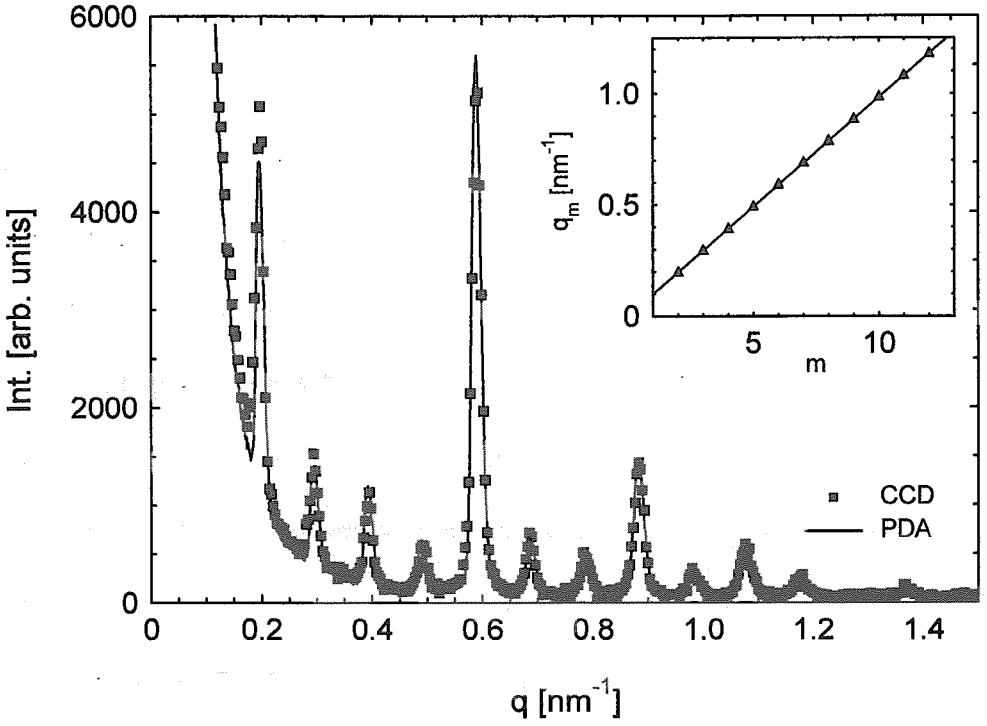

Figure 13. SAXS data measured from dried chicken tendon collagen using a CCD detector and a PDA detector at a sample-to-detector distance of 110 cm. The intensities were scaled with suitable factors to superimpose both curves, background scattering was not subtracted. The inset shows the position q_m of the Bragg peak maxima as a function of the order *m* of the peak. The slope of the linear fit curve is inversely proportional to the d-spacing.

Figure 12 displays a small angle diffraction image which was acquired from a dry chicken tendon using the CCD detector with an exposure time of 100 s and a sample-to-detector distance of 110 cm. A large number of meridional reflections, which arise due to the periodic arrangement of collagen units along the fiber axis, could be detected. The repeat distance, which was obtained by using a PMMA-latex of known particle size as a cross-calibrant, was determined to 643 Å. We observed a slow degradation of the

collagen sample, so its repeat distance should be rechecked from time to time, if it is to be used as a SAXS calibrant. Figure 13 shows a one-dimensional slice of those diffraction data together with the diffraction pattern measured by the PDA detector. As can be seen, the patterns from both detector systems coincide well. In addition, the measured interpeak distances are highly periodic (cf. inset in Figure 13, which shows that both detectors are free from a significant spatial distortion. Together with other cross-calibrated samples (e.g. lead stearate, ordered block copolymer) the chicken tendon collagen is routinely used for angle calibration and for the exact determination of the center coordinates of the incident beam. Note that the measured higher order peaks in Figure 13 are considerably broadened, mainly due to the beam polychromaticity (cf. discussion of this point in connection with Figure 3). The first order Bragg peak of collagen could not be resolved at a camera length of 110 cm. Upon increasing the distance between sample and detector to 170 cm, the resolution of the SAXS camera can be increased to ca. 800 Å.

As an example for time-resolved SAXS measurements, Figure 14 displays experimental data acquired during the isothermal crystallization of a poly(ethylene terephthalate) (PET) sample.[16] Using a dual-chamber temperature jump unit, the sample was first molten at 280°C in the upper chamber, and then rapidly transferred into another chamber (which is aligned in the X-ray beam), where the isothermal crystallization was carried out at 225°C. Successive SAXS profiles were collected by the PDA detector with an acquisition time of 10 s per scan. During the induction period only diffuse scattering curves without maxima were observed. Above 90 s, a distinct scattering maximum appears. It progressively moves to higher scattering angles with time and simultaneously the integral scattering intensity (invariant Q) increases. The

angle position of the broad diffraction peak is related to the average separation (long period L) of crystalline regions within a lamellar stack. Using a correlation function approach,[17] the change of morphological parameters (such as lamellar and amorphous layer thickness) could be extracted from the experimental data as a function of time.

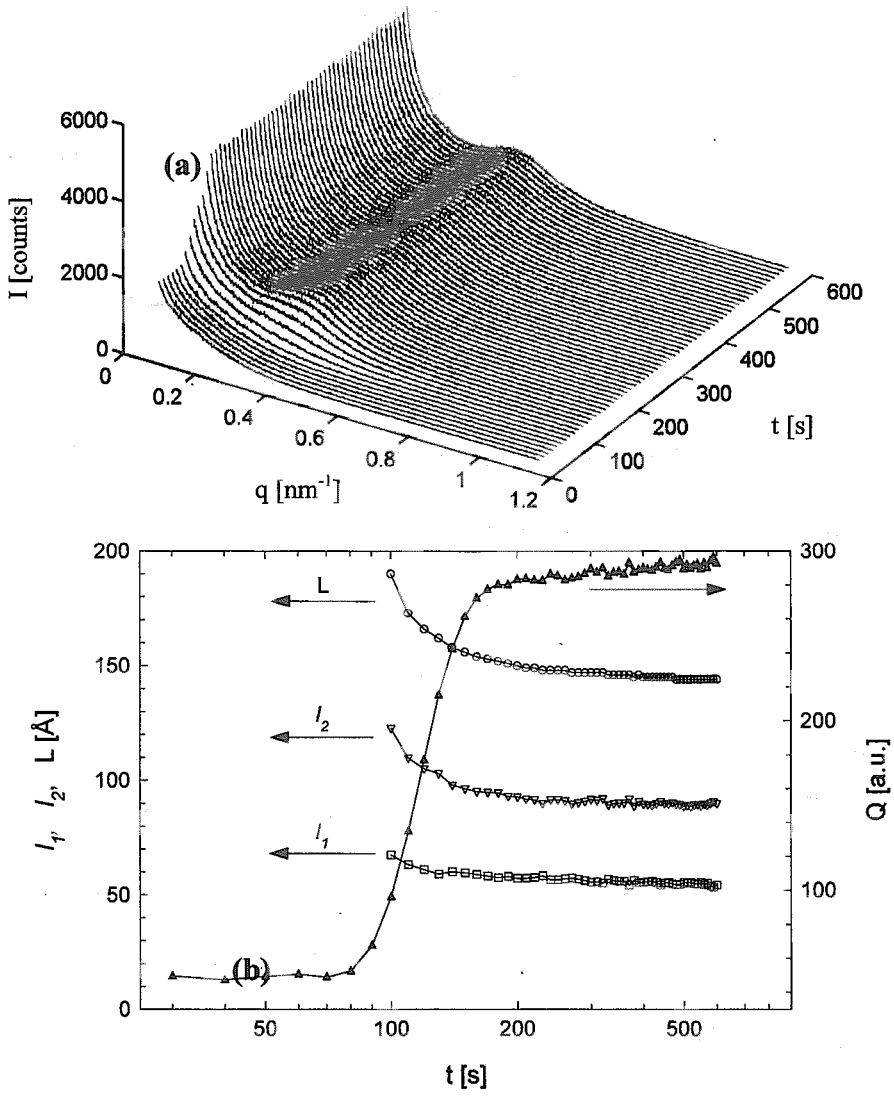

Figure 14. **(a)** Time-resolved SAXS patterns as collected during the isothermal crystallization of PET at 225°C. **(b)** Morphological parameters which were obtained from the data analysis: Long period L, lamellar thickness l_1, and amorphous layer thickness l_2. Q denotes the scattering invariant.

Upon decreasing the sample-to-detector distance to ca. 10 cm, wide-angle diffraction (WAXD) measurements can be performed. As already discussed in connection with Figure 3, a desmearing of the experimental data due to the wavelength spread in the incident beam is required when well-ordered samples are to be investigated. Corrections for the polarization factor and for smearing and distortion of the data due to the oblique incidence of the scattered beam on the flat detectors (because the solid angle subtended by one pixel on the detector changes with the scattering angle) are also required.[2,18] Furthermore, the $1/r^2$-dependence of the scattered intensity, as well as the angle-dependence of the absorption factor (inside the sample and between sample and detector) have to be considered. Note that all those points are of no concern for SAXS, due to the validity small angle approximation in that regime. A typical application of WAXD which was performed at BL4C1 is the time-resolved study of the thermal imidization of a precursor polymer to yield the corresponding polyimide. Some of the time-resolved WAXD measurements are shown in Figure 15. In this measurement the film sample was heated with 2.0 K/min to 380°C in the upper chamber under nitrogen atmosphere, dwelled at that temperature for 30 min, and cooled down to room temperature. WAXD profiles were collected by the PDA detector with an acquisition time of 10 s per scan. During early stage of heating up to around 120°C only poorly developed structural features were observed. Above 124°C distinct diffraction peaks appear, indicative of the structural evolution induced by the thermal imidization. For the newly developed each diffraction peak, its angle position changed and the intensity became strong as temperature elevated. The angle position corresponds to the Bragg d-spacing. Further, the coherence length L_c was estimated. As representative

examples the d-spacings and L_cs determined for the Peak 1 and Peak 3 are plotted in Figure 15 as a function of temperature.

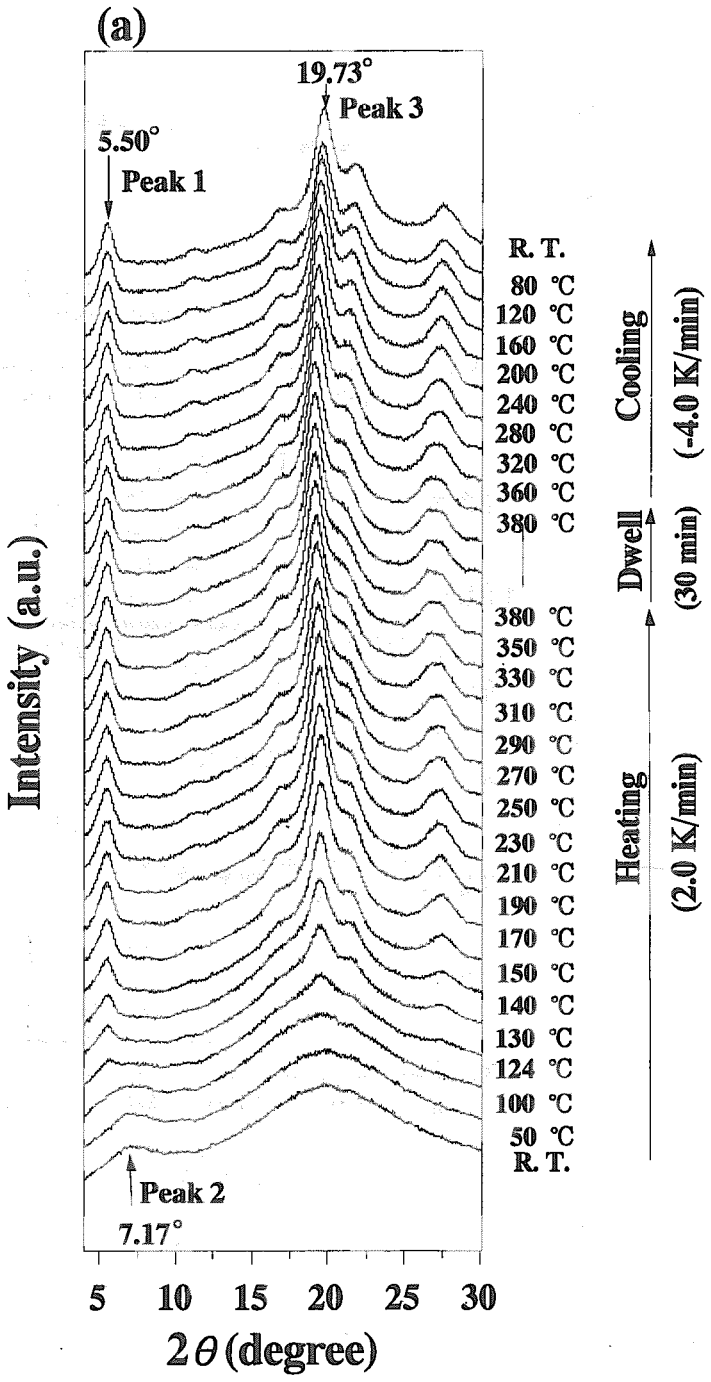

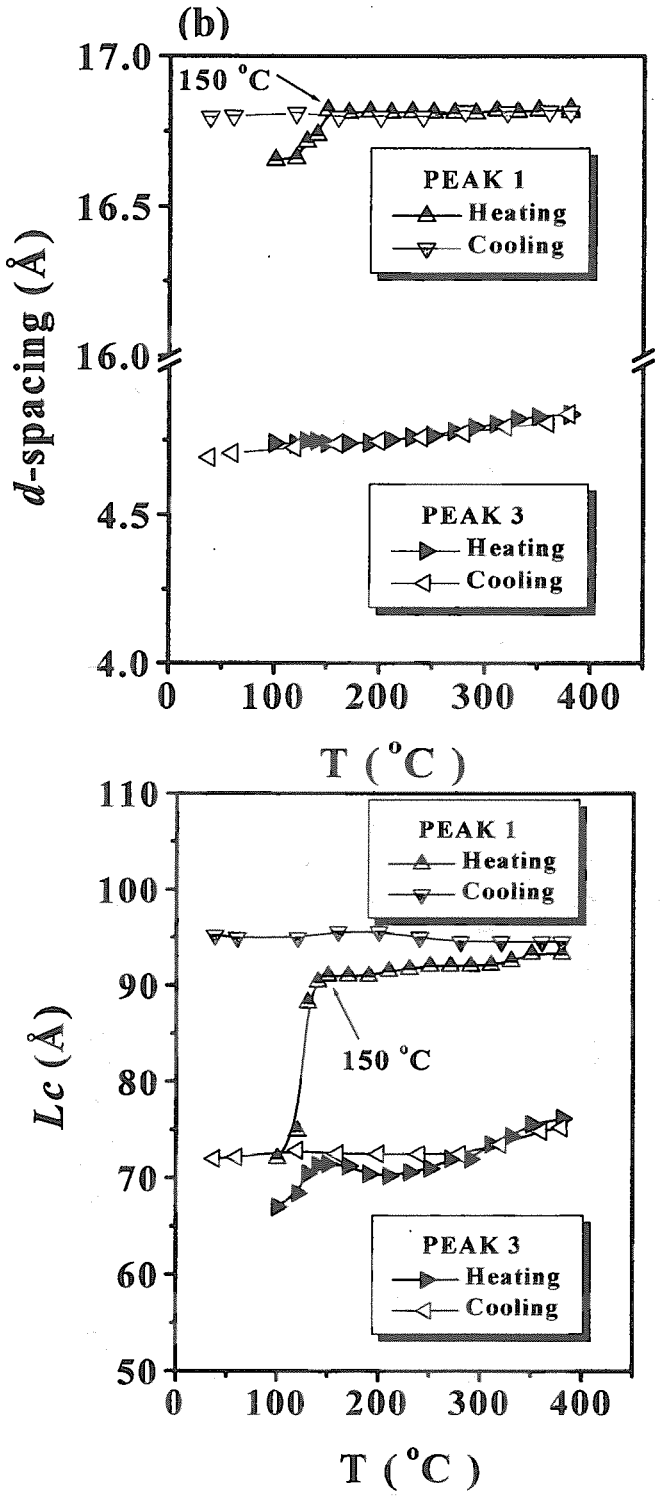

Figure 15. **(a)** WAXD patterns measured during thermal imidization of PMDAODA-34 precursor polymer and subsequent cooling. **(b)** Morphological parameters which were obtained from the data analysis: *d*-Spacing and coherence length L_c.

7. Conclusions

The beamline BL4C1 (SAXS-1 Beamline) of PAL is the first dedicated synchrotron small-angle X-ray scattering station in Korea, which meets the basic requirements of the rapidly growing domestic SAXS user community. The X-ray source is a bending magnet which produces white radiation with a critical energy of 5.5 keV. A synthetic double multilayer monochromator is adopted, which selects quasi-monochromatic radiation with a bandwidth of ca. 1.5 % that is sufficient for most SAXS measurements and allows a considerably higher flux at the sample as compared to monochromators using single crystals. Higher harmonics from the monochromator are rejected by reflection from a flat mirror, and a slit system is installed for collimation. A CCD system, two one-dimensional photodiode arrays (PDA) and imaging plates (IP) are available as detectors, depending on the SAXS users' needs. The CCD and PDA detectors are suitable for diffraction measurements but give unsatisfactory data from weakly scattering samples due to their high intrinsic noise. By using the IP system smooth scattering curves could be obtained in a wide dynamic range.

In order to increase the photon flux at the sample position, a toroidal mirror will be installed at the beamline, using a 2 : 1 focusing geometry. Another slit will be added to further reduce the parasitic scattering at smallest angles. To increase the angle resolution, the maximum camera-to-sample distance will be extended to 3 m. Another area detectors, Gabriel-type gas-filled proportional counters (1-D and 2-D) will be available for measuring samples with low scattering intensities. It is also planned to facilitate simultaneous SAXS/WAXD measurements. Absolute scattering intensities

will be obtainable through cross-calibrated standard samples. These upgrading works will be completed by August of 2002.

The second SAXS beamline BL4C2 (SAXS-2 beamline) is under construction. The major part of the beamline construction was done now. This is another bending magnet based beamline but the optics is based on a double crystal monochromator, two toroidal focusing mirrors and three sets of slits. The energy resolution of the monochromatized X-ray source will be <0.01 %. Its end station (i.e., experimental hutch) is under design, which will be filled by specially designed optic tables with a SAXS/WAXD camera system and a 4-circle diffractometer. A CCD area detector and gas-filled wire area detectors (1-D and 2-D) will be available by the end of 2002.

A third SAXS beamline (SAXS-3 beamline) is also planned to construct on one of undulator insertion devices in 2005. The beam flux at the experimental station would be at least two orders higher than those of the SAXS-1 and SAXS-2 beamlines. Further, the beamline will have much higher energy resolution and be equipped with the state of art 1-D and 2-D detectors which can allow rapid time-resolution and give the highest spatial resolution.

The SAXS beamlines become very important advanced tools for structural investigations on various commodity and advanced materials in Korea. Together with the SAXS facilities at PAL, the wide-angle and small-angle neutron scattering beamlines at the Hanaro Center of Korea Atomic Energy Research Institute open a wide view of features to the fundamental and applied researches of functional and high performance materials.

Acknowledgments

This work was supported in part by the Ministry of Science & Technology and POSCO, by the Center for Integrated Molecular Systems (Korea Science & Engineering Foundation), and by the Ministry of Education (BK21 Functional Polymer Thin Films).

References

(1) A. Guinier and G. Fournet, *Small Angle Scattering of X-rays*, Chapman & Hall, London 1955.

(2) O. Glatter and O. Kratky, Eds., *Small Angle X-ray scattering*, Academic Press, London 1982.

(3) L. A. Feigin and D. I. Svergun *Structure analysis by small-angle X-ray and neutron scattering*, Plenum Press, New York, 1987.

(4) H. Brumberger, Ed., *Modern Aspects of Small-Angle Scattering*, Kluwer Academic Press, Dordrecht 1995.

(5) R.J. Roe, *Methods of X-ray and Neutron Scattering in Polymer Science*, Oxford Univ. Press, Oxford 2000.

(6) S. Doniach, *Chem. Rev.*, **101**, 1763 (2001).

(7) P. Cebe, B. S. Hsiao (ed.), and D.J. Lohse, Eds., *Scattering from Polymers: Characterization by X-rays, Neutrons and Light*, ACS Symposium Series 739, Oxford Univ. Press 1999, and further references given therein.

(8) B. Chu and B. S. Hsiao, *Chem. Rev.*, **101**, 1727 (2001).

(9) T.-Y. Lee, J. Choi, Y. Chung, J.Y. Huang, J.M. Lee, S.H. Nam, H.S. Youn, *Nuclear Instruments and Methods in Physics Research A*, **467–468**, 47 (2001).

(10) N. Dingenouts, J. Bolze, D. Pötschke, and M. Ballauff, *Adv. Polym. Sci.*, **144**, 1 (1999), and further references given therein.

(11) A.P. Hammersley, S.O. Svensson, A. Thompson, H. Graafsma, Å. Kvick, and J. Moy, *Rev. Sci Instr.*, **66**, 2729 (1995).

(12) R.G. Gilbert, *Emulsion Polymerization*, Academic Press, London, 1995.

(13) N. Dingenouts and M. Ballauff, *Langmuir*, **15**, 3283 (1999)

(14) T. Fujisawa, Y. Inoko, and N. Yagi, *J. Synchr. Rad.*, **6**, 1106 (1999).

(15) N. Dingenouts, *Röntgenkleinwinkelstreuung als Methodik der Strukturanalyse teilgeordneter Systeme*, Shaker Verlag, Aachen 1999.

(16) S.W. Lee, B. Lee, and M. Ree, *Macromol. Phys. Chem.*, ***201***, 453 (2000).

(17) G.R. Strobl and M. Schneider, *J. Polym. Sci.*, **18**, 1343 (1980).

(18) P. Norby, *J. Appl. Cryst.*, **30**, 21 (1997)..

1. Workshop

Abstract & Papers

Neutron Activation Analysis

This is a blank page.

JP0250098

1.14 Introduction of the Neutron Activation Analysis Facilities in High Flux Engineering Test Reactor

Feng Mingquan

(Nuclear Power Institute of China, Chengdu, 610005, P.R. China)

Abstract

Neutron activation is used for minimum element analysis widely in agriculture, biological medicine, geology and metallurgy. Based on High Flux Engineering Test Reactor, the "rabbit" facilities and neutron activation analysis system for the minimum impurity analysis of silicon doping and production of short-life isotopes were developed by Nuclear Power Institute of China (NPIC). They include "rabbit" irradiation rig and supporter in reactor vessel; sample entry and distributor; active gas purifier; sample stripped and storage; pneumatic transportation and γ spectrum analysis system. Each inner dimension of three irradiation boxes is 15mm in diameter and 30mm in length; the speed of pneumatic transportation is at ≤15mm/sec. Thermal neutron (E<0.625ev) flux of the "rabbit" channel is at $(0.6\sim1.4)\times10^{14}$n/cm^2.sec.

The "rabbit" facilities are applied to analysis of minimum elements (such as Ag Se Cr Sn Sb Fe Zn Co) for silicon doping. Production of short-life isotopes and other application are developing.

Keywords: HFETR Rabbit facilities Activation analysis

1 Introduction

Neutron activation is a high sensitive and non-destructive analysis method. It is widely used for minimum element analysis in agriculture, biological medicine, geology, metallurgy, and archaeology as well as environment control. Because of high thermal neutron flux in High Flux Engineering Test Reactor (HFETR), irradiation time of specimen can be shortened in seconds for neutron activation analysis. The sensitivity of analysis can be improved too. The neutron activation analysis systems (rabbit facilities) in HFETR have been established in order to develop the

utilization of HFETR. The main purpose is for the analysis of minimum impurity element in silicon neutron irradiation processing and the production of short-life isotope indicators with high specific activity.

2 Design of the Rabbit Facilities

Taking some particularities in HFETR as following pressured tank type reactor, no any horizontal irradiation channel and neutron energy spectrum harder into account, it must be complied with the design principles as follow:

a. more than 8m vertical irradiation rig to be used;

b. irradiation rig must be bear pressure more than 1.65Mpa;

c. γ heating of specimen low;

d. accurate irradiation time and location;

e. high fly speed of specimen;

f. leakage of activated gases as low as possible;

g. radioactive ray disturbance of γ spectrometry measurement small;

h. operation of the whole system easily;

i. Safety and reliability of rabbit facilities.

3 Outline of the Rabbit Facilities

3.1 Technological process

The facilities consist of sample entry; active gases purifier, irradiation rig, sample distributor, sample stripped, storage, γ spectrum analysis, and pneumatic transportation as well as control protection system. The flow

diagram of the facilities shows in Fig.1. When rabbit (sample box) run

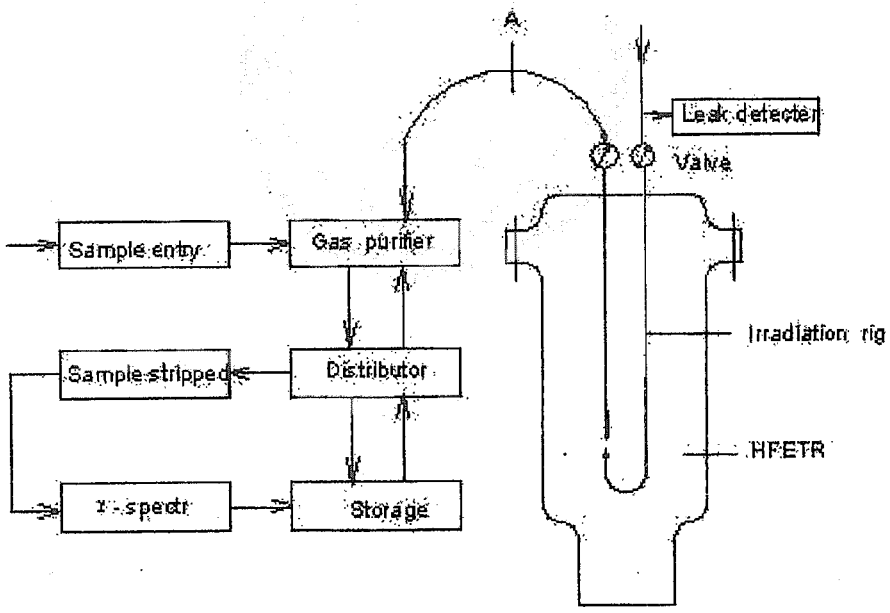

Fig 1. Flow diagram of the rabbit facilities

into point A of arch transportation tube, it slows down to irradiation rig controlled by buffer gas. The rabbit from the rig enters purifier for clean, then pass distributor or to be stripped and measured either to be stored. For protecting vibration of the rig from water flowing in the core, 32 anti-shake rings are fixed at a space of 200mm in axial and a supporter is installed at the middle of the rig in reactor vessel. The rig is 8750mm in length and 63mm in diameter. Its cross section shows in Fig.2. The two safety valves are mounted respectively rabbit tube and gas tube at the top of HFETR, and controlled by the threshold signal from minimum humidity analysis instrument for avoid coolant water into rabbit system

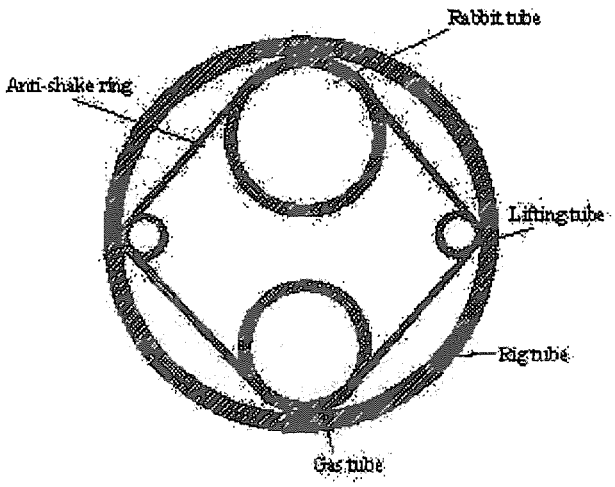

Fig2. Cross section of the rig

and out of the core. In order to detect rabbit pass through point A and control irradiation time, a photoelectric device is mounted at point A of arch rabbit tube.

3.2 System parameters

a. irradiation channel: Be reflector R-11 channel;

b. thermal neutron flux: (0.6~1.4)× 10^{14}n/cm^2.s;

c. size of sample box: ϕ15×30mm;

3 boxes can be irradiated simultaneously

d. speed of transportation: ≤15m/s;

e. pressure of pneumatic transportation: ~0.2Mpa;

f. flow of coolant gas: ~8.5m^3/h;

3.3 Characteristics of the Facilities

a. high thermal neutron flux;

b. The all process (including sample enter, irradiation, exit and stripped) automatically.

c. the run line and location of sample box visible with photoelectric;

d. accurate irradiation time;

e. better gas quality purified by oil-water separator;

f. sample box exit the rig, then safety valves closed within 1 second after alarm.

4 Applications of the Facility

The rabbit facilities are applied to analysis of minimum elements for improving quality of single crystal silicon neutron irradiation processing. The typical analysis results are shown in table 1. Production of short-life

Table 1. the results of neutron activation analysis for silicon doping

	Company A-1	Company A-2	Company B-3	Company B-4	Company *
Co	$\leq 1.2\times10^{-9}$	$\leq 1.0\times10^{-9}$	$\leq 1.4\times10^{-9}$	$\leq 1.3\times10^{-9}$	$\leq 5.0\times10^{-8}$
Ag	$\leq 3.9\times10^{-8}$	$\leq 3.4\times10^{-8}$	$\leq 4.6\times10^{-8}$	$\leq 4.4\times10^{-8}$	$\leq 2.8\times10^{-8}$
Se	$\leq 3.6\times10^{-7}$	$\leq 3.7\times10^{-7}$	$\leq 4.7\times10^{-7}$	$\leq 5.2\times10^{-7}$	/
Cr	$\leq 1.0\times10^{-8}$	$\leq 1.2\times10^{-8}$	$\leq 1.4\times10^{-8}$	$\leq 1.6\times10^{-8}$	$\leq 1.0\times10^{-8}$
Sn	1.2×10^{-7}	1.0×10^{-7}	$\leq 8.7\times10^{-7}$	$\leq 9.1\times10^{-7}$	/
Sb	1.0×10^{-9}	1.4×10^{-9}	1.0×10^{-9}	1.2×10^{-9}	$\leq 2.0\times10^{-8}$
Fe	$\leq 3.2\times10^{-7}$	$\leq 3.8\times10^{-7}$	$\leq 6.9\times10^{-7}$	$\leq 6.5\times10^{-7}$	$\leq 2.5\times10^{-7}$
Zn	$\leq 1.1\times10^{-8}$	$\leq 3.2\times10^{-8}$	$\leq 1.1\times10^{-8}$	$\leq 1.2\times10^{-8}$	/

Note: * analyzed by mass spectrometry,

isotopic indicators and other application are developing. The table 2 shows the calculation results for production of some short-life isotopic indicators.

Table 2. calculation results for production of short-life isotopic indicators

isotopic indicators	half-life	reaction cross sect. 10^{-24}cm	abundance %	irradiation time	Specific activity Bq/g
^{24}Na	15.02h	0.53	100	1h	3.15×10^{10}
^{32}P	14.28d	0.18	100	1d	8.14×10^{9}
^{42}K	12.36h	1.46	6.7	1h	4.10×10^{9}
^{46}Sc	83.8d	29.00	100	1d	1.61×10^{11}
^{51}Cr	27.7d	15.90	4.35	1d	1.03×10^{10}
^{64}Cu	12.7h	4.40	69.2	1h	7.73×10^{10}
^{76}As	1.10d	4.30	100	1h	4.48×10^{10}
^{82}Br	1.50d	2.70	49.6	1h	9.96×10^{9}
^{86}Rb	18.65d	0.41	17	1d	9.03×10^{8}
^{89}Sr	50.53d	0.01	82.56	1d	1.92×10^{7}
^{90}Y	2.67d	1.28	100	1d	9.92×10^{10}
^{110m}Ag	250.4d	4.50	48.18	1d	1.66×10^{9}
^{115}Cd	2.23d	0.30	26.7	1d	5.92×10^{9}
^{122}Sb	2.72d	6.25	57.25	1d	2.00×10^{11}
⋮	⋮	⋮	⋮	⋮	⋮
⋮	⋮	⋮	⋮	⋮	⋮
^{140}La	1.68d	9.00	99.91	1h	3.32×10^{10}
^{197}Pt	18h	0.79	25.30	1h	1.16×10^{9}

Note: in the case of thermal flux at 5×10^{13}n/cm^2.s

5 Conclusion

The rabbit facilities in HFETR have been completed some tests and neutron activation analysis. It fulfils the requirements of design, manufacture and installation as well as the demands of the reactor for safety operation. There is a good prospect for neutron activation analysis and other application.

JP0250099

1.15 CURRENT STATUS AND PROGRESS OF RESEARCH AND DEVELOPMENT OF NAA AT GA. SIWABESSY REACTOR*)

By

Sutisna[1], Saeful Yusuf[1], Rukihati[1], Sri Wardani[2], Amir Hamzah[2], Th. Rina M[2]
[1]Research and Development Center for Materials Science and Technology
[2]Center for Development of Research Reactor Technology

ABSTRACT

Progress of R & D on Neutron Activation Analysis (NAA) at G.A. Siwabessy research reactor briefly presented in this paper. We describe a current status and research progress that cover of application of NAA technique, a software development and an improvement of laboratory capability. Future program and collaboration plans are also presented. Application of Instrumentation Neutron Activation Analysis (INAA) technique has been used on environmental study to solve a pollution problem, especially for a trace elements determination on water and soil samples. Trace elements determinations have been carried out in Ciliwung river water sample using a combination of INAA and pre-concentration method. River water sample was taken from a five sampling site of Ciliwung River, from Kedung Badak at Bogor area to Marina Beach at Jakarta area. We have been determine some toxic elements such as As, Ag, Mn, Fe, V, Hg, Co and Zn which have quantities depended on sampling site. The analytical results show some elements have quantity higher compare to government regulation value. Soil analysis has been carried out in Puspiptek area using non-destructive method. In this study we applied an enrichment factor to estimate a pollution level of the soil. Meanwhile the software developments have been done to support the environmental study. Examination of this software was done using standard reference materials of NIES CRM 3, NIST SRM 1646a, NIST SRM 1573a and NIST 1648 and we compare our result to a certified value of NIES and NIST. Quantitative analysis results show that elements of Cr, Co, Sb, As, Cd, Mn, Sc, Se, V and Na have a good enough precision and accuracy of about 5 – 10%. Meanwhile for other elements, such as Hg and Zn, they have a precision and accuracy of about 11 – 15 %. A capability of the NAA laboratory is going to improve by applying a quality system based on ISO/DIS 17025. At present time, we are going ahead with our laboratory accreditation program to obtain international recognition for our laboratories. We also introduce a k_0 and PGAA method to develop INAA technique. Some research work have been prepared with Environmental Management Center (EMC) and Osaka University in order to determine trace elements contained on suspended particulate matter at Jakarta Metropolitan area.

Key words: INAA, Environmental pollution, Pollutant, Trace elements analysis, Enrichment factor

INTRODUCTION

The GA. Siwabessy research reactor located at Serpong, Indonesia, is one of three-research reactor operated in Indonesia. The reactor irradiation facilities includes in a core irradiation position, four hydraulics transfer system and one pneumatic transfer system. The reactor also has a neutron beam facility for research and development in materials science.

*) Presented in *The 2000 Workshop on the Utilization on Research Reactor*, Taejon, November 20-24, 2000, Korea

The main utilization of GA Siwabessy reactor is in the R & D of science and nuclear technology, such as: radioisotope production for medical purpose, application of neutron beam for materials science and technology research, fuel elements testing, nuclear instruments examination and, neutron activation analysis.

The activities of neutron activation analysis in GA. Siwabessy reactor have been doing since 1990. The NAA was intensive applied in field of wide range for instance an environmental study, geological, biological and industrial materials. In the last five years, we focused in analysis of trace elements in environmental samples such as: airborne particulate matter, water, soil and sediment. We believe that the analysis results will be a great help for the environmental monitoring management.

In this paper we present a briefly a progress of R & D in the NAA and the future program.

RESEARCH PROGRESS

Environmental Study

Utilization of INAA technique in the environmental is intensive used to solve a pollution problem, especially in a contaminated air, water and soil. The research has a priority on evaluation and determination of elements that have potentially a toxic effect to human.

Water is an object that very important to be study because it is potentially contaminated by pollutant released from industrials activities, such as textile industry, dry battery factory and automotive assembly. Quantity of toxic elements contained in the water polluted is very small and some times very difficulty to determine by non-nuclear method. Combination of pre-concentration method and INAA technique could improve a sensitivity determination. We use this method for trace elements determination on water sample.

We have been determine a Ag, As, Co, Mn, Fe, Hg, V, and Zn on the Ciliwung river water sample taken from five sampling point, i.e., Kedung Badak (KBK), Pancoran Mas (PMS), Tanjung Barat (TBR), Kampung Melayu (KMB) and Pantai Marina (MAR). Figure 1 shows an elemental distribution for all sampling point [1].

According to the Indonesian Government Regulation No. 20/1990 about Category A Water Quality, the concentrations of Fe, Mg and Mn were significant higher than its value permitted. A quantity of As in all sampling point is in the range of permitted value, except for

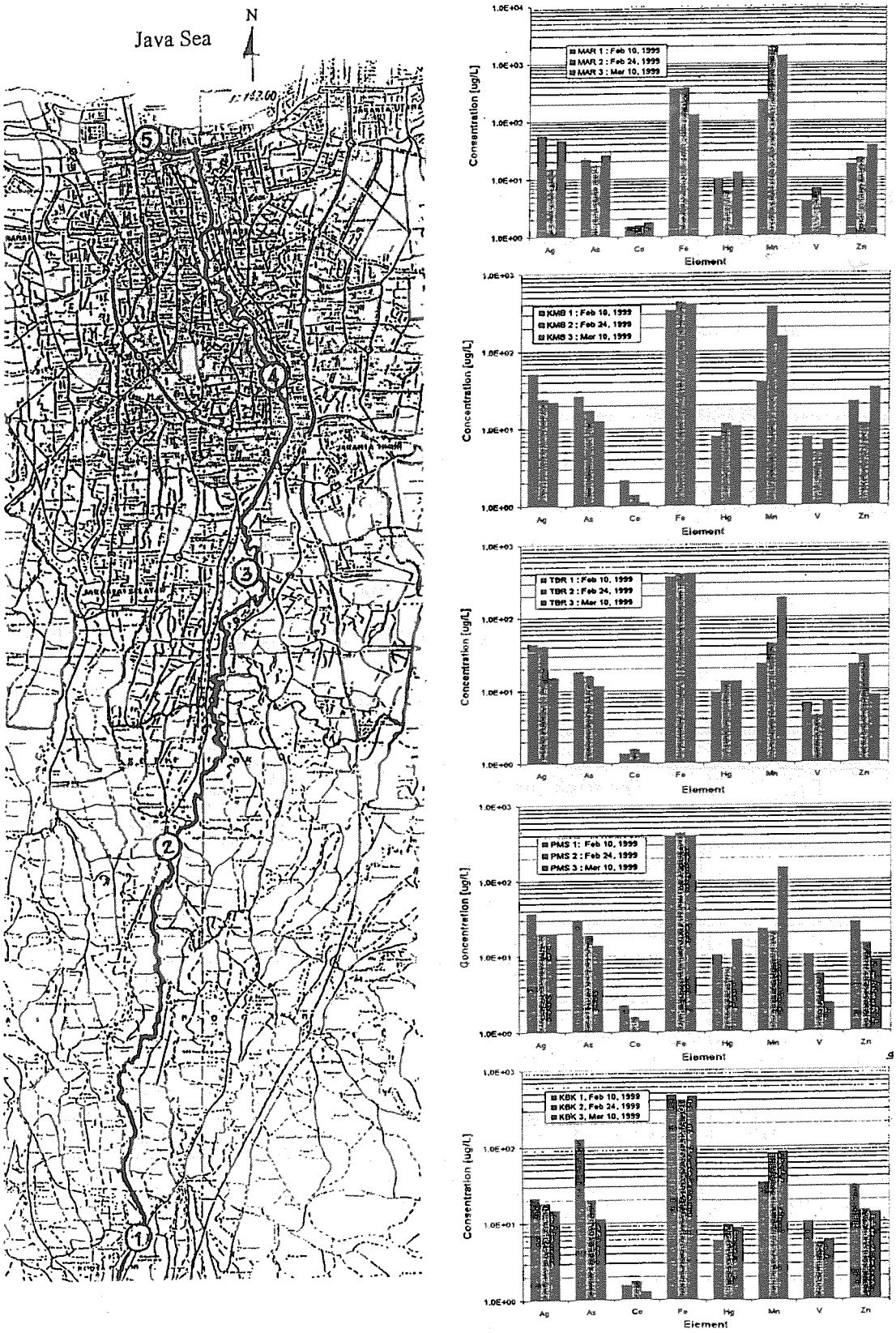

Figure 1 : The distribution of elements detected at five sampling point, i.e : (1) Kedung Badak, (2) Kampung Melayu Besar, (3) Tanjung Barat, (4) Pancoran Mas and (5) Pantai Marina [1].

the first sampling at Kedung Badak sampling point. Its value is three times comparing to others value. In case of Mn, it has a quantity relatively high for all sampling point, especially at Pantai Marina sampling point. From this analysis results we conclude that the Ciliwung River was polluted with some toxic elements that probably coming from human activities as well as the industrial activity alongside the river.

Soil analysis has been doing since 1966, which involve an Environmental Management Center (EMC) and Center for Development of Radioactive Waste Management (CDRWM). Determinations of elements in surface soil have been done using INAA technique, which involve a non-destruction method. Soil samples were collected from nine sampling point at PUSPIPTEK area. In this study, we use CRM IAEA Soil 7 as comparator to control the analytical results. The enrichment factor was used to estimate the enrichment level of element. This factor is calculated for each element in the samples, and we use the Al reference element as proposed by Vinogradov [2]. The enrichment factor close to unity would indicate that a particular element is identical to its appearance in the crustal origin. While as the enrichment factor of ten or greater is indicative that the source of the element is

Table 1. Some analytical result of elements concentration in certified reference material of IAEA CRM Soil 7 [1].

No.	Elements	Our result [μg/g]		IAEA [μg/g]	
		Mean	Range value	Mean	Range value
1.	Al*	4.3	3.9 - 4.7	4.7	4.4 - 5.1
2.	Ce	52.4	50.1 - 54.7	61.0	50.0 - 63.0
3.	Co	7.6	7.4 - 7.8	8.9	8.4 -10.1
4.	Cr	52.9	50.8 - 55.0	60.0	49.0 - 74.0
5.	Cd	1.1	0.6 - 1.6	1.3	1.1 - 2.7
6.	Eu	0.9	0.6 - 1.1	1.0	0.9 - 1.3
7	Fe*	2.6	2.4 - 2.9	2.6	2.5 - 2.6
8.	Hf	5.5	5.0 - 6.4	5.1	4.8 -5.5
9.	La	27.0	36.8 - 30.0	28.0	27 - 29
10.	Mn	654	612 - 694	631	604.0 - 650.0
11.	Sb	1.8	1.6 - 2.7	1.7	1.4 -1.8
12.	Sc	7.9	5.8 - 9.7	8.3	6.9 - 9.0
13.	V	60.6	53.5 - 67.7	66	59.0 - 73.0
14.	U	3.0	1.7 - 3.9	2.6	2.2 -3.3
15.	Zn	94.6	83.9 - 105.6	104	101.0 - 113.0

*Unit in %

anthropogenic in nature. That is, its source is not from the natural environment [2-4].

The analysis results of CRM IAEA Soil 7 show in Table 1. Meanwhile the elemental concentration and the enrichment factor of elements detected presented in Table 2. A total of 16 elements were analyzed in the soil samples. Six of them, i.e., Al, Fe, Mn, Na, K and Ti, have a concentration range of 0.1% - 16.2% and the others were in order of mg/kg. The result shows that the enrichment factor of all elements is less than 10. It indicated that it is not any anthropogenic contribution [5].

NAA software development

We develop ourselves a new software for gamma rays analysis to support R & D in INAA. The research had been successfully establishing software for neutron activation analysis. Examination of program obtained has been done using some materials that its properties and its characteristic are known. The materials were used are Standard Reference Materials (SRM) as well as Certified Reference Materials (CRM). The software performance is demonstrated with of capability to identify a nuclide. Identification capability of new software was compared to the Gamma Trac software, and we define a quantity of nuclide identification in %

The comparison result show that the new software is better than Gamma Trac software for identification of long half life radionuclide, i.e., 93.3% for new software and 66.6% for Gamma Trac. Meanwhile in case of short half-life radionuclde, new software is worse (65.3%) than the Gamma Trac (80.9%) [6]. Analytical result shows that a precision and accuracy are good enough, however some software module should be improve. Quantitative analysis result shows that the elements of Cr, Co, Sb, As, V, Cd, Mn, Sc, Se and Na have a deviation of 5% ~ 13%. Meanwhile the Hg and Zn have a deviation of 11% ~15% as shown in the Table 3 [7].

Improvement laboratory capability

In a free market era, a competition of testing and calibration laboratory for services and analysis is going to hard. The laboratory must provide a result data that have a high confidence level. According to those reason, we study and develop a method and procedure of materials testing and characterization that compliant to national and international quality standard. Standardized procedure has been carried out for analysis of rear earth element in

Table 2: Analysis result of soil samples taken from PUSPIPTEK area. The enrichment factor (EF) value was obtained by calculation. All values are in mg/kg unit, except denoted by * in % [5].

Ele-ment	Guest House		Block IV		Power House		Water Tower		P3M		LAGG		LSDE		P3KIM		LUK		Range value	
	Mean	EF	Mean	EF	Mean	EF	Mean	EF	Mean	EF	Mean	EF	Mean	EF	Mean	EF	Mean	EF	Min	Max
Al*	15.2	1	16.2	1	15.6	1	15.3	1	15.9	1	8.8	1	14.5	1	13.5	1	15.1	1	8.8	16.2
As	8.9	0.8	8.6	0.8	5.6	0.5	12.9	1.2	8.9	0.8	20.4	3.3	7.5	0.7	6.1	0.6	6.4	0.6	5.6	20.4
Ce	70.9	0.7	60.1	0.5	70.5	0.6	72.1	0.7	73.7	0.7	45.7	0.7	52.2	0.5	46.7	0.5	60.5	0.6	45.7	73.7
Co	31.6	0.3	22.3	0.12	21.8	0.2	17.9	0.2	39.7	0.3	23.2	0.3	28.5	0.3	32.7	0.3	33.0	0.3	17.9	39.7
Cr	22.2	0.05	22.4	0.05	8.6	0.02	8.9	0.02	17.8	0.04	28.5	0.1	23.3	0.05	17.7	0.05	17.6	0.04	8.6	28.5
Fe*	8.1	1.0	7.4	0.9	7.2	0.9	5.0	0.6	8.3	1.0	8.1	1.7	8.6	1.1	8.0	1.1	9.3	1.2	5.0	9.3
Hf	6.0	0.5	6.5	0.5	6.6	0.5	10.7	0.8	7.1	0.5	5.8	0.8	5.3	0.4	5.0	0.4	4.9	0.4	4.9	10.7
K	824	0.03	577	0.02	392	0.01	33851	1.2	515	0.02	3767	0.2	1355	0.05	963	0.04	465	0.02	392	33851
La	21.2	0.3	17.3	0.2	18.6	0.2	25.4	0.3	16.8	0.2	17.9	0.4	19.0	0.2	17.6	0.2	22.4	0.3	16.8	25.4
Mn*	0.3	1.7	0.3	1.4	0.1	0.6	0.3	1.3	0.3	1.3	0.2	1.4	0.3	1.5	0.2	0.9	0.2	1.1	0.1	0.4
Na	437	0.03	445	0.03	253	0.02	3173	0.2	251	0.02	7351	0.9	2815	0.2	1079	0.1	158	0.01	158	3173
Sc	29.2	1.9	29.2	1.8	29.9	1.9	18.5	1.2	31.9	2.1	25.3	2.9	26.6	1.9	26.0	1.9	37.9	2.6	18.5	37.9
Th	9.7	0.8	9.3	0.7	0.9	0.7	14.4	1.1	11.0	0.8	6.8	0.9	9.6	0.8	9.5	0.8	7.8	0.6	6.8	14.4
Ti*	0.9	0.9	0.9	0.9	0.9	0.9	0.5	0.6	1.0	1.0	0.6	1.1	0.9	1.0	1.0	0.1	1.4	1.4	0.5	1.4
U	1.7	0.8	1.7	0.8	2.0	0.9	2.5	1.2	2.1	0.9	1.3	1.0	2	1.0	2.2	1.2	0.9	0.4	0.3	2.5
V	233	1.1	162	0.7	183	0.9	138	0.6	270	1.2	161	1.3	290	1.4	253	1.3	256	1.2	137	290

Table 3: Quantitative result of elemental analysis in SRM 1646a, SRM 1648, SRM 1573a and CRM No. 3 samples compare to Gamma Trac and NIST certified. Concentration unit is in μg/g [6,7].

Element	SRM 1646a			SRM 1648			SRM 1573a			CRM No. 3		
	NIST	Gamma Trac (dev.)	Our software (dev.)	NIST	Gamma Trac (dev.)	Our software (dev.)	NIST	Gamma Trac (dev.)	Our software (dev.)	NIES	Gamma Trac (dev.)	Our software (dev.)
Cd	0.148 ± 0.007	-	0.133 (10.1%)	75.7± 7	82.2 (10.4%)	82.35 (9.8%)	1.52± 0.64	-	1.675 (10.2%)	0.026	0.029 (11.5%)	0.293 (12.5%)
Mn	234.5± 2.8	250 (6.95%)	257.48 (9.8%)	860	936.54 (8.9%)	946.5 (10.06%)	246± 8	265.93 (8.1%)	270.3 (9.8%)	69± 5	76.25 (10.5%)	26.45 (10.8%)
Mo	1.8	1.989 (10.5%)	1.97 (9.5%)	-	-	-	-	-	-	-	-	-
Se	0.193± 0.028	0.207 (7.3%)	0.210 (8.8%)	27± 1	24.5 (9.3%)	24.9 (7.8%)	0.054± 0.03	-	-	-	-	-
Cr	40.9± 1.9	37.7 (7.8%)	37.30 (8.8%)	403± 12	368.5 (8.56%)	367.5 (8.9%)	1.99± 0.06	-	-	-	-	-
As	6.23± 0.21	5.52 (11.35%)	5.80 (6.9%)	115± 10	-	103.5 (10%)	0.122± 0.004	-	0.123 (9.87%)	-	-	-
Sb	0.3	0.273 (9%)	0.271 (9.6%)	45	49.32 (9.6%)	49.14 (9.2%)	0.063± 0.006	0.069 (9.5%)	0.068 (7.9%)	-	-	-
Co	5	4.9 (2%)	4.75 (5%)	18	18.47 (2.6%)	19.08 (6%)	0.057± 0.02	0.63 (10.5%)	-	0.87± 0.05	0.80 (8.1%)	0.963 (10.7%)
Ba	210	214.5 (2.1%)	205 (2.4%)	737	-	-	-	-	-	-	-	-
Hg	0.04	-	-	-	-	-	0.034± 0.004	0.0375 (10.3%)	0.0383 (12.5%)	-	-	-
Zn	48.9± 1.6	52.5 (7.4)	53.3 (9%)	0.476± 0.014	0.566 (9%)	0.572 (10.9%)	309± 0.7	340.2 (10.19%)	344.54 (11.59%)	20.5± 1.0	22.06 (9.8%)	22.653 (10.5%)
V	44.84± 0.76	-	-	140± 3	151.5 (8.2%)	152.8 (9.1%)	0.835± 0.010	-	-	-	-	-

geological materials. We applied a quality system of ISO Guide 17025 to prepare this procedure [8]. Validation and evaluation of data resulted have been done using a statistical approach using control chart. In this activity, evaluation of elements in certified reference materials of CRM SY-3 and CRM Soil-7 has been carried out. Quantitative determination of elements were done by an instrumental neutron activation analysis using a comparative method to laboratory standard which involve a utilization of coaxial and planar type HPGe detector. Standard procedure obtained was applied to evaluate a rear earth element concentration in monazite minerals. The experimental result show some rear earth elements such as Ce, Dy, Eu, Hf, Lu, La, Nd, Sm and Yb can be evaluated quantitatively by planar type detector. Meanwhile Al, Co, Cr, Cd, Fe, Mn, Sc, V and Zn are given a best result if it evaluated by coaxial type detector. From six monazite minerals evaluated using method recommended, we obtained that a concentration of some rear earth elements have value of La [4.4 – 11.9] %, Ce [7.1 – 10.1] %, Sm [0.7 – 11] %, Gd [0.4 – 1.8] %, Nd [3.5 – 5.6] %, Yb [0.3 – 0.4] % and Lu [0.08 – 4.8] %. We have a conclusion that the implementation of quality system on materials shows a consistency of analytical result [9].

In the present time, the complete quality system document is intensive going to prepare consist of a quality manual, a standard operational procedure and a work instruction.

Preparation for development of the PGAA facility

In the development of analytical method, the PGAA is not only a complement of Instrumental Neutron Activation Analysis (INAA), but also becomes a potential method in the field of materials characterization. The PGAA has characteristic of non-destructive multielements analysis which can not be analyzed by INAA. It able to analyze a H (biological and polymer), C, N and S (important in industrial material such as Iron and Stainless Steel), B and Be (reactor material) and Si (high purity material) element which are difficult to determine by INAA technique.

Indonesia National Nuclear Energy Agency (Batan) has commitment to develop and applied a nuclear science and technology for peace and to improve a quality life. According to this program, in 1992 Batan constructed a neutron guide hall provided with some instruments for a research and development of materials science. One of the beam port at TPN2 is free and could be used to setup PGAA facility. The location of the beam port is about 30 meter from

the reactor core and to be made low γ-rays. This condition can support the PGAA installation because they will give a lower background and can improve an analytical sensitivity.

We have been determined a thermal neutron flux distribution at the end of beam port as a preliminary study. We calculated the neutron flux in this beam port is about 2.6 x 10^7 $n.cm^{-2}.det^{-1}$ at reactor power operation of 15 MW.

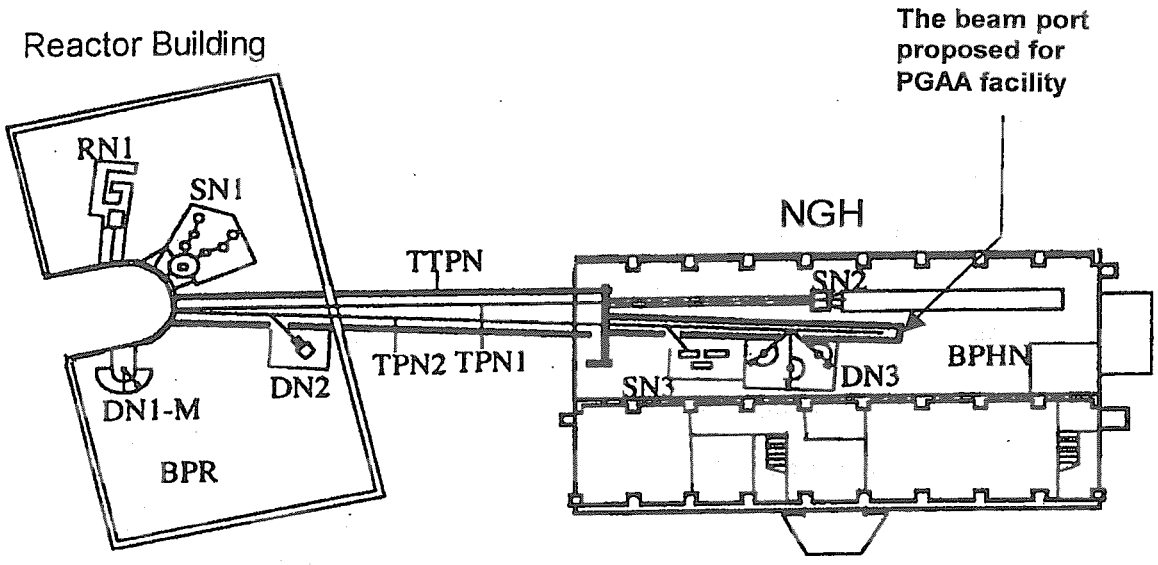

Figure 2: Schematic diagram of neutron spectrometry facility at National Nuclear Energy Agency of Indonesia.

Future program

A. Air particulate matter study

Research cooperation was carrying out with Environmental Management Center (EMC) in an air pollution study for Jakarta Metropolitan Area. In this study we choice two sampling point, i.e. the Jakarta City and Serpong, as urban and rural area respectively. and we use INAA and ICP-MS methods to determine some elements interested. The result show a total suspended particulate matter (TSP) volume taken from Jakarta was 6 – 10 times higher than Serpong area. We have been determine an elements of Ag, As, Al, Ba, Cd, Co, Cr, Cs, Cu, Fe, In, K, Mg, Mn, Na, Ni, Pb, Rb, V and Zn [10]. We shall continue this research cooperation and will be expanded with Osaka University, Japan. In this research we shall used a new type of air sampler unit developed by Department of Environmental, Osaka University. Trace elements analysis should carry out in Suspended Particulate Matter taken from 20

sampling site at Jakarta Metropolitan region. The instrumental neutron activation analysis should be used intensively to support this research.

B. Implementation of a Quality System

In the 2003, Indonesia will access to global market that has a strong competition in the product and services marketing. Accordance with this challenge, we have to improve our laboratory capability by implementation of suitable quality system, software upgrading and hardware. Quality system in neutron activation laboratory has applied in aim to get an accreditation status according to ISO Guide 17025.

Meanwhile to support our quality system program, we are going to involve in IAEA RCA on QA for Nuclear Analytical Technique in the near future.

C. The k_o standardization

Elemental quantitative determination based on comparative method almost depends on the standard reference materials, and also time consumed, especially for multi-elements determination. Meanwhile an application of numerical calculation was supported by utilization high-speed computer grows increasingly in all discipline, including neutron activation analysis application based on workstation computer. According to those methods, we planed to improve the NAA technique by implementation of k_o method in own facility. The NAA group committed to prepare a time schedule of 5 years covered some activities: (i) to study a flux characteristic of irradiation position, especially in a R1 to R4 position of the GA. Siwabessy reactor at Serpong. (ii) Standardization and implementation of k_o and provide a NAA program, (iii) to test of NAA program obtained using some standard reference materials with applied Quality Assurance and Quality Control program. (iv) Application of k_o in material analysis. Some contact person and scientist are needed to guide a Batan staff. Perhaps in 5 years future the k_o methods could be install and could handle an elemental analysis problem in the field of industry and environmental.

D. Establishment of the PGAA facility

According to recommendation from Dr. Chushiro YONEZAWA (JAERI experts), we shall continue the PGAA program. We plan to construct a simple PGAA facility using Ge detector gamma spectrometer, neutron and gamma-ray shielding materials, and start the

PGAA research. Technical skill will be improved using this simple facility and the facility should be improved gradually.

ACKNOWLEDGEMENT

I would like to express special thank to Dr. Hudi Hastowo and Dr. Wuryanto for their support, and would like to acknowledge other members of NAA group members for useful discussion.

REFERENCES

1. Sutisna, Istanto, N.M. Ekasari, "*Heavy Metal Content Analysis of The Ciliwung River Using Neutron Activation Technique*", Technical Report, Research and Development Center for Materials Science and Technology, Serpong 1999.
2. A.P. Vinogradov, *"The Geochemistry of Rare and Dispersed Chemical Elements in Soils*", 2nd Ed. (English Translation), Consultants Bur., New York, 1959.
3. Alice. Sirinuntavid, Paphot Provantosai, "*Application of Instrumental Neutron Activation Analysis for Elemental Determination of Airborne Particulate Matter in Thailand*", Regional Workshop on the Utilization of Research Reactors, Jakarta, November 24 – 28, 1996.
4. M. Rashid, A. Khalik, A. Rahmalan, "*Elemental Analysis of Inhalable Particulates in An Industrialized Ares of Pasir Gudang*", Regional Workshop on the Utilization of Research Reactors, Jakarta, November 24 – 28, 1996
5. Dhandang Purwadi, R. Muhammad Subekti, Amir Hamzah, Kristedjo, *"Software Development for Gamma Spectrum Analysis Which is Resulted by Neutron Activation*", in Print, Jakarta 2000.
6. Adel Fisli, Rukihati, Sutisna, Sudiati, Edison Sihombing, "*Determination of Elemental Concentration in Soil of Puspiptek Area by Instrumental Neutron Activation Analysis*", Prosiding of The 2nd National Seminar on Spectroscopy, 1996.
7. Sri Wardani, "*Laporan dan Kertas Kerja Riset Unggulan Terpadu*", Kantor Menteri Negara Riset dan Teknologi & Lembaga Ilmu Pengetahuan Indonesia, Jakarta 2000
8. ISO Guide 17025
9. Sutisna, Rukihati, Saeful Yusuf, Adel Fisli, saryati, *"Application and Development of Quality System for Material Testing*", Technical Report, Research and Development Center for Materials Science and Technology, Serpong 1999.
10. Rukihati, Sutisna, Ruska P.P., Arlinah, Hari Wahyudi, Liliansari, *"Air Pollution Monitoring Using Instrumental Neutron Activation Analysis and Nuclear Related Analytical Technique*", Presented on Asia Symposium on Research Reactor V, Taejon, Korea, May 29-31, 1996

JP0250100

1.16 Application and Facility of Neutron Activation Analysis in HANARO Research Reactor

Yong Sam Chung

Korea Atomic Energy Research Institute
P.O.Box 105 Yusong, 305-600, Taejon, Korea

Summary

The facilities for neutron activation analysis in the HANARO research reactor are described and the main applications of NAA in Korea are reviewed. The sample irradiation tube, automatic and manual pneumatic transfer system, were installed at three irradiation holes at the end of 1995. One irradiation hole is lined with a cadmium tube for epithermal NAA. The performance of the NAA facility was examined to identify the characteristics of tube transfer system, irradiation sites and custom made polyethylene irradiation capsule. The available thermal neutron flux with each irradiation site are in the range of $3 \times 10^{13} \sim 1 \times 10^{14}$ n/cm^2 · s and cadmium ratios are 15～250.

For an automatic sample changer for gamma-ray counting, a domestic product was designed and manufactured. An integrated computer program(Labview) for the calculation of content was developed.

Neutron activation analysis has been applied in the trace component analysis of nuclear, geological, biological, environmental and high purity materials and various polymers for research and development. Improvement of analytical procedures and establishment of an analytical quality control and assurance system were studied. Applied research and development for the environment, industry and human health by NAA and its standandization was carried out. For the application of the Korea Laboratory Accreditation Scheme(KOLAS), evaluation of measurement uncertainty and proficiency testing of reference materials was performed. Also to verify the reliability and validity of analytical results, intercomparison studies between laboratories were carried out. In this paper, analytical services, national cooperation and the results of the researches are summarized.

I. Facilities for Neutron Activation Analysis

There are three irradiation holes(NAA 1-3) for Neutron Activation Analysis(NAA) in the HANARO research reactor as shown in Figure 1. The pneumatic transfer system(PTS) had been mainly used to sample irradiation of NAA and has been operated since the end of 1996. A Neutron beam facility is planned for prompt gamma neutron activation analysis from 2001. One of the irradiation holes(NAA 2) is a Cd lined tube for epithermal NAA. PTS consists of two modes ; PTS #1 is handled manually as a a simple shuttle system, and PTS #2 is controlled by a preset computer program ; start from a sample loader via an automatic sample loader, deverter, two reactor core, radiation detector, delay stacker, two counters with and without window, finish to discharged receiver. The control program is written in Microsoft's Visual Basic for Windows which is an extension of Quick Basic and employs many of the structured features of C and other high level languages.

At the initial stage of HANARO, the samples are transferred by fresh air. Air pressures of 0.6 bar and 1 bar are used to transfer the irradiation capsule(sample of less than 30 g). A 42 cc irradiation capsule is available for manual PTS. Up to one hundred 27 cc irradiation capsules can be loaded for automatic PTS at a time. The layout of PTS is presented in Figure 2. The operation of the program starts from the main menu of the Windows screen display.

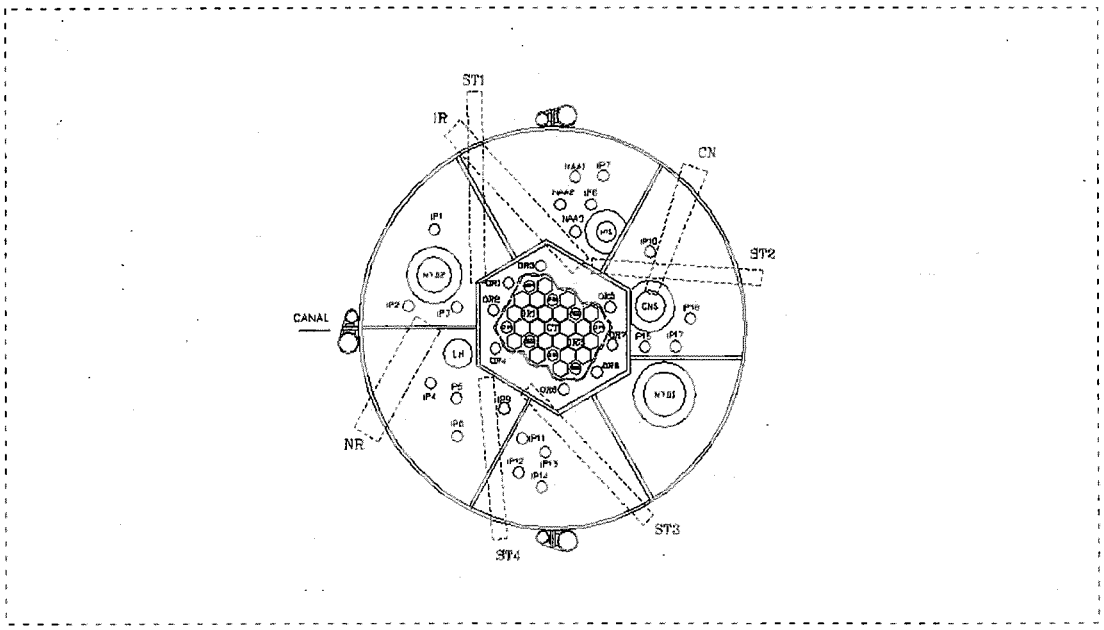

Fig. 1. Comfiguration of NNA Irradiation Holes in HANARO.

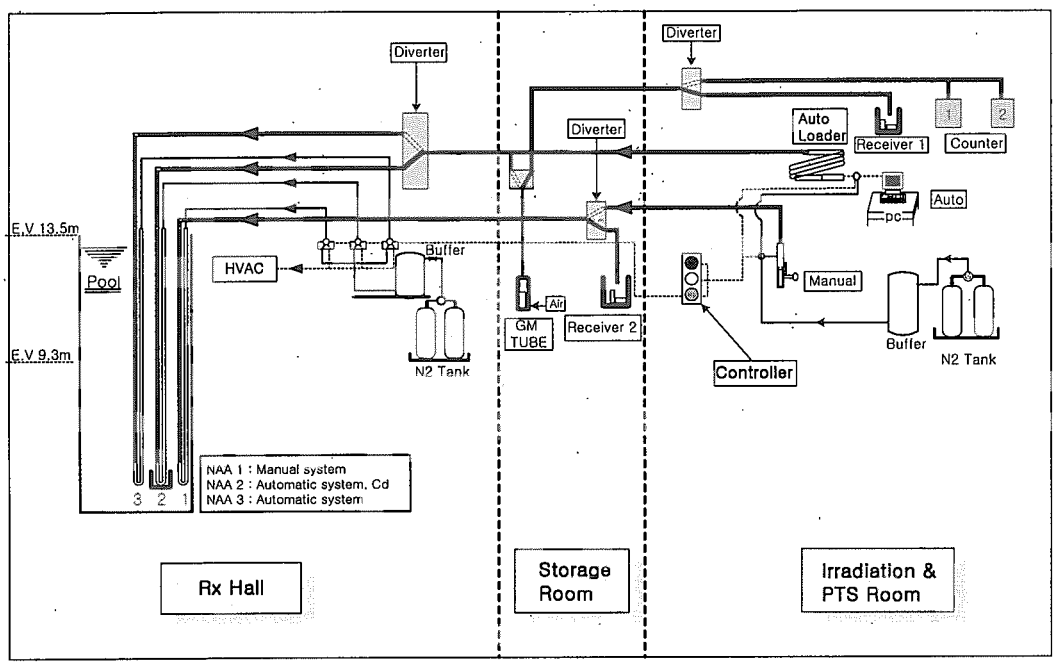

Fig. 2. Layout of Irradiation Facility(PTS) for Neutron Activation Analysis in HANARO.

The available neutron flux with each irradiation site and the general characteristics of pneumatic transfer system are in the range of $3 \times 10^{13} \sim 1 \times 10^{14}$ n/cm^2 · s and presented in Table 1 with cadmium ratios and temperature of irradiation tubes.

We examined the characterization of the three irradiation sites and two kinds of polyethylene irradiation capsules. Firstly, the temperature of three irradiation sites were measured with irradiating time. In the case of PTS#1, the internal temperature of the PE capsule was rose from 50 to 70 ℃ with increase of thermal power.

Table 1. Measured Thermal, Epithermal and Fast Neutron Flux of NAA Irradiation Holes and Cadimium Ratios at 22MW Thermal Power.

Irradiation Hole	Neutron flux, n/cm^{2}sec.			Cadimium Ratio(Au)	Temperature ℃
	Thermal, Φ_t	Epithermal, Φ_e	Fast, Φ_f		
NAA 1	$1.75 \pm 0.02 \times 10^{13}$	$3.62 \pm 2.13 \times 10^{10}$	$3.25 \pm 0.14 \times 10^{10}$	205	40 ~ 70
NAA 2 (Cd lined)	$5.78 \pm 0.56 \times 10^{11}$	$3.40 \pm 0.41 \times 10^{10}$	$3.85 \pm 0.31 \times 10^{9}$	35	> 80
NAA 3	$7.60 \pm 0.06 \times 10^{13}$	$4.35 \pm 1.85 \times 10^{11}$	$6.80 \pm 0.70 \times 10^{11}$	13	> 70

Table 2. Analytical Results of Trace Elements in Polyethylene Rabbit and Various Polyethylene Samples by INAA and ICP. Concentration in ppb.

Element	Rabbit	HN1	HN2	TR1	TR2	TR3	LG1	LG2
Ca(ppm)	-	150	160	270	<3.7	<23	230	300
Mg(ppm)	140	110	110	3.6	150	0.28	23	26
Al(ppm)	74	76	52	8.7	57	0.20	13	23
Cl(ppm)	38	100	79	19	53	0.19	140	140
Ti(ppm)	6.1	4.1	5.2	1.4	4.1	0.17	9.4	13
Cu	-	<280	<240	<130	680	54	<170	<240
V	20	<4	<3	<2	440	1.5	<2	<2
Mn	170	<6	<6	6.78	<19	4.4	8.8	10
Na(ppm)	1.3	0.26	0.43	<0.02	0.20	1.0	0.65	0.92
Fe(ppm)	2.3	1.5	<0.75	<0.84	<0.46	<0.55	0.52	0.81
Mo	280	-	-	-	<1100	<1600	<260	<260
As	0.51	<0.71	0.66	<.1.3	1.2	<1.2	<0.35	<0.43
Br	90	<2.4	3.0	5.0	4.6	5.4	8.00	51
Sb	3.1	<1.1	2.9	2.3	<1.8	<2.4	4.4	55
La	10	<0.16	<0.14	<0.18	1.1	9.9	1.3	0.72
Au	0.44	0.028	<0.015	<0.015	0.059	0.067	<0.009	<0.019
Cd	30	<24	<28	<12	<32	<51	<6.7	<15
Cr	310	21	20	37	<7.5	18000	5.2	12
Ga	2.9	<38	<42	<26	<25	<6.2	<1.3	<1.5
Hf	0.66	<0.72	<0.69	<0.71	<0.64	2.5	<0.4	<0.75
Hg	1.7	<2.9	<2.8	<2.1	<2.2	<3.0	<1.1	<1.6
Co	4.3	9.2	8.6	3.8	5.5	6.3	2.8	3.4
Zn	60	<74	110	<70	160	74	<30	55
Cs	1.3	<3.1	7.1	<2.5	<1.2	<1.4	<0.71	<2.6
Eu	-	<2.0	1.7	1.1	<1.1	<1.3	<0.86	<0.34
Ba	0.18	0.11	840	<860	<270	<310	<190	<210
Sc	-	<0.06	0.23	0.20	<0.044	<0.061	0.076	0.057
K	250	<2600	<5500	<1060	<3300	<530	<820	<240
Zr	-	<660	800	<760	<210	<260	<280	<300
Ce	50	9.5	<5.9	17	<4.5	<9.5	<2.8	<2.8
Sm	0.07	0.23	<0.11	<0.13	0.10	0.27	0.13	0.060
Rb	-	<24	<47	57	<21	100	<17	<20
Th	1.4	<1.2	<1.1	<0.84	<0.59	<0.90	<0.31	<0.48
W	1.1	<4.3	<4.0	<3.4	<2.9	<5.0	<0.85	<1.4

Two kinds of irradiation capsules(rabbit) were manufactured using a high density polyethylene material produced by the domestic industry. Also five kinds of inner sample capsules and two kinds of outer capsules made of pure high density polyethylene were manufactured. Some stability and physical properties such as heat-resistance, radiation-resistance and mechanical characteristics were checked to estimate a suitable irradiation condition. The physical properties of the polyethylene capsule are as follows ; melting index(20.7), density(0.95), melting point(131.6℃). The analytical results of trace elements in the polyethylene rabbit and various polyethylene materials by INAA

and ICP are presented in Table 2.

Recently, the connection part of 13 diverters using the coupling method were converted and an examination of stability and transfer functions was carried out to improve the NAA facility in HANARO as shown in Figure 2. The PTS #1 receiver and controller for the return of a sample rabbit irradiated for a long period of time was manufactured and installed in the sample storage room. The PTS #2 receiver, which was semi-automatically operated for short irradiation(1-2 min.) was manufactured and set up in a shielded box in the hood. Software programs for the operation of PTS #2 were developed and upgraded. The air pressure system was changed to nitrogen gas to decrease the level of background radiation.

For an automatic sample changer for gamma-ray counting, a domestic product was designed and manufactured. An integrated computer program(Labview) for the calculation of content was developed.

II. Application of Neutron Activation Analysis in Korea

The Application of NAA in KAERI started after the operation of TRIGA-II(250 KW) in 1962. Since 1972, neutron activation analysis using TRIGA-III(2 MW) has made remarkable progress both in its methodology and applications in industry, agriculture, geology, environmental pollution, biology, archaeology, forensic science and many other fields in Korea. Now we are using an advanced research reactor(HANARO, 30 MW). There are two NAA groups ; the Korea Atomic Energy Research Institute (KAERI) and the Korea Institute of Geology, Mining and Materials(KIGAM) as well as many users at universities and other organizations. In the future, the applied field of NAA will be extended and users will increase. Table 3 are summarises the utilization of NAA in HANARO[1, 2]. Examples of applications of NAA from 1970 to 1995 in Korea are as follows :

• *Nuclear Materials* : Trace impurities in nuclear fuel and materials such as uranium oxide, graphite, reactor coolant and alloy metals were determined using radiochemical NAA mainly. For the analysis of boron, a prompt gamma counting technique was also studied in the 1980s. To improve analytical accuracy, spectral and isotope interference occuring from uranium fission products were studied and an interference calibration program was developed and an anticoincidence counting method was studied.

• *Environmental Science* : For a long-term study of environmental pollution monitoring, trace and toxic elements in enviromental samples such as air dust, coal and fly-ash, soil, sediment, plants and sea and river water, rain- and snow fall samples were analyzed. Recently, KAERI has been participating in international cooperative research which organized by the IAEA(sub-project on air pollution, UNDP/RCA/IAEA Project). The migration of trace elements was studied using a radioactivable tracer method.

• *Biological and Medical Science* : Analysis of a number of animal and plant tissues,

serum and blood, fishery, etc. are carried out. Analysis of trace elements in cancer tissues was performed together with the Korea Cancer Center Hospital.

• *Industrial Science* : Analysis of the composition of high purity materials, noble metals, rare earth elements and inorganic compounds are carried out. Analytical quality service for QA/QC in industries are supported. Trace element analysis of high purity metals and a study on improvement of accuracy were performed ; an analytical method of high purity silicon semiconductor was developed by INAA and analytical methods of high purity Mo, Ni, Ta were also developed by RNAA.

Table 3. Utilization of Neutron Activation Analysis Facility.

1) Number of Samples

Items \ Year		1996	1997	1998	1999
Research & Development	INT	800	1,200	1,381	2,500
	EXT	80	200	813	1,900
	Total	880	1,400	2,194	4,400
Analytical Services	INT	130	166	381	750
	EXT	50	209	354	800
	Total	180	375	735	1,550

2) Contents of Analysis

Items \ Year	Objects	Users
Research & Development	· Environmental Samples: Airborne Particulates · Biological Samples: Rice, Algae, Foodstuff, Hair · Rocks, Soils, Sediments · PTS Examination · Measurement of Neutron Flux, Cadimium Ratios · Data Intercomparison of Reference Materials · International CRP · Plastic Samples · Proficiency Test of Reference Materials	· Institutes (KAERI, KRISS, KIGAM, KORDI, etc.) · Industries (LG Corp., Samsung, EnTec, etc.) · Universities (Seoul, Yonsei, Kyungsan, Chungnam, etc.)
Analytical Services	· Impurities in Iodine · Flyash, Air Dust, Air Filter, Resin, Human Hair · Ground Water, Waste Water, Sludge, Sediments · Bentonite, Granite, Silicate, Rock, Soil, Sand · Dry Bid Sample · Reactor Coolent, Fuel Materials, Irradiation Test · Flux Monitors, Fission Track Analysis · HP SiC Plate & Tube · Impurities in RI Medicines · Tooth Sample Irradiation · Impurities in Iodine, Molybdenum, Nickel	· Institutes (KAERI, KRISS, KIGAM, KORDI, etc.) · Industries (LG Corp., Samsung Elect., KIA Motors,Samrim Corp., Sampung Industry, etc.) · Universities (Seoul, Yonsei, etc.)

• *Geological Science* : To improve analytical sensitivity, nuclear and spectral interference related to spectrum analysis and irradiation methods were studied. The composition of trace elements in soils, rocks, minerals, etc. were determined using thermal and epithermal neutron activation analysis. Analysis of rare earth elements in cosmic materials such as meteorites were carried out as the Apollo project. The isotopes from the reactions of fast neutrons were studied and the interference was also corrected, and 40 elements in geological samples were determined.

• *Life Science* : For clinical, nutritional and contamination research, the concentration level of essential, toxic elements and heavy metal in biological samples such as foodstuff, rice, human milk, human hair, tabacco and smoke, Korean Ginseng, etc. were analyzed by INAA and RNAA. Iodine analysis of the colostrum and mature milk of Korean lactating mothers related to diseases and metabolism of infants was performed.

• *Archaeology, Forensic Science* : The origin and classification of Korean antiques was investigated using chemometrics and multivariate analysis of multi-elements composition in the pottery and coinages in the laboratories of universities, institutes and museums. To study individual identification for criminal investigation, several kinds of human hair samples were analyzed by INAA.

• *Certification of Reference Materials* : Cross-checking and identification of standards has been performed and obtained good scores in international and domestic intercomparison and certification of reference materials. Our laboratory has participated in the IAEA's data intercomparison study(AQCS).

III. Applications of Neutron Activation Analysis in HANARO

In the last years, basic and applied research for an analytical quality control system and trace component analysis of nuclear, geological, biological, environmental and high purity materials and various polymers has been carried out using a neutron activation analysis facility in HANARO, major contents are summarized.[3-23]

1) Improvement of analytical procedures and establishment of an analytical quality control system.

With the analysis of six kinds of biological and environmental standard reference materials(NIST SRM : Peach Leaves, Citrus Leaves, Total Diet, Bovine Liver, Oyster Tissue, Wheat Flour), the analytical error was identified(15 elements were within 10% of the relative error, and 20 elements were within 15% of the relative standard deviation). A radiochemical separation procedure(RNAA) for U and Th to improve analytical sensitivity(> 0.5 ng) was developed by using the co-precipitation and ion exchange resin methods, and the ENAA method for I and Sr determination(sensitivity : >0.1 ppm) was also examined.

In connection with fundmental qualification for the application for the Korea Laboratory Accreditation Scheme(KOLAS), education and training for practical

application, evaluation of measurement uncertainty and proficiency test reference materials were performed.

To verify the reliability and validity of the analytical results, intercomparison studies between laboratories for twelve kinds of samples such as dust, soil, coal fly ash, sediment, algae, etc., were carried out. All results obtained were excellent and a typical result of urban dust was plotted in Figure 3.

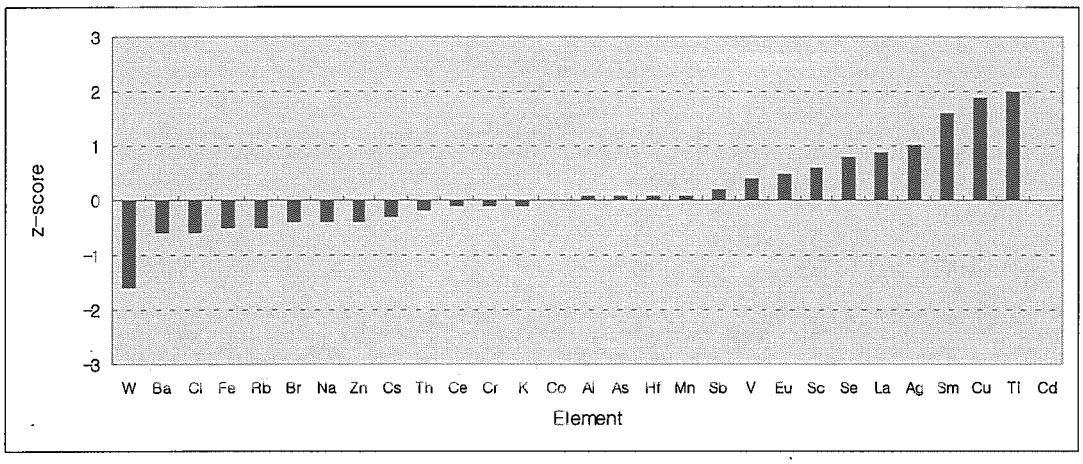

Fig. 3. Evaluation of z-score for the elements measured in urban dust.

2) Applied research and development in the fields of the environment, industry and human health.

A study on the development of analytical methods and the standardization of a procedure for the analysis of airborne particulate matter were carried out using standard reference materials(NIST SRM 1648, NIES CRM-8) and laboratory intercomparison work. Air pollution monitoring was performed using a Gent stacked filter unit low volume sampler and polycarbonate membrane filter(coarse particle : 2.5~10 μm, fine particle : <2.5 μm). To compare air quality, airborne particulates with two particle sizes were collected from urban, rural and industrial areas from May 1997 to 2000. The concentrations of impurities in the blank filters were estimated and used for correction. The concentrations of 25 heavy metals, trace elements and the mass of airborne particulate matter($PM_{2.5}/PM_{10}$) and elemental black carbon were measured. From the measured data, a presumption of the source origin and a correlation pattern between PM and the elements was statistically treated with the calculation of enrichment factor and correlation coefficient. The results of air monitoring are plotted in Figure 4 and 5.

Concerning applied research on human health and the environment using NAA of biological samples, five kinds of biological standard reference materials were analyzed and the measurement error of the analytical results was evaluated.

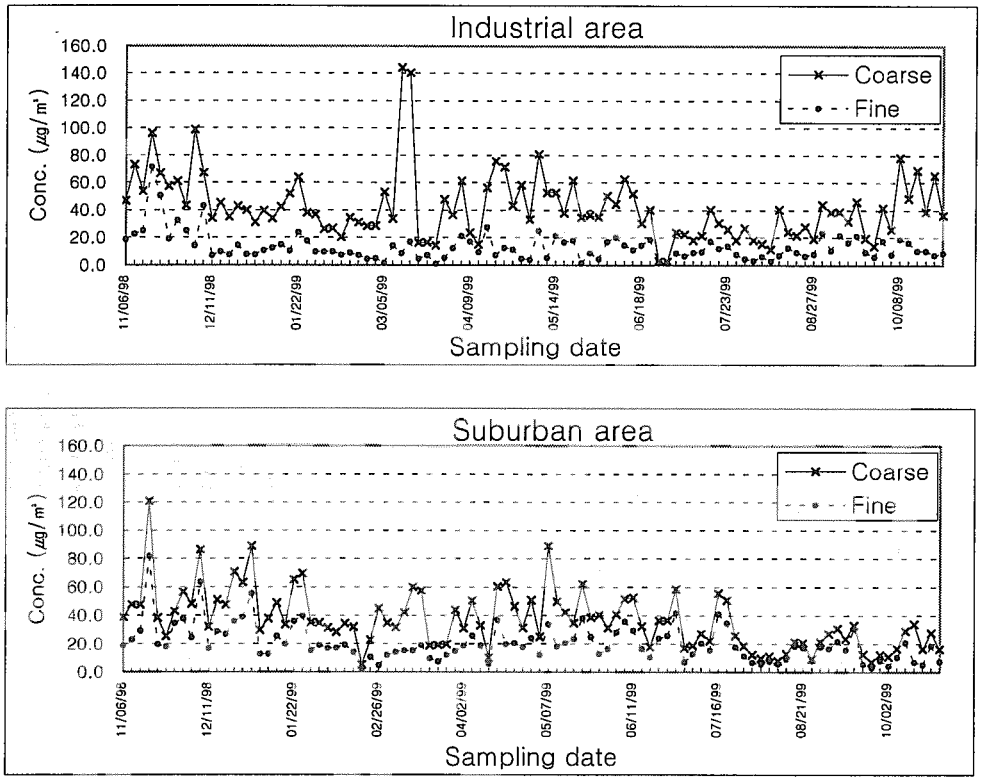

Fig. 4 Mass concentration of fine and coarse fraction with sampling date.
(`98.11 - `99.10)

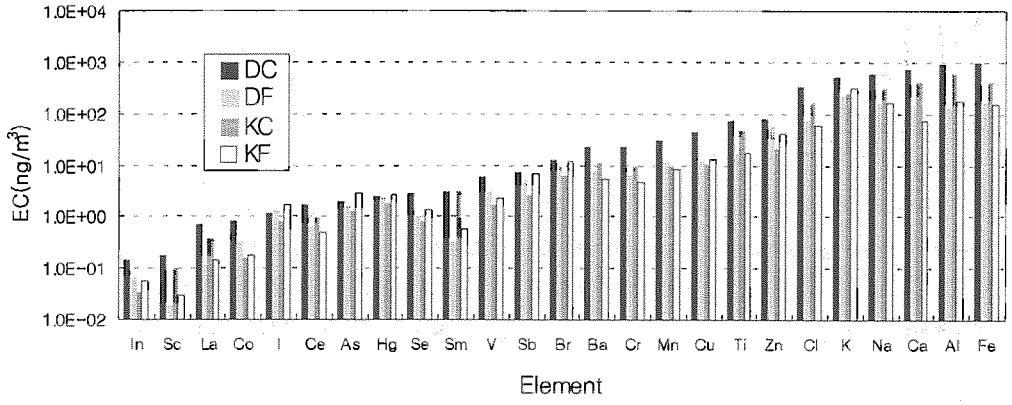

Fig. 5. Average elemental concentration of airborne particulate matter collected in urban and industrial areas('98. 11 - '99. 10).

The amounts of trace elements in the air dust samples collected from inside a foundry working place were analyzed and the distribution of trace elements in the hair and blood of corresponding workers were measured to investigate a correlation. In addition, identification of the elemental distribution in healthy supplementary foodstuffs, comparison of the component elements of six kinds of herb medicines in Korea and

China, the distribution of trace elements in the Korean total diet(Table 4) and representative foods were studied.

Table 4. Analytical Result of Korean Total Diet by NAA.

Element	Nuclide	Concentration of element		
		Range	Mean Value	Standard Deviation
		< ppm >		
Al	Al-28	16.1～18.3	17.6	1.28
Br	Br-80/Br-82	9.59～10.6	9.95	0.58
Ca	Ca-49/Ca-47	1358～1496	1418	70.9
Cl	Cl-38	10870～11780	11353	458
Fe	Fe-59	23.7～26	25.2	1.32
I	I-128	1.50～1.77	1.64	0.19
K	K-42	5394～5706	5579	134
Mg	Mg-27	807～896	850	44.4
Mn	Mn-56	8.46～8.78	8.65	0.16
Na	Na-24	10080～10470	10298	162
Rb	Rb-86	5.43～5.49	5.46	0.03
Sr	Sr-87m/Sr-85	5.3～5.80	5.55	0.36
Zn	Zn-65	31.57～33.74	32.48	1.13
		< ppb >		
As	As-76	493～603	526	51.8
Co	Co-60	29.6～31.6	30.8	1.06
Cr	Cr-51	348～420	393	39.4
Cs	Cs-134	10.6～11.6	11.1	0.71
Sc	Sc-46	3.2～3.6	3.43	0.21
Se	Se-75	223～328	276	74.5
Sm	Sm-153	46.1～47.5	46.8	0.99
Th	Pa-233	2.38～2.82	2.6	0.3
U	Np-239	31.5～38.6	35	5.0

In connection with the analysis of trace elements in plastics(raw material and fabricated products) using NAA, identification of the results by NAA and comparison with those by the XRF and ICP methods, the optimum analytical conditions for NAA were determined, a new freezing-crushing technique for the preparation of a polymer sample was developed, analysis of inorganic components and additive agents in plastic materals(PE, PP) was carried out for the manufacture of irradiation rabbits and sample capsules, and the elution charateristics of toxic elements in plastic materials was also evaluated.

IV. Future Plan

We will carry out analysis of airborne particulate matter as well as other environmental and biological samples for air and marine environmental pollution studies. This workscope is also involved as a part of our long term nuclear research and development project related to intensive study on the application of NAA. Particularly, we are interested in the applications as well as the supporting system for analytical quality control of NAA involving the PGAA facility. Continously, to improve the analytical accuracy and detection limit, we are making plans for the development of various irradiation facilities and equipment, and research of analytical techniques using ko-standardization method. However, to make the above project a success application of international standards is essential, i.e., standardization and harmonization of analytical techniques in sampling and sample preparation, analytical procedures and data evaluation. Collaboration with RCA member states, IAEA and other nations will be promoted.

V. References

[1] Yong Sam Chung, Annual Report of Korea Atomic Energy Research Institute, KAERI/RR-1745/96

[2] Yong Sam Chung, Technical Report of Korea Atomic Energy Research Institute, KAERI/TR-898/97].

[3] Yong Sam Chung, Technical Report of Korea Atomic Energy Research Institute, KAERI/TR-2031/99].

[4] Y.S. Chung, Y.J. Chung, E.S. Jung and S.Y. Cho ;'Comparison and Determination of Environmental Standard Samples by Instrumental Neutron Activation Analysis', *J. Radioanal. Nucl. Chem.*, 217, 1, (1997) 71-76.

[5] Y.S. Chung, Y.J. Chung, K. H. Cho and J.H. Lee ;'Determination of Trace and Toxic Elements in Korean Rice CRM by INAA, ICP and AAS', *J. Radioanal. Nucl. Chem.*, 215, 1 (1997) 129-134.

[6] S.Y. Cho, O.D, Awh and Y.S. Chung ; 'Trace Element Exposure in Human by Instrumental Neutron Activation Analysis of Hair', *J. Radioanal. Nucl. Chem.*, 217, 1.(1997) 107-109.

[7] Y.S. Chung, Y.J. Chung, E.S. Jeong and S.Y. Cho ; 'Study on Air Pollution Monitoring in Korea using Instrumental Neutron Activation Analysis', *J. Radioanal. Nucl. Chem.*, 217, 1 (1997) 83-89.

[8] S. Y. Cho, S. G. Jang and Y. S. Chung ; 'Human Hair Identification by Instrumental Neutron Activation Analysis', *J. Radioanal. Nucl. Chem. Letters*, 229, 1-2 (1998) 143-147.

[9] J. H. Lee, J. S. Kim, K. H. Cho, J. C. Woo, M. S. Han and Y. S. Chung ; 'Determination of Trace Elements in High Purity Copper by INAA, GFAAS and ICP-AES', *J. Radioanal. Nucl. Chem.*, 234, 1-2 (1998) 77-83.

[10] S. J. Moon, J. Y. Kim, Y. J. Chung, Y. S. Chung, 'The Iodine Contents in Common Korean Foods', *Korean J. Nutrition*, 31, 2, (1998) 206-212.

[11] S. J. Moon, J. Y. Kim, Y. J. Chung, Y. S. Chung, 'The Determination of Iodine in

Human Milk and Cow Milk by Iodide Specific Ion Electrode and Neutron Activation Analysis', *Korean J. Nutrition*, **31**, 2, (1998) 213-219.

[12] Y.S.Chung, J.H.Moon, Y.J.Chung, Y.J.Park, K.Y.Lee, Y.Y.Yoon, S.H.Lee, K.T.Kim, 'Intercomparison and Determination of Sediment by Instrumental Neutron Activation Analysis', *Journal of the Korean Socirty of Groundwater Environment*, **5**, 2 (1998) 116.

[13] Y. S. Chung, J. H. Moon, Y. J. Chung, S. Y. Cho, S. H. Kang, 'Study on Air Pollution Monitoring in Korea using Low Volume Air Sampler by Instrumental Neutron Activation Analysis', *J. Radioanal. Nucl. Chem.*, **240**, 1 (1999) 79.

[14] Y. S. Chung, J. H. Moon, Y. J. Chung, K. Y. Lee, Y. Y. Yoon, 'Determination of Toxic and Trace Elements in Algae by Instrumental Neutron Activation Analysis', *J. Radioanal. Nucl. Chem.*, **240**, 1(1999) 95.

[15] K. Y. Lee, S. K. Shim, Y. Y. Yoon, Y. S. Chung, G. H. Lee, 'An accurate and Sensitive Analysis of Trace and Ultra Trace Metallic Impurities in Plastics by Neutron Activation Analysis', *J. Radioanal. Nucl. Chem.*, **241**, 1 (1999) 129.

[16] Y. S. Chung, J. H. Moon, Y. J. Chung, Y. J. Park, 'Determination of Uranium in Groundwater by Instrumental Neutron Activation Analysis', *Journal of the Korean Socirty of Groundwater Environment*, **5**, 4 (1999) 210.

[17] K. Y. Lee and Y. S. Chung, 'Analysis of Inorganic Elements in Polymer Materials by NAA', *Polymer Science and Technology*, 10, 3 (1999) 395.

[18] Y. S. Chung, J. H. Moon, K. W. Park, K. Y. Lee, Y. Y. Yoon, 'Data Intercomparison and Determination of Toxic and Trace Elements in Algae by Instrumental Neutron Activation Analysis', *Analytical Science & Technology*, **12**, 4 (1999) 346.

[19] Y.H.Seo, B.K.Lee, Y.S.Chung, Y.J.Chung, J.H.Moon, K.Y.Lee, S.K.Shim, W.Hong, H.W.Choi and K.H.Kim, Interlaboratory Comparison for the Sampling and Chemical Species Measurement of PM_{10}, *Journal of Korean Society for Atmospheric Environment*, 15, 4 (1999) 485.

[20] Y.S.Chung, J.H.Moon, Y.J.Chung, K.W.Park, K.Y.Lee, Y.Y.Yoon, S.K.Shim, K.H.Cho, M.S.Han and J.H.Lee, Multielement Analysis in Airborne Particulate Matter(PM_{10}) by INAA, ICP and AAS, *Journal of Korean Society for Atmospheric Environment*, **15**, 4 (1999) 495.

[21] Y.S.Chung, J.H.Moon, S.H.Kim, K.W.Park and S.H.Kang, Intercomparison and Determination of Trace Elements in Urban Dust by Neutron Activation Analysis, *Analytical Science & Technology*, **13**, 2 (2000) 179.

[22] Y.S.Chung, J.H.Moon, S,H.Kim, K.W.Park, S.H.Kang and S.Y.Cho, Study on Airborne Particulate Matter($PM_{2.5}/PM_{10}$) Monitoring in Urban and Rural Area by using gent SFU sampler and INAA, *Journal of Korean Society for Atmospheric Environment*, **16**, 5 (2000).

[23] Y.S.Chung, J.H.Moon, S.H.Kim, K.W.Park, S.H.Kang and S.Y.Cho, Evaluation of Daily Intake of ^{238}U and ^{232}Th in a Korean Mixed Diet Sample Using RNAA, *Journal of the Korean Nuclear Society*, **32**, 5 (2000) 477.

JP0250101

1.17 The Use of Neutron Activation Analysis in Environmental Pollution Studies

A. M. Yusof[1], S. K. Gill[1], S. Salleh[1], S. Akyil[2] ,S. Hamzah[3], S. A. Rahman[3] and A. K. H. Wood[3]

[1]Department of Chemistry, Universiti Teknologi Malaysia, 81310 UTM Skudai, Johor, Malaysia
[2]Institute of Nuclear Sciences, Ege University, 35100 Bornova, Izmir, Turkey
[3]Malaysia Institute of Nuclear Technology Research, PUSPATI Complex, 43000 Bangi, Selangor, Malaysia

Abstract

Environmental samples and localized species from a marine environment, water samples for public drinking, sediment core samples from a polluted marine environment, soil samples from tin-tailing dump sites, air particulate matter and leachates from landfills were analyzed for their trace, toxic elemental contents, chemical species and natural radioactivity in an attempt to assess the safety levels of these pollutants in these matrices by means of instrumental neutron activation analysis (INAA) and other related nuclear techniques. Complementary techniques such as the graphite furnace atomic absorption spectrometry (GFAAS), ICP-MS, ion chromatography and pre-concentration steps particularly in the speciation studies were also incorporated in these studies for specific elemental determinations prior to irradiation in a neutron flux of about 5.1×10^{8} $n.m^{-2}.s^{-1}$ from a TRIGA Mk.II reactor. Pre-concentration of the chemical species of As and Se was done using a mixture of ammonium pyrrolidinethiocarbamate-chloroform (APDTC-$CHCl_3$) while activated carbon derived from agricultural wastes was used in the iodine speciation. Some of the specific chemical species have to be separated prior to the final quantitative determination to reduce interference and enhance the sensitivity of the INAA technique. These include arsenic, selenium and iodine species present in various matrices. The more toxic inorganic arsenic, selenium, iodine and a host of other trace elements were detected in these samples by quantifying their respective γ-rays emitted from the radioisotopes. The amounts of As(III) present vary from about 1.8 ng/g to 15.5 ng/g in localized marine species, 0.1 ng/g to more than 5.0 ng/g in treated public drinking water while the more toxic inorganic Se(IV) is present in the range of 1.5 μg/L to about 4.5 μg/L. The distribution patterns of pollutants were presented on maps and deductions were made from these patterns to address pollution issues.

Results obtained from the analysis of sediment core samples taken from a fairly polluted marine environment were analyzed for the REE contents to determine the concentrations of La, Ce, Sm, Eu, Tb, Dy and Yb using instrumental neutron activation analysis. Core samples were divided into strata of between 2 to 3 cm intervals and prepared in the powdered form before irradiating them in a neutron flux of about 5.0×10^{12} $n.cm^{-2}.s^{-1}$ in a TRIGA Mk.II reactor. Down-core concentration profiles of La, Ce, Sm, Eu, Tb, Dy and Yb in 3 core sediments from three sites are obtained. The shale- normalized REE pattern from each site was examined and later used to explain the history of sedimentation by natural processes such as shoreline erosion and weathering products deposited on the seabed and furnishing some baseline data and/or pollution trend occurring within the study area. The shale-normalized REE patterns also showed that LREE in the sediment samples exhibit enrichment relative to HREE particularly, La and Sm showing enrichment compared to the ratios in shale. REE concentrations of 124 μg/g at the surface of sediment collected at two of the three sites were found to decrease to 58 and 95 μg/g, respectively. This was of particular interest when it is used to explain the anomalies occurring in the marine sediment as a result of geochemical processes over a long period of time. The air pollution trend in the Asia Pacific region was also studied for source emission identification with samples collected using the Gent Stack Sampler and modeling was done using the Chemical Mass Balance-7 and Statgraphic software. About 100 filters were analyzed and close to about 60% of the mass within the particulate matter group has been identified. All determinations were validated using suitable SRMs.

Introduction

Most of the major sources of pollution are anthropogenic in origin and they particularly affect not only the estuarine and coastal areas but other areas. With most of the pollutants likely to originate from industrial discharges, metals and metal species have resulted in a sharp increase in environmental contamination. The aquatic and marine environment, particularly sediments, localized and freshwater species, even the waters from these areas, have traditionally been surveyed for environmental assessments. Marine life found on the sea beds and freshwater species have been subjected to either direct or indirect contamination and the pollutants will eventually find their way into the human food chain through the consumption of marine derived foodstuffs such as popular localized species and seaweed. Freshwater species are commonly found in disused tin-mining pools which provide natural habitats for aqua-culture activities where most of the freshwater fishes are bred. With many fishing villages found along the coastal areas and some of them are near an industrial zone, this study area was thought to be ideal in terms of anthropogenic activities-pollution-human surrounding relation.

Much attention has been given to the long-lived ^{129}I radionuclide with a half-life of 1.6×10^7 y since it behaves similarly to its stable isotope of ^{127}I in the biogeochemical cycle. Its introduction into the atmosphere is mainly through the spontaneous fission of uranium and by cosmic ray interactions with xenon. Iodine concentrations in soil are much higher than in the parent rock materials due to the transfer of iodine, evaporated from the ocean [1], into soil through wet and dry deposition and decomposition of iodine-containing vegetation. From the natural leaching process, dissolved iodine finds its way into the underground water system. In drinking well waters, the concentrations of iodine range from 0.5 to 35 $ng.mL^{-1}$ and this is extremely low compared to seawater.[2,3] Since iodine is an essential element for human especially in thyroid gland functions, the iodine intake by human beings from drinking water is important from the health view point.

Landfills, either sanitary or conventional is still the preferred method for municipal solid waste disposal though incineration and composting has gained grounds as the suitable alternative to landfill depending on limitations of available space for landfill sites. Most landfills accept wastes of all kinds including hazardous wastes generated as a result of the extensive use of heavy and toxic metals in modern society. The changed flow path of these toxic contaminants in their soluble forms may be harmful for the balance of biological systems at different levels, micro-organisms, human beings and the whole eco-systems, since the toxicity of these contaminants is determined by their concentrations and chemical forms. Some would find their way into water system and will enter the human food paths through direct or indirect ingestion. These contaminants in their enriched forms will be dispersed in the water system and eventually pollute the ground water often used as water intake sources. Chemical components in leachates from

hazardous wastes landfills in Japan were studied to determine their components and their effects on human beings.[4]

The use of rare earth elements (REE) as an indicator in the understanding of the accretionary processes of the earth's crust has been investigated during the last two decades, nevertheless continuing work has been done in view of the potential of REE to elucidate the geo-chemical processes involved in depositional processes on the ocean floor. Sedimentation history and the knowledge of the abundance and distribution of the major sources of pollution, especially toxic and heavy metals which are anthropogenic and also natural in origin has shown to be very helpful in explaining the geo-chemical and environmental investigations. A fairly polluted marine environment in the waters in the Straits of Johore, Malaysia, a shallow channel in the continental shelf connecting the South China Sea to the east with the Straits of Malacca to the west situated at the southern tip of the Malaysian peninsular in Johore has been investigated to look into the possibility of using rare earth elements (REE) as an anthropogenic indicator. Determination of the natural processes controlling REE distributions will assist in the recognition of man-made inputs to the marine system[5], in this case industrial effluents discharge into the marine system. The chemistry of the REE, especially their similar chemical properties and low solubility that allow only limited elemental fractionation during weathering and diagenesis, make these elements useful as geochemical indicators in sediments and in sedimentary rocks.[6] Of particular interest are the abundance and distribution patterns of rare earth elements in marine minerals and sediments in order to identify the source of these elements, the mechanism of their incorporation and the depositional environment. REE can also be a powerful tool to define the remobilization mechanism during diagenesis and weathering of sediments. Moreover REE are used as indicators of the behavior in the environment of transuranic elements on the account of the similarity in their physico-chemical properties.[7]

Shale-normalized REE patterns have been conveniently used to explain some oceanic processes governing the mechanism by which the sedimentation occurred over a period of time and the environment in which these processes took place. Murray *et al.*[8] have shown that specific depositional environments of chert and shale could be deduced from their REE chemistry, and differences in the REE relative fractionations and total abundance in marine cherts and shales reflect the depositional location of the sediments. Sholkovitz[9] observed that shale-normalized REE patterns of shelf and slope sediments are enriched in light REE (LREE) relative to heavy REE (HREE). Significant LREE enrichment in marine sediments has also been investigated for use in making assumptions in the interpretation of many processes associated with the fractionation of REE in oceanic waters and sediments.[9]

A comprehensive study on the geochemistry of sediments in these straits was reported by other workers[10] and the report in this study concerns the rare earth elements patterns in the sediment cores of three sites located in the vicinity of an industrial area. Total rare earth element

(REE) concentrations were used to develop correlations between the Ce/Ce* anomalies and the distribution patterns of some of the light rare earth elements (LREE) and the heavy rare earth elements (HREE). Several interpretations of the results are obtained such as vertical profiles of REE (La, Ce, Sm, Eu, Tb, Dy and Yb) using concentrations data at all the sites, correlation study using certain standard elements such as Sm and elemental distribution based on total REE concentrations according to area to trace the history of sedimentation by natural processes such as shoreline erosion and weathering products on the seabed.

Technical Study

Samples and Standards

Aquatic samples used in this study were obtained from specific water bodies such as disused tin-mining pools as in the case of the determination of selenium species in these samples. Since the concentration of selenium species in natural waters is governed by the rate of seepage from seleniferous environments, water bodies in disused tin-mining pools could be a good source of selenium input as a result of the landuse activity related to dredging. The aquatic species found in these water bodies range from algae undergrowth found along the perimeter of the pools to a common, hardy freshwater fish, the *Tilapia nilotica*. This particular fish from the *tilapia* family is found in abundant in disused tin-mining pools and because of its rapid breeding nature, they are also bred in man-made ponds and is a major contribution to the local aqua-culture industry.

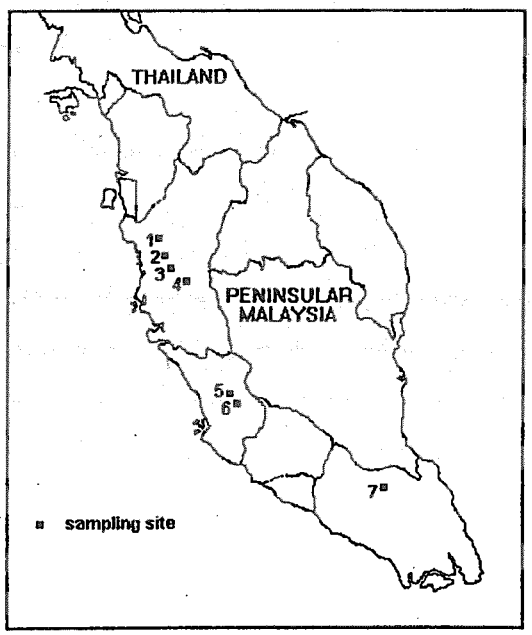

Figure 1. Locations of disused tin-mining pools

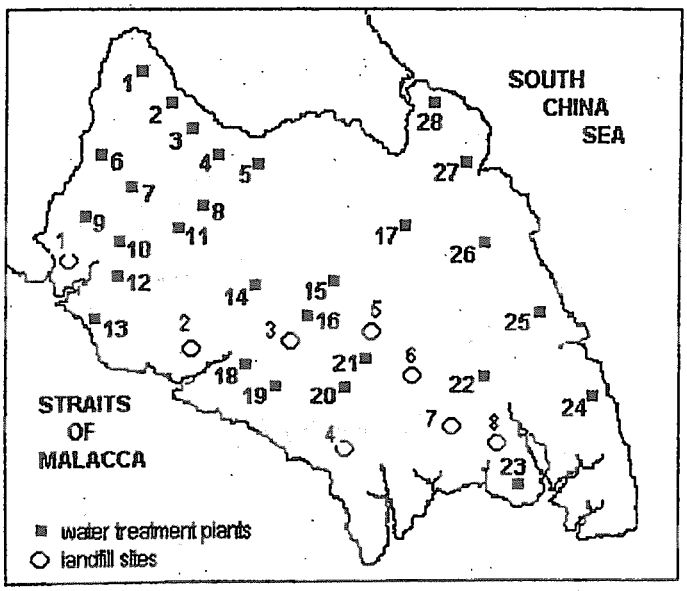

Figure 2. Treatment plants for raw and treated for water sampling

Water samples from disused mining pools were collected from seven different locations throughout the Malaysian peninsula, as shown in Fig. 1, with one location chosen as a control. Samples from water treatment plants were collected from 27 sampling sites chosen in the state of Johore, as depicted in Fig. 2, in an effort to evaluate the treatment process at the plants. The nature of activities in the vicinity of the reservoirs or rivers feeding the treatment plants has a profound effect on the arsenic and radium concentrations in the water samples depending on the locality of the raw water intake points. Preparation of samples for analyses was done within 72 h to avoid any changes in the metal species. Synthetic drinking water used as a reference sample was prepared by spiking with 100 $\mu g.dm^{-3}$ of As(III) and As(V) each according to a prescribed method.(Lo *et al*). [11]

All fish samples were collected from a fresh catch and selected to ensure only fish of similar sizes were used in the study. Samples were also taken from a man-made pond to be used as a control. The fish samples were cut and separated into three parts, namely the head, flesh and bones using pre-cleaned stainless steel blades. The wet weights were recorded before freeze-drying them using an Edward Mudalyo freeze-dryer and later ground to <200 mesh size with a Herzog HSM-100 grinder. Samples were sealed in pre-treated polyethylene containers for further analysis. For quality assurance controls, a CRM *Lobster Hepatopancreas* marine reference material (TORT-1) supplied by the National Research Council of Canada (NRCC) and standard selenic acid (H_2SeO_3) were used.

The well and river water samples used in this study were collected from 26 sites (10 from wells and 16 from rivers) in the State of Perak, Malaysia. Well water samples were collected using pre-washed plastic buckets while river water samples were taken from water intake points

designated by the state water authority. Only surface waters were used in this study since no depth profile analysis was planned.

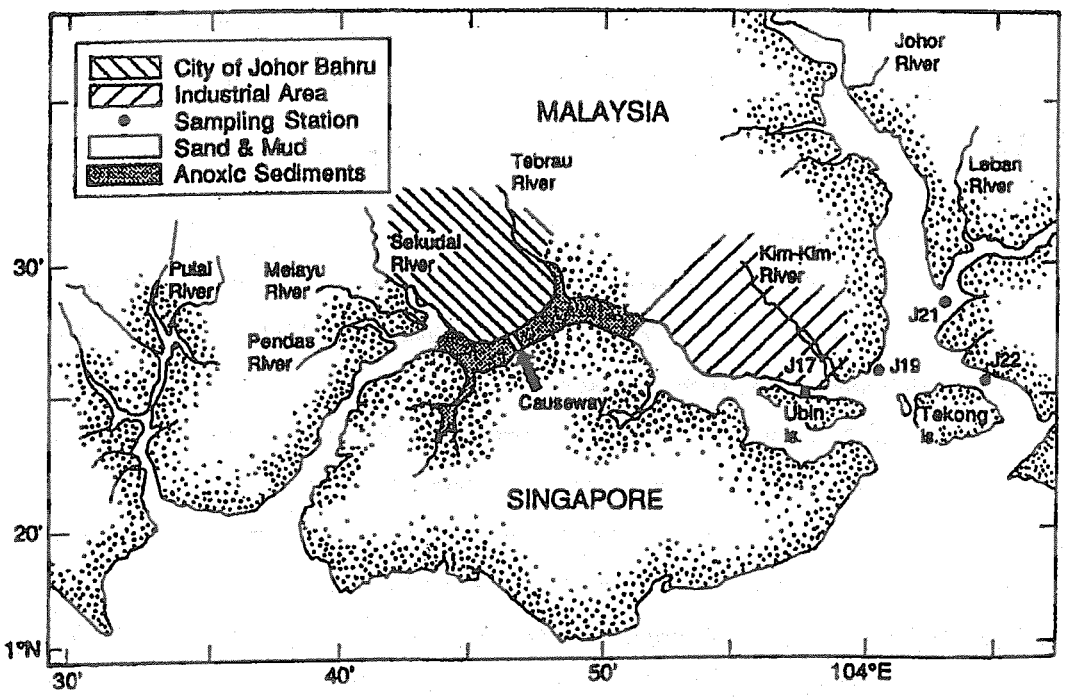

Fig. 3. Sampling locations of core sediment samples (*courtesy of Wood et al* [10])

Sediment cores were collected at the 3 locations as shown in Fig. 3 in July 1993. Three core sediments were identified as J-17 (N1°25' E103°58'), J-19 (N1°26' E104°0') and J-21 (N1°28' E104°3'). The core sediment samples collected at a sea depth of between 5 to 10 m from the Johore Straits between Malaysia and Singapore using a box corer of 20 x 30 cm cross-sectional area were taken to a depth of 60 cm. with the central core cut into strata between 2- and -3 cm intervals. The procedures adopted in the coring activities followed those of the University of Washington and was carried out by a team of workers from the Malaysian Institute for Nuclear Technology Research (MINT), Universiti Pertanian Malaysia (UPM) and School of Oceanography, University of Washington.[10] Analytical accuracy was obtained by using standard reference materials IAEA Soil-7 or prepared standards consisting of a combination of solutions evaporated onto filter papers. This area is one of the most important Malaysian continental shelf areas where increasing economic development along the coast may threaten preservation of valuable biological resources in adjacent sea waters. An industrial settlement is situated on the south-eastern part of the tip of the peninsula. (Fig. 3)

As for leachates, water samples were collected from waterways found in the vicinity of the landfill areas. (Fig. 2) Sampling was done about one hour after a heavy down pour because the leachates would have a better chance of seeping into the nearby waterways. Synthetic leachate

used as a reference sample was prepared and spiked with 100 $\mu g.L^{-1}$ each of As(III) and Se(IV) according to a prescribed procedure.[11] Mixed standards were prepared in the laboratory using As_2O_3 for As(III), $Na_2HAsO_4.7H_2O$ for As(V), SeO_2 for Se(IV) and Na_2SeO_4 for Se(VI) species. Nearshore Seawater (CASS-2) purchased from the United States National Institute of Standards and Technology (NIST) was used as SRM and treated similarly as the water samples prior to the final analysis using neutron activation technique.

Samples Treatment and Preparations

In the speciation studies of inorganic selenium in aquatic species, all reagents used were of analytical grade (Analar), purified prior to use and prepared by diluting Analar acids (15.8 M HNO_3, 11.8 M HCl and 18.1 M H_2SO_4), base (7.1 M NH_4OH) or salt (NH_4COOCH_3) with quartz-distilled water (Q-H_2O) to the appropriate concentrations. The chelating resin Chelex-100, in the sodium form used in the total inorganic selenium separation step, was obtained from Sigma Chemicals. Aqueous stock solutions of Se(IV) were prepared by dissolving H_2SeO_3 in Q-H_2O and made up to the mark. Ammonium pyrrolidinecarbodithioate (APCDT) used in the extraction step was obtained from Fluka. Sample solutions for the extraction step with APCDT-$CHCl_3$ and preconcentration with Chelex-100 were prepared by dissolving 1 g of the dried material with 10 mL of HNO_3 (70%) in a Teflon™ pressure decomposition vessel of a CEM Model MDS-81D microwave digester and the details are described elsewhere.[12] All CRMs and standards used in this study were similarly treated for consistency. Since inorganic selenium species exist in the Se(IV) and Se(VI) forms, the extraction was done on the Se(IV). The Se(VI) determination was achieved by first reducing the Se(VI) to Se(IV) with 25% sodium thiosulphate ($Na_2S_2O_3$) solution. The difference in the two selenium concentrations constitutes the Se(VI) in the samples investigated. The details of the extraction procedure for the Se(IV) species is described elsewhere.[13] The ion-exchange procedure using the chelating resin Chelex-100 was carried out to preconcentrate the elements prior to the total inorganic species determination. The procedure followed that of Kingston *et al* [14] with some modifications. The final solution obtained after the phase separation was used in the irradiation step to determine the inorganic Se content in the samples.

The charcoals used in the adsorption of iodine species from river and well water samples were derived from used palm oil kernel and were prepared according to the method described by Hussain and Ui.[15] The most suitable activated charcoal was chosen based on their physical characteristics related to pore size and type and the best iodine number obtained. The substrate used in this work is designated as PK-ZC-H-450 (palm kernel-zinc chloride activated-acid treated-at 450°C). All reagents were of analytical grade (Analar) and supplied by Sigma Chemicals. Standard iodine solutions were prepared indirectly by dissolving it together with the

iodide salt solution. About 20 g of KI was dissolved in between 30-40 mL of DDW in a 1 L flask and later 12.7 g of I_2 added followed by shaking until all the iodine was dissolved. A standard iodate solution was prepared by the dissolution of 0.12 g of Analar KIO_3 supplied by Sigma Chemicals in DDW in a 1 L flask. The dilution made up to the mark gives a standard stock solution of 100 $\mu g.mL^{-1}$. Required standard of varying concentrations were prepared accordingly by using certain dilution factors. A schematic representation of the separation procedure is shown in Fig.4. After filtration the filter was freeze-dried using an Edward Mudalyo freeze-dryer and stored for further analysis.

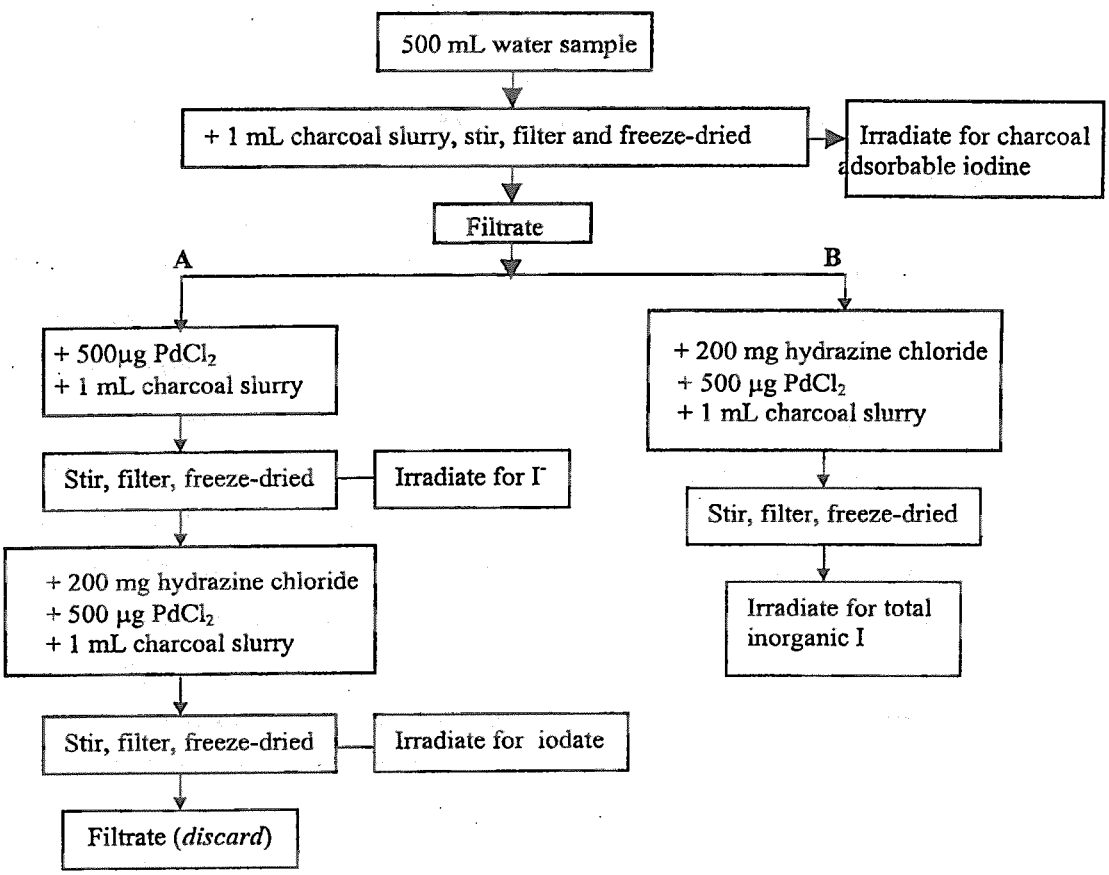

Fig. 4. Separation scheme of iodine species in river and well water samples

Sediments core samples collected were oven-dried for at least 2 weeks at 60° C or until a constant dry weight was observed followed by grinding using a grinder mill (Herzog) to get the homogenous powdered form of approximately < 200 mesh size (±75 µm) prior to further analyses as in the case of rare earth elements determination and distribution patterns studies. Further treatment, as in the case of speciation of Se(IV) in marine sediments, was required whereby the sample solutions for the extraction step with DBDTC-Pp were prepared by dissolving 1 g of the dried material with a mixture of 6.0 mL of HNO_3 (70%), 4.0 mL of $HClO_4$ (60%) and 2.0 mL of

HF (48%) in a Teflon™ pressure decomposition vessel of a CEM Model MDS-81D microwave digester. The resultant solutions were allowed to cool to ambient temperature before filtering them through a Whatman 0.45μm membrane filter followed by the addition of 1.5 mL of 30% H_2O_2 and finally made up to 250 mL with DDW for subsequent analyses. All SRMs and standards used in this study were similarly treated for consistency. The extraction procedure for the Se(IV) species requires the preparation of a fresh batch of DBDTC solution and the sample solution was first adjusted to pH 2.0 with 2.0 M HCl. About 2.0 mL of 2% DBDTC, 4.0 mL of 12% EDTA and 6.0 mL of 5% phenolphtalein were added to 250 mL of sample solution in a conical flask. The samples were stirred with a magnetic stirrer for about 1 min. and the precipitate formed was separated by filtration through a 0.45μm membrane and freeze-dried using an Edward Mudalyo freeze-dryer prior to the irradiation step.

The determination of inorganic As and Se in leachates was done according to the method similarly described for sediment samples. Details for the extraction procedures for inorganic As species were described by Yusof *et al.*[12,16,17] Inorganic Se(IV) species were extracted by a modified method involving co-precipitation with sodium dibenzylcarbodithioate-phenolphthalein (NaDBDTC-Pp) on the aqueous solution. A 100 mL aliquot of sample solution was acidified to pH 2 with concentrated HNO_3 in a conical flask. About 4 mL of 5% Na-DBDTC solution was added to the aliquot followed by 8 mL of 12% EDTA and 10 mL of phenolphthalein and the mixture was stirred with a magnetic stirrer for 10 min. and then left standing for 60 min. for the precipitate to settle. The precipitate obtained was filtered through a 0.45 μm Whatman membrane filter, washed with 2 mL of 0.01 M HNO_3 making sure that no precipitate was left in the flask and later freeze-dried prior to the irradiation step. The total inorganic selenium contents were determined similarly but the Se(VI) species from a fresh batch of 100 mL aliquot adjusted to pH 2 was first reduced to the Se(IV) state by adding 10 mL of 6M HCl and heated to about 70°C in a water-bath for 10 min. The difference in the total Se(IV) and the actual Se(IV) content determined earlier gives the Se(VI) concentration.

Irradiation and Counting

Irradiation of all samples were carried out in a TRIGA Mk.II reactor at the Malaysian Institute of Nuclear Technology and Research (MINT). Liquid samples solution of 1 mL from the final solutions were pipetted into vials of *i.d.* 10mm x 20mm, heat-sealed to prevent any leakages which might lead to reactor contamination and packed into larger vials before irradiating them in a neutron flux of 5.1×10^{12} $n.cm^{-2}.s^{-1}$. Between 0.15 and 0.25 g of the dried sediment samples were weighed into flip-top polyethylene vials (Olympia) and placed into larger vials before irradiating them. An irradiation period usually of 6h. followed by 2 weeks of cooling is normally required for the determination of Se species while it required only about 3 days of cooling after an

irradiation period of 6h. before the concentration of the As species is determined.[12,16] Irradiation of up to 6 h followed by varying cooling times were performed on the sediment samples to measure longer-lived isotopes of La, Ce, Sm, Eu, Tb and Yb. The short-lived isotope of Dy was counted for 5 min. immediately after an irradiation time of 1 min. followed by a cooling time of 20 min. Signals from the 559 keV γ-rays from ^{76}As and 264.7 keV and 136.0 keV from ^{75}Se were used in the quantitative determination of the inorganic As and Se species respectively. Counting was done over a period of 3600 s to ensure good statistics. The gamma spectrometry equipment used in the counting procedure consists of a large coaxial hyperpure germanium detector (HPGe) Model GC-1520, with a resolution of 1.9 keV at 1332 keV ^{60}Co connected to a pre-amplifier, amplifier and an ADC ND592 (Nuclear Data) analyzer connected to a ND6000 (Nuclear Data) multichannel analyser.

Output and Benefits of Study

Inorganic Se in Aquatic Species

Selective separation and extraction of the Se(IV) species from aqueous media by APDC and subsequent adsorption on C_{18}-bonded silica gel prior to determination by GFAAS[18] enabled concentrations of Se(IV) as low as 50 ng/L to be detected. Preconcentration of Se(IV) with the formation of a complex with 3-phenyl-5-mercapto-1,3,4-thiadiazole-2(3H)-thione potassium salt (Bismuthiol-II) have been successfully used by Sakai *et al* [19] where the complex was later adsorbed onto activated carbon and irradiated in a thermal neutron beam using the short-lived ^{77m}Se with a half-life of 17.5 s to calculate the amount of Se(IV) present in water samples. However, the success of the preconcentration and extraction step by APCDT-$CHCl_3$ followed by neutron activation analysis on aqueous samples for inorganic arsenic determination[13] prompted the application of this technique to the quantitative analysis of Se(IV) and Se(VI) in biological samples.

The *Lobster Hepatopancreas* TORT-1 SRM used in this study has a certified Se concentration of 6.88±0.47 μg/g and the value obtained in this study using the Chelex-100 chelating resin separation is 6.22±0.49 μg/g. This is equivalent to about 90.33% recovery and considered quite substantial, thus enabling this procedure to be used throughout the study. The microwave digestion with programmed heating was chosen instead of the normal heating to prevent massive loss of the volatile materials during the digestion step. The reproducibility of this technique in arsenic speciation was reported by Yusof *et al.*[13] Table 1 shows the concentrations of total inorganic Se in different parts of the *Tilapia nilotica* species using the Chelex-100 separation procedure. Comparatively, different parts of the fish seem to indicate

Table 1
Concentrations of total inorganic selenium in different parts of the *Tilapia nilotica* species

	Concentrations of inorganic Se (ng/g)		
Locations	Bone	Flesh	Head
1	297±27	410±31	93±6
2	331±28	410±31	92±7
3	367±29	275±23	82±6
4	294±26	289±22	80±7
5	381±39	327±26	88±7
6	344±24	316±28	94±8
7	362±30	287±21	76±5
8	428±36	371±24	73±5
9	349±27	255±17	75±5
10	349±24	248±17	76±6
11	417±33	257±19	77±6
12	287±22	267±47	84±7

Table 2
Concentrations of Se(IV) and Se(VI) in the bones of the *Tilapia nilotica* species

Locations	Se(IV) ng/g	Se(VI) ng/g	Se(IV)/Se(VI)
1	47±3	233±18	0.202
2	16±1	280±21	0.057
3	34±3	293±23	0.116
4	48±4	221±19	0.217
5	40±3	302±25	0.132
6	128±10	195±25	0.656
7	43±4	279±23	0.154
8	37±4	318±28	0.106
9	24±3	287±27	0.084
10	16±2	290±26	0.055
11	15±1	358±29	0.042
12	15±1	241±20	0.062

JAERI—Conf 2001—017

special preference in the accumulation of the inorganic Se species. In general, the bones have relatively higher concentrations of inorganic Se than the flesh with the head showing the least affinity for this element. This trend is prevalent in all the samples taken from all the locations. Other parts of the fish might show different preference but since only the bone, head and flesh parts are normally used in the preparation of food, other parts are not relevant and therefore discarded.

The Se(IV) and Se(VI) concentrations determined in the bone, flesh and head of the *Tilapia nilotica* species are presented in Tables 2, 3 and 4 respectively. The values given are expressed in μg/g dry weight. The normal weight used in the preparation of food is about five times more than the dry weight. Figures obtained for the Se(IV) concentrations in various parts of the *Tilapia nilotica* species show that the reduced form of the Se species is very much lower than the Se(VI) species. The bones of the *Tilapia nilotica* species have a greater tendency to concentrate the inorganic Se as compared to the head and flesh parts. This was also reflected in the figures obtained for the total inorganic Se contents using the Chelex-100 preconcentration step as shown in Table 1. The overall results indicate that most of the Se occur as the Se(VI) species and this is reflected in the low Se(IV)/Se(VI) ratio in the three parts of the *Tilapia nilotica* species investigated. The low Se(IV)/Se(VI) ratio also suggests that high oxidizing environment prevails in these water bodies thus favouring the formation of the Se(VI) than the Se(IV) counterpart. The inorganic Se uptake by the *Tilapia nilotica* species depends on the chemical forms of the element and its quantity, microbiological activities in the water and the age of the fish.

The extraction procedure used in waters from disused tin-mining pools and water treatment plants to separate the inorganic arsenic species from natural waters was found to be effective, as depicted by the percentage recoveries in Table 5. The percentage recovery for standard As(III) species was 100.6% and is comparable to 100.4% obtained in another study by Yusof *et.al.*[13] and 102.2% by Subramanian *et.al.* [20] This method enabled the elimination of interfering alkali metals especially ^{23}Na, alkaline-earth metals and the halogens especially ^{81}Br, both of which produce high-intensity γ-peaks from the ^{24}Na and ^{82}Br resulted from the high neutron capture cross-sections during the irradiation step. With the elimination of bromine, possible overlapping of the 556 keV peak from ^{82}Br on the 559 keV peak from ^{76}As is overcome. The presence of other metal ions such as Pb^{2+}, Cu^{2+}, Sn^{2+} and Sn^{4+} which could affect the degree of extraction of As(III) with the dithiocarbamate due to competitions by these ions was eliminated by using EDTA as the masking agent. The As(III) is readily extractable from the aqueous solution compared to the As(V) species, hence it was therefore more effective to reduce the As(V) to its lower oxidation state of As(III) using a suitable reducing agent such as $Na_2S_2O_3$ followed by extraction of the total As(III). The difference in the As(III) concentrations from the two water sample aliquots constitutes the As(V) present.

Table 3
Concentrations of Se(IV) and Se(VI) in the flesh of the *Tilapia nilotica* species

Locations	Se(IV) ng/g	Se(VI) ng/g	Se(IV)/Se(VI)
1	2±0.15	395±28	0.005
2	1±0.05	390±25	0.002
3	2±0.05	260±23	0.008
4	2±0.05	214±19	0.009
5	3±0.08	312±28	0.010
6	3±0.06	301±28	0.010
7	2±0.05	272±23	0.007
8	3±0.05	355±35	0.008
9	1±0.04	240±22	0.004
10	9±0.15	213±19	0.042
11	4±0.08	242±23	0.017
12	3±0.05	212±20	0.014

Table 4
Concentrations of Se(IV) and Se(VI) in the head of the *Tilapia nilotica* species

Locations	Se(IV) ng/g	Se(VI) ng/g	Se(IV)/Se(VI)
1	14±0.5	68±5	0.206
2	15±0.8	72±6	0.208
3	12±0.9	56±4	0.214
4	11±0.9	58±6	0.190
5	11±0.8	56±5	0.196
6	13±0.7	68±5	0.191
7	15±0.7	51±4	0.294
8	11±0.6	49±5	0.244
9	10±0.6	53±4	0.189
10	9±0.3	57±5	0.158
11	10±0.6	50±4	0.200
12	15±0.9	55±4	0.273

Table 5. Percentage recoveries of APCDT-$CHCl_3$ extraction of As(III) and As(V) with and without EDTA

sample	As(III) added ($\mu g.L^{-1}$)	As(V) added ($\mu g.L^{-1}$)	% recovery of As(III)	% recovery of As(V)
seawater[a]	100	100	71.5±1.7	75.5±1.9
well-water[a]	100	100	79.8±1.8	87.9±2.0
seawater[b]	100	100	100.7±2.5	96.5±2.2
well-water[b]	100	100	101.3±2.7	98.7±2.3

a - without EDTA; at room temperature
b - with EDTA; at room temperature

Table 6. Concentrations of As(III) and As(V) species in water samples from mining pools

Site	pH	Temp. (°C)	As(III) ($pg.L^{-1}$)	As(V) ($pg.L^{-1}$)	As(III)/As(V)
1	7.54	30.5	44.2± 5.90	221.0± 5.90	0.20
2	7.30	29.0	157.3±20.2	557.0± 77.1	0.28
3	7.54	30.3	731.0±50.3	1017± 41.5	0.72
4	7.33	30.5	255.8±31.0	235.5± 23.3	1.09
5	6.80	31.7	689.3±66.0	595.0± 45.2	1.16
6	7.50	30.3	238.1±34.3	2320± 59.0	0.10
7	7.65	29.0	170.7±19.5	1115±120	0.15

ND – not detectable

The overall concentrations of the inorganic arsenic species in water samples taken from mining pools as shown in Table 6, range between a minimum of 265.2 $pg.L^{-1}$ to a maximum of 2558.1 $pg.L^{-1}$ that is between 0.265 $\mu g.L^{-1}$ to about 2.26 $\mu g.L^{-1}$ and the average total inorganic arsenic for most surface waters is about 1.0 $\mu g.L^{-1}$. [21] In this study only three sites (5,6, and 7) as shown in Fig. 1, recorded total arsenic concentrations exceeding 1.0 $\mu g.L^{-1}$ and this reflected the nature of the soil in these particular areas as compared to the others. In terms of inorganic arsenic contents related to water quality, and under normal circumstances of an aquatic environment, the As(V) concentrations would far exceed the As(III) concentrations. However several factors, such as the external introduction of arsenic species from the surrounding areas where the sites are located, competing processes which can modify the concentrations of the

arsenic species in natural waters, such as lack of oxygen since most of the pools have depths of more than 30 m, leading to a low oxidizing environment and would shift the As(III)/As(V) ratio from less than 1.0 for a normal condition to more than 1.0 as illustrated by sites 4 and 5. The shift from a more dominant As(V) to one which is more dominant in As(III) can be found in certain reduced environments especially for water samples taken from deep wells or from surface waters of tropical gyres where the high internal cycling of phosphorous-based compounds inputs result in the rapid uptake of As(V) by phytoplanktons in the warm waters and excreting it as the As(III) reduced species.[22] Sites 4 and 5 could be comparable to a rather confined water body with little or no flow, thus depriving the aquatic environment with reduced oxygen required to sustain life. In terms of water quality the dissolved oxygen in waters taken from these sites is relatively low thus providing an environment not suitable for the formation of the more stable higher oxidation state of As(V). It can be inferred that water samples with As(III)/As(V) ratios of less than unity originate from a normal surface water environment suitable for aquatic life.

The charcoal prepared and used in the speciation of iodine from well and river waters had the highest iodine capacity of 838.2 (mg I g^{-1} carbon) compared to other substrates prepared under different conditions.[23] Prior to using the PK-ZC-H-450 activated charcoal as the adsorbant, recovery experiments were performed for iodine, iodate and iodide species by spiking the prepared standards in DDW and subjecting them through the same chemical separation using the adsorbant as filters. Each iodine species fraction after removal of the charcoal through filtration was irradiated to determine the percentage retained by the charcoal for various species. More than 52.1% iodine was retained in the prepared charcoal, while the percentage is lower for iodate (45.9%) and iodide (41.6%) species. The percentage of iodine species retained by the prepared charcoal appeared to be relatively lower compared to the commercially available substrates used by Woittiez *et al.*[23] However, Mukherjee *et al.*[24] reported that charcoal derived from agricultural wastes and impregnated with $ZnCl_2$ as the activating agent during the carbonation process resulted in a degradation of the cellulose material, causing the structural framework to expand and resulting in improved pore size. This could be the reason for the relatively lower retantion for most iodine species in the substrates used in this work.

The $PdCl_2$ used in the iodate and total inorganic iodine separation was maintained at 500 μg to achieve quantitative recovery as mentioned by Woittiez *et al.*[23] The chemical treatment used in the sequential separation of the iodine species follows that of Woittiez *et al.*[23] except in the quantitative analysis where instead of iodine tracers, prepared standards were irradiated together with the separated iodine species. The amount of hydrazine added was also not critical as it did not give any significant change in the concentration of iodate or iodide determined in the water samples.[23] All separation procedures were performed at the natural pH of between 6.3 – 7.5 of the river and well water samples. Quality assurance control tests were performed by standard addition as no standard reference materials were available for comparison. The concentrations of

various iodine species obtained from the neutron activation analysis of the filter were tabulated in Table 7 for river water samples and in Table 8 for well water samples.

Table 7. Concentrations of charcoal-adsorbable iodine, iodide, iodate and total inorganic iodine for river water samples

Sample location	Temp. (°C)	pH	Charcoal-adsorbable iodine (μg/L)	Iodide (μg/L)	Iodate (μg/L)	Total inorganic iodine (μg/L)	Ratio (sum species/ total)
R1	24.0	7.4	0.197±0.02	0.067±0.01	0.121±0.01	0.313±0.02	1.23
R2	25.0	7.0	0.121±0.01	0.038±0.01	0.115±0.01	0.325±0.01	0.84
R3	25.0	7.0	0.159±0.01	0.067±0.01	0.121±0.01	0.293±0.01	1.18
R4	24.0	7.2	0.144±0.01	0.120±0.01	0.101±0.02	0.258±0.02	1.41
R5	25.0	7.0	0.180±0.01	0.014±0.02	0.100±0.02	0.249±0.01	1.18
R6	26.0	7.0	0.188±0.02	0.083±0.01	0.091±0.01	0.288±0.01	1.26
R7	24.0	7.2	0.190±0.01	0.055±0.01	0.129±0.01	0.345±0.01	1.08
R8	26.0	7.4	0.135±0.01	0.135±0.01	0.137±0.01	0.352±0.01	1.16
R9	23.4	6.4	0.182±0.01	0.047±0.01	0.090±0.01	0.242±0.01	1.32
R10	23.3	7.8	0.110±0.02	0.063±0.01	0.098±0.01	0.263±0.01	1.03
R11	24.0	7.2	0.153±0.01	0.078±0.02	0.112±0.01	0.299±0.02	1.15
R12	27.0	6.3	0.146±0.02	0.077±0.01	0.108±0.01	0.227±0.01	1.46
R13	29.0	6.3	0.199±0.01	0.069±0.01	0.122±0.01	0.238±0.01	1.64
R14	22.4	6.4	0.173±0.01	0.132±0.02	0.123±0.02	0.300±0.01	1.43
R15	24.1	6.5	0.160±0.01	0.125±0.01	0.110±0.01	0.303±0.01	1.30
R16	23.2	6.8	0.154±0.01	0.041±0.02	0.100±0.01	0.3100.01	0.95

R = river

The study serves as an indication of the presence of iodine and its species in different drinking water sources and it also attempts to relate the different geochemical surroundings from where these waters were drawn. Well waters seem slightly more acidic than river waters due to the reduced aeration taking place in well waters. More bacterial actions, either aerobic or anaerobic, would have taken place in stagnant waters as in the case of well waters, thus giving rise to acidic by-products associated with organic material breakdown.[25]

Charcoal-adsorbable iodine, mainly I_2 in solution, is the quantity of iodine remaining on the activated charcoal filter after filtration from the river and well water samples without changing their natural pH values. It was observed in Tables 7 and 8 generally, that the amounts of charcoal-adsorbable iodine in river water samples were higher compared to well waters. Hoede *et al.*[26] have reported on the simultaneous decrement of iodate species with an increase of iodide species in reducing environments of marine sediment during a study conducted in Indonesian waters. The same trend is also observed in this work in well water samples with relatively higher reducing conditions compared to river waters. The reduced iodine species of iodide were much higher than those determined in river waters. Much of the acidic by-products produced by

bacterial actions at the bottom of the well must have provided the reducing environment that can convert the higher oxidation state iodine species into the reduced forms of iodide. The slightly higher temperature of the well water is expected since the water samples were drawn from the sub-surface epilimnion strata. Natural convection of the water has brought up some of the bottom water rich in reduced iodine species to the top. The same is not true in river waters since constant aeration has provided the iodine species with oxygen-rich water thus maintaining them in the oxidized forms of iodate and charcoal-adsorbable iodine.

Table 8. Concentrations of charcoal-adsorbable iodine, iodide, iodate and total inorganic iodine for well water samples

Sample location	Temp. (°C)	pH	Charcoal-adsorbable iodine (μg/L)	Iodide (μg/L)	Iodate (μg/L)	Total inorganic iodine (μg/L)	Ratio (sum species/ total)
W1	29.0	5.9	0.077±0.01	0.312±0.01	0.108±0.01	0.214±0.01	2.32
W2	28.0	5.3	0.022±0.01	0.297±0.01	0.063±0.01	0.101±0.02	3.78
W3	28.0	5.4	0.079±0.01	0.298±0.01	0.097±0.01	0.153±0.01	3.10
W4	29.0	5.0	0.032±0.01	0.301±0.01	0.073±0.02	0.158±0.02	2.57
W5	34.0	4.5	0.058±0.01	0.313±0.01	0.112±0.01	0.198±0.01	2.44
W6	27.0	5.2	0.021±0.02	0.288±0.01	0.080±0.01	0.220±0.01	1.77
W7	26.0	5.5	0.035±0.01	0.277±0.01	0.091±0.01	0.122±0.02	3.30
W8	26.0	5.4	0.063±0.01	0.270±0.01	0.110±0.01	0.180±0.01	2.46
W9	26.2	5.8	0.078±0.01	0.286±0.02	0.092±0.02	0.192±0.02	2.38
W10	25.9	5.5	0.020±0.01	0.312±0.01	0.090±0.01	0.215±0.01	1.96

W=well

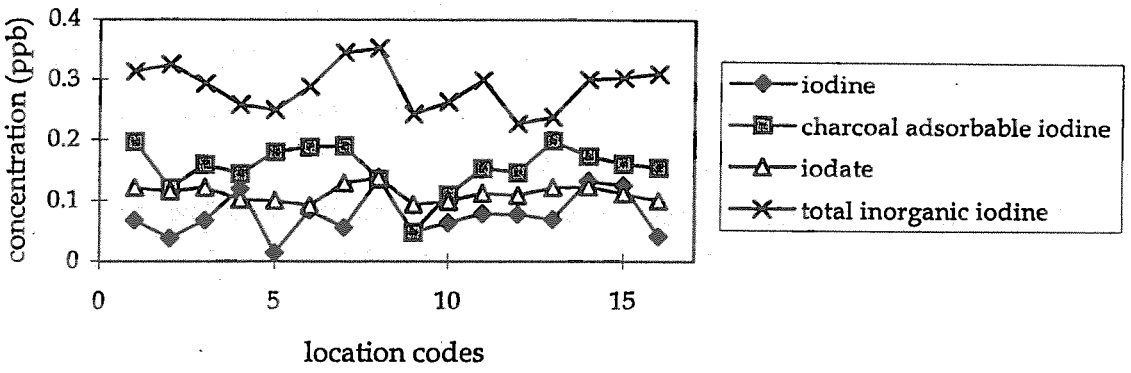

Fig. 5. The distribution of iodine species in river water samples according to locations

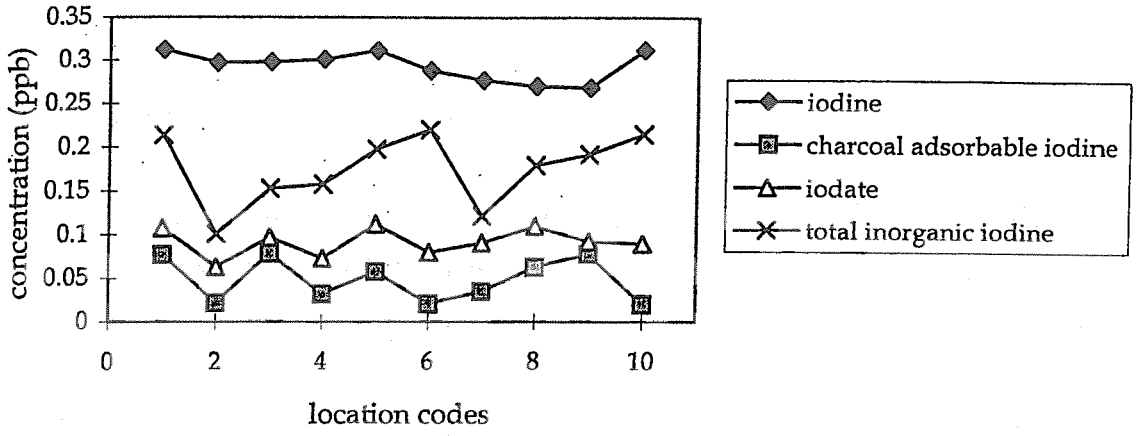

Fig. 6. The distribution of iodine species in well water samples according to locations

Figures 5 and 6 show the distribution of the various iodine species in river and well water samples according to the sampling locations. The analysis of iodine species in water samples taken from the same locations showed that the concentration patterns were almost identical. There were no abnormalities in terms of relative concentrations of the iodine species. This serves to illustrate that any incremental in the concentrations of the reduced iodine species is consistent with the simultaneous decrease of their oxidized forms.

The efficiency of the procedure described in the speciation of Se(IV) in marine sediments was tested by comparing the certified selenium contents in both the SRMs of BCSS and MESS-2 with those obtained in this work. Table 9 shows the percentage recoveries of total selenium in both the SRMs. It was found that a percentage of 95.4 and 93.1 for BCSS and MESS-2 respectively provided good quality assurance controls and these figures were used throughout this work for consistency. The relatively good recoveries for Se(IV) using phenolphtalein as a coprecipitant was also reported by Saleh *et.al*[27] where more than 90% of the spiked Se(IV) was recovered. Linder *et.al* [28] adopted the coprecipitation technique using only DBDTC to extract twelve heavy metals in pharmaceutical products with recoveries of more than 90%.

Table 9. Percentage recoveries of selenium in standard reference materials

SRM	certified values ($\mu g.g^{-1}$)	determined values ($\mu g.g^{-1}$)	% recovered
BCSS	0.43±0.06	0.41±0.07	95.4
MESS-2	0.72±0.09	0.08±0.08	93.1

The use of microwave digestion with programmed heating was chosen instead of the normal heating to prevent massive loss of the volatile materials during the digestion step. The reproducibility of this technique was reported by Yusof *et.al*[13] in the speciation of arsenic in seawater and some localized marine species.

Some of the concentrations for Se(IV), expressed in $\mu g.g^{-1}$ or ppb, determined at different sediment strata for the four locations are given in Table 10. There is no distinct pattern observed for all the four sites in terms of Se(IV) distribution implying that the concentrations of Se(IV) in the sediment were subjected to constant changes in the inorganic selenium input. Except for samples taken at location J19, the rest showed varying amounts of inorganic selenium inputs possibly originating either from the industrial settlement between SJ2 and J17 or pollutants trapped within the bay area where J21 is located. There is a possibility that location J19 is located in the path of a fairly constant sea current originating from the bay area as well as moving along the straits. The distribution of Se(IV) is quite constant at J19 with time since the lower strata represents the accumulation trend of pollutants in the past. Fig. 7 shows the distribution pattern of Se(IV) concentrations for the four sites for comparison.

Table 10. Concentrations of Se(IV) in sediment strata at different locations

Locations Strata (cm)	SJ2 ($\mu g.g^{-1}$)	J17 ($\mu g.g^{-1}$)	J19 ($\mu g.g^{-1}$)	J21 ($\mu g.g^{-1}$)
0 - 02	50.17±0.08	20.79±0.03	13.36±0.07	ND
02 - 04	19.93±0.09	40.24±0.07	16.93±0.02	ND
04 - 06	24.95±0.05	16.62±0.03	16.24±0.05	ND
06 - 08	30.56±0.08	12.93±0.05	37.29±0.09	ND
08 - 10	35.83±0.09	20.13±0.06	18.48±0.05	ND
10 - 12	47.79±0.08	33.10±0.08	17.50±0.05	ND
12 - 14	19.55±0.06	25.78±0.06	16.20±0.09	12.57±0.05
14 -16	17.28±0.04	17.55±0.04	11.48±0.07	10.23±0.03
16 - 18	-	-	17.17±0.05	3.93±0.05
18 - 20	-	-	12.62±0.09	ND
20 - 23	-	-	12.25±0.06	11.64±0.07
23 - 26	-	-	15.47±0.08	30.03±0.06
26 - 29	-	-	17.86±0.02	9.07±0.07
29 - 32	-	-	11.48±0.09	13.55±0.08
32 - 35	-	-	17.17±0.05	15.93±0.05
35 – 38	-	-	20.15±0.07	-
38 - 41	-	-	30.93±0.06	-

Note : ND – not detectable

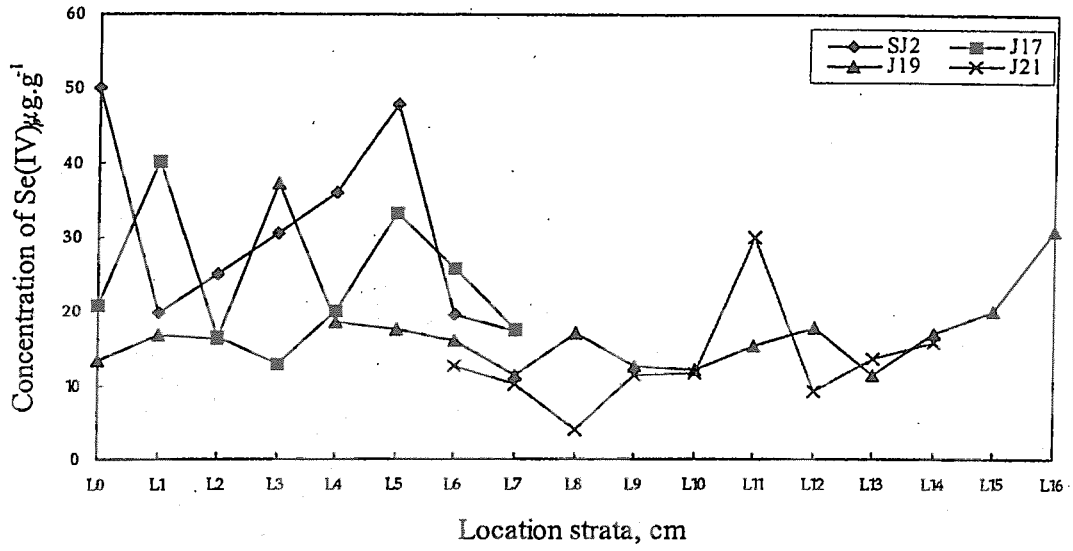

Fig. 7. Distribution pattern of Se(IV) concentrations at different depths

The accumulation of Se(IV) at SJ2 recorded relatively higher concentrations of Se(IV), between 17.28±0.04 $\mu g.g^{-1}$ to 50.17±0.08 $\mu g.g^{-1}$. There is no clear trend in the accumulation pattern except that this location is within the industrial belt along the coast and it is quite natural that it acts as a receiving basin for most pollutants. It was reported by Cobo *et.al*[29] that in fresh water the usual range of inorganic selenium is between 0.02 - 1.0 $ng.mL^{-1}$ and in sea water 0.004 ng. mL^{-1} at the surface and 0.06 $ng.mL^{-1}$ in the deep ocean, mostly in the selenite form. Groundwater in contact with different geological environments may reach much higher concentrations of inorganic selenium, sometimes as high as 6000 $ng.mL^{-1}$.[30] Since the sediments obtained varies in nature, from high in organic materials to mostly clay, it was anticipated that the determination of Se(IV) and/or Se(VI) was somewhat suppressed by the interference of dissolved organic carbon (DOC) as reported by Workman and Soltanpour[31] when they found out that recoveries of Se(IV) and Se(VI) in some extracts were poor. All these factors could have contributed to the non-uniformity of Se(IV) species in different sediment strata resulting in uneven accumulation and distribution of the inorganic selenium species as indicated in this study.

The analytical results for some of the REE elements for sediment core samples taken at sites J-17, J-19 and J-21 (as shown in Fig.3) are presented in Tables 11, 12 and 13 respectively and are expressed in $\mu g.g^{-1}$. A better representation of the variation in down-core concentrations and distribution of the REEs can be seen from the profiles as shown in Fig. 8 for the three sites J-17, J-19 and J-21. The extent of change in the concentrations of the REEs with depth is better demonstrated by these profiles and can be used to distinguish enrichments due to anthropogenic input from those due to natural processes, especially if the age of the sediment layers can be

estimated by using accumulation rates, surface layer mixing depths and rates obtained from radionuclide activity profiles.

Table 11. Concentrations (μg/g) of REE in core sediment collected at site J-17

Depth (cm)	La	Ce	Sm	Eu	Tb	Dy	Yb
0-2	73.53±8.18	70.61±1.29	9.95±0.36	0.66±0.08	0.74±0.22	3.86±0.66	3.12±0.20
2-4	66.36±5.40	62.94±0.94	10.31±0.26	0.63±0.05	0.77±0.13	3.40±0.50	2.96±0.18
4-6	65.97±5.41	74.35±1.00	10.05±0.25	0.75±0.05	0.80±0.16	4.09±0.56	3.05±0.18
6-8	47.88±4.12	68.61±0.96	6.49±0.21	0.68±0.05	0.81±0.16	3.81±0.47	2.64±0.17
8-10	57.20±7.22	72.99±1.31	7.61±0.26	0.71±0.08	0.61±0.25	3.11±0.48	2.01±0.16
10-12	59.15±4.94	68.81±1.00	8.33±0.23	0.79±0.05	0.61±0.15	3.31±0.42	3.62±0.23
12-14	54.97±4.75	76.51±1.08	8.32±0.22	0.77±0.06	1.24±0.19	3.06±0.57	3.25±0.20
14-16	22.30±10.67	55.94±2.58	6.28±0.60	0.65±0.15	N.D.	N.D.	N.D.
16-18							
18-20							
20-23							
23-26							
26-29	46.51±4.18	66.57±0.89	7.79±0.21	0.82±0.05	1.20±0.18	4.08±0.50	2.37±0.14
29-32	29.18±9.55	68.28±2.70	7.78±0.53	0.67±0.14	N.D.	N.D.	2.53±0.52
32-35							
35-38	40.23±4.43	77.00±1.16	7.42±0.22	0.51±0.06	0.57±0.18	3.33±0.47	1.59±0.09
38-41	49.44±3.79	72.24±0.09	6.73±0.19	0.82±0.05	0.76±0.13	3.96±0.52	2.22±0.13

ND – not determined

Table 12. Concentrations (μg/g) of REE in core sediment collected at site J-19

Depth (cm)	La	Ce	Sm	Eu	Tb	Dy	Yb
0-2	50.08±0.52	59.10±1.01	8.15±1.13	0.48±0.04	0.70±0.11	2.94±0.47	2.30±0.11
2-4	57.85±0.55	51.81±0.97	10.27±1.16	0.60±0.04	0.66±0.11	3.75±0.47	2.20±0.12
4-6	63.54±0.56	59.88±1.01	11.97±1.25	0.62±0.04	0.47±0.09	3.77±0.44	2.54±0.13
6-8	ND	58.44±1.96	11.28±2.17	0.73±0.08	0.75±0.21	3.22±0.88	ND
8-10	56.84±0.54	62.69±1.00	12.79±1.19	0.73±0.04	0.66±0.10	3.02±0.49	2.11±0.12
10-12	53.77±0.50	67.21±1.04	9.18±1.10	0.65±0.05	0.69±0.12	4.00±0.50	1.92±0.10
12-14	49.33±0.48	55.70±0.94	8.69±1.05	0.59±0.04	0.43±0.11	3.49±0.45	1.92±0.10
14-16	51.66±0.47	63.57±1.01	10.16±1.05	0.62±0.05	0.51±0.12	3.72±0.39	2.14±0.10
16-18	44.84±0.45	56.52±0.98	6.81±0.78	0.65±0.04	0.42±0.07	3.22±0.46	1.97±0.12
18-20	42.52±0.43	61.50±1.00	11.06±0.97	0.74±0.05	0.70±0.10	3.06±0.46	1.85±0.10
20-23	46.43±0.44	60.55±1.00	9.81±0.95	0.59±0.04	0.67±0.15	4.11±0.45	1.99±0.10
23-26	44.96±0.44	62.21±1.00	7.01±0.86	0.71±0.05	0.86±0.18	3.39±0.42	1.88±0.09
26-29	50.26±0.46	64.60±1.00	7.99±0.81	0.69±0.05	0.55±0.09	3.80±0.40	2.03±0.10
29-32	37.79±0.40	52.86±0.92	8.69±0.85	0.52±0.04	0.52±0.07	3.37±0.56	1.73±.0.09
32-35	28.57±0.32	57.05±0.85	9.87±0.89	0.70±0.05	0.74±0.12	3.77±0.52	1.35±0.07
35-38	27.88±0.31	61.50±0.93	9.09±0.87	0.85±0.05	0.95±0.13	3.85±0.50	1.39±0.07
38-41	26.38±0.29	59.90±0.94	8.38±0.92	0.77±0.05	0.63±0.10	4.20±0.36	1.43±0.07
41-44	24.58±0.28	59.17±0.92	7.82±1.44	0.79±0.05	0.73±0.11	3.77±0.46	1.40±0.07
44-47	25.06±0.28	57.52±0.92	6.43±0.62	0.70±0.05	0.56±0.12	2.99±0.40	1.55±0.08

ND – not determined

Table 13. Concentrations (μg/g) of REE in core sediment collected at site J-21

Depth (cm)	La	Ce	Sm	Eu	Tb	Dy	Yb
0-2	38.42±1.49	69.97±0.98	7.23±0.11	0.78±0.06	0.55±0.12	4.24±0.49	2.83±0.26
2-4	32.67±6.13	67.68±4.14	7.66±0.46	N.D.	N.D.	N.D.	2.42±1.14
4-6	35.66±1.39	62.18±0.91	6.67±0.09	0.70±0.05	0.78±0.13	4.46±0.48	2.20±0.22
6-8	37.92±1.52	62.17±0.94	6.51±0.09	0.68±0.06	0.63±0.15	5.22±0.49	2.31±0.24
8-10	34.17±1.61	61.71±0.99	6.18±0.09	0.69±0.06	0.52±0.14	4.79±0.46	2.88±0.29
10-12	29.59±1.25	66.62±0.92	5.88±0.08	0.79±0.05	0.62±0.11	4.82±0.38	2.47±0.21
12-14	28.44±1.31	59.06±0.91	4.95±0.08	0.74±0.06	0.57±0.15	5.07±0.41	2.06±0.22
14-16	25.18±1.07	64.52±0.93	4.32±0.07	0.63±0.05	0.56±0.13	4.53±0.45	1.79±0.20
16-18	17.73±0.95	61.93±0.94	3.69±0.07	0.74±0.06	0.69±0.17	3.91±0.41	1.96±0.20
18-20	17.59±0.90	63.38±0.93	3.58±0.06	0.77±0.06	0.59±0.13	5.40±0.44	1.26±0.15
20-23	11.84±0.70	38.68±0.80	2.56±0.05	0.48±0.04	0.80±0.13	2.95±0.35	0.87±0.13
23-26	8.40±0.63	33.38±0.79	1.99±0.05	0.36±0.04	0.32±0.09	2.66±0.29	0.74±0.12
26-29	7.89±0.57	27.45±0.72	1.70±0.05	0.41±0.04	0.32±0.08	2.26±0.31	0.54±0.11
29-32	6.54±0.71	24.52±0.77	1.53±0.05	0.33±0.05	0.34±0.16	2.40±0.26	0.68±.0.14
32-35	8.18±0.81	26.16±0.79	1.74±0.05	0.27±0.06	N.D.	1.68±0.33	0.98±0.20
35-38	7.37±0.53	27.98±0.71	1.52±0.05	0.31±0.06	0.17±0.09	2.04±0.31	1.05±0.15
38-41	10.03±0.80	41.76±0.82	1.92±0.05	0.35±0.06	0.40±0.09	2.59±0.37	0.86±0.19

ND – not determined

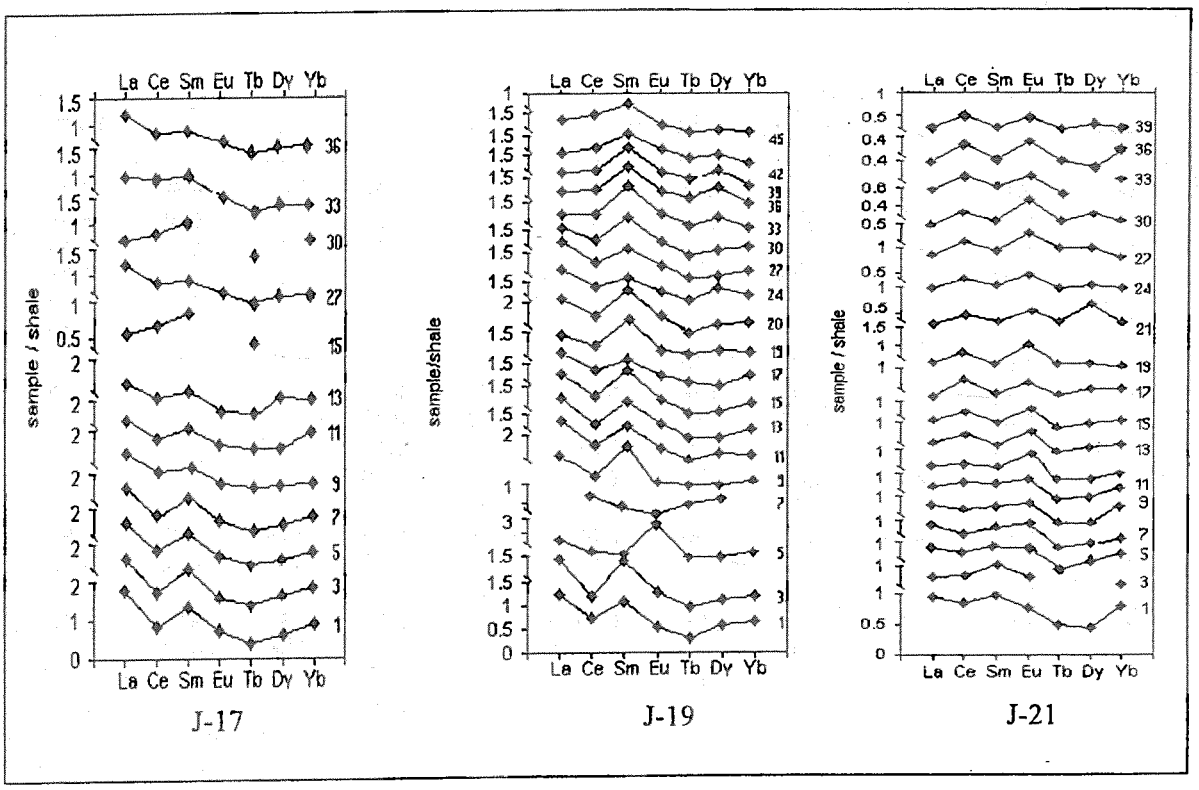

Fig. 8 Distribution patterns of shale-normalized REE placed in stratigraphic order for core samples taken at three sites (J-17, J-19 and J-21)

In general the concentrations of other REEs determined at sites J-17 and J-19 have not extremely changed with depth though the concentrations of La, Sm and Yb at these two sites

seemed to decrease with increasing depth (Tables 11 and 12). On the other hand all REEs at site J-21 exhibit decreasing concentrations from surface to the bottom of the sediment (Table 13). Incidentally, concentrations of REE except Eu and Dy at site J-17 were higher than sites J-19 and J-21. It is evident that the REEs are more enriched in the surface of sediments compared to the lower strata. This enrichment reflects the preferential scavenging of REEs from the seawater rendering the continual accumulation of these REES at the upper part of the sediment core. De Baar et al[13] have reported that REE concentrations were found to increase with the depth of sea water column taken from the Pacific and Atlantic Ocean basins. Increasing of REE concentrations in the surface of core sediments are supported by these results since the higher concentrations of REEs in the deeper sea water column enables scavenging of REEs to occur at the top sediment layer as compared to sediments taken at a depth of between 5 to 10 m as described in this work. It was found that except La and Sm, REE concentrations in core sediments were lower than those in average shale given by De Baar *et al*[32] and Sholkovitz.[33]

Table 14. The total REE values, Ce/Ce* anomalies, La/Sm and Yb/Sm ratios at all depths of 3 core sediment samples

Depth	J-21				J-19				J-17			
(cm)	ΣREE	Ce/Ce*	La/Sm	Yb/Sm	ΣREE	Ce/Ce*	La/Sm	Yb/Sm	ΣREE	Ce/Ce*	La/Sm	Yb/Sr
1	124	0.89	5.32	0.39	124	0.60	6.14	0.28	162	0.50	7.39	0.31
3	110	0.97	4.26	0.32	127	0.44	5.63	0.21	147	0.48	6.44	0.29
5	113	0.86	5.35	0.33	143	0.53	5.31	0.21	159	0.58	6.56	0.30
7	115	0.82	5.82	0.35	74				131	0.75	7.38	0.41
9	111	0.89	5.53	0.47	139	0.52	4.44	0.17	144	0.67	7.52	0.26
11	111	1.09	5.04	0.42	137	0.63	5.86	0.21	145	0.60	7.10	0.43
13	101	1.04	5.75	0.42	120	0.56	5.67	0.22	148	0.71	6.60	0.39
15	102	1.28	5.83	0.42	132	0.60	5.08	0.21	85	1.12	3.55	
17	91	1.68	4.80	0.53	114	0.64	6.59	0.29				
19	93	1.74	4.91	0.35	121	0.66	3.84	0.17				
21	58	1.56	4.63	0.34	124	0.62	4.73	0.20				
24	47	1.85	4.21	0.37	121	0.70	6.42	0.27				
27	41	1.66	4.63	0.32	130	0.65	6.29	0.25	129	0.72	5.97	0.30
30	36	1.75	4.27	0.45	105	0.66	4.35	0.20	108	1.06	3.75	0.33
33	39	1.53	4.69	0.56	102	0.84	2.90	0.14				
36	40	1.83	4.85	0.69	106	0.94	3.07	0.15	131	0.94	5.42	0.21
39	58	2.04	5.22	0.45	102	0.98	3.15	0.17	136	0.76	7.34	0.33
42					98	1.04	3.14	0.18				
45					95	1.05	3.90	0.23				

The total rare earth element concentrations, ΣREE values, as given in Table 14, indicate that the mechanism of REE incorporation could be lithologically dependent[4]. The ΣREE in sediments is correlated with the depth of the sediment strata. ΣREEs decrease with increasing distance from the surface to deeper layers for each sediment core. REE concentrations of 124 μg/g at the

surface in samples taken at sites J-21 and J-19 sediments decreased to 58 and 95 μg/g, respectively. However, ΣREE concentrations in sediment taken at site J-17 showed little variation. This results reflect the dominant role of REE at the surface layers and the significant role of seawater in the contribution of REE to the sediment. It was also observed that at intervals where Ce/Ce* anomalies increase the corresponding ΣREEs are found to decrease. Murray *et al*[8] reported that REE vary in marine sediments in a consistent fashion that can be directly related to depositional environment as in the case of the study area.

A comparison on the distribution of REEs in core sediments investigated in this study to those obtained from average shale and mean crustal materials and SRM Soil 7 was made and are given in Table 15. Almost all of the average concentrations of REEs determined in this work fall within the range reported by other workers[34-36] except for Eu which recorded a lower average concentration of about 0.66±0.14 μg/g but having a good agreement with values found in SRM Soil 7. This is attributed to the similar conditions existing between this area and those reported by other workers.[34-36] The Ce/La ratios calculated from the average concentrations in the core sediment samples gave a value of 1.55 which in this case is almost comparable to those found in the average shale and crustal materials, indicating the low probability of Ce enrichment due to its possible reduction to the lower valence state. It also suggests that there were little external inputs, especially from the effluents of a large oil refining complex situated to the south of Singapore island due to strong local undercurrents which prevent transport of the effluent around the island and into the Johore Straits.(Fig. 3) These observations were also reported by Wood *et al.*[10]

Table 15. Comparison of the concentrations (μg/g) of REE in core sediments with those in average shale and mean crustal materials

	Straits of Johore		Average shales	Mean crustal materials		SRM Soil-7
Element	Range	Average	B, M&M or T&W	M&M	B	SRM
La	6.54 – 73.50	38.52±2.60	24 - 92	30	32	28
Ce	24.52 – 77.00	59.89±1.11	50 - 96	60	68	61
Sm	1.52 – 12.79	7.14±0.48	6.2	6.0	7.9	5.1
Eu	0.27 – 0.85	0.64±0.06	1.0 - 1.2	1.2	2.1	1.0
Tb	0.17 – 0.86	0.66±0.14	ND	ND	ND	0.6
Dy	1.68 – 5.22	3.61±0.46	ND	ND	ND	3.9
Yb	0.54 – 3.62	2.06±0.18	2.4	0.5	3.3	2.4

B=Bowen (1979)[34]; M&M=Mason and Moore (1982)[35]; T&W=Turekian and Wedepohl (1961)[36]

REEs behaviors were also investigated with correlation between concentrations of Sm and these elements. Figs. 9, 10 and 11 show the concentrations of REEs plotted against those of Sm for sediments of varying depths. Sm was chosen because it is roughly in the middle of the series;

and precision and accuracy of Sm data are relatively good. Sm shows no anomalous behavior as exemplified by Ce and Eu.[37,38] Correlation coefficients were calculated for all REEs at all three sites. Site J-21 exhibits a highly significant positive correlation between selected REEs and Sm.

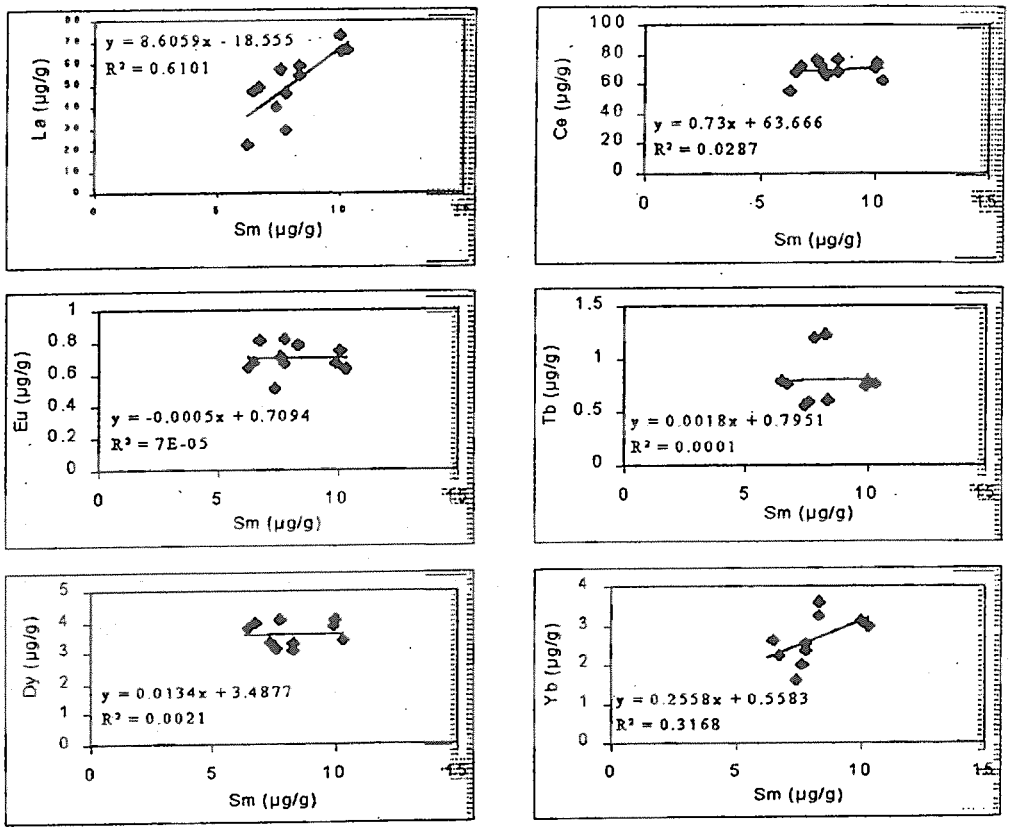

Fig. 9. Plot of REE (La, Ce, Sm, Eu, Tb, Dy, Yb) concentrations versus those of Sm for site J-17

The reasonably strong correlation was observed between (La, Yb) and Sm for site J-21. Correlation coefficients were found as r = 0.96 for La and 0.88 for Yb. Quite reasonably good correlations were observed between (Ce, Eu, Dy) and Sm at site J-21 as well where Ce, Eu and Dy are positively correlated with values of r = 0.78, 0.74 and 0.69 respectively. Almost all the REEs investigated at site J-19 did not display any good correlation except for La with a slight positive value of 0.27. This was rather insignificant because the distribution of La concentrations relative to Sm was not very good. A similar slightly positive correlative phenomenon was again observed at site J-17 for La with a correlation coefficient of 0.61. Generally the correlation between REEs and Sm for sites J-17 and J-19 was found to exist at a decreased level of significance. This could probably be due to external inputs from industrial effluents originating from the nearby industrial area as depicted in Fig.3.

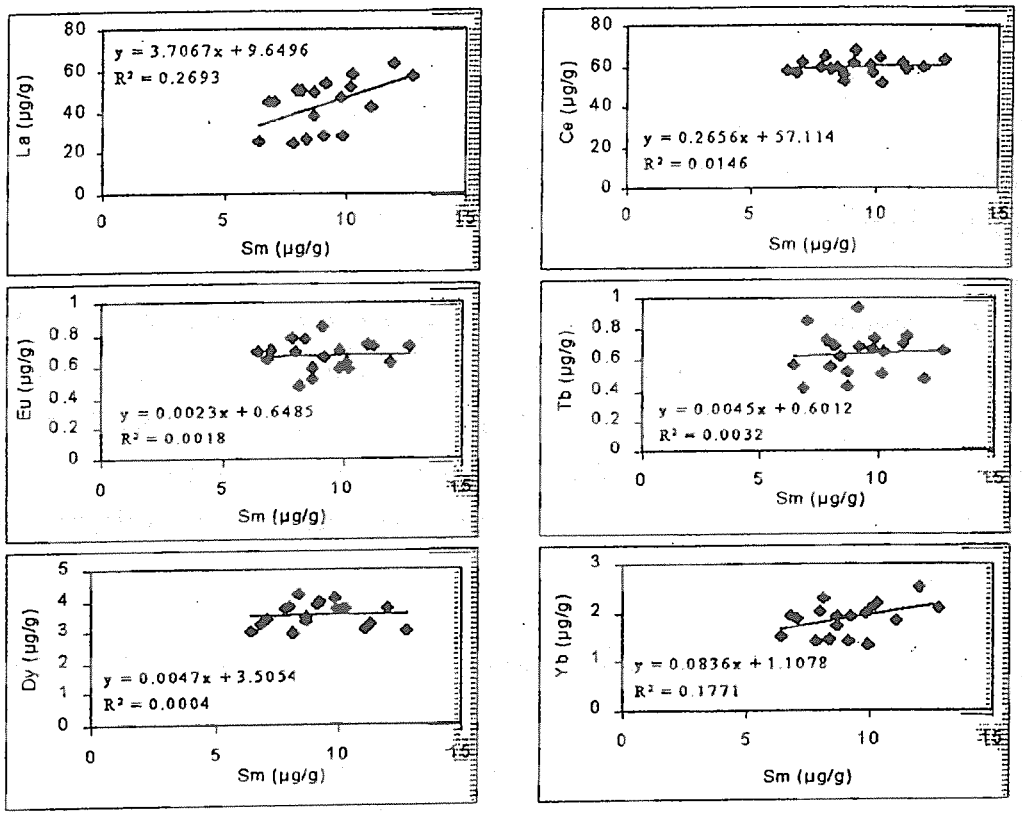

Fig.10. Plot of REE (La, Ce, Sm, Eu, Tb, Dy, Yb) concentrations versus those of Sm for site J-19

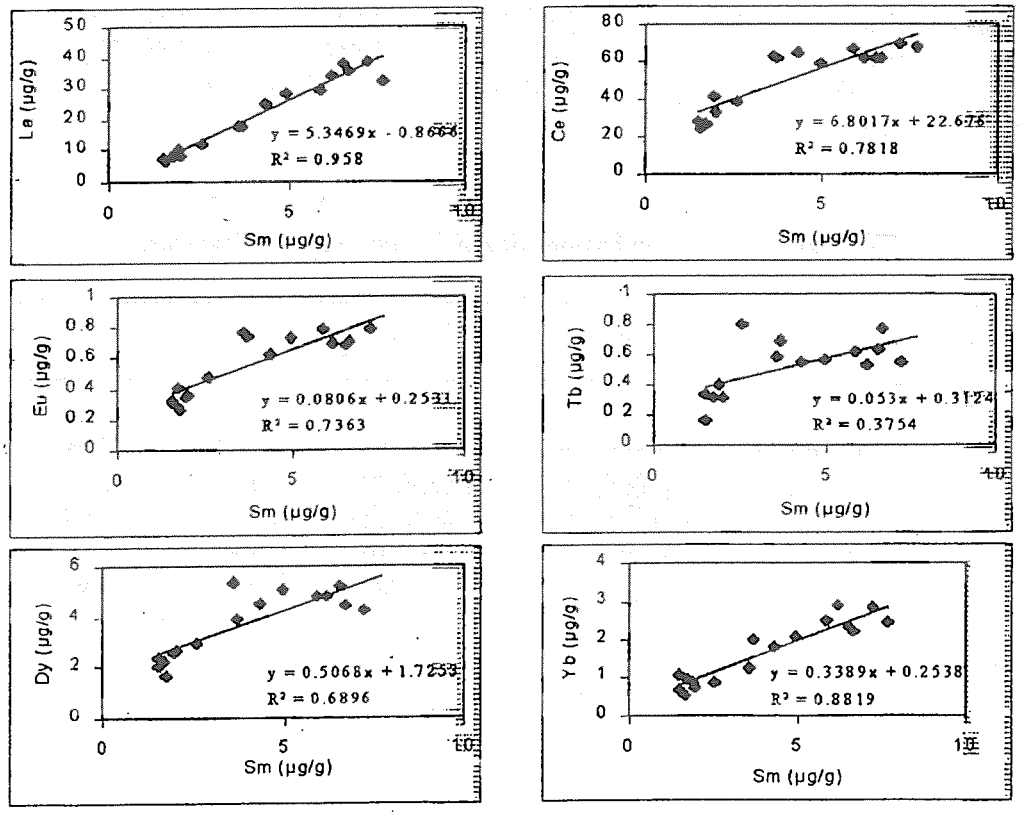

Fig.11. Plot of REE (La, Ce, Sm, Eu, Tb, Dy, Yb) concentrations versus those of Sm for site J-21

The 8 landfill sites chosen, as shown in Fig. 2 were scattered over an area of about 18950 km^2. All the 8 sites chosen are situated near rivers or streams which have water intake points somewhere along the length of the waterways. Hence this study is not only looking at the extent of pollution at water intake points by some trace elements leachates but also quantifying the dominant metal species present in the soluble toxic form using techniques with high efficiency and accuracy.

A SRM of Nearshore Seawater used in this study gave a total recovery of ≥95%, as shown in Table 16 suggesting good reproducibility in the techniques used. The same method for Se(IV) extraction and determination by co-precipitation with sodium dibenzyldithiocarbamate-phenolphthalein (NaDBDTC-Pp) on acidified aqueous solutions prepared from BCSS-2 Nearshore Seawater and MESS-2 Marine Sediment reference materials was employed in another study with good recoveries for total selenium.[17]

Table 16. Percentage recoveries of spiked As(III) and Se(IV) in aqueous solutions and in SRM

Sample	Species	Concentration in solutions or SRM ($\mu g.mL^{-1}$)		% recovery
		Before	After	
Spiked water	As(III)	1.0000	0.9584	95.84±1.50
Spiked water	Se(IV)	1.0000	0.9463	94.63±1.30
CASS-2 (*certified*)	$As_{(total)}$	0.97±0.02	0.93±0.04	96.10±2.75

Table 17. Concentrations of As(III) and As(V) in leachates

Location	As(III) μg/L	As(V) μg/L	Total As μg/L	pH	As(III)/As(V)
1	0.70±0.04	0.83±0.04	1.53±0.04	6.2	0.84
2	0.69±0.06	0.96±0.02	1.65±0.04	6.8	0.72
3	0.88±0.06	0.81±0.07	1.69±0.08	7.0	1.09
4	1.17±0.07	1.19±0.06	2.36±0.04	6.0	0.98
5	0.80±0.03	0.98±0.04	1.78±0.04	6.0	0.82
6	1.24±0.04	1.05±0.05	2.29±0.05	6.8	1.18
7	0.82±0.04	0.84±0.09	1.66±0.06	7.7	0.98
8	0.56±0.03	0.66±0.06	1.22±0.09	6.6	0.85

Concentrations from 8 locations of As(III), As(V) and the total inorganic arsenic species expressed in $\mu g.L^{-1}$ or ppb in leachate samples are given in Table 17 while those of Se(IV), Se(VI) and total inorganic selenium are given in Table 18. Water may be purposely or inadvertently used as carriers for soluble toxic inorganic arsenic and selenium depending on the source, especially from landfills located near rivers or streams and which will be loaded with these species after a heavy down pour. The determination and quantification of these species in water samples taken from water intake points need to be done to ensure that the treatment of raw water for public consumption is efficient in the reduction of the level of toxic inorganic species especially arsenic and selenium species. The pH of leachate samples range from 6.2 to 7.7 which is about the pH of normal freshwater. The fluctuations in pH in the leachates did not have any significant impact on the inorganic arsenic or selenium species concentrations.

Table 18. Concentrations of Se(IV) and Se(VI) in leachates

Location	Se(IV) μg/L	Se(VI) μg/L	Total Se μg/L	pH	Se(IV)/Se(VI)
1	0.71±0.04	0.89±0.04	1.60±0.04	6.2	0.80
2	0.99±0.06	0.76±0.02	1.75±0.08	6.8	1.30
3	1.36±0.14	2.33±0.61	3.69±0.08	7.0	0.58
4	1.10±0.07	1.34±0.06	2.44±0.08	6.0	0.82
5	1.03±0.04	0.92±0.08	1.95±0.12	6.0	1.12
6	1.36±0.14	1.29±0.61	2.65±0.15	6.8	1.05
7	0.92±0.10	2.05±0.23	2.97±0.34	7.7	0.45
8	0.63±0.03	0.98±0.13	1.60±0.17	6.6	0.64

All the samples have As(III) concentrations of more than 0.5 μg/L. Though the concentration of total arsenic in most natural water systems are in the range of 10^{-9} - 10^{-8} g/L,[39] the maximum admissible concentration for inorganic arsenic in public drinking water as recommended by the World Health Organization (WHO) is 50 μg/L.[40] All water samples taken near the landfill sites have values of total inorganic arsenic of less than 50 μg/L. The highest concentration recorded was 2.36±0.04 μg/L. While the total inorganic arsenic species might be less than the maximum acceptable limit imposed by WHO, EEC and the US[40] guidelines, the chemical environment could be different, one which is favouring the formation of the more toxic As(III) species at several sites. The balance between the corresponding existence of As(III) and As(V) species in water samples could be viewed from the As(III)/As(V) ratio. A ratio value of more than unity indicates predominantly higher concentration of the more toxic As(III) species. This could be the significant factor in determining the water quality of rivers used as intake

points. For example there are two sites with As(III)/As(V) ratio of more than unity and perhaps water taken from rivers situated near these sites require special attention during the treatment process in order to reduce the more toxic As(III) species to reasonable levels before distribution to the public. Under normal conditions, the As(III) species is a thermodynamically unstable oxidation state and the expected As(III)/As(V) would be less than unity. However because of the continuous discharge of arsenic compounds from the solid wastes dumped in these landfills, and also because of the anaerobic conditions in the waste pile, more of the As(III) would be preferably formed thus pushing the As(IIII)/As(V) to more than unity. Several competing biogeochemical processes taking place in the waste pile under anaerobic conditions could modify the concentrations of the dissolved ions in leachates giving rise to the concentration of the more toxic As(III) species.

The corresponding inorganic selenium species in water samples mixed with leachates taken from the same locations are given in Table 18. The same justification for the variation in Se(IV) and Se(VI) concentrations could be used to explain the distribution of these species in water samples taken from nearby streams and rivers at landfill sites. While some locations exhibited fairly low Se(IV)/Se(VI) ratios (locations 3, 7 and 8) three locations (2, 5 and 6) as shown in Fig. 2, have Se(IV)/Se(VI) of more than unity. Again these variations in Se(IV) and Se(VI) concentrations could be brought about by the intense contact of groundwater, especially after a heavy downpour or possibly resident groundwater, with the solid waste high in selenium contents reacting in different geological environments. Eleazer *et al*[41] reported an average pH of about 7.5 for the decomposition of organic refuse leaving the by-products in the form of soluble ions, perhaps metal ions which can easily be washed down into the leachates and consequently into the groundwater. It was also reported that coated paper, old newsprint, old corrugated containers and office paper represent 4.2, 6.6, 12.2 and 3.3% of municipal waste respectively and with the high content in chemicals especially in the treatment of the pulp and coatings, the anaerobic degradation will contribute to the accummulation of inorganic Se(IV), Se(VI) and other species in the leachates and with the right amount and flow of groundwater, these species will be washed down the waterways into streams and rivers. Very low levels of inorganic selenium species, in the range of 0.02 – 1.0 $ng.mL^{-1}$ are normally present in freshwater but the increased concentration of the lower oxidation state of the Se(IV) species described a different picture in terms of water quality where these landfills are closely situated. It will have a significant impact on the quality of the raw water used for public consumption and also on the cost of operation at water treatment plants. Though the maximum admissible limit for total selenium in drinking water is about 10 $\mu g.L^{-1}$[40] the total inorganic selenium however is much lower.

Basically out of the 8 locations where this study was carried out, most of them showed high As(III)/As(V) and Se(IV)/Se(VI) ratios indicating rather abnormal conditions for natural

groundwaters to exist. Naturally these abnormalities have been traced to sources with anthrapogenic inputs originating from landfills.

Future Studies

Much of the future studies using research reactors as far as this group is concerned would be focussed on environmental related areas including monitoring work, assessment of environmental safety and risk and to a certain extent inter-laboratory exercise. Some work on air pollution studies and its trend within the Asia Pacific region is under way using INAA as the main technique of analysis of elements in the finest air particulate matter (PM 2.5) and also in the coarser particles complemented with ICP-MS and ion chromatography. The air pollutants will be collected using a Gent Stack Sampler and softwares such as Chemical Mass Balance – 7 and Statgraphic will be used for source emission identification.

Further work in the marine environment will be pursued diverting from the usual sediment analysis to the more general marine materials to be collected within the Straits of Malacca. Elemental analysis will be performed using normalization procedure to address anthropogenic contaminants. This study will also attempt to investigate the multiple oxidation state of various elements such as U, As, Sb, Fe, Mn and Cr within the sediment column profile. Perhaps an extended application of INAA is the determination of anthropogenic elements in coral rings. The elemental contents in each ring would correspond to the historical profile of pollution trend within the study area. And this leads to the question of bio-indicator studies using marine species as the possible subject to map the pollution trend along the coastal areas. Substantial amount of sample collection has to be planned to provide enough input for modeling studies to be conducted such as using the MINTEQA 2 software for water quality studies.

Conclusions

The simplicity of the preconcentration step using a complexing agent such as APCDT as in the case of the inorganic selenium species determination in aquatic species followed by INAA have eliminated the problem associated with interfering metallic ions and with sufficient cooling time after the irradiation (usually two weeks) most of the 264.7 and 136.0 keV photopeaks would be visible for peak area estimation. This was also true in the speciation studies of inorganic Se in marine sediments. Some of the intriguing problems in the sample preparations, namely the dissolution of the sediments with little or minumum loss of the volatiles, have been partly overcome by using programmed microwave digestion. The problem would not be as demanding

if the determination of Se(IV) was done on seawater though some precautionary steps have to be taken to address the interfering alkali, alkaline earth and halogens.

The efficiency of the separation process in the speciaiton of inorganic As in the water quality studies of waters from disused tin-mining pools and in drinking water was evaluated using spiked standards for As(III) and As(V) and the method proved to be useful in low levels arsenic species determination. Water quality for water samples taken from different aquatic environment was also examined by assessing the concentrations of dissolved species which was also used as an indicator of the redox status of the water bodies.

Instrumental neutron activation analysis (INAA) is used because of its sensitivity for multi-elemental non-destructive analysis to address the quantitative aspect of the trace elements contents in samples used in various studies. By using charcoal derived from agricultural waste material, a study on the speciation of iodine was possible and the use of INAA further complemented the quantitative analysis.

References

1. J. E. LOVELOCK, R. J. MAGGS, R. J. WADE, (1973) Nature, 241, 194.
2. V. W. TRUESDALE, (1978) Mar.Chem., 6, 1.
3. V. W. TRUESDALE, C. P. SPENCER, (1974) Mar.Chem., 2,33.
4. A. YASUHARA, (1995) Toxicol.Environ.Chem., 51, 113-120.
5. R. W. MURRAY, T. B. M. BUCHHOLTZ, D. C. GERLACH, G. PRICE RUSS III, D. L. JONES, (1991) Geochim.Cosmochim.Acta, 55, 1875-1895.
6. G. Th. KLAVER , T. C. E. VAN WEERING, (1993) Marine Geology, 111, 345-359.
7. V. C. CRESPI, N. GENOVA, L. TOSITTI, O. TUBERINI, G. BETTOLI , M. ODDONE, S. MELONI, A. BERZERO, (1993) J. Radioanal. Nucl. Chem., Articles, 168, No.1, 107-114.
8. R. W. MURRAY, T. B. M. BUCHHOLTZ, D. L. JONES, D. C. GERLACH, G. PRICE RUSS III, (1990) Geology, 18, 268-271.
9. E. R. SHOLKOVITZ, (1990) Chem.Geol., 88, 333-347.
10. A. K. H. WOOD, Z. AHMAD, N. A. M. SHAZILI, R. YAAKOB, R. CARPENTER, (1997) Continental Shelf Research. 17, No.10, 1207-1228.
11. J. M. LO, J. C. YU, F. I. HUTCHINSON, and C. M. WAI, (1982). Anal.Chem., 54, 2536-2541.
12. A. M. YUSOF, M. MISNI, A. K. H. WOOD, (1997) J. Radioanal.Nucl. Chem. 216, No.1 59-63.

13. A. M. YUSOF, Z. B. IKHSAN, A. K. H. WOOD, (1994) J.Radioanal.Nucl.Chem., 179, No.2, 277.
14. H. M. KINGSTON, I. L. BARNES, T. J. BRADY, T. C. RAINS, M. A. CHAMPS, (1978) Anal.Chem., 50, 2064.
15. A. HUSSAIN, S. Y. UI, (1993) Proc.Malaysian Sci.Tech.Congress, Vol.1, 188.
16. A. M. YUSOF, N. A. RAHMAN and A. K. H. WOOD, (1994). Biological Trace Element Research, 43, 2.
17. A. M. YUSOF, Z. HANAFIAH and A. K. H. WOOD, (1998). The Sci.of the Tot.Environ. 214, 247-252.
18. R. E. STURGEON, S. N. WILLIE, S. S. BERMAN, (1985) Anal. Chem., 57, 6.
19. Y. SAKAI. K. TOMURA, K. OHSHITA., (1994) J. Radioanal.Nucl.Chem., 187, 441.
20. K. S. SUBRAMANIAM, J. C. MERANGER, R. F. McCURDY, (1984) Atomic Spectroscopy, 5(4), 192-194.
21. K. H. WEDEPOHL, S. W. STEARNS., (1994) Env.Science and Technology, 28(3), 534-537.
22. M. O. ANDREAE, (1986) Organometallic compounds in the environment : Principles and reactions. In: P. J. Craig (Ed.). Organoarsenic Compounds in the Environment. John Wiley and Sons, New York.
23. J. R. W. WOITTIEZ, H. A. van der SLOOT, G. D. WALS, B. J. T. NIEUWENDIJK, J. ZONDERHUIS, (1991) Marine Chemistry, 34, 247.
24. S. MUKHERJEE, S. BHATLACHAY, (1974) J.Phys.Chem., 2, 1725.
25. S. E. MANAHAN, Fundamentals of Environmental Chemistry, (1993) Lewis Publishers, Michigan, U.S.A. *pp*394.
26. D. HOEDE, J. WIJKSTRA, van der SLOOT, (1987) Netherlands Energy Research Foundation Rep.ECN-203, 231.
27. A. I. SALEH, J. R. W. WOITTIEZ, G. D. WALS, H. A. DAS, (1990) J.Radioanal.Nucl.Chem., 140(2), 357.
28. H. R. LINDER, H. D. SELTNER, B. SCHREIBER, (1978) Analytical Chemistry, 50(7), 896.
29. M. G. COBO, M. A. PALACIOS, C. CAMARA, F. REIS, P. H. QUEVAUVILLER, (1994) Anal.Chim.Acta 286, 371.
30. J. GLOVER, O. LEVANDER, J. PARIZEK, V. VOUK, (1979) Handbook on the Toxicology of Metals, Elsevier, Amsterdam, p555.
31. S. M. WORKMAN, P. N. SOLTANPOUR, (1980) Soil Sci.Soc.Am.J., 44, 1331.
32. H. J. W. De BAAR, M. P. BACON, P. G. BREWER, (1985) Geochim.Cosmochim.Acta, 49, 1943-1959.

33. E. R. SHOLKOVITZ, (1988) Am.J.Sci., 288, 236-281.
34. H. J. M. BOWEN, (1979) "Environmental Chemistry of Elements", Academic Press, London, pp 333.
35. B. MASON, C. B. MOORE, (1982) "Principles of Geochemistry", 4th. edn. J. Wiley and Sons, New York, pp 344.
36. K. K. TUREKIAN, K. H. WEDEPOHL, (1961) Bulletin of the Geological Society of America, 72, 925-965.
37. A. MATSUDA, Y. MATSUI, (1966) Geochim.Cosmochim.Acta. 30, 239-250.
38. K. TOYODA, Y. NAKAMURA, A. MASUDA, (1990) Geochim. Cosmochim.Acta, 54 1093-1103.
39. W. M. MOK, N. K. SHAH,. AND C. M. WAI, (1986). Anal.Chem., 58: 110-113.
40. I. M. SAYRE, (1988). J.Am.Water Works Assoc., 80(2): 53-59.
41. W. E. ELEAZER, W. S. ODLE, Y. S. WANG, M. A. BARLAZ, (1997) Environ.Sci.Technol. 31, 911-917.

JP0250102

1.18 Utilization of NAA in Thailand

Chastbongkoch Srinyawach

Office of Atomic Energy for Peace

Bangkok 10900 , Thailand

ABSTRACT

Although it is more than sixty years old ,Neutron Activation Analysis (NAA) is still widely used and continues to develop all over the world. Up to now, no other new analytical methods have been able to replace it for some applications. In Thailand ,NAA is avery popular nuclear technique for analysis of Trace elements in various samples and various fields by using the Thai Research Reactor-1/modification-1(TRR-1/M-1) as following: 1. Geological field, 2.Environmental field ,3.Biological field, 4.Industrial field and 5. Training and Technology Transfer

Introduction

The Office of Atomic Energy for Peace (OAEP) was established after the worldwar II under the program of "Atoms for Peace" proposed by the United States of America (USA) to the United Nation (UN): the program aimed to promote the peaceful use of atomic energy for the benefit of humankind and to discourage nations from obtaining or building destructive weapons.

On October ,27,1962 , The operation of the Thai Research Reactor to the criticallity was successful. The Thai Research Reactor-1 /modification-1(TRR-1/M-1) is a light water reactor (TRIGA MARK III)which has a power of 2 MW steady state and could be increased to 2,000 MW in pulsing state. The maximum nuetron flux at 1 MW is approximately 10^{13} $n/cm^2/sec$.. The TRR-1/M-1 utilization has been achieved in many area ie. isotope production , research in the field of chemistry, reactor characteristic studies and physics experiments, personnel training in reactor operation, industry and economy serving. All of these are Neutron Activation Technique.

Irradiation facilities

The TRR-1/M-1 has 7 facilities depending on the purpose of the activities as following :

1. In- core pneumatic transfer system
2. Out-core pneumatic transfer system
3. Rotary specimen rack system
4. Accessory tubes facility

5. Cadmium accessory tubes facility
6. Thermal column facility
7. Wet tubes facility

1.In- core Pneumatic Transfer system

This facility is used for producing the very short-lived radioisotopes . The specimen will be conveyed to and from reactor core, The major components as following :

- specimen capsule (rabbit)
- blower and filter assembly
- valve assembly
- terminus assembly
- receive-sender assembly
- control assembly
- specimen transfer box (optimal)

The system is controlled from the receiving area and may be operated either manually or automatically with an electric timing device in corporate into the system so that the specimen capsule is ejected automatically from the core from predetermined time span, A solinoid-operated valve controls the air flow . The system operates on a pressure differential drawing the specimen capsule into and out of the core by vacuum. Thus , the system is always under a negative pressure , so that any leakage is always into the tubing system. All the air from the pneumatic is passed through a filter before it is discharged or recycled back through the system. The thermal neutron flux are 0.9-2.9x10^{13}n/cm^2/sec.and the epithermal flux are 3.1x10^{11}-

$1.3x10^{12}$ n/cm^2/sec. The very small amount of sample and very short-lived radionuclides approved for this facility.

2.Out-core Pneumatic Transfer system

This facility cannot be used now because of the coorosive damage inside of the tubes.

3.Rotary Specimen Rack system (RSR)

There are 41 holes irradiation by this facility . The intermediate and long-lived radionuclides can be produced. The thermal neutron flux is approximately $3.1\text{-}3.5x10^{12}$ n/cm^2/sec. , and the epithermal flux is $6.9\text{-}8.8x10^{10}$ n/cm^2/sec.

4.Accessory tube facility

There are 2 tubes (A1,A4) in this facility and similar to the RSR for producing the intermediate and long –lived radionuclides and for the elements which have a thermal neutron cross-section better than epithermal neutron cross- section. The thermal flux are approximately $2.4x10^{11}$, $3.5x10^{10}$ n/cm^2/sec. and epithermal flux are $5.4x10^{9}$,$7.9x10^{8}$ n/cm^2/sec..

5.Cadmium accessory tubes facility

This facility has 2 cadmium covered tubes (CA2, CA3) and suitable for the irradiation of the resonance neutron active elements which produce the intermediate or long-lived radionuclides . there are only epithermal and fast neutron which have a epithermal flux in CA2 $2.2X10^{9}$ n/cm^2/sec. and in CA3 $1.2X10^{9}$ n/cm^2/sec.

6.Thermal column facility

The core was moved to the center of the pool. This facility was temporarily neglected.

7.Wet tubes facility

This facility has 5 big tubes (P1-5)diameter are about 4 inches and 8 small tubes (W1-8) diameter are about 2 inches. The big ones were established for topaz irradiation which have the approximately thermal flux 2.0-3.9x10^{11} n/cm^2/sec.. Small tubes were established for biological samples irradiation which have a long time loading . The thermal and epithermal flux are 0.45-0.55x10^{12} n/cm^2/sec and 0.45-0.55x10^{12} n/cm^2/sec.respectively.

Previous and Current status of NAA in Thailand

The utilization of NAA for studying on determination of multi elements in various samples have been carried out for many years at OAEP. Up to now such analytical technique has still been performed an important role on many researches and application works of OAEP. The following is a summary of these applications.

Field	Kind of sample	Element	Technique	Remark
Geological	Monazite Zircon Sandstone Xenotime Tin slag	U, Th, REE, Zr, Hf, V,W,Y,U,Th,Sn,Sc ,K,Ba,REE Y,REE, U,Th,	INAA	
Environmental	Water Airborne particulate matter Coal and fly ash emitted to atmosphere	Cd,Co,Hg,Se,Zn Al,As,Cr,K,Mg,Mn, Sb,Si,Sr,V Al,Br,Ce,Cr,Cs,Eu ,Gd,Hf,La,Mn,Sc, Sm,Sr,In,Tm,V,Fe,	INAA and RNAA INAA INAA	river water and sea water

	Lignite	Na,K,Ti,Rb,Ta,Th, Ca,Si,Yb,Zr	INAA	Research with the national oceanic and atmospheric administration , USA to develop the mathematic model for the meteorology
		Br	INAA and RNAA	
	Soil and sediment	U,Th,Al,As,Co,Cu, Mn,Mo,Na,Se,Zn,		
	Coal and ash	K,Th,U,V	INAA	

Biological	Vegetable	Br,As,Hg,	RNAA	
	Blood,	Mn,Cu,Zn,Fe,Mo,	RNAA	
	Body fluids	Cu	RNAA	
	Gallstone	P,Ca,Mg,Na,Zn, Ag,Se	INAA,RNAA	
	Urine,	P	RNAA	
	Rice,	N	RNAA	
	Fish,	U,Br, Co,Zn,Hg	INAA,RNAA	
	Teak,	Au	RNAA	
	Human hair	Hg	RNAA	

Industrial	Modular Cast Iron Iron alloy	Ce,La Fe,Al.As.Cu,Ce, Mn,V,W	NAA	
Training and Technology Transfer	Environmental sample such as soil and sediment and underground water	Sc,Cr,Mn,Zn and U	INAA RNAA	

Future Utilization Plan of NAA in Thailand

Some activities as mention above are still continued . Especially ,for the environmental field , rainwater and the food stuff are the interesting materials for the future projects.

JP0250103

1.19 NEUTRON ACTIVATION ANALYSIS AT THE DALAT NUCLEAR RESEARCH RACTOR

NGUYEN VAN MINH
Nuclear Research Institute, Dalat, Vietnam

INTRODUCTION

Neutron Activation Analysis (NAA) is one of the most sensitive, rapid, accurate methods for determination of major, minor and trace elements in different materials. This method is playing an important role of nuclear and non- - nuclear analytical methods, which are being carried out at Dalat Nuclear Research Institute (DNRI). A Review is made of current status of the activities and the results in studying and developing NAA at DNRI and applying this method to different sectors of science and technology in Vietnam.

I. The irradiation facilities and their characteristics for NAA

The Dalat Nuclear Research Reactor, former TRIGA Mark II reactor, was built in 1963 with thermal power of 250 kW. It was reconstructed and upgraded in 1984 with the power of 500 kW.

The Dalat Nuclear Research Reactor has two dry channels (7-1, 13-2), a thermal column and one wet channel (1-4). Inside of the reactor there are a neutron trap and a rotary specimen rack in the graphite reflector consisting of 40 irradiation positions.

Since 1984 the reactor has been operated mainly in continuous runs of 100 hours one every 4 weeks for radioisotope production, neutron activation analysis and other related studies. In the neutron activation analysis we have carried out the following methods: Instrumental Neutron Activation Analysis (INAA), Radiochemical Neutron Activation Analysis (RNAA), Ko – standardization method (Ko-NAA) and Prompt Gamma Neutron Activation Analysis (PGNAA).

The characteristics and the parameters of neutron spectrum for activation Analysis of Dalat nuclear research reactor are shown in Table 1.

Table 1: Irradiation facilities and their characteristic parameters of Dalat reactor

Irradiation positions	Thermal neutron flux ($n.cm^{-2}s^{-1}$)	Average Rcd Value	Note
Neutron trap	2.21×10^{13}	2.93	Wet channel with beryllium moderator, diameter: 64 mm, length: 600 mm for RI and NAA
Rotary Specimen Rack	4.27×10^{12}	3.0	40 irradiation holes, diameter 40 mm, length: 30 mm for NAA and RI
Channel 1 – 4	1.28×10^{13}		Wet channel, diameter: 32 mm; length: 600 mm for NAA and RI
Channel 7 –1	4.5×10^{12}	2.1	Dry channel with pneumatic transfer system for NAA
Channel 13 – 2	4.6×10^{12}	2.2	Dry channel with pneumatic transfer system for NAA
Thermal column	5.5×10^{9}	1.94	Dry channel with pneumatic transfer system for NAA
Horizontal (tangential) beam tube No-3	2.3×10^{6}		For PGNAA

II. Development of methodology for NAA at NRI

Since neutron will activate almost all the elements present in the sample by different nuclear reactions. The activation techniques are developed at DNRI in more than fifteen last years such as INAA, RNAA. Besides, the other techniques have also been established and studied such as Ko – standardization method and the prompt gamma neutron activation analysis (PGNAA).

II.1. Instrumental Neutron Activation Analysis (INAA) [1]

Advantages of INAA technique are non-destructive, reduction of the time and well suited for on line analysis.

For determination of elements which have short live radionuclides, in the few past years we developed capacity for analyzing of samples including establishment of facilities for rapid INAA by using the pneumatic transfer systems of the channels 13-2, 7-1 and thermal column. The samples are irradiated in these channels for from 3 seconds to 30 min and after appropriate cooling time the samples are directly measured on the HPGe detector.

For determination of elements which have long live radionuclides, the irradiation process of the samples is carried out in the rotary specimen rack or at neutron trap.

The irradiation time depends on characteristics of the nuclide of elements and the sample to be analyzed.

II.2. Radiochemical Neutron Activation Analysis (RNAA)

The need for chemical separation in activation analysis arises from the peculiar characteristics of gamma ray spectrum. There are counts from zero to full energy peak of a gamma ray instead of the peak alone. This gives rise a continuous base line and other peaks in this energy range and lead to interference with the detection and measurement of other peaks of low energy. Thus radiochemical separation have remained an integral part of activation analysis even after the introduction of high-resolution detector.

Techniques of separation in NAA

The choice of the techniques for a chemical separation depends on a number of factors such as the elements to be separated, time available for the separation and the extent of decontamination required. The techniques of separation in RNAA at DNRI have been developed such as precipitation, chromatography, extraction, ion exchange, etc. for the individual or groups of elements in different samples. The inorganic or organic compounds such as MnO_2, SnO_2, $ZrPO_4$, SBW, AG x1-8, Dowex 50, HAP... have been studied for their possible use in radiochemical separation.

The pre-concentration chemical separation in NAA for determination of the trace elements can be carried out before or after irradiation of the samples.

The RNAA techniques for determination of trace elements in different materials at DNRI are summarized in Table 2 :

Table 2: Summary of radio-chemical separation techniques in RNAA at DNRI

Matrix (elements analyzed)	Sample opening	Separation techniques
Rock sample (REE)	Fusing with Na_2O_2	Anion ex.chromat (NO^{3-}) in methanol – nitric medium
Rock sample (Ga, Cu, Co, Cd, Fe, Mn)	HF-HNO_3 treatment	Anion ex.chromat. (Cl^-), elution with different gradient concent. of HCl
Rock sample (Ag)	Fusing with Na_2O_2	Filter through the PbCl filter in 4N HNO_3
Rock sample (W, Mo, Sn, Th)	HF-HNO_3 treatment	MnO_2 sorp. in 1M $HClO_4$
Environmental sample (about 20 elements)	HF-HNO_3 treatment	HAP sodium removal; anion ex. elution (Cl^-)
Water sample (Hg, Cd, Sb, Cu, Mn...)		Scavenging on active carbon of chelat complex of dithiz. with ion of elements
Water sample (As)		Co-precipitate with $Fe(OH)_3$
Biological samples (about 30 elements)	$H_2SO_4 – H_2O_2$	Anion ex.chromat. (Cl^-) Cation ex.chromat. using citrat, EDTA, KSCN
Rock sample (Au)	Hf-HNO_3 treatment	Concentration on anion ex.chromat. (Cl^-) in 4N HNO_3
Soil sample (about 30 elements)	HF-HNO_3 treatment	Anion ex. (Cl^-); cation, in ex. chromat; extraction with TBP, DDC CCl_4

III. Typical results and application of NAA at DNRI

III.1. Application of NAA in geochemistry

Application of NAA in geological and geochemical study has played a very important role in our country. In combination with Vietnamese geologists, every year thousands samples of rocks and minerals have been determined. The DNRI's directions for the application of NAA to geochemistry at present are following:

+) The investigation of the distribution of rare earth elements (REE) in some minerals such as monazite and zircon in beach sand to get the information about the relation between monazite and zircon and their origin [2].

+) Determination of noble metals such as Au, Ag, Pt [6, 7].

+) Determination of Uranium, Thorium and the related elements.

+) Determination of trace elements and heavy metals[8].

+) Determination of major and minor elements.

Etc.

Table 3. Results of analysis for geological samples from 1986 to Oct. 2000 [3]

Year	Number of samples
1986	100
1987	200
1988	490
1989	2400
1990	2600
1991	2700
1992	3300
1993	950
1994	834
1995	927
1996	821
1997	976
1998	773
1999	1120
2000	897

III.2. Application of NAA in environmental research [4, 5]

Results obtained of the application of NAA to environmental research at DNRI recently are focused on:

1. The concentration of toxic elements and radio nuclides in environmental objects in different areas of Vietnam.

2. Supporting the sustainable development of agriculture and improving the quality of human life;

3. Investigation of environmental pollution by heavy metals and other toxic elements coming from industrial manufacturing and development. The samples of soil, water, plant, aerosol have been collected in different areas of Vietnam for determination of toxic elements and radio nuclides.

Some results of aerosol and water samples at environmental monitoring stations and lakes in Dalat, Nha trang and HCM City are given in Tables 4, 5 and 6.

Table 4. Element composition of aerosol collected in Dalat and Ho Chi Minh City, determination by NAA and related method

Element	Concentration range (ng/m^3)	Element	Concentration range (ng/m^3)
Al	1200 – 7200	Mg	320 – 880
Ba	12 – 40	Mn	24 – 64
Br	10 – 18	Na	450 – 1150
Ca	1600 – 5600	Nd	0.6 – 2.2
Cd	0.004 – 0.030	Sb	800 – 4400
Ce	1.6 – 4.2	Sc	4 – 44
Cl	1000 – 1200	Se	0.3 – 0.8
Co	0.5 – 1.5	Sm	0.02 – 0.06
Cu	0.8 – 6.8	Ta	0.04 – 0.10
Fe	160 – 40000	Tb	0.02 – 0.06
Hf	0.08 – 0.35	Ti	160 – 400
Hg	0.004 – 0.04	U	0.06 – 0.20
I	0.3 – 0.4	V	8 – 42
K	600 - 2200	Yb	0.024 – 0.092

Table 5. Composition of heavy metals in fresh water of Dalat, determination by RNAA and related method (μg/l)

Sample	Pb	Cd	Cu	Zn	As	Hg
Suoi-vang Lake	6.33	0.94	7.16	12.8	2.64	1.22
Tuyen -lam Lake	10.6	1.41	5.75	22.1	3.95	0.98
Chien -thang Lake	10.8	0.86	7.50	12.8	5.60	1.66
Ta -in stream	15.3	1.65	9.95	12.5	6.90	1.22
VN. Standard (1995)	50	10	100	1000	50	2
Inter. Standard (1963)	50	10	1000	5000	50	-

Table 6. Composition of heavy metals in seawater of Nha trang, determination by RNAA and related method (μg/l)

Element	Drying season	Raining season
As	3.9	2.5
Co	5.3	7.1
Cu	3.1	3.1
Fe	13415	13651
Mn	258	288
Pb	0.9	0.4

III.3. Application of NAA in biology

We use NAA method to analyze the heavy – toxic metals; radio nuclides and trace elements in biological materials for investigation of their distribution in plants, foods, foodstuffs... such as U, Th, Cs, Sr, Hg and Hg(methyl) in human urine and hair of women living in different areas of Vietnam [5]. The main directions of application of this method in present and future at DNRI are:

- Determination and assessment of the nutritional roles of microelements in agriculture plants growing in different kinds of soil.
- Determination and assessment of the concentration and distribution of elements in food used for feeding domestic animals and livestock.
- Quality control for heavy and toxic metals in foodstuffs including products for export.

IV. Conclusions

After more than 15 years of NAA activities by using Dalat reactor, it has seen that this method has a very important role to study and apply for determination elemental compounds in geo – bio – environmental samples. Every year we have analyzed thousands samples for different sectors of science and technology in Vietnam.

For the further achievements in the development and application of NAA, DNRI wishes to strengthen the co-corporation with other Institutions in the region as following problems:

- To introduce and implement the new NAA techniques and procedures in the practice (RNAA, INAA, PGNAA).
- To exchange the experience in the applications of NAA in different fields of science such as geochemistry, environmental, biology, purity materials etc. by scientific visits, training courses and workshops.

References

[1]. N.T.Anh: Report on investigation and development of nuclear analytical techniques in 1997 at Nuclear Physics Department, NRI.

[2]. N. V. Suc, N.M. Sinh: Determination of REE in Vietnamese monazite samples by RNAA. J. Radioanal.Nucl.Chem. Letters 164 (5) 321-325 (1992).

[3]. N. Q. Hien, N. V. Minh, C. M. Khoa, L. Hai: Brief review of research and development activities in radiochemistry, NAA and radiation chemistry at NRI; J. of Chemistry, T.35, No-3b, 59-63, 1997.

[4]. L.T. Mua, N.N. Tuan, N.M. Sinh: Determination of nutrient and toxic elements in seafood by RNAA method. J.of Chemistry, T.33, No-4, 66-69, 1995.

[5]. N.V. Hung, N.V. Suc, N.V. Minh: Determination of the iodine in human urine by neutron activation. Jour. of Chemistry, T.33, No-4, 74-76,1995.

[6]. N.V. Minh, N.V. Suc: Determination of Au, Ag and Pt in geological samples by NAA technique. Journal of Chemistry, T.33, No-3,39-40,1995.

[7]. N.V. Minh, N.V. Suc: The fast determination of Ag in geological samples by NAA. J. of Chemistry, T.34, No-1,39-40,1996.

[8]. N.V. Minh: Study of optimal conditions for simultaneous determination of Zn and Cd in geological samples by RNAA. J. of Chemistry, T.33, No-1, 1996.

JP0250104

JAERI－Conf 2001－017

1.20 NAA Supporting system of JAERI

F. SASAJIMA, H. SAWAHATA*[1], K. ONIZAWA*[2], S. ICHIMURA
A. OHTOMO, Y. HORIGUCHI, Y. ITO*[1], M. TAKAYANAGI

Department of Research Reactor

Japan Atomic Energy Research Institute (JAERI)
2-4 Shirane, Shirakata, Tokai-mura, Ibaraki-ken 319-1195, JAPAN

*[1] The University of Tokyo, Research Center for Nuclear Science and Technology
*[2] Radiation Application Development Association

ABSTRACT

Neutron Activation Analysis (NAA) has been performing as a major part of irradiation utilization at research reactor in JAERI. To carry out NAA in the reactor, researchers have been required to be versed in advanced technique also being enough experienced at same time, therefore, we started to develop a support system that will enable to carry out NAA easily even by a beginner. NAA supporting system is the system in which even the user who has not much experience in the NAA can conveniently and accurately carry out the multi-element analysis of the sample. We carried out verification test of this system using irradiation device, measuring device, automatic sample changer and analyzer equipped in the JRR-3M PN-3 facility, and analysis software KAYZERO/SOLCOI based on the k_0 method. With these equipments, calibration of the germanium detector, measurement of the parameter of the irradiation field and analysis of three kinds of environmental standard sample were carried out. The k_0 method adopted in this system is primarily utilized in Europe recently, and it is the analysis method, which can conveniently and accurately carried out the multi element analysis of the sample without requiring individual comparison standard sample. By this system, total 28 elements were determined quantitatively, and 16 elements with the value guaranteed as analytical data of the NIST (National Institute of Standards and Technology) environment standard sample were analyzed in the accuracy within 15%(max.).

Keyword: Neutron Activation Analysis, JRR-3M, PN-3, INAA, k_0, Support, System

INTRODUCTION

For joint use of JRR-3M, INAA support system is applied to the PN-3 facility. This system was automates the operating procedure of irradiation, measurements, analysis, etc. as much as possible, and it would enable to use INAA conveniently even by beginners. As an analysis method, the k_0 method which does not require individual standard reference material is applied in order to obtain the fixed quantity of the elements easily.

INAA SUPPORTING SYSTEM

1. Irradiation facility

JRR-3M is a light water moderated and cooled swimming pool type reactor, operating with maximum thermal power of 20MW. The reactor is operated on 5weeks/1cycle, with about 26 continuous days at full power operation followed by 9 days for maintenance and refueling. There are a lot of experimental facilities in JRR-3M, as shown in Figure 1, involving 9 vertical holes installed for irradiation usage in the core and heavy water tank region and 9 horizontal tubes for neutron beam experiments. The PN-3 facility for the irradiation of INAA is installed in the D_2O tank region.

1.1 Irradiation hole

The PN-3 facility provides well-thermalized neutrons with Φ_{th}=2x10^{13}(n/cm^2 s), Φ_f=1x10^9(n/cm^2 s), R_{cd}=300. Homogeneity of the thermal flux in the facility is less than 1%. An irradiation rabbit for the PN-3 facility, which is made of polyethylene, has the dimension of 17mm diam. and 30mm long. The specifications of the irradiation hole are shown in Table 1.

1.2 Irradiation device

The irradiation device is composed of PN-3 irradiation tube, automatic rabbit loader, remover, solenoid valve and control equipment using sequencer, etc. The device has 3 operating modes; the automatic, semiautomatic and manual modes. The automatic operation can control a series of processes from irradiation to measurement at preset sample conditions. This mode suites to the process for a group of samples at the same conditions. The semiautomatic operation is used when conditions to be carried out for each sample are different individually. The manual mode is used only to operate by some skilled operators, particularly for the recovery when minor troubles occur in the device. The PN-3 facility allows the irradiation times of 3s up to 1200s. For short-lived nuclides, the sample in the rabbit must be off from the core within about 7s, followed by quickly measuring with the sample encapsulated. If necessary, it is also possible to repeatedly irradiate the same sample. On processing, necessary information can be collected, *e.g.* irradiation start date/time, irradiation finish

time, exposure time, measurement start date/time, output of neutron detector, etc. PN-3 irradiation device is shown in Photo 1.

2. Measuring system

2.1 Gamma-ray spectroscopy system

The system has 2 Gamma-ray spectrometers; one for short-lived nuclide and the other for normal measurements. The former spectrometer for short-lived is for immediate measurement after irradiation. For the later case, samples are measured by replacing from the rabbit into polyethylene bag, subsequently setting them on the shelf. Especially, it has been composed of the Gamma-ray spectrometer using DSP(digital signal processor) that is latest measurement equipment in proportion to the measurement of high count rate such as short-lived nuclide. The block diagram of the Gamma-ray spectroscopy system is shown in Figure 2.

2.2 Automatic sample changer

The automatic sample changer is composed of leads shield (10cm), 5 axis arm robot, controllers, sequencers, gravimeters for liquid nitrogen, etc. Up to 100 samples can be set into the changer. The changer has random sample accessibility and allows placing the sample at a measurement position. The sample-to-detector distance (0mm–300mm) is variable at 10mm intervals. Photograph of the automatic sample changer is shown in Photo 2.

2.3 Gamma-ray spectrum analysis software

Software GENIE-2000[4] for the spectrum analysis is a commercially available package running on personal computers under Microsoft Windows NT/95. Multi-user environment by ETHENET is available, enabling the data analysis and monitor through the network.

3. Data analysis system

The data analysis system is calculated for quantitative analysis by k_0 method or relative method, after the analysis sample is measured. Irradiation and measurement data necessary for the data analysis can be automatically received from INAA support system. As an analysis method of INAA, it is carried out based on the convenient and accurately procedure of the k_0 method. In this system, it is analyzed using evaluated marketing software SAMPO-90[5], KAYZERO/SOLCOI. Flowchart of INAA support system is shown in Figure 3.

3.1 Peak analysis

The peak analysis needs SAMPO-90 spectral format and analytical result used in the KAYZERO/SOLCOI. Therefore it is used after conversion of the gamma-ray spectrum into the type of data, which can be read in KAYZERO/SOLCOI. And, conversion software in proportion to several

kinds binary file is prepared in order to convert the gamma-ray spectrum type.

3.2 Calibration of the Ge detector by SOLCOI

The SOLCOI determines effective solid angles and coincidence correction factors. Since accuracy of a detector is indispensable for k_0 method, a detector must be accurately calibrated beforehand for general users.

3.3 Calculation of the reactor parameter

The reactor parameter is a coefficient for correcting neutron spectrum of reactor, and it is shown in the thermal-to-epithermal neutron flux ratio (f) and the slope of 1/E distribution (α). These parameters (f, α) must be also measured beforehand for general users.

3.4 Analysis

KAYZERO software, which performs qualitative/quantitative analysis based on the k_0 method in this system, provides a list of concentrations and/or detection limits of all measurable elements. However, there are some difficulties in transporting analysis results automatically to KAYZERO from INAA support system, which runs under DOS. As a solution of this problem, original software, which will perform analysis automatically by k_0 method, will be prepared.

3.5 Analytical database

Analytical databases are that it accumulates data such as analysis condition, result of analysis, gamma-ray spectrum got by this system. And does the data base construction which faces every analysis sample. It will be improved in order to conjugate as a reference for deciding beginners or analysis conditions of the inexperience sample, etc.

EVALUATION

As verifying performance of the analyzing system, its accuracy and confidence were confirmed analysis on SRM-1633b (Coal Fly Ash) `1577b (Bovine Liver) `SRM-1515 (Apple Leaves) environmental standard reference by NIST. The samples were irradiated for 30 sec and 20 min at the bottom position of JRR-3M PN-3 facility, and then their radioactivity were measured by calibrated system. Fig. 4 - 6 show the results of each sample analyzed with the k_0 method. In the present study, 28 elements in the 3 samples could be quantitatively analyzed by the system, especially we found out that almost of the elements could be done within approximately 10 % accuracy except for few elements of outermost 15 %.

FURTHER DEVELOPMENT

It is understood that the improvement of INAA support system based on the k_0 method is convenient instruments for the NAA users. An attempt to apply the support system to the PN-3 facility in JRR-3M of JAERI has been made at present, and its application for JRR-4 will be done in future. Further development and improvement of this system will be preceded in order to utilize NAA more conveniently and accurately.

REFERENCES

(1) KAYZERO/SOLCOI User's Manual, DSM Research (1996)
(2) F. DE. CORTE and A. SIMONITS, VADE MECUM FOR k_0-USERS (1994)
(3) F. DE CORTE, "The k_0 Standardization Method", Rijksuniversiteit Gent (1987)
(4) Genie-2000 Spectroscopy System/Operations, Canberra Industries, (1997)
(5) SAMPO 90 User's Manual, Canberra Industries, (1991)

Table 1 Specification of PN-3 facility

Position / Item	Bottom	Middle
Φ_{th}	1.9×10^{13}	1×10^{12}
Φ_f	6.0×10^{9}	10^{8}
R_{cd}	300	700 ~
Irradiation time	max. 20 min.	
Irradiation tube size	Φ 20 mm	
Irradiation rabbit		

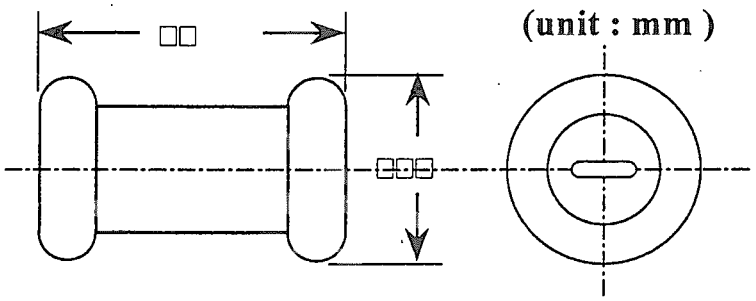

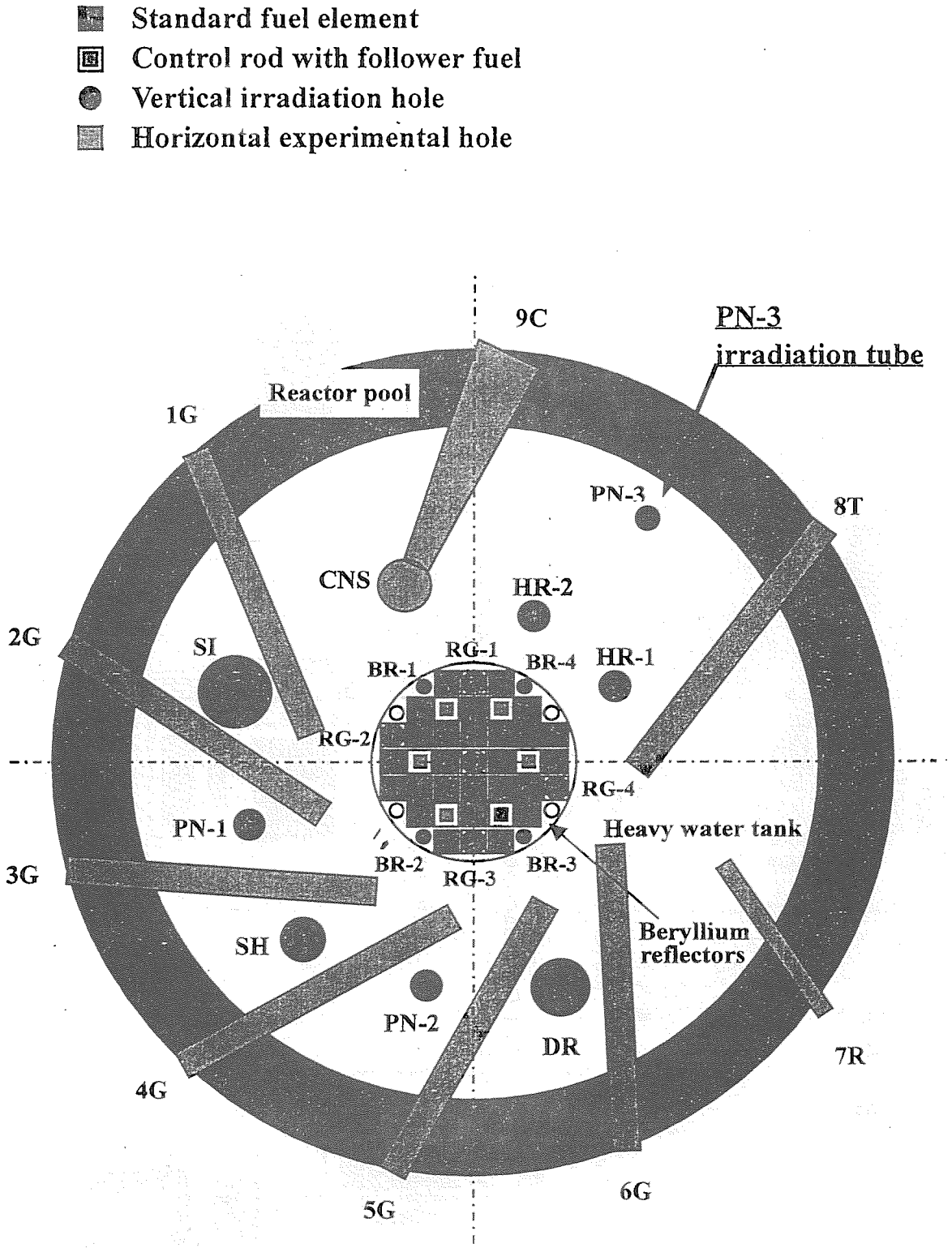

Fig.1 JRR-3M Reactor core and utilization facilities

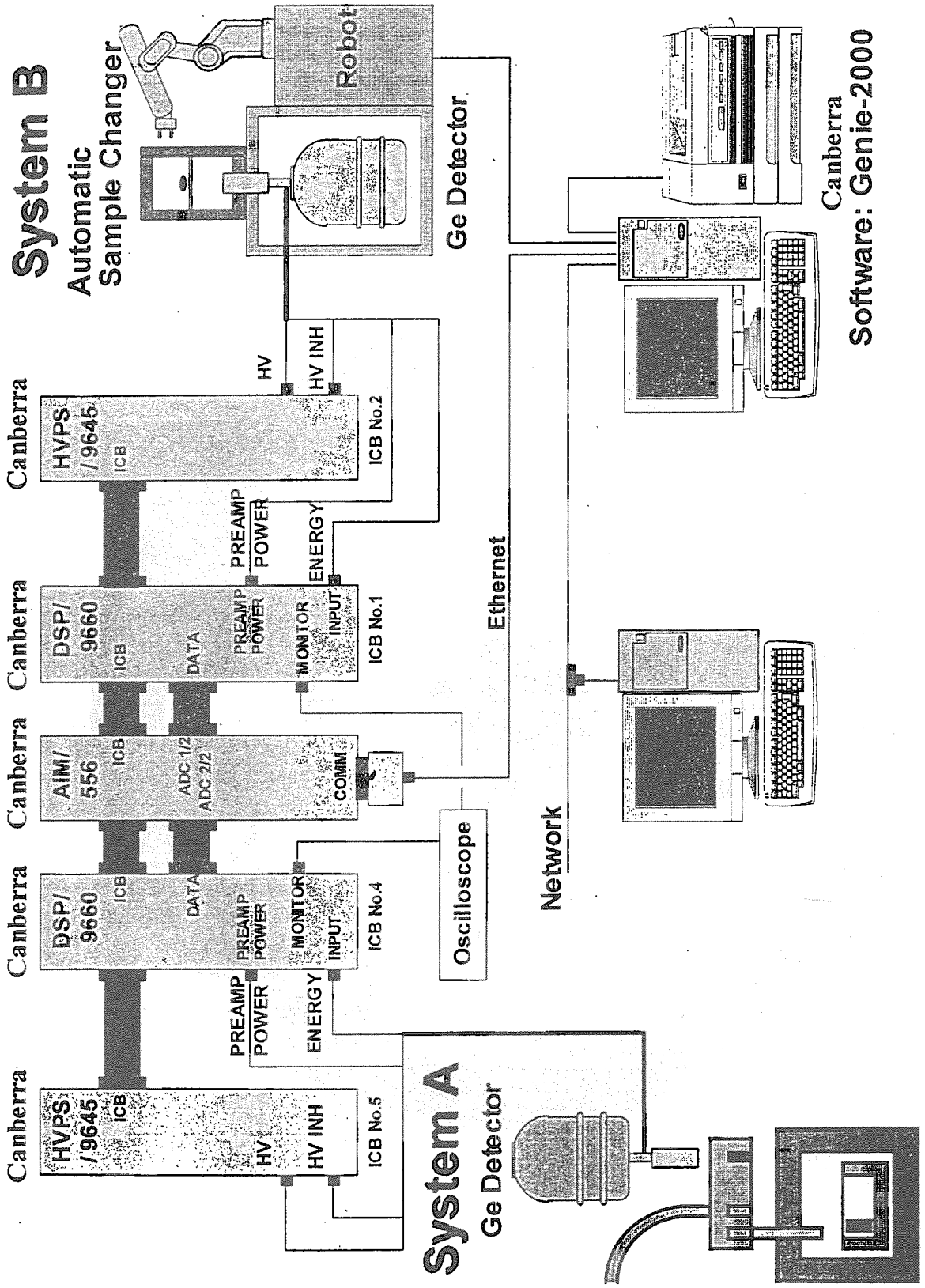

Fig.2 Gamma-ray Spectroscopy System

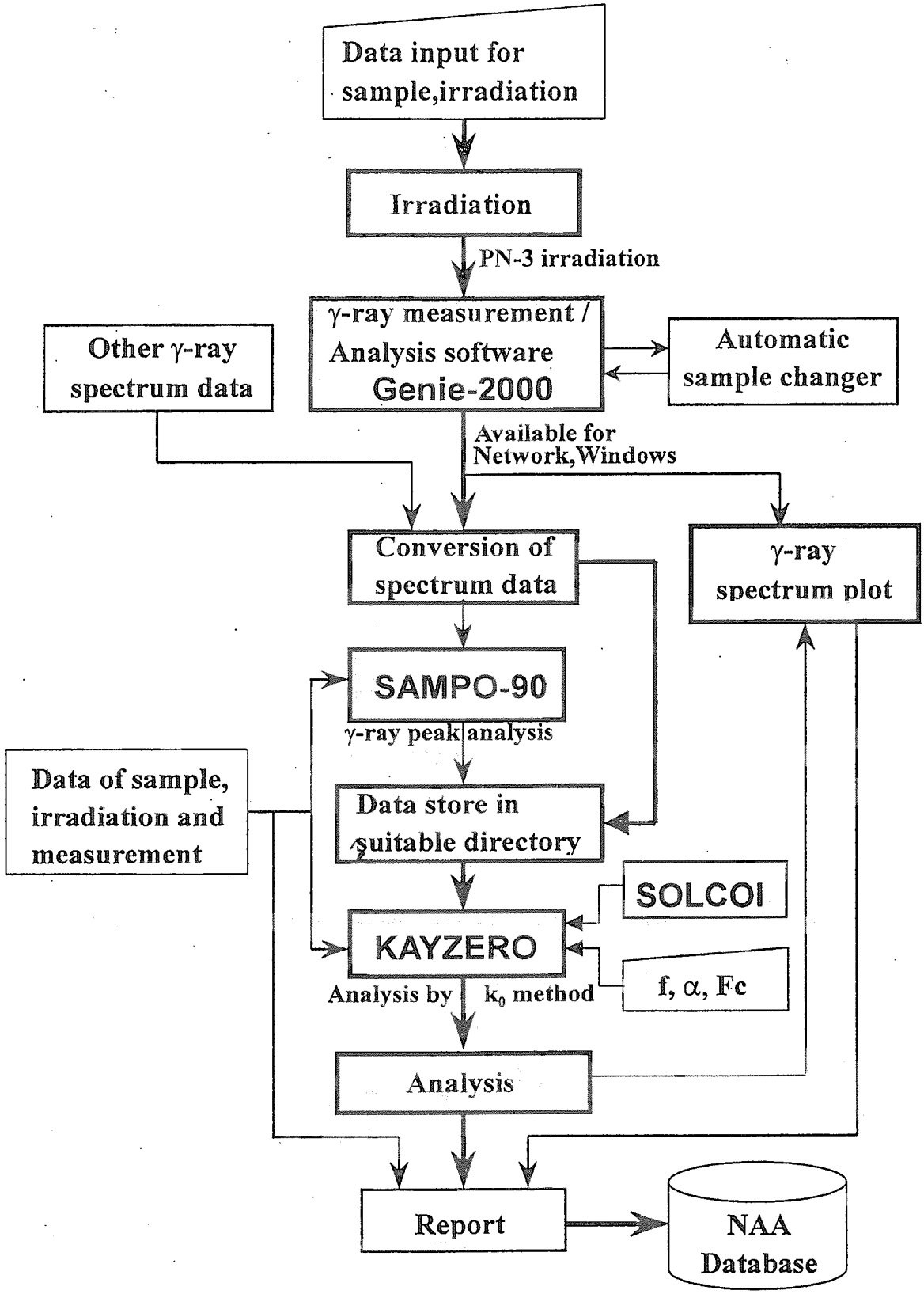

Fig. 3 Flowchart of INAA supporting system

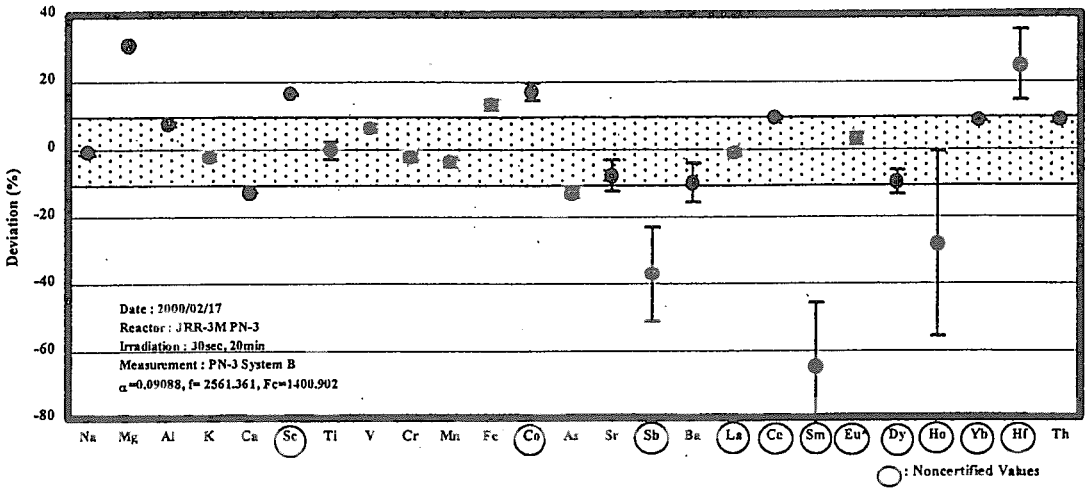

Fig.4 Comparison of Analytical results (NIST SRM-1633b)

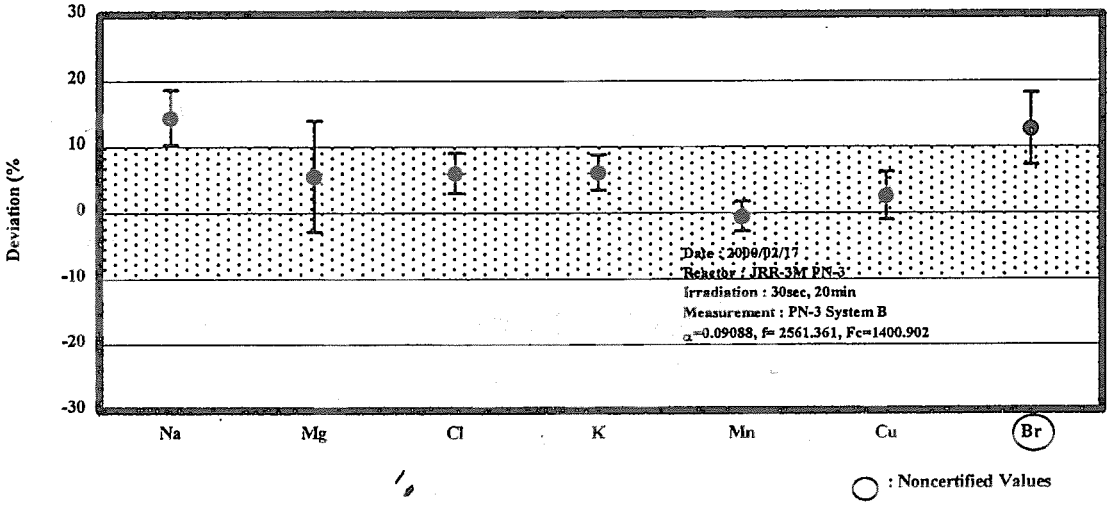

Fig.5 Comparison of Analytical results (NIST SRM-1577b)

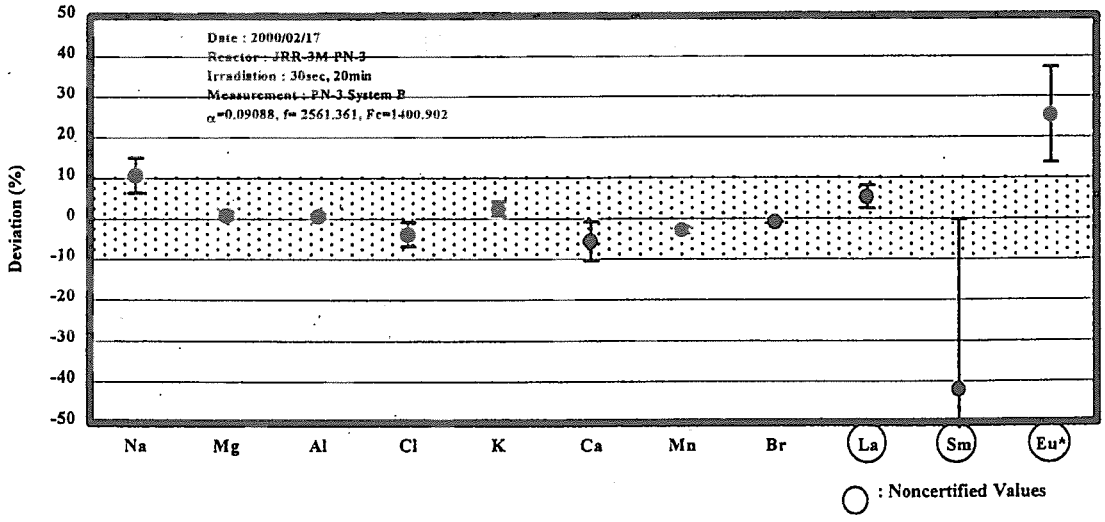

Fig.6 Comparison of Analytical results (NIST SRM-1515)

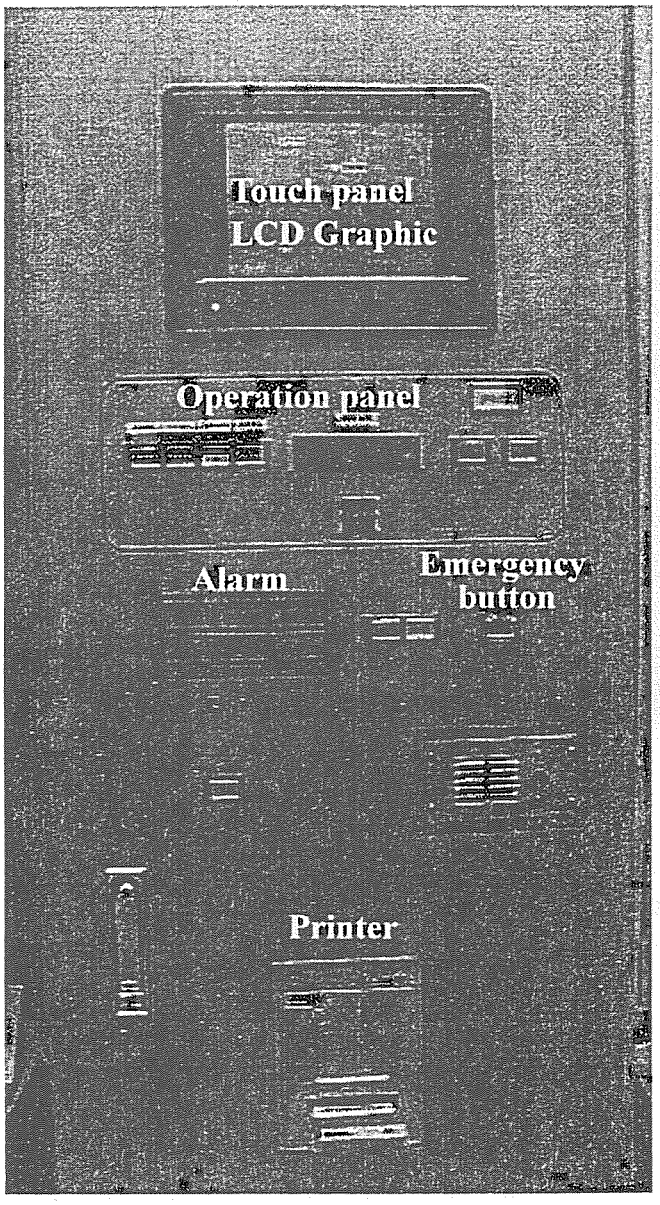

Specification

- Easy operation
- Operation by auto/semi-auto/manual mode
- Monitoring of operation condition and process data
- Repeatedly irradiation
- Interlock by dose rate
- Quick measurement for short-live nuclide
- Etc.

Photo 1　PN-3 irradiation device

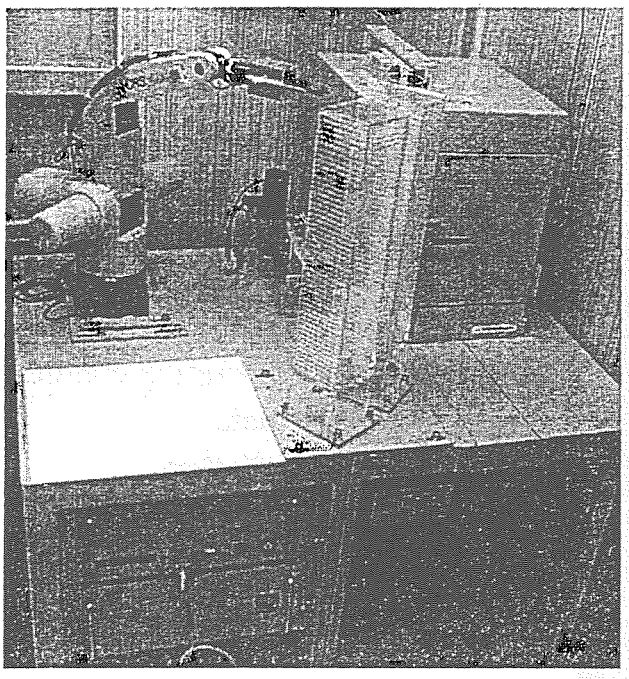

Specifications

- Measurement method : Random Access
- Sample number : 100 sample (max.)
- Thickness of Shield : Pb 100mm (low B.G.)
  Cu 5mm
- Shielding door : Manual / Automatic door
- Measurable distance : 0 - 300 mm
  Manual : 200 mm x 200 mm x 3 mm
  Auto : 100 mm x 100 mm x 3 mm
- Robot : 5 degrees of freedom
  Repeatability : +/- 0.05 mm
- Others
  - Balances for liquid N_2 level
  - Adjustable of Ge Det. height
  - Controls : Sequencer
  - Communication : RS-232C

Photo 2 Automatic sample changer

JP0250105

1.21 Air Pollution Study by NAA in Korea

Moon Jong Hwa
Korea Atomic Energy Research Institute,
P.O.Box 105 Yusong, Taejon, 305-600, Korea.
E-mail : jhmoon1@kaeri.re.kr

Abstract

The aim of this research is to enhance use of a nuclear analytical technique(instrumental neutron activation analysis) in the field of air pollution studies through a feasibility study of the usefulness of a routine monitoring tool in assessing and comparing air pollution levels in the region, in order to identify critical air pollution sources. For the collection of airborne particulate matter(APM) for the fine (<2.5 μm EAD) and coarse particle (2.5-10 μm EAD) fractions, the Gent stacked filter unit low volume sampler and two types of Nuclepore polycarbonate filters were employed. Samples were collected on selected sampling dates(working and non-working days) at two regions(suburban residential site and industrial complex of Taejon city in the Republic of Korea). Trace elements in the samples collected were analyzed by INAA. Variations of the concentrations of particulate matter, elements and elemental carbon were measured monthly and enrichment factors with the sampling sites were calculated. The analytical data were treated statistically to estimate the relationship between two variables, the concentrations of elements and two particulate matters. The results were used to describe the emission sources and their correlations.

I. Introduction

Due to recognition and regulation for environmental pollution, which is caused by rapid industrialization and urbanization, vehicle increment, etc., public concerns about clean, comfortable surroundings have increased. For this reason, intensive efforts to control pollution sources and to examine contamination levels through the analysis of various environmental samples are being followed up. Therefore, measurement of elemental concentrations in environmental samples including air, soil and water, is very important in solving pollution problems. In particular, airborne particulate matter(APM) consists of various elements both

artificial as well as of natural origin. When the level of total suspended particulate matter(TSP) and/or the content of specific elements in PM_{10} (<10 μm) are high, the short and long term effects on human health are insidious and important. However, sampling of PM_{10} is the first step in estimating the effects of air pollution and mass concentrations of PM_{10} are generally less than 0.1 mg/m^3. So the method of analyzing the elements should be sensitive and precise, and also be able to identify multi-elements simultaneously because of the diversity of elements in the samples. Instrumental neutron activation analysis(INAA) using thermal neutrons in a nuclear reactor as an irradiation source, and high resolution semiconductor detectors as measuring equipment, is the most suitable method for satisfying the above mentioned requirements. INAA for airborne particulate matter can analyze up to ppm. ppb level of concentrations for 30. 40 trace elements simultaneously.[1-7] The results can be used to conduct epidemiological studies, to investigate source identification and apportionment, to study long-range transport phenomena, and to establish a more cost-effective plan to control air pollution. Air pollution sources can also be identified by employing a statistical method of analytical data such as the Enrichment Factor, Receptor Modeling and Chemical Mass Balance Methods.[8-10] If the concentrations of several elements in air samples that are specifically related to emission sources are measured, the above statistical techniques can be used to identify the fingerprinting of air pollution from the results. For these emission source studies, collection of comprehensive analytical data is required continuously. The selection of a sampling site, sampling methods and air sampler depend on the purpose of research and the elements to be analyzed.

In this study, INAA was applied for the determination of trace elements in airborne particulate samples, to identify emission sources, to assess and compare air pollution levels for two regions in Taejon city of Korea. That is, airborne samples collected at two sites were analyzed using this method and monthly variations, distribution of the concentration of elements and the enrichment factor were evaluated to verify the emission sources and to estimate their correlation.

II. Experimental

2.1. Sampling and sample preparation

For the collection of airborne particulates for the fine (<2.5 μm EAD) and coarse particle (2.5-10 μm EAD) fractions, the Gent SFU sampler(low volume air sampler with fine and coarse fraction) with polycarbonate filters(ϕ 47 mm, 0.4 and 8 μm pore size, Nuclepore) according to the recommended method[11] was used. Samples were collected on selected sampling dates(working and non-working days) at two regions, a suburban residential area and industrial

complex in the middle of Korea. The sampler was placed about 4m above the ground. Atmospheric conditions such as temperature, humidity, wind direction, wind velocity and change in weather conditions were recorded regularly during the collection of samples. The flow rate was adjusted to 18 *l*/min at the beginning of sampling and collected for 24 hours twice a week from November 1998 to October 1999. The total volume of air sampled through the filter was calculated from the reading of the volume meter and compared with the obtained value from the average of the initial and final flow rate. The collected samples were pre-stored for 24 hours in a controlled atmosphere(20℃, 50% relative humidity) and prepared in polyethylene vials after weighing in the same conditions. Electrostatic charges are controlled by ^{210}Po radioactive source. For both fine and coarse filters, each filter was cut into three parts, half for the analysis of medium-long half-life nuclides, a quarter for the short half-life nuclides and the rest for storage.

Before elemental analysis of the sample collected, the reflectance of fine particle filters was measured using Smoke Stain Reflectometer(Model 43D) according to recommended procedure for calculation of concentration of the elemental carbon.[12]

2.2. INAA analysis of sample

Collected samples were irradiated with thermal neutrons using the Pneumatic Transfer System(PTS, Φ_t = 1.75 x 10^{13} n/cm^2.s, R_{cd} ~ 250) at the HANARO research reactor at the Korea Atomic Energy Research Institute. Samples were irradiated at the same position to minimize geometric errors. For neutron flux monitoring, activation wires (Reactor Exp. Inc., R/X activation wire, 99.99% purity) such as Au-Al, Co, Fe and Mn were used. Analytical conditions were optimized after considering the preliminary results.

The measurements were carried out using a high purity Ge detector of 25% relative efficiency and 1.9 keV resolution(FWHM) at 1332 keV of ^{60}Co and peak to Compton ratio is 45:1, coupled to a personal computer and 8K-multichannel analyzer (EG&G ORTEC, 919A MCB). Energy and efficiency calibration were done using multi-nuclide reference sources (NEN Products Inc., NES-602, 1" diameter disc type) certified by NIST. GammaVision software (EG&G ORTEC) for energy and efficiency calibrations, the acquisition of gamma spectra and peak analysis were used.

2.3. Data Treatment

Under the same analytical conditions, such as irradiation cooling and counting time, the elemental concentrations in both samples and blank filters were measured. Concentration of the elements was calculated using the new Windows PC-code, Labview software of KAERI

with the nuclear data library[13, 14] which was developed at this laboratory for rapid and simple data treatment with the gamma ray spectrum obtained at preset analytical conditions. The detection limits for the elements were calculated by Currie's quantitative definition[15] with 10% allowable uncertainty. The detection limits of trace components were in the range of 10 - 0.01 ppm which were 0.5 - 0.01 times the measured concentrations. The assessment of measurement uncertainty were evaluated as a combined uncertainty including most of the sources of standard uncertainty to be considered in INAA.[16] The analytical data were treated statistically using Microsoft Excel(version 7.0).

The concentrations of elemental carbon, EC, were determined for fine particle ($PM_{2.5}$) by W. Maenhaut and D. Cohen's suggestion [12] using the reflection method on Nuclepore filter as follows :

$$EC(\mu g/cm^2) = [100/2F\ \varepsilon]\ Ln\ [R_0/R]$$

where, F is a correction factor of order 1, ε is the mass attenuation coefficient in m^2/g, R_0 is the unloaded filter reflectance and R is the loaded filter reflectance for a given wavelength.

III. Results and Discussion

3.1 Analytical quality control

After the optimum analytical conditions such as neutron flux, irradiation facilities, irradiation time, cooling time, counting time, etc were pre-estimated according to previous procedures[17-19], the standard reference material(NIST, the National Institute of Standards and Technology, U.S.A., SRM 1648, urban particulate matter) was used for analytical quality control . The concentrations of 37 elements in the certified reference material were determined. The concentrations of 12 elements were statistically compared with the certified values.[20] The relative errors of Al, Cd, Cr, K, Na, V agreed within 5% and those of As, Fe, Zn agreed within 10%. The concentration of 19 elements were compared with the recommended values. The relative errors of Ba, Br, Cl, Co, Cs, Mn, Rb, Th, Ti, W agreed within 5%. The relative standard deviations were within 15% except Au, As, Cl, Cu, Dy, Hg, In, Ta, Ti and W. In addition the results of the combined uncertainty at a 95% confidence interval and the detection limit for each element under analytical conditions were evaluated. The filter blank values of major impurities are used for the correction of individual concentrations.[19] The concentrations of interfering elements such as Al, Cl, Mn, Br, Na were low relative to other filter types.[21]

3.2 Mass concentrations of APM

The mass concentrations of APM were measured during the sampling period and the variations in particle size, sampling date and sampling site is presented in Figure 1. The mass concentration of the coarse fraction(DC) was in the range of 15.2 - 50.9 $\mu g/m^3$ and that of the fine fraction(DF) was in the range of 9.3 - 33.1 $\mu g/m^3$ in the industrial area. On the other hand, the mass concentration of the coarse fraction(KC) was in the range of 3.1 - 24.6 $\mu g/m^3$ and that of fine fraction(KF) was in the range of 10.3 - 36.3 $\mu g/m^3$ in the suburban area. The average of the mass concentrations yearly and monthly were also compared in accordance with sampling site and particle size and are presented in Figure 2. The concentration of coarse samples collected from March to May are relatively higher than other sampling periods. This is probably caused by the phenomena of "yellow sand storm" from continental Asia. The annual average mass concentrations of total suspended particulate matter(PM_{10}) in the suburban and industrial areas are 36.2 $\mu g/m^3$ and 41.9 $\mu g/m^3$, respectively. The mass concentration of the coarse fraction is higher than that of the fine fraction in the industrial area, whereas the result of the suburban area is the opposite.

3.3 Elemental concentrations in APM

The distribution and variation of the annual average concentrations of elements were obtained from the average of measured values weekly and the results together with its ratio are summarized in Figures 3 and 4. The concentrations of 25 elements, Al, As, Ba, Br, Ca, Ce, Cl, Co, Cr, Cu, Fe, Hg, I, In, K, La, Mn, Na, Sb, Sc, Se, Sm, Ti, V and Zn were analyzed. In comparison with particle size, most of the elemental concentration of the coarse fraction in the industrial area were higher than those of suburban area except Fe, but in the case of the fine fraction, the trend is reversed. In comparing sampling sites, most of the elemental concentrations of the coarse fraction in the industrial area were higher than those of the fine fraction except iodine, but in the case of suburban area, the concentrations of elements such as As, Br, Co, Cu, Hg, I, In, K, Sb, Se, V and Zn in the fine fraction were high.

Figure 5 showed the ratio of elemental concentrations for working day to non-working day. There are some differences with sampling site and particle size. In the industrial area, the concentration of elements like Ba, Ca, Ce, Cl, Co, Cr, Fe, Hg, In, Mn, Se, Sm, Ti, V, Zn in the coarse fraction of the working day were higher than the non-working day, whereas in the case of the fine fraction, elements like Ce, Fe, I, Mn, Ti, V, Zn showed the same results. In the suburban area, the concentration of elements like Ba, Br, Ca, Ce, Cl, Co, Cu, Fe, Hg, K, La, Mn, Na, Sc, Se, Zn in the coarse fraction and elements of Ce, Cr, Hg, La, Sm, Zn in the fine fraction of the working day were higher than the non-working day. The patterns of elemental distribution in the two areas were different from each other.

3.4 Elemental carbon in APM

The monthly average concentrations of elemental black carbon (BC) were determined for the fine fraction according to suggested methods and are plotted in Figure 6. The average concentrations of elemental black carbon at the industrial and suburban areas were in the range of 1.86 - 5.84 $\mu g/m^3$ and 1.90 - 7.24 $\mu g/m^3$, respectively. The amounts of elemental black carbon during the fall and winter seasons were relatively higher than those of other seasons. In general fine particles originate mainly from combustion processes and also the elemental black carbon fraction consists of soot aggregates originating from smoke, coal and wood burning, vehicle exhaust, industry, etc. The yearly concentration of elemental black carbon in the fine fraction at the industrial and suburban areas were about 22.7 % and 17.1 %, respectively. The value of winter was higher than in other seasons. Figure 7 shows the ratio of elemental black carbon for working day and non-working day at the industrial and suburban areas.

3.5 Enrichment factor

In order to find out the major emission sources, enrichment factors(EF) were calculated from measured elemental concentrations using Mason's crustal abundances [22] for the sampling period. An enrichment factor is given by the double ratio of the element of interest in the sample to a reference element in the sample divided by the ratio of the same element found in a reference material(e.g. rock, soil, etc) ; $EF = (X_i/C_i)_{APM} / (X_i/C_i)_{REF}$. Sc is taken as the reference element because it is supposed to be a unique element in soil. In general, most of the crustal elements (Al, Si, Ca, K, Fe, Mn, Ti, etc.) have EF values close to unity, higher EF values of elements indicates that they are not of crustal origin. Therefore, it can be classified to two group from the EF value of measured element ; the anthropogenic origin and the crustal origin. The average EF values calculated for particle size and sampling site are presented in Figure 8 and Figure 9. These values were in the range 10^0 - 10^4 and the industrial area showed generally higher values than those of the suburban area. High EF values of As to Se are observed at both areas, and they are assumed to be anthropogenic elements. Also the EF values of the fine fraction are higher than those of the coarse fractions in anthropogenic elements with respect to the elements of crustal origin generally. The ratio of the elemental concentration for working day to non-working day is presented Figure 10. The difference in EF values with sampling site and particle size can be clearly seen. This trends suggest that this result is available to investigate air pollution sources and levels for the evaluation of environmental conditions.

3.6 Correlation Patterns

The correlation coefficient measures the extent of association in the linear relationship between two variables. A Linear regression equation is obtained to describe the functional nature of the relationship between elements of crustal and anthropogenic origin involving industry and motor vehicles. We focus on typical elements like Al, Sc, Fe, K, La, Br, As, Cr, Sb, Zn as possible emission sources from two areas. In Table 1, the correlation coefficients are given for each pair of elements and APM for the sampling period. From the result of the correlation analysis, the group of variables can be distinguished as a weak(<0.4), moderate and strong(>0.8) linear relationship according to particle sizes. However, these relationship is a manifold pattern according to sampling dates, areas and particle sizes. In addition to investigating the correlation of these elements, the correlation patterns of elements associated with soil and other pollution sources are plotted.

The correlation between elemental black carbon and fine particles of APM at the two areas are plotted in Figure 11. The correlation coefficients of the industrial and suburban area were 0.67 and 0.70, respectively. Therefore the linear relationships are strong for all of the industrial and suburban area. The above relationship allows prediction of a correlation between concentrations of the other elements and the measured elements as well as the long term pattern of the specific elemental concentration in the environment.

IV. Conclusion

To enhance the use of nuclear analytical techniques(NAT), for air pollution studies and to study the feasibility of the use of INAA as a routine monitoring tool to find out environmental pollution sources, the concentrations of 25 trace elements in airborne particulate matter collected for two sampling dates and particle sizes at two different locations using a low volume air sampler were measured. The statistical results of analytical data obtained by INAA were used to investigate the emission sources of air pollution and relevant environmental information. Consequently, neutron activation analysis using a research reactor proved to be a useful tool for environmental pollution monitoring.

Acknowledgement : This research project has been carried out under the Nuclear R&D Program by Ministry of Science and Technology, Republic of Korea, and a part of the international cooperative research program(RCA/IAEA sub-project) on air pollution.

V. References

[1] R. Dams, J. A. Robbins, K. A. Rahn and J. W. Winchester, *Anal. Chem.*, **42**, (1970) 861.

[2] W. H. Zoller and G. E. Gordon, 'INAA of Atomospheric Pollutants Utilizing Ge(Li) γ -ray Detector', *Anal. Chem.*, **42**, (1970) 257.

[3] E. S. Gladney, W. H. Zoller, A. G. Jones and G. E. Gordon, 'Composition and Size Distribution for Atmospheric Particulate Matter in Boston Area', *Environ. Sci. Technol.*, **8**, (1974) 551.

[4]A. Alian and B. Sansoni, 'A Review on Activation Analysis of Airborne Particulate Matter', *J. Radioanal. and Nucl. Chem., Articles*, **89**, (1985) 191.

[5] A. Alian and B. Sansoni, 'Activation Analysis of Airborne Particulate Matter', Central Department for Chemical Analysis, Report Jul-Spez-475, ISSN 0343-7639, Kernforschungsanl -age Julich GmbH, D-5170 Julich, Federal Republic of Germany, 99 (1988).

[6] W. D. Ehmann and D. E. Vance, 'Advances in Neutron Activation Analysis', CRL Critical Reviews in *Anal. Chem.*, **20**, (1989) 405.

[7] J. Tolgyessy and E. H. Klehr, 'Nuclear Environmental Chemical Analysis', Ellis Harwood Series in Analytical Chemistry, John Wiley and Sons (1987).

[8] P. K. Hopke, 'Receptor-Modelling in Environmental Chemistry, Chemical Analysis., 76 (1985).

[9] K. H. Wedepohl, Origin and Distribution of the Elements, Pergamon Press, London, 999 (1968).

[10] IAEA, 'Sampling and Analytical Methodologies for Instrumental Neutron Activation Analysis of Airborne Particulate Matter', Training Course Series No.4, IAEA-TCS-4, Vienna, 1992.

[11] IAEA Report ; 'Regional RCM on Applied Research on Air Pollution using Nuclear-related Analytical Techniques in the Asia and Pacific Region', 1995.

[12] Meeting Report of Mid-Term Review Meeting Joint UNDP/RCA/IAEA sub-Project on Air Pollution and its trends, Sigapore 18-22 October 1999.

[14] G. Erdtmann ; 'Neutron Activation Tables', Vol.6, New York (1976).

[15] IAEA ; 'Handbook on Nuclear Activation Analysis Data', IAEA Tec. Rep. No. 273 (1987).

[16] L. A. Currie ; *Anal.Chem.*, **40** (1968) 586.

[17] Quantifying Uncertainty in Analytical measurement, EURACHEM/CITAC, 1999.

[18] Y. S. Chung, Y. J. Chung, E. S. Jeong and S. Y. Cho ; 'Determination of Trace Elements in Airborne Particulates by INAA', *J. Kor. Nucl. Soc.*, 27, 2 (1995) 234.

[19] Y. S. Chung, Y. J. Chung, E. S. Jung and S. Y. Cho ;'Comparison and Determination of Environmental Standard Samples by Instrumental Neutron Activation Analysis', *J. Radioanal.Nucl. Chem.*, 217, 1 (1997) 71-76.

[20] Y. S. Chung, Y. J. Chung, E. S. Jeong and S. Y. Cho ; 'Study on Air Pollution Monitoring in Korea using Instrumental Neutron Activation Analysis', *J. Radioanal. Nucl. Chem.*, 217, 1 (1997) 83-89.

[21] IAEA, Survey of Reference Materials "Biological and Environmental Reference Materials for Trace elements, Nuclides and Microcontaminants" IAEA-TECDOC-854 vol.1, Vienna (1995); IAEA, Survey of Reference Materials "Biological and Environmental Reference Materials for Trace elements, Nuclides and Microcontaminants" IAEA-TECDOC-880 vol.2, Vienna (1996).

[22] Zeev B. Alfassi, Activation Analysis, vol. 2, CRC Press, 1990.

[23] B. Mason ; *Principles of Geochemistry*, 3rd ed. 1966.

Table 1. Correlation Coefficients between of Elements and PM (a) DC, (b) DF, (c) KC, (d)KF

	Sc	Al	Fe	k	La	As	Cr	Sb	Zn	PM_{10}
Sc	1.00									
Al	0.93	1.00							(A)	
Fe	0.92	0.90	1.00							
k	0.92	0.72	0.87	1.00						
La	0.98	0.69	0.90	0.96	1.00					
As	0.75	0.51	0.65	0.71	0.74	1.00				
Cr	0.46	0.03	0.73	0.47	0.49	0.29	1.00			
Sb	0.52	0.57	0.62	0.65	0.59	0.37	0.45	1.00		
Zn	0.61	0.24	0.83	0.67	0.67	0.42	0.85	0.65	1.00	
PM_{10}	0.78	0.68	0.84	0.89	0.85	0.60	0.65	0.73	0.73	1.00

	Sc	Al	Fe	k	La	As	Cr	Sb	Zn	$PM_{2.5}$
Sc	1.00									
Al	0.87	1.00							(B)	
Fe	0.77	0.59	1.00							
k	0.64	0.38	0.38	1.00						
La	0.76	0.27	0.29	0.63	1.00					
As	0.51	0.49	0.52	0.55	0.34	1.00				
Cr	0.13	0.28	0.36	0.01	0.14	0.17	1.00			
Sb	0.25	0.29	0.34	0.39	0.58	0.42	0.38	1.00		
Zn	0.46	0.44	0.76	0.41	0.17	0.48.	0.27	0.37	1.00	
$PM_{2.5}$	0.40	0.35	0.38	0.70	0.20	0.76	0.05	0.39	0.45	1.00

	Sc	Al	Fe	k	La	As	Cr	Sb	Zn	PM_{10}
Sc	1.00									
Al	0.96	1.00							(C)	
Fe	0.97	0.60	1.00							
k	0.91	0.57	0.87	1.00						
La	0.97	0.13	0.96	0.21	1.00					
As	0.60	0.24	0.61	0.44	0.57	1.00				
Cr	-0.11	-0.04	-0.06	-0.06	-0.11	-0.14	1.00			
Sb	0.36	0.21	0.48	0.50	0.09	0.24	0.14	1.00		
Zn	0.05	0.36	0.66	0.72	0.62	0.45	0.12	0.80	1.00	
PM_{10}	0.88	0.54	0.89	0.86	0.35	0.57	-0.10	0.51	0.71	1.00

	Sc	Al	Fe	k	La	As	Cr	Sb	Zn	$PM_{2.5}$
Sc	1.00									
Al	0.94	1.00							(D)	
Fe	0.93	0.85	1.00							
k	0.48	0.40	0.52	1.00						
La	0.90	0.80	0.89	0.57	1.00					
As	-0.37	0.48	0.65	0.55	0.65	1.00				
Cr	0.52	-0.20	-0.21	-0.19	-0.14	-0.18	1.00			
Sb	-0.36	0.16	0.25	0.20	0.24	0.24	-0.22	1.00		
Zn	-0.33	0.25	0.49	0.68	0.50	0.59	-0.23	0.59	1.00	
$PM_{2.5}$	0.32	0.34	0.43	0.74	0.47	0.63	-0.27	0.46	0.83	1.00

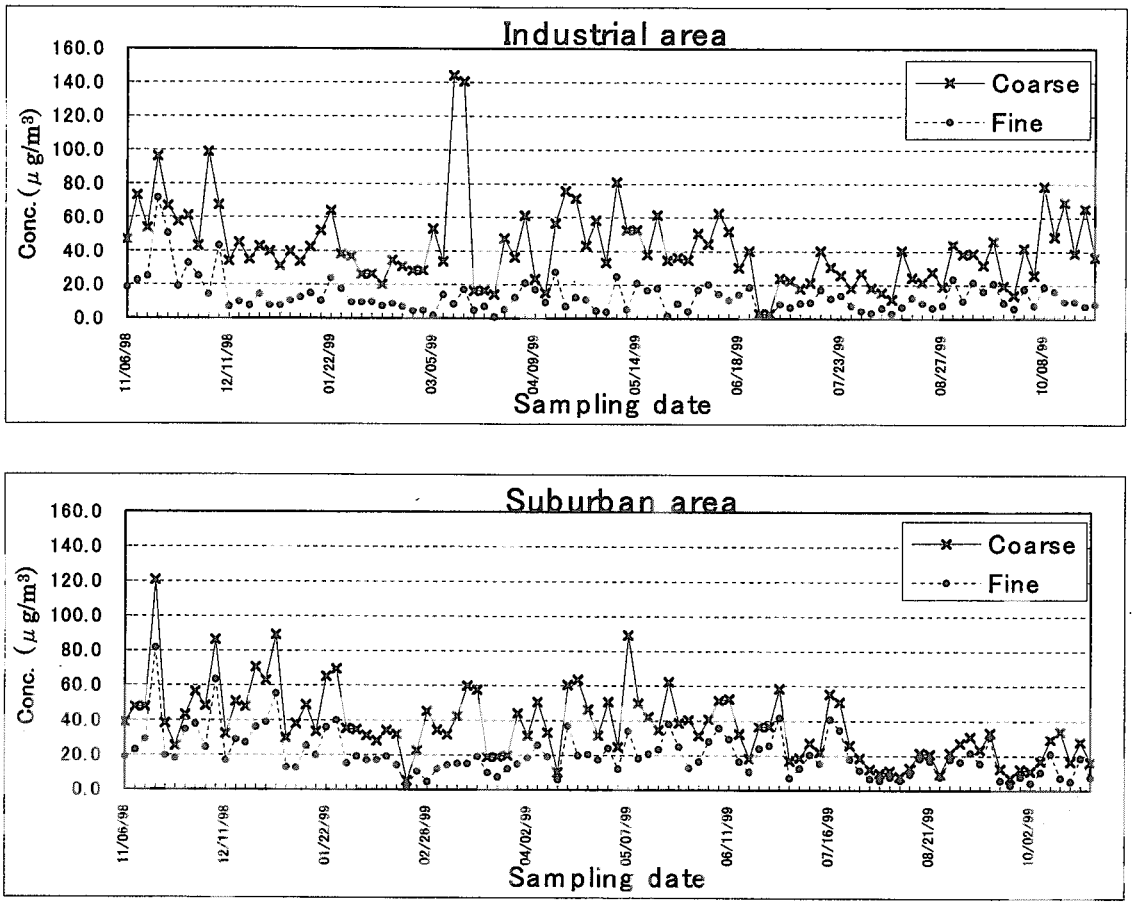

Fig. 1 Mass concentration of fine and coarse fraction with sampling date.
(`98.11 - `99.10)

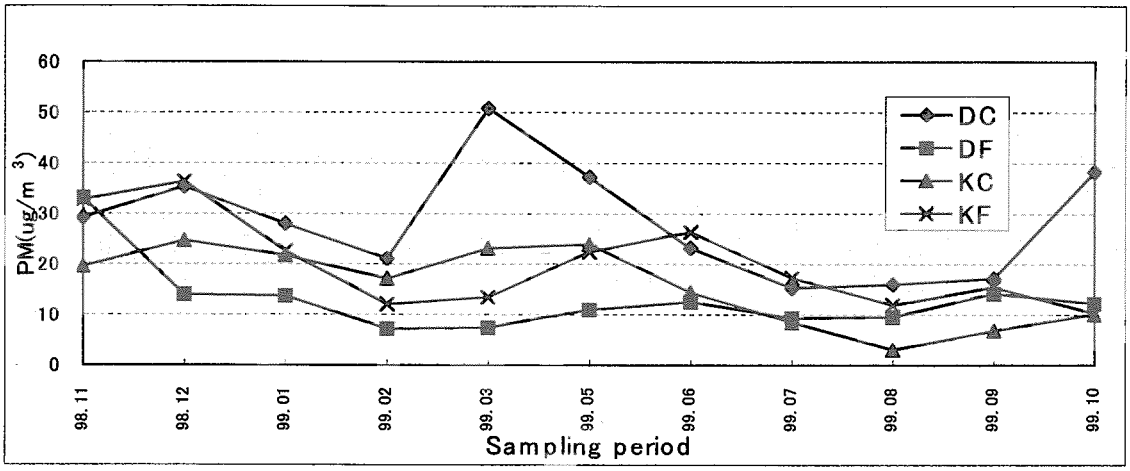

(μ g/m^3)

Site	Range	Mean	Std.	Geo. Mean
DC	15.2-50.9	28.71	10.79	26.86
DF	7.2-33.1	13.24	6.77	12.17
DC+DF		41.95		39.03
KC	3.1-23.9	16.10	7.37	13.90
KF	10.3-36.3	20.12	8.40	18.61
KC+KF		36.22		32.51

Fig. 2 Monthly variation of mass concentration of APM at industrial and suburban areas.

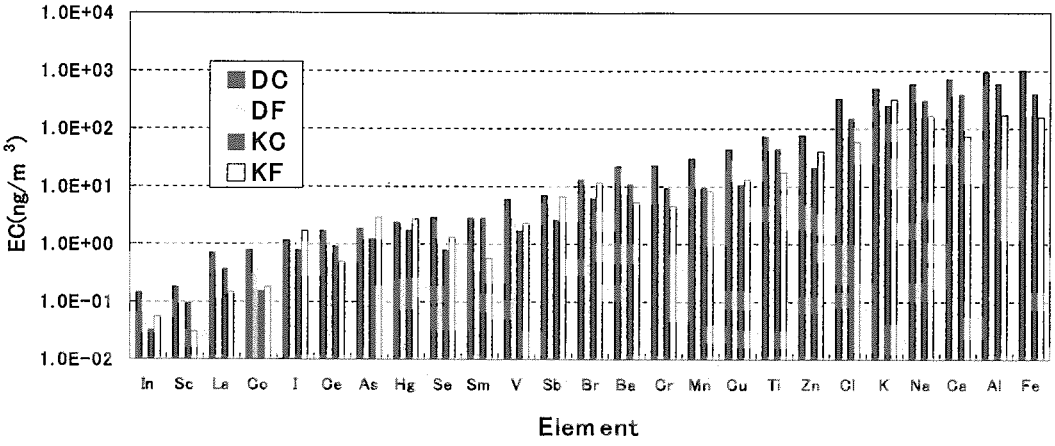

(ng/m^3)

Elements	DC	DF	KC	KF
In	0.15	0.07	0.03	0.06
Sc	0.18	0.02	0.10	0.03
La	0.71	0.12	0.38	0.15
Co	0.80	0.33	0.16	0.18
I	1.14	1.29	0.80	1.68
Ce	1.71	0.68	0.94	0.50
As	1.90	1.58	1.29	2.92
Hg	2.42	2.32	1.77	2.71
Se	2.87	1.01	0.81	1.33
Sm	2.93	0.33	2.93	0.57
V	5.98	2.96	1.73	2.29
Sb	7.02	5.15	2.67	6.70
Br	13.22	9.95	6.26	11.62
Ba	22.46	7.60	11.21	5.33
Cr	23.11	6.15	9.53	4.61
Mn	29.94	11.13	9.66	8.27
Cu	43.43	12.24	10.73	13.02
Ti	73.84	16.98	45.89	17.62
Zn	76.51	53.53	21.27	40.47
Cl	329.25	72.82	156.63	58.76
K	497.51	212.98	254.71	317.58
Na	598.96	162.94	319.79	167.47
Ca	723.50	149.55	406.14	73.72
Al	934.21	134.26	606.95	171.47
Fe	1021.67	167.45	405.77	155.98

Fig. 3 Average concentration of measured elements at industrial and suburban areas.

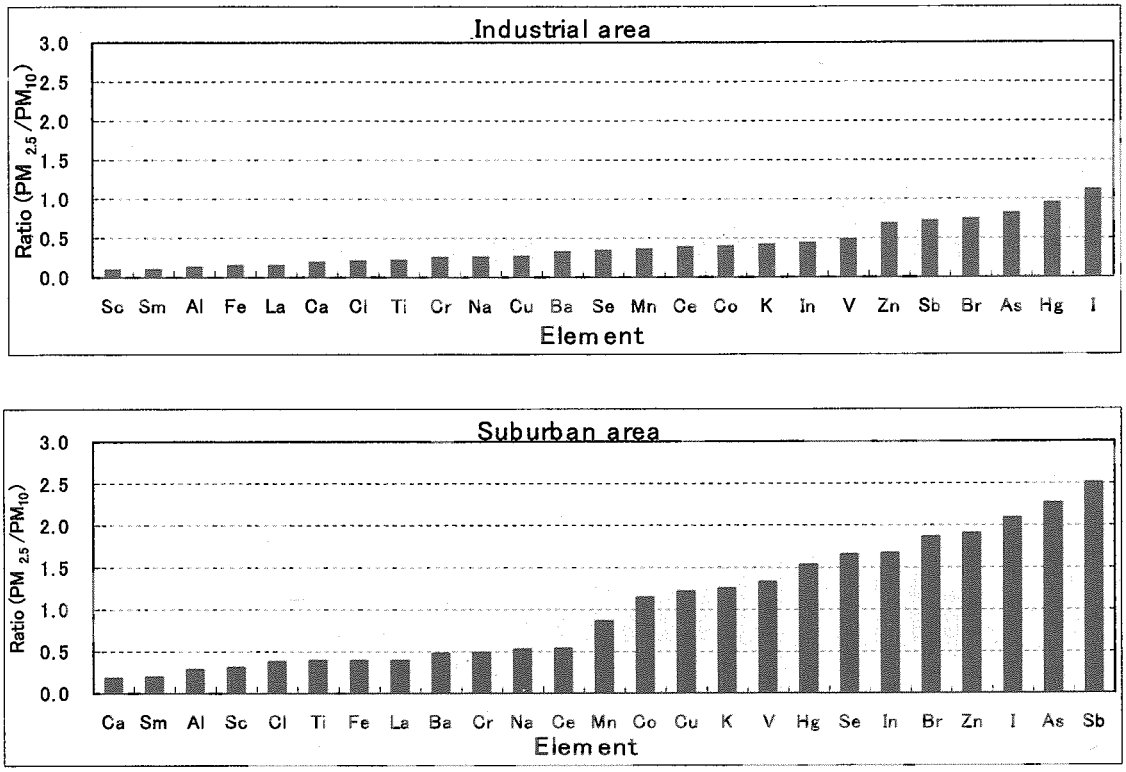

Fig. 4 Ratio of elemental concentration between $PM_{2.5}$ and PM_{10}.

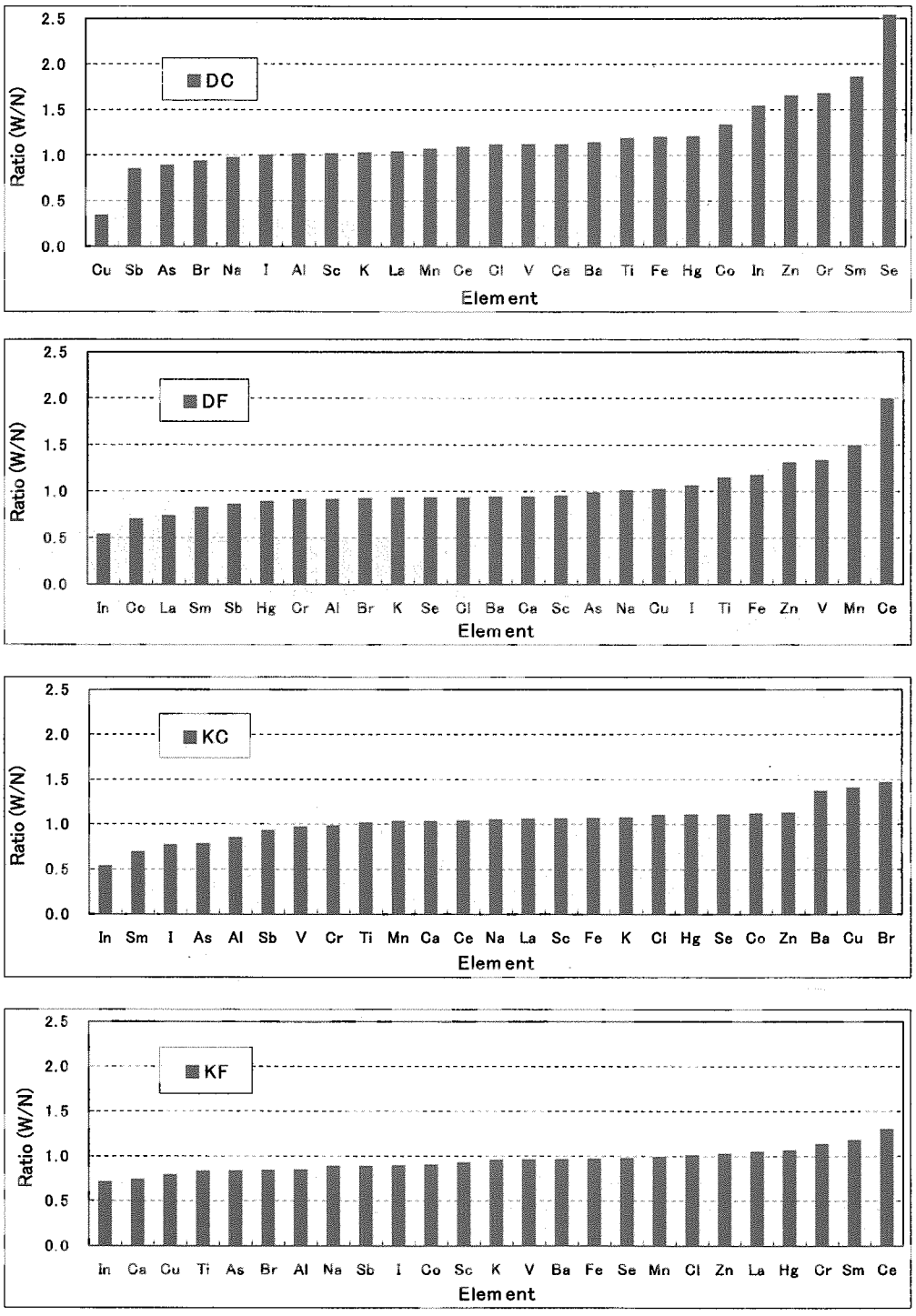

Fig. 5 Ratio of elemental concentration for working to non-working day.

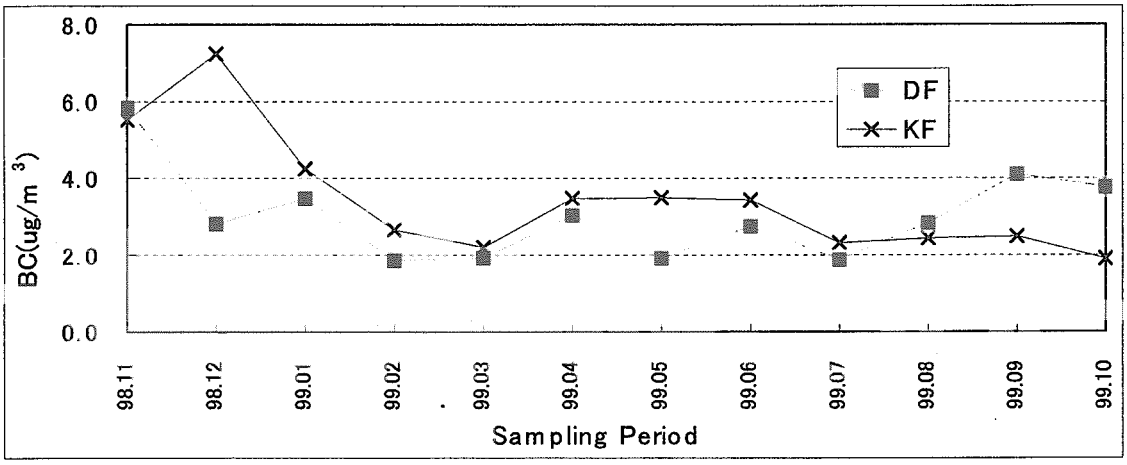

Fig. 6. Monthly variatuion of black carbon concentration. ($PM_{2.5}$)

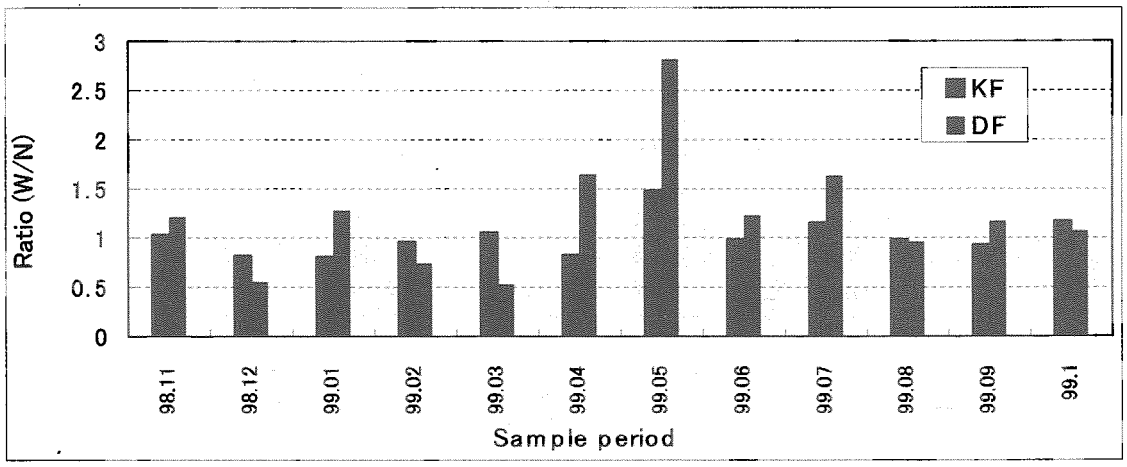

Fig. 7 Ratio of black carbon concentration($PM_{2.5}$) for working to non-workingday.

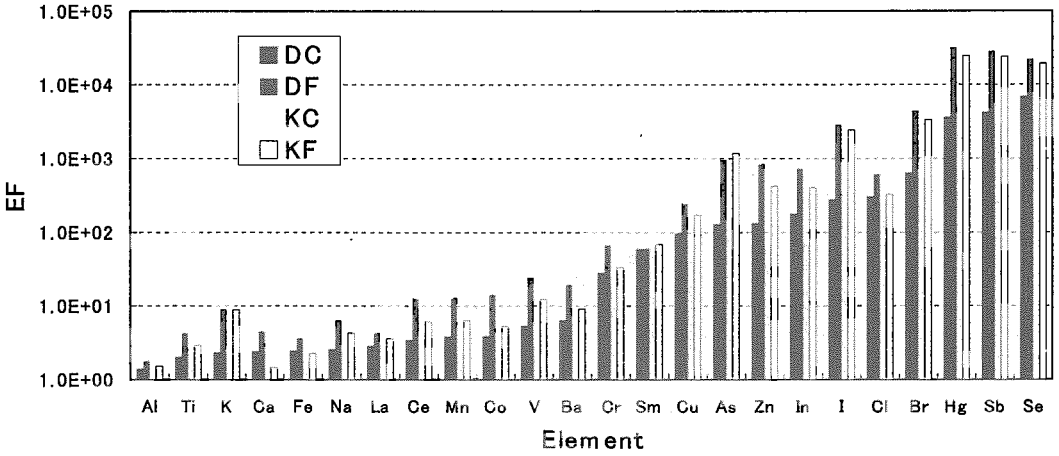

Element	DC	DF	KC	KF
Al	1.40	1.83	1.65	1.53
Ti	2.04	4.27	2.31	2.90
K	2.33	9.10	2.18	8.88
Ca	2.42	4.56	2.48	1.47
Fe	2.48	3.71	1.80	2.26
Na	2.57	6.37	2.50	4.29
La	2.86	4.30	2.83	3.57
Ce	3.45	12.60	3.48	6.04
Mn	3.83	12.97	2.25	6.31
Co	3.87	14.41	1.40	5.24
V	5.38	24.29	2.84	12.30
Ba	6.42	19.80	5.84	9.08
Cr	28.05	68.12	21.09	33.40
Sm	59.23	61.01	108.20	68.32
Cu	95.86	246.33	43.17	171.60
As	128.06	970.97	158.43	1174.13
Zn	132.70	846.64	67.22	418.88
In	179.87	738.59	73.87	403.07
I	277.64	2866.23	355.92	2432.79
Cl	307.49	620.16	266.56	327.52
Br	641.78	4408.51	553.77	3368.11
Hg	3680.13	32153.56	4900.64	24583.41
Sb	4263.90	28500.21	2956.83	24266.05
Se	6973.51	22387.28	3578.02	19341.62

Fig. 8. Enrichment factor of measured elements.

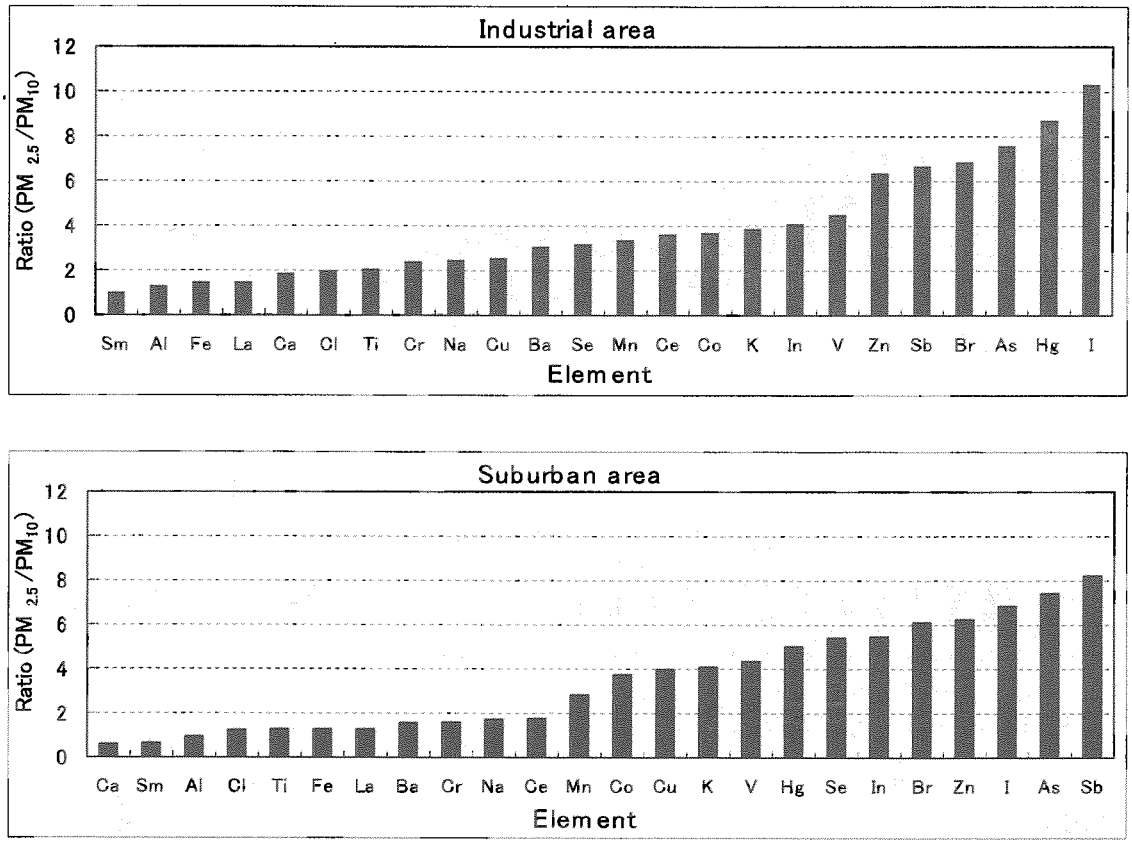

Fig.9. Ratio of enrichment factor between $PM_{2.5}$ and PM_{10}.

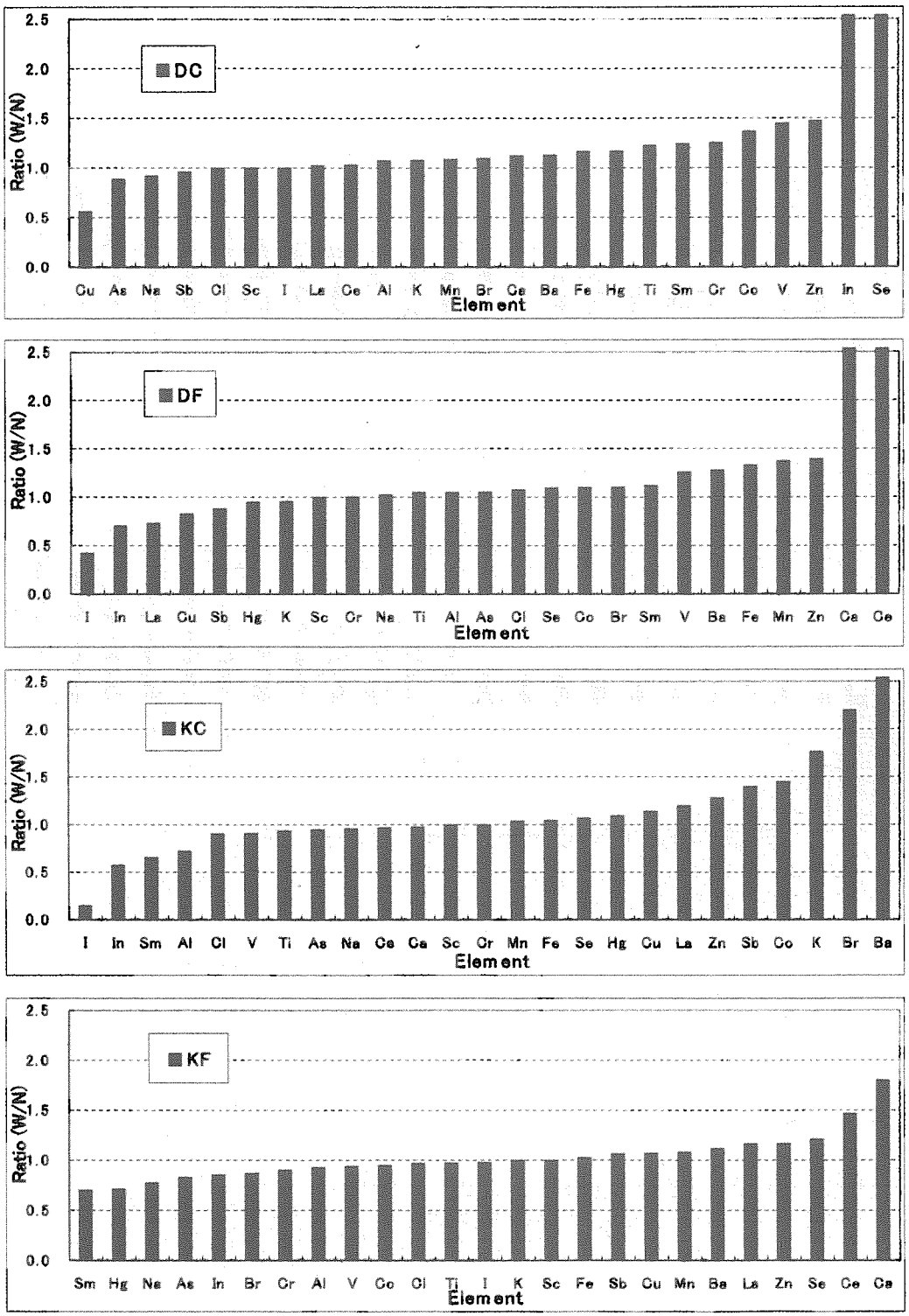

Fig. 10. Ratio of enrichment factor for working to non-working day.

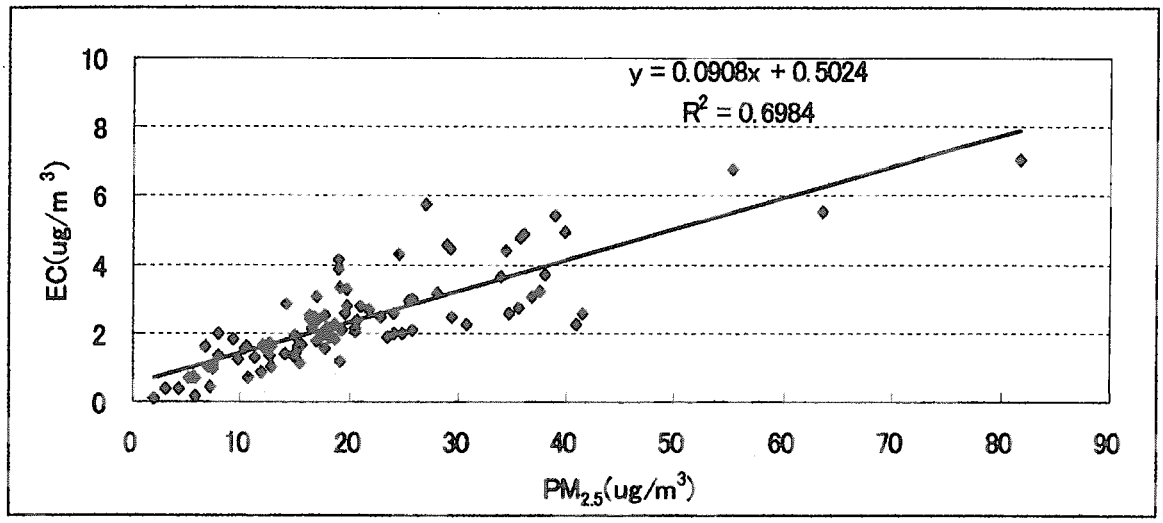

(a) Correlation between Elemental Carbon and PM2.5 at suburban area.

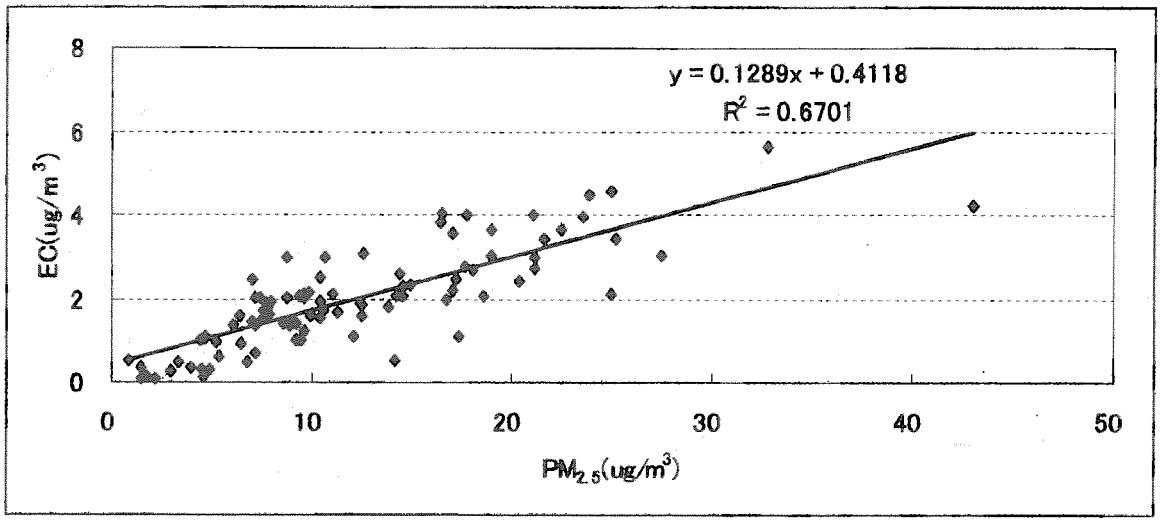

(b) Correlation between Elemental Carbon and PM2.5 at industrial area.

Figure 11. Correlation between Elemental Black Carbon and PM2.5

JP0250106

1.22 Probabilistic Risk Analysis of Airborne Toxic Metals in Korean Industrial Complex

Jin-Hong Lee Mi-Suk Jang
Department of Environmental Engineering, Chungnam National University,
Daeduck Science Town, Taejon 305-764, Korea

Abstract

The research centered on the concentration profiles and probabilistic risk analysis of toxic metals for ambient air in Taejon industrial complex, one of the most polluted industrial complexes in Korea. Airborne concentrations of toxic metals for the analysis were obtained from about two-year sampling and analysis in the complex. The long-term arithmetic means of human carcinogens such as arsenic, hexavalent chromium and nickel subsulfide were 5.53, 2.16 and 3.46 ng/m^3 while the means of probable human carcinogens such as beryllium, cadmium and lead were 0.08, 2.35, 293.29 ng/m^3, respectively. And the long-term arithmetic mean concentration of non-carcinogenic toxic metal, manganese was 55.91 ng/m^3. The point risk estimate for the inhalation of carcinogenic metals was 6.2 10^{-5}, about 90% of which was due to the inhalation of human carcinogens, arsenic and hexavalent chromium. From a probabilistic risk analysis, the 50th－95th percentile cancer risks for men and women were estimated to be 2.8 10^{-5}～9.6 10^{-5} and 2.5 10^{-5}～8.5 10^{-5}, respectively. About 70% of the 50th percentile risk for both men and women came from human carcinogens such as arsenic and hexavalent chromium. A comparison of the probabilistic risk estimates with point risk estimate showed that the probabilistic analysis can provide a more complete assessment of risk and more useful information to risk manager and the public. However, uncertainty remains and improved Korean probabilistic density functions (PDF) are needed for factors such as inhalation rate, exposure frequency, cancer potency factors and reference doses.

Key words : probabilistic risk analysis, airborne toxic metals, industrial complex

Ⅰ. Introduction

In spite of low concentrations of toxic metals in urban air, the magnitude of health risk associated with may be not smaller than that with other hazardous air pollutants.

Especially, it has been expected that the risk from industrial complexes might be much higher by toxic metals including carcinogenic ones. However, unfortunately there has been few of domestic studies on the concentration profiles and risk analysis of airborne toxic metals in such areas. Thus, few of long-term concentration profiles for toxic metals in ambient air has been made. Therefore, this study focuses on about two-year analysis by using ICP-MS for the concentrations of twenty-two metals including six airborne carcinogenic metals in Taejon industrial complex, which is one of the most polluted industrial complexes in Korea. ICP-MS has much more excellent detection limits and reproducibility for almost every metal than any other analytical technique. In addition, the study centers on a probabilistic risk analysis of the inhalation of airborne toxic metals based on the concentration profiles. For carcinogenic metals, the risk is assessed quantitatively by using dose-response model selected as the best for each metal. If a substance is identified as a potential human carcinogen, its carcinogenicity may be related to the chemical form of a substance and the route of exposure. This type of information with regard to carcinogenic uncertainty is incorporated into hazard quantification. The carcinogenic group of toxic metal is also emphasized with regard to the hazard quantification.

Ⅱ. Material and Methods

The suspended particulate matters were collected on quartz micro-fiber filter (Whatman QMA, 8" 10") by a high volume air sampler (Sierra Andersen: SAUB-10H model). The sampling was carried out in Taejon industrial complex two or four times per month during weekdays from April, 1997 to December, 1998. Sampled air per filter was computed by using flow recorder from the start to the end of sampling. Whenever motor brush of sampler was changed, flow rate was adjusted by orifice calibrator (GMW-25). Twenty-two metal elements were analyzed by ICP-MS (FISONS PQ3 STE model) and ICP-AES (SHIMADZU ICPS 1000-Ⅲ model) after the pre-treatment of mixed acid extraction using microwave digestion system[1]. Risks were calculated by the following equations, adapted from EPA guidance[2]:

$$Risk = \left(\frac{C \cdot IR \cdot EF \cdot ED}{BW \cdot AT}\right) \cdot CPF$$

$$HI = \left(\frac{C \cdot IR \cdot EF \cdot ED}{BW \cdot AT}\right) \div RfD$$

Where Risk = upper bound lifetime cancer risk (unitless)

HI = non-carcinogenic hazard index (unitless)

C = pollutant concentration in ambient air (mg/m^3)

IR = daily inhalation rate (m^3/day)

EF = exposure frequency (days/year)

ED = exposure duration (years)

BW = body weight of an exposed individual (kg)

AT = averaging time (lifetime for carcinogen, exposure duration for non-carcinogen) (days)

CPF = inhaled cancer potency factor $(mg/kg/day)^{-1}$

RfD = inhaled reference dose (mg/kg/day)

Table 1. Fixed assumptions and PDFs used as inputs to estimate risk

Parameter	Distribution type	Distribution parameters	Source
Arsenic (ng/m³)	LN	GM = 3.09 GSD = 3.38	70 Samples
Beryllium (ng/m³)	LN	GM = 0.07 GSD = 1.97	65 Samples
Cadmium (ng/m³)	LN	GM = 1.68 GSD = 2.61	70 Samples
Hexavalent chromium[a] (ng/m³)	LN	GM = 1.53 GSD = 2.29	68 Samples
Nickel subsulfide[a] (ng/m³)	LN	GM = 2.75 GSD = 2.09	69 Samples
Manganese (ng/m³)	LN	GM = 45.63 GSD = 1.93	70 Samples
Men inhalation rate (m³/day)	LN	GM = 15.07 GSD = 1.11	(3)
Women inhalation rate (m³/day)	LN	GM = 11.15 GSD = 1.14	(3)
Exposure frequency (days/yr)	TR	Min = 180 Best = 345 Max = 365	(4)
Men body weight (kg)	LN	GM = 64.96 GSD = 1.13	(5)
Women body weight (kg)	LN	GM = 54.28 GSD = 1.13	(5)
Cancer potency factor $(mg/kg/day)^{-1}$	Point value	Adjusted IRIS Value[b]	(6)
Reference dose (mg/kg/day)	Point value	Adjusted IRIS Value[b]	(6)

LN : Lognormal; TR : Triangular; GM : Geometric Mean; GSD : Geometric Standard Deviation.

a) Each chemical form of a metal was assumed to be ten percent of total amount.

b) Adjusted IRIS value for reference Korean of a 60-kg body weight over a 70-year life span

Exposure assumptions and concentrations used for probabilistic risk analysis are shown in Table 1. Probabilistic calculations were done by running Crystal Ball (Decisioneering, version 4.0) Monte Carlo simulator. The simulation software sampled all distribution variables 10,000 times using Latin hypercube strategy. The point risk estimate was computed by same software for reference Korean of a 60-kg body weight with 20 m^3/day of daily inhalation rate. Results of probabilistic calculations are shown in Table 2.

Table 2. Monte Carlo carcinogenic risk estimates in Taejon industrial complex

Percentile	Risk estimate	
	Men	Women
5 percentile	9.8×10^{-6}	8.6×10^{-6}
10 percentile	1.2×10^{-5}	1.1×10^{-5}
25 percentile	1.8×10^{-5}	1.6×10^{-5}
50 percentile	2.8×10^{-5}	2.5×10^{-5}
75 percentile	4.6×10^{-5}	4.0×10^{-5}
90 percentile	7.2×10^{-5}	6.4×10^{-5}
95 percentile	9.6×10^{-5}	8.5×10^{-5}
Average	3.8×10^{-5}	3.4×10^{-5}

Ⅲ. Results and Discussion

The arithmetic mean concentration of ambient particulate matters was 99.4 $\mu g/m^3$ during the sampling period in the study area. The minimum is 36.4 $\mu g/m^3$ while the maximum is 200.1 $\mu g/m^3$, respectively. The seasonal concentration of airborne particulate matters was minimum in every summer, which might be due to mainly washout effect by high rainfall intensity. About two-year arithmetic means of human carcinogens such as arsenic, hexavalent chromium and nickel subsulfide were 5.53, 2.16 and 3.46 ng/m^3 while the means of probable human carcinogens such as beryllium, cadmium and lead were 0.08, 2.35, 293.29 ng/m^3, respectively. And the long-term arithmetic mean concentration of non-carcinogenic toxic metal, manganese was 55.91 ng/m^3. The concentrations of soil related metals, that is, Al, Ca, Fe, K, Mg, Na and Si

were to be much higher. Among those metals the maximum concentration of 1,730 ng/m^3 was for Al while the minimum concentration of 435ng/m3 was for Mg, respectively. By analyzing main emission sources in Taejon industrial complex, it was judged that arsenic was emitted from agricultural chemical manufacturing, copper related and/or alloy steel industry, chromium from chemical and metal coating industry, and finally lead from diesel engine exhaust, coal combustion, and storage battery manufacturing, respectively.

The point risk estimate for the inhalation of carcinogenic metals was 6.2 10^{-5}, about 90% of which was due to the inhalation of human carcinogens, arsenic and hexavalent chromium. From a probabilistic risk analysis, the 50th～95th percentile cancer risks for men and women were estimated to be 2.8 10^{-5}～9.6 10^{-5} and 2.5 10^{-5}～8.5 10^{-5}, respectively. About 70% of the 50th percentile risk for both men and women came from human carcinogens such as arsenic and hexavalent chromium. A comparison of the probabilistic risk estimates with point risk estimate showed that the probabilistic analysis can provide a more complete assessment of risk and more useful information to risk manager and the public.[7] However, uncertainty remains and improved Korean probabilistic density functions(PDF) are needed for factors such as inhalation rate, exposure frequency, cancer potency factors and reference doses.

Since December of 1999, a study on the concentration profiles of trace metals for ambient air over Taejon metropolitan city is going on by using INAA, which is funded by ANARO Steering Committee. The committee and ANARO User Association has been operated actively since autumn of 1999. Recently, air pollution studies in Korea have concentrated on the following topics:

1) Ozone related problems, especially for World Cup 2002 in Korea;
2) Non-criteria hazardous air pollutants including VOCs;
3) PM-2.5;
4) The analysis and data interpretation of a large number of samples by INAA;
5) Receptor modeling including CMB modeling, and so on.

INAA has very low detection limits and needs very small amount of airborne particulate sample for the analysis. However, it is difficult to analyze metals such as lead, nickel, cadmium and silica, which are very important metals for either risk assessment or receptor modeling. Thus, it is necessary to use other analytical tool like ICP-MS as a complement.

References

1. Greenberg AE, Clesceri LS, Eaton AD. Standard Method(18th edition). American Public Health Association 1992:3.6
2. U. S. EPA. Risk Assessment Guidance for Superfund. U. S. EPA 1989
3. U. S. EPA. Exposure Factors Handbook(Draft). U. S. EPA 1996
4. Smith RL, Use of Monte Carlo simulation for human exposure assessment at a superfund site. *Risk Analysis* 1994:14(4):433-439
5. KRISS. Investigation of Standard Korean Body, KRISS, 1992
6. U. S. EPA. IRIS (Integrated Risk Information System). U. S. EPA 1999
7. Finley B, Paustenbach, D. The benefits of probabilistic exposure assessment: three cases studies involving contaminated air, water, and soil. *Risk Analysis* 1994:14(1):53-73

JP0250107

1.23 Application of NAA in the Field of Environmental Geology

Kil Yong Lee, Yoon Yeol Yoon

Environmental Geology Division, Korea Institute of Geoscience & Mineral Resources(KIGAM), 30 Gajung-dong, Yuseong-gu, Daejeon 305-350, Korea(E-mail: kylee@kigam.re.kr)

ABSTRACT

NAA is a very useful technique for the nondestructive analysis of trace elements in environmental and geological materials. Sampling and preparation procedures were established to analysis of various major and trace elements in environmental and geologic materials. About 40 elements in pine needle, rice and a few crops and the soils have been analyzed at different sites. The pine needle, rice and other crops were investigated whether they can be feasible or not as bio-monitors. NAA procedure was optimized for sample types and elements analyzed. ICP and XRF also applied to analysis of some samples and the results were compared with NAA. The elemental distributions and relationship between plants and soils were also investigated. NAA appeared to be a very fruitful method to analysis environmental and geologic materials. It was found that pine needles and rice could be able to use as indicator plants for pollution monitoring in Korea.

INTRODUCTION

The aim of present work is to investigate applicability of NAA in the field of environmental geology. Their are so many samples such as soil, air, water(groundwater) to be analyzed in the environmental geology field. It is very difficult to study of environmental pollution, because the sampling, pretreatment and analytical procedures are very tedious and complicate works. For a meaningful evaluation of degree of environmental pollution in a site it is necessary to analysis enormous and various samples such as air, water, and soil and to know various climate parameters. It has been well known NAA has peculiar advantages, nondestructive and multielemental and sensitive analysis. Several studies reported considering the biomonitor using plants such as spruce, moss, lichen, and so on. In the present work, pine needle, rice and some common crops grown in Korea were analyzed by NAA and compared other analytical methods. Pine needle was chosen as a possible biomonitor of pollution because it is largely present in anywhere of our country, and it is evergreen tree and the needle possess a high surface homogeneity. Rice, soybean and red pepper were also chosen as possible biomonitors, because they have similar motive with pine needle. Optimum conditions for the analysis of the plants and soils by NAA such as sampling, preparing, irradiation and cooling procedures have been studied. Feasibility as bio-monitors of these plants has also been discussed.

Sampling and Preparation

Pine Needle

The sampling sites were urban, suburban and rural regions and sampling time were spring, summer, fall and winter. Needle samples were taken from twenty pine trees in a site. Sampling was done on Korean pine (Pinus denaiflora) at a height of 1.5 to 2 m above ground, taking only a year old needle which is more yellowish than old needle and has two scales on it. Needle samples were put in a clean PE bag and the bag was stored an ice chest. After the transferring the needle samples in laboratory, the samples were stored in refrigerator and the temperature was controlled to 4 ❶. Each needle sample was split into two parts. Only a part was cleaned successively with 1% HCl and deionized water. Both cleaned and uncleaned needle samples were then dried in a freeze dryer at -50❋C for 2 weeks. Dried needle samples were pulverized with a ball mill to make fine powder (-150 mesh) and mixed in a mixer mill to improve homogeneity.

Soil and Crops

Soil samples were taken from 5-15cm deep field ground around the root of each crop. The soil sample was sieved with 2mm sieve and store in a clean PE(polyethylene) zipper bag. In our laboratory, the soil samples were dried at 60 for 72 h in an electric oven and then they were pulverized under 150 ﷺ particle and homogenized. All crops were freeze dried and pulverized, homogenized. In case of root samples(rice, soybean), they were washed with distilled water to remove soil on their surface before drying.

NAA

Pine Needle and crops

500mg of the each sample powder was placed in PP(polypropylene) vial and the vial was sealed. An SRM(NIST-1575, pine needle) was also prepared. The sample and SRM were irradiated for 2min and 30 minutes for short and long lived nuclide at a PTS(pneumatic transfer system) in a research reactor (HANARO). Thermal and epithermal neutron flux densities were 1.8 x 1013 and 1.2 x 1010, respectively. Activity measurements of the irradiated needle samples and SRMs were carried out with three different decay intervals. For the short lived nuclide the 2min irradiated samples were counted two times, after 5 and 30min decay. And for medium and long lived nuclide, 30min irradiated samples were counted 3 times, after 2, 7, and 20days decay.

Soil

100mg of the each soil sample was placed in PP(polypropylene) vial and the vial was sealed. An SRM(NIST-coal) was also prepared. Irradiation and counting of soil samples were carried out with the same method of crop samples.

Fig. 1 and 2 show the preparation procedure of pine needle sample and NAA procedure, respectively.

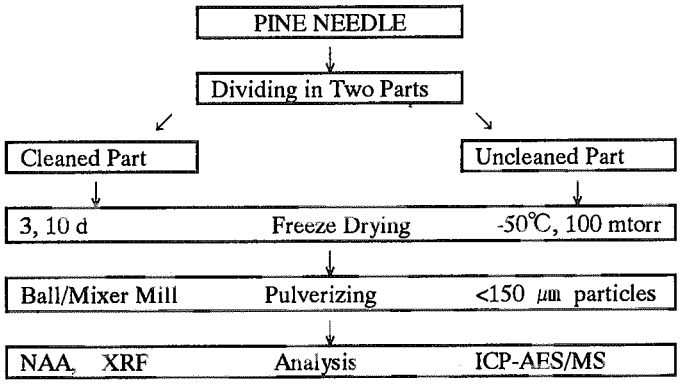

Fig. 1. Flow chart for preparing of pine needle.

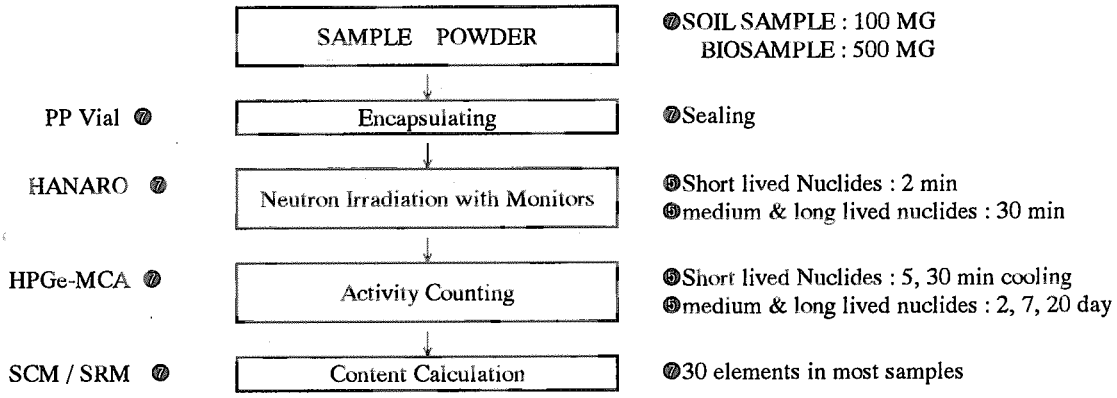

Fig. 2. NAA Procedure of soil and plant samples.

Results and Discussion

Collected sample must be representative of the site, and contamination of analytes must be suppressed contamination of analytes must be suppressed during sampling and analysis. Table 1 shows the NAA results of pine needle samples taken from three different regions at four seasons. Almost all of the elements examined, except for a few elements related to lithosphere such as as Ca, Co, Fe, Rb, and Sc, have different content values with region and needle body or surface. Some elements such as As, Br, Cr, W, and Zn show significantly higher contents in urban and sub-urban regions than in rural region. Fig. 3 shows the content ratio on needle surface and body in urban region with seasons based on fall. The content ratio with seasons is very different on needle surface and body.

Table 1. NAA results of pine needle samples(*ppm*)

Region	Element	Fall		Winter		Spring		Summer	
		Uncleaned	cleaned	uncleaned	cleaned	uncleaned	cleaned	uncleaned	cleaned
Urban	As	0.29	0.15	0.39	0.19	1.3	0.62	0.54	0.19
	Au	0.0058	0.0035	0.011	0.0025	0.012	0.0066	0.010	0.0054
	Br	4.7	3.6	3.8	2.2	5.2	4	6.6	5.1
	Ca	5100	3700	4700	3300	5300	4700	4000	3400
	Ce	0.72	0.18	0.74	0.32	0.93	0.66	0.62	0.38
	Co	0.35	0.31	0.32	0.29	0.36	0.31	0.29	0.3
	Cr	4.1	4	3.6	3.4	3.9	2.3	3.6	3.4
	Eu	0.01	0.01	0.01	0.01	0.01	0.01	0.01	0.01
	Fe	110	95	120	89	240	180	170	140
	K	7600	7200	6600	5200	5000	4600	4700	4800
	La	0.48	0.18	0.58	0.18	0.59	0.38	0.51	0.2
	Na	53	24	86	29	130	79	110	110
	Rb	17	13	9.6	7.8	6.1	4.8	7.4	7.2
	Sb	0.1	0.09	0.1	0.09	0.16	0.1	0.23	0.16
	Sc	0.03	0.02	0.03	0.02	0.08	0.04	0.06	0.05
	Sm	0.04	0.02	0.05	0.04	0.1	0.05	0.05	0.02
	Th	0.05	0.05	0.06	0.02	0.17	0.07	0.1	0.06
	W	0.26	0.15	0.31	0.14	0.21	0.23	0.18	0.06
	Zn	74	62	60	57	80	75	36	30
Sub-urban	As	0.2	0.12	0.51	0.09	0.69	0.2	0.24	0.12
	Au	0.0074	0.0049	0.0056	0.0016	0.0053	0.0048	0.0039	0.0015
	Br	5.1	5	5.9	3.7	3.5	3.2	3.9	3.4
	Ca	4900	3800	4400	3400	3200	2800	4500	3700
	Ce	0.65	0.41	0.74	0.38	0.69	0.63	0.69	0.35
	Co	0.49	0.36	0.52	0.32	0.36	0.31	0.41	0.38
	Cr	1.8	1.9	1.9	1.7	1.9	1.6	2.7	2.5
	Eu	0.01	0.01	0.02	0.01	0.01	0.01	0.02	0.01
	Fe	170	130	160	120	160	130	160	110
	K	6600	6400	6800	4300	6200	5100	3400	2700
	La	0.79	0.36	0.52	0.22	0.7	0.6	0.38	0.22
	Na	180	140	49	39	80	51	110	110
	Rb	12	11	15	12	10	10	7.1	3.8
	Sb	0.09	0.06	0.06	0.06	0.11	0.09	0.18	0.1
	Sc	0.03	0.02	0.03	0.02	0.04	0.02	0.03	0.03
	Sm	0.01	0.005	0.08	0.04	0.06	0.02	0.05	0.02
	Th	0.09	0.08	0.06	0.02	0.09	0.05	0.14	0.07
	W	0.82	0.07	0.49	0.15	0.07	0.04	0.13	0.06
	Zn	78	54	75	59	68	62	74	69
Rural	As	0.08	0.05	0.08	0.04	0.32	0.19	0.28	0.09
	Au	0.0030	0.0013	0.0040	0.0010	0.0050	0.0020	0.0021	0.0018
	Br	2.7	2.3	3.3	2.5	3.8	3.7	3.4	2.6
	Ca	3500	2800	3700	2700	3800	2800	2900	2600
	Ce	0.56	0.5	0.59	0.48	0.55	0.53	0.63	0.23
	Co	0.57	0.48	0.61	0.58	0.65	0.54	0.35	0.33
	Cr	3.3	3.3	2.6	2.6	3	2.7	2.8	2.5
	Eu	0.01	0.01	0.01	0.01	0.01	0.01	0.01	0.01
	Fe	130	98	100	77	130	94	160	100
	K	5700	5600	5800	5200	5200	5100	4800	4500
	La	0.26	0.17	0.36	0.12	0.26	0.17	0.21	0.15
	Na	86	30	50	38	74	62	120	50
	Rb	13	11	8.9	8.3	8.4	6.7	6.9	5.4
	Sb	0.04	0.04	0.04	0.04	0.1	0.07	0.1	0.05
	Sc	0.05	0.03	0.05	0.03	0.04	0.04	0.05	0.02
	Sm	0.04	0.02	0.02	0.02	0.04	0.03	0.02	0.01
	Th	0.05	0.04	0.05	0.04	0.07	0.05	0.07	0.04
	W	0.29	0.09	0.15	0.04	0.1	0.03	0.13	0.03
	Zn	33	21	35	27	35	23	26	24

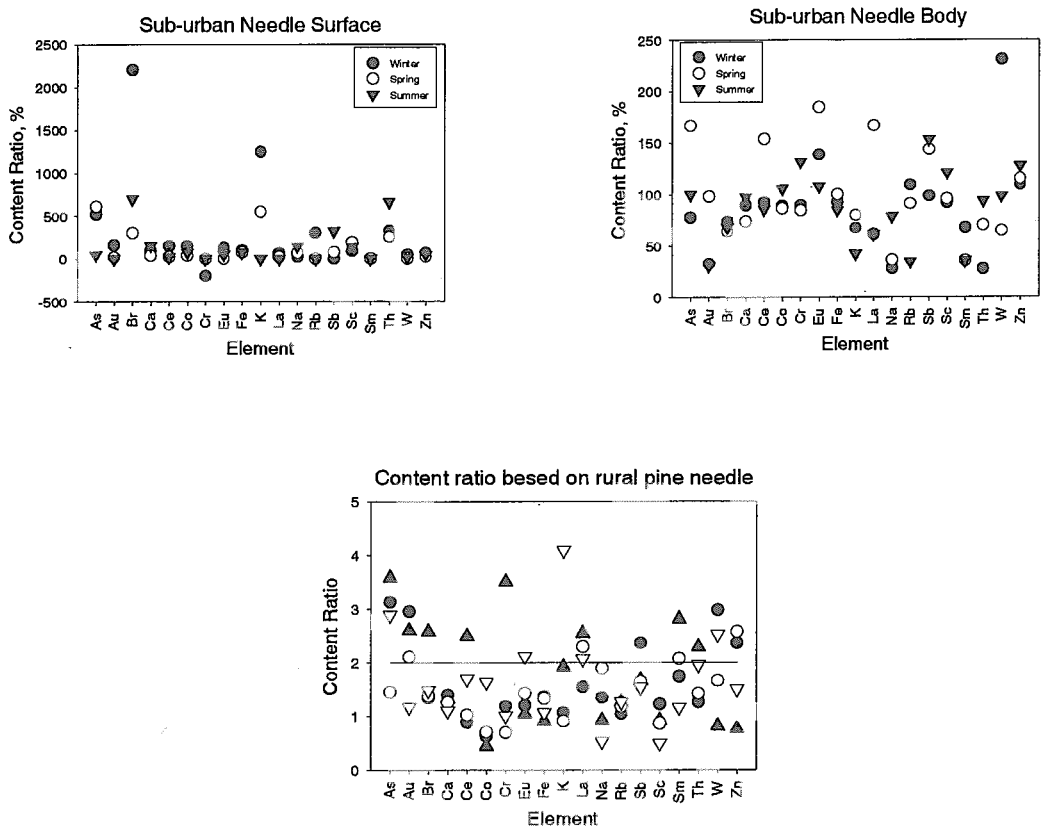

Fig. 3. The mean content ratio on needle body and surface in urban and sub-urban based on rurals'.(circle : needle body, triangle : surface, closed form : urban, opened form : sub-urban)

As we can see in table and figures, the concentration of elements on pine needle body and surface are very different with growing regions and sampling seasons.

The concentration ratios of major elements, rare earth elements and trace elements in the part of rice based on soil were presented in Fig. 4, 5 and 6, respectively. Fig. 7 and 8 also show the concentration of several elements in soybean and other crops. In Fig. 4 and 6, we can see that the trends of concentration ratios for major and trace elements are very similar in three regions. However, in Fig. 5, the concentration ratios of rear earth elements have different characteristics with regions and rice parts.

In case of soybean in Fig. 7, almost all elements except for Ca, K and Zn have similar trends for the concentration ratios. The trends are also similar in other crops of Fig. 8.

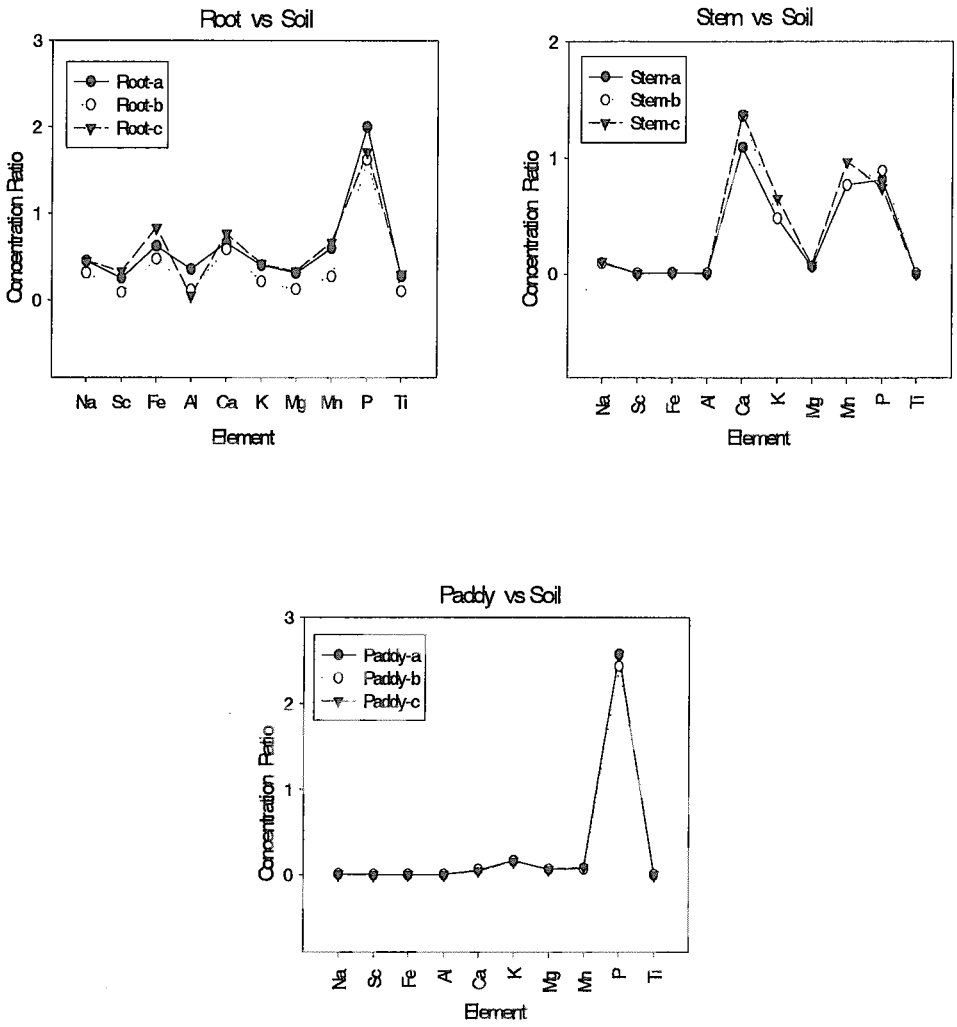

Fig. 4. Concentration ratio of major elements in the part of rice based on soil from three regions.

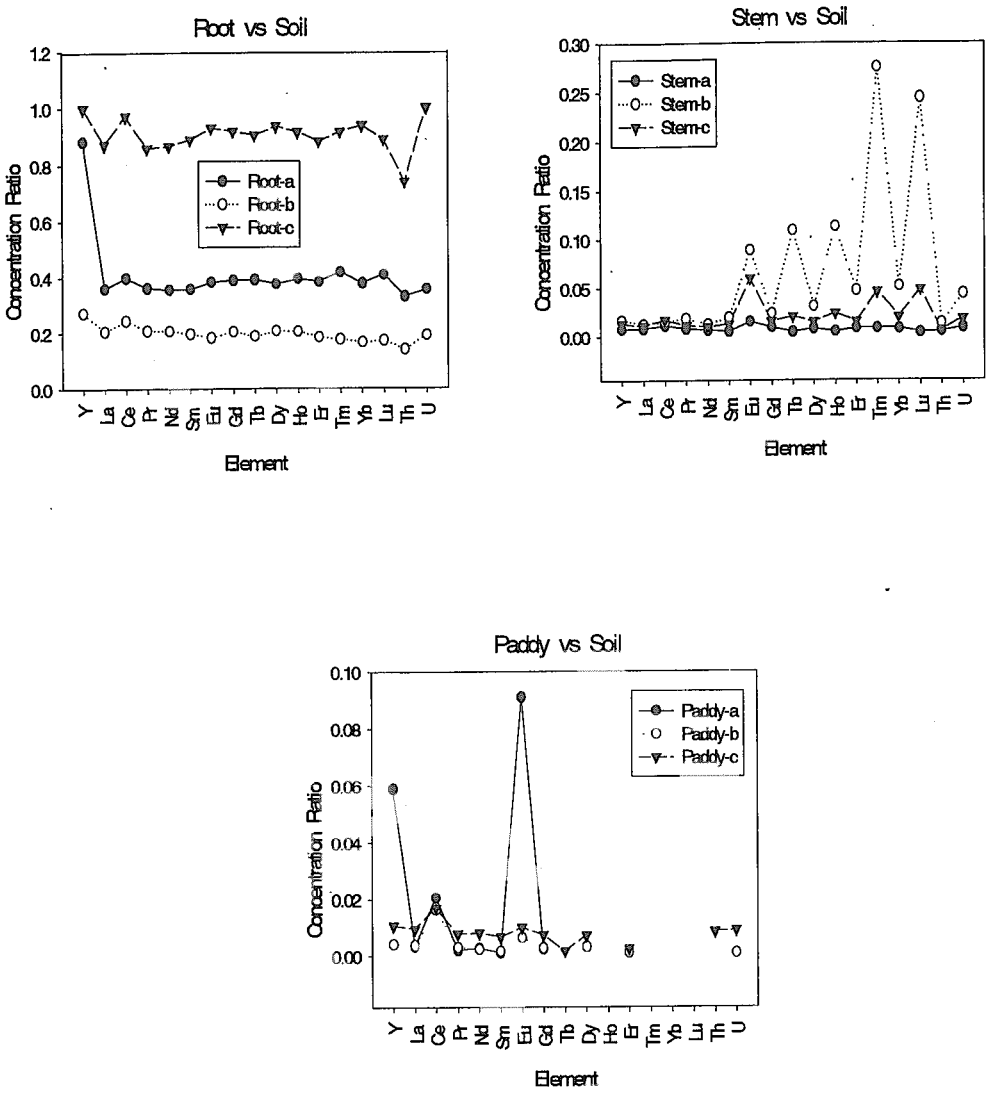

Fig. 5. Concentration ratio of rare earth elements in the part of rice based on soil from three regions.

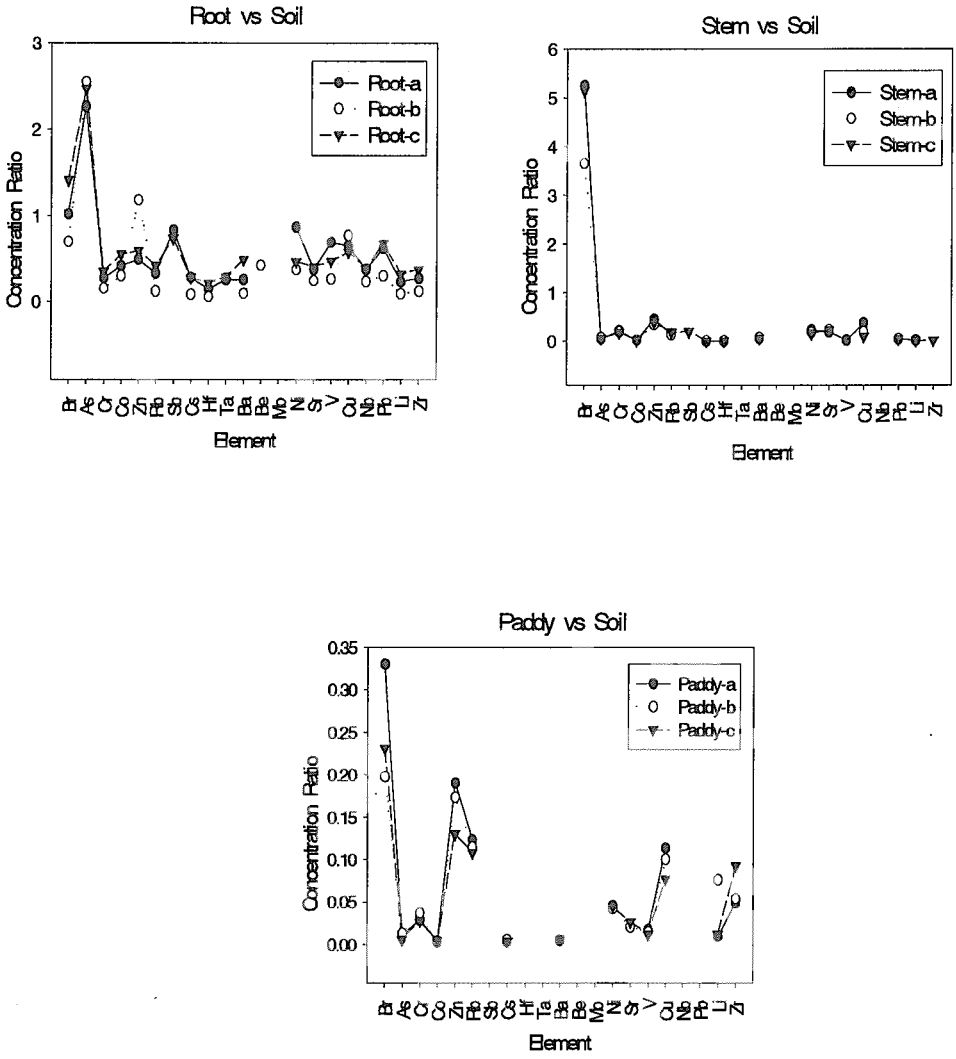

Fig. 6. Concentration ratio of trace elements in the part of rice based on soil from three regions.

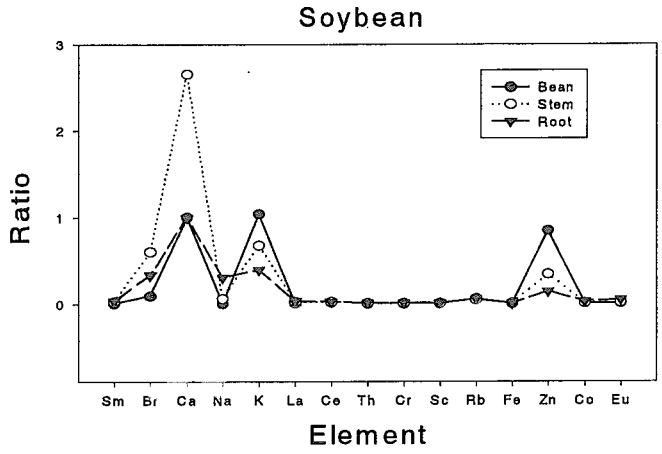

Fig. 7. Concentration ratio of trace elements in the part of soybean based on soil from three regions.

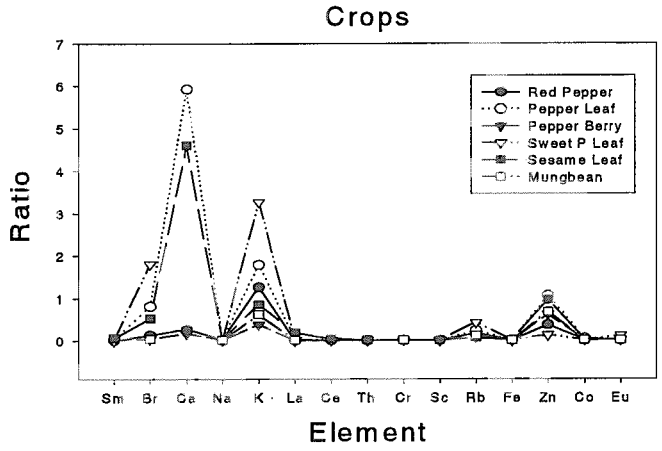

Fig. 8. Concentration ratio of trace elements in the part of crops based on soil from three regions.

Conclusion

In the present work we investigated sampling, preparing and analysis procedures of soil and several plants for NAA. Elemental concentrations in pine needle were compared with seasons and sites. Cleaning effect of surface on pine

needle were also investigated. Concentration ratios based on soil in each part of crops also investigated. Sampling and preparing procedures of the samples could be optimized for NAA. Therefore in conclusion this work confirms the validity of pine needle and rice as environmental biomonitor for pollution caused by various elements. And NAA could be applied to analysis the environmental geologic samples.

JP0250108

1.24 Application of NAA in High Purity Materials

Yoon-Yeol Yoon, Kil-Yong Lee

Korea Institute of Geoscience and Mineral Resources(KIGAM), 30 Kajung-dong, Yusung-gu, Daejon Korea 305-350

The analysis of trace impurities in high purity materials is important. Some impurities could change the property of the device. But these materials are extremely difficult to dissolve and could be contaminated by chemical pretreatment. Therefore, limiting the application of analytical methods that rely on the sample being in solution. NAA has been found to be extremely useful in the determination of trace impurities in high purity materials. Because this method possesses several important advantages such as freedom from blank, multi-elements determination and chemical contamination free. Using these characteristics, some high purity materials were analyzed by the radiochemical neutron activation analysis(RNAA). The impurities in some refractory metals such as Mo, W, Ta, Nb and Ti, Ni, were separated using ion exchange and solvent extraction method. The chemical yield was acquired by tracer analysis method and the analytical accuracy was confirmed by analyzing certified reference materials. And also, impurities distribution characters were investigated by analyzing semiconductor silicon wafers using instrumental neutron activation analysis(INAA).

Introduction

High purity refractory metals are attracting attention as they have useful properties such as corrosion resistance, good thermal conductivity, high melting point and superior gettering characteristics. In order to increase the usefulness as a base material for electronics, and for chemical and nuclear reactor equipment, impurities in high purity materials should be minimized. Neutron activation analysis is well known to be a excellent method for the analysis of trace impurities in high purity metals. On irradiation with reactor neutrons, high matrix activity makes difficult for the analysis of impurities in the sample. So, radiochemical separation procedure has to be applied.

In the analysis of refractory metal, separations on a strong anion exchange resin from a mixture of hydrofluoric acid and hydrochloric acid have become classical techniques. The behavior of elements in these systems has been studied in detail by several authors. The high distribution coefficient of tantalum and niobium in concentrated hydrofluoric acid enable their quantitative separation from a large number of elements which are of interest as relevant

impurities. And also, the impurities in tungsten and molybdenum are separated using anion and cation exchange resin. High purity nickel sample is separated using solvent extraction with 2-benzylpyridine(BPy). And impurities distribution characters are investigated by analyzing semiconductor silicon wafers using instrumental neutron activation analysis(INAA).

Experimental

Reagents and Instruments ; The reagents used for the radiochemical separation methods were GR grade reagents and ion exchanges were 200~400 mesh size anion(Dowex 1X8, cloride form) and cation(Dowex 50X8, hydrogen form). The ion exchange resins were classified by sedimentation and then conditioned by successive washing with the eluents. The prepared resins were poured into column tube to make a column length of 8 cm. Ion exchange column was pre-equilibriated by passing sufficient volume of eluent through the resin column at a flow rate of 2 *ml/min*.

For the detection of γ-rays emitted from radio-tracers, high purity germanium detector was used. The detector efficiency was 30% and energy resolution was 1.9 keV at 1332 keV. Measured γ-ray spectrum was amplified and stored at 4k channel multichannel analyzer. The peak identification and activity determination of each nuclides were done by the "Gamma Vision" EG&G Ortec software.

Tracer Experiments ; High purity Nb and Ta materials were dissolved with 10 *ml* mixture of concentrated hydrofluoric and nitric acid(9:1 volume ratio). The appropriate activities of each tracer were then added. The solution sample was dried by heating and redissolved in 5 *ml* of 2M hydrofluoric acid. The solution was passed through the anion exchange resin column and separated each tracers successively with appropriate eluents. This separation procedure was shown in Fig. 1. And also, analytical procedure of the trace impurities in high purity molybdenum and tungsten were shown in Fig. 2 and 3. The most important trace impurities, U and Th, were quantitatively separated with hydrochloric and hydrofluoric acid eluents. Another important chemical and electrical material, titanium was also analyzed by ion exchange method. This procedure was shown in Fig. 4. In this method, hydrobromic acid eluent was effectively separated trace impurities from the matrix.

Solvent extraction method applied for the analysis of high purity nickel samples was shown in Fig. 5. Nickel sample was dissolved in 0.1M hydrochloric acid and impurities were effectively separated from the matrix by 1M KSCN/1M BPy solvent.

Semiconductor silicon wafer was divided into three parts; central sample was taken from a site less than 1 cm from the center, middle one from a site 5~6 cm from the center and outer part from a site less than 1 cm from the edge. All the samples were treated by washing, etching

and rinsing procedures, sequentially. The distribution of impurities was investigated by analyzing above three kinds of samples.

Results and Discussion

As niobium and tantalum have similar chemical properties, the separation scheme in the present work has been developed based on tantalum separation, the main impurity, from niobium. For the separation of impurities of niobium and tantalum, four kinds of elueints were used. At first 2M hydrofluoric acid was eluated and 32M hydrofluoric acid was eluated. After then, the mixture of 0.5M hydrofluoric acid and 3M hydrochloric acid, the mixture of 1M ammonium fluoride and 4M ammonium chloride were passed through the anion exchange column successively. The recovery yield of each nuclide was shown in table 1. In this table, most impurities were quantitatively separated. Using this separation scheme, two kinds of 99.9% high purity tantalum samples were analyzed and the results were shown in table 2.

Molybdenum and tungsten produce high activity by neutron activation. So, radiochemical separation method was applied. The important alpha emitting trace impurities, uranium and thorium, and some other elements were quantitatively separated from matrix element using anion and cation exchange resin and the separation yields were represented in table 3 and 4.

Due to low specific weight, high corrosion resistance and melting point properties of titanium, it was widely used in various fields. Their property was affected by the presence of some trace impurities. When titanium was exposed to reactor neutron, it produce long-lived scandium radionuclides by (n,p) reaction. The scandium was effectively separated from trace impurity using cation exchange resin and 6.5M hydrobromic acid. The separation yield was shown in table 5. Using this procedure, two kinds of 99.99% high purity titanium was analyzed and the results were shown in table 6. Nickel is another important metal used in catalyst, magnet and electronic equipment. For the analysis of high purity nickel radiochemical neutron activation analysis using solvent extraction was applied. The separation of cobalt and other 27 elements was studied using tracers. The major interfering nuclide, cobalt, was extracted into organic phase in the form of $BPy_3Co(SCN)_2$ and other trace impurities are quantitatively separated into aqueous phase. The distribution coefficient of each element in two kinds of organic phase are represented in table 7 and analytical results of four kinds of high purity nickel samples are shown in table 8.

The distribution of impurities in semiconductor silicon wafer was investigated using INAA. Surface contaminated elements were studied by washing samples with deionized water, aceton, trichloroethylene and etching with the mixture of concentrated nitric and hydrofluoric acid. The analytical results of above experiment are shown in table 9.

By the radiochemical neutron activation analysis(RNAA), it has been found that RNAA is

the most powerful tool for the element analysis in various high purity metal samples. Trace impurities in high purity metal samples could be analyzed by RNAA and considerable improvement in the detection limit achieved.

Reference

1. J. Hoste, F. DeCorte, W. Maenhaut, "Application of Nuclear Activation Analysis: High Purity Materials", Treatise on Analytical Chemistry, I.M. Kolthoff, P. elving, V. Krivan ed., 2nd ed. Part I, Vol. 14, Wiley Intersciencs, New York, 1986, p.645.
2. R. Caletka, R. Hausbeck, V. Krivan, *J. Radioanal. Nucl. Chem.*, **120** (1988) 319.
3. R. Caletka, V. Krivan,, *Talanta*, **30** (1983) 465.
4. M. Ebihara, *J. Radioanal. Nucl. Chem.*, **111** (1987) 385.
5. S. Zuha, A. Rusheed, *J. Radioanal. Nucl. Chem.*, **133** (1989) 241.
6. K.S. Park, N.B. Kim, H.J. Woo, K.Y. Lee, Y.Y. Yoon, S.K. Chun, *J. Radioanal. Nucl. Chem.*, **168** (1993) 497.
7. K.S. Park, N.B. Kim, H.J. Woo, K.Y. Lee, Y.Y. Yoon, W. Hong, *J. Radioanal. Nucl. Chem.*, **179** (1994) 81.
8. K.S. Park, N.B. Kim, Y.S. Kim, K.Y. Lee, H.W. Choi, Y.Y. Yoon, *J. Radioanal. Nucl. Chem.*, **123** (1988) 585.
9. N.B. Kim, K.S. Park, H.J. Woo, K.Y. Lee, Y.Y. Yoon, D.K. Kim, *J. Radioanal. Nucl. Chem.*, **160** (1992) 539.
10. K.S. Park, N.B. Kim, K.Y. Lee, Y.Y. Yoon, S.K. Chun, J.H. Lee, *J. Radioanal. Nucl. Chem.*, **192** (1995) 155.
11. Y.Y. Yoon, K.Y. Lee, G.H. Lee, *J. Radioanal. Nucl. Chem.*, **210** (1996) 55.
12. K.S. Park, N.B. Kim, H.J. Woo, D.K. Kim, J.K. Kim, H.W. Choi, *J. Radioanal. Nucl. Chem.*, **151** (1991) 373.

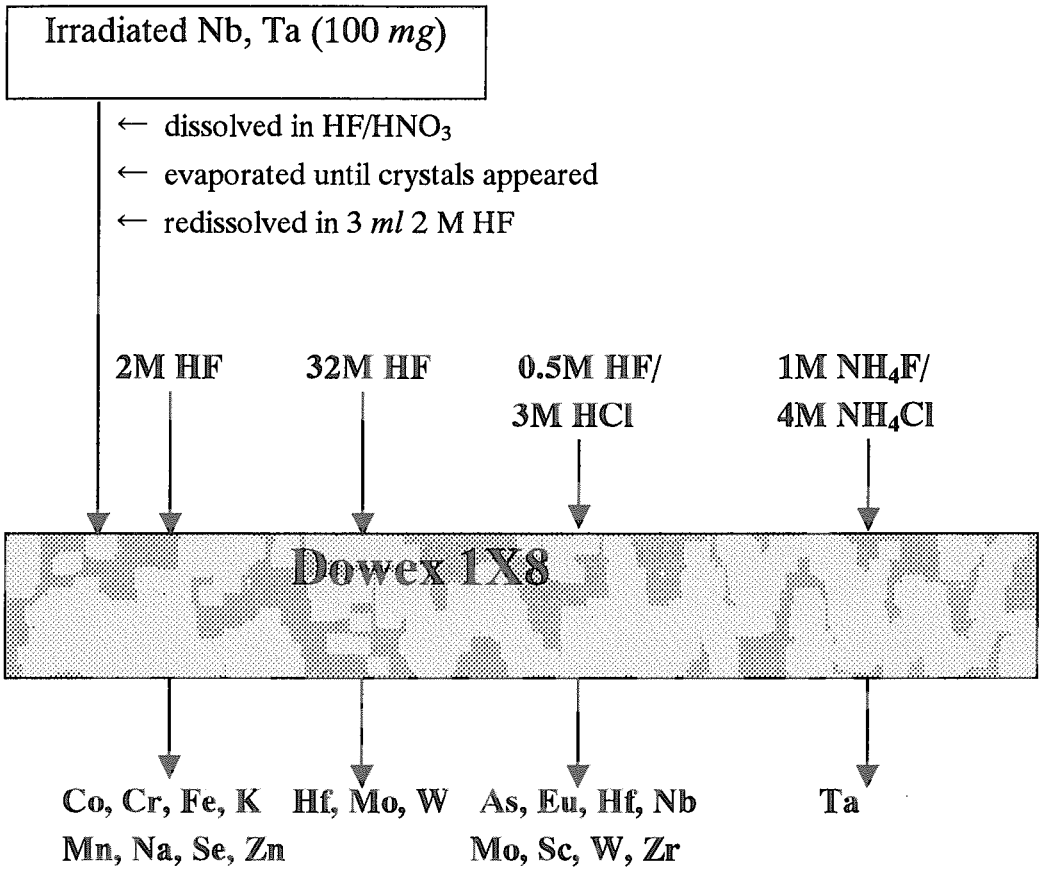

Fig. 1. Flow chart for the separation of impurities in niobium and tantalum.

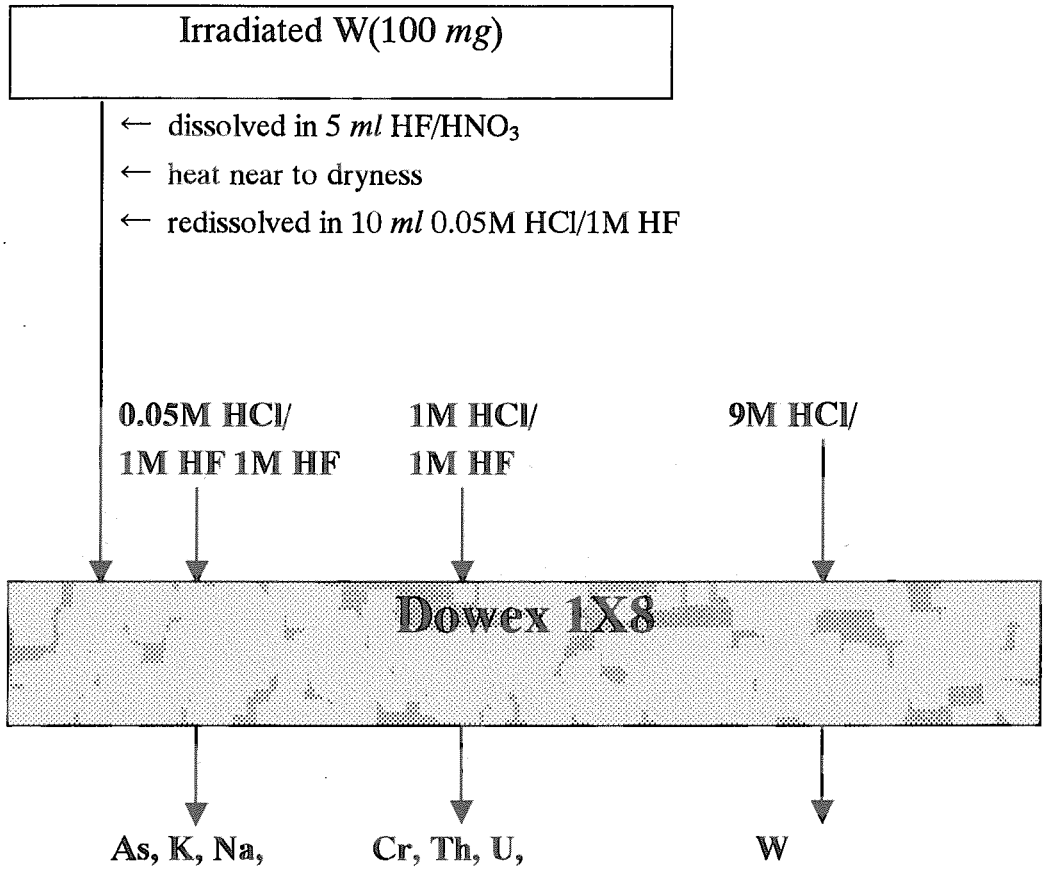

Fig. 2. Flow chart for the separation of impurities in tungsten.

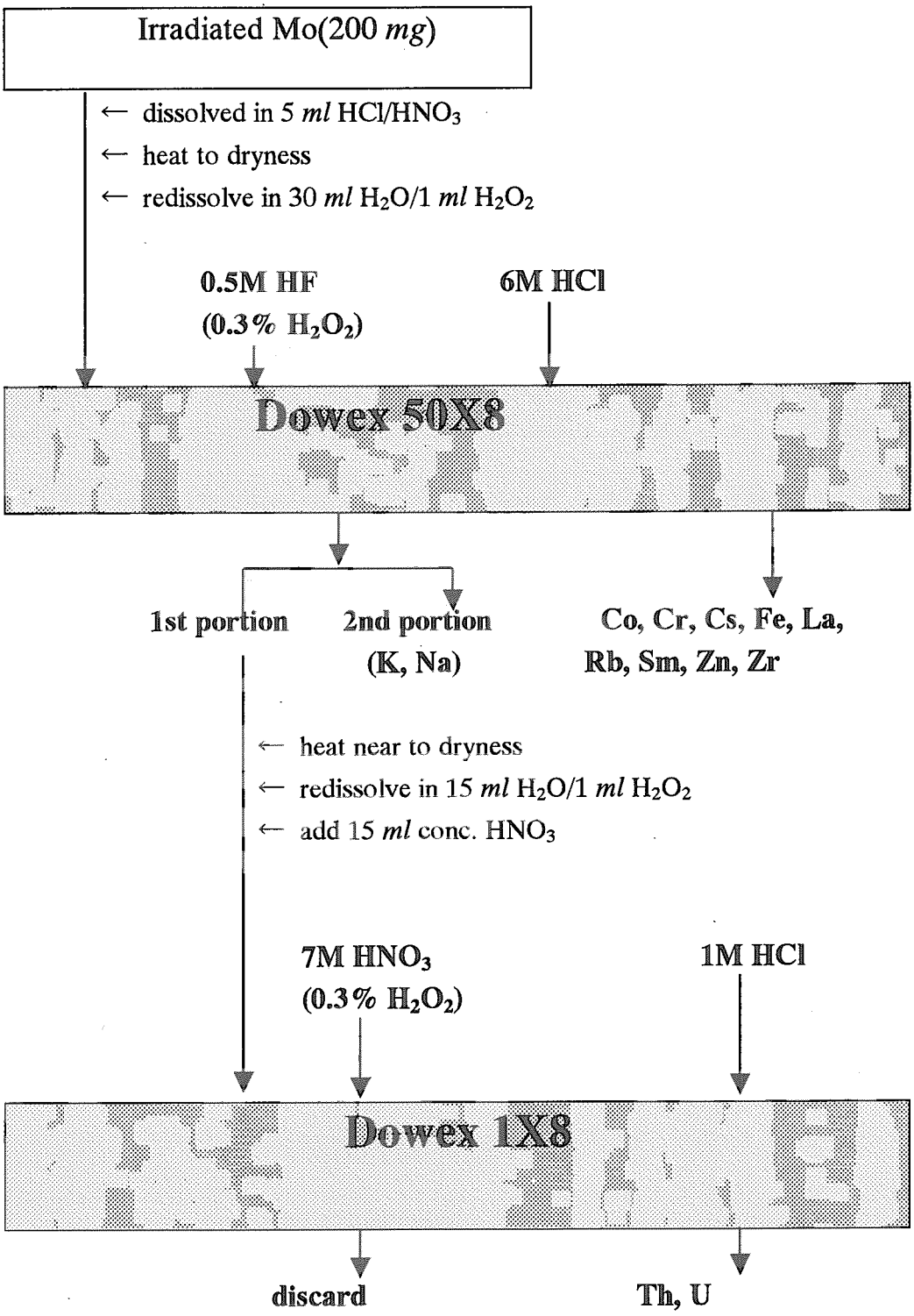

Fig. 3. Flow chart for the separation of impurities in molybdenum.

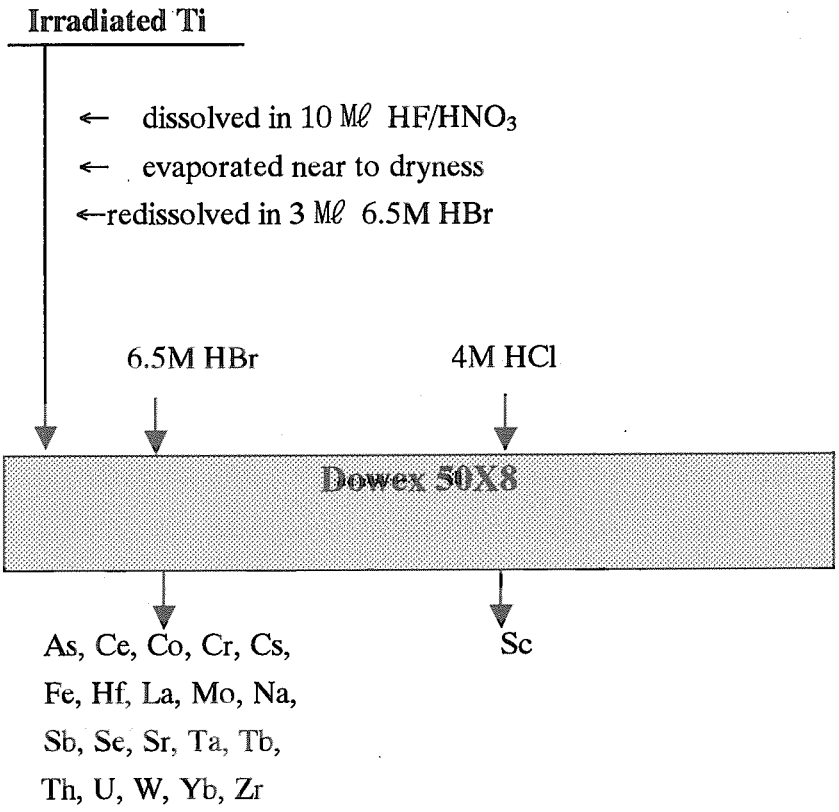

Fig. 4. Flow chart for the separation of impurities in titanium.

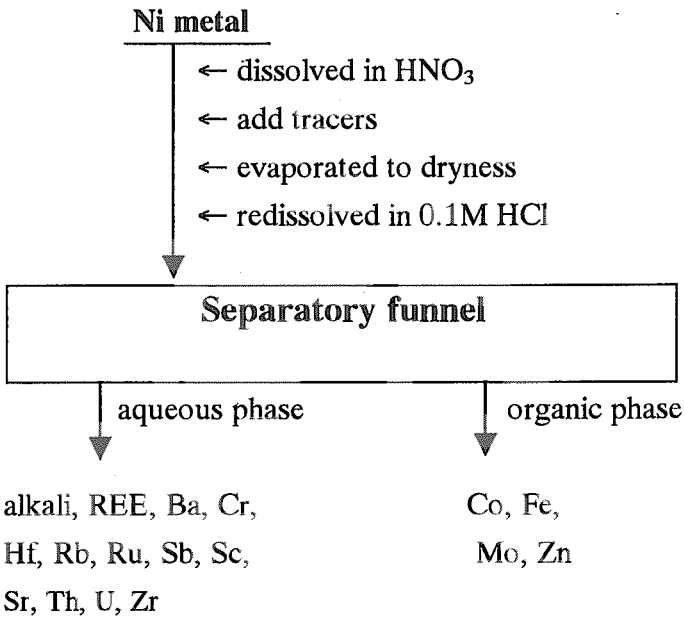

Fig. 5. Flow chart of radioactive tracer work for the separation of impurities from Co in case of using 1M-KSCN and 1M BPy.

Table 1. Separation yields of impurities from tracer work.(%)

nuclide	2M HF	32M HF	0.5M HF/ 3M HCl	1M NH_4F/ 4M NH_4Cl
Co-60	99.9			
Cr-51	98.1			
Fe-59	98.2			
K-42	99.7			
Mn-54	99.6			
Na-24	99.4			
Zn-65	100.4			
Mo-99	-	96.8		
W-187	-	98.1		
Hf-181	-	99.9		
As-76	-	-	99.3	
Eu-152	-	-	98.8	
Hf-181	-	-	100.0	
Mo-99	-	-	97.6	
Nb-94	-	-	100.0	
Sc-46	-	-	99.3	
W-187	-	-	99.4	
Zr-95	-	-	99.9	
Ta-182	-	-	-	99.7

Table 2. Analytical results of impurities in tantalum.(ppm)

element	sample 1	sample 2
As	0.0041±0.0010	0.011±0.003
Co	<0.003	0.027±0.001
Cr	1.9±0.3	14±1
Eu	<0.1	0.0040±0.0003
Fe	<3	16±1
Hf	0.38±0.03	0.0030±0.0005
K	1.9±0.3	16±1
Mn	0.080±0.003	0.65±0.02
Mo	110±8	1.4±0.2
Na	2.2±0.1	3.6±0.1
Sc	<0.002	<0.002
W	0.55±0.04	0.22±0.02
Zn	<0.2	<0.2
Zr	<2	<2

* sample 1 : Johnson & Matthey Co.(BN-625291, 99.95%)
sample 2 : Shoa Cabot Supermetals Co.(DCUH-8-1481LDX, 99.9%)

Table 3. Recovery yield of tungsten tracer work.

element	added(ug)	found(ug)	yield(%)
Na	22.2	21.7±1.2	97.3±5.3
K	96.1	94.2±2.9	98.0±3.0
As	10.2	10.0±0.2	98.0±2.0
U	15.5	14.8±0.9	95.5±5.8
Th	33.3	33.0±0.6	99.1±1.8
Cr	141.7	137.9±6.6	97.3±4.7

Table 4. Recovery yield of Mo tracer work.

element	added(ug)	found(ug)	yield(%)
U	21.1	20.7±1.0	98.1±4.7
Th	42.9	36.0±3.6	84.1±8.4
Co	3.8	3.77±0.03	99.2±0.8
Cr	120.4	117.4±6.5	97.8±5.4
Cs	27.0	26.6±0.8	98.5±3.0
Fe	203.8	191.7±11.4	94.1±5.6
K	123.7	122.9±1.2	99.4±1.0
La	1.15	1.16±0.03	100.9±2.6
Na	22.8	21.8±1.3	95.6±5.7
Rb	83.6	80.1±4.5	95.8±5.4
Sm	15.4	15.9±0.7	103.0±4.5
Zn	45.6	44.8±1.9	98.2±4.2
Zr	251.3	251.9±2.5	100.2±1.0

Table 5. Separation characteristics of elements by Ti tracer work.

(Recovery Yield, %)

Element	Cation Column		
	Resin	6.5M-HBr100 Mℓ)	4M-HCl(100 Mℓ)
Sc	-	-	100
Ba	-	100	-
Ce	-	99	1
Co	-	100	-
Hf	-	100	-
Nd	-	100	-
Pa	-	98	2
Sb	-	100	-
Se	-	98	2
Ta	-	100	-
Tb	-	100	-
Yb	-	99	1
Zr	-	100	-

Table 6. Analytical results of high purity titanium metals by NAA.

(unit : ppm)

Element	Johnson & Matthey		Supetter Target(Japan)		Maximum
	INAA	RNAA	INAA	RNAA	Limit
As	<0.04	0.026	<0.08	<0.04	
Co	<0.18	0.037	<0.06	<0.03	
Cr	3.6	4.8	1.8	2.0	2
Cs	<0.27	0.017	<0.13	<0.04	
Fe	150	150	<56	<30	2
Hf	<0.49	0.39	<0.08	<0.02	
Mo	<16	<2.9	<2.8	1.2	
Na	120	118	<0.2	<0.03	0.1
Sb	<0.2	0.15	<0.13	<0.06	
Se	<1.3	<0.69	<0.58	<0.22	
Ta	<0.18	0.16	<0.08	<0.02	
W	<0.1	0.27	<0.25	<0.01	
Zr	<5	3.6	<6.8	<3.4	
Ce	<0.9	<0.6	<0.36	<0.28	
Tb	<0.16	<0.06	<0.09	<0.03	
Yb	<0.19	<0.09	<0.09	0.04	
Th	<0.16	<0.08	<0.07	<0.03	0.001

Table 7. Distribution coefficient of some elements in 0.1M HCl/1M BPy

element	D(benzene)	D(benzene/acetone)
As	0.01	0.01
Ba	0.02	0.03
Ce	0.01	2.64
Co	43	90
Cr	0.09	0.01
Eu	0.01	0.01
Fe	14.3	140
Hf	<0.01	4.6
K	<0.01	<0.01
La	<0.01	<0.01
Lu	<0.01	<0.01
Mo	39	0.23
Na	<0.01	<0.01
Nd	0.02	0.03
Np(U)	0.02	0.02
Pa(Th)	0.13	0.05
Rb	0.02	0.02
Ru	0.18	10.6
Sb	0.06	0.03
Sc	0.01	0.05
Se	0.02	0.03
Sr	0.02	0.04
Ta	0.01	0.04
Tb	0.01	0.03
W	0.03	0.03
Yb	0.02	0.02
Zn	55.6	120
Zr	0.00	0.02

Table 8. Analytical result of high purity nickel(μg/g)

element	1	2	3	4	5
As	0.17±0.05	0.028±0.003	0.09±0.01	0.37±0.05	(0.4)
Ba	<25	<25	<25	<35	
Ce	0.4±0.1	0.049±0.004	0.08±0.01	0.15±0.04	
Cr	6±1	<0.4	0.75±0.08	3.2±0.6	(3)
Eu	0.6±0.1	0.57±0.03	1.1±0.8	1.50±0.06	
Hf	<0.04	<0.06	<0.05	<0.04	
K	0.25±0.09	0.5±0.1	<0.3	32±1	
La	0.021±0.006	0.016±0.004	0.012±0.002	0.030±0.005	
Lu	<0.005	<0.04	<0.006	<0.006	
Na	0.7±0.1	1.3±0.1	0.32±0.05	3.4±0.5	
Nd	<2	<3	<2	<3	
U	<0.1	<0.2	<0.2	<0.2	
Th	1.5±0.2	1.30±0.03	1.4±0.3	3.9±0.2	
Rb	<1	<2	<1	<3	
Ru	<0.2	<0.3	<0.2	<0.2	
Sb	3.3±0.5	0.6±0.2	0.6±0.1	0.4±0.1	(<0.5)
Sc	0.015±0.003	0.016±0.004	0.076±0.009	0.04±0.01	
Se	<0.1	0.11±0.01	0.4±0.1	0.21±0.03	0.2
Sr	<30	<30	<25	<25	
Ta	<0.1	<0.1	<0.1	<0.1	
Tb	0.58±0.06	4±2	3.5±0.8	2.6±0.4	
W	0.40±0.03	<0.06	<0.04	<0.06	
Yb	0.22±0.01	0.053±0.003	0.28±0.04	0.028±0.003	
Zr	21±8	<30	9±1	<30	

* 1. Japan High Purity Chemical Institute Inc.
2. Johnson & Matthey Co., nickel oxide
3. Johnson & Matthey Co., nickel foil
4. NIST SRM-673 nickel oxide
5. NIST value
() : recommended value

Table 9. Analytical results for semiconductor wafers.

(unit : ppt)

element	central region		middle region		outer region	
	washing	etching	washing	etching	washing	etching
p-type wafer						
Au	0.40	0.12	0.48	0.11	0.44	0.11
Br	150	41	1400	33	960	31
As	71	8.9	120	11	68	12
W	150	14	370	14	480	14
Co	87	65	51	48	86	57
Cr	760	160	830	160	1200	120
Eu	120	52	70	50	140	37
La	970	180	150	110	170	110
Sc	27	2.5	8.3	2.3	6.2	2.7
Zn	1500	270	2000	260	1800	280
U	350	160	270	160	290	200
Th	75	9.7	88	12	120	9.9
Hf	43	8.9	36	11	89	8.0
Sb	190	63	96	58	70	53
Fe(ppb)	59	12	130	13	280	16
n-type wafer						
Sb(ppm)		180		170		160

JP0250109

1.25 The Study of Trace Element Distribution in Biological Samples with NAA for Human Health

Seung Yeon Cho, Sang Hun Kang, and Yong Sam Chung*

Dept. of Environmental Engineering, Yonsei University
**Korea Atomic Energy Research Institute*

A one day representative mixed diet of an adult Korean was collected from the data based on the food intake of 108 healthy subjects between the ages 20 and 50. Sampling for the Korean total diet was carried out by the way of using a market basket study based on the Korean standard food consumption scheme reported by the Korean Nutrition Society. Average consumption frequency of different food items for a one day representative mixed diet of an adult Korean and the amount of each item to prepare a one day Korean representative total diet are surveyed. The analytical methods involve both instrumental and radiochemical neutron activation techniques developed for the determination of the elements Cs, I, Sr, Th and U in various kinds of food samples. Concentrations of trace elements including 5 important elements for radiological protection, U, Th, Cs, Sr and I in the Korean total diet and the 4 most frequently consumed Korean foodstuffs have been analyzed by neutron activation analysis. Detection limits for U, Th, Sr and I were improved to ppb levels by radiochemical separation after neutron irradiation. Five biological NIST reference materials were also analyzed for quality control of the analysis. Seventeen trace elements in the Korean total diet and four Korean representative foodstuffs were also analyzed quantitatively by instrumental neutron activation analysis.

The elemental distributions in supplemental healthy food and Korean and Chinese origin oriental medicine were also identified. The amount of trace elements ingested with the hair analysis of oriental medicine takers were estimated. The amounts of trace elements inhaled with the analysis of foundry air, blood and hair of foundry workers were also estimated. The basic estimation method in view of health and environment with the neutron activation analysis of biological samples such as foods and hair was established with the result.

Nationwide usage system of the NAA facility in Hanaro in many different and important areas of biological area can be initiated with the results. The output of the project can support public health, environment, and medical research area. The results

can be applied for the process of micronutrients enhanced health food production and for the health safety and health status enhancement with the additional necessary data expansion and the development of various evaluation technique.

Introduction

The advances in trace element analytical techniques have led to the re-examination of much of the published data for trace elements in foods and body fluids[1-3]. Determination of trace mineral intake is important not only for assessing nutritional status but also for estimating the metabolic parameters of uptake and deposition of radionuclides such as ^{137}Cs, ^{131}I, ^{90}Sr, ^{232}Th and ^{238}U in the human body. To control the radiation hazard, it is important to have reliable data on food types in which these radionuclides tend to accumulate, once they are released in the environment. A proper control can be exercised on the distribution of various food types in case of a nuclear emergency with established reliable data. It is also important to have accurate knowledge of the biokinetic behaviour of the above radionuclides in humans for realistic assessment of radiation dose[4].

Studies on intakes for different age groups are scarce in the literature. This paper describes the daily intake of 22 elements for Korean adults. Quantitative data were collected by performing instrumental and radiochemical neutron activation analysis(INAA & RNAA) following collecting of a Korean representative total diet.

Experimental

Sample Collection

Sampling for the Korean total diet was carried out by using a market basket study based on the Korean standard food consumption scheme reported by the Korean Nutrition Society[5]. Average consumption frequency of different food items for a one day representative total diet of

an adult Korean which obtained from a food intake by study group for a week was used and the amount of each ready-to-eat food item was mixed to prepare a one day Korean total diet.

Sample Preparation

Immediately after the completion of the initial blending of the prepared one day Korean representative total diet in a blender with titanium blades, an analytical sub-sample representing about 20% of the total diet was withdrawn using a large plastic spoon and placed in a container for freeze-drying. Samples were initially frozen at -80℃ for 3 hours and freeze-dried for 30 hours at the same temperature. The four most popular Korean representative foodstuffs were also collected and freeze-dried. Their weight loss after freeze-drying is listed in Table 1. Samples of meat and fish cannot be dried fully because of their large oil content. Solvent (chloroform:methanol, 2:1 V/V) was added to the samples containing a large amounts of oil component with the ratio of 1:3 and shaken well. Oils in upper level were discarded and the remaining solution was stored for a day and freeze-dried. Freeze-dried samples were ground well to get sample homogeneous for the analysis. Samples were stored in polyethylene vials at 2 - 4 ℃ for short term storage and in a Teflon™ vial at below -15℃ for long term storage to avoid absorption or evaporation which may cause a change of elemental concentrations.

Table 1. Weight loss after freeze-drying of the Korean total diet and Korean representative foodstuffs

	Habitat	Wet Diet	Freeze-drying
Total Diet	Korea	1120.0 g	130.2 g
Boiled Rice	Kanghwa	268.1 g	76.8 g
Kimch'i	Chungju	315.0 g	27.4 g
Mackerel	East Sea	309.2 g	142.2 g
Beef & Pork	Wonju	338.4 g	138.3 g

Neutron Activation Analysis

Samples were irradiated with thermal neutrons from the HANARO research reactor (20 MW) at the Korea Atomic Energy Research Institute. The Pneumatic Transfer System (PTS) was used for sample irradiation. Samples were irradiated at the same geometrical position to minimize the geometry error. For neutron flux monitoring, activation wire (Reactor Exp. Inc., R/X activation wire, 99.99% purity) such as Au, Cu, and Mn were used to monitor the thermal neutron flux (Φ_t = 1.7×10^{13} $cm^{-2} \cdot s^{-1}$). Samples were allowed to decay for an appropriate time to ensure satisfactory detection limits. Radiochemical separation processes were needed to quantify the ultra-trace elemental concentrations of Th, U, Cs and I in Korean total diet.

Radioactivity Measurement

Gamma-ray spectra and activity for the irradiated samples were obtained with the following equipment. The crystal of the high purity germanium semi-conductor detector (EG&G ORTEC, GMX-25190P) was surrounded with a 10 cm thick lead shielding box (75x90x90 cm) with its inner wall lined with 0.1 cm Cd and Cu plate to reduce the influence of the external radiation. Gamma-ray interactions with surrounding material were also considered. The detector is a coaxial type with 25% relative efficiency and 1.9 keV resolution (FWHM) at 1332 keV (^{60}Co) and a peak to Compton ratio of 45:1. The detector was connected to a personal computer and a 8K-multichannel analyzer (EG&G ORTEC, 919A MCB, Maestro-II) to complete the γ-ray spectrometer for activity measurement and data analysis. Energy and efficiency calibrations were done with the radioactive multinuclide reference source (NEN Products Inc., NES-602, 1″ diameter disc type) certified by NIST. The dead time of detector was maintained under 5% as much as possible. Decay and pile up correction were done automatically.

Data Treatment

Concentrations of elements were calculated with a new graphical programme, POWER NAA, coded with LabView version 5.0 for rapid and simple data treatment after obtaining the γ-ray spectrum under the preset analytical condition. The program is run with the counting condition, automatic identification of nuclides and their γ-ray energies, decay time correction for short half-life nuclides in order to calculate activities, elemental concentrations, counting errors and detection limits. Elemental concentration was calculated from peak area which is measured by γ-ray activity along with the related nuclear data[6,7].

Results and Discussion

Five biological reference materials such as NIST SRM 1548(total diet), NIST SRM 1567a(wheat flour), NIST SRM 1547(peach leaves), NIST SRM 1566a(oyster tissue) and NIST SRM 1577b(bovine liver) were analyzed mainly by instrumental neutron activation analysis for quality control (Table 2-6). The elemental concentrations, relative standard deviations, and relative errors to certified values were calculated. After the repetitive analysis($\geq$5 times), the relative standard deviations were within 10% except for Fe(12.4%) in SRM 1548, Rb(11.7%) and V(23.9%) in 1567a, Ce(14.4%) and La(15.7%) in 1547 and V(12.9%), Rb(15.8%) and Sc(10.8%) in 1566a. The relative errors to certified values are within 5% except for K(7.2%) and Zn(10.9%) in 1548, Mn(10.2%) and Rb(7.9%) in 1567a, Cl(13.2%), Fe(9.3%) and Rb(5.8%) in 1547, Cd(5.4%), Cl(7.6%), Co(5.7%), Cr(6.6%), Cu(7.2%), K(10.2%) and Zn(23.1%) in 1566a and Cu(8.7%), K(7.1%), Rb(8.6%) and Zn(9.4%) in 1577b. Analytical results of elemental distribution in Korean total diet and four Korean representative foodstuffs are listed in Table 7-11.

Table 2. Analytical Result of Total Diet, NIST SRM 1548 by NAA

(unit : ppm)

Element	Certified Value(S.D.%)	This Work		Relative Error(%)
		Range	Mean(S.D.%)	
Ca	1740 (4)	1676~1765	1735 (0.08)	0.31
Cl	8700 (5)	8210~8883	8460 (5.63)	2.76
Fe	32.6 (11)	30.4~36.4	34.2 (12.4)	4.83
K	6060 (5)	5049~5958	5621 (1.28)	7.24
Mg	556 (5)	521~568	551 (5.98)	0.95
Mn	5.2 (8)	5.00~5.39	5.25 (0.4)	0.94
Na	6250 (4)	6352~6605	6460 (2)	3.36
Se	0.245 (2)	0.24~0.27	0.26 (4.9)	4.79
Zn	30.8 (4)	32.5~36.3	34.2 (7.89)	10.9
Al	[33]	32.6~37.7	34.4 (10.4)	
Cs	[0.014]	0.0141~0.0149	0.014 (5.5)	
Rb	[4.8]	4.78~5.01	4.92 (3.32)	
Sn	[3.6]	3.10~3.49	3.29 (8.31)	

[ ] : reference value

Table 3. Analytical Result of Wheat Flour, NIST SRM 1567a by NAA

(unit : ppm)

Element	Certified Value(S.D.%)	This Work		Relative Error(%)
		Range	Mean(S.D.%)	
Al	5.7 (22)	5.25~5.99	5.72 (8.09)	0.3
Ca	191 (2)	178~200	188 (5.04)	1.47
Cu	2.1 (10)	2.01~2.27	2.14 (8.40)	1.86
Fe	14.1 (4)	12.9~15.1	14.3 (0.69)	1.7
K	1330 (2)	1239~1303	1271 (3.56)	4.46
Mg	400 (2)	401~414	405 (2.15)	1.3
Mn	9.4 (5)	8.42~8.48	8.45 (0.18)	10.2
Na	6.1 (13)	6.13~6.36	6.25 (1.35)	2.42
Rb	0.68 (4)	0.66~0.78	0.73 (11.7)	7.92
Se	1.1 (18)	1.10~1.19	1.15 (3.26)	4.39
Zn	11.6 (3)	12.0~12.2	12.2 (1.11)	4.71
Cl	[565]	528~547	535 (0.08)	
Co	[0.006]	0.0058~0.0062	0.006 (4.69)	
V	[0.011]	0.0138~0.018	0.0154 (23.9)	

Table 4. Analytical Result of Peach Leaves, NIST SRM 1547 by NAA

(unit : ppm)

Element	Certified Value(S.D.%)	This Work		Relative Error(%)
		Range	Mean(S.D.%)	
Al	249 (3)	242～253	249 (2.61)	0.05
Ba	124 (3)	124～129	126 (2.63)	1.8
Ca	15600 (1)	14720～15210	14950 (0.95)	4.17
Cl	360 (5)	306～322	312 (1.02)	13.2
Fe	218 (6)	234～242	238 (2.35)	9.25
K	24300 (1)	23090～23190	23137 (0.12)	4.79
Mg	4320 (2)	4150～4450	4307 (2.79)	0.31
Mn	98 (3)	93.7～96.7	95.1 (2.23)	2.95
Na	24 (8)	22.4～23.4	22.8 (2.98)	5.15
Rb	19.7 (0)	18.9～22.1	20.9 (8.89)	5.84
Sr	53 (8)	47.3～54.2	51.7 (9.38)	2.44
V	0.37 (8)	0.34～0.38	0.37 (6.06)	0.97
Zn	17.9 (2)	16.8～18.7	17.7 (2.64)	1.21
Br	[11]	10.5～12.0	11.4 (2.37)	
Ce	[10]	9.19～11.7	10.8 (14.4)	
Co	[0.07]	0.071～0.076	0.074 (3.92)	
Cr	[1]	1.16～1.20	1.18 (1.14)	
La	[9]	9.44～12.0	11.1 (15.7)	
Nd	[7]	6.84～7.69	7.22 (5.29)	
Sc	[0.04]	0.045～0.054	0.050 (6.85)	
Sm	[1]	1.14～1.22	1.19 (3.87)	
Tb	[0.1]	0.10～0.11	0.11 (3.98)	
Th	[0.05]	0.049～0.0548	0.051 (0.42)	

Table 5. Analytical Result of Oyster Tissue, NIST SRM 1566a by NAA

(unit : ppm)

Element	Certified Value(S.D.%)	This Work		Relative Error(%)
		Range	Mean(S.D.%)	
Ag	1.68 (9)	1.55～1.78	1.66 (4.51)	1.07
Al	202.5 (6)	193～213	204 (2.42)	0.84
As	14 (9)	13.7～15.2	14.4 (3.63)	3.05
Ca	1960 (10)	1857～1983	1936 (4.6)	1.22
Cd	4.15 (9)	4.36～4.39	4.37 (0.58)	5.4
Cl	8290 (9)	7501～7932	7656 (3.66)	7.64
Co	0.57 (19)	0.60～0.61	0.60 (1.8)	5.7
Cr	1.43 (32)	1.47～1.57	1.52 (4.92)	6.6
Cu	66.3 (6)	60.7～62.4	61.5 (1.93)	7.2
Fe	539 (6)	529～570	552 (3.5)	2.39
K	7900 (6)	6720～7726	8.45 (0.18)	10.2
Mg	1180 (14)	1139～1204	1165 (0.85)	1.24
Mn	12.3 (12)	11.8～12.3	12.0 (2.77)	2.28
Na	4170 (3)	4047～4271	4185 (3.19)	0.35
Se	2.21 (11)	2.20～2.48	2.30 (8.12)	4.01
V	4.68 (3)	4.13～4.97	4.57 (12.9)	2.26
Zn	830 (7)	1004～1034	1022 (2.08)	23.1
Au	[0.01]	0.013～0.017	0.015 (6.27)	
La	[0.3]	0.29～0.30	0.30 (0.91)	
Rb	[3]	2.76～3.46	3.11 (15.8)	
Sc	[0.06]	0.059～0.069	0.066 (10.8)	
Sm	[0.06]	0.058～0.061	0.059 (1.32)	

Table 6. Analytical Result of Bovine Liver, NIST SRM 1577b by NAA

(unit : ppm)

Element	Certified Value(S.D.%)	This Work		Relative Error(%)
		Range	Mean(S.D.%)	
Ca	116 (3)	113	113	2.5
Cl	2780 (2)	2633～2685	2657 (0.85)	4.42
Cu	160 (5)	173～175	174 (0.73)	8.73
Fe	184 (8)	179～197	188 (2.97)	2.21
K	9940 (0)	9060～9572	9238 (3.92)	7.07
Mg	601 (5)	594～658	620 (1.5)	3.12
Mn	10.5 (16)	9.82～10.4	10.1 (2.89)	3.41
Na	2420 (2)	2299～2391	2345 (1.42)	3.11
Rb	13.7 (8)	13.8～16.4	14.9 (9.13)	8.59
S	7850 (1)	8013～8235	8124 (1.93)	3.49
Se	0.73 (8)	0.66～0.76	0.72 (2.33)	1.5
Zn	127 (13)	130～146	139 (7.84)	9.37
Co	[0.25]	0.26～0.27	0.26 (0.81)	
V	[0.123]	0.108～0.115	0.110 (6.81)	

Table 7. Analytical Result of Korean Total Diet by NAA

Element	Range	Mean Value	Standard Deviation
<ppm>			
Al	16.1~18.3	17.6	1.28
Br	9.59~10.6	9.95	0.58
Ca	1358~1496	1418	70.9
Cl	10870~11780	11353	458
Fe	23.7~26.0	25.2	1.32
I	1.59~2.01	1.81	0.30
K	5394~5706	5579	134
Mg	807~896	850	44.4
Mn	8.46~8.78	8.65	0.16
Na	10080~10470	10298	162
Rb	5.43~5.49	5.46	0.03
Sr	5.3~5.80	5.55	0.36
Zn	31.6~33.7	32.5	1.13
ppb			
As	493~603	526	51.8
Co	29.6~31.6	30.8	1.06
Cr	348~420	393	39.4
Cs	10.6~11.6	11.1	0.71
Sc	3.2~3.6	3.43	0.21
Se	223~328	276	74.5
Sm	46.1~47.5	46.8	0.99
Th	2.38~2.82	2.6	0.3
U	31.5~38.6	35	5.0

Table 8. Analytical Result of Korean Boiled Rice by NAA

Element	Range	Mean Value	Standard Deviation
<ppm>			
Al	0.87～1.19	1.03	0.23
Ca	83.3～87.2	85.2	2.77
Cl	298～331	316	16.6
Fe	2.22～2.34	2.28	0.085
K	757～786	775	12.3
Mg	65.9～68.9	67.1	1.61
Mn	3.23～3.36	3.27	0.07
Na	109～112	110	1.25
Zn	16～17.3	16.6	0.69
< ppb level >			
As	103～142	130	18.1
Au	0.17～0.23	0.2	0.04
Br	645～742	679	43.9
Co	4.64～5.5	5.01	0.44
I	77～120	100	30
Mo	268～384	326	82.0
Rb	452～510	486	24.2
Sc	1.8～2.46	2.17	0.34
Sr	77～91	840	10
Th	0.1～0.12	0.11	0.02
U	2.7～4.2	3.5	1.0

Table 9. Analytical Result of Korean Kimch'i by NAA

Element	Range	Mean Value	Standard Deviation
<ppm>			
Br	182~210	197	11.6
Ca	4022~4480	4284	236
Cl	115900~120500	118433	2335
Cr	1.10~1.44	1.30	0.16
Fe	49.2~54.8	51.4	2.97
K	27320~30770	29535	1604
Mn	26.6~30.6	29.1	2.22
Na	97790~104500	99843	3167
Rb	22.8~28.0	26.1	2.47
Sr	22.3~25.2	23.8	2.06
Zn	42.5~46.5	44.7	1.70
<ppb>			
Co	346~392	365	23.1
Cs	69.5~71.8	70.9	12.4
Sc	30~33.8	31.6	1.75
Th	4.1~5.75	4.9	1.2

Table 10. Analytical Result of Mackerel by NAA

Element	Range	Mean Value	Standard Deviation
<ppm>			
Al	12.6～15.8	13.8	1.77
As	6.28～6.92	6.50	0.37
Br	16.3～18.5	17.3	1.01
Ca	3448～3973	3675	2706
Cl	22980～24170	23747	665
Cr	0.88～1.37	1.14	0.21
Fe	45.3～49.4	47.6	1.75
K	11250～11790	11510	223
Mg	649～694	675	23.4
Na	2183～2289	2230	53.3
Rb	1.06～1.39	1.17	0.15
Se	2.91～3.10	2.99	0.10
Sr	6.4～7.54	7.0	0.8
Zn	35.7～39.8	37.3	1.89
<ppb>			
Au	1.2～1.7	1.45	0.35
Co	587～638	614	27.1
Cs	53.6～66.2	61.1	5.47
Sc	3.2～3.8	3.5	0.42
Th	0.85～1.07	0.96	0.15

Table 11. Analytical Result of Korean Mixed Pork and Beef by NAA

Element	Range	Mean Value	Standard Deviation
<ppm>			
Al	17.6~21.4	19.5	2.68
Br	13.3~13.9	13.5	0.24
Cd	1.55~1.58	1.56	0.02
Cl	26020~26840	26343	437
Fe	39.8~46	43.4	2.81
K	11500~11930	11625	205
Mg	603~674	635	36.1
Na	2110~2205	2162	41.1
Rb	18.6~21.6	20.8	1.45
Zn	119~131	124	5.83
<ppb>			
As	72.5~107	85	15.7
Co	13.6~17.3	15.4	1.74
Cr	337~683	515	143
Cs	34.6~46.2	40.2	5.62
Hg	33.8~36.9	35.4	2.19
I	150~250	200	70
Se	449~606	527	79.1
Sm	7.2~7.3	7.25	0.07
Sr	640~870	760	150
Th	0.44~0.53	0.48	0.05

Analytical results can be classified into four groups such as essential minor elements(group 1 : Ca, K, Mg, Na), essential trace elements(group 2 : Fe, Mn, Se, Zn), toxic trace elements(group 3 : Al, As, Cd, Cr, Hg) and trace elements which are important for radiological protection(group 4 : Cs, I, Sr, Th, U). Elemental distribution of group 1 was in a range from a few hundred to several ten thousand ppm. The concentration of Ca in Kimch'i was the highest among Korean staple foodstuffs. Elemental distribution in group 2 was below several tens ppm. Elemental

distribution of group 3 was below a few ppm except for Al. Arsenic concentration in mackerel was ten times higher than that of the Korean total diet. These results suggest that a specific enriched element in food because of environment can be accumulated in the body system by an individual's eating habit. Elemental distribution in group 4 of the Korean total diet was in the order of U< Cs < Th < I< Sr. High U concentration in the Korean total diet was probably from groundwater used to prepare the Korean total diet. To identify the amount of U contribution from water many different Korean total diet samples must be prepared for analysis with various sources of water such as tap, surface, bottled and ground water. Iodine concentration in the wet Korean total diet can be 235 μg/day which is greater than WHO's adult recommended value, 150 μg/day. This shows Korean's eating habit of large consumption of seaweeds and fishes.

The NAA results obtained from the various samples such as total diet, oriental medicine, indoor air and human hairs are summarized in Table 12. We can say that trace elements introduced to human body through inhalation and ingestion reflect elemental distribution in human hair.

Table 12. Elemental Concentrations in Different Biological Materials and Air to See Elemental Deposition in Hair

Element	Ingestion [ppm]		Inhalation [ng/㎥]		Hair [ppm]		
	Total Diet	Tonic	Ambient Air	Foundry Air	Common Person	Foundry Worker	Tonic Taker
Al	17.6	307	2305	-	25.9	14.6	20.7
As	0.526	0.159	9.09	163	0.234	0.107	0.232
Br	9.95	8.29	8.02	133	1.21	1.76	29.7
Ca	1418	5012	407	-	909	1097	2190
Cl	11353	759	577	-	142	598	597
Cr	0.393	1.09	5.73	1510	-	1.01	-
Cu	-	15.6	40.2	-	14.6	-	32.8
I	1.64	-	4.13	-	0.724	1.50	1.63
K	5579	5570	346	-	16.7	-	-
Mg	850	1399	-	-	114	175	396
Mn	8.65	162	13.9	-	1.19	1.20	2.13
Sb	-	0.031	5.59	40	0.328	0.08	-
Sc	0.003	0.048	0.054	74	-	0.06	-
Sr	5.55	21.9	-	6680	4.94	-	22.0
Th	0.0026	0.133	0.086	121	-	-	-
U	0.035	-	0.694	-	-	-	-
Zn	32.5	52.3	91.3	26800	410	241	205

Conclusions

Concentrations of trace elements including 5 important elements for radiological protection such as U, Th, Cs, Sr and I in the Korean total diet and four Korean representative foodstuffs have been analyzed by neutron activation analysis and their results were listed in Table 2-6. RNAA was used for Th, U, Sr and I determination because of their low concentration(-ppb) in food and detection limits for U, Th, Sr and I were improved by radiochemical separation after neutron irradiation.

References

1. Report of a Joint WHO/IAEA Collaborative Study, Geneva, World Health Organization, 1989.
2. Trace elements in human nutrition and health, Geneva, World Health Organization, 1996
3. G. V. Iyengar, Radiat. Phys. Chem., 51 (1998) 545.
4. ICRP, Report of the Task Group on Reference Man, ICRP publication 23, Pergamon Press, Oxford, 1975
5. Recommended Dietary Allowances for Koreans, 6th Revision, the Korean Nutrition Society, 1996
6. G. Erdtmann, Neutron Activation Tables, Vol. 6, New York, 1976
7. Handbook on Nuclear Activation Analysis Data, IAEA Tech. Rept. No. 273, 1987

This is a blank page.

1.Workshop

Abstract & Papers

Research Reactor Utilization
(BNCT)

This is a blank page.

JP0250110

1.26 Current Status of Operation and Utilization with Several Research Reactors in China

Xu Hanming
China Institute of Atomic Energy
102413 Beijing 275(33) ,PRC
xuhanming@iris.ciae.ac.cn

A general overview of operation and utilization in this year with several research reactors in China are given. The involved reactors are HWRR, SPR, HFETR and MJTR. As a result of great efforts on the upgrading of safety system and renewal of old equipment, a good availability of reactor operation has been achieved compared to that in previous years. The research and production work have been accomplished on schedule.

Utilization on these four reactors including PWR fuel element and material testing, radioisotope production, silicon doping, neutron activation analysis, etc. Some work on neutron scattering are also briefed.

1. Introduction

Facing sustained requirements from unclear technology and nuclear power development, the aged reactors in China are still asked to continue their service on a safe operation basis before the new research reactor CARR is constructed. The basic strategy to accomplish the above purpose is to renew essential equipment and to strengthen aging management. Efforts on this aspect look effective as the practical situation in the recent years has shown. In this paper, status of operation and utilization is described for four research reactors, named HWRR, SPR, HFETR and MJTR.

2. General Situation of the Reactor Operation

As mentioned above, all the four research reactors were designed and

constructed in the old years when the safety requirements and regulations were not completely and well established. In addition, aging problems further worsen safety and availability of these reactors. Based on these facts, under the organizing and audit of National Nuclear Safety Administration (NNSA), a retroactive safety review was performed for each of those reactors. As a result of this activity, a series of equipment renewal and upgrading items were established in order to make the safety level of those old reactors close to or approaching modern requirements. After implementation of the equipment renewal and upgrading, which took more or less than one year for each reactor, the safety level and availability have been significantly improved. For example, the operation duration, which is affected both by the tasks of the reactor utilization and by the reliability of the components and systems, is increased in 2000 by 10 to 20 percent compared to that of past years. The number of unexpected reactor scram has also been significantly decreased.

Table 1 gives basic parameters for the four reactors and also a list of equipment renewal. A brief description of the general situation in 2000 for each reactor is followed after the Table.

Table 1 Basic Data and Safety Upgrading for Four Reactors

Reactor	Basic Data	Increase System	Renewal	Other Improve
HWRR	D_2O coolant Pool type 15MW from 1958	Emergence recirculation Earthquake safety rod Two set diesel units Safety injection		Emergence operation procedure
SPR	H_2O coolant Pool type 3.5MW from 1964	UPS system Period protection Pool level protection	Motors of secondary pumps Venting fans	Change protection logic
HFETR	H_2O coolant Tank type 125MW from 1979	Residual heat removal Emergence electricity Secondary emergence cooling		
MJTR	H_2O coolant Pool type 5MW from 1991	Partially improvement		

Heavy water Research Reactor (HWRR)

In this year, the reactor operates one cycle each month regularly including power operation, maintenance and experiment preparation during shut down duration. The accumulated operation duration in 2000 is about 20% longer than ever. Due to reactivity requirement by the testing and irradiating material, the average burn-up of the discharged spent fuel has to be decreased from 8000 to 6500 MW⊙d/t. There are three unexpected reactor scram in this year all due to instability or prompt loss of offsite power. Two principles are followed for aging management of HWRR. The first is to implement an elaborated maintenance plan. Actually during shut down duration three main pumps and two of the main heat exchangers have been routinely maintained and cleaned, resin of the ion-exchanger for the primary coolant purification system has been replaced, and under-water in-core inspection has been carried out regularly. The second is to apply a strategy based on reduced power operation. Quantitative study on the corrosion and erosion of essential components shows that aging progress is not linearly dependent on the reactor operation duration T. For a fixed value of PT, the larger the power P (and the coolant flow rate), the more severe the erosion. Therefore, instead of design power of 15 MW, the reactor is now usually operated at a power not higher than 7.5MW unless the operation is engineered for some kinds of special purposes. By these methods, it is believed that HWRR can be safely operated till the new reactor CARR is constructed.

Swimming Pool Reactor (SPR)

Similarly, SPR has also been improved in safety and availability after the equipment renewal and upgrading were accomplished. In this year, there are three times of unexpected reactor scram, two due to loss of off site power in very short time and the another is due to operator's error. The maintenance plan has been strictly implemented, including clean-up of two heat exchangers, protective repair of the main pump axle sealing, and inspection and adjustment of other equipment. SPR will also be long term shut down after CARR go to operation. However, the difficulties for its continuing operation during this period not only stem from aging problem, but also from insufficient fuel element

storage inventory. The fuel element inventory in storage is not enough to support the reactor operation up to the year of 2007. A fuel element fabrication project of 10% enriched U-Mg alloy has been commenced recently to guarantee the fuel supply for SPR operation in the coming years.

High Flux Engineering Testing Reactor (HFETR) and Ming Jiang Research Reactor (MJTR)

HFETR has been designed with capability of operation at partial loading. So, based on the task, the reactor has been recently operated at a power of 50 to 60 MW instead of its rated power 125MW. MJTR is operating at power of 5 MW. This couple of reactors applies same type of tubular fuel assembly composed of six tubes with different diameters. An unified fuel management strategy is applied for this reactor couple. Fresh fuel assemblies are loaded into HFETR, stay there up to an average relative burn-up of about 38%, then after discharging and cooling, the spent fuel from HFETR were reloaded into MJTR for continued burning. The ultimate relative burn-up will reach a value of more than 45%. HFETR mainly used for power reactor fuel and material testing and for other utilization requiring high neutron flux, while MJTR mainly used for isotope production and silicon doping. By this way the fuel can be used more economically.

3 Radioisotope Production, Silicon Doping and Other Application

Research reactor are still important facility irreplaceable for production of radioisotope, silicon doping and other irradiation products.

Table 2 shows the capability and also the practical annual yield around recent years. The real production amount in recent years keeps almost constant. Reactor produced radioisotopes are supplied for more than three thousands of domestic hospitals, therefore continuing operation of research reactors has significant importance even only from this point.

Table 2 Isotope Production in China

Isotope	Installed capability, Ci	Actual production yield, Ci	remarks
^{60}Co	3,000,000	1,500,000	
^{192}Ir	1,500,000	1,200,000	
^{131}I	3000	2,500	
^{125}I	200	60	
^{99}Mo	14000	3,000	NPIC, gel-type
		3,000	CIAE, fission-type
^{113m}In	400	50	For well logging
^{32}P	400	80	
^{89}Sr	10	10	
^{153}Sm	1000	300	
^{131}Ba	300	100	
^{186}Re	50	nonscheduled	
^{90}Y		nonscheduled	For ^{90}Y applicator
^{14}C		nonscheduled	For labeling compounds

Production of doped silicon in 2000 is maintained on an amount of less than 100 tons.

Fig.1 shows artificial gem produced by SPR.

4 Fuel Test for Nuclear Power

China follows an energy source policy of developing nuclear power to proper extent. There is a research and develop plan in field of PWR fuel performance study in accordance with that policy. The research reactors play an important role in this regard.

(a) HFETR has a fuel testing loop in its core with a loop power of 500kW and pressure of 15.5MPa. Twelve fuel rods with different dimension and various core pellets manufacture technology have been loaded in it. The target of the testing is to reach an average (maximum) burn –up of 51 (60) GW d/tu. Up to now, an average (maximum) burn-up of 36 (40) GW d/tu has already been reached.

(b) HWRR is being used for the transient performance study for PWR fuel assembly. The study is divided into two phases. In the first phase which will be ended in next year, the power ramp of the fuel rod will be realized by means of movement of silver absorber. The re-fabrication technology for the spent fuel assembly has already been practiced during this phase. In the second phase, which is scheduled one year later, the power transient will be achieved by means of filling gas absorber He-3 into the loop.

Fig.2 gives a simplified diagram of transient performance study facility, which is scheduled to be loaded into HWRR by the end of this year. The movement of the silver absorber will result in a ramp of linear power density of the testing rod from 200W/cm to 450W/cm within the environment of HWRR core in about two minutes. Up to now, the preparation of the whole test section has been completed, the in-core physics parameters has been experimentally determined, and the safety report for transient testing has been prepared. The project is now being reviewed and waiting for approval.

(c) HWRR is also used for in-core testing of the instrumented fuel elements. In order to master the on-line measurement technique for the central line temperature of the UO_2 pellet and the interior gas pressure from the fission product, special kind of instrumented fuel element has been developed. Pellet of this fuel is made of 10% enriched UO_2 with a linear power density of 220 to 240 W/cm when it is located in the HWRR core. This testing capsule is also scheduled in the coming December to load into HWRR.

5 Neutron Scattering

Due to the equipment problems of cold neutron source on HWRR, main attention is now focused on establishment of new experiment facility on CARR. In spite of the equipment difficulties on HWRR, efforts is still given on some topics with SANS as follows.

(a) SANS study of artificial articular cartilage has been started in cooperation with University of Science and Technology Beijing. Since the equipment of SANS in HWRR is not in good condition, preliminary experiment

has been performed in NIST, United States. The first step in this study, which has been completed in this year, is the determination of optimized measurement means.

(b) As part of the cooperative research project between Asian countries on SANS, CIAE has tested and applied the neutron camera supplied by JAERI, and found the camera is very effective in sample positioning for SANS experiment.

6 BNCT

Research and develop with BNCT has been highly concerned in China. However, no definite decision of the technique line for BNCT has been made yet. Several possibilities have been considered while each of them has problems which should be further studied. The most probable approach among them is to install a tentative BNCT beam tube on a MNSR modification, or to use one of the tubes of CARR for this purpose.

7 Conclusion

Recognizing the fact that the role of research reactors is irreplaceable by other kind of facilities in fulfilling their fixed scientific and engineering functions, and that aging problem is impairing safety operation and utilization of research reactors, China has made efforts both in design and construction of a new research reactor CARR and in upgrading and renewal of equipment and systems in old reactors. Operation and utilization of old reactors has been improved due to these efforts in recent years.

BNCT is highly concerned not only by nuclear engineer but also by medical doctors and hospitals in China. International experience and cooperation will be well utilized. Progress in this field will be further reported in the coming workshop.

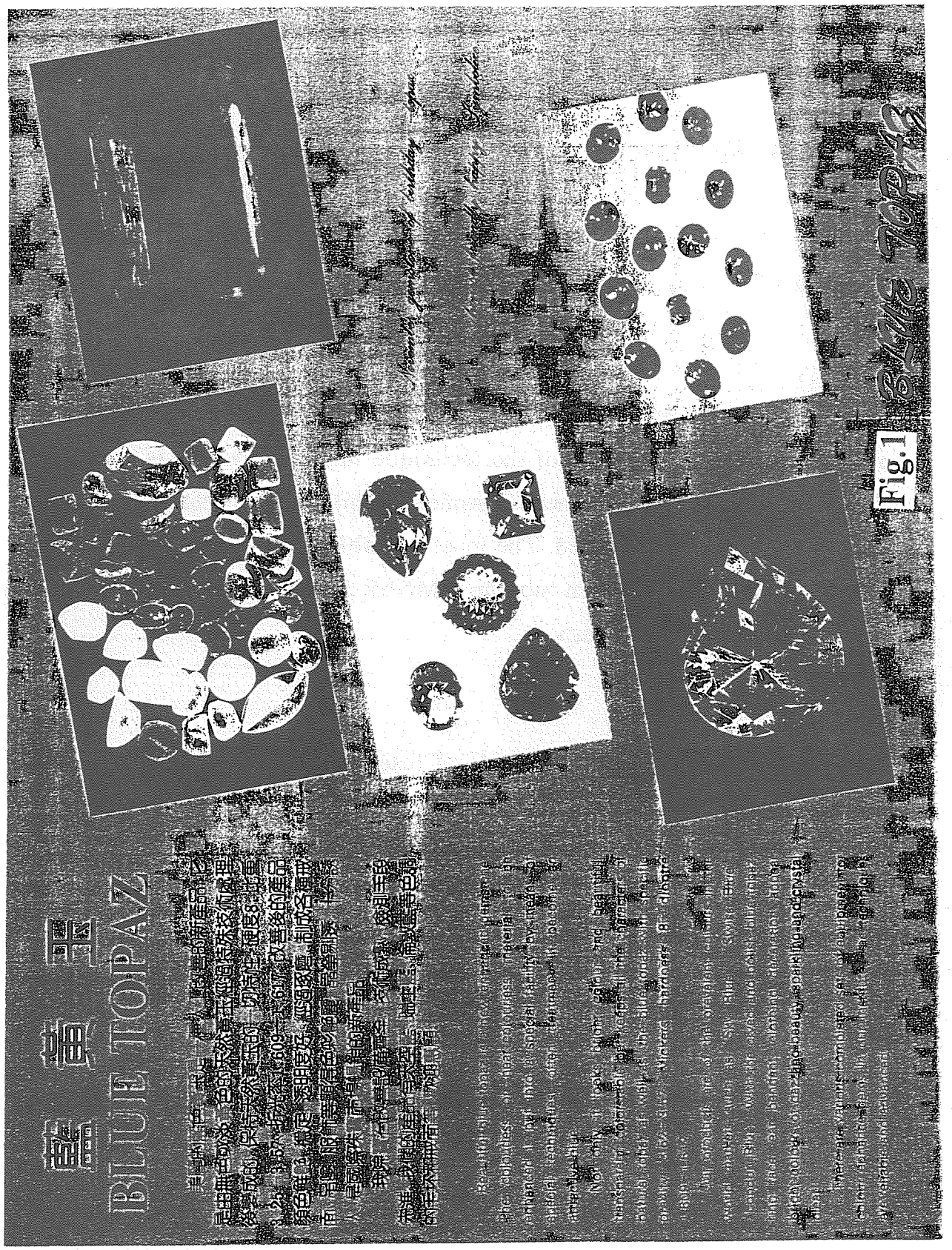

Fig.1

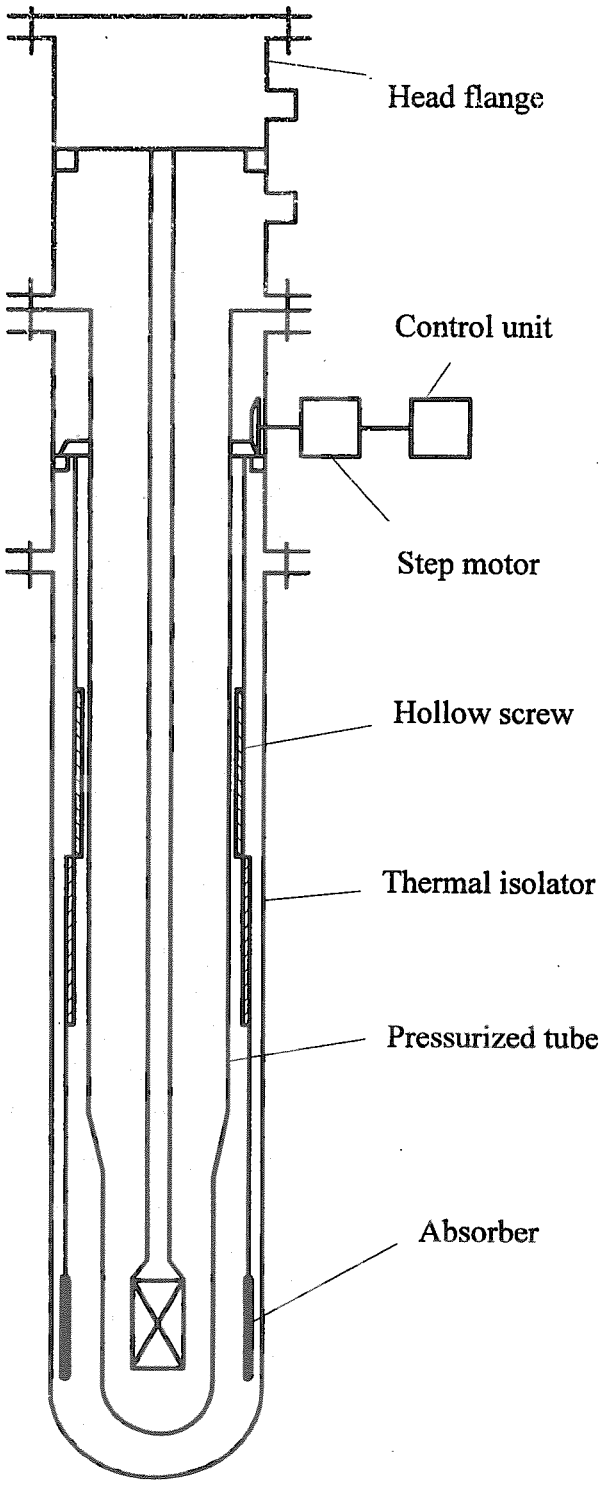

Fig.2 Diagram of In-pile Transient Test Facility

JP0250111

1.27 PRESENT STATUS OF RESEARCH AND TEST REACTORS IN JAERI

Mitsugu Sato,
Shinsho Kobayashi
And
Masaji Takayanagi

Department of Research Reactor
Tokai Research Establishment, JAERI
Tokai-mura, Naka-gun, Ibaraki-ken 319-1195 JAPAN

ABSTRACT

Several research and test reactors have been constructed in Japan Atomic Energy Research Institute (JAERI) and extensively utilized for various studies. At present, four reactors, the upgraded Japan Research Reactor No.3 (JRR-3), the Japan Research Reactor No.4 (JRR-4), the Japan Materials Testing Reactor (JMTR) and the Nuclear Safety Research Reactor (NSRR) are in operation, and a new High Temperature Engineering Test Reactor (HTTR) is under commissioning test. This paper introduces the research and test reactors in JAERI and describes the present operational status of them.

1.INTRODUCTION

Since 1956, many research and development works in the field of the nuclear energy have been carried out in JAERI. Four multi-purpose research reactors (JRR-1, JRR-2, JRR-3 and JRR-4), one material testing reactor (JMTR), one pulse reactor (NSRR) and one power demonstration reactor (JPDR) were successively

constructed in Tokai and Oarai Research Establishment. A high temperature gas-cooled reactor (HTTR) is under commissioning test in Oarai Research Establishment.(see OHP-1)

JRR-1 is the first nuclear reactor in Japan, JRR-2 is the first multi-purpose and high-performance research reactor in Japan and JPDR is the first nuclear power reactor in Japan. They were already shut down with the completion of their operating mission and JRR-2 has been utilized for the development of decommissioning technology of research reactors.(see OHP-2)

Upgraded JRR-3 (JRR-3M) has been operated and utilized for about 12 years. The operation of JMTR using the low enriched silicide fuel was started in 1992. JRR-4 changed fuels from high-enriched fuels to low enriched ones and resumed the operation successively in 1998.(see OHP-3)

2.OVERVIEWS

2.1 JRR-3M

The old JRR-3 was domestically designed and constructed as the first Japan made reactor in 1962 and used in various research fields for about twenty-one years.(see OHP-4)

In order to satisfy the requirements of the date for neutron utilization, JRR-3 was modified to the upgraded research reactor as the JRR-3M. JRR-3M is a light water moderated and cooled swimming pool type reactor with the maximum thermal output of 20MW. JRR-3M got the first criticality in March 1990.

At first, JRR-3M used fuel elemwnt of material testing reactor (MTR) type with low enriched (19.75wt%) UAl_x-Al dispersion type fuel material. But, in 1999, the fuel material was changed from UAl_x-Al to U_3Si_2-Al in order to reduce the number of discharged fuel elements by increasing an amount of uranium loading.

The isometric view of JRR-3M reactor pool is shown in OHP.-4. Five irradiation holes in core region and 4 holes in beryllium reflector region are furnished, and eight irradiation facilities are installed in the heavy water reflector tank. They are being utilized for fuel and material irradiation tests, RI production, neutron transmutation doping for silicon semiconductors, activation analysis and so on.

Nine beam tubes, including the tube (9C) of the cold neutron source (CNS) facility, are installed tangentially for neutron beam experiments.(see OHP-5) The beam tubes 8T and 9C are followed by two and three neutron guide tubes, respectively, which lead thermal (8T) and cold (9C) neutron beams to experimental instruments in the beam hall. There are about thirty beam experimental facilities such as many kinds of neutron scattering experimental facilities, neutron radiography facility and neutron-induced prompt gamma-ray analysis facility.

JRR-3M has been operated about 70 cycles of four weeks continuous operation for about 12 years. Some troubles happened in this operation but many of them are troubles of initial stage on the operation. There is no serious trouble. Due to the high performance of JRR-3M, the number of beam experimental users are remarkably increasing through the past operation years.

2.2 JRR-4

JRR-4 is a light water moderated and cooled swimming pool type reactor. It was originally constructed for the purpose of shielding experiments of nuclear ship and has been operated and utilized since 1965. JRR-4 is operated daily with the thermal output of 3.5MW. The main utilization fields of JRR-4 are activation analysis, RI production, neutron transmutation doping for silicon semiconductors and educational training of reactor engineers (including trainees from abroad).

The reactor core components of JRR-4 are shown in OHP-6.

Although JRR-4 started its operation with high-enriched fuel elements, in 1998, JRR-4 modified to use low enriched silicide fuels in order to follow the worldwide reduced enrichment program and upgrade the utilization facilities. Now, the reactor is renowned for the research reactor that is utilizing the boron neutron capture therapy (BNCT) facilities.

2.4 NSRR

NSRR is a modified TRIGA-ACPR (Annular Core Pulse Reactor) which was constructed for investigating the reactor fuel behavior under reactivity initiated accident (RIA) conditions. The cross section of NSRR reactor core is shown in OHP-7. NSRR can be operated in steady power mode of less than 300KW and in pulse power mode of maximum peak power of 23,000MW.

NSRR is mainly used for the pulse irradiation to determine the threshold energy for fuel failure and to investigate its mechanism and failure consequences under RIA conditions.

It is expected to establish the experimental data base for the evaluation of fuel integrity during RIA,especially on the high burnup fuel and plutonium mixed oxide fuel.

2.5 JMTR

JMTR is a light water moderated and cooled tank type reactor with maximum thermal output of 50MW, and has been operated and utilized since 1971. The reactor core components of JMTR are shown in OHP-8.

The reactor core is installed in a reactor pressure vessel consists of twenty-two standard fuel elements, five control rods followed by fuel elements and beryllium

reflectors. Fuel elements are of ETR type and the fuel materials were changed from high enriched (93wt%) U-Al alloy type fuel to low enriched (19.75wt%) U_3Si_2-Al dispersion type fuel in 1994 through medium enriched (45wt%) UAl_x-Al dispersion type fuel which became utilized in 1986.

At present, JMTR is continuously operated for twenty-five days with LEU fuel elements.

A lot of irradiation facilities are installed as follows; many capsule irradiation holes, two hydraulic rabbit irradiation facilities and one shroud irradiation facility (OSF-1). Many kinds of reactor fuels and materials for testing are irradiated under various conditions such as high temperature, high pressure and so on. Irradiation tests of blanket materials for fusion reactor are being carried out.

2.6 HTTR

HTTR is a graphite moderated and helium gas cooled test reactor with thermal output of 30MW and outlet coolant temperature of 950C using the LEU pin-in-block type fuel. Its construction work started in 1991. HTTR attained the first criticality in 1997, and now is carrying out the commissioning test. OHP-9 shows the reactor core components and fuel element of HTTR.

After the completion of the test, research and development works for establishing and upgrading the basic technology of high temperature gas-cooled reactors (HTGRs) will be carried out and innovative basic researches will be conducted under high temperature condition by utilizing HTTR.

3.CONCLUSION

At present, five research and test reactors are in operation or under commissioning test in JAERI. They are contributing to the basic researches as well as engineering researches & developments (R&Ds) in both nuclear and non-nuclear energy fields. After the completion of JRR-3M, the research fields have been widely expanding, therefore, advanced technologies which can comply with the demands from users are requested.

JAERI is making efforts not only to continue the stable operation but also to conduct R&Ds in order to improve and develop the utilization technology.(see OHP-10)

JP0250112

1.28 Overview of HANARO

Byung-Jin Jun and Hark-Rho Kim
HANARO Center, Korea Atomic Energy Research Institute
P.O.Box 105, Yusong, Daejon, KOREA

ABSTRACT

A general overview of the HANARO is given. Design features of the HANARO are described. Also, main utilization areas of fuel and material tests, radioisotope production, neutron beam application, neutron activation analysis, etc., are briefly summarized.

1. INTRODUCTION

Two TRIGA reactors of 250kW and 2MW were operating at the time of HANARO project. TRIGA Mk-II of 250kW opened the nuclear era in Korea and was used for manpower development. It reached an initial criticality in 1962. TRIGA Mk-III of 2MW which had an initial criticality in 1972, played an important role in enhancing nuclear research in Korea.

HANARO which would replace two prior TRIGA reactors, was designed for multipurpose applications to satisfy national requirements and to promote national development. Demonstration of our capability for safe and peaceful use of nuclear energy and technology was also very important for this project. Therefore, HANARO can be said to represent the crystallization of our efforts and technology around 1990.

HANARO project started at 1985 and got a construction permit on 1987. In 1993, installation of reactor structure started. HANARO reached the first criticality in February 1995. Most part of the project except fuel and component supply was achieved inside Korea.

2. DESIGN FEATURES

HANARO is an open tank in pool type reactor. It is cooled and moderated by light water. Heavy water reflector surrounds the core.

Fuel is 19.75w/o enriched U_3Si dispersed in Al matrix. There are two kinds of fuel

assembly, hexagonal 36-element assembly in triangular array and circular 18-element assembly in two concentric annular rings. Hexagonal assembly has two kinds of fuel element, standard and reduced, with different radius of fuel meat, whereas circular assembly has only standard elements. U density and loading amount in the fuel element are 3.15gU/cc and 69.8(standard)/52.4gU(reduced), respectively. The fuel element has 8 fins to enhance the capability of heat removal and structural strength. The core consists of 23 hexagonal sites to load 36-element assemblies or irradiation capsules and 8 circular sites to load 18-element assemblies. 4 control absorber rods (CARs) and 4 shutoff rods (SORs) made of Hf have annulus shape and positioned at circular sites. In addition, there are 8 circular sites adjacent to the core called outer core; 4 are fuel sites and 4 are irradiation sites.

HANARO has a compact core and wide reflector region to have many experimental holes with different neutron spectrum. Three central flux traps located at the central region of the core have high fast neutron flux over $2x10^{14}$ n/cm^2-sec. They can be utilized for material and fuel test. Four holes in outer core region can give high epithermal neutron flux. These sites are utilized for fuel or material test and radioisotope production. In the heavy water reflector region, 25 holes having high quality thermal neutron flux are prepared for radioisotope production, neutron activation analysis, fuel test loop, neutron transmutation doping, cold neutron source. In addition to the above vertical holes, there are 7 horizontal beam tubes for research in neutron scattering, neutron radiography, medical application, and neutron guide tubes.

The core is cooled by upward forced convection for inherent safety against cooling pump failure or channel blockage accident. The reactor structure has a double containment of cooling water to protect against hypothetical accidents such as LOCA or pool failure. Control rods are driven from the core top and has long lifetime. Digital control is adopted for the stable neutron flux and compact operation room.

Figure 1 shows the plan view of the HANARO.

3. UTILIZATION FIELDS

3.1 Material and Fuel Test

Material and fuel tests have been performed using instrumented or non-instrumented capsules. Instrumented capsule for material test has a characteristic of 5 stages independent temperature control and maximum temperature control up to 500°C. It has

12 thermocouples and 5 micro-heaters. It is utilized for structural materials of nuclear power reactors such as reactor pressure vessel, reactor core materials, CANDU pressure tube, etc.

Non-instrumented capsule for fuel test with a total length of 960mm and an outside diameter of 56mm is utilized for burnup test of newly developed fuels such as DUPIC, advance PWR and metallic fuels.

Atomized research reactor fuel is developed in KAERI as part of RERTR program. It is stable to high burnup and has high thermal conductivity. The irradiation test for this fuel has been performed at HANARO. The test consists of mini-assembly test, mini-plate test in cooperation with ANL, high power full length bundle test and U-Mo full length bundle test.

3.2 Radioisotope Production

There are 4 concrete and 17 lead cells for radioisotope production. Many RIs are produced for medical and industrial use to suffice domestic demand. Those are Tc-99m, I-131, Dy-165, Au-198, Cr-51, P-32, Ir-192, Co-60, etc.

In addition to routine RI production, new application such as Ho-166 has been developed. Research projects to realize fission moly, I-125 production, high activity cobalt, etc. are steadily in progress. Production of I-125, P-33, Sr-89, Sm-153 as non-sealed sources and Re-186, Re-188, Yb-169, Se-75, Gd-153, Eu-152, Sb-125, No-63 and Tm-170 as sealed sources are planned in the future.

3.3 Neutron Beam Application

A High Resolution Powder Diffractometer (HRPD) and a Four Circle Diffractometer (FCD) are in full service. HRPD is applied in the area of crystal structure and phase transition studies, magnetic structure studies, hydrogen and hydride studies, etc. FCD is utilized for single crystal analysis, measurement and analysis of texture, etc. A Small Angle Neutron Spectrometer (SANS) is ready for commissioning. It will be utilized for analysis of defects in metallic and ceramic materials, structural studies of biological macromolecules, etc. A Neutron Radiography Facility (NRF) has been occasionally used for the demand from industry and its upgrade for the dynamic image is underway. Current application areas are nuclear industry, aerospace industry, metallurgy, etc. Table 1 summarizes design characteristics of neutron beam facilities.

Facilities for Boron Neutron Capture Therapy (BNCT) and Prompt Gamma Neutron

Activation Analysis (PGNAA) are under construction, and will be available for user in the next year. Characteristics of BNCT facility and PGNAA system are as follows.

- BNCT facility
  - Thermal neutron flux ≥ higher than $2x10^9$ n/cm^2-sec
  - Thermal-to-fast neutron flux ratio ≥ 100
  - Gamma dose ≤ 0.5Gy/hr
  - Irradiation time ≤ 2 hours
  - Irradiation without interruption of reactor shutdown
  - Temporal surgical operation at site

- PGNAA system
  - Sensitivity of boron concentration measurement ≤ 1 ppm
  - Measurement time ≤ 10 min.

A polarized neutron spectrometer is being installed. Installation of a reflectometer and a triple axis spectrometer is planned for the next step. Then all beam ports in the reactor hall will be occupied, and we will judge the proper time to install cold neutron source and neutron guide tubes for the quantum jump in neutron beam experiments.

3.4 Neutron Activation Analysis

There are three holes for neutron activation analysis in the reflector region. Neutron flux and cadmium ratio is given in Table 2.

Application areas of NAA are wide as follows:

- trace analysis of impurities in nuclear materials
- trace element analysis of heavy metals and toxic materials in environmental samples
- analysis of micro-elements in geological mineral samples
- analysis of composition in cosmic materials
- analysis of heavy metal and specific element related with agriculture and life science
- analysis of forensic, medicines, archaeology and material science

The record of neutron activation analysis has shown a very sharp increase every

year especially in its application to the environmental research.

3.5 Neutron Transmutation Doping

A feasibility study for the NTD utilizing two large holes in the reflector region is underway. The holes are capable of irradiating up to 6- and 8-inch crystals, but the facility will be designed to irradiate 5- and 6-inch crystals considering the current market demand. Annual capacity of the NTD service is estimated about 50 tons.

4. CONCLUSION

HANARO is successfully operating since its first criticality in February 1995 and widely utilized or to be utilized in the areas of material/fuel irradiation test, radioisotope production, neutron beam research, medical research, neutron activation analysis, neutron transmutation doping.

Users are increasing rapidly as experimental facilities are steadily added, modified, and upgraded. New technologies, especially in non-nuclear R&D area, are continuously being developed using HANARO.

It is believed that HANARO will play a key role in basic and applied sciences in both nuclear and non-nuclear areas in Korea.

Table 1. Design Characteristics of HRPD, FCD, SANS and NRF in HANARO

Beam Facility	Design Characteristics
HRPD	$2\theta_M$ 44°, 65°, 90°, 120° Wavelength 0.980-2.510Å Min. step size 0.01° Qmax(A-1) 11.105 Beam collimation α_1 = 6', 10', 20', open (50') α_2 = 30', open α_3 = 10' Neutron flux at sample table (S)[1] 2.6×10^6 (n/cm^2/s) Resolution ($\Delta d/d$) 2.00×10^{-3} ($\tan\theta_B/\tan\theta_M$ =1.10) Detectors 32 He-3 Multi-detectors Linear-PSD (600mm, 200mm) Sample Environment CCR:10K-RT Electromagnet : 1 Tesla, 10K-RT Furnace : up to 1300K 1) Ge(331) (vertically focused), $\alpha_1=\alpha_3$=10', α_2=30' and β=20' The transmissions of the Soller collimators and the filter are not included.
FCD	Take-off angle –45° Monochromators Ge(331) in transmission Ge(113) in reflection Wavelength 0.99 Å for Ge(331) 1.30 Å for Ge(113) Beam collimation α_1 = 20, 30, open α_2 = 55, α_3 = 17 Eff. beam dimension 25mm dia. at the Sample Table[1] Neutron flux at sample 6.61×10^5 n/cm^2/s Scanning mode coupled or independent 1) Measured at 20MW with Au-foil activation analysis
SANS	Beam Port CN Gamma/Fast neutron flux filter Liquid nitrogen cooled Bi/Be filter Super-mirror V-Bender Monochromator Mechanical velocity selector (Dornier) Wavelength range 0.4nm to 0.8nm variable $\Delta\lambda/\lambda$ (FWHM) = 10% Detector 2D-PSD(He-3), 65x65 cm^2 with 0.5x0.5 cm^2 resolution Sample size 0.5 to 2.0cm diameter Q-range 0.06 to 8 nm^{-1} Calculated flux at sample Qmin(nm^{-1}) I_s(n/sec) 0.06 2×10^3 0.1 3×10^4 1.0 3×10^5
NRF	Exposure Room 1st 2nd Collimation ratio 206 >290 Φ_{th} (n/cm^2/s) 1.13×10^7 5.07×10^6 Beam uniformity (σ) - 7% Cadmium ratio -45 Neutron-γ ratio 3.9×10^6 (n/mrem/cm^2) Eff. beam size (cm) 250x350 350x450 ASTM Designation NC-H-C = 75-8-7

Table 2. Characteristics of NAA holes in HANARO

Irradiation Hole	Neutron Flux (n/cm^2-s)			Cadmium Ratio (Au)
	Thermal	Epithermal	Fast	
NAA1	2.1×10^{13}	3.6×10^{10}	3.3×10^{10}	205
NAA2 (Cd lined)	5.8×10^{11}	3.4×10^{10}	3.8×10^{09}	35
NAA3	7.6×10^{13}	4.4×10^{11}	6.8×10^{11}	13

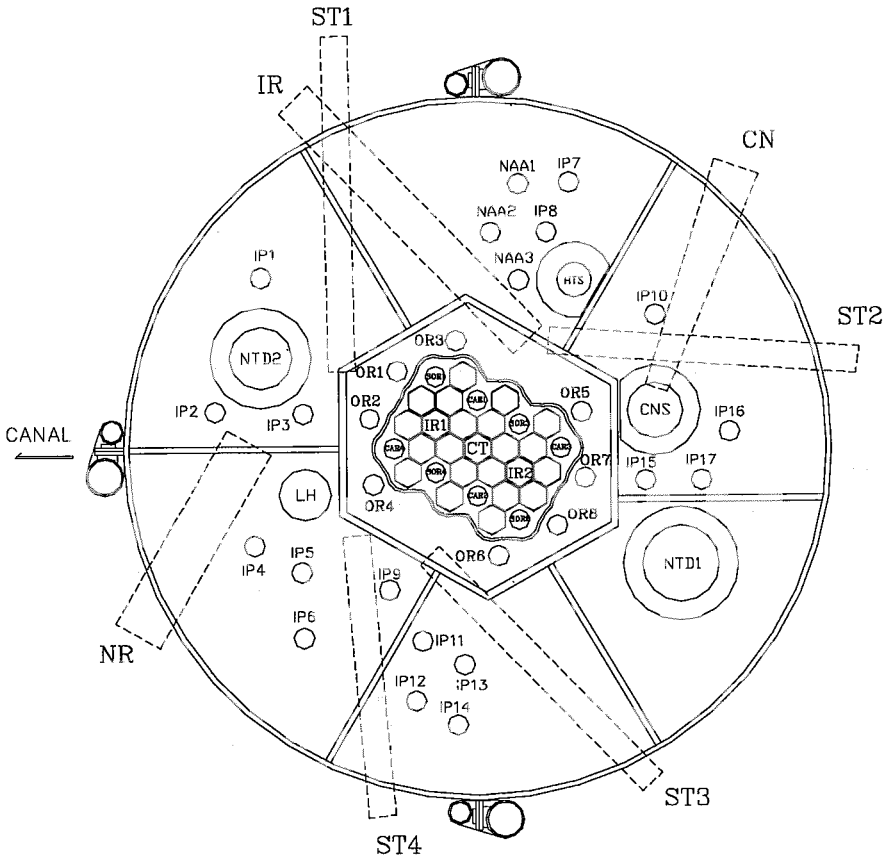

Figure 1. Plan View of HANARO

JP0250113

1.29 Utilization of Beam Ports of MINT Research Reactor

Adnan Bokhari, Mohammad Suhaimi Kassim

Malaysian Institute for Nuclear Technology Research (MINT)
Bangi, 43000 Kajang, Malaysia

Abstract

The first application of MINT TRIGA Reactor (commissioned in 1982) has been with the standard irradiation locations in the core and reflector in support of projects involving neutron activation analysis and production of radioisotopes. As neutron beams experimental facilities, four beam tubes and one thermal column are available, fabrication of beam instruments was initiated in 1984. A neutron radiography facility, which is being used by experimenters in the areas of non-destructive testing, has been installed in 1985. The construction of the small angle neutron scattering (SANS) on the radial piercing beam port was completed in 1995. Some of the devices already in operation but considerable effort is still needed, before the research programs planned for these instruments can be initiated in their full extend. The paper also describes briefly about the prospect of installing a BNCT facility at the reactor.

1. Introduction

The original role of MINT TRIGA Reactor, commissioned in 1982, was manpower training facility in preparation for the introduction of nuclear power program in Malaysia. That nuclear power program never realized over the years, and the mission was later changed towards supporting activities relating to the non-power application of isotopes and radiation technologies.

The reactor, with a maximum steady state power of 1 MWth, consists of a circular core containing a circular grid plate and a graphite assembly surrounding the core. To facilitate neutron beam experiments, the reactor is equipped with four beam ports installed at mid-core height and a thermal column. The location of the beam ports and the thermal column is shown in figure 1. The different designs of the ports give rise to differences in the neutron beams obtainable. The flux available at the entrance to the beam ports are approximately ranges from 1 x 10^{12} n/cm^2/s to 2 x 10^{12} n/cm^2/s. Presently, only two beam ports are utilized for the neutron beam experiments, namely neutron radiography and small angle neutron scattering.

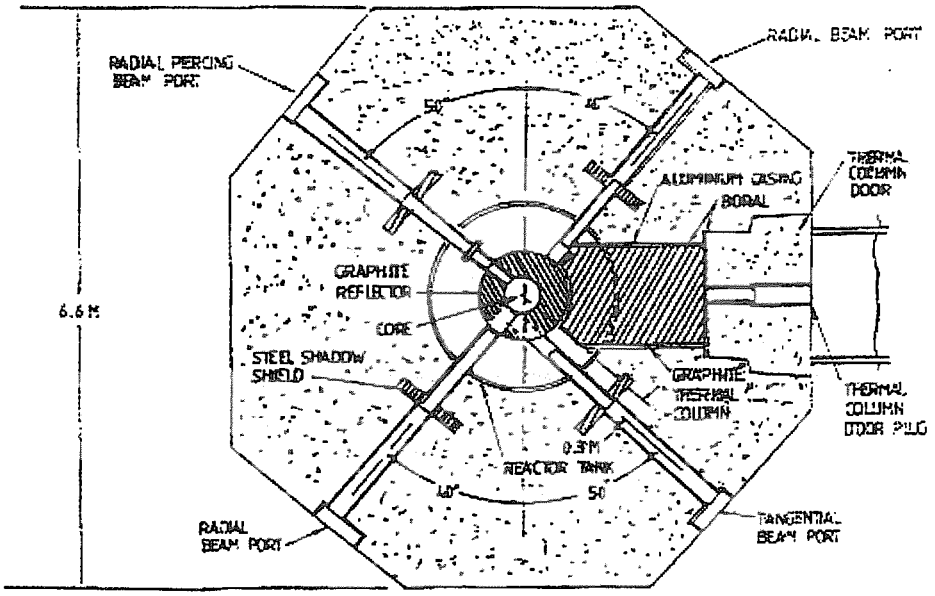

Fig. 1. The location of the beam ports and the thermal column

2. Neutron Radiography

Neutron radiography has been typical utilization of many research reactors for several decades. The neutron radiography activity in Malaysia started in 1983 with the main aim of constructing a permanent neutron radiography facility as to encourage industrial application of NDT to industry. Before undertaking final design of the facility, an experimental neutron radiography facility was constructed using concrete blocks, so that the blocks could be move around to obtain different arrangement and thickness for shielding confirmation. The construction completed in the first quarter of 1984 and was the first attempt at neutron beam utilization on the reactor. Besides for the shielding calculation, the purpose of this facility was to familiarize the neutron radiography group on several aspect of neutron radiography such as collimator design and exposure geometry.

From the data available, a permanent facility was constructed at beam port 3. The choice of beam port 3 as the location of neutron radiography facility was based upon the unavailability of the piercing beam port which has higher neutron flux intensity, which was intended for construction of a small angle neutron scattering. Figure 2 shows the schematic diagram of NuR2.

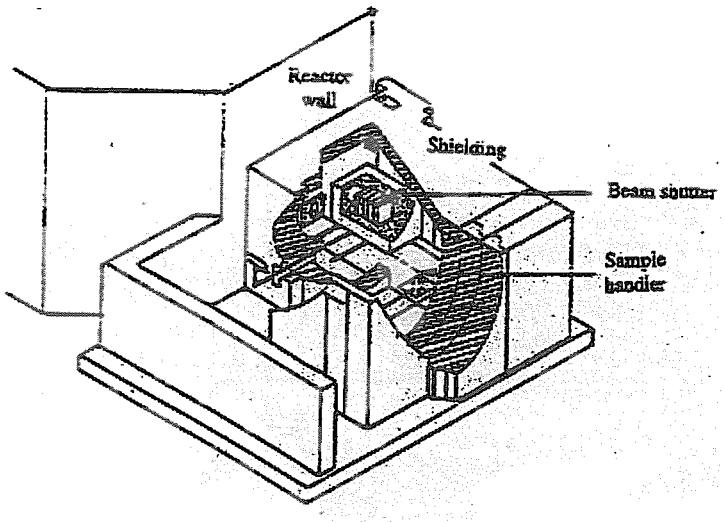

Fig.2. Cut-away isometric view of NuR2

The characteristics of Nur2 are listed below:

Collimator type	-	Step divergent
Length	-	200 cm
Inlet aperture	-	5.4 cm
L/D ratio	-	37
Thermal neutron flux	-	1 x 10^5 n/cm^2/s
Gamma dose rate	-	36.7 R/hr

The quality of the radiograph produced now is comparable to that of other similar facilities elsewhere. NuR2 has been used for number of purposes such as examination historical artifacts on archeological objects, during the early years of completion. The limited number of opportunities to apply the technique to industrial applications in the country did not warrant expansion of the facility. Its further promotion has been has not been encouraging. A part of small space handler to accommodate big samples, this is also due to the immobile nature the reactor based neutron radiography facility. It may also be due to industry immaturity to fully utilize neutron radiography for final product inspection.

3. Neutron Scattering

The use of neutron beams for research reactors to study the physical properties of materials has been a primary area of reactors since the early development. In view of this, a neutron scattering community at MINT, with the assistant of an expert from IAEA in late 1985, began planning for the construction of a small angle neutron scattering (SANS) facility at the radial piercing beam port of the reactor for carrying out neutron scattering experiment in the country.

The design, construction and installation of SANS instrument were completed in 1995. The isometric view of the SANS instrument set-up is shown in fig.3 The instrument consists principally of a monochromator system, a collimator, a sample handler and a detector system.

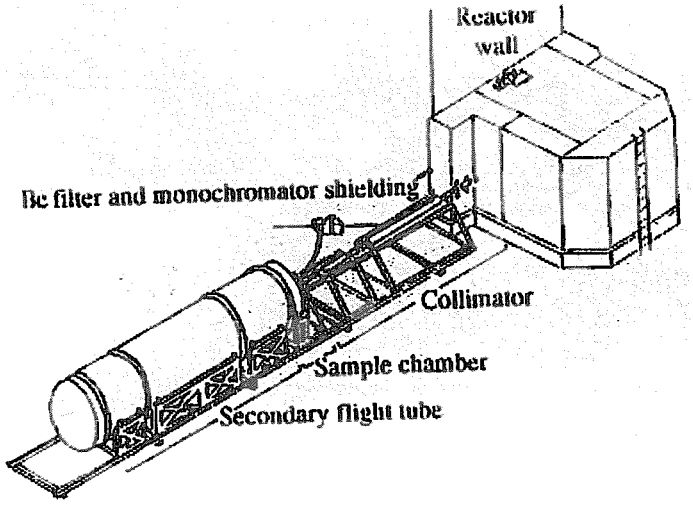

Fig. 3. An isometric view of the SANS instrument

The coarse collimator, which is placed inside the beam port of the reactor, is made of an aluminum tube of diameter 110 mm and length 1.5 mm. The monochromator which is composed of three layers of highly oriented pyrolitic graphite crystals is mounted on a remote-controlled goniometer and a turntable. The main collimator consists of three stainless steel tube (two length 1.0 m and one of 2.0 m) containing cadmium diaphragms mounted on separate stands on a rail, which allows variation of collimation length by removal of one or more elements. Presently, sample is placed in air at the exit of the main collimator. The secondary flight path, which is covered by layer of paraffin wax, consists of two sections of 1.0 m lengths and one of 2 m to enable length adjustment. The neutron detection system is made of ^{3}He filled position sensitive detector.

3. The Prospect of BNCT Facility at MINT Reactor

At present, there is in no major group in Malaysia working on BNCT approach in treatment of cancer patients. Today's standard treatments, conventional radiotherapy techniques using Co-60 source is the main approach by doctors in providing treatment to many kind of cancers. Although the TRIGA reactor is equipped with a thermal column, which is suitable for modification for BNCT facility, there are several factors that need to be established before a BNCT facility for medical treatment can be considered. The most important factor is the establishment of infrastructure such as formation of collaboration between doctors and scientists to develop specialists in BNCT technology. This includes the training of professionals including in BNCT related fields such dosimeter calculation, radiation shielding and so on.

Basically, the health service in Malaysia is geared toward providing basic health care to the population. Presently, there is no cancer registry established in the country to determine the number of cancer patients especially those that require BNCT treatment. The lack of information regarding the cancer patients may probably contribute to the lack of interest among the scientists and academicians to initiate BNCT studies in the country.

To begin the BCNT study, a student at Radiophamacytical School in one of the local university is currently reported to be working for early investigation of BNCT technology such as in basic information in dosimetry calculation. In addition, a substantial funding is being requested for such studies in the next Eighth Malaysian Plan which begins next year to enable such activity to be carried out at the MINT reactor.

Conclusion

MINT TRIGA Reactor has been in operation for more than 18 years, mostly for the purpose of neutron activation analysis, production of radioisotopes and neutron beams experiments. At present there is no major activity being carried out toward the establishment of BNCT facility at the reactor.

References

A. G. Ramli (1994), Paper presented at Workshop on Research Reactor Utilization, ANSTO, Australia, 27 April – 13 May

M. A. M. Sufi, et al: J. Appl. Crst. (1997), 30,884-888

JP0250114

1.30 CURRENT STATUS OF OPERATION AND UTILIZATION OF THE DALAT RESEARCH REACTOR

Nguyen Nhi Dien
Nuclear Research Institute, Dalat, Vietnam

ABSTRACT

The Dalat Nuclear Research Reactor (DNRR) is a 500 kW swimming pool type reactor used the Soviet WWR-M2 fuel elements, moderated and cooled by light water. It was upgraded from the USA 250 kW TRIGA Mark-II reactor. The first criticality of the renovated reactor was in November 1983 and its regular operation at nominal power of 500 kW has been since March 1984.

The DNRR is operated mainly in continuous runs of 100 hrs, once every 4 weeks, for radioisotope production, neutron activation analyses and other research purposes. The remaining time between two continuous runs is devoted to maintenance activities and also to short run for physics experiments. From the first start-up to the end of November 2000, it totaled about 22,000 hrs of operation at nominal power.

After 10 years of operation with the core of 89-fuel element configuration, because of the decrease of the excess reactivity of the reactor core to value of 3%, in April 1994, refueling work was done. At present, the reactor has been working with 100-fuel element configuration. In order to prepare a plan for the second reloading at the end of 2001, fuel management including calculation and experiment researches have been carried out. The system for fuel burn-up measurement has been set up recently.

The current status of operation and utilization and some activities related to the reactor core management of the DNRR are presented and discussed in this paper.

I. INTRODUCTION

The Dalat reactor was reconstructed and upgraded from the former 250 kW TRIGA Mark-II reactor, launched into first criticality in November 1983 and put into operation at nominal power of 500 kW in March 1984. The reactor loaded with the Soviet WWR-M2 fuel elements of 36% enrichment, moderated and cooled by light water. Since the first start-up, the reactor has been used extensively and successfully for radioisotope production, neutron activation analysis, manpower training and other research purposes. Over recent years, the DNRR and its associated technological systems have been thoroughly examined and refurbished to ensure and strengthen its safe operation. And the reactor as the most important scientific tool of the nuclear sector in our country has played an important role in the research and development of nuclear technique applications in Vietnam. The main characteristics of the DNRR are shown in *Table 1.*

Table 1. Main characteristics of the DNRR

Parameter	*Period of determination*	
	Before April 1994	*After April 1994*
Thermal Power, *kW*	500	500

Core configuration, *Number of fuel elements*	89	100
Fuel enrichment, *% U-235*	36	36
Reactivity reserve, β_{eff}	9.17 (1984), 5.8 (1990), 3.8 (3/1994)	6.5 (4/1994), 4.8 (12/1996), 3.2 (11/2000)
Control rod worth, β_{eff}		
• *Safety and shim rods (B_4C)*	2.7 - 3.5	2.7 - 3.1
• *Automatic regulating rod (St. steel)*	0.47 - 0.49	0.504
• *Four shim rods (total)*	10.67 - 12.47	11.26
• *Two safety rods (total)*	5.0	5.36
Xenon poisoning effect, β_{eff}	1.62 ± 0.15	1.65 ± 0.06
Thermal neutron flux, $n.cm^{-2}.s^{-1}$		
• *Neutron trap*	2.13×10^{13}	2.21×10^{13}
• *Wet channel 1-4*	1.02×10^{13}	1.28×10^{13}
• *Dry channel 7-1*	3.8×10^{12}	4.5×10^{12}
• *Dry channel 13-2*	4.0×10^{12}	4.6×10^{12}
• *Rotary specimen rack*	3.27×10^{12}	4.0×10^{12}
• *Thermal column*	5.5×10^{9}	5.8×10^{9}
• *Horizontal beam tube No.3*	2.3×10^{6}	2.3×10^{6}
• *Horizontal beam tube No.4*	1.8×10^{7}	1.8×10^{7}

II. REACTOR DESCRIPTION AND ITS OPERATION

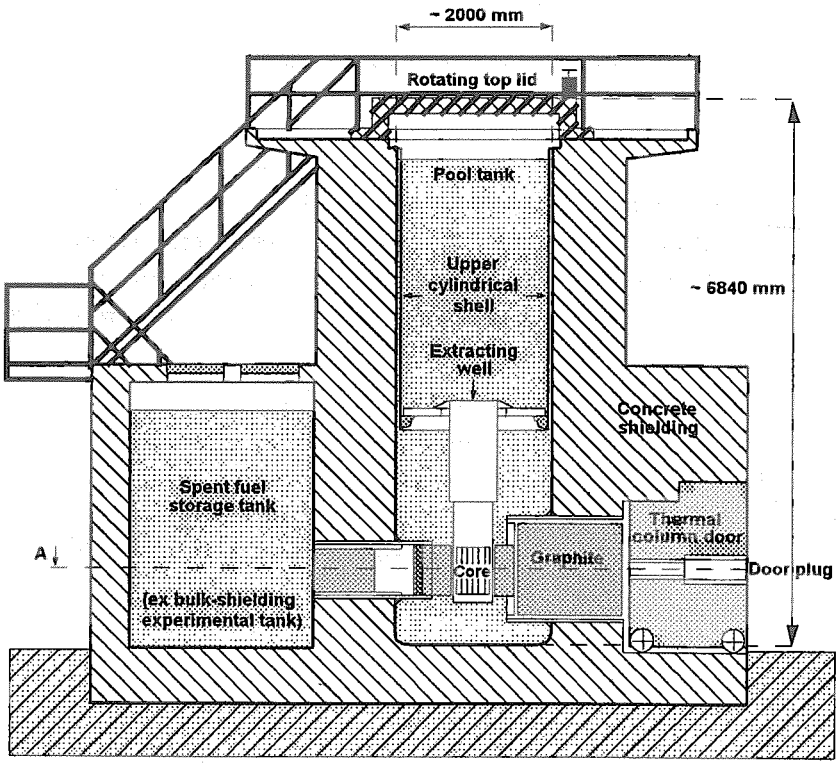

Fig. 1. Vertical section view of the Dalat research reactor

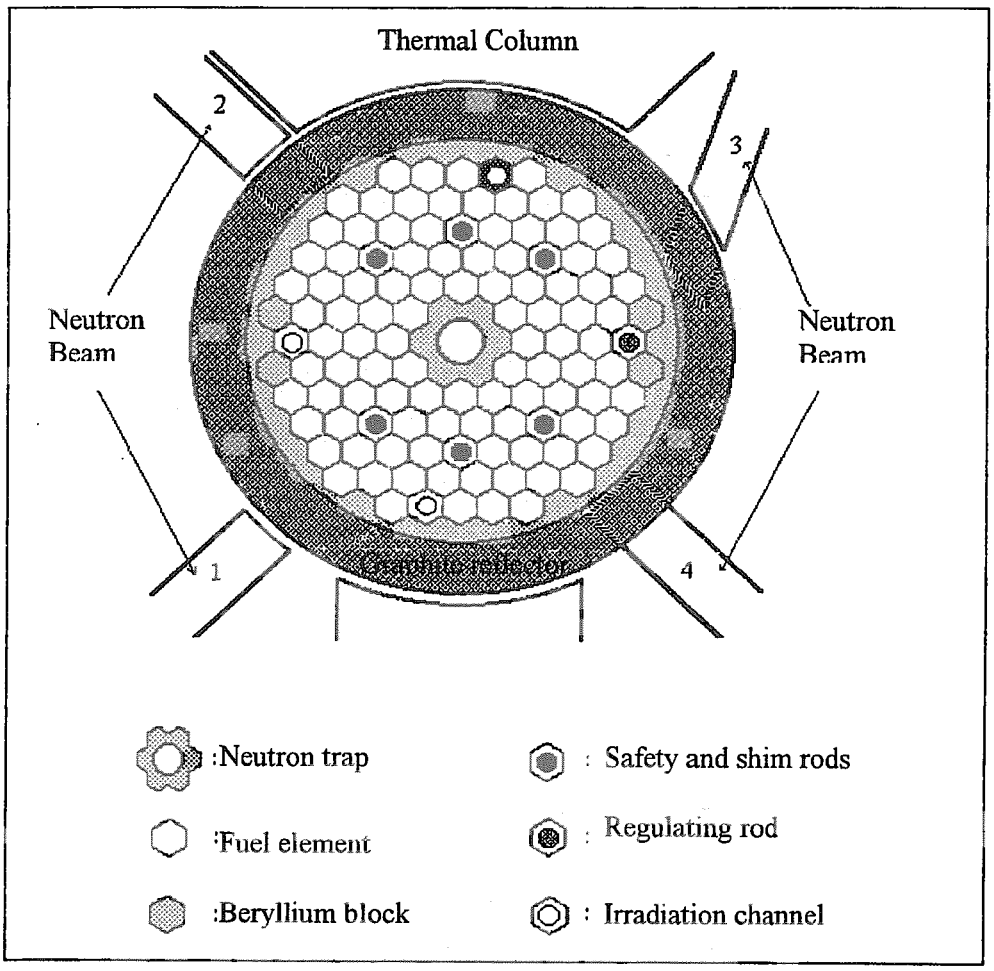

Fig. 2. Cross-section view of the Dalat reactor core

The Dalat reactor consists of a cylindrical aluminum tank 6.26 m high and 1.98 m in diameter of the original TRIGA Mark II reactor. The reactor core, positioned inside the graphite reflector, is suspended from above by an inner cylindrical extracting well in order to increase the cooling efficiency for copping with higher thermal power of the reactor. The vertical section of the reactor is shown in *Figure 1* and the cross-section view of the reactor core in shown in *Figure 2*.

In the framework of the reconstruction and renovation project of the 1982-1984 period, the reactor core, the control and instrumentation system, the primary and secondary cooling systems, as well as other associated systems were newly designed and installed. Some structures of the reactor such as the reactor aluminum tank, the graphite reflector, the thermal column, four horizontal beam tubes and the radiation concrete shielding have been remained.

The DNRR is operated mainly in continuous runs of 100 hrs, once every 4 weeks, for radioisotope production, neutron activation analyses and other research purposes. The remaining time between two consecutive runs is devoted to maintenance activities and also to physics experiments. From the first start-up of the reactor in March 1984 to the end of November 2000, it totaled about 22,000 hrs of operation at nominal power of 500 kW, giving a yearly average of 1300 hrs. Throughout the entire period, the reactor has proved to be safe

and reliable, as it has never suffered from any incident which significantly affected the environment, and annual operation schedules have been rigorously respected *(Table 2)*.

Table 2. Operation data of the Dalat Reactor

Year	*Operation time (hrs)*	*Released Energy (MWd)*	*Accumulated released energy (MWd)*	*Number of scram*		
				Electric network failure	*Other reasons*	*Total*
1984	1120	18.6	18.6	11	17	28
1985	1771	31.7	50.3	5	8	13
1986	1387	26.9	77.2	6	4	10
1987	993	17.9	95.1	6	4	10
1988	1286	25.2	120.3	14	4	18
1989	1343	26.3	146.6	9	2	11
1990	1505	30.4	177	13	5	18
1991	1654	33.9	210.9	8	2	10
1992	1486	30.4	241.3	8	2	10
1993	966	17.7	259	1	2	3
1994	1302	26.8	285.8	11	1	12
1995	1351	27.9	313.7	9	2	11
1996	1370	28.1	341.8	7	3	10
1997	1206	24.7	366.5	9	1	10
1998	1203	24.9	391.4	2	4	6
1999	1215	25.1	416.5	9	4	13
Nov. 2000	1013	20.8	437.3	8	0	8

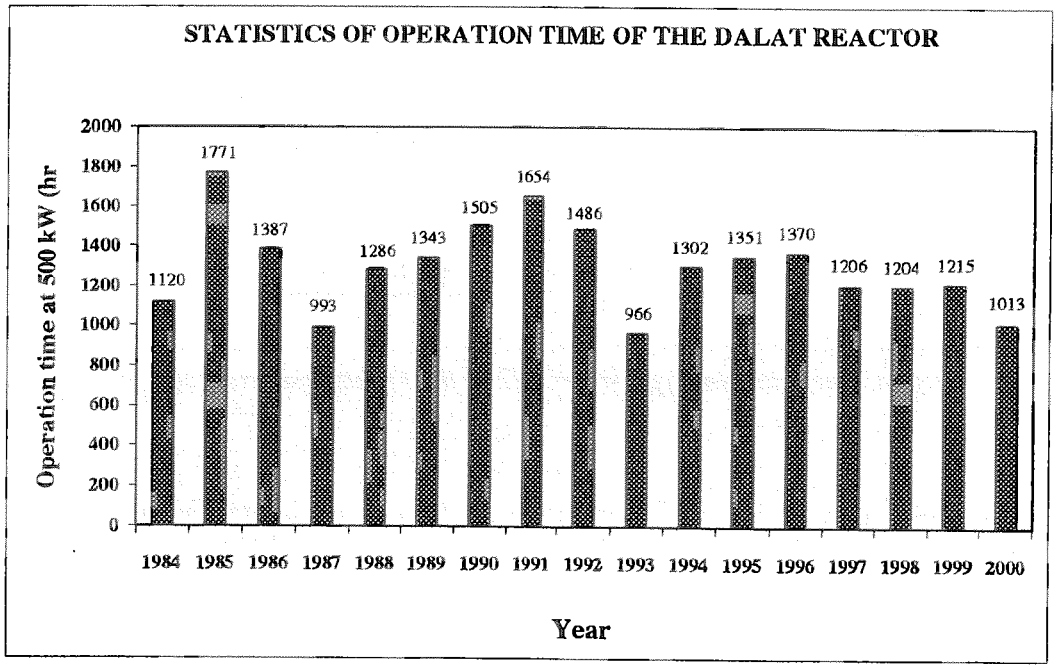

Fig. 3. Statistics of reactor operation time from 1984 to November 2000

III. FUEL MANAGEMENT

The fuel elements of the DNRR are of Soviet-designed standard type WWR-M2, enriched to 36% in U-235. Each element composes of 3 concentric layers: 2 circular inner tubes and one hexagonal outer tube. The fuel layer with a thickness of 0.7 mm is wrapped between two aluminum alloy cladding layers of 0.9 mm thickness *(Fig. 4)*.

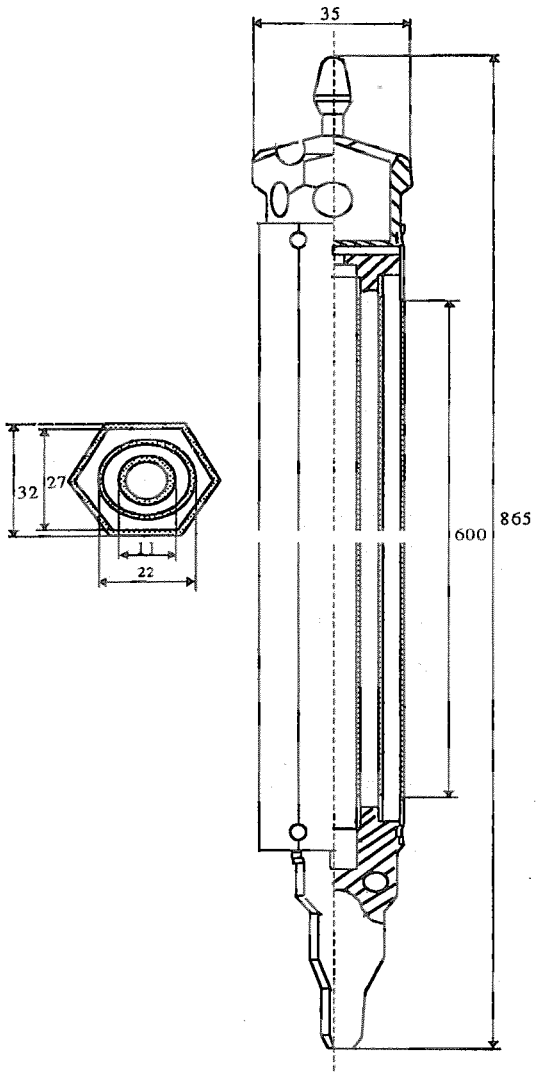

Fig. 4. Fuel element type WWR-M2 of the Dalat research reactor

Up to 1994, after 10 years of operation with 89 fuel elements, the reactivity reserve has lowered at a level, which required fuel reloading. In April 1994, refueling work was implemented. Based on theoretical calculations, a reloading scheme was adopted, which consisted of adding 11 new fuel elements in the core periphery at previous beryllium element locations. Control measurements were made after reloading operations have confirmed the theoretical calculation validity. This fuel reloading ensured the reactor to be exploited efficiently for about 7 years before the next refueling, which scheduled for the second half of 2001. At present time, the reactor has been working with 100-fuel element configuration.

To prepare a future plan for the second reloading, fuel management activities by calculation and experiment measurements have been done. The code HEXA-BURNUP has been developed to solve the problem of in-core fuel management optimization basing on the perturbation theory and binary shuffle technique. The code can search an optimal fuel loading pattern with the lowest power peaking factor for any available set of fuel elements. To determine the number of fuel elements to be discharged at the end of cycle, which satisfies with operational constraints, several different reloading schemes with the different number of discharged fuel elements are investigated. Some experiments have been done for checking calculation results and evaluating the safety of the reactor.

Table 3 presents the experimental and calculation values of the maximum fuel surface temperature at some positions in the core at different reactor power levels. Determination of the fuel surface temperature is carried out by replacing the fuel elements at measuring positions with a thermocouple instrumented fuel element, which consists of 9 thermocouples placed on the surface of this element in the axial direction.

Table 3. Maximum fuel surface temperature distribution

Reactor power (kW)	*Inlet water temperature (^0C)*	*Maximum fuel surface temperature (^0C)*		*Deviation between calculation and experiment*	
		Experiment	*Calculation*	*^0C*	*%*
Position 5-6					
250	19.2 ± 0.1	61.2 ± 0.4	66.5	5.3	8.7
400	19.7 ± 0.1	80.8 ± 0.2	85.1	4.3	5.3
500	20.7 ± 0.4	92.3 ± 0.6	96.3	4.0	4.3
Position 3-4					
250	19.7 ± 0.1	48.0 ± 0.2	51.4	3.4	7.1
400	20.3 ± 0.1	60.8 ± 0.4	63.6	2.8	4.6
500	21.4 ± 0.3	67.4 ± 0.3	71.4	4.0	5.9
Position 1-1					
250	21.1 ± 0.1	46.3 ± 0.9	49.0	2.7	5.8
400	21.6 ± 0.1	56.6 ± 0.3	60.5	3.9	6.9
500	22.7 ± 0.2	63.8 ± 0.3	67.4	3.6	5.6

Table 4. Relative distribution of fuel burn-up

Pos.	*Relative Burn-up*	
	Experiment	*Calculation*
5-6	1.28 ± 0.14	1.42
3-4	1.11 ± 0.13	1.03
4-1	0.72 ± 0.10	0.71
5-3	0.88 ± 0.11	0.78
7-3	0.93 ± 0.12	1.00
4-6	1.03 ± 0.15	1.15
4-4	1.10 ± 0.16	0.97
2-3	0.95 ± 0.14	0.93

Table 5. Reactivity distribution of fuel elements

Pos.	*Reactivity (β_{eff})*	
	Experiment	*Calculation*
4-5	0.38 ± 0.03	0.47
7-3	0.20 ± 0.03	0.24
7-2	0.28 ± 0.03	0.26
7-9	0.18 ± 0.03	0.23
7-4	0.50 ± 0.21	0.53
1-1	0.41 ± 0.21	0.36
5-6	0.76 ± 0.21	0.75
3-4	0.30 ± 0.21	0.38

We have also developed a method for measuring the radial distribution of fuel burning-up. The method allows to determine the relative burn-up distribution of fuel elements

by counting the neutron density of the reactor at subcritical states directly through detectors of the control and instrumentation system. The experimental and calculation results are presented in *Table 4*. *Table 5* shows the fuel reactivity worth distribution. The reactivity worth of a fuel element is measured from the difference in critical positions of control rods before and after the fuel element is withdrawn from the core. It can be seen that the calculation and experimental results are in a good agreement except at some positions around the control rods.

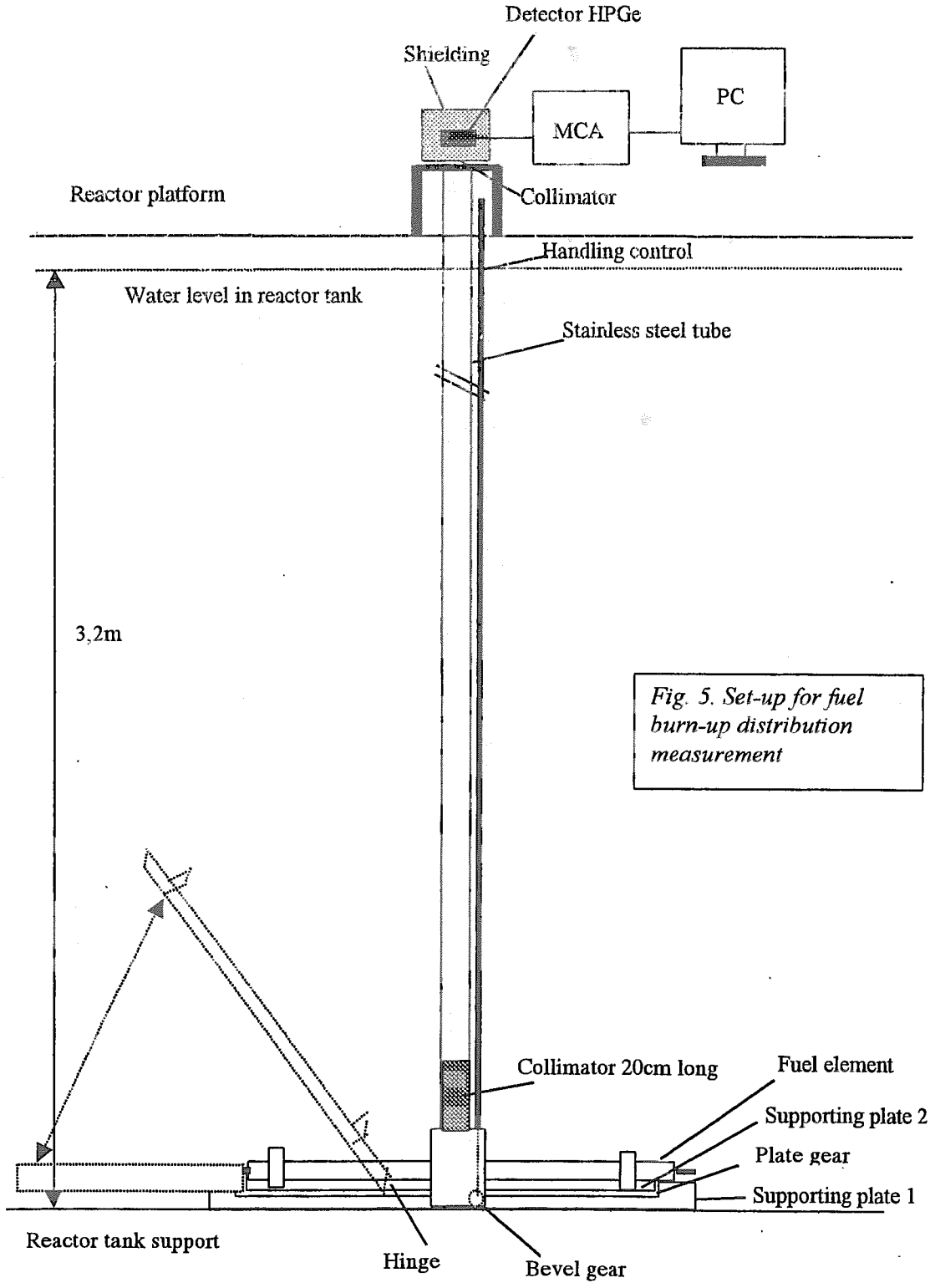

Fig. 5. Set-up for fuel burn-up distribution measurement

Recently, the burn-up distribution has been studied using the gamma scanning method. The measurement system is shown in *Figure 5.*

Gamma spectra, treated by a multichannel analyzer can be used to evaluate the component of fission and activation products in fuel elements. It means based on the analyzing the gamma spectra, we can define the burn-up of each fuel element. It is clear that the activity of long-lived fission product - Cs^{137} has concern with fuel burn-up. But because of the difficulty with the efficient standardization of the measurement system, the relative method is usually used. By relative method, ratios of Cs^{134}/Cs^{137}, Eu^{154}/Cs^{137}, Cs^{134}/Sb^{125} can be used for evaluating the fuel burn-up. In our case, we are interested in using Cs^{134}/Cs^{137} ratio because radioactivity of Cs^{137} can measured after several days of fuel cooling and Cs^{134} can be measured after one month of fuel cooling with our existing $70cm^3$ HPGe system. Preliminary results of measurement are shown in *Figure 6.* And *Figures 7 and 8* show the curves of variation of Cs^{134} and Cs^{137} activity by fuel burn-up using PHDOSE program.

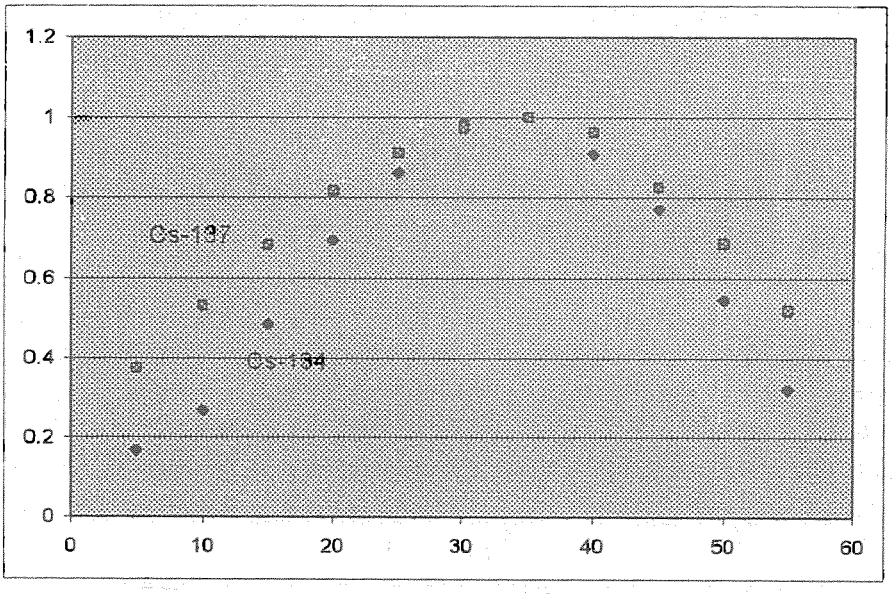

Fig. 6. Distribution of Cs^{134} and Cs^{137} in fuel element No. 6-5

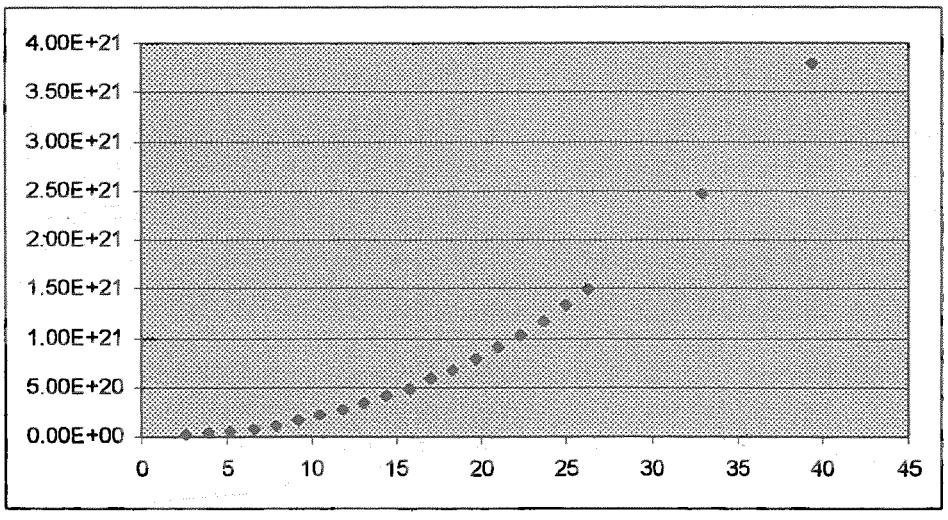

Fig. 7. Variation of Cs^{134} activity by fuel burn-up using PHDOSE

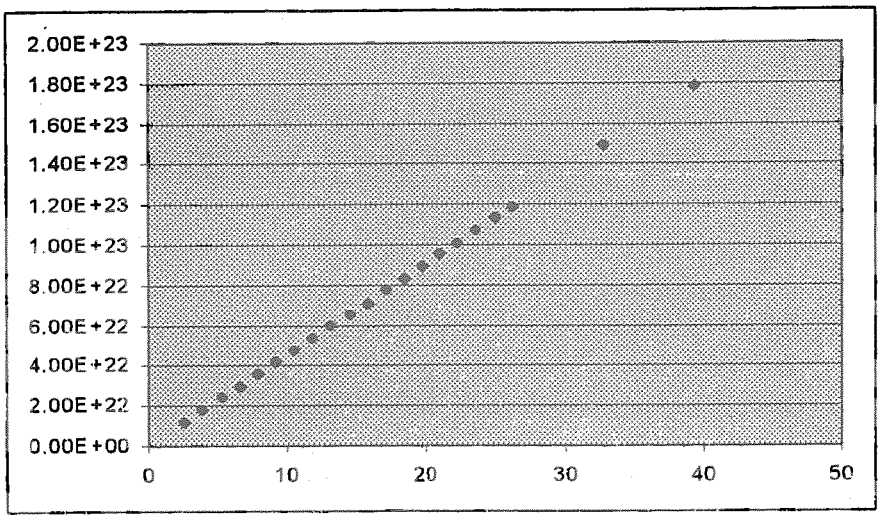

Fig. 8. Variation of Cs^{137} activity by fuel burn-up using PHDOSE

IV. REACTOR UTILIZATION FOR SERVICE OF SOCIETY

For the past years, Dalat Nuclear Research Institute has pushed forward applications of nuclear techniques for answering country's needs. Practically, many products and services have been introduced in our society.

Radioisotopes and radiopharmaceuticals are routinely delivered to more than twenty hospitals in the country, allowing them to diagnose and treat thousands of patients. Continuous efforts have been produced to assist local hospitals in setting up nuclear medicine departments in such aspects as laboratory design, instrument procurement, training, radiation protection. For other nuclear technique users, the assistance is delivered in any needed aspect.

In the nuclear analytical field, requests of many branches of the national economy for various types of samples have been answered. Nuclear techniques have an advantage in serving geology and oil field study. Environmental studies are carried out efficiently with nuclear and associated methods.

V. CONCLUSION

The Dalat reactor has been safely operated for more than 16 years. To achieve that, maintaining and upgrading the reactor technological facilities have been done with a high quality. Besides, reactor researches have also provided the important bases for safety evaluation and in-core fuel management to ensure its safe operation and effective exploitation.

Taking this opportunity, we would like to express our thanks to Japanese Government for co-ordination and financial support for this collaboration program.

REFERENCES

[1] Nguyen Nhi Dien, The Dalat Research Reactor – Operation Status and Fuel Management. The ITC on the Technical and Administrative Preparations Required for Shipment of Research Reactor Spent Fuels to Its Country of Origin, Illinois, USA, 3 – 14 May, 1999.

[2] Do Quang Binh et al, Experience in operation and fuel management at the Dalat Nuclear Research Reactor. The 2-nd International Topic Meeting on Research Reactor Fuel Management, Bruges, Belgium, March 29-31, 1998.

JP0250115

1.31 BNCT Project in Thailand

Sakda Charoen

Office of Atomic Energy for Peace

Vibhavadi Rangsit Road, Chatuchak, Bangkok, THAILAND

Tel. (662) 562 – 0127 Fax. (662) 562 – 0127

e – mail : sakda@oaep.go.th

ABSTRACT

Boron Neutron Capture Therapy (BNCT) is considered as an intra cellular internal radiation therapy for brain tumor treatment. The grate potential advantage of BNCT is its cell level selective destruction of tumor tissue without significant damage to healthy brain tissue.

BNCT Project in Thailand was established in 1996. The working group was set up to study and plan for this project. The BNCT facility was planned to install in a new research reactor of Ongkarak Nuclear Research Center. The project is in the process of detail design and will be ready for operation in the near future. Feature and activities of BNCT Project are presented.

Introduction

BNCT is used in nuclear medicine for brain tumor treatment. Alpha particles and recoiling lithium－7 nuclei from reaction between boron－10 and thermal neutrons have a high linear energy transfer and an associated high relative biological effectiveness. The great potential advantage of BNCT is its cell level selective destruction of tumor tissue without significant damage of healthy brain tissue. It is well known that for successful brain tumor treatments, it is essential to secure a sufficient radiation dose. This depends on an adequate accumulation of boron in the tumor cells and a satisfactory neutron fluence at the target area.

To develop and promote utilization of research reactor in Thailand, BNCT project was decided to include in Ongkarak Nuclear Research Center (ONRC) project. BNCT facility was planned to install in a new research reactor.

ONRC Research Reactor

The reactor system shall be a multipurpose, pool type reactor, cooled and moderated by light water, reflected by beryllium and heavy water (D_2O), that will use low－enriched uranium (LEU) fuel. This uranium erbium zirconium hydride fueled TRIGA reactor shall have a steady state thermal power rating of 10 MW, and shall be capable of generating a neutron flux suitable for the following functions :

- Beam experiments : Neutron Diffraction (HRPD), Neutron Radiography (NR), and Prompt Gamma Neutron Activation Analysis (PGNAA.)
- Radioisotope production for medical, industrial and agricultural uses.

- Neutron transmutation doping (silicon.)
- Applied research and technology development in the nuclear field.
- General training to master the fundamental principles of the reactor and its operation.
- Training in reactor physics (neutron physics, thermal hydraulics, reactor experiments, etc.)
- The capability for later modification to perform medical therapy for patients using the boron neutron capture (BNCT) technique, and/or small angle neutron scattering (SANS.)

Flux. The 10 MW core shall be capable of generating the neutron fluxes shown in table, in support of the various functions.

REACTOR FLUX

Location	Flux
H_2O flooded irradiation facility	$\geq 1.0 \times 10^{14}$ (E < 0.42 eV)
Fast neutron irradiation facility	$\geq 1.0 \times 10^{13}$ (E > 2 MeV)
Epithermal irradiation positions	$\geq 1.0 \times 10^{13}$ (0.82 MeV > E > 0.42 eV)
Beam tubes (thermal)	$\geq 0.5 \times 10^{12}$ (E < 0.42 eV)
Neutron transmutation doping (NTD)	$\geq 1.6 \times 10^{13}$ (E < 0.42 eV)

The reactor system is located within the Reactor Island Building's reactor hall. The system consists of a nuclear research reactor, immersed in water – filled, stainless steel lined pools, that are supported and contained by a steel – reinforced concrete biological shield. The reactor system includes those portions of the primary coolant and D_2O piping within the shield, and to the

portions of the primary coolant and D_2O piping within the shield, and to the first weld outside the shield. The shield, which is approximately 1000-mm high, uses high－density concrete for portions of the lower half (approximately 5000-mm height), in the area surrounding the reactor pool. The shield and the pool water provide sufficient radiation shielding from the various sources within the pools to allow personnel to work safely at any location in the reactor hall. Bridges over the reactor pool allow personnel safe access to all reactor components.

Beam Ports

Beam Port 1. This is a tangential beam port that is designed for neutron diffraction with a high－resolution powder diffractometer.

Beam Port 2. This is a tangential beam port that is designed for neutron radiography.

Beam Port 3. This is a tangential beam port that is designed for prompt gamma neutron activation analysis.

Beam Port 4. This radial beam port is reserved for boron neutron capture therapy (BNCT.)

Beam Port 5. This tangential beam port is reserved for small angle neutron scattering.

Beam Port 6. This radial beam port is reserved for future use.

Beam Port Plugs. The heavy port plugs will be designed such that radiation levels outside the beam ports will be comparable to that of the reactor shield structure. These plugs will be stored in receptacles in the biological shield when not in use. The receptacles will be located within a practical distance from the floor, and on the side of the shield near the east wing.

Beam Port Shutters. The lead shutters will be designed to provide adequate temporary shielding during installation of beam tube experiments. The reactor is assumed to be shutdown during such periods.

BNCT Neutron Beam Facility

BNCT Beam Port. The portion of the BNCT beam port within the reactor pool is an enclosed box, which is normally water－filled to minimize liner and concrete activation. When water filled, a small flow rate will be provided from the water cleanup system to assure proper water quality is maintained within the enclosure. This portion of the BNCT port has the plumbing required to permit draining, flushing, and gas filling.

The box is welded to the reactor structure on the two sides of the shroud not in contact with the D_2O tank. The arrangement has a single aluminum barrier, and no water, between the core and the box. The design of the box, and the reactor structure's installation, will minimize the water gap between the box and liner to maximize the number of useful neutrons available for BNCT use.

Where attached to the shroud, the box inside height, 854-mm, is concurrent with the core height to maximize the available neutrons ; the box enlarges to 1000-mm square where it fits against the pool liner. To avoid the possibility of overloading the shroud when either air or water－filled, the BNCT port top plate has "wings" that transfer loads around the square shroud, and through the ¾ cylindrical shroud, to the D_2O tank's top plate.

Two layers of removable aluminum blocks are provided at the periphery of the core adjacent to the BNCT port.

Progress activities of BNCT project

Nov. 1996	Set up working group for BNCT project
Sep. 1997	A staff of BNCT working group scientific visit on BNCT Facility at KURAI, Japan
Jan. 1998	Invite expert Dr. T. Kobayashi from KURAI, Japan for Conceptual Design of BNCT Facility and lecture on "Boron Neutron Capture Therapy"
Sep. 1999	Invite IAEA Expert Professor Pekka Hiismaki from VTT Chemical Technology, Finland for Conceptual Design of BNCT Facility
Dec. 1999	Lecture on "The Finnish BNCT Programme Before and After the Treatment of the First Glioma Patient" by Prof. Pekka Hiismaki
Mar. 2000	Lecture on "Boron Neutron Capture Therapy" by Prof. Yoshimobu Nakagawa, Japan.
Mar. 2000	Seminar on "Clinical Practice in BNCT to the Brain" by Prof. Yoshimobu Nakagawa, Japan
Present	BNCT neutron beam facility is in the process of detail design.

Future Plan

Since our BNCT project is in the process of detail design. The BNCT neutron beam facility will be designed and provided by the contractor. The design of BNCT supporting facility eg. irradiation room, treatment room,

preparation room, etc. will be also done for the next phase. The collaboration among the participating countries on the BNCT facility design will be needed.

Our further activities will continue with the design of BNCT neutron beam facility and other supporting facilities.

Propose for collaboration

Workshop on BNCT Facility Design

Since many participating countries are interested in BNCT technology and almost of them do not have this facility. To prepare and modify the existing reactor facility for BNCT, it need to plan for the design of BNCT facility. The facility for BNCT should comprise of neutron beam facility, irradiation room, treatment room, preparation room, etc. which have to be carefully designed.

To hold workshops on BNCT facility design at the country which the BNCT facility existed would be very useful for the participating countries who are interested in this field.

Sub－workshop on Demonstration of Clinical Treatment by BNCT

BNCT Technology is not widely utilized in many countries. To demonstrate of clinical treatment by BNCT for nuclear physicists, nuclear medicine doctors, etc. would be beneficial for them to gain more experience in this Technology.

This sub－workshop would be also helpful for the participating countries in preparing a working staff, instruments and equipments for implemention of the project.

Conclusion

To expand the utilization of a new 10 MW research reactor of ONRC project, OAEP has planned to install BNCT facility in the project. The ONRC project are during the detailed design phase, the BNCT neutron beam facility will be provided by the contractor. OAEP has to design the BNCT supporting facilities eg. irradiation room, treatment room, preparation room, etc. which need some advice and assistance form the experienced countries. The collaboration among participating countries will be beneficial for implementation of our BNCT project.

JP0250116

1.32 Development of BNCT Facility at the Indonesian Research Reactor[1]

Hudi Hastowo

Center for Development of Research Reactor Technology,
National Nuclear Energy Agency of the Republic of Indonesia (P2TRR-BATAN),
Kawasan PUSPIPTEK Serpong, Tangerang, 15310, INDONESIA.
Phone: +62-21-7560908, Facsimile: +62-21-7560573.
E-mail: prsg@cbn.net.id

Abstract

Batan has an intention to develop BNCT facility at one of the research reactor available in Indonesia. Study on utilization of the BNCT facility has a good response from hospital nearby research reactor facility.

In order to realize development of the BNCT facility, a feasibility study to define which reactor in Indonesia will be used for that purpose has been done. The result indicates that the TRIGA Kartini reactor in Yogyakarta will be the most suitable for that purpose in comparison with the other reactors. Further action plans for that program has been defined as much as reasonable with availability of fund can be provided.

With a support of JAIF Japan, a JAERI's expert on BNCT has visited Indonesia to explain basic requirement for the BNCT and he has also intensively discussed with Indonesian reactor engineers as well as medical doctor to explain the latest status of the BNCT facility available in JAPAN. Under bilateral JAERI-Batan cooperation program, scientist exchanges from both institutions has been focused and also will be utilized to support development of the BNCT facility in Batan's reactor.

Up to know Batan is expecting the IAEA Technical Cooperation Program on BNCT for the fiscal year 2001. Under this program, another aspects of BNCT technology i.e. radiation dose and radiobiology, as well as radio-pharmaceutical aspects will be developed. Visit of foreign experts to Indonesia and also joint research work between Batan facility and foreign research institute will be done.

This report will describe status report on development of the BNCT facility in the Indonesian research reactor, mainly from reactor engineering aspects, and also further cooperation with an international institution being sought.

Key-words: bnct, research reactor, Indonesia.

1. Introduction

As a result of a good promotion on application of the nuclear technology for medical purposes as well as availability of the BATAN's reactors to supply radioisotopes to hospitals, nuclear medicine has progressively growth in Indonesia. Ups to now, 19 hospitals in

[1] Presented to the Workshop on Utilization of Research Reactors, Taejon, Korea, 20 – 24 November 2000.

Indonesia have been facilitated with nuclear medicine. Further support of BATAN to that hospitals in the form of providing nuclear-medical equipment such as thyroid up-take and renograph unit have a good response by medical doctor at those hospitals. Numbers of patients treated by nuclear techniques in those hospitals have increased significantly.

Progress on development of the BNCT treatment to cure cancers have been achieved by developed countries such as Japan, USA, European Countries, etc has attracted BATAN to consider possibility to develop BNCT facility in Indonesia. Whenever this idea was communicated to the oncologist, they give a good response. This idea is inline with evident given by oncologist regarding incidence for cancerous tumors and other brain tumors in Indonesia. Data from Sardjito hospital in Yogyakarta stated 30 brain tumor patients in 1998 have been treated using combination of surgery and photon irradiation, and the results were unsatisfied.

Feasibility study to develop BNCT at the Indonesian Research Reactor has done last year. With support of the Japan Atomic Industrial Forum (JAIF) one JAERI experts on BNCT facility has been assigned to support this feasibility study. With support of the Japan Atomic Energy Research Institute (JAERI) author has a chance to visit BNCT facility in Japan and also to gather latest information on BNCT facility, especially on the preparation of the reactor and beam design to facilitate BNCT treatment.

Further steps on development of the BNCT facility have been defined in accordance with Batan's 5-year development program. Since limited funds available for the near future, up to 4-5 years from now on, the activities on the BNCT program will be stressed to the engineering design. The main goal with be achieved is within 4-5 years from now-on, Basic Engineering Design of the BNCT facility will be finalized.

2. Feasibility study of the BNCT facility in Indonesia

Three research reactors are available in Indonesia, those reactors are: TRIGA type reactor Bandung, Kartini (TRIGA) reactor Yogyakarta, and Multipurpose Research Reactor (MTR-type) RSG-GAS located in Serpong Nuclear Research Center [1]. Further detail description and also its status are described below.

a. TRIGA reactor in Bandung

TRIGA reactor Bandung has been operated since 1964. On the early period of its operation the reactor has a nominal power of 250 kW. Last 1971; the reactor was then upgraded to 1000 kW with replacement of the reactor core and its fuel elements; instrumentation and other related process system equipment. Finally, after replacement of reactor liner and reflector, on last June 2000 the reactor has been successfully operated at 2000 kW. The TRIGA Bandung reactor has utilized for radioisotope production purposes, neutron beam experiment and also training for reactor operator; as well as doing some reactor physics experimental activities. This reactor has 4 beam tubes, 3 radial and 1 tangential tube, thermal column and thermalizing column.

Several types of radioisotopes have been produced using this reactor. Radioisotope for medical purposes, such as: ^{131}I and ^{99}Mo/^{99m}Tc. Other radioisotope has been produced either for hydrology (^{82}Br) or R & D on agriculture; ^{32}P.

This reactor has a laboratory for NAA and equipped with a nuclear counting system as well as personnel to perform neutron flux measurement and neutron dosimetry. A big hospital with nuclear medicine facility is available around 5 km from the reactor site. This hospital is also used as a teaching hospital by faculty of medicine, Padjadjaran University.

Up to 1990, medical radioisotope as well as radioisotope for other purposes in Indonesia were fulfilled by this reactor. Whenever the new reactor RSG-GAS, 30 MW and the radioisotope laboratory in Serpong at that time become in operation, radioisotope required for medical as well as for industry and other purposes were then fulfilled by this new reactor. Since then the TRIGA reactor in Bandung is mainly used to perform R & D on new radioisotope and also this reactor is used as a back-up when the RSG-GAS reactor in the shut down period.

b. Kartini reactor in Yogyakarta

Kartini research reactor is a 100 kW TRIGA operated since 1979 in Yogyakarta. This reactor is equipped with in-core as well as in reflector irradiation facilities. The irradiation facilities are equipped also with rabbit system and also gamma spectrometry system as well as delayed neutron-counting system. So that this reactor can be used to perform NAA (Neutron Activation Analysis) and also U-Th analysis (using delay neutron counting technique) from the mining. This reactor has 4 beam tubes, these tubes are equipped with a neutron-radiography facility, and sub-critical assembly. The thermal column and thermalizing column are available in the reactor, see Figures 1 & 2.

The Kartini reactor is operated by Center for Research and Development of Advanced Technology of Batan, which is very closed in relationship with Gadjah Mada University. Based on this situation, the Kartini reactor is used as a training facility for student from the Gadjah Mada University.

Several hospitals, either government or private own hospitals are located near by this reactor facility in the distance less then 10-km. One of those hospitals is a teaching hospital of Faculty Medicine, Gadjah Mada University. This reactor is located just five minutes by car from Yogyakarta airport, and this area also very well connected to the other city in Indonesia with transportation facility.

c. Multipurpose Research Reactor RSG-GAS

The RSG-GAS reactor is located in Serpong Research Center; it has nominal power 30 MW. The RSG-GAS reactor is a plate type/MTR type reactor using LEU fuel in form of U_3O_8-Al and U_3Si_2-Al. This reactor is equipped with irradiation facility as well as equipment for neutron beam experimental purposes, see Figure 3.

This reactor was officially inaugurated on August 1987 and reactor utilization for radioisotope production was started on December 1990. Up to know this reactor produced the entire radioisotope used in Indonesia, either for medical purposes as well as for industrial purposes. Some of the radioisotopes produced from this reactor are also exported to foreign country. The reactor equipped with 6 beam tubes, one of this up to know is still unused. The other beam tubes used for radioisotope production (^{125}I), and neutron beam experiments purposes, i.e. neutron radiography, powder diffractometer, triple axis spectrometer, neutron guide tube, etc.

This reactor is also has a facility for fuel element irradiation under high pressure and temperature condition as occurred in the NPP. This reactor has equipped with a power ramping facility, a facility to stimulate power ramping on the BWR or PWR fuel element under irradiation condition.

This reactor is located in Serpong, a suburb of Jakarta for about 35-km in SouthWest direction. Several big hospitals either private or government own are available in Jakarta, however due to traffic condition in near by Jakarta, at least one and half hour is required to go from the nearest hospital in Jakarta to the reactor facility in Serpong vice versa.

Survey to the Indonesian research reactor for the BNCT treatment facility have done with the following requested criteria used as considerations:

a. Neutron flux requirement:
Neutron flux might be used at the front of beam tube or other facility should be around 10^8 - 10^9 n/cm^2.s for thermal or epithermal [2,3]. It was considered also possibilities to modify such of beam-tubes arrangement if it would be needed to reach that requirement. It was considered also volume of the beam and available space in front of beam tube to allow activities for BNCT treatment.

b. Reactor utilization program:
Since the BNCT treatment requires preparation in the reactor area/ room, neutron as well as gamma beam shutter is absolutely needed, other wise reactor should be started-up and shut-down to perform this treatment or single purpose only.

c. Supporting facility:
The most important supporting facility is neutron flux measuring laboratory and boron concentration measurement facility. All of the reactor facilities have a laboratory to perform neutron flux as well as neutron spectrum measurement. The available equipment to measure boron concentration in the tissue as well as in the blood is ICP-MS, and this equipment is available in Serpong facility.

d. Potential users of the BNCT/hospital:
Positive response of the medical staff in the hospital, their expertise as well as facility available on that hospital is considered as a supporting items to decide utilization of the reactor for BNCT.

e. Transportation for patient especially from hospital to the facility vv.
A good transportation facility is required for patients before and after treatment. It is assumed that only one facility will be made available in Indonesia, so that a good transportation mode from other city to this facility is available.

With a support of JAIF, a BNCT expert of JAERI has visited Indonesia and spent around one week at the RSG-GAS reactor in Serpong beginning of last year. He has performed intensive discussion with the Indonesian reactor engineered and he explains basic requirement for the BNCT facility. He has visited also TRIGA reactor in Yogyakarta and performed technical discussion with reactor engineers and medical doctor/oncologist of the Sardjito hospital and Faculty of Medicine, Gadjah Mada University. With support from JAERI, Japan, author has spent 2 weeks in JAERI facility to gather further detail information regarding BNCT technology, and he has also visited several institutions operated these facilities. During his visit to Japan, discussions with specialist expert on neutron beam design as well reactor engineers have been done in order to finalize decision on which reactor the BNCT facility will be installed.

Result on this survey indicated that the RSG-GAS reactor is not suitable to perform BNCT treatment due to some reasons:

a. Neutron beam as well as volume of the neutron beam available in the front of beam tube is only 10^7 and it is not sufficient [4]. Beam-tube modification is very difficult and also not possible since utilization program of the reactor.
b. Neutron and gamma beam shutter is required because of utilization program of this reactor will be disturbed by BNCT treatment. However, construction of the beam shutter in this room/hall is not possible since available space on this area as well as bearing capacity of that floor is limited.
c. Transportation of the patient being treated from hospital to the reactor facility is rather difficult since arrangement of the reactor building, and also traffic from Jakarta to the reactor site vice versa are not comfortable.

Since the RSG-GAS reactor is not suitable for the BNCT facility, other two TRIGA reactors are considered to be used for that purposes. Further activity on preparation of the beam design for BNCT will be concentrated to the TRIGA reactor. Using TRIGA reactor, BNCT facility should be installed in front of the thermal column.

Availability of the supporting facility as well as a good response of oncologist and other medical staff of the Sardjito hospital and Gadjah Mada University to the BNCT program is indicating that utilization of TRIGA reactor in Yogyakarta will be feasible. From the transportation point of view, Yogyakarta is more accessible and also less traffic dense than Bandung. Furthermore, results of the FiR-1 TRIGA Mark II reactor 250 kW for epithermal BNCT treatment facility gave an indication that TRIGA Kartini reactor in Yogyakarta more preferable than TRIGA Bandung reactor.

4. Further step on BNCT activities in Indonesia

The BNCT facility in Indonesia is planned in operation within next 5 years from now on. Based on the literature survey referring to the other facilities now are available [2,3,5,6] or being available in the near future [7], epithermal neutron beam is more preferable rather than thermal neutron beam. To follow on the tendency, BNCT facility for the Indonesian TRIGA reactor is planned to use epithermal neutron beam.

Since the BNCT program has started several activities now were identified and also initiated. The main activities can be described as follows:

a. Up-rating Kartini reactor.
Power up-rating from 100 kW to 250 kW is underway. In general this activity would not have a technical problem because previously the reactor was designed at that power level. However to fulfill licensing requirements, Safety Analysis Report of this reactor as well as Environment Impact Analysis Report should be issued and approved by the relevant institution.

b. Beam design
The thermal column of TRIGA reactor will be modified to produce epithermal neutron beam required for the BNCT facility. Material in the thermal column will be changed in order to get epithermal neutron beam. As the first step, the reactor physics calculation using montecarlo code MCNP is initiated. To get a better result and also to speed up the calculation process, shifter material or moderator and also photon γ-shield have used in the Finnish reactor [8] will be considered. Calculation model as described by Matsumoto [9,10] will be applied on this work. Completion of this work will be followed with the next step to perform engineering design to prepare basic and detail design. Preparation of the reactor physics calculation as well as engineering activities of the neutron beam design is planned for two years. This activity will be followed by construction, testing and commissioning of the equipment, including also phantom measurement.

c. Neutron dosimetry and treatment planning
At the reactor facility, neutron flux and spectrum measurements have done using foil and wire activation detectors. Laboratory with nuclear counting system is available, included also sample changer to perform multiple sample analysis. Neutron flux measurement using SPND is also used in the experimental facility. Since manpower to perform these activities is also available, the most important activity to be done in the field of neutron dosimetry is improvement on accuracy and to speed-up the measurement result. The other aspect of dosimetry for BNCT as described by Watkin [11] will be considered and prepared.
Dose treatment planning can be done through calculation process and it will be checked or verified using measurement.

d. B concentration measurement
B concentration in tissue and blood can be measured using PGAA and ICP-MS/AES. Up to know PGAA system is still being prepared, it is expected that within 5 years from now, the equipment is ready and well-trained personnel are available to determine B concentration in tissue as used in other facility [12].
The ICP-MS is available and also well-trained personnel are ready to perform light element identification and measurement.

e. Radiobiology and pre-clinical experiment
Radiobiology and pre-clinical experiment for animal will be continued, as previously done using TRIGA reactor in Bandung. This experiment should be done in cooperation with medical doctor or oncologist to get better result.

f. Man power improvement
Since the BNCT facility is considered as a priority of the Batan's program, activity for preparation of this facility will be done not only by staff of the Kartini reactor but also done by personnel from other centers such as from Serpong facility.
Sending them to the foreign facility as well as receiving expert from other country through bilateral arrangement and IAEA technical assistance does enhancement of the manpower capability.
Through JAERI-BATAN arrangement one Batan's staff has received training on neutron dose measurement for BNCT treatment beginning of this year, and another Batan's staff will be trained on the field of neutron beam design at the beginning of 2001. Under IAEA TC program for 2001, is planned to accept experts on the fields of radiobiology, dose calculation/measurement, and radio-pharmaceutical aspect.

4. Conclusions

Development of the BNCT facility at the Indonesian research reactor is just being started. The Kartini reactor in Yogyakarta is the most suitable for BNCT facility in comparison with others. Since several circumstances of the current economical situation, the next 5-year planning has a target to finalized engineering design of this facility. Several technical activities have been initiated and further support from foreign countries is sought to improve manpower required for realizing the program.

Reference

[1] Hastowo, H., Utilization of Research Reactor and its R & D Program in Indonesia, paper presented to the Project Formulation Meeting on the Reactor Utilization, Taejon, Korea, March 1998
[2]. Torii, Y., et al., BNCT Irradiation Facility at JRR-4, paper presented to the ASRR-6, Mito, Japan, 29 – 31 March, 1999
[3]. Yokoo, K., et al., The Installation of a New Medical Irradiation Facility at JRR-4, paper presented to the Workshop on the Utilization of Research Reactor, Yogyakarta, Indonesia, 8 – 11 February 1999.
[4]. Ikram, A., personal communication, 1999
[5]. Constantine, G., "The physics and technology of NCT, an overview", Advance in Neutron Capture Therapy, Volume I, Medicine and Physics, Edited by B. Larsson et al., pp. 301 – 310, Elsevier Science, 1997.
[6]. "Boron Neutron Capture Therapy – BNCT", Annual Report 1998, Operation of the High Flux Reactor, Joint Research Centre, European Commission, EUR 18714 – EN.
[7]. Savolainen, S., et al., "The Finnish boron neutron capture therapy program, an overview on scientific projects", Advance in Neutron Capture Therapy, Volume I, Medicine and Physics, Edited by B. Larsson et al., pp. 342 – 347, Elsevier Science, 1997.

[8]. Auterinen, I., and Hiismäki, P., Epithermal BNCT Neutron Beam Design for a TRIGA II Reactor, Advances in Neutron Capture Therapy, Edited by A.H Soloway at al., pp. 81 – 84, Plenum Press, New York, 1993

[9]. Matsumoto, T, et al., Design Studies of an Epithermal Neutron Beam for Neutron Capture Therapy at the Musashi Reactor, Journal of Nuclear Science and Technology, Vol. 32, No. 2, pp. 87 – 94, Feb. 1995.

[10]. Matsumoto, T, Design of Neutron Beams for Boron Neutron Capture Therapy for TRIGA Reactor, Journal of Nuclear Science and Technology, Vol. 33, No. 2, pp. 171 – 178, Feb. 1996.

[11]. Watkin, P., et al., "Dosimetry for BNCT in theory and practice", Advance in Neutron Capture Therapy, Volume I, Medicine and Physics, Edited by B. Larsson et al., pp. 141 – 146, Elsevier Science, 1997.

[12]. Yonezawa, C., et al., "Application of Neutron-induced Prompt Gamma-Ray Analysis for Determination for B-10 in BNCT", Cancer Neutron Therapy, Edited by Mishima, pp. 221 – 225, Plenum Press, New York, 1996.

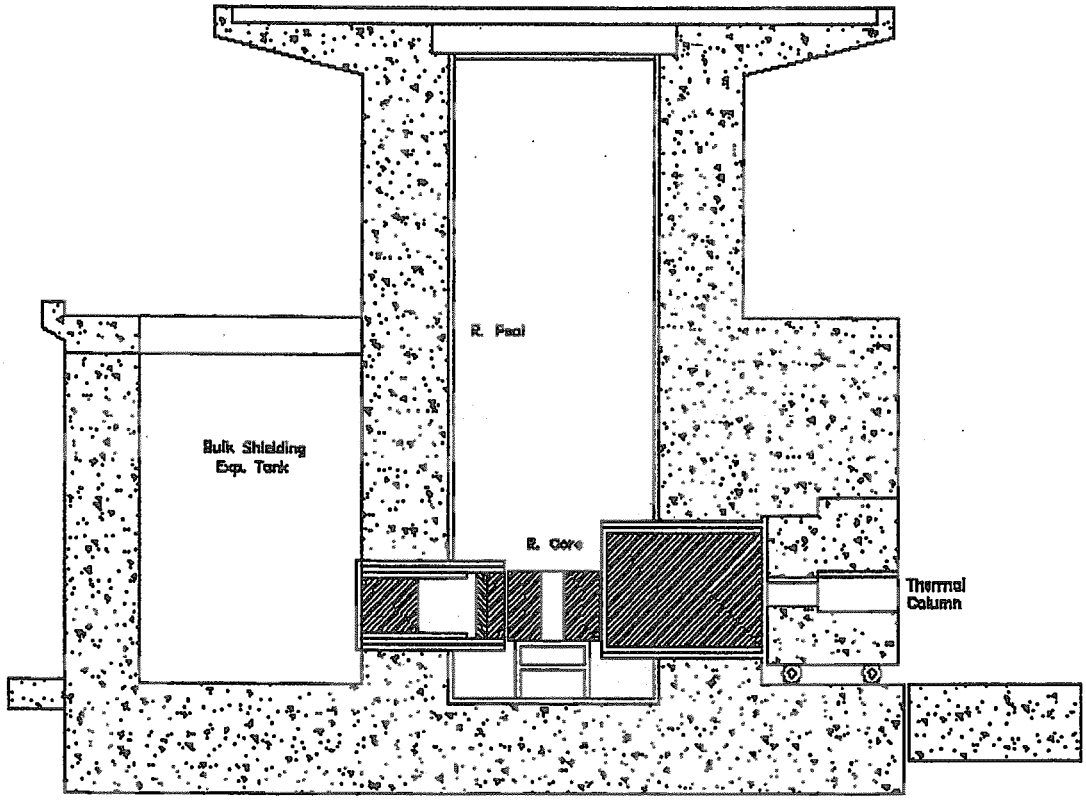

Figure 1. Vertical cross-section of the TRIGA Kartini reactor

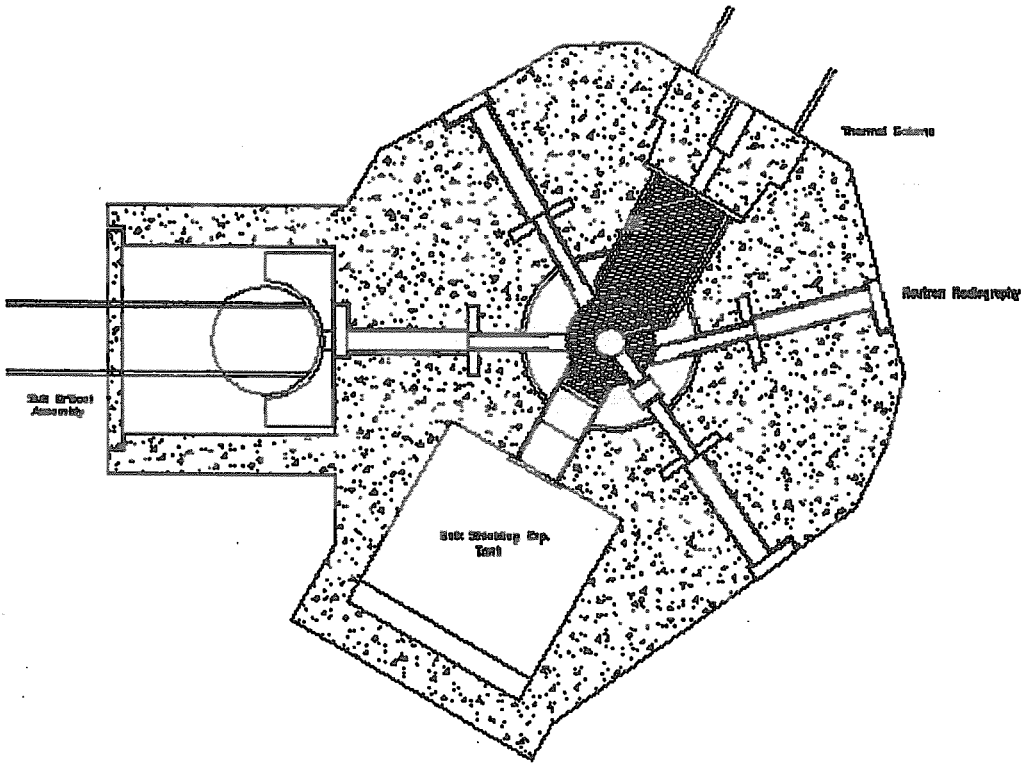

Figure 2. Horizontal cross-section of the TRIGA Kartini reactor

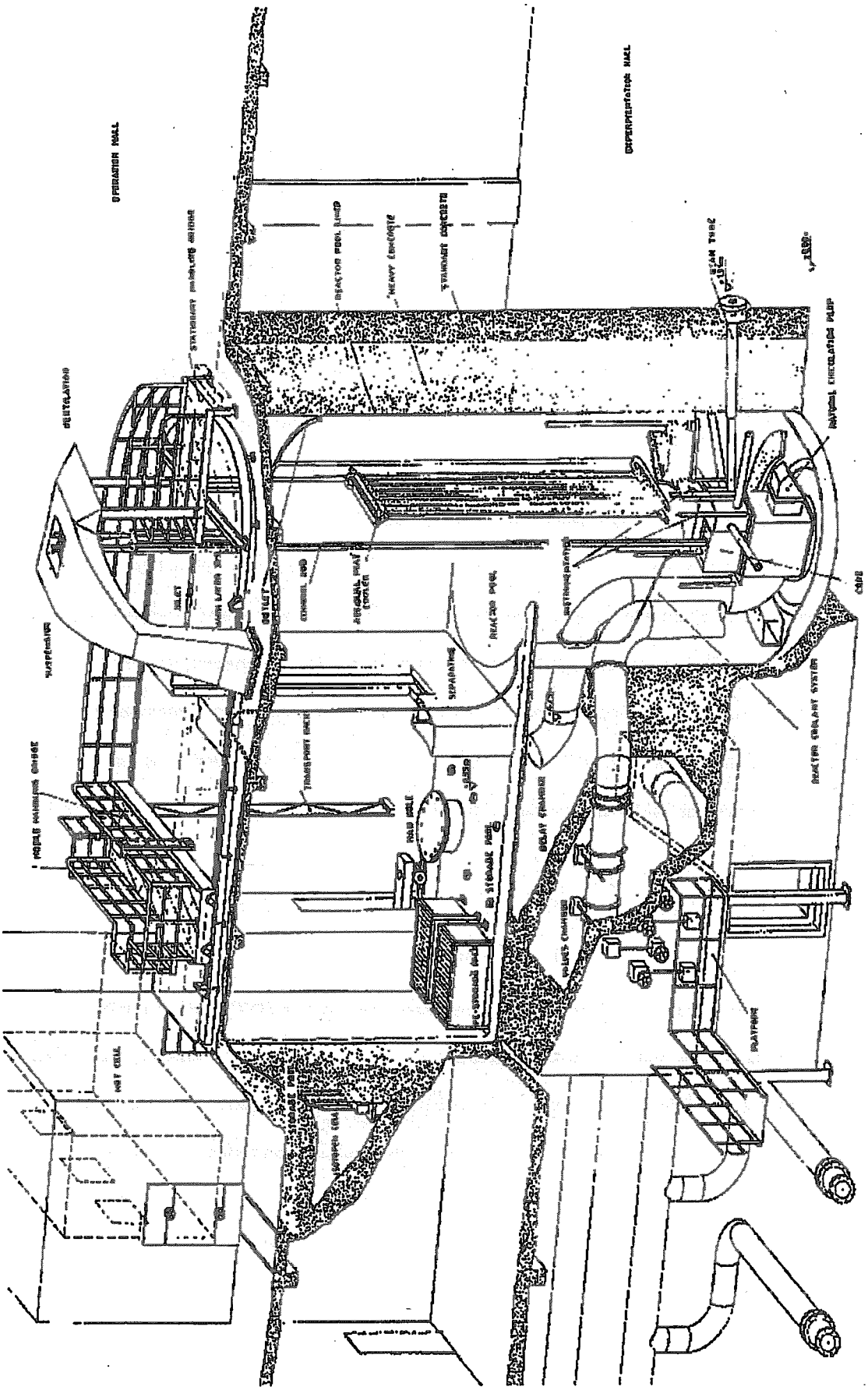

Figure 3. Isometric drawing of the RSG-GAS reactor

JP0250117

1.33 Development of PGNAA Facility in HANARO

H. D. Choi*, S. H. Byun, G. M. Sun,

M. S. Kim†, and B. J. Jun†

Department of Nuclear Engineering, Seoul National University, Seoul 151-742, Korea

†HANARO Center, Korea Atomic Energy Research Institute, Taejon 305-600, Korea

A prompt gamma neutron activation analysis(PGNAA) system is being set up in HANARO, a multipurpose research reactor in the Korea Atomic Energy Research Institute. The beam is polychromatic thermal neutrons diffracted vertically by a set of pyrolytic graphite crystals at the Bragg angle of 45° from a horizontal beam line. Prior to assembling, measurements of the neutron spectrum and gold wire activation confirmed that a sufficient neutron flux can be obtained. A tapered collimator is positioned between graphite crystals and the Teflon sample holder, being composed of alternating layers of borated plastic, lead and polyethylene. The detection system consists of a 43% n-type HPGe detector, signal electronics and a fast ADC. At present, graphite crystals and collimator with the surrounding shield on the beam line are set up and measurements of beam characteristics are progressing. Thermal neutron flux of 6.1×10^{7} n/cm^{2}s and the Cd-ratio of 364 are achieved at sample position while the reactor is operating at 24MW in November 2000. The first application of the system will be analyzing ^{10}B in biological samples.

1. Introduction

Determining ^{10}B concentration in treating area is necessarily required in BNCT before implementing the irradiation in order to decide the neutron irradiation time and to evaluate the therapeutic effect[1]. For measuring ^{10}B, PGNAA method and ICP(inductively coupled plasma) atomic emission spectroscopy are widely used, among which PGNAA method has the merit of matrix-independent result in short turn-around time[2].

In PGNAA method, concentration of component nuclide in the sample is analyzed by detecting prompt gamma-rays which are emitted promptly within the order of 10^{-14} sec after a neutron is absorbed by the nuclide. This method is particularly suitable for analyzing the elements of B, Cd, Sm, Gd etc. which have large neutron

*corresponding author : (email) choihdg@snu.ac.kr

capture cross sections, and also for the elements like H, C, N, S etc. which do not lead to radioactive isotopes by neutron absorption[3].

The performance of a PGNAA facility depends on obtaining a high flux thermal or cold neutron beam with fast neutron and gamma backgrounds removed to a sufficient degree. The pioneering facilities mostly adopted direct neutron beam from the ports, while the recent trend is developing facility by using cold neutrons as the construction of cold neutron beam lines is widespread over the research reactor sites[4,5,6]. In HANARO, developing PGNAA facility was initiated by the requirement of ^{10}B analysis along with the plan of BNCT facility[7]. The present facility adopts the method of Bragg diffraction by using pyrolytic graphite(PG) crystal for extracting thermal neutrons from a direct beam line[8,9]. The facility, however, has the unique feature of utilizing diffracted polychromatic neutrons without filtration[10,11].

In the design stage, thermal neutron flux was predicted to be above 10^7 n/cm^{2}s for the case of Bragg angle 45° by calculating the theoretical reflectivity of mosaic PG crystal and by simulating the beam divergence effect with Monte Carlo method. The prediction was afterwards confirmed by a prototype experimental setup[10]. At present, measuring the characteristics of neutron beam is finished for varying conditions of extraction methods such as the thickness of crystal and the focusing geometry. Since all other components of the facility are ready to assemble, the installation is planned to finish by the end of 2000.

2. System features

2.1. Thermal neutron extraction

The schematic diagram of PGNAA facility in HANARO is shown in Fig. 1. The PGNAA device is installed at the wall end of the ST1 horizontal neutron beam port, and shares the neutron beam with the polarized neutron spectrometer(PNS). The cross section of ST1 port exit is $70^w \times 120^h$ mm^2, whose central part of $70^w \times 60^h$ mm^2 will be used for PNS, while the area of top-and-bottom edges is assigned to PGNAA facility. The thermal neutrons in the horizontal beam line are diffracted upwards as shown in the figure. For the diffracting crystal, pyrolytic graphite(PG) is chosen for its high reflectivity. The mosaic spread of PG is 0.8°. It is chosen to give the maximum flux at the sample position, predicted through a detailed optimizing calculation of two conflicting effects from reflectivity and beam divergence[11]. PG crystals are located at the both top and bottom edge regions at the exit of ST1 port. One piece of crystal is 2 mm thick and 25 mm wide by 50 mm long. A double

layer of 3 pieces occupies the beam cross section of $70^{w}\times30^{h}$ mm^2. The two side-pieces are inclined with respect to the central piece and hence they are shaped in concave form in order to achieve focusing the diffracted neutrons at sample position. Before mounting, the inclination of the side-pieces are fine-tuned by using a parallel light beam. The reflected light image was observed at the sample distance on an optical table. By varying the tilting angle of side-pieces, tilting position was fixed when both images from the side pieces coincide with that from the center piece.

The PG crystal mount is located 4 m from the nose of ST1 beam tube. It is attached to a two-axis goniometer of manual driven type. After installing a BF_3 detector wrapped with Cd-sheet having a pin-hole at the detection position, the angle of goniometer is adjusted by maximizing the neutron count rate at sample position.

Between PG crystals and sample, beam collimator is installed to limit the beam cross section at sample location which is 1.5 m from crystal. The collimator has layered structure of alternating rings made of borated plastic, lead, and polyethylene, respectively, to reduce thermal neutron, gamma ray and fast neutron. The diameter of alternating ring is gradually decreased to reduce to a circle of 20 mm diameter at sample position.

2.2. Shielding, sample holder and detection system

The PGNAA device needs shielding around the collimator, the beam shutter, the stopper, and also around the diffracted beam line and the HPGe detector. Since the PG mount and collimator are near the exit of beam port, the background level is inaccessibly high. To shield the high level background, heavy concrete blocks containing B_4C powder are installed around the ST1 beam line. For shielding of diffracted beam line and detector, neutron is shielded at first and gamma-ray at next. The material for thermal neutron shielding contains boron or lithium of which absorption cross section is high. The boron shields neutron effectively but produces more secondary gamma-ray. Therefore, borated plastic in which B_4C is mixed by 66 % weight fraction is used in shielding for the beam shutter, the beam stopper and the regions where the production of secondary gamma-ray does not influence the detector. The LiF tiles($100\times100\times10$ mm^3) are used for locations near sample and detector entrance where the production of secondary gamma-ray has to be suppressed. The 95% enriched ^{6}Li is used only for the detector window while natural lithium is used in other places. The ^{6}LiF tile is produced from the sintering process after converting the commercial $^6Li_2CO_3$ powder to ^{6}LiF by use of hydrofluoric acid. The shield for gamma-ray is lead of thickness 10 cm minimum.

The gamma-ray detection system is shown in Fig. 2. The gamma-ray detector is n-type HPGe with relative efficiency of 43%. A charge sensitive preamplifier with resistive feedback is to be used. To increase the

maximum tolerable count rate of the spectroscopy system, an amplifier with gated integrator and a fast ADC with a constant conversion time of 1.5 μsec have been chosen.

3. System performance

Since the details of the neutron spectrum obtained by diffraction are unknown, a measurement by time-of-flight(TOF) spectrometer has been carried out, the result of which is shown in Fig. 3. Due to the difficulty of installing TOF spectrometer at ST1 line, the measurement was performed at the neighboring CN beam line. The neutron spectrum is obtained for 90° diffraction by PG crystal. The relative proportion of neutron flux for each diffraction order is determined from the measured area of Bragg peak with proper correction for the effects of chopper transmission and detection efficiency etc. Table 1 shows the comparison of the measured result with that obtained by theoretical calculation using integrated reflectivity. For the case of Bragg angle of 45°, both results confirm that there is little contribution from the 1st order diffraction but those from the 2nd, 3rd and 4th order are the majority.

The beam profile at the sample position is measured by use of a pin-hole BF_3 detector. The result is shown in Fig. 4. It is evident in the figure that a flat distribution is achieved in a region of 20 mm diameter. For clear cut of beam cross section, a final slit will be located at the exit side of beam shutter.

To determine the neutron flux and Cd-ratio, gold-wire of 0.1 mm diameter and 0.5 mm thick Cd sheet are used. For the rotary shutter of ST1 beam port set at full open position, the results of measuring diffracted neutron flux at the sample position are listed in Table 2 for several PG crystal configurations. When the PG crystals are used in single layer and flat geometry, the flux and Cd-ratio are 2.2×10^7 n/cm^{2}s and 292, respectively. For the double layered PG, the crystal thickness is doubled and the gain in flux reached to 1.6 which is slightly larger than the theoretical gain 1.4. By considering the non-proportional increase in Cd-ratio, considerable amount of background fast neutron leaking into the sample region exists in parallel with those scattered from the crystals. The flux gain by tilting the side crystal pieces to produce focusing effect is 1.7 which is equal to the calculated gain by Monte Carlo method. The increase of Cd-ratio by only a factor of 1.2 requires further study. The achieved neutron flux 6.1×10^7 n/cm^{2}s and the Cd-ratio 364 are of sufficient quantity and quality required for analyzing ppm level ^{10}B in the course of BNCT[1], and prove a unique neutron beam environment which is not seen in the existing PGNAA facilities utilizing thermal neutron.

The test performance of gamma spectroscopy system is summarized in Table 3. The relative efficiency of the purchased HPGe detector is 43% and the resolution for 1332 keV gamma-ray was measured to be consistent with the vendor's value 1.9 keV.

4. Conclusion

The characteristics of neutron beam for use in HANARO PGNAA facility are measured and described. The optimized beam flux at the sample position is 6.1×10^7 n/cm^{2}s and the Cd-ratio is 364, at 24 MW of reactor power. Hence it is verified that the 90° diffracted beam by PG crystals has suitable qualifications for applying to PGNAA. By this year's end, assembling all components is carried out with a view of application to ^{10}B analysis in biological samples.

References

1. T. Kobayashi and K. Kanda, Nucl. Instr. and Meth. **204** (1983) 525.
2. T.U. Probst, Fresenius J. Anal. Chem. **364** (1999) 391.
3. R.M. Lindstrom, Proceedings of the International Workshop on Cold Neutron Utilization, Taejon, Korea (1998) 205.
4. C. Yonezawa, A.K.H. Wood, M. Hoshi, Y. Ito and E. Tachikawa, Nucl. Instr. and Meth. **A329** (1993) 207.
5. R.M. Lindstrom, R. Zeisler, D.H. Vincent, R.R. Greenberg, C.A. Stone, E.A. Mackey, D.L. Anderson and D.D. Clark, J. Radioanal. Nucl. Chem. **167** (1993) 121.
6. K. Ünlü, C. Rios-Martinez and B.W. Wehring, J. Radioanal. Nucl. Chem. **193** (1995) 145.
7. H.D. Choi, S.H. Byun and B.J. Jun, Proceedings of 6th Meeting of the International Group on Research Reactors, Korea (1998) 449.
8. D.F.R. Mildner, R. Berliner, O.A. Pringle and J.S. King, J. Appl. Cryst. **14** (1981) 370.
9. K.J. Riley and O.K. Harling, Nucl. Intstr. and Meth. **B143** (1998) 414.
10. H.D. Choi, S.H. Byun, B.J. Jun and M.S. Kim, Proceedings of 10th International Symposium on Capture Gamma-Ray Spectroscopy and Related Topics, USA (2000) 731.
11. S.H. Byun and H.D. Choi, J. Radioanal. Nucl. Chem., **244** (2000) 413.

Table 1. Comparison of the measured and calculated relative fractions of the diffracted neutron flux from each diffraction order for a double layer of PG crystals.

Diffraction Order (n)	Wavelength [Å]	Energy [meV]	$\phi_D(n)/\phi_D$*		$\phi_D(n)/\phi_{th}$**
			Calculation [%]	Measurement [%]	Calculation
1	4.74 ± 0.07	3.6 ± 0.1	5.9	5.0 ± 0.1	0.0014
2	2.37 ± 0.03	14.6 ± 0.4	22.2	25.4 ± 0.2	0.0052
3	1.58 ± 0.02	32.8 ± 0.9	30.9	37.9 ± 0.2	0.0072
4	1.19 ± 0.02	58.3 ± 1.6	24.3	22.9 ± 0.2	0.0057
5	0.95 ± 0.01	91.1 ± 2.5	12.4	8.2 ± 0.1	0.0029
6	0.79 ± 0.01	131.2 ± 3.7	4.3	0.5 ± 0.1	0.0010

* $\phi_D(n)$: neutron flux from n-th order diffraction, ϕ_D : sum of all $\phi_D(n)$'s.
** ϕ_{th} : total thermal neutron flux of incident beam.

Table 2. Thermal neutron beam characteristics measured at the sample position.

Crystal shape	Number of crystal layer	Neutron flux [n/cm^{2}s]	Flux gain	Cd-ratio
Flat	1	2.2×10^7	•	292
	2	3.5×10^7	1.6	315
Tilted	2	6.1×10^7	1.7	364

Table 3. Result of performance test of the γ-ray spectrometer for 1332 keV γ-rays.

	Warranted	Measured	
		Factory	This study
Resolution (FWHM)	1.90 keV	1.83 keV	1.90 keV
Relative efficiency	30 %	43.1 %	43.1 %

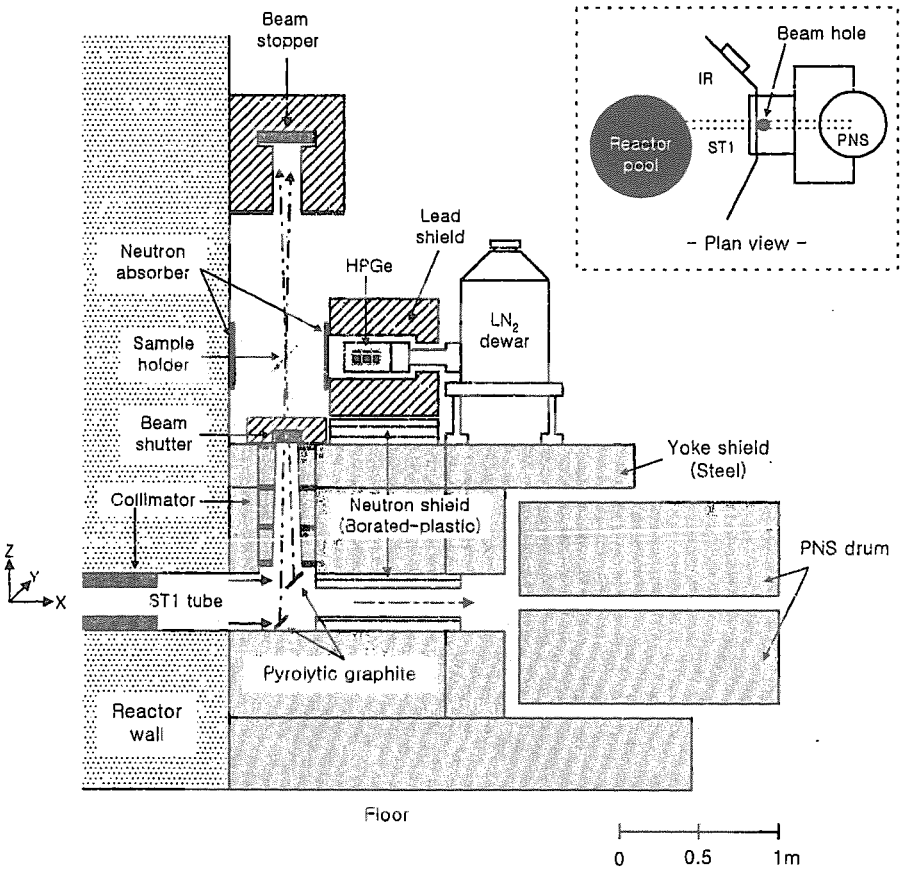

Fig. 1. A schematic layout of the PGNAA system on the ST1 beam port of HANARO. Additional shielding around the sample and the beam path is not shown here.

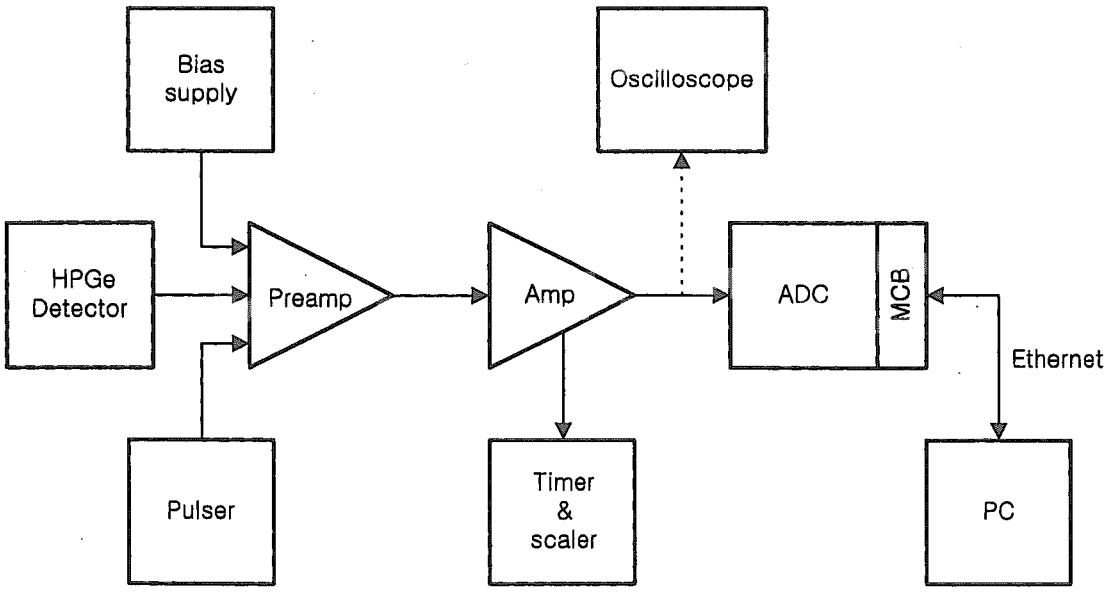

Fig. 2. Block diagram of the detection system for PGNAA.

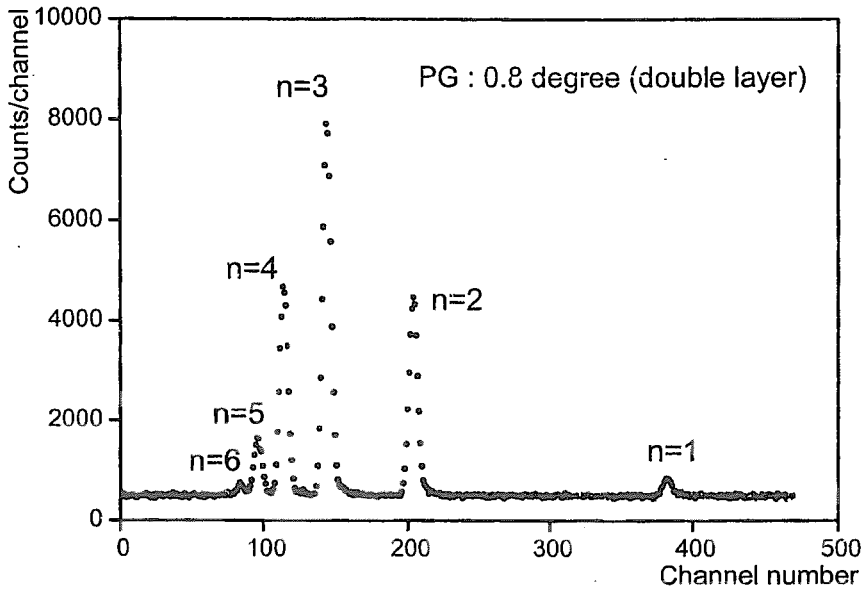

Fig. 3. The TOF neutron spectrum of the diffracted polychromatic beam at the Bragg angle of 45° obtained by using a double layer of PG crystals having 0.8° mosaic spread.

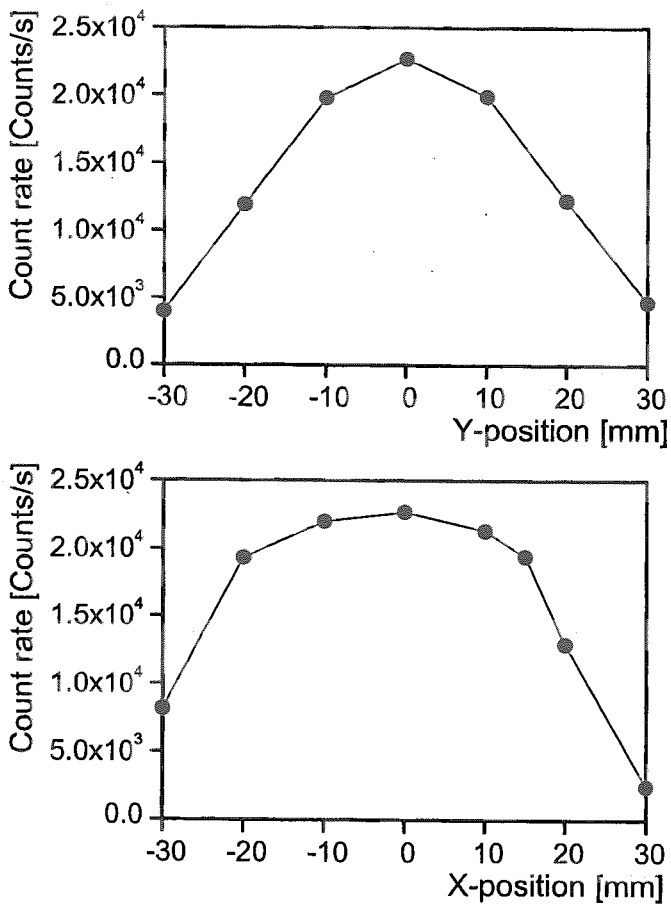

Fig. 4. Neutron profile at the sample position, measured by a BF_3 pin-hole detector.

JP0250118

1.34 JRR-4 Medical Irradiation Facility

Y. Torii, K. Yamamoto, N. Hori, H. Kumada, Y. Horiguchi
Japan Atomic Energy Research Institute
Tokai-mura Naka-gun Ibaraki 319-119 JAPAN

1. ABSTRACT

JAERI started Boron Neutron Capture Therapy (BNCT) at JRR-2 in 1990. JRR-2 was performed 33 BNCT until 1996 when JRR-2 operation was terminated for decommissioning the reactor. JRR-4 was constructed to research the reactor shielding of the first Japanese nuclear ship "Mutsu" in 1965. JRR-4 was modified for reducing fuel enrichment and constructing a new medical irradiation facility at 1997 when after the terminating operation of JRR-2. The medical irradiation facility is especially using for BNCT of brain cancer. JRR-4 medical irradiation facility was designed for both using of thermal neutron beam and epi-thrmal neutron. Thermal neutron is using for conventional Japanese BNCT as inter operative irradiation therapy. Epi-thermal neutron beam will be using advanced BNCT for deep cancer and without craniotomy operation for irradiation at the facility. The first medical irradiation for BNCT of JRR-4 was carried out on October 25, 1999. Since then, seven times of irradiation was performed by the end of June 2000. In BNCT irradiation, boron concentration and thermal flux measurements were performed by JAERI. Boron concentration of patient brood was measured using prompt gamma ray analysis technique. Thermal neutron flux was measured by gold wire activation method using beta – gamma coincidence counting system. There data were furnished to medical doctor for determination the irradiation time of BNCT.

2. OUTLINE OF JRR-4

JRR-4 was constructed for the purpose of shielding design study for nuclear ship. It was a swimming pool type research reactor using light water for its moderator and coolant. Its maximum thermal power is 3.5MW and first criticality on January 28, 1965. The operation of JRR-4 using HEU fuel terminated at the beginning of 1996. A new medical irradiation facility was constructed and the operation of the reactor resumed with LEU fuel in July 1998. The new facility at JRR-4 was designed to be capable of providing both thermal and epithermal neutron beams. Bard eyes view of JRR-4 is shown Fig. 1.

3. IRRADIATION FACILITY

The cross section of JRR-4 medical irradiation facility is shown in Fig.1. The heavy water tank is structurally composed aluminum and heavy water layer. The material of ammonium was selected for fast neutron absorber. The heavy water layers are separated and optimum heavy water

thickness can be chosen for both thermal and epithermal beams according to the need of each treatment. The tank is installed together with a cadmium filter, which is set for beam condition changing thermal mode to epi-thermal mode.

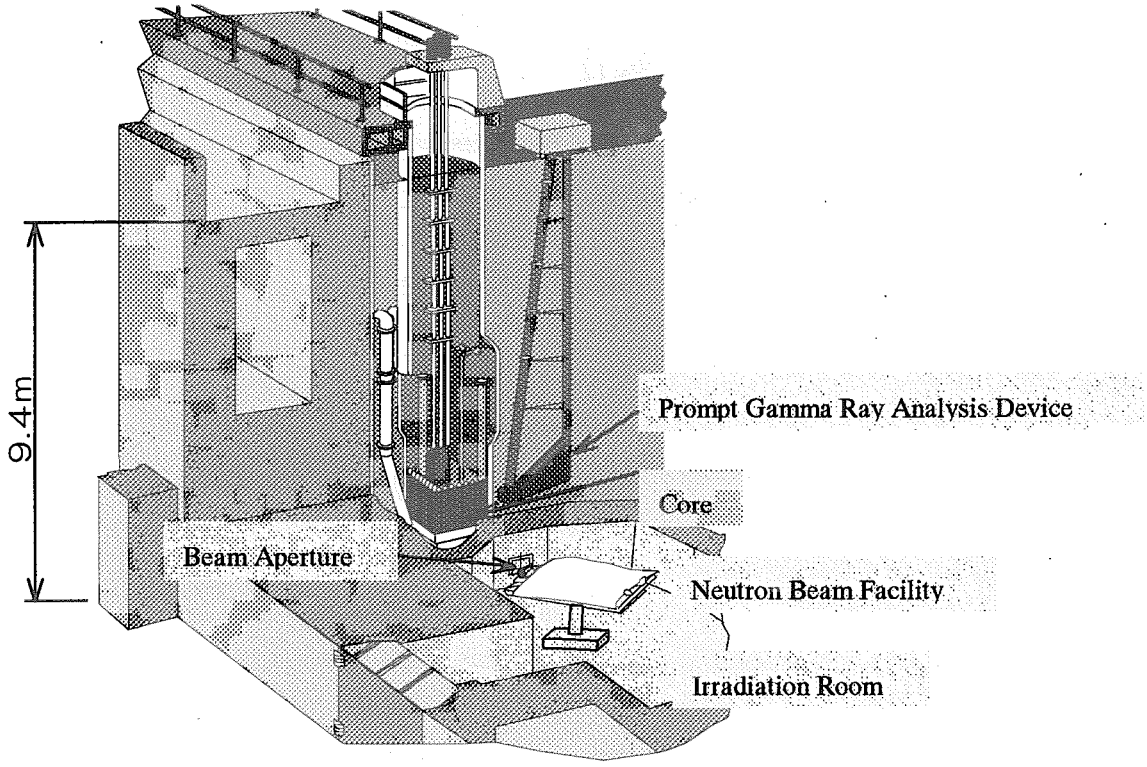

Fig.1 Bard eyes view of JRR-4

The beam experimental elements consist of Bismuth filter for reducing gamma-ray dose, Lead and graphite for neutron reflectors, LiF and B_4C for decreasing activation of structural materials, LiF collimator at beam port, and Borated polyethylene and lead blocks set for shielding around the beam port. The irradiation room have sufficient space for setting angle of patients which is possible to adjust within 90 degree to left side, and 60 degree to right side. The medical treatment room and patient-monitoring area were also prepared adjacent to the irradiation room. Patient monitoring area was installed video monitor, neutron and gamma rays area monitor in the irradiation room.

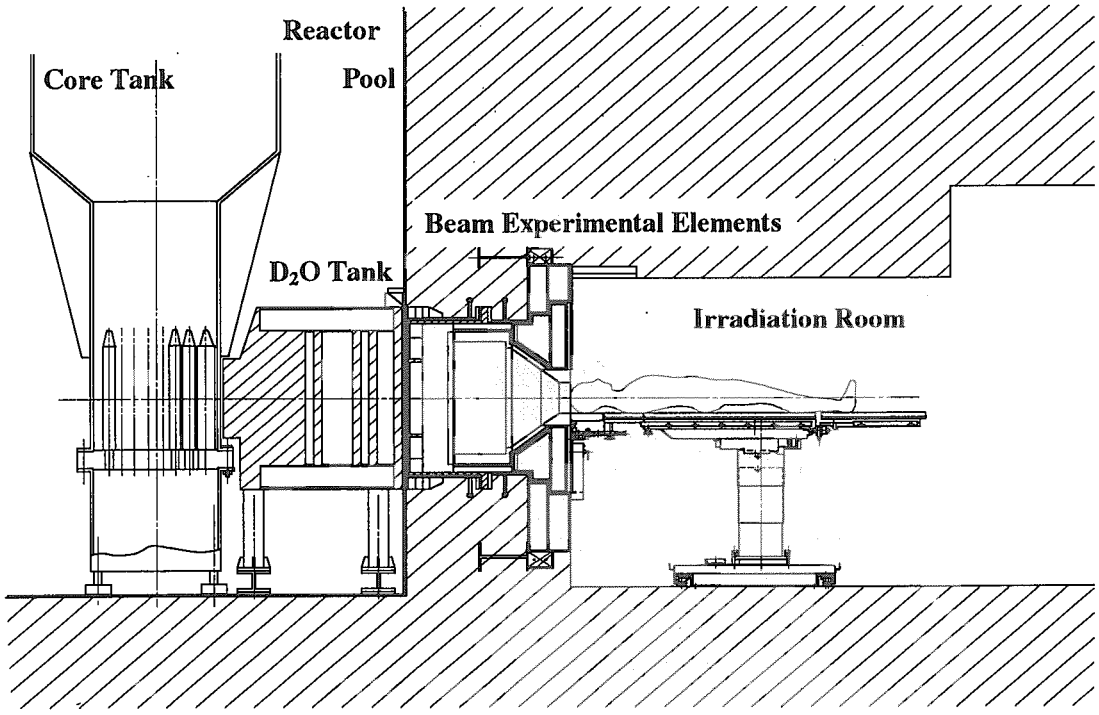

Fig. 2 Cross Section of JRR-4 Medical Irradiation Facility

4. Boron Concentration Measurement

The boron concentration of patient blood was measured using prompt gamma ray analysis (PGA) device. JRR-4 has no horizontal experiment tube, which can use for PGA. Therefore, thermal neutron is transferred in the neutron guide tube using the neutron mirror (the super mirror) to the top of reactor pool, and the prompt gamma-ray analysis is carried out. Neutron guide tube with the super mirror consists 8m length was adopted in order to obtain sufficient thermal neutron flux at measurement position which is necessary for the analysis of the boron concentration. As a super mirror of the neutron guide tube, flat surface glass that alternately coated 124 layers of nickel and titanium was used, it has the performance of two times further than the nickel mono layer. Crystalline Bismuth was installed in the neutron beam aperture in order to shield the gamma ray, which comes from reactor core. The boron concentration measurement at JRR-4 is performed by taking the ratio of the peak areas of B-10 and hydrogen. The method of using the ratio is not affected to difference of sample value and neutron flux density. A Ge detector measures the prompt gamma ray that the sample radiates. By this spectral data, boron peak area and hydrogen peak area are calculated to obtain the peak area ratio (B/H ratio). The boron peak becomes trapezoid-shaped by the Doppler shift because radiation of prompt gamma-ray from the Li-7 particle with high speed motion. Fitting function was defined in order to accurately integrate trapezoid-shaped peak area, and nonlinear fitting program to this function as known Error Function was developed. This program similarly carries out the fitting of hydrogen peak area to the Gaussian curve, and the area would be

calculated. We made a calibration curve using standard boron acid solution and blood with BSH(mercaptoundecahydrododecaborate). Patients boron concentration of blood was measured using B/H ratio to concentration calibration curve. The required measurement time is only 5min for obtain sufficient accuracy from 1 cm^3 blood sample.

5. Thermal Neutron Flux Measurement

Thermal neutron flux is measured using Au foil activation method with coincidence counting device. Absolute activity measurement is usually carried out finding efficiency of the detector. But the determination of the efficiency is very difficult because usually the shape of sample and standard radiation source are different and the standard radiation source has error to definition of the accuracy. The use of coincidence courting method often affords the most practical technique for measuring the absolute activity of a given radioisotope source. Beta – gamma coincidence counting as shown as follows. The system has auto sample changer therefore it is available for much samples measurement.

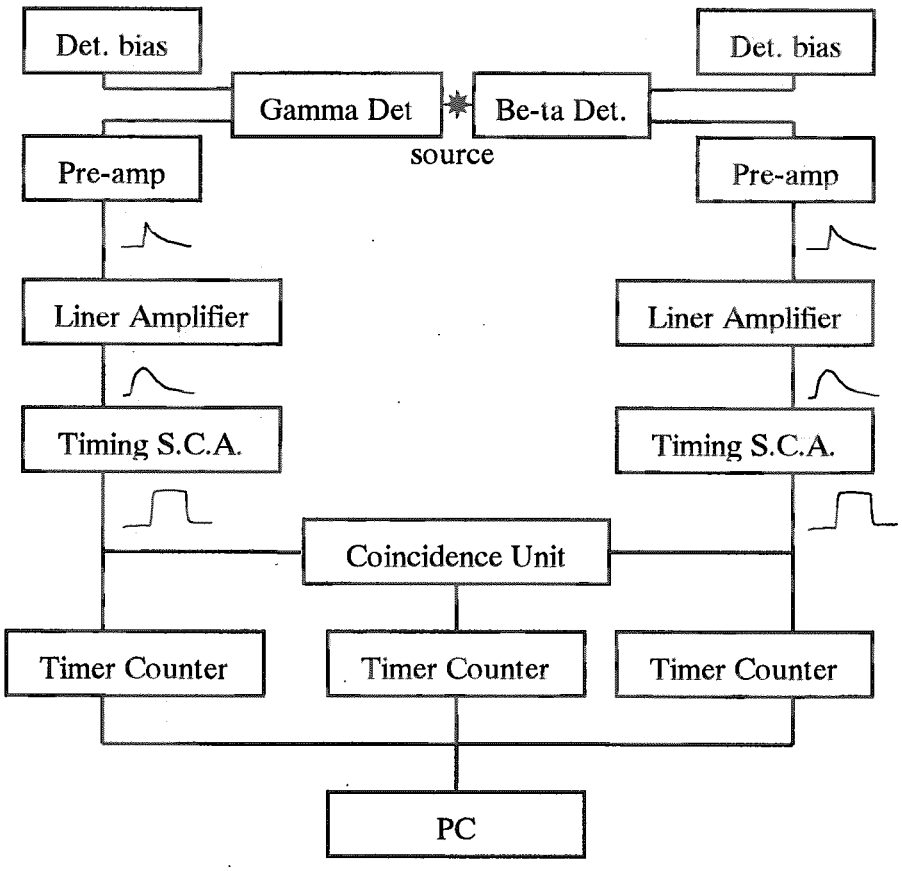

Fig. 3 Beta Gamma Coincidence counting system

6. Conclusions

The first medical irradiation for BNCT of JRR-4 was carried out on October 25, 1999. In that case, the patient was treated by the Tsukuba University group used mixed thermal and epithermal neutron generated the above TNB I. And as for reactor power, 2MW was selected in order to get necessary time for dose determination. The status of irradiation of first patient is shown Fig. 3. Since then, total seven times of BNCT irradiation were performed at JRR-4 by Dr. Matsumura as Tsukuba Univ. and Dr. Nakagawa as national Kagawa children's hospital by the end of June 2000. In the BNCTs, we carried out boron concentration and neutron flux. The doctors used these data for determination of irradiation time.

Reference

1) K. Yokoo, T. Yamada et al., Advances in Neutron Capture Therapy. Vol. I, Medical and Physics, ed. by B. Lasson et al., 1997, 326-230
2) T.Kishi, Y.Torii et al., Abstract of Eighth International Symposium on Neutron Capture Therapy for Cancer. La Jolla, California, USA, September 13 –18 abstract, 1998, p83
3) Y.Torii, T.Kishi et al., JAERI-Conf 99-006, 1999, 228-231
4) K. Yokoo, Y. Torii et al., Measurement of Thermal Neutron Flux for BNCT in JRR-2, JAERI-M 94-058, 1994
5) Glenn F. Knoll, Radiation Detection and Measurement Second edition, 1989

JP0250119

1.35 Development of Computational Dosimetry System and Measurement of Dose Distribution in Water Head Phantom for BNCT in JAERI

H. KUMADA[1], K. Yamamoto[1], Y. Torii[1], A. Matsumura [2],
T. Yamamoto [2], Y. Nakagawa [3], Y. Horiguchi[1]

1: Japan Atomic Energy Research Institute,
Ibaraki 319-1195, Japan
2: Institute of Clinical Medicine, University of Tsukuba,
Ibaraki 305-8575,Japan
3: National Kagawa Children's Hospital,
Kagawa 765-8501, Japan

Abstract

A new medical irradiation facility has been installed in JRR-4 in 1998. By using this facility, it is possible to initiate the research and development of BNCT with epithermal neutron beam more suitable for deep brain tumor. A new treatment planning software: Computational Dosimetry System (JCDS), which can calculate the dose distribution in a patient head accurately by MCNP Monte-Carlo code, is in progress its development for carrying out BNCT in JRR-4. Also, Free beam and phantom experiments at neutron beam facility in JRR-4 are being performed in order to measure neutron and gamma distribution concurrently, because the experimental data can be applied to verification of JCDS.

In this report, the current status of the development of JCDS and results of the experiments will be described.

Keywords: BNCT, JRR-4, BNCT, Epithermal Neutron Beam, Treatment Planning, JCDS, Computational Dosimetry, Phantom experiment

Introduction

It is necessary to adequate estimate irradiation dose in patient head in order to carry out BNCT. In IOBNCT that carried out currently in Japan, thermal neutron flux distribution and gamma dose in patient head are measured by using Au wires and TLDs respectively. Also Boron concentration is determined by using PGA. By these data acquired, irradiation dose in the head can be estimated and irradiation time are decided. It is important to comprehend the thermal neutron flux distribution in the head due to attribute to the dosimetry. Therefore thermal neutron flux and gamma dose distribution are measured by experiments of water head phantom so that dose distribution in the head are grasped accurately. These measurement data not only can be used to the dosimetry for the actual BNCT is executed at JRR-4, but also is able to be applied for verification of JCDS.

By using medical irradiation facility that was installed at JRR-4, it is possible to carry out BNCT with epithermal neutron beam as well as thermal neutron BNCT. However, at the epithermal neutron BNCT, dosimetry measurement at inner brain was impossible, therefore it is necessary to precise calculate dosimetry for preparation of treatment planning before BNCT operation. Currently new treatment planning software; Computational Dosimetry System (JCDS), which can calculate the dose distribution in the patient head by Monte Carlo Code and support to prepare treatment planning beforehand, is being developed in JAERI in order to carry out the epithermal neutron BNCT.

Water Head Phantom Experiments

Grasping of thermal neutron flux distribution and gamma dose distribution in patient head are very important for the dosimetry at BNCT irradiation. Thermal neutron and gamma dose have a great influence on irradiation dose in the head because Nitrogen dose, Boron dose and gamma dose mainly attribute to irradiation dose. Nitrogen dose and Boron dose are depend on thermal neutron fluence proportionally, and gamma dose is calculated from integration of gamma-ray fluence which is generated from secondary source of Hydrogen to neutron capture reaction. Therefore, water head phantom experiments are carried out for measurement of thermal neutron flux and gamma dose distributions in order to comprehend dose distribution in the head precisely.

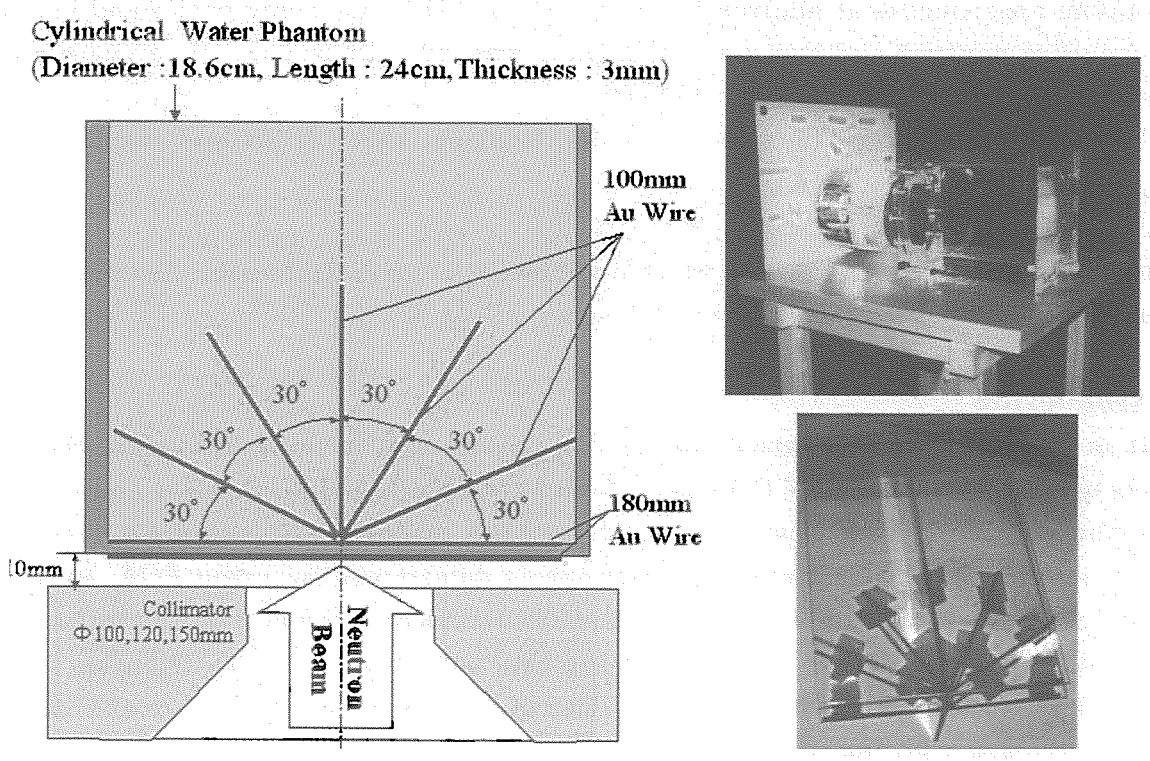

Fig.1 Configuration of Au wires for measurement two-dimensional distribution of thermal neutron flux in water phantom

A cylindrical water phantom of 18.6cm diameter and 24cm depth was put from the beam port with the gap for 1cm. Au wires and/or TLDs are inserted within the phantom for measurement thermal neutron flux and gamma dose distributions respectively. By disposing Au wires as radial in the phantom, it is possible to measure the flux distributions as two-dimensional in order to accurate estimate the irradiation dose in patient head at BNCT. (Fig.1) The phantom within Au wires or TLDs are irradiated at respective beam modes at neutron beam facility.

Fig.2 is shown the thermal neutron flux distribution with Thermal Neutron Beam mode 1 (TNB1 mode) and Epithermal Neutron Beam mode (ENB mode) with 15cm collimator. At TNB1 mode, maximum thermal neutron flux is approximately 6.0×10^{9} cm-2・sec-1 in the vicinity of about 5mm depth from the phantom surface, and maximum thermal neutron flux at ENB mode is about 4.0×10^{9} cm-2・sec-1. It is possible to recognize that the depth of peak region is about 2cm from phantom surface and is deeper than TNB1 one.

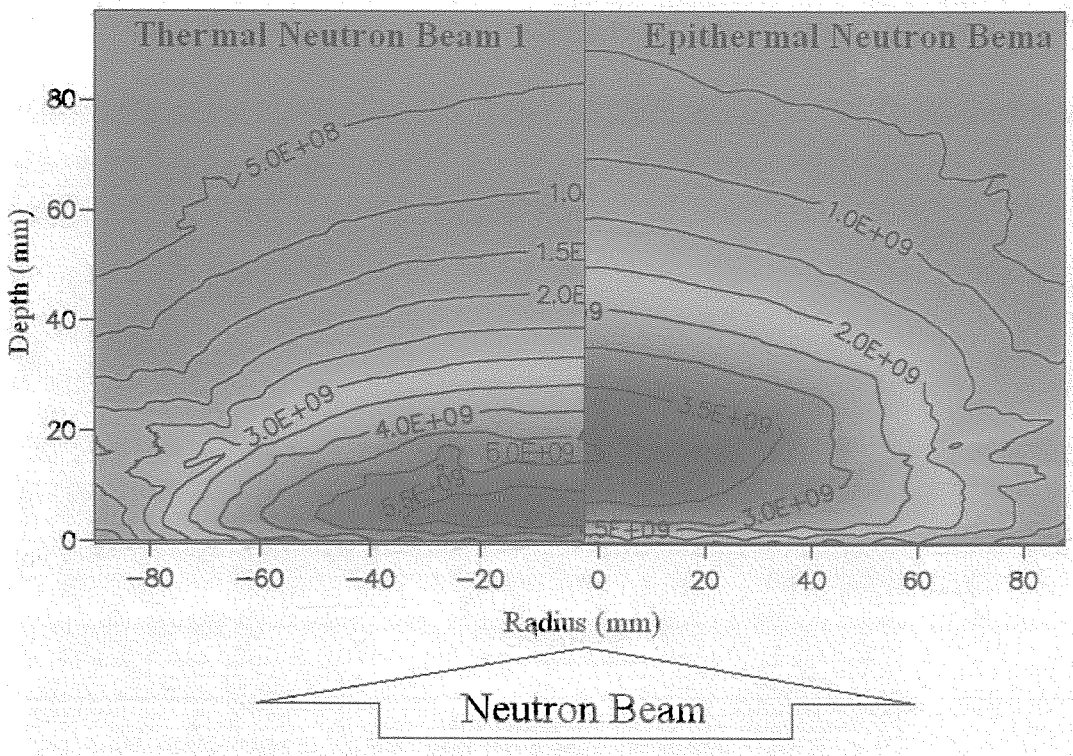

Fig.2 Thermal neutron flux distribution in water phantom that compared TNB1 mode with ENB mode at ϕ150mm collimator.

Development of Computational Dosimetry System in JAERI

Computational Dosimetry System (JCDS) that is necessary to carry out the epithermal neutron BNCT is be developing in JAERI. JCDS can estimate of dose distribution in the patient head by Monte Carlo code. By using JCDS at BNCT operation, adequate irradiation conditions such as beam mode, patient irradiation position and irradiation time can be decided and treatment planning is able to be prepared beforehand.

JCDS is comprised of three components such as Preprocessing, Dose calculation processing, and Post-processing. Preprocessing could create detailed numerical models for dose calculation by MCNP. The tissue components such as soft tissue, bone and air can be automatically selected from the CT data set, On the other hand, the tumor volume and the region of interest (ROI) can be specified by MRI images, because MRI allows differentiating among normal tissue and for example tumor. Therefore, by using CT and MRI data set together, it is possible to make a 3-D patient head image easily and correctly. This 3-D model is editable to simulate the surgical processes, such as skin flap opening and bone removal. By these procedures, a calculation condition is specified, and a numerical model for the calculation is generated (Fig.3).

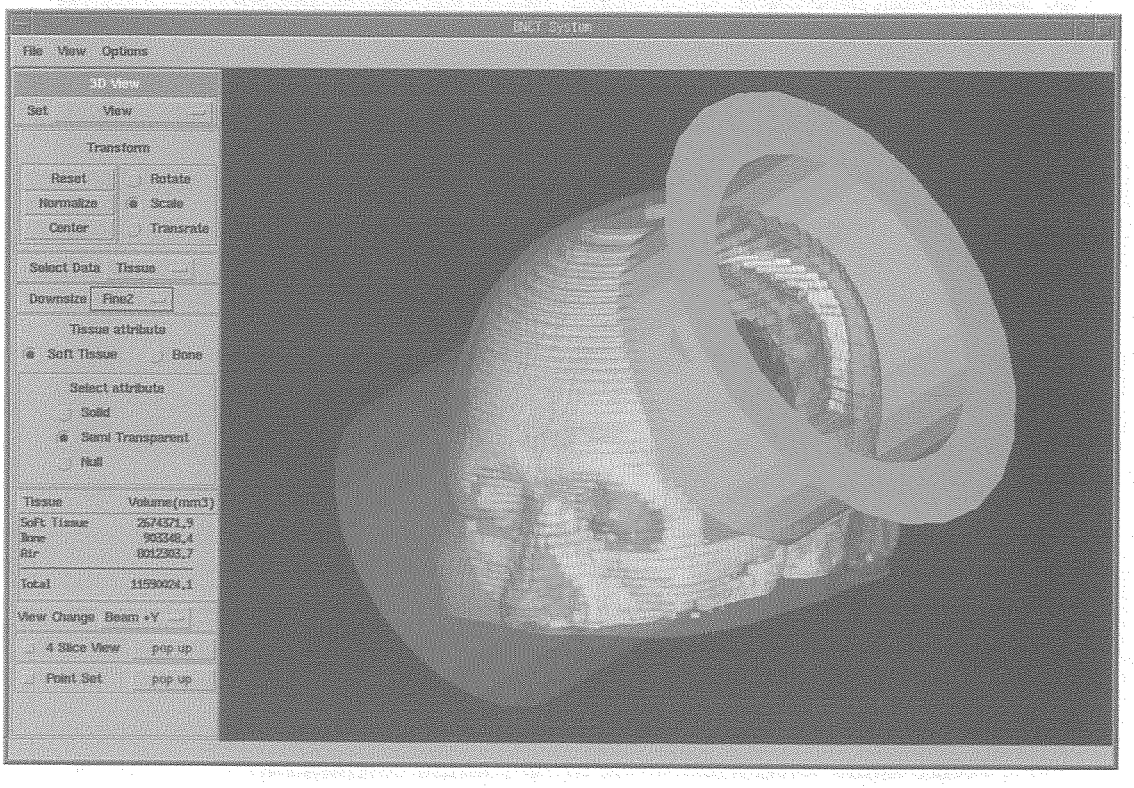

Fig.3 3D patient head model determined calculation conditions for the dosimetry by MCNP.

Utilizing the numerical models from preprocessing, the neutron and gamma ray distributions are calculated by MCNP Monte Carlo code. By Post-processing, Fig.4 is shown the dose distributions so obtained can be displayed on the 3-D head image or CT and MRI images as a contour, and total dose to normal tissue, tumor and target volume and any ROI are displayed. Finally, Post-processing can provide adequate information for preparation of treatment planning. By using JCDS, irradiation conditions such as beam mode, irradiation time, and beam angle with a patient are decided, and a treatment planning for BNCT operation can be prepared.

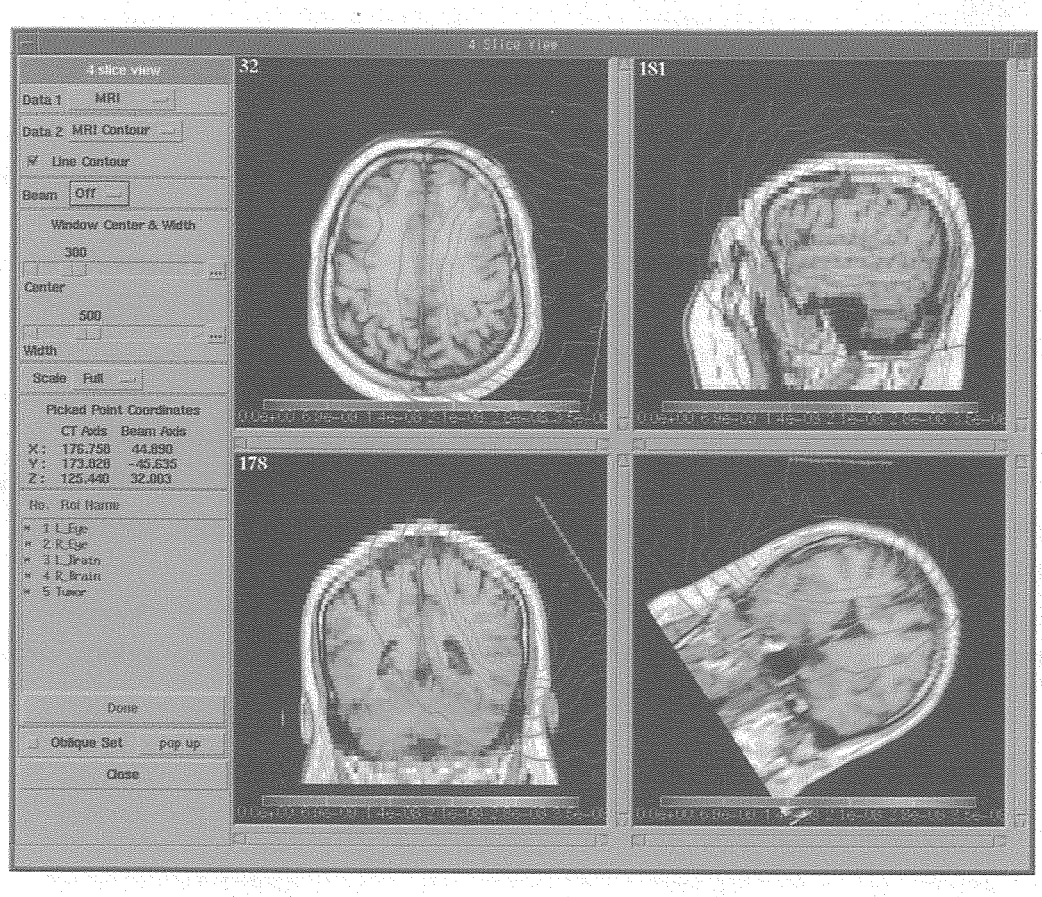

Fig.4 Dose distribution drawn on MRI medical images as a contour

System Characteristics

This system will be designed to work with the UNIX and Windows operating System. For the purpose of efficient utilization, the system will operate on a network. Virtual CT or MRI images are available simultaneously in order to create a numerical model precisely for MCNP calculation. It is possible to use JCDS for BNCT with craniotomy currently done by Japanese medial group because the 3-D head image could be edited to simulate surgical procedures. By applying JCDS to the thermal neutron BNCT, the more precise posterior evaluation of BNCT can be performed. JCDS could transfer the information that is necessary to the patient setting to the Patient Setting System that can support more accurate setting to the actual irradiation position.

Conclusion

New treatment planning software; JCDS is in progress its development in JAERI in order to carry out BNCT with the epithermal neutron beam. At present, JCDS is being verified for precise dosimetry and calculation more. Several data acquired from water phantom experiments and actual BNCT carried out currently are applied for verification the system.

Reference

1) Y. Torii, T. Kishi et al., JAERI-Conf 99-006, 1999, p228-231
2) JAERI-Conf 2000-013 Proceedings of Neutron Irradiation Technical Meeting on BNCT, March 13, 2000, p25-36
3) K. Yokoo, Y. Torii, F. Samaria, K. Koibuchi et al., JAERI-M 94-058 Measurement of Thermal Neutron Flux for BNCT in JRR-2, 1994,
4) H. Kumada, Y. Nakagawa, A. Matsumura et al., 1998 Abstract of Eighth International Symposium on Neutron Capture Therapy for Canner. La Jolla, California, USA, September 13-18 abstract, 1998, p58
5) K. Yamamoto, H. Kumada, Y. Torii, et al., Program & Abstracts Ninth International Symposium on Neutron Capture Therapy for Cancer. 2000, p243-244
6) H. Kumada, K. Yamamoto, Y. Torii, A. Matsumura, et al., Program & Abstracts Ninth International Symposium on Neutron Capture Therapy for Cancer. 2000, p281-282
7) N. Hori, T. Yamamoto, A. Matsumura, et al., Program & Abstracts Ninth International Symposium on Neutron Capture Therapy for Cancer. 2000, p263-264

JP0250120

1.36 Carboranyl Tetrahydroisoquinolines. Synthesis and the X-ray Structural Study of 1-(*o*-Carboran-1-ylmethyl)-1,2,3,4-Tetrahydroisoquinolines

Jong Dae Lee,[†] Chai-Ho Lee,[‡] Seung-Hoon Lee,[§] Sang-Moo Lim,[@] Sungil Cho,[#] and Sang Ook Kang[†]

[†]Department of Chemistry, Korea University , 208 Seochang, Chochiwon, Chung-nam 339-700, Korea. [‡]Department of Chemistry, Wonkwang University, Iksan, Jeonbuk 570-749, Korea. [§] National Cancer Center, Ilsan, Goyang, Kyungi-do, Korea. [@]Korea Cancer Center Hospital, Gongnung, Seoul, Korea. [#]Department of Chemical Engineering, Junnong-dong 90, Seoul City University, Seoul 130-743, Korea.

Synthesis of the first fully characterized boronated tetrahydroisoquinolines is reported. Thus, tetrahydroisoquinolines containing 1-(*o*-carboran-1-ylmethyl)-1,2,3,4-tetrahydroisoquinolines have been synthesized from the corresponding arylethylamines to provide carboranes attached to functional group capable of being covalently incorporated into structures of potential use in boron neutron capture therapy (BNCT). The carboranyl functionalities were attached at the 1-position of the tetrahydroisoquinoline molecule. Experimental details and analytical data leading to the identification of the reported compounds are provided. Additionally, the X-ray diffraction structure of **9b** is reported.

Introduction

1,2,3,4-Tetrahydroisoquinolines present in mammalian brain plays a major role in therapy of variety of neurological disorders.[1] In particular, 1-arylmethyl-1,2,3,4-tetrahydroisoquinolines 1 has been reported to be a potent dopamine antagonists as neuroleptic agents.[2] As part of a program of synthesis and evaluation of tetrahydroisoquinolines in the treatment of cancer,[3] we have proposed that compounds containing *o*-carborane cages linked to 1-tetrahydroisoquinolines would form a useful method of delivering borons in brain tumors. Therefore, the aim of this work was to synthesize and determine the characteristics of 1-(*o*-carboran-1-ylmethyl)-1,2,3,4-tetrahydroisoquinolines containing *o*-carboranes as a new boron-rich class of tetrahydroisoquinoline analogues, which may allow the advantage of BNCT.[4]

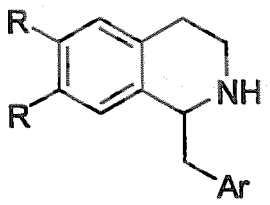

1

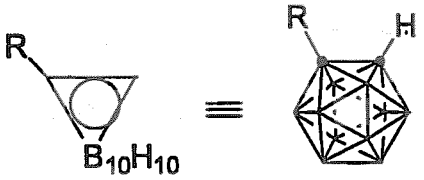

2a, R = H
b, R = Me

In this paper, we discribe the synthesis of 1-(*o*-carboran-1-ylmethyl)-1,2,3,4-tetrahydroisoquinolines 7 and 9 which benzyl groups of 1 are replaced by the boron clusters, for new BNCT agents and dopamine antagonists. And key spectral properties for 7 and 9 are presented along with the data obtained from the single crystal X-ray structural determination of 9b.

Result and Discussions

Synthesis of 1-(*o*-carboran-1-ylmethyl)-1,2,3,4-tetrahydroisoquinolines (7). The general synthetic strategy for the preparation of the starting materials used to prepare the reported *o*-carboranylacetaldehydes (5) relied on the methods developed by Rudolph. The synthesis of 5 was accomplished in three steps (Scheme 1).

Scheme 1

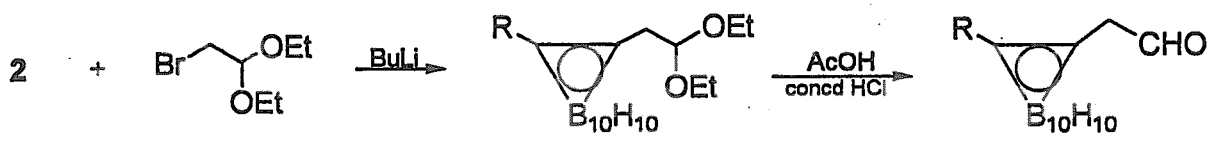

3

4a, R = H
b, R = Me

5a, R = H
b, R = Me

The synthesis was initiated by the monoalkylation of *o*-carborane derivatives (2). When *o*-carborane was reacted with an equimolar quantity of *n*-butyllithium in a mixture of ether and benzene (1:2 ratio), followed by reaction with 3, diethyl acetal (4) was formed in high yield. The resultant diethyl acetal (4) was reacted with acetic acid in the presence of concentrated HCl. The *o*-carboranylacetaldehyde (5) was formed in excellent yield.

With this carboranylacetaldehyde (5) now available, the Pictet-Spengler reacton (dipolar cyclocondensation) with the arylethylamine (6) was investigated (reaction 1). Dipolar cyclocondensation of arylethylamine with aldehyde proceeds under mild conditions; this methods of hetero-cyclic ring formation was investigated as a route to the target compounds. Thus, this condensation was finally achieved in 50-60% yield by refluxing the mixture of 5 and 6 in a formic acid solution.

All products in the synthesis were examined by ^{1}H NMR and IR spectroscopy. The introduction of the *o*-carborane cage into a molecule can be identified by particular features of their spectra. In the IR the B-H stretch at ca. 2600 cm^{-1} is relatively strong. In the ^{1}H NMR spectrum, however, the hydrogens attached to the boron in the carborane cage appear as a broad unresolved band in the region 1.3-3.2 ppm.

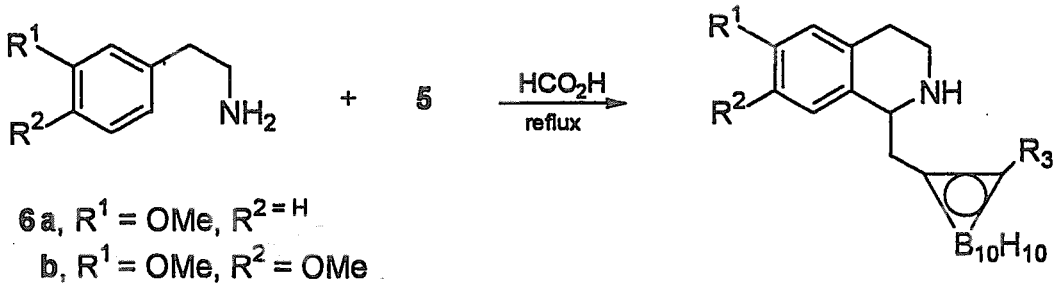

(1)

6a, R^1 = OMe, R^2 = H
b, R^1 = OMe, R^2 = OMe

7a, R^1 = OMe, R^2 = H, R^3 = H
b, R^1 = OMe, R^2 = H, R^3 = Me
c, R^1 = OMe, R^2 = OMe, R^3 = H
d, R^1 = OMe, R^2 = OMe, R^3 = Me

To provide a *o*-carborane with tetrahydroisoquinoline directly attached to C-1, a strategy based on an α-sulfamidoalkylation reaction was employed (Scheme 2). Following the standard method for the synthesis of tetrahydroisoquinoline from sulfamides (**6**) and acetal (**4**) at elevated temperatures in the presence of a formic acid solution, the tetrahydroisoquinoline (**9**) was formed from sulfamide (**6**) and *o*-carboranylacetal (**4**) in 80-90% yield. A formic acid solution of an sulfamide **6** and acetal **4** was heated at refluxed to give the corresponding **9** in 80-90% yield.

Scheme 2

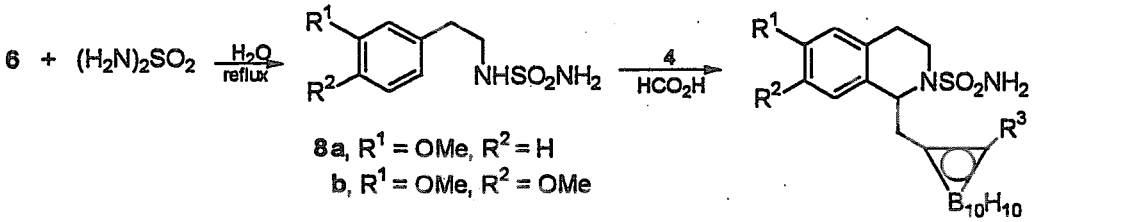

8a, R^1 = OMe, R^2 = H
b, R^1 = OMe, R^2 = OMe

9a, R^1 = OMe, R^2 = H, R^3 = H
b, R^1 = OMe, R^2 = H, R^3 = Me
c, R^1 = OMe, R^2 = OMe, R^3 = H
d, R^1 = OMe, R^2 = OMe, R^3 = Me

Conclusions

Compounds 7 and 9 are the first fully characterized boronated tetrahydroisoquinolines to be reported and contains one *o*-carborane cage covalently linked to the tetrahydroisoquinoline periphery. These boronated tetrahydroisoquinolines may be useful as a tumor-selective sensitizer for boron neutron capture using thermal neutrons to activate ^{10}B through the $^{10}B(n, \alpha)^7Li$ reaction. Studies evaluating the *in vitro* and *in vivo* localizing ability of 7 and 9 are currently being carried out and will be reported in an appropriate venue in the near future.

References

1. Yates, F. S. in *Comprehensive Heterocyclic Chemistry*, Boulton, A. J.; McKillop, A. Eds.; Pergamon Press: Oxford, 1984; pp. 511-524.
2. Shamma, M. *The Isoquinoline Alkaloids, Chemistry, and Pharmacology*, Academic Press, New York, 1972.
3. Stork, G.; Guthikonda, R. N. *J. Am. Chem. Soc.* 1972, *94*, 5109.
4. Soloway, A. H.; Tjarks, W.; Barnum, B. A.; Rong, F.-G.; Barth, R. F.; Codogni, I. M.; Wilson, J. G. *Chem. Rev.* 1998, *98*, 1515.

JP0250121

1.37 Neutronic Design Approach to a Small Medical Reactor for BNCT

Nam Zin Cho
Korea Advanced Institute of Science and Technology
Department of Nuclear Engineering
373-1 Kusong-dong, Yusong-gu, Taejon, Korea 305-701
Email : nzcho@mail.kaist.ac.kr

Abstract

To provide high quality neutron beams for BNCT using a small reactor, two types of reactor cores are designed: a square core with rod-type fuel in hexagonal cells and a rectangular slab core with plate-type fuel.

1. Introduction

BNCT is a binary radiation therapy modality that brings together two components that when kept separate have only minor effects on cells. The first component is a stable isotope of boron, ^{10}B that can be concentrated in tumor cells. The second is a beam of low-energy neutrons. ^{10}B in or adjacent to the tumor cells disintegrates after capturing a neutron. This interaction produce high energy, high linear energy transfer, short-range radiation of ^{4}He nuclei(i.e. α particles) and recoiling ^{7}Li ions that would be confined to the tumor and destroy its cells.

Currently available epithermal neutron beams are produced directly from the reactor core but they are not sufficiently intense to meet the anticipated demand for BNCT treatments. There is another method of generating an epithermal neutron beam, namely a ^{235}U fission plate set in the thermal column of low-power reactor. To get a high-intensity, high-quality epithermal neutron beam for BNCT, fission converter-based epithermal neutron beam has been designed for the MIT Research Reactor, the Brookhaven Medical Research Reactor (BMRR) and the Musashi Reactor.

This paper describes two types of medical reactors, square core reactor and plate type fuel based reactor respectively. One (type 1) is a square core with four assemblies and inner D_2O tank. The ^{235}U loading of the core is consist of 1056 fuel rods using U_3Si-Al cylindrical type fuel. The other, type 2, is a based on plate type U_3Si_2-Al fuel, has four epithermal neutron beam collimators. Both types have a maximum operating power of 300kW.

2. Design Goals

Thermal neutrons are attenuated exponentially in tissue with half-value layers of 1.5 to 2.5cm and

could effectively irradiate tumors <3-cm depth. Thermal neutrons are appropriate for use in irradiating skin tumors or tumors in small animals such as rats and mice. Epithermal neutrons have a lower probability of interacting with and damaging the skin as they enter. This probability then gradually decreases with greater depths. These would be used to treat tumors from 2- to 8-cm depth.

Neutron beams used for BNCT are designed to meet the best dosimetric conditions for patients. The design goals in this study are a thermal neutron flux $>3.0\times10^{9}$ n/cm^2·sec, the dose from fast neutrons $<3.0\times10^{-13}$ Gy·cm^2/n, the dose from gamma rays $<2.0\times10^{-13}$ Gy·cm^2/n, and an epithermal flux $>1.0\times10^{9}$ n/cm^2·sec for type 1 and $>1.0\times10^{10}$ n/cm^2·sec for type 2. Forward directed beams (ratio of neutron current-to-flux, J/φ, close to 1) offer better dosimetry in the target than do isotropic beams.

3. Designs and Results

The design results of the two types of nuclear reactors, a square reactor with two epithermal neutron beams and two thermal neutron beams, and a plate fuel based reactor with four epithermal neutron beams, are as follows. The square reactor(type 1) provides an epithermal neutron beam of $>3.2\times10^{9}$ n_{epi}/cm^2·sec intensity with low contamination by fast neutrons($<1.6\times10^{-13}$ Gy·cm^2/n_{epi}) and gamma rays($<1.0\times10^{-13}$ Gy·cm^2/n_{epi}) and a thermal neutron beam of 8.9×10^{9} n_{th}/cm^2·sec intensity with low contamination by fast neutrons ($<1.1\times10^{-13}$ Gy·cm^2/n_{th}) and gamma rays($<1.2\times10^{-13}$ Gy·cm^2/n_{th}). Both neutron beams are highly forward-directed with low contamination by fast neutrons and gamma rays.

On the other hand, type 2 reactor provides an East-West regional epithermal neutron beam of 1.7×10^{10} n_{epi}/cm^2 sec intensity with low contamination by fast neutrons($<2.2\times10^{-13}$ Gy·cm^2/n_{epi}) and gamma rays($<1.4\times10^{-13}$ Gy·cm^2/n_{epi}) and a North-South regional epithermal neutron beam of 1.3×10^{10} n_{epi}/cm^2·sec intensity with low contamination by fast neutrons ($<3.0\times10^{-13}$ Gy·cm^2/n_{th}) and gamma rays($<2.0\times10^{-13}$ Gy·cm^2/n_{th}).

The heat generated in the core can be removed by natural convection through a pool of light water. The proposed design in this study could be constructed for a dedicated clinical BNCT facility that would operate very safely.

4. Conclusions

The two types of reactor cores designed produce high quality neutron beams for use for BNCT. Type 1 reactor provides very good epithermal neutron beams and also provides relatively good thermal neutron beams. Type 2 reactor designed to provide epithermal beams produce epithermal flux in excess of 1×10^{10} n/cm^2, surpassing the neutronic design goals. The neutron beams of both reactors are forward-directed with low contamination by fast neutrons and gamma rays. The low operating power of 300kW allows the proposed reactors to be installed in a medical facility dedicated to BNCT.

This is a blank page.

2. Summary Reports

This is a blank page.

2.1 SUMMARY REPORT FROM THE WORKSHOP ON THE RESEARCH REACTORS

NOVEMBER 20 – NOVEMBER 24, 2000

TAEJON, KOREA

This document presents a summary on the implementation of the ninth Workshop on the Utilization of Research Reactors held in Taejon from November 20 to November 24, 2000. It was attended by scientists and specialists from Australia, China, Indonesia, Japan, Korea, Malaysia, Thailand and Vietnam.

Dr. Chang In Soon - president of KAERI, welcomed participants, and opening remarks by the Ministry of Science and Technology of Korea and Science and Technology Agency of Japan followed. Three general lectures were composed of topics closely related with research reactor – UMo fuel development, BNCT for malignant brain tumor, and new technology for the medical application of RI.

The workshop discussed three different fields of activities, namely, neutron scattering, neutron activation analysis, and research reactors and utilization technology (BNCT). A summary of the discussions, progress reports and future programs of each group are presented below.

I. NEUTRON SCATTERING

A sub-workshop on the utilization of SANS instruments and the evaluation of data was held from November 20 to 23 in KAERI, Daejon (Korea). Topics ranged from the study of the structure of polymer materials to the porosity of glassy-carbon materials. Participants gained valuable experience in the design of SANS experiments, sample preparation, data reduction and analysis.

Progress Report on Collaborative Activities for 1999/2000

Two approved projects that cover a number of research topics are currently in progress: (1) Small-angle Neutron Scattering (SANS), and (2) Structural Analysis of Functional Materials. Reports on these projects were presented and discussed.

1. Small-Angle Neutron Scattering

Regional collaborative activities in SANS are identified under four headings.

1.1 SANS Instrument Calibration

The scattering intensity from a polystyrene-h/polystyrene-d (PSH/PSD) binary polymer mixture prepared by Prof. Matsushita (Nagoya University) was calibrated on the SANS-J instrument at JAERI and data collected on the SANS instrument at KAERI. The results obtained were of excellent quality

and, therefore, the sample is suitable for use as one of the primary absolute cross-section standards for instruments in the region. In addition, an inter-laboratory comparison for instrument q calibration using silver behenate was successfully completed for the SANS instruments at KAERI, JAERI, BATAN and ANSTO.

MILESTONE

- Under the FNCA programme, all SANS instruments in the region have been calibrated in q.
- A series of standards for the absolute cross-section. This will be achieved by a thorough evaluation of all available standards including water, LUPOLEN and porous silica.

1.2 SANS and Soft Condensed Matter

There are three topics under investigation: strain induced crystallisation of natural rubber; miscibility of polymer blends; and microstructure of polymer gels. SANS data have been collected on these three systems and data analysis is in progress. Detail of the investigations is contained in the Summary Report of the Sub-workshop on Neutron Scattering.

MILESTONE

- Detailed analysis and interpretation of the SANS data with assistance from specialist research collaborators in the participant's institute. For example, SANS results from polymer blends must be interpreted with the assistance of a specialist polymer chemist.
- Sharing the results of all studies between participating countries.

1.3 SANS and Condensed Matter

Because of the potential industrial importance, glassy-carbon systems prepared from the combustion of palm-oil tree waste materials are under investigation. The effect of polymer binder on the microstructure of the system is important to their end-use in industrial application such as a catalyst.

MILESTONE

Porosity will be the first structural feature studied using the SANS technique.

- The results of a systematic structural study of a wide range of glassy-carbon polymer samples will be compared with results from other techniques.
- As a collaborative project SANS beam time will be sought at regional facilities.
- The data analysis will be carried out and results shared between participating countries.

1.4 SANS Data Reduction and Analysis

It is crucial to the success of SANS experiments to accurately correct the scattering data for instrumental and background effects. To date, this correction has been accomplished using a number of strategies adopted by individual institutes and it is recognised that there are distinct advantages in

sharing these strategies.

The analysis of the corrected data has been undertaken with a variety of computer programs including IGOR, JAERI and ILL software packages. Each package has advantages.

MILESTONE

- Standardization of data reduction procedures will be in accordance with those established at JAERI.
- The IGOR® software package will be adopted for the analysis of corrected scattering data wherever possible, and programs for a variety of analyses shared amongst institutes in the region.
- Standard data storage format in the short term requires a detailed description of all instrument and data parameters. In the future an international standardized data format may be adopted.

2. Structural Analysis of Functional Materials

The following projects were discussed and the agreements is that all will be continued.

2.1 High Tc Superconductor

There are two topics on the high Tc superconductor project, both based on the BSCCO (2223) system. The first topic was the preparation of Pb and Sb doped BSCCO system by Vietnam researchers. Samples of $Bi_{2-x-y}Pb_xSb_ySr_2Ca_2Cu_3O_z$, where x = 0.1 - 0.8 and y = 0.1 – 0.4 were synthesized. After processing, the temperature dependent resistivity of these samples was measured using the four-probe technique and the phase identification carefully studied using X-ray diffraction. In contrast to the BPSCCO samples, the BSSCCO sample displayed a new phase, called 4441, in the X-ray diffraction pattern and the T_c^{on} attained approximately 140K.

The second topic is the mechanism study of Co-doped BSCCO (2223). As agreed in 1999 Workshop on the Utilization of Research Reactor, the Joint Research Project on high temperature superconductor would be continued on the investigation of Co substitution for Cu in BSCCO (2223). The samples of $Bi_2Sr_2Ca_2(Cu_{(1-x)}Co_x)_3O_y$ where x = 0.0, 0.01, 0.02, 0.04, 0.06, and 0.08 were prepared by solid state reaction. Samples were sintered between 828-853C and then quenched in liquid nitrogen. Physical properties of the specimens were examined by standard four-probe technique to determine the critical temperatures. Phase identifications were performed using the X-ray diffraction technique. It was found that at a certain sintering temperature, increasing the amount of cobalt impurities suppressed the critical temperatures.

MILESTONE

- Bulk specimens of Sb and Co doped Pb-BSCCO (2223) synthesized under the proper conditions by Thailand and Vietnam researchers.
- Neutron diffraction results obtained by Indonesian researchers.

2.2 Permanent Magnet

The neutron diffraction pattern of commercially available permanent magnets of the Nd-Fe-B system will provide information on its phase separated structure that will be valuable for development of its utilization.

2.3 Superionic Conductors

In view of the application of Cu- and Ag-based superionic conductors as devices (e.g. capacitors and batteries) study of (i) detailed structure investigation (especially for the non-stoichiometric compounds) using HRPD, and (ii) investigation of the influence of stoichiometry on dielectric and electrical properties, could improve the quality of the bulk materials.

3. Presentations

1. Introduction of SANS Measurement (Dr. Robert KNOTT)
2. Introduction of SANS Facility in HANARO (Mr. SEONG Baek-Seok)
3. Introduction of Data analysis (Prof. HASEGAWA Hirokazu)
4. Explanation of HANARO SANS facility for data analysis (Dr. HAN Young-Soo)
5. Neutron Scattering in Australia (Dr. Robert KNOTT)
6. The Study of Artificial Articular Cartilage – PVA-Hydrogel by SANS (Mr. Tonghua YANG)
7. Current Status of Neutron Scattering in Indonesia (Dr. Abarrul IKRAM)
8. Current Status of Neutron Scattering in JAERI (Dr. HAMAGUCHI Yoshikazu)
9. Current Status of Neutron Scattering in KAERI (Mr. LEE Chang-Hee)
10. Current Status of Neutron Scattering in Malaysia (Dr. Abdul Aziz Bin MOHAMED)
11. Optimisation of Data Acquisition System For Mysans (Malaysian Small Angle Neutron Scattering) – Graphical User Interface (GUI) Personnel Computer Based (Dr. Abdul Aziz Bin MOHAMED)
12. Present Status of Neutron Scattering in Thailand (Mrs. Archara SANGARIYAVANICH)
13. High temperature superconductors of Pb and Sb doped Bi-Sr-Ca-Cu-O system (Ms. Phuong Thi Thu TRAN)
14. Introduction of the Research on Polymer Blends (Prof. HASEGAWA Hirokazu)
15. Residual Stress Analysis by Neutron Scattering (Mr. MINAKAWA Nobuaki)
16. SAX Facility at PAL and Its Applications in Materials Science (Prof. REE Moon-Hor)

4. New Collaborative Project Planned for 2001 and Beyond

The SANS collaborative research project is in the third year of an approved four year program. The project is achieving the stated goals of regional capability development and application to the study of polymers and related materials. In 2001 the focus will be on data analysis and interpretation, and linking with industrial partners.

The future activities in neutron scattering were discussed. In order to highlight the socio-economic benefits of neutron beam applications it was decided to include neutron reflectometry and residual stress/texture diffractometry as strong candidates for future plans. At the 2001 workshop submissions on the two techniques will be made and further discussion will be held. In the meantime participating countries will evaluate the potential application of these techniques in their respective end user communities.

4.1. Residual Stress/Texture Diffractometry

This project is potentially useful for a collaborative research program particularly for participating countries with a heavy-industry base. The residual stress technique is important in solving many problems including the aging of power generation and petrochemical plants, and the failure welded components. In 2001, participating countries will prepare project plans and discuss the possibility of commencing the research project in 2002.

4.2. Reflectometry

Reflectometry is a rapidly emerging technique with wide applications in many fields of scientific and industrial research. For example, reflectometry provides detailed structural information on thin films on surfaces such as detergents, polymers, semiconductors and biomaterials. In 2001, participating countries will prepare project plans and discuss with each other the possibility of commencing the research project in 2002.

5. We plan to publish our activity in Neutron News and to distribute our newsletter in 2001.

6. Recommendation

The neutron scattering group strongly recommends that a sub-workshop for the utilization of SANS instruments and cooperative research using SANS instrument will be held jointly with the 2001 Workshop on the Utilization of Research Reactor. The title of 'NEUTRON SCATTERING' would like to be modified to 'NEUTRON BEAM APPLICATIONS'.

2.2 SUMMARY REPORT OF SUB-WORKSHOP ON THE UTILIZATION OF SANS INSTRUMENT AND EVALUATION OF DATA

November 20-23, 2000

KAERI, TAEJON, KOREA

The Sub-Workshop was held over 4 days from Nov. 20 to 23, 2000, in KAERI-TAEJON (Korea). The participants were a total of 17 from Australia, China, Indonesia, Malaysia, Thailand, Vietnam, Japan and Korea.

Experiments and data analysis on the standard polymer samples and samples from several countries of table 1 were performed using the HANARO SANS instrument. In addition, two lectures on the analytical technique of SANS data and the talks on the introduction of SANS instrument and characterization of prepared samples were presented.

EXPERIMENTS

All the samples measured in this workshop are listed in the table 1 below.

Table 1. The SANS samples provided by participants

Number	Country	Name	Sample	Comments
1	Australia	Dr. Robert Knott	Deuterated PS in THF	
2			THF solvent	
3	China	Mr. Tonghua Yang	PVA-hydrogel	20kGy & 60kGy
4	Indonesia	Dr. Abarrul Ikram	Porous silica	
5	Japan	Dr. Hamaguchi Yoshikazu & Prof. Hasegawa Hirokazu	PSD/PSH	
6			PS-PEP	Edge view & Through view
7			Poly ball SS175	
8			DPB/HPI	
9			PS/PI	
10	Malaysia	Dr. Abdul Aziz Bin Mohamed	Carbon-glassy	4 samples
11	Thailand	Mrs. Archara SANGARIYAVANICH	Natural Rubber	

The number of samples prepared by participating countries exceeded the time available on the SANS instrument and careful selection, therefore, was required. The following samples were selected:

- Before the sub-workshop, data were collected on the two samples- Silver Behenate from Dr. Robert Knott and Poly ball ss175 in JAERI. The purpose of the experiments was to calibrate the SANS instrument in q and to check the smearing effect.
- Samples of natural rubber were prepared in Thailand. The strength of natural rubber is important in

engineering applications. It is known that the strength of rubber increases under strain and this effect can be explained by strain induced polymer crystallization. The purpose of the SANS experiments was to observe this effect. In the experiment, various SANS patterns were collected under normal and applied strain conditions.

- Samples of glassy-carbon were prepared in Malaysia. These samples originated from palm-oil fruit bunch waste products. The proposal is to process the waste products and develop value-added industrial materials for carbon-based conducting applications. SANS experiments were carried out to determine the porosity of the samples.
- A series of PVA-hydrogels were prepared in China. The development of dressings for damaged human tissue is important. In order to understand the relationship between clinical effectiveness and polymer structure, a series of gamma initiated PVA-hydrogels were prepared for study.
- The miscibility of polymers of different composition is important to the polymer industry particularly for manufacturing of consumer products with defined properties, as well as for the re-cycling of polymer materials. A deuterated polystyrene sample (MW approximately 100,000) was prepared in Australia to investigate the conformation of an important polymer in a good solvent (tetrahydrofuran).
- A sample of poly balls was prepared by Prof. Hideki Matsuoka, Kyoto University to observe the resolution of the SANS instrument. Regular spherical particles provide a characteristic SANS pattern.
- A sample of DPB/HPI (polybutadiene-d/ polyisoprene-h) polymer blend was prepared by Prof. Hasegawa to investigate the microstructure of a miscible polymer blend.
- The following SANS instrument calibration samples were investigated:
    - a PSH/PSD (polystyrene-h/polystyrene-d) binary polymer mixture supplied by Prof. Matsushita (Nagoya Univ.) for absolute intensity calibration.
    - a PS-PEP (polystyrene-poly (ethylene-alt-propylene)) block copolymer supplied by Prof. Hasegawa (Kyoto Univ.) for q calibration.
    - porous silica (supplied by Indonesia) for q calibration
    - silver behenate (prepared by Australia) for q calibration.

The SANS instrument was configured with a neutron wavelength of 0.644 nm and a q-range 0.05 nm^{-1} to 0.8 nm^{-1}. Under the guidance of KAERI scientists, participants observed the preparation of some samples, operation of the SANS instrument and collection of raw data. Total experiment time was about 96 hours.

DATA ANALYSIS

- The data collected on the silver behenate, PS-PI, and Porous silica sample were corrected for instrumental effects and independently analyzed for the q position of the diffraction peak as well as the uniformity of the scattering pattern.
- The PSH/PSD standard sample was corrected for instrument and background effects and the radius

of gyration and scattered intensity at zero q were determined.

- The Poly Ball ss175 was corrected for smearing effect of instrument and background effects.
- Data from the PS-PEP standard sample were corrected and analysed to demonstrate the two orthogonal views of scattering from a lamella structure.

  Data from the various samples provided by participants were corrected and analysed to explore the microstructural features of the sample.

RESULTS

- The results for the inter-laboratory comparison for q calibration using silver behenate, PS-PI, and Porous silica indicate excellent agreement. The expected diffraction peak of silver behenate at 1.1 nm^{-1} was closely observed on the three instruments. The diffraction peak of PS– PI sample at 0.272 nm^{-1} was clearly observed on the KAERI SANS and SANS-J. The results to calibration in q were a good agreement with JAERI, ANSTO, and BATAN.
- The results from the PSH/PSD standard sample were excellent quality and therefore provide a useful intensity standard for SANS instruments in the region. The measured radius of gyration was 5.27 nm and a good agreement with the result from JAERI.
- The results from the edge-view and through view of the PS-PEP standard sample clearly displayed the lamella structure.

  The results from various samples provided by participants displayed a number of interesting features.
- 4 glassy-carbon samples with various aging time were measured and the peak shift was observed with varying aging time. This result showed that the porosity of glassy-carbon increased with increasing aging time.

SANS SOFTWARE

The reduction of two-dimensional raw data to one-dimensional data was performed using KAERI and ILL software.

Through the discussion among the participants it was decided by the group to standardize on the macro package on IGOR® software for data analysis wherever possible. The programs for standard data analysis (Guinier Fits etc) will be shared amongst participants.

PROPOSAL FOR FUTURE ACTIVITIES

All participants discussed the next year program and future activities. Strong agreement was made to have a workshop on the analysis of SANS data taken this sub-workshop and new data from now to next year. Based on the proposal made with last meeting and strong recommendation for the socio-economic contribution of each activity in this program at the Thailand meeting at November, 2000, two fields are recommended as a candidate for future program. One of them is residual stress measurement combined with texture analysis and the other is reflectometry. As a result of continued discussion, it was decided to have specialists' talks on these two fields in next year meeting.

CONCLUSION

At the sub-workshop on the utilization of SANS instrument for polymer studies, participants gained valuable experience in the design of SANS experiments, sample preparation, data analysis and planning for future activities.

II.NEUTRON ACTIVATION ANALYSIS

1. Summary of the Workshop

A session of neutron activation analysis (NAA) of the 2000 workshop on Utilization of Research Reactors held in Daejon on 20-24 November 2000 was attended by 14 participants from 7 countries (China, Indonesia, Japan, Korea, Malaysia, Thailand and Vietnam). The NAA session started with country reports presented by individual participating countries, followed by invited lectures. After these presentations, the future activity of the NAA group was discussed. In the following, presentation and discussion taken place in the NAA session are summarized in this order.

2. Country Reports

At the workshop held in Yogyakarta, 1999, a long-standing project concerning NAA was finalized and future activities were discussed. In the previous report, several plans were proposed after the intense discussion. Following this, a theme of "supporting system for the neutron activation analysis" was chosen for the 2000 workshop. Unfortunately, this theme was not well announced and, therefore, was not well understood by most participating countries before attending the workshop. In place of this theme, the current situation of reactor facilities related with NAA and/or research activities of NAA were presented by several countries. Followings are brief summaries of presentations of individual countries;

a. China ("Introduction of the Neutron Activation Analysis Facilities in High Flux Engineering Test Reactor" by M. Feng).

Several facilities such as pneumatic transfer (rabbit) system and NAA system in a high flux test reactor at the Nuclear Power Institute of China (NPIC) were introduced.

b. Indonesia ("Current status of Research and Development of Neutron Activation Analysis Group at GA Siwabessy Reactor" by Sutisna).

Progress of R & D on NAA at Siwabessy research reactor was presented. Ko method is being developed for further utilization of NAA.

c-1. Japan ("Current Activity and Problem of Neutron Activation Analysis in Japan" by M. Ebihara).

The present situation concerning NAA in Japan is summarized and a possible problem about NAA in future is pointed out.

c-2. Japan ("NAA Supporting System of JAERI" by F. Sasajima)

A supporting system developed at JAERI is introduced. This system includes Ko method, data analysis, automatic sample changer and gamma ray acquisition. Some data for SRM samples obtained by using this system were shown.

d. Korea ("Application and Facility of Neutron Activation Analysis in HANARO Research Reactor" by Y.-S. Chung)

The facilities for NAA in HANARO research reactor are described and the main application of NAA in Korea are reviewed. Automatic sample changer and integrated computer software for data calculation were acknowledged to be highly effective for efficient use of NAA.

e. Malaysia ("The Use of Neutron Activation Analysis in Environmental Pollution Studies" by A. M. Yusof)

Analytical data for various environmental samples were presented and the usefulness of NAA for multi-elemental analysis of these samples was emphasized.

f. Thailand ("Utilization of NAA in Thailand" by C. Srinyawach)

It was shown that how extensively and effectively the Thai Research Reactor-1 (modification-1) (TRR-1/M-1) was used in a variety of research fields.

g. Vietnam ("Neutron Activation Analysis using the Dalat Nuclear Research Reactor" by M. V. Nguyen)

Facilities related NAA at Dalat nuclear research institute was presented. Ko method has been tried using homemade software. PGA has also been initiated.

3. Invited Talks

A session of invited talks consists of 6 presentations. In each presentation, a specific research subject was clearly outlined and a contribution of NAA to its subject was emphasized. From these presentations, the usefulness, the effectiveness and the advantage of NAA in a variety of fields of applications were impressed. Titles, speakers and brief summaries of invited talks are following;

a. "Air Pollution Study by NAA in Korea" by J. -H. Moon.

The recent air pollution in Taejon and the surrounding areas including industrial complex was examined by using INAA. Data and their interpretation were presented.

b. "Probabilistic Analysis of Airborne Toxic Metals in Korean Industrial Complex" by J. -H. Lee.

Concentration profiles and probabilistic risk analyses of toxic metals for ambient air in Taejon industrial complex were presented.

c. "How Important can Neutron Activation Analysis be in Coming Century? - In a Case of Planetary Science" by M. Ebihara.

It was demonstrated that NAA would be of great importance in planetary science in the 21st century when a large variety of extraterrestrial materials were returned to the earth by space missions.

d. "Application of NAA in Environmental Geology" by K. -Y. Lee.

A large number of environmental and geological materials were analyzed by different analytical methods including NAA. From these analyses, it was concluded that NAA is the most effective method for analyzing these samples. Promising candidates as indicator plants for pollution monitoring were proposed.

e. "Application of NAA in High Purity Materials" by Y. -Y. Yoon.

Several examples of analyses of high purity materials for trace impurities were presented, demonstrating that radiochemical neutron activation analysis can be the best choice for these analysis.

f. "The Study of Trace Element Distribution in Biological Samples with NAA for Human Health" by S. -Y. Cho.

It was shown that NAA of biological samples were essential for estimating the uptake rate of trace elements into human bodies. Such estimation was emphasized to be very important for public health.

4. Discussion for Future Activities

As this is the first year after the completion of the previous project and past activities with that project were evaluated at the last meeting in Yogyakarta, we have not tried to review them. Instead, we have rather extensively discussed the future activities which we could have in the next couple of years. It must be

needless to admit that we have initiated our discussion after the recognition of the last report of this workshop, in which evaluation of past activities (1992-1998) and proposal for future activities were printed.

After the discussion, we have come to the following conclusions;

(i) This workshop is very important and efficient for promoting NAA in participating countries.

(ii) In order to promote NAA in each country, a supporting system is highly desirable. It was acknowledged that Ko method could be one of the best choices.

(iii) As admitted in the previous report, we need to prepare environmental samples and geological samples for the inter-laboratory comparison of NAA data.

The followings are some additional explanations for these conclusions.

It is now well recognized that not only in participating countries of this workshop but also in worldwide that mono-standard method like Ko method is very useful for end-users of NAA. The largest reason to prevent Ko method from being widely distributed is its high price for software package. There are several other problems with commercial Ko softwares: the software is written on old operation system (OS) (DOS) and the software cannot be run on computers with modern CPUs. Considering these situations, it is highly desirable that non-commercial software of Ko method which can be run on modern computers with "MS-windows" as OS is developed.

It can be agreed that NAA has been almost established as an analytical tool. This doesn't mean that an effort for refining the NAA procedure is no more necessary. NAA, especially INAA seems to be one of instrumental analytical methods, but it is not so instrumental as other real instrumental analytical methods like ICP-MS and XRF. Considering that NAA is admitted to be the best reliable method for elemental analysis and that NAA values are usually used for evaluating analytical data obtained by other methods, we definitely need to make effort to keep the analytical capability by NAA at the best level. Inter-laboratory comparison of analytical data by NAA has been carried repeatedly in the past and needs to be continued in future, considering that such an activity is very essential to keep the analytical level reasonably high. For inter-laboratory comparison, well-prepared common samples are needed.

Neutron activation analysis is particularly efficient for the analysis of solid samples such as geological samples and dust particles. These samples can be subjected to INAA without any further processing. In ICP-MS, a competitive analytical method to NAA, such solid samples need to be completely decomposed and dissolved into solution. During these procedures, contamination of impurities and/or loss of samples are more or less probable and tend to yield less reliable data. In this sense, NAA can be the best method for air pollution monitoring by measuring dust particulates. To monitor the pollution level in nation-wide of each country, a large number of samples need to be analyzed. INAA coupled with Ko method must be capable of matching such a requirement.

5. Proposals for Future Activities

Based on the discussion stated above, we would propose the following subjects for future activities.

(i) Non-commercial Ko software will be developed. This software should be user-friendly, written on "MS-windows" as OS, run on computers with latest CPUs and able to be distributed to any user with no cost. Considering the current progress in participating countries, Japan and Vietnam are required to participate in this development. We estimate one and a half year for the completion of this project under

the best condition. Korea can join this project, especially in upgrading the data calculation algorithm.

(ii) Meanwhile, three kinds of reference materials as common samples will be prepared and/ or distributed. These common samples as follows;

a. Averaged Asian food diet sample. Each participating country is required to send its food diet sample to Malaysia by January 31, 2001. Malaysia is responsible to make well-mixed samples, which is designated here as an averaged Asian food diet sample, and send a portion of it to every participating countries. It is also required for Malaysia that the homogeneity of mixed sample is good enough for INAA work (an error due to heterogeneity must be less than 1%).

b. Geological reference samples. Korea is responsible to distribute Korean geological reference samples (eight samples in total) prepared by Korean Institute of Geology, Mining and Materials (KIGAM) by the end of February. Basic description of each sample (type of rock, sampling site, grain size, etc.) should be noticed at the same time.

c. Pollution samples (air particulates). Preparation of common samples of this category is not intended. Instead, air particulate samples will be collected in each participating country. In order to make the later discussion more meaningful, several conditions for collecting the samples should be unified. Korea is responsible for distributing pre-fixed conditions to each participating country by the end of this year 2000. It must be considered that a specified dust sampler is not available in any country.

(iii) These samples will be analyzed by using conventional NAA which is used in individual institutes/laboratories. Ko method may be applied in Japan and Vietnam. Results will be discussed in the next workshop. If any country likes to have some particular samples analyzed by other countries for confirmation of data, such a request is highly welcome and asked to announce to other countries. Communication by using e-mail helps fast and effective exchange of data and idea.

(iv) Once a Ko software is newly developed, it is required to distribute to all participating countries. The software will be immediately evaluated by analyzing the common samples which are already distributed and analyzed in individual countries. If any bug or bug-like defect is found, it should be noted to developers. With several catching-ball communications, the software will be completed in a reasonable time.

(v) By using the final version of Ko software, air particulate samples as well as the common samples are to be analyzed. Data from all participating countries for the common samples will be compared with each other for evaluating the usefulness of the newly developed Ko software. Data for airborne particulate samples also are compared for discussing the degree of air pollution in participating Asian countries.

III. RESEARCH REACTOR UTILIZATION (BNCT)

Sixteen scientists from seven countries of China, Indonesia, Japan, Korea, Malaysia, Thailand and Vietnam made presentations in this section. The participating countries reported the current status of their research reactor as well as the recent achievements in the design, construction, research, and clinical trials of BNCT.

1. Country Progress Report

- China upgraded the safety system and renewed the old equipment in research reactors. As a result, good availability of the reactor operation has been achieved. Research and utilization of four reactors, which are HWRR, SPR, HFETR and MJTR, are on schedule. Research and development in BNCT has been greatly concerned, however, no definite decision on BNCT technique line has been made.
- Japan presented the present status of research and test reactors in JAERI. Also reported is JRR-4 BNCT Facility. In JRR-4, ever since the first medical irradiation for BNCT was carried out Oct. 25, 1999, seven times of treatments were performed by the end of June 2000. By using prompt gamma ray analysis, boron concentration in the patient's blood was measured by gold wire activation method using beta-gamma coincidence counting system. This data was furnished to medical doctor for irradiation time determination.
- Ever since Korea built HANARO, which is a multipurpose research reactor and whose design feature is rather unique, the experimental facilities such as HRPD, FCD are in service and SANS is ready for commissioning, Neutron Radiography is occasionally used by the demand of industry. BNCT and PGNAA are under construction, and will be available to user next year. Other spectrometers like PNS etc. are planned for the next step and proper installation time of CNS and neutron guide tube are in consideration. Material irradiation test for the newly developed research reactor fuel and structural material for nuclear power reactors, RI production, and neutron activation analysis has increased. A feasibility study for the NTD is underway.
- Malaysia reported that the construction of the small angle neutron scattering (SANS) on the radial piercing beam port was completed in 1995 and some devices are already in operation but considerable effort is still required before the research program for this instrument is made in their full extent.
- Vietnam presented the status of operation, utilization and some activities related to the core management of the Dalat Nuclear Research Reactor (DNRR). It will reach about 22,000 hours of operation at nominal power by the end of November this year.
- Thailand reported that they established the working group for BNCT project in 1996. Detail design is now underway and the BNCT facility will be provided to expand the utilization of a new 10 MW research reactor of ONRC project.
- Indonesia reported that Batan has an intention to develop BNCT facility at one of the research reactors. Study indicates that the TRIGA Kartini reactor in Yogyakarta will be the most suitable

one. Depending on the availability of fund, further action plans for this program will be defined. They expect scientist exchange program to be utilized to support development of the BNCT facility under the bilateral JAERI-BATAN cooperation program. They also expect the IAEA Technical Cooperation on BNCT in 2001.

- Korea introduced the recent progress in developing the BNCT facility in HANARO. They installed radiation filter made of single crystals of silicon and bismuth. It effectively attenuates fast neutrons and gamma, but it allows effective penetration of thermal neutrons. Water shutter for continuous operation of reactor is installed. The thermal neutron flux of 2.6 x 10^9 n/cm^2-s is estimated at the irradiation position.
- Korea also reported that a prompt gamma neutron activation analysis (PGNAA) system is being set up in HANARO. Polychromatic thermal neutron beam diffracted vertically by a set of pyrolytic graphite crystals at a Bragg angle of 45 deg. from a horizontal beam line. Thermal neutron flux of 6.1x10^7 n/cm^{2}s and the Cd-ratio of 364 are achieved at sample position.
- Japan introduced JRR-4 BNCT Facility. JRR-4 medical irradiation facility was designed to use thermal, epithermal or mixed neutron beam. The first medical irradiation for BNCT of JRR-4 was carried out on Oct. 25, 1999. In BNCT irradiation, boron concentration was measured by prompt gamma neutron activation analysis and thermal flux distribution in the irradiation position was measured by gold wire activation method using beta-gamma coincidence counting system.
- Dr. Nakagawa who is the leader in BNCT worldwide introduced BNCT in Japan from the viewpoint of clinical application. This kind of clinical information seems to be very important to Neurosurgeon.
- A Korean professor introduced newly developing boron compounds. These boronated tetrahydorisoquinolines may be useful as a tumor-selective sensitizer for BNCT. Studies evaluating the in vitro and in vivo localizing ability are currently being carried out and will be reported in near future.
- A Korean medical doctor pointed in his presentation that the I-BPA-Fructose is a promising tumor imaging radiopharmaceutical for BNCT research.
- Japan introduced a new treatment planning software, Computational Dosimetry System (JCDS) and experiments being done to verify the JCDS in JRR-4.
- A Korean professor introduced image data formats for dose planning and DICOM (Digital Image Communication in Medicine), which is standard protocol for medical images and related information.
- A Korean professor introduced the small medical reactor for BNCT in terms of neutronic design approach.

2. Discussions:

The information presented by every country in the BNCT session seems to be very useful to those who are planning to have BNCT facility. Especially, presentations by Dr. Nakagawa who is

the pioneer in this field, Mr. Torri and Mr. Kumada conveyed very useful information. When the future plan was made last year, it was agreed to have discussion on BNCT this year, Neutron Radiography next year and Reactor Core Management in 2002. Although BNCT is not scheduled for future workshops, since BNCT is very useful and interesting, and some countries are planning to have BNCT facilities, continued information exchange through communication link or network would be very beneficial to the member states. Consideration in this matter will be commissioned to future program under the FNCA framework.

- Korea pointed that the workshop on BNCT is not necessary to continue next year or in near future because any significant progress among member states except Japan would not be expected within short time period. If the initiation of BNCT facility in China, Indonesia or Thailand is made, or if some clinical trial is made in Korea, then another workshop can be applied.
- Malaysia suggested the continuation of our workshop as agreed last year, and one or two lectures about BNCT development could be inserted into the workshop.
- Japan suggested inclusion of the progress and new ideas on BNCT into our country report in order to continue the information exchange on BNCT.
- Vietnam also agreed to put the report for BNCT in the country report even though BNCT is not in consideration now.
- Indonesia expressed that the way to support the society using research reactor is the production of radioisotopes for medical & industrial purpose, and they intended to have BNCT facility and had good response from medical doctors. Also expressed that they would like to put the topic of radioisotope as an item for the next workshop.
- Japan realized that many Asian countries are interested in BNCT. Therefore, they expressed their hope to develop collaboration with other countries in this subject.
- Thailand decided to have BNCT facility in their reactor. Since BNCT is a new technology and it involves many fields, they would like to have collaboration with the countries that have experience. They would like to have workshop on the design of BNCT facility as well.
- Dr. Nakagawa made comment that BNCT is not familiar to people and medical doctors, and therefore it is necessary to keep them informed of the correct status of BNCT. Also comment made was that if we have more clinical data and result in future, it would be important for the medical doctors to know them. Mr. Torri said that he was willing to collaborate in the measurement technology with any country anytime and anywhere.
- China was pleased to deliver three remarks. The first one is that the most realistic option in China is to install BNCT in CARR that is under design and second possibility is to construct a small reactor for BNCT. In near future, they will have decision and hope to report the BNCT progress in their country report. The second remark is that production of RI in China is supposed to be not so efficient due to various reasons. The third is that China has experience in NAA field and they are happy to communicate with other country, if they have chance.
- Japan is willing to provide communication network to deliver important information about

BNCT. They can open and even allow the tour to KUR or JRR4 facilities while an actual BNCT is underway under the FNCA framework or other cooperation programs. Also they told that they could even receive patients up to about five in a year from FNCA member states. Financial support for the treatment and some part of the hospital fee just after the BNCT in Japan would be possible.

- Korea mentioned that it would be good for Thailand to utilize STA program, or IAEA fellowship or expert mission to consult the design, instead of workshops.
- Thailand told that they had difficulty in setting up the requirements for BNCT and which type of BNCT facility they had to have due to lack of medical doctors with enough knowledge in BNCT.
- Indonesia expressed that good communication network is indispensable. And medical doctors in Indonesia are very interested in that information.
- China is much interested in the application of their Miniature Neutron Source Reactor to the BNCT, which seems to be more attractive to medical doctors.
- Korea pointed out that there was a misunderstanding in the design of neutron beam for BNCT, and what matters is whole brain irradiation vs. local (or focal) irradiation not the use of thermal vs. epithermal neutron.
- Japan indicated that the focal irradiation is seemed better than whole brain irradiation, but the use of neutrons with higher penetration power is the better.

Since all project leaders participating in this workshop except Australia were in this section, pre-discussion was made for the future activity on the Utilization of Research Reactors. Japan explained about the recommendations from the review committee of Japan. The criticism can be summarized that the themes has been rather oriented to the interest of researcher, the number of topics has seemed rather many, but it has been not so clear that how the results have been contributed to the end user or public. Close link with the activities of other international organization such as IAEA was also emphasized.

- Japan proposed RI using PZC for the Tc generator and NAA for its application to environmental research and mine exploration, as future activity.
- Korea, as the lead country of an IAEA/RCA project on research reactor, explained the scheduled activities in this region by the IAEA/RCA and the Japanese extra-budgetary program of IAEA, considering the close link with other international activities. It was found that the workshop on the research reactor core management in 2002 would be overlapping. Korea also expressed that they prefer to discuss radioisotope rather than neutron radiography in 2001, and proposed to include the discussion on the neutron radiography at the IAEA/RCA workshop on neutron scattering in 2001 rather than in the workshop under the FNCA framework.
- Japan explained that new proposal for FNCA workshop such as Establishment and Transfer of Tc-99m Generator Technology and Utilization of NAA would not be accepted in 2001

because the budget of 2001 is already fixed. It may be considered for the topic of 2002 workshop.

- It was understood that the topic of the next year program would be Neutron Scattering, Neutron Activation Analysis and Neutron Radiography.
- The contact point for Neutron Scattering and NAA already have been established. If we will have workshop for Neutron Radiography next year, then we need to assign contact points for NR.

3. Results

- Communication network especially in BNCT is necessary. Contact person of each country is to be assigned. List server is also necessary.
- The BNCT of Japan are open to member states. Japan is willing to help member states for the facility development or for learning on the patient treatment.
- The progress of BNCT in each country will be included in the status report of each country.

IV. ROUND TABLE DICUSSION

All participants attended the round table meeting lead by project leaders of member states. Leaders of three sections summarized their activity during the workshop focusing on the future activities, and discussion followed.

Dr. Machi – the coordinator of FNCA, presented summary of the first FNCA meeting held in Bangkok in November 2000. He told that FNCA was recognized as an efficient mechanism of cooperation in nuclear technology for the social and economic development. The recommendation from the FNCA meeting to this workshop was almost the same with that from the project review committee of Japan as Mr. Kaieda explained at the BNCT section and his iterated explanation after Dr. Machi's presentation. Linkage with end user was emphasized for all future activities. Several impressive examples demonstrating the advantage of nuclear technology for various applications were presented. Dr. Machi also explained about the proposal of Japan on RI and NAA as the future activities.

The project leader of Korea proposed an activity on RI in 2001 instead of neutron radiography for the better linkage with the backup supply of RI of which topic will be discussed at an expert meeting of IAEA/RCA in Bangkok on sharing of resources in May 2001. He also requested the project leaders, since most of them are Project Coordinators of IAEA/RCA as well, to support the inclusion of neutron radiography at the IAEA/RCA workshop on neutron scattering in Korea in 2001. Discussion to avoid overlapping in the neutron scattering by this workshop and by the IAEA/RCA followed.

A few participants pointed out the possible problem or difficulty to provide budget for our activities within limited time if the topics or contents of activities in near future are changed. It was understood that it depends on the time span, plan and financial issue of the project.

Dr. Machi emphasized the importance of close communication among experts in each specific field. For this purpose, he suggested assignment of contact point of each country in each field and a leader among them.

The project leader of China announced that China would host this workshop in 2001.

The conclusions of the round table meeting are as following:

- The topics of 2001 will be,
  1) Neutron Activation Analysis focusing on the environmental research and mine exploration.
  2) Radioisotope for the realization of Tc generator technology using PZC.
  3) Neutron Scattering focusing to its application to end-user.
- The venue of 2001 workshop will be in China.
- The recent development on BNCT will be included in the country reports, and a communication network will be provided.

New projects such as establishment and transfer for Tc-99m generator production technology and application of NAA for environment monitoring and mineral resources exploration were agreed and a recommendation of the new projects will be submitted to the coming coordinator meeting.

Appendix

Schedule of the 2000 Workshop on the Utilization of Research Reactors
November 20 - November 24, 2000
Taejon, korea

Group: Neutron Scatterong

Time	Nov. 20, 2000 Monday	Chairperson
09:00 - 09:30	[Room: Seminar room 2F Main Building KAERI] Registration	Dr. KIM S. Y.
09:30 - 10:10	**Welcoming Remark** Dr. CHANG In Soon **Opening Remark** Mr. SHIGEYAMA Masaru **Opening Remark** Mr. LEE Moon Ki	
10:10 - 10:30	*Coffee Break*	
10:30 - 11:00	**General Lecture** Dr. KUK Il Hyun	Mr. KAIEDA K. Mr. JUN B. J.
11:00 - 11:30	**General Lecture** Dr. NAKAGAWA	
11:30 - 12:00	**General Lecture** Dr. PARK Kyung bae	
12:00 - 12:20	Video Presentation	
12:20 - 12:30	Group Photo	
12:30 - 13:30	*Lunch*	
13:30 - 13:40	[Room: Meeting room of RI Building] Confirmation of Chairperson	Dr. HAMAGUCHI Mr. LEE C. H.
13:40 - 14:40	Country Report: Australia Country Report: Korea	
14:40 - 15:00	*Coffee Break*	
15:00 - 16:30	Country Report: Japan Country Report: Korea	Dr. IKRAM A. Mr. MINAKAWA N.
16:30 - 17:00	Demonstration Experiment	

Time	Nov. 21, 2000 Tuesday	Chairperson
09:00 - 11:00	[Room: Meeting room of RI Building] SANS Experiments (Continue)	
11:00 - 12:00	Demonstration of Data Analysis	
12:00 - 13:00	*Lunch*	
13:00 - 14:40	Country Report: Australia Country Report: Korea Country Report: Indonesia Country Report: Japan Country Report: Korea	Dr. MOHAMED A. Mrs. SANGARIYAVANICH
14:40 - 15:20	*Coffee Break*	
15:20 - 16:20	Country Report: Malaysia Country Report: Thiland Country Report: Vietham	Dr. KNOTT R.B. Mr. YANG T.
16:20 - 17:30	Reports on the Cooperative Research Project	

Time	Nov. 22, 2000 Wednesday	Chairperson
09:00 - 12:00	[Room: Meeting room of RI Building] Continuation of SANS Experiment	
12:00 - 13:00	*Lunch*	
13:00 - 15:00	Country Report: Japan Country Report: Japan	Mr. SEOK S. B. Ms. TRAN P. TT.
15:00 - 15:30	*Coffee Break*	
15:30 - 16:30	Country Report: Korea	Prof. HASEGAWA H. Ms. LEE C. H.
16:30 - 17:30	Discussion of the Future Program	

Time	Nov. 23, 2000 Thursday	Chairperson
09:00 - 12:00	[Room: Meeting room of RI Building] Discussion(Continued)	
12:00 - 13:00	*Lunch*	
13:00 - 14:00	Report on Sub- Workshop	
14:00 - 14:30	*Coffee Break*	
14:30 - 15:30	Discussion of the Report and Future Plan	
15:30 - 17:00	WS Report & Summary	

Time	Nov. 24, 2000 Friday	Chairperson
09:00 - 10:00	[Room: Conference room of Hotel Spapia] Summary of WS Activity & Reports	Mr. KAIEDA K. Mr. JUN B. J.
10:00 - 12:00	Future Plan	
12:00 - 13:00	*Lunch*	
13:00 - 14:00	[Room: Conference room of Hotel Spapia] Finalization of WS Report	Mr. KAIEDA K. Mr. JUN B. J.
14:00 - 15:00	**Closing Session**	

Appendix

Schedule of the 2000 Workshop on the Utilization of Research Reactors
November 20 - November 24, 2000
Taejon, korea

Group: Neutron Activation Analysis

Time	Nov. 20, 2000 Monday	Chairperson
09:00 - 9:30	[Room: Seminar room 2F Main Building KAERI] Registration	Dr. KIM S. Y.
09:30 - 10:10	**Welcoming Remark** Dr. CHANG In Soon **Opening Remark** Mr. SHIGEYAMA Masaru **Opening Remark** Mr. LEE Moon Ki	
10:10 - 10:30	*Coffee Break*	
10:30 - 11:00	**General Lecture** Dr. KUK Il Hyun	Mr. KAIEDA K. Mr. JUN B. J.
11:00 - 11:30	**General Lecture** Dr. NAKAGAWA	
11:30 - 12:00	**General Lecture** Dr. PARK Kyung bae	
12:00 - 12:20	Video Presentation	
12:20 - 12:30	Group Photo	
12:30 - 13:30	*Lunch*	
13:30 - 13:40	[Room: Seminar room of NETEC] Confirmation of chairperson	Mr. NGUYEN M. V. Mr. LEE K. Y.
13:40 - 13:50	Overview	
13:50 - 15:20	Country Report: China Country Report: Indonesia Country Report: Japan	
15:20 - 15:40	*Coffee Break*	
15:40 - 16:40	Country Report: Korea Country Report: Malaysia	Mrs. SRINTAWACH. C. Mr. MOON J. H.

Time	Nov. 21, 2000 Tuesday	Chairperson
09:00 - 10:00	[Room: Seminar room of NETEC] Country Report: Thiland Country Report: Vietham	Mr. FENG M. Mr. LEE J. H.
10:00 - 10:30	*Coffee Break*	
10:30 - 12:00	Country Report: Japan Country Report: Korea Country Report: Korea	Mr. SUTISNA Mr.YOON Y. Y.
12:00 - 13:00	*Lunch*	
13:00 - 15:00	Country Report: Japan Country Report: Korea Country Report: Korea	Prof. ALIAS M. Y. Mr. CHO S. Y.
15:00 - 15:30	*Coffee Break*	
15:30 - 16:00	Country Report: Korea	Dr. CHUNG Y.S. Mr. SASAJIMA F.
16:00 - 16:30	Discussion in Technical Matter	

Time	Nov. 22, 2000 Wednesday	Chairperson
09:00 - 10:30	[Room: Meeting room of HANARO Reactor Building] Visit to HANARO and BNCT Facility	
10:30-11:00	*Coffee Break*	
11:00 - 12:00	Demonstration of Facility	
12:00 - 13:00	*Lunch*	
13:00 - 14:00	General Discussion	Prof. EBIHARA M. Dr. CHUNG Y. S.
14:00 - 15:00	Discussion of the Future Program	
15:00 - 15:30	*Coffee Break*	
15:30 - 16:30	Discussion of the Future Program	Prof. EBIHARA M. Dr. CHUNG Y. S.
16:30 - 17:00	Review of Final Report	

Time	Nov. 23, 2000 Thursday	Chairperson
09:00	[Departure at Hotel Spapia] **Technical Tour** Young- Kwang Nuclear Power Plant	

Time	Nov. 24, 2000 Friday	Chairperson
09:00 - 10:00	[Room: Conference room of Hotel Spapia] Summary of WS Activity & Reports	Mr. KAIEDA K. Mr. JUN B. J.
10:00 - 12:00	Future Plan	
12:00 - 13:00	*Lunch*	
13:00 - 14:00	[Room: Conference room of Hotel Spapia] Finalization of WS Report	Mr. KAIEDA K. Mr. JUN. B. J
14:00 - 15:00	**Closing Session**	

Appendix

Schedule of the 2000 Workshop on the Utilization of Research Reactors
November 20 - November 24, 2000
Taejon, korea

Group: Research Reactor Utilization(BNCT)

Time	Nov. 20, 2000 Monday	Chairperson
09:00 - 9:30	**[Room: Seminar room 2F Main Building KAERI]** Registration	Dr. KIM S. Y.
09:30 - 10:10	**Welcoming Remark** Dr. CHANG In Soon **Opening Remark** Mr. SHIGEYAMA Masaru **Opening Remark** Mr. LEE Moon Ki	
10:10 - 10:30	*Coffee Break*	
10:30 - 11:00	**General Lecture** Dr. KUK Il Hyun	Mr. KAIEDA K. Mr. JUN B. J.
11:00 - 11:30	**General Lecture** Dr. NAKAGAWA	
11:30 - 12:00	**General Lecture** Dr. PARK Kyung bae	
12:00 - 12:20	Video Presentation	
12:20 - 12:30	Group Photo	
12:30 - 13:30	*Lunch*	
13:30 - 13:40	**[Room: Seminar room of NETEC]** Confirmation of Chairperson	Mr.CHAROEN S. Mr. LEE B. C.
13:40 - 15:10	Country Report: China Country Report: Japan Country Report: Korea	
15:10 - 15:30	*Coffee Break*	
15:30 - 16:30	Country Report: Malaysia Country Report: Vietnam	Dr. HASTOWO H. Mr. TORII Y.

Time	Nov. 21, 2000 Tuesday	Chairperson
09:00 - 10:30	**[Room: Seminar room of NETEC]** Country Report: Thiland Country Report: Indonesia Country Report: Korea	Dr. XU H. Mr. KUMADA H.
10:30 - 11:00	*Coffee Break*	
11:00 - 12:00	Country Report: Korea Country Report: Japan	Mr. KAIEDA K. Mr. LIM S. M.
12:00 - 13:00	*Lunch*	
13:00 - 14:30	Country Report: Japan Country Report: Korea	Mr. BOKHARI A. B. Prof. CHOI H. D.
14:30 - 15:00	*Coffee Break*	
15:00 - 17:00	Country Report: Korea Country Report: Japan Country Report: Korea Country Report: Korea	Dr. NGUYEN N.D. Mr. KANG S. U.

Time	Nov. 22, 2000 Wednesday	Chairperson
09:00 - 10:30	**[Room: Meeting room of HANARO Reactor Building]** Visit to HANARO and BNCT Facility	
10:30 - 11:00	*Coffee Break*	
11:00 - 12:00	Discussion	
12:00 - 13:00	*Lunch*	
13:00 - 14:30	Discussion	Mr. KAIEDA K. Mr. JUN B. J.
14:30 - 15:00	*Coffee Break*	
15:00 - 16:00	Discussion of the Future Program	
16:00 - 17:00	Review of Final Report	

Time	Nov. 23, 2000 Thursday	Chairperson
09:00	**[Departure at Hotel Spapia]** **Technical Tour** Young- Kwang Nuclear Power Plant	

Time	Nov. 24, 2000 Friday	Chairperson
09:00 - 10:00	**[Room: Conference room of Hotel Spapia]** Summary of WS Activity & Reports	Mr. KAIEDA K. Mr. JUN B. J.
10:00 - 12:00	Future Plan	
12:00 - 13:00	*Lunch*	
13:00 - 14:00	**[Room: Conference room of Hotel Spapia]** Finaiization of WS Report	Mr. KAIEDA K. Mr. JUN B. J.
14:00 - 15:00	**Closing Session**	

Appendix

LIST OF PARTICIPANTS
2000 WORKSHOP ON THE UTILIZATION OF RESEARCH REACTORS
November 20 - 24, 2000
Taejon, Korea

No	Country	Field	Name	Organization and Position	Telephone & Facsimile No. E-mail address
1	Australia	NS	Dr. KNOTT Robert Barry	Principal Research Scientist, Physics Division, Australian Nuclear Science and Technology Organization (ANSTO)	Private Mail Bag, Menai NSW 2234, Australia T: + 61- 2- 9717- 3218 F: + 61- 2- 9717- 9262 *robert.knott@ansto.gov.au*
2	China	NAA	Mr. FENG Mingquan	Senior Engineer, Reactor Operation and Application Sub-Institute Nuclear Power Institute of China(NPIC)	*P.O.Box 291-109 Chengdu Sichuan 610005 China* T: + 86- 28- 55582199- 44474 F: + 86- 28- 5582223 *fengmg@npic.ac.cn*
3	China	BNCT	Dr. XU Hanming	Chief Engineer, Reactor Engineering Department, China Institute of Atomic Energy (CIAE) CNNC	*P.O.Box 275(33), Beijing China* T: + 86- 10- 6935- 7582 F: + 86- 10- 6935- 8140 *Xuhanming@iris.ciae.ac.cn*
4	China	NS	Mr. YANG Tong Hua	Nuclear Physics Division China Institute of Atomic Energy (CIAE) CNNC	*P.O.Box 275(33), Beijing China* T: + 86- 10- 6935- 7564 F: + 86- 10- 6935- 7008 *Thyang@iris.ciae.ac.cn*
5	Indonesia	NAA	Mr. SUTISNA	Leader of Natural Materials Group Department of Industrial Materials R & D Center for Materials Science & Technology, BATAN	Kawasan Puspiptek Serpong Tangrang 15314 Indonesia T: + 62- 21- 756- 0562 Ext. 2111 F: + 62- 21- 756- 0926 *tisna@link.net.id*
6	Indonesia	NS	Dr. IKRAM Abarrul	Head of Neutron Scattering Laboratory, R & D Center for Materials Science & Technology, BATAN	Kawasan Puspiptek Serpong Tangrang 15314 Indonesia T&F: + 62- 21- 756- 0926 *nsibatan@centrin.net.id*
7	Indonesia	BNCT	Mr. HASTOWO Hudi	Director, Center for Development of Research Reactor Technology, P2TRR- BATAN	Kawasan Puspiptek Building No.31Serpong Tangrang 15310 Indonesia T: + 62- 21- 756- 0908 F: + 62- 21- 756- 0573 *prsg@cbn.net.id*
8	Malaysia	BNCT	Mr. BOKHARI Adnan	Reactor Manager, Division of Technical Service Malaysian Institute for Nuclear Technology Research (MINT)	Bangi 43000 Kajiang Selangor Malaysia T: + 60- 3- 892- 82988 F: + 60- 3- 892- 53037 *abokhari@mint.gov.my*
9	Malaysia	NS	Mr. MOHAMED Abdul Aziz Bin	Senior Research Officer, NDT-Radiation Technology, Industrial Technology Division Malaysian Institute for Nuclear Technology Research (MINT)	Bangi 43000 Kajiang Selangor Malaysia T: + 60- 3- 892- 50510 F: + 60- 3- 892- 50907 *Aziz__mohd@mint.gov.my*
10	Malaysia	NAA	Prof. MOHD YUSOF Alias	Professor, Universiti Teknologi Malaysia Inst. of Environmental & Water Resource Management, Faculty of Civil Engineering	81310 UTM Skudai Johor Malaysia T: + 607- 5504500/ 3079 F: + 607- 5566162/ 3075 *alias@kimia.fs.utm.my*
11	Thailand	NS	Ms.SANGARIYAVANICH, Archara	Senior Nuclear Physicist, Physics Division, Office of Atomic Energy for Peace (OAEP)	Vibhavadi Rangsit Rd., Chatuchak BANGKOK 10900 Thailand T: + 66- 2- 5620119 F: + 66- 2- 5620118 *archara@oaep.go.yh*
12	Thailand	NAA	Ms.SRINYAWACH Chastbongkoch	Project Leader, Chemical Research section Chemistry Division	Vibhavadi Rangsit Rd., Chatuchak BANGKOK 10900 Thailand T: + 66- 2- 5620121 F: + 66- 2- 5613031 *Chastbon@oaep.go.th*
13	Thailand	BNCT	Mr. CHAROEN Sakda	Head, Isotope Production Section Isotope Production Division	Vibhavadi Rangsit Rd., Chatuchak BANGKOK 10900 Thailand T: + 66- 2- 5620121/ 5795230- 4 F: + 66- 2- 5613013/ 5620127 *sakda@oaep.go.th*

Appendix

LIST OF PARTICIPANTS
2000 WORKSHOP ON THE UTILIZATION OF RESEARCH REACTORS
November 20 - 24, 2000
Taejon, Korea

No	Country	Field	Name	Organization and Position	Telephone & Facsimile No. E-mail address
14	Vietnam	NAA	Mr. NGUYEN Minh Van	Scientific Researcher, Center for Analytical Techniques and Environmental Research Nuclear Research Institute (NRI)	01 Nguyen Tu Luc Street Delat Vietnam T: + 84- 63- 832630 F: + 84- 63- 821107 *luonghoan@fpt.vn*
15	Vietnam	BNCT	Dr. NGUYEN Nhi Dien	Director, Nuclear Research Institute (NRI)	01 Nguyen Tu Luc Street Delat Vietnam T: + 84- 63- 828620 F: + 84- 63- 821107 *nndien@hcm.vnn.vn*
16	Vietnam	NS	Ms. TRAN Phuong Thi Thu	Engineer, Nuclear Physics Division Nuclear Research Institute (NRI)	01 Nguyen Tu Luc Street Delat Vietnam T: + 84- 63- 822191 F: + 84- 63- 821107 *nrigovn@hcm.vnn.vn*
17	Japan	M	Mr. SHIGEYAMA Masaru	Technical Official, International Affairs and Safeguards Division, Atomic Energy Bureau, Science and Technology Agency (STA)	2-2-1 Kasumigaseki Chiyoda-ku Tokyo 100- 8966 Japan T: + 81- 3- 3581- 2597 F: + 81- 3- 3581- 5198 mshigeya@sta.go.jp
18	Japan	M	Dr. MACHI Sueo	Senior Managing Director Japan Industrial Forum., Inc.	1-7-6, Torano-mon Minato-ku Tokyo 105- 0001 Japan T: + 81- 3- 3508- 7932 F: + 81- 3- 3508- 9021
19	Japan	BNCT	Mr. KAIEDA Keisuke	Projector Leader Special Senior Staff Nuclear Material Control Center	2-53 Shirakata Shirane Tokai-mura Naka-gun Ibaraki-Ken 319- 1106 Japan T: + 81- 29- 306- 3136 F: + 81- 29- 282- 8004 *kaieda@jnmcc.or.jp*
20	Japan	M	Mr. SATO Kenji	Deputy General Manager, Research Reactor Administration Division, Dept of Research Reactor, JAERI	2-4 Shirakata Shirane Tokai-mura Naka-gum Ibaraki-ken 319- 1195 Japan T: + 81- 29- 282- 6895 F: + 81- 29- 282- 5258 *kjsato@nems.jaeri.go.jp*
21	Japan	NS	Dr.HAMAGUCHI Yoshikazu	Senior Scientific Advisor Dept of Research Reactor, JAERI	4-20-16-403 Honcho Tanashi Tokyo 188- 0011 Japan T: + 81- 424- 66- 9361 F: + 81- 424- 66- 9361 *hayo@hh.iij4u.or.jp*
22	Japan	NS	Mr. MINAKAWA Nobuaki	Sub-leader, Research Group for Neutron Scattering at Ultralow Temperature Advanced Science Research Center, JAERI	2-4 Shirakata Shirane Tokai-mura Naka-gun Ibaraki-ken 319- 1195 Japan T: + 81- 29- 282- 5997 F: + 81- 29- 282- 5939 *minakawa@kotai3.tokai.jaeri.go.jp*
23	Japan	NS	Prof. HASEGAWA Hirokazu	Associate Professor, Department of Polymer Chemistry, Graduate School of Engineering, Kyoto University	Yoshida-honmachi Sakyo-ku Kyoto 606- 8501 Japan T: + 81- 75- 753- 5614 F: + 81- 75- 753- 4864 *hasegawa@alloy.polym.kyoto-u.ac.jp*
24	Japan	M	Mr. OHTOMO Akitoshi	Deputy General Manager, Research Reactor Utilization Div., Dept of Research Reactor, JAERI	2-4 Shirakata Ibaraki-ken 319- 1195 Japan T: + 81- 29- 282- 6765 F: + 81- 29- 282- 6763 *ohtomo@jrr3fep2.tokai.jaeri.go.jp*
25	Japan	NAA	Mr. SASAJIMA Fumio	Research Reactor Utilization Div., Dept of Research Reactor, JAERI	2-4 Shirakata Shirane Tokai-mura Naka-gun Ibaraki 319- 1195 Japan T: + 81- 29- 282- 6586 F: + 81- 29- 282- 6763 sasajima@jrr3fep2.tokai.jaeri.go.jp

Appendix

LIST OF PARTICIPANTS
2000 WORKSHOP ON THE UTILIZATION OF RESEARCH REACTORS
November 20 - 24, 2000
Taejon, Korea

No	Country	Field	Name	Organization and Position	Telephone & Facsimile No. E-mail address
26	Japan	BNCT	Mr. SATO Mitsugu	Deputy General Manager, JRR-3 Operation Div., Dept of Research Reactor, JAERI	2-4 Shirakata Shirane Tokai-mura Naka-gun Ibaraki-ken 319- 1195 Japan T: + 81- 29- 282- 5095 F: + 81- 29- 282- 5933 *sato@jrr3fep2.tokai.jaeri.go.jp*
27	Japan	NAA	Prof. EBIHARA Mitsuru	Associate Professor, Department of Chemistry, Graduate School of Science Tokyo Metropolitan University	1-1 Minami-Ohsawa Hachioji Tokyo 192- 0397 Japan T: + 81- 426- 77- 2553 F: + 81- 426- 77- 2525 *ebihara-mitsuru@c.metro-u.ac.jp*
28	Japan	BNCT	Mr. TORII Yoshiya	Deputy General Manager, Research Reactor Utilization Div., Dept of Research Reactor, JAERI	2-4 Shirakata Shirane Tokai-mura Naka-gun Ibaraki-ken 319-1195 Japan T: + 81- 29- 282- 5592 F: + 81- 29- 282- 6763 *torii@jrr3fep2.tokai.jaeri.go.jp*
29	Japan	BNCT	Mr. KUMADA Hiroaki	Researcher, Research Reactor Utilization Div., Dept of Research Reactor, JAERI	2-4 Shirakata Shirane Tokai-mura Naka-gun Ibaraki-ken 319-1195 Japan T: + 81- 29- 282- 5593 F: + 81- 29- 282- 6763 *kumada@jrr3fep2.tokai.jaeri.go.jp*
30	Japan	BNCT	Dr. NAKAGAWA Yoshinobu	Vice President, National Kagawa Children's Hospital	2603 Zentsuji-cho Zentsuji-shi Kagawa 765-8501 Japan T: + 81- 877- 62- 0885 F: + 81- 877- 62- 5384 *nakagawa@kagawasyo.hosp.go.jp*
31	Japan	M	Mr. SHIRAI Eiji	Executive Director, Radiation Application and Development Association (RADA)	2-4 Shirakata Shirane Tokai-mura Naka-gun Ibaraki-ken 319-1195 Japan T: + 81- 29- 282- 6300 F: + 81- 29- 282- 1182 *shirai@jrr3fep2.tokai.jaeri.go.jp*
32	Japan	M	Mr. ISSHIKI Masahiko	Director, Radiation Application and Development Association(RADA)	2-4 Shirakata Shirane Tokai-mura Naka-gun Ibaraki-ken 319-1195 Japan T: + 81- 29- 282- 6300 F: + 81- 29- 282- 1182 *issiki@ jrr3fep2.tokai.jaeri.go.jp*
33	Korea	M	Mr. CHANG In Soon	President, Korea Atomic Energy Research Institute(KAERI)	P.O.Box 105 Yusung Taejon 305-600 Korea T: + 82- 42- 868- 2121 F: + 82- 42- 861- 9611 *ischang@kaeri.re.kr*
34	Korea	M	Mr. KIM Seong Yun	Principal Researcher, HANARO Center Korea Atomic Energy Research Institute(KAERI)	P.O.BOX 105 Yusung Taejon 305-600 Korea T: + 82- 42- 868- 2126 F: + 82- 42- 861- 8292 *sykim@kaeri.re.kr*
35	Korea	M	Mr. LEE Moon Ki	Director, Nuclear Policy & R&D Division Ministry of Science and Technology	Government Complex-Kwachon Kwachon Korea 427- 760 T: + 82- 2- 503- 7646- 8 F: + 82- 2- 507- 0558 *mklee@most.go.kr*
36	Korea	M	Mr. KUK Il Hyun	Vice President, HANARO Center, Korea Atomic Energy, Research Institute(KAERI)	P.O.BOX 105 Yusung Taejon 305-600 Korea T: + 82- 42- 868- 2334 F: + 82- 42- 868- 8501 *ihkuk@kaeri.re.kr*

Appendix

LIST OF PARTICIPANTS
2000 WORKSHOP ON THE UTILIZATION OF RESEARCH REACTORS
November 20 - 24, 2000
Taejon, Korea

No	Country	Field	Name	Organization and Position	Telephone & Facsimile No. E-mail address
37	Korea	M	Mr. PARK Kyung Bae	General Manager, RI Team, Korea Atomic Energy Research Institute (KAERI)	P.O.BOX 105 Yusung Taejon 305-600 Korea T: + 82- 42- 868- 8120 F: + 82- 42- 868- 8448 *kbpark@nanum.kaeri.re.kr*
38	Korea	BNCT	Mr. JUN Byung Jin	General Manager, HANARO Management Team, HANARO Center, Korea Atomic Energy Research Institute (KAERI)	P.O.BOX 105 Yusung Taejon 305-600 Korea T: + 82- 42- 868- 8493 F: + 82- 42- 861- 0209 *bjjun@nanum.kaeri.re.kr*
39	Korea	NAA	Mr. CHO Seung Yeon	Professor, Dept of Environmental Science, Yonsei University	234 Maeji-ri Hungup-myun Wonju-si Kangwon-do 222- 701 Korea T: + 82- 33- 760- 2437 F: + 82- 33- 766- 2551 *sycho@dragon.yonesei.ac.kr*
40	Korea	BNCT	Mr. CHOI Hee Dong	Professor, Dept of Nuclear Engineering, Seoul National University	Seoul National University 151- 742 Korea T: + 82- 2- 880- 7205 F: + 82- 2- 889- 2688 choihdg@snu.*ac.kr*
41	Korea	NAA	Mr. CHUNG Yong Sam	Projector Manager, NAA Project, HANARO Center, Korea Atomic Energy Research Institute (KAERI)	150 Puckjindoug Yusungku Taejon Korea 305-353 T: + 82- 42- 868- 8412 F: + 82- 42- 868- 8610 *yschung@kaeri.re.kr*
42	Korea	NAA	Mr. MOON Jong Hwa	Researcher, NAA Project, HANARO Utilization Team, Korea Atomic Energy Research Institute (KAERI)	P.O. Box 105 Yusung Taejon 305-600 Korea T: + 82- 42- 868- 8534 F: + 82- 42- 868- 8448 *Jhmoon1@kaeri.re.kr*
43	Korea	NAA	Mr. LEE Kil Yong	Project Manager, Environmental Geology Division, Korea Institute of Geology, Mining and Materials (KIGAM)	30 Gajung-Dong Yusung Taejon 305-350 T: + 82- 42- 868- 3652 F: + 82- 42- 861- 9727 *kylee@kigam.re.kr*
44	Korea	NAA	Mr. YOON Yoon Yeol	Senior Researcher, Environmental Geology Division, Korea Institute of Geology, Mining and Materials (KIGAM)	30 Gajung-Dong Yusung Taejon 305-350 T: + 82- 42- 868- 3654 F: + 82- 42- 861- 9727 *yyyoon@kigam.re.kr*
45	Korea	NAA	Mr. LEE Jin Hong	Assoc. Prof, Dept of Environmental Eng. Chungnam National University	220 kung-Dong Daeduck Science Town Taejon 305-764 T: + 82- 42- 823- 7546 F: + 82- 42- 822- 5610 *jinlee@cnu.ac.kr*
46	Korea	BNCT	Mr. PARK Seung Hun	Professor, School of Electronics and Information, Kyung Hee University	1 Seocheon-ri Giheung-eup Yogin Gyeonggido T: + 82- 31- 201- 2568 F: + 82- 31- 205- 9062 *parksh@khu.ac.kr*
47	Korea	BNCT	Mr. LEE Byung Chul	Senior Researcher, HANARO Management Team, HANARO Center, Korea Atomic Energy Research Institute (KAERI)	P.O.Box 105 Yusung Taejon 305-600 Korea T: + 82- 42- 868- 8489 F: + 82- 42- 868- 8341 *Bclee2@nanum.kaeri.re.kr*
48	Korea	BNCT	Mr. LEE Seung Hun	M.D, National Cancer Center Hospital	809 Madu 1-dong Ilsan-ku Koyang Gyeonggido 411-351 T: + 82- 31- 920- 1660 F: + 82- 31- 920- 1759 *nsish@kcchsun.kcch.re.kr* *tomsj@chllian.net*

Appendix

LIST OF PARTICIPANTS
2000 WORKSHOP ON THE UTILIZATION OF RESEARCH REACTORS
November 20 - 24, 2000
Taejon, Korea

No	Country	Field	Name	Organization and Position	Telephone & Facsimile No. E-mail address
49	Korea	BNCT	Mr. LIM Sang Mu	M.D, Korea Cancer Center Hospital	215-4809 Kongreung-dong Nowon-ku Seoul T: + 82- 2- 970- 1213 F: + 82- 2- 978- 2005 *Smlim328@kccnsun.kcch.re.kr*
50	Korea	BNCT	Prof. CHO Nam Zin	Professor, Dept of Nuclear Engineering Korea advanced institute of Science and Technology (KAIST)	373-1 Kusong-dong Yusong-gu Taejon 305-701 Korea T: + 82- 42- 869- 3819 F: + 82- 42- 869- 3810/ 8860 *nzcho@mail.kaist.ac.kr* *nzcho@sorak.kaist.ac.kr* *http://nurapt.kaist.ac.kr*
51	Korea	BNCT	Prof. KANG Sang Ook	Professor, Dept of Chemistry Korea University	208 Seochang, Chochiwon, Chung-nam 339-700, Korea T: + 82- 41- 860- 1334 F: + 82- 41- 867- 5396 sangok@tiger.korea.ac.kr
52	Korea	NS	Mr. LEE Chang Hee	Project Manager, Neutron Beam Application, HANARO Center, Korea Atomic Energy Research Institute (KAERI)	P.O.Box 105 yusung Taejon 305- 600 Korea T: + 82- 42- 868- 8443 F: + 82- 42- 868- 8448 *leech@kaeri.re.kr*
53	Korea	NS	Prof. REE Moon Hor	Professor, Dept of Chemistry Pohang University of Science and Technology	San 31 Hyoja-dong Pohang 790- 784 T: + 82- 54- 279- 2120 F: + 82- 54- 279- 3390 ree@postech.edu
54	Korea	NS	Mr. SEONG Baek Seok	Senior Researcher, Neutron Beam Application, Korea Atomic Energy Research Institute (KAERI)	P.O.Box 105 Yusung Taejon 305- 600 Korea T: + 82- 42- 868- 8442 F: + 82- 42- 868- 8448 *bsseong@kaeri.re.kr*
55	Korea	NS	Mr. HAN Young Soo	Senior Researcher, Neutron Beam Application, HANARO Center, Korea Atomic Energy Research Institute (KAERI)	P.O.Box 105 Yusung Taejon 305- 600 Korea T: + 82- 42- 868- 8441 F: + 82- 42- 868- 8448 yshan@kaeri.re.kr
56	Korea	NS	Mr. CHOI Young Nam	Senior Researcher, Neutron Beam Application, HANARO Center, Korea Atomic Energy Research Institute (KAERI)	P.O.Box 105 Yusung Taejon 305- 600 Korea T: + 82- 42- 868- 8439 F: + 82- 42- 868- 8448 dragon@kaeri.re.kr
57	Korea	NS	Mr. LEE Jeong Soo	Senior Researcher, Neutron Beam Application, HANARO Center, Korea Atomic Energy Research Institute (KAERI)	P.O.Box 105 Yusung Taejon 305- 600 Korea T: + 82- 42- 868- 8435 F: + 82- 42- 868- 8448 Jslee3@kaeri.re.kr
58	Korea	NS	Mr. SHIM Hae Seop	Senior Researcher, Neutron Beam Application, HANARO Center, Korea Atomic Energy Research Institute (KAERI)	P.O.Box 105 Yusung Taejon 305- 600 Korea T: + 82- 42- 868- 8437 F: + 82- 42- 868- 8448 hsshim@kaeri.re.kr
59	Korea	NS	Dr. KIM Shin Ae	Post Doctor, Neutron Beam Application, HANARO Center, Korea Atomic Energy Research Institute (KAERI)	P.O.Box 105 Yusung Taejon 305- 600 Korea T: + 82- 42- 868- 8438 F: + 82- 42- 868- 8448 ex-sakim@kaeri.re.kr
60	Korea	NS	Mr. NAM Ki Young	Post Doctor, Neutron Beam Application, HANARO Center, Korea Atomic Energy Research Institute (KAERI)	P.O.Box 105 Yusung Taejon 305- 600 Korea T: + 82- 42- 868- 8439 F: + 82- 42- 868- 8448 *ex-namky@kaeri.re.kr*

Field: NS - Neutron Scattering, NAA - Neutron Activation Analysis, BNCT - Research Reactor Utiliztion(BNCT), M-Management.